











東京帝國大學  
理 科 大 學 紀 要

第 參 拾 七 冊

THE  
JOURNAL  
OF THE  
COLLEGE OF SCIENCE,  
IMPERIAL UNIVERSITY OF TOKYO.

Vol. XXXVII.

東京帝國大學印行  
PUBLISHED BY THE UNIVERSITY.

TOKYO, JAPAN.

1914-1917.  
TAISHO 8-6.

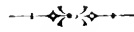
## Publishing Committee.

Prof. **J. Sakurai**, *LL. D.*, *Rikugakuteikushi*, Director of the College (*ex officio*).

Prof. **I. Ijima**, *Ph. D.*, *Rikugakuteikushi*.

Prof. **F. Ōmori**, *Rikugakuteikushi*.

Prof. **S. Wataŕe**, *Ph. D.*, *Rikugakuteikushi*.



12970

## CONTENTS.

---

- Art. 1.—Researches on the electric discharge of the isolated electric organ of *Astrape* (Japanese electric ray) by means of oscillograph. (With 30 plates). By K. FUJI.—Publ. Dec. 11th, 1914.
- Art. 2.—Recherches sur les spectres d'absorption des ammine-complexes métalliques. I. By Y. SHIBATA.—Publ. Sept. 30th, 1915.
- Art. 3.—Considerations on the problem of latitude variation. By K. SOTOME.—Publ. Nov. 30th, 1915.
- Art. 4.—On the distribution of cyclonic precipitation in Japan. By T. TERADA, T. YOKOTA and S. OGIKI.—Publ. Jan. 27th, 1916.
- Art. 5.—On the relatively Abelian corpora with respect to the corpus defined by a primitive cube root of unity. By T. TAKENOUCHI.—Publ. Mar. 30th, 1916.
- Art. 6.—Numerical calculation of the Jacobian ellipsoids. By R. KAMEBA.—Publ. July 20th, 1916.
- Art. 7.—On the elastic equilibrium of a semi-infinite solid under given boundary conditions, with some applications. By K. TERAZAWA.—Publ. Dec. 7th, 1916.
- Art. 8.—Recherches sur les spectres d'absorption des ammine-complexes métalliques. II. By Y. SHIBATA.—Publ. Dec. 29th, 1916.
- Art. 9.—On rapid periodic variations of terrestrial magnetism. By T. TERADA.—Publ. May 25th, 1917.
- Art. 10.—On the photographic action of  $\alpha$ ,  $\beta$  and  $\gamma$  rays emitted from radioactive substances. (With 3 plates). By S. KINOSHITA and H. ICHII.—Publ. Nov. 20th, 1917.
-



# Researches on the Electric Discharge of the Isolated Electric Organ of *Astrape* (Japanese Electric Ray) by Means of Oscillograph.

By

K. Fuji, *Rigakushū*.*With 30 Plates.*

## Contents.

	Page
I. Introduction. ... ..	1
II. Description of the fish, and preparation of the organ. ... ..	3
III. Plan of the experiments. ... ..	6
IV. Formula expressing the discharge curve. ... ..	14
V. Relation between the form of stimulus and the discharge caused by it. ...	26
VI. Discharge by two successive stimuli. ... ..	42
VII. Fatigue phenomenon. ... ..	65
VIII. Speed of propagation of excitation through the nerve. ... ..	70
IX. Miscellaneous problems. ... ..	72
Summary. ... ..	77
Appendix. Tables of experimental data and calculated numbers. ...	80

## I. Introduction.

It is now some twenty years since the discharge curves of electric fishes began to be investigated by such physiologists as Gotch, Schönlein, Garten, Koike, Cremer and others. The method of Gotch consisted in tracing the curve, point by point, by means of a ballistic galvanometer, a single point being determined by each discharge. Schönlein applied Bernstein's rheotome; Garten and Koike used the capillary electrometer and the string

galvanometer, whereas Cremer employed his string electrometer. Although the method of experiments used by Gotch was certainly the most ingenious at that time, the curves obtained are not sufficiently accurate to be analysed quantitatively. The method of Schönlein is inferior to that of Gotch, for the form of the discharge curves obtained by his method cannot fail to be much affected by the fatigue of the tissues. As the capillary electrometer, the string galvanometer and the string electrometer cannot faithfully follow so quick a change in the electromotive force as happens in the case of the discharge phenomena in question, the curves obtained by them are only qualitative.

In April 1906, in conjunction with Mr. S. Oinuma, now *Igakuhakushi*, the author began his experiments on the same subject by means of an oscillograph in the Physiological Institute of the Imperial University of Tōkyō. In the course of this investigation, his collaborator went to Europe, and the author was then obliged to continue the experiments alone.

The electric fish used by us was one of the electric rays called *Astrape japonica*, which was brought from Misaki, a fishing town in Sagami peninsula. Perhaps on account of the imperfectness of our aquarium, the fish could not be kept in a healthy state except for a few months in Spring and Autumn; and in these most favourable periods, even a single fish sometimes could not be obtained. On account of these and other hindrances, and although lengthy and exhaustive experiments were continued up to 1910, the problems first proposed could not be thoroughly investigated. The results so far obtained by these experiments are now presented in this paper.

With regard to the form of the discharge curve which will be discussed in § IV., it is very interesting to note that some physiological phenomena can be explained from the standpoint of the theory of probability. It is a known fact that many quantities characterising a class of animals or plants are subject to individual variations; and if the observations are taken on a sufficiently large number of individuals of the same class, the values representing any of these characteristics distribute themselves, among the number of

individuals taken, in such a manner that the variation appears to occur in accordance with the law of errors. Since now the tissues of an organism consist of a large number of structural elements, it is natural to suppose that a characteristic belonging to these elements varies in different individuals according to a similar law. Then, it may be remarked, that the treatment of the physical phenomenon in a tissue must be based on the principle of probability, and especially in the treatment from the standpoint of the "all or none"\* theory, the application of this principle must be effective and indispensable, for a physical phenomenon exhibited by a tissue must be the integral effect of the phenomena occurring in each of the component elements.

## II. Description of the Fish, and Preparation of the Organ.

The structure of the electric organ in *Astrape japonica* was recently described in detail by K. Ishimori<sup>†</sup>, and therefore need not be entered into here. However, a few points having direct bearing on the present investigations may here be recorded.

The external aspect of the fish and its electric organs are represented in Plate I. The length of the mature fish is about 25 cm.,

---

\* Lucas inferred from his investigation on the contraction of a skeletal muscle, *M. cutaneous dorsii*, of the frog (Journal of Physiology, Vol. 33, 1909.), that, when a stimulus greater than a certain threshold value is given to a single nerve-fibre, the excitation evoked in it appears to have a definite value independent of the intensity of the stimulus. Then, it seems very probable that, with regard not only to a nerve but to tissues in general, the excitation evoked at a point in the excitatory elements follows the so-called "all or none" law. In other words, there exist only two alternatives, *i.e.*, whether the excitation does occur in a definite intensity or not at all,—no intermediate value being possible. In this view, the propagation of the excitation should take place by the successive action of the excited point towards its neighbour, the propagation in reverse direction being impossible in virtue of the existence of the refractory period. The energy of the excitation of each portion should be supplied by some chemical change in it, and therefore its intensity should depend on the physiological state of that portion only. A case may occur, that an excitation is enfeebled on its way to propagation, by passing through a portion in an abnormal state, to such a degree as is incapable of evoking the excitation of the neighbouring portion. Then the farther propagation is impossible and stops there. For proper understanding of the discussions throughout this paper, it is necessary to keep these considerations in mind.

† Beiträge zur Physiologie. Festschrift zu Ehren der 25 Jährigen Lehrtätigkeit von Kenji Osawa.

measured from head-end to tip of tail. The electric organ is present in a pair in the form of large flat bodies, situated one on each side and lateral mainly to the head and the branchial regions. The upper and lower surfaces of the organ are in direct contact with the integument of the fish. Each organ is an assemblage of vertical hexagonal prisms about 200 in number. The height of the prisms measures 1–1.5 cm. Each prism consists of a pile of disc-like body called the *electric plate* numbering about 400. The plates consist each of a clear jelly-like mass inclosing a number of large nuclei and are surrounded as well as separated from one another by a connective-tissue layer in which the nerves and the blood vessels find their course. From the *Lobus electricus* of the brain, there arise on each side five special nerves, the electric nerves, which supply the organ in question. Distally the nerves undergo successive branching, finally to terminate in fine network on the ventral side of each electric plate. In the discharge of electricity the side of the plate just mentioned is always negative, while the dorsal side without the nerve-endings is positive.

Before explaining the plan of the experiments, we shall describe the method of preparing the organ for the purpose. Except when the spontaneous discharge was to be studied, the organ was separated from the body and the whole or a part of it was used according to circumstances. When the fish was brought from the aquarium to the laboratory, in order to avoid the setting in of fatigue, the brain was extracted by applying a cork-borer to the head and then striking its upper end with a hammer. The spinal cord was next destroyed by pushing a wire into the spinal canal. Having thus avoided the reflex action of the nervous centre, the organ was separated from the fish.

The electric discharge of the organ is evidently a very complex phenomenon, for it must be the integral effect of unit discharges of the electric plates. When a stimulus is given at a point in the nerve-trunk, the excitation is distally transmitted through nerve-fibres of different lengths, and as the speed of transmission through them is finite, it should arrive at the different electric plates not simultaneously but at different periods. Hence it is



advantageous, for the investigation of the discharge curve, to stimulate the organ not through the nerve-trunk but directly, so that each plate may receive the stimulus at the same instant. For the direct stimulation of the muscle, it is customary to use *curara* in order to benumb the nerve-endings. In the case of the electric organs, however, there is known no such drug that can be used with the same effect. Hence the term *direct stimulation* used in this paper in relation to the electric organ has a somewhat different meaning from that used in the case of a muscle. Though the stimulating electric current is sent directly through the electric organ, the stimulus is probably in the main imparted to it through the nerve-fibres distributed in it. Nevertheless, in that way the condition of simultaneous stimulation can be better fulfilled than when the stimulation is given through the nerve-trunk. Moreover, when the nerve-trunk is left attached to the organ, the discharge current flowing through the nerve-trunk is very liable to act as a second stimulus and to cause a *secondary discharge* of considerable magnitude, by which a tertiary discharge is called forth, and so on. This makes the phenomenon very complex. But, in the case of direct stimulation of the organ, if the nerve-trunk be carefully taken away from the organ, and if its temperature be kept sufficiently low, there will result only a very weak secondary discharge (Plate I., Fig. 2). In accordance with these considerations, we employed direct stimulus in general, except when the property of the nerve was to be investigated. In the former case the five trunks of the nerves were cut off as near as possible to the organ, and the whole or a part of it was utilised. In the latter case, when the stimulus was to be sent through the nerve-trunk, about a quarter of the organ with one nerve-trunk was employed.

### III. Plan of Experiment.

The diagram of the plan of the experiment is represented in Fig. 1.

The oscillograph used by us was that designed by Duddell and made by The Cambridge Scientific Instrument Company, and that which is known as the high frequency type. The period of strips in an undamped state measures about  $1/10000$  sec. By means of this instrument, an alternating current having a period 50 times that of the strips may be photographed without an appreciable error.\* As the duration of a discharge of the organ measures about  $1/100$  sec., the curve obtained by this instrument may be relied on for quantitative analysis. As the instrument is designed for an alternating current, it has a pair of strips, one for the current and the other for the applied E. M. F. In our experiments, when the organ was stimulated directly, only one of them was employed, the stimulating current and the resulting discharge current being made to flow through the same strip; and when the stimulus was sent through the nerve-trunk, one of the strips was used for the stimulus and the other for the discharge. The fact that both the stimulus and the discharge may be photographed upon one and the same film is very convenient for accurate work. The sensitivity of the oscillograph is about 26 mm. for 0.1 ampere, the film being at a distance of 50 cm. from it. The resistance of each strip is about 8 ohms.

The light source  $Q$  for illuminating the oscillograph consists of a hand-regulating arc lamp of 15 amperes, the image of which is formed on a slit  $s$  by a lens  $L$ .

The registering drum  $D$  is supported within a camera and has a circumference of 50 cm. (Plate III., Fig. 1). This is revolved by a small motor  $M$  of  $1/30$  H.P. The number of revolutions used was 5–20 per. sec., according to circumstances. A photographic film was wound around the drum and kept in position by means of two india-rubber rings which keep each side of the film pressed

---

\* Zeitschrift für Instrumenten-Kunde, S. 240, Bd. 21, 1901.

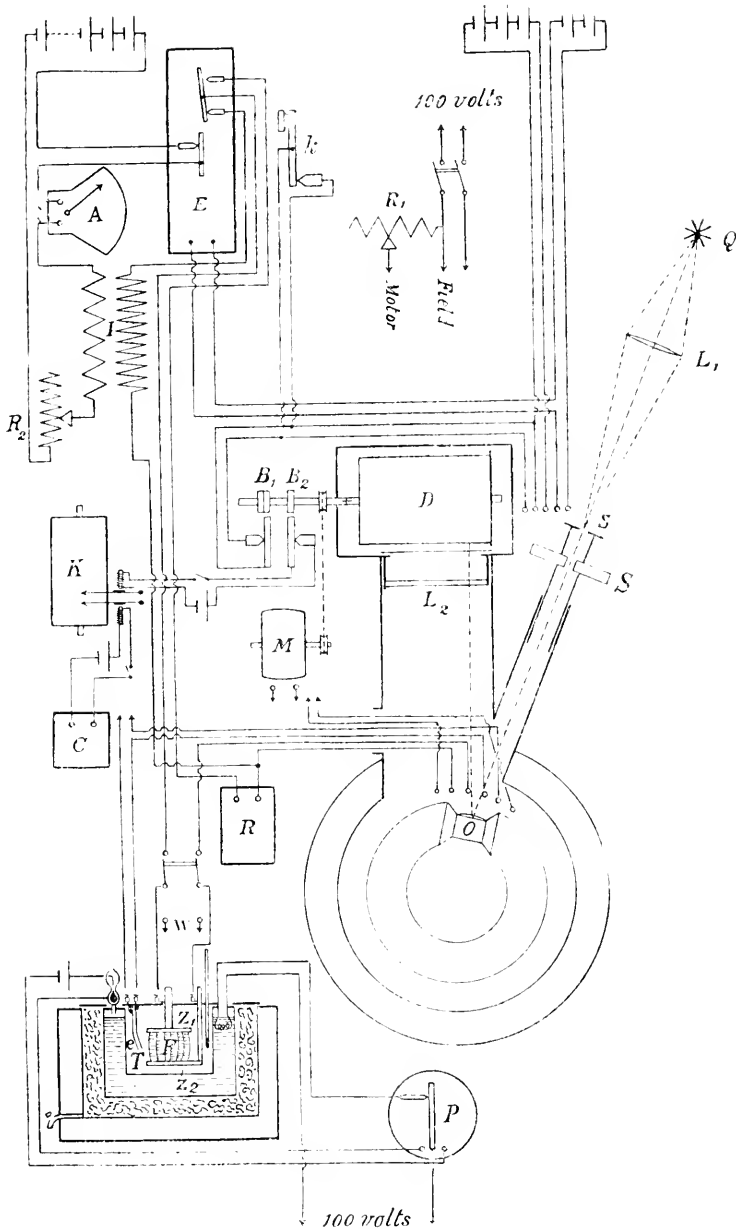


Fig 1. The Plan of Experiment.

- |                                     |                                      |                                     |  |
|-------------------------------------|--------------------------------------|-------------------------------------|--|
| <i>O</i>                            | Oscillograph.                        | <i>Z<sub>1</sub>, Z<sub>2</sub></i> | Zinc electrodes for electric organ.                          |
| <i>Q</i>                            | Arc lamp.                            | <i>P</i>                            | Relay for thermostat.  |
| <i>L<sub>1</sub></i>                | Converging lens.                     | <i>E</i>                            | Stimulation-apparatus.                                       |
| <i>s</i>                            | Slit.                                | <i>I</i>                            | Induction coil.  |
| <i>S</i>                            | Shutter.                             | <i>A</i>                            | Ammeter.   |
| <i>L<sub>2</sub></i>                | Cylindrical lens.                    | <i>R<sub>2</sub></i>                | Regulating resistance for primary current of induction coil. |
| <i>D</i>                            | Registering drum.                    | <i>k</i>                            | Morse key.   |
| <i>M</i>                            | Motor.                               | <i>K</i>                            | Chronograph.   |
| <i>R<sub>1</sub></i>                | Regulating resistance for motor.     | <i>C</i>                            | Chronometer.   |
| <i>B<sub>1</sub>, B<sub>2</sub></i> | Break-circuit contrivances.          | <i>R</i>                            | Resistance box.  |
| <i>F</i>                            | Organ-preparation.                   | <i>W</i>                            | To Kohlrausch bridge.  |
| <i>T</i>                            | Thermostat.                          |                                     |  |
| <i>e</i>                            | Electrodes for indirect stimulation. |                                     |  |

firmly against the drum and also by a thin piece of bamboo which presses the two overlapping ends of the film. When the stand supporting the drum is pulled, the axis of the drum is disconnected from its driving shaft by means of a special contrivance (Plate IV., Fig. 1, *a*), and the drum with its stand may be taken out of the camera, the operation being accomplished in the dark without any trouble.

On the shaft of this registering apparatus, there are two break-circuit contrivances like that of a chronometer (Plate IV., Fig. 1, *b*; *b*<sub>2</sub>; Fig. 2), one for the chronograph by which the number of revolutions of the drum is measured, and the other for the shutter described below.

A kymograph *K* made by Zimmermann, with accompanying time-markers, was used as the chronograph, the record being obtained on smoked paper. When the speed of the rotation of this instrument is increased to its maximum, the number of revolutions of the registering drum may be accurately determined to three figures.

The organ-preparation was supported between two zinc plates that served as electrodes. To secure a good contact, and also to avoid the effect of polarisation, if such existed, the surfaces of the zinc plates were covered with kaolin paste, soaked with a saturated solution of zinc sulphate, and then with a layer of the same material kneaded with a physiological solution of sodium chloride.

Since it is found that the form of the discharge curve is much affected by the change of temperature, the organ is put into an electrically regulated thermostat. As the favourable range of temperature for our investigation was found to be 8°C.—15°C., and because in the warm season this range of temperature is lower than that of the room, the thermostat must be so designed as to ensure that a constant temperature lower than the surrounding temperature be maintained. For this purpose the author constructed a special thermostat shown in Fig. 1. The moist chamber, in which the organ supported by the zinc electrodes is put, is surrounded by a jacket of transformer oil, in which a toluene regulator and an

electrically-heated resistance are immersed. Outside of this comes a layer of ice, and the whole is protected from external heat by an air jacket. The thermostat works well for 6—7 hours without any fresh supply of ice.

Next we shall describe the construction of a shutter designed by the author (Plate II.). The function of this shutter is as follows. (*a*) When a certain place on the film just comes to receive light from the oscillograph, the shutter opens, (*b*) then the stimulation-apparatus is set in work, whereby the organ is excited and the oscillograph prints the motion due to the stimulation and the discharge current, and (*c*) when the drum has made just one revolution after the shutter first opened, it is made to close so as to protect the film from unnecessary exposure to light. The operations *a* and *c* are accomplished by sending to the electro-magnets on the shutter instantaneous breaks of current, which occur once in each revolution of the registering drum. Fig. 4 in Plate IV. represents the construction of the shutter. It consists essentially of two almost identical aluminium sectors *A* and *B*, placed one behind the other with a circular hole in each of them, and two electro-magnets *A'* and *B'*, one for each sector. When the sectors, by means of cords, are pulled to the left against the action of the springs, and there held in position by the detents attached to the armatures of the electro-magnets, the shutter is ready for action. When the current is broken for an instant, at the break-circuit contrivance attached to the shaft above mentioned, only the electro-magnet *A'* belonging to the front sector is put into action and the sector *A* is released and turns to the right, and then a free passage of light through the shutter is admitted, (operation *a*). By a simple mechanism attached to the front sector, the electric connection is changed automatically, without interrupting the current in the operation, so that at the next break of the current, which takes place after one revolution of the drum, the back sector is released and the passage of light is intercepted (operation *c*). The contrivances for these operations are illustrated diagrammatically in Fig. 2. The mechanism of the operation *b* will be described under the paragraph of the

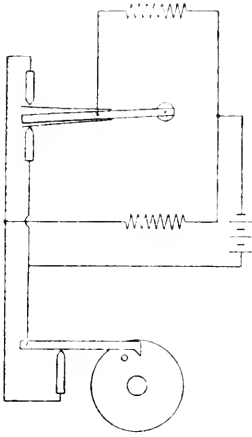


Fig. 2. Connections of shutter.

Before describing the stimulation-apparatus, we shall explain the form of stimulus used in our experiments. The stimulation ordi-

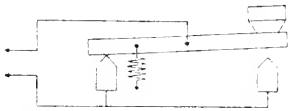


Fig. 3. Connection of Morse key for time-shutter.

narily used was an induced current in the secondary circuit of a Du Bois Reymond's induction coil usually employed by physiologists. When the primary current is suddenly opened, the secondary current increases from zero to a maximum value in a very short period, and then decreases exponentially to zero. By shunting the secondary current at a desired instant in its decreasing stage, it can be made to decrease to zero suddenly. Such a current was ordinarily used as our stimulus in direct stimulation. In many experiments the strength and the duration of such a secondary stimulating current were changed and their influence upon the discharge curve was investigated. The oscillogram in Plate I. (Fig. 2) shows a form of such stimulus followed by the discharge current of the organ in response to it. Here we may remark that we can see in this oscillogram how well the shutter works. In the indirect stimulation, however, the induced current caused by an instantaneous contact in the primary circuit of the induction coil is ordinarily used. This forms a stimulus of very short duration as shown in Fig. 4. For brevity we shall hereafter call such

stimulation-apparatus. The shutter does not work unless a Morse key *k* is pressed which serves as a shunt to the break-circuit contrivance. By adjusting the phase of the break with reference to the drum, the shutter may be opened when any desired position on the film comes to receive light from the oscillograph. For the sake of economy of time and of film, a series of discharges are photographed in order on one film, by thus shifting the phase of break with reference to the drum. The shutter may be used as a time-shutter if desired, when it is connected to the ordinary Morse key as shown in Fig. 3.

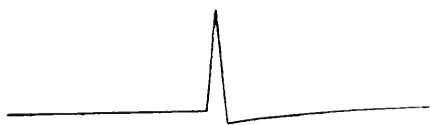


Fig. 4. Momentary stimulus.

a stimulus the *momentary stimulus*. Sometimes it was required to experiment with two such momentary stimuli separated by a given interval of time.

In the direct stimulation of the organ, the secondary of the induction coil, the organ and the oscillograph must be connected in a series. But when the discharge is to be photographed, it is necessary to exclude the secondary coil from the circuit and to introduce a proper resistance if required. For, if the secondary coil is in the circuit, its enormous self-induction influences and modifies the form of the discharge curve, so that, after a stimulus is given, the exclusion of the secondary coil is necessary.

To fulfil the requirements above mentioned, a stimulation-apparatus represented in Plate III. and Plate V. was designed. A brief description of the apparatus will be given below.

A small car *A* having three wheels *B* on each side lies on a pair of cylindrical rails *C*. The rails have grooves in their upper and lower sides to guide the motion of the wheels. A helical spring is wound round each rail and pushes the car to the left end of the rails. An armature made of laminated iron is fixed to the right end of the car. An electro-magnet fixed on the right end of the apparatus, whose core consists of a bundle of soft iron wires, attracts the armature and keeps the car at the right end of the rails against the action of the helical springs. The current of the electro-magnet flows through the breaking contrivance of the shutter. When the shutter is opened (operation *a* before mentioned), the electro-magnet releases the car (operation *b*) and the latter is pushed away along the rails by the action of the helical springs. The car has a knocking contrivance on its lower side called a *knocker*, whose function will be explained later on. In order to protect the car from damage caused by a strong collision against the stop at the end of its leftward motion, a special device is attached to the stop. This consists of a pair of jaws closed by a strong spring. When the car comes against the stop, a plate forming part of the car plunges into the jaws and dissipates

its energy by friction. Behind the electro-magnet, there is a circuit-breaker for opening the current of the electro-magnet. To its lever, an armature made of laminated iron is fixed, so that when the armature is pushed against the electro-magnet, the contact on the upper end of the lever makes the current by means of which this armature as well as the armature fixed to the car is kept in position at the same time, and the magnetic circuit is thus closed through these armatures and the cores of the electro-magnet. The service of this contrivance is twofold. When the current through the electro-magnet is broken at the shutter, this armature, together with that of the car, is released, and the magnetic circuit is broken at once, so that, on account of the increase of the demagnetising force, the electro-magnet loses its magnetism very soon. This is essential for the quick and unfailing action of the stimulation-apparatus. The second service of this contrivance is evident, for when once the circuit is opened at this place, it does not close again.

On the base-board of the stimulation-apparatus and under the rails before mentioned, lie three grooves each furnished with a millimetre-scale along its length and each parallel to the rails. Into these grooves fits any one or a combination of small mechanisms, which are put into action by the knocker attached to the car. The position of these mechanisms can be read to one-tenth of a millimetre by means of verniers attached to them.

One of these mechanisms is called a *circuit-breaker* and is used for breaking the primary circuit of the induction coil. Plate V., Fig. 2 shows the construction of the circuit-breaker. The circuit is to be broken at the contact between a knock-down lever  $l$  and the platinum point of an adjustable screw  $s$ . The lever  $l$  is kept vertically and pressed firmly against the screw by a holder  $h$  by means of a spring. When the car moves leftwards, the knocker kicks down the lever  $l$  and the contact is broken. The peculiar form of the end of the lever and of the holder protects the former from making a second contact with the screw.

Plate V., Fig. 3 is another mechanism which we shall call the *connection-changer*. The rôle of this is to short circuit the secondary



coil at the proper instant after the primary current is broken and then to exclude the secondary coil from the oscillograph circuit. Since the latent period of the discharge measures about  $80 \times 10^{-4}$  sec., this change of connection may be made without disturbing the discharge current. Referring to the figure, *A* and *B* are two springs attached to an arm of a T-shaped lever. At first, the spring *A* is in contact with *A'*. In this case the organ, the oscillograph and the secondary of the induction coil are in a series. When the knock-down lever is kicked, the spring *B* comes into contact with *B'* and then *A* parts from *A'*. At the moment when *B* touches *B'*, the secondary coil is short circuited, and when *A* parts from *A'*, it is excluded from the oscillograph circuit. Then the organ, the oscillograph and an appropriate inductanceless resistance are in a series, ready to receive the response of the organ. *C* is a catcher of the knock-down lever to prevent it from rebounding. The mechanism here mentioned is the final form used by the author. In the earlier experiments mercury contacts were employed, but the trembling of the surfaces of the mercury which generally formed a very complex stimulus could not be avoided. Next we attempted simply to cut the secondary current instead of short circuiting the secondary coil, but the spark at the instant of breaking the circuit, prevented the instantaneous decrease of the current. After such experiences, the author was convinced that it is very dangerous to presume on the form of the stimulus by theoretical considerations only; actual experimental evidence is indispensable. Plate V., Fig. 4 is a contrivance for giving two successive momentary stimuli with any desired interval of time. Two electric contacts are made between the ends of the levers and the knocker of the car. Usually such stimuli are given to the nerve and consequently in this case the connection-changer is not necessary. The distance of the two points of contacts may be adjusted from zero to 25 mm. and may be read to one-tenth of a millimetre by means of a vernier.

These mechanisms are fitted into the grooves fixed on the base-board of the apparatus. The grooves being provided with millimetre-scales, their positions may be read to one-tenth of a

millimetre by means of verniers. When in good working-condition, the length of one millimetre on this apparatus corresponds to  $4.4 \times 10^{-4}$  sec.

#### IV. Formula Expressing the Discharge Curve.

From the oscillogram in Plate I., we see that the discharge curve, caused by a direct stimulus, resembles the probability curve of Gauss, except that it is not symmetrical with respect to the maximum ordinate. After some assumptions, a formula is obtained for expressing the curve that agrees very closely with the experimental curve.

In the first place it is assumed that the discharge of each electric plate, caused by a single stimulus, is of very short duration. It is a known fact that only the first small time-interval of a closing current influences the height of the discharge curves, and this will be discussed more fully afterwards. When this fact is considered, it will not be unnatural to suppose, that a stimulus of such short duration causes a discharge of an instantaneous nature. In the second place it is assumed that the interval between the stimulus and the discharge of a single plate in response to it, which interval may be called the *latent period of a single plate*, may have various values, and among them there is a certain value, which predominates in number, so that other values deviate more or less from it according to the law of errors, though in a somewhat modified form. This predominating latent period may be called the *modal latent period*, which, as will be explained afterwards, represents the interval between the stimulus and the instant corresponding to the maximum point of the discharge curve. In biological phenomena there exist many instances which are governed by a law that involves the idea of probability. The phenomenon of contingency and of correlation treated by Pearson and others are such examples. Here it is simply assumed that a similar relation exists in the quantity—the *latent period of a single plate*.

In Gauss's probability curve, the freedom of deviation from its most probable value is symmetrical with respect to it. In the

discussion here, the discharge of any single plate cannot of course occur before a stimulus is given, so that the freedom of deviation from the modal value can never be symmetrical. There must exist a certain instant before which the discharge can never occur. We shall call this instant the *origin of the discharge*. This origin may be at the instant of stimulation or it may be later.

To adapt the present case to that of Gauss's it is assumed that the equivalent elementary interval with respect to the deviation is proportional to the interval between the origin and that instant.

Denoting the latent period of a single plate by  $x$ , the above assumption gives

$$Jx = kx,$$

$$i. e. \quad J \log x = k,$$

where  $k$  is a proportional constant. This means that, when the logarithm of  $x$  is taken as the measure of the abscissa, the case becomes identical with that of Gauss's.

The well known curve of probability is expressed by

$$y = Ae^{-b^2x^2}, \dots \dots \dots (1)$$

where the origin of  $x$  is at the maximum of  $y$ . Transforming the origin to  $-x_0$ , then

$$y = Ae^{-b^2(x-x_0)^2}$$

is obtained. Substituting the logarithm of  $x$  and of  $x_0$  instead of them, the above reduces to

$$y = Ae^{-b^2 \log^2 \frac{x}{x_0}} \dots \dots \dots (2)$$

Since the total electromotive force at any instant must be proportional to the number of plates simultaneously discharged at that instant, then, when  $y$  is taken as the electromotive force at a point on the discharge curve and  $x$  as the time-interval measured from the origin of the discharge to that point, the curve expressed by the above formula ought to represent the discharge curve obtained by the oscillograph.

Before entering into an examination of experimental curves, the method for determining the constants  $A$ ,  $b^2$  and  $x_0$  must be treated.

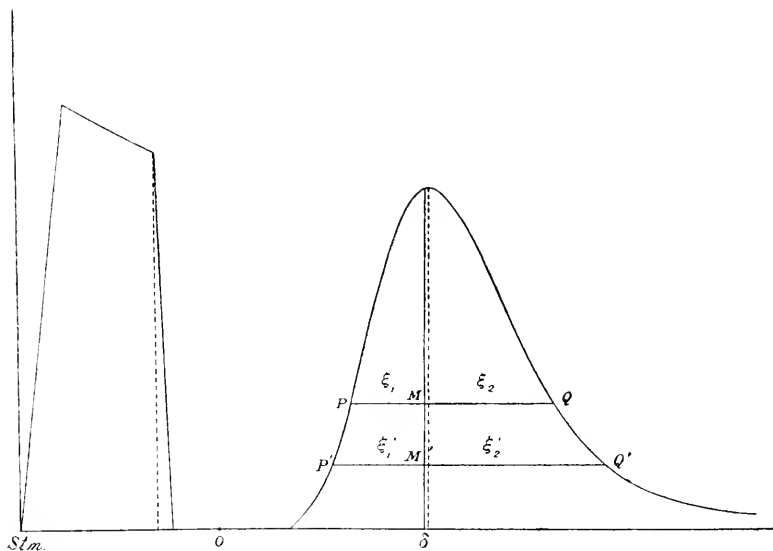


Fig. 5.

To determine  $x_0$ , take two points  $P$  and  $Q$  with the abscissae  $x_1$  and  $x_2$  on the curve in question on its ascending and descending branches where the values of  $y$  are equal. Then it is obvious that

$$\frac{x_2}{x_1} = \frac{x_0}{x_1} \quad \text{or} \quad x_1 x_2 = x_0^2. \dots\dots\dots (3)$$

Let  $M$  be the intersection of  $PQ$  with the maximum ordinate of the curve. Measure  $PM$  and  $QM$ , which may be called  $\xi_1$ ,  $\xi_2$ , then

$$(x_0 - \xi_1)(x_0 + \xi_2) = x_0^2,$$

or

$$x_0 = \frac{\xi_1 \xi_2}{\xi_2 - \xi_1} \dots\dots\dots (4)$$

Thus we can determine the value of  $x_0$ , so that the position of the origin is made known. Then we can calculate  $b^2$  by the following formula.

$$b^2 = \frac{\log_{10} A - \log_{10} y}{(\log_{10} x - \log_{10} x_0)^2} \times 0.4343, \dots\dots\dots (5)$$

where  $x$  and  $y$  are the co-ordinates of  $P$  or  $Q$ .

Since the denominator of the fraction of  $x_0$  in (4) is very small, errors incurred in measuring  $\xi_1$  and  $\xi_2$  influence very much the value of  $x_0$ . Evidently the error due to  $\xi_2 - \xi_1$  is made smaller, the lower the points  $P$  and  $Q$  are taken; but near the foot of the curve on its descending branch, there exists probably secondary discharge, and therefore we cannot take  $P$  and  $Q$  too low. It may be shown that in the calculation of  $b^2$ , it is least affected by the error in  $y$ , caused by the error on the position of the  $x$ -axis, when  $y$  is equal to  $4e^{-1}$ . So also, for the determination of  $x_0$ , we prefer the points  $P$  and  $Q$  whose heights are equal to  $4e^{-1}$ . Since it is very difficult to accurately determine the position of the maximum ordinate, and since the error in its determination influences the difference  $\xi_2 - \xi_1$  doubly, we must make full allowance for the existence of an error of not insignificant importance in  $x_0$  due to this cause. To eliminate this error as far as possible, we take another pair of points  $P'$  and  $Q'$  of equal heights and calculate  $x_0$  as above. If the values of  $x_0$  in the two cases do not coincide, let us assume that the discrepancy is due solely to the error of the position of the maximum ordinate, say  $\delta$ . Correcting for this amount and equating the values of  $x_0$  in the two cases, we have

$$\delta = \frac{\xi_1' \xi_2' (\xi_2 - \xi_1) - \xi_1 \xi_2 (\xi_2' - \xi_1')}{2(\xi_2' \xi_1' - \xi_2 \xi_1)}, \dots\dots\dots (6)$$

where the terms of the second order are neglected.

First the agreement between the theoretical and the experimental curve was examined on Oscillogram No. 54 (Plate XIII.). This was a series of experiments for finding the relation between the magnitude of the stimulation current and the discharge in response. The stimuli were direct and their durations were taken pretty long in order to avoid the effect of small changes in them.

The following are the data of the experiment:—

#### Oscillogram No. 54.

Object of experiment:	Relation between the intensity of the stimulation current and the magnitude of the discharge.
-----------------------	---

Date of experiment: Nov. 6, 1909.

Organ: Left organ (whole) of a fish of middle size.

Temperature of the organ:  $8.5^{\circ}$ — $7.2^{\circ}$ C.

Resistance of the organ: About 240 ohms.

Reading on the first rail of the stimulation-apparatus (circuit-breaker): 64.0 mm.

Reading on the second rail of the stimulation-apparatus (connection-changer): 60.0 mm.

No. of stimulus in order of time.	1	2	3	4	5	6	7	8
Primary current of induction coil in amp.	1.5	2.0	2.5	3.0	3.5	4.0	4.5	4.95
Number of revolutions of registering drum.	6.51	6.38	6.50	6.53	6.40	6.18	6.00	6.36

The ordinates of the points on the curves were measured for every one mm. of abscissa on the oscillogram, and they were plotted on a section paper, the value of the abscissa being converted to the unit of  $10^{-4}$  sec. (Plate VI.). The following table shows the constants obtained by applying the method above described on the reproduced curves:—

TABLE I.

No.	L. P. in $10^{-4}$ sec.	M. L. P. obs. in $10^{-4}$ sec.	$\delta$ in $10^{-4}$ sec.	M. L. P. corr. in $10^{-4}$ sec.	$A$ in mm.	$b^2$	$x_0$ in $10^{-4}$ sec.
1	76.8	107.5	Too low to be measured.		1.6		
2	79.2	106.4			5.0		
3	73.9	107.8	+ 0.68	108.5	10.1	4.60	59.2
4	71.9	107.1	+ 1.12	108.2	17.3	4.69	59.8
5	73.6	109.6	— 0.10	109.5	26.7	5.63	64.2
6	69.7	108.5	+ 1.40	109.9	35.7	5.37	60.8
7	68.3	106.6	+ 1.06	107.7	44.8	4.49	54.8
8	67.5	109.9	+ 1.46	111.4	55.6	5.95	61.8

L. P. means *latent period* (ordinary usage).

M. L. P. means *modal latent period*.

Full details of calculations are given in the Appendix.

Referring to the table we see that the value of the modal latent period is tolerably constant in spite of the wide changes of the magnitude of the stimulus, while the latent period decreases with the height of the discharge curve. The small increase of the modal latent period may be due to the progressive decrease of temperature, as is given in the data of the experiment. In this case it is a remarkable fact, that  $\delta$  is always positive except in Curve No. 5, and the constancy of the modal latent periods corrected becomes rather worse than that of the observed modal latent periods. The values of  $x_0$  and of  $b^2$  vary with the increase of the height of the stimulus and the values of  $b^2$  are equal to 5.0 in order of magnitude. Here we may remark; that it is very difficult to determine accurately the value of  $x_0$ , but  $b^2$  may compensate for the error of  $x_0$  in the final result. So we cannot put too much weight on the changes of the value of  $x_0$  and of  $b^2$ . At anyrate we calculated the values of  $y$  for every one-thousandth of a second, from the values of constants in the table, and plotted these calculated values on the reproduced curves. These are shown in Plate VI. The agreement between the calculated and the observed curves is very satisfactory except for a small part on both feet of the curves, where the calculated points are in general lower than the observed. The discrepancy on the descending foot may be due to the superposed secondary discharge.

Next Oscillogram No. 37 (Plate XIII.) was examined. This was a series of experiments for investigating the relation between the duration of the stimulating current and the magnitude of the discharge. The durations of the stimuli were very small compared with those of Oscillogram No. 54. The curves on the oscillogram were measured and reproduced in the same way as in No. 54 (Plate VII.).

In this series of experiments, the previous method for the determination of  $x_0$  failed to give consistent values to  $x_0$  on account of the smallness of  $\xi_2 - \xi_1$ , or, in other words, the values of  $x_0$  were greater than those of No. 54. After many laborious trials, we at last found that, when we took the origin of the discharge at the beginning of the stimulus, the square root of the product of  $x_1$  and

$x_2$  for any value of  $y$ , agreed very closely with the observed modal latent period. So assuming that the origin of discharge was at the beginning of the stimulus, we calculated as in No. 54.

The following table shows the constants of the curves:—

TABLE II.

Oscillogram No. 37. Left organ (whole) of a fish, the same preparation as No. 35 and No. 36.

Temperature of the organ: 11° C.

No.	M. L. P. obs. in $10^{-4}$ sec.	Mean of $\sqrt{x_1 x_2}$ .	$b^2$ .	$A$ in mm.
1	123.0	122.0	23.7	31.5
2	124.2	124.6	25.8	30.8
3	125.7	126.6	27.1	28.3
4	126.7	127.4	27.4	27.5
5	125.4	126.6	26.1	25.0
6	128.2	128.2	27.0	23.3
7	129.5	129.2	26.3	19.0
8	127.5	128.2	27.8	12.5

The data and the details of the observed and the computed numbers given in the Appendix.

Here the modal latent period is tolerably constant as in No. 54, having a tendency to increase a little with the progress of the experiment. The constant  $b^2$  increases with the decrease of the breadth of the stimulus \*or the height of the discharge.\*

Calculating with these constants the values of  $y$  for every one-thousandth of a second, and plotting the values obtained on the reproduced curves, the agreement of the points is very satisfactory as we may see in the figures (Plate VII.).

\* For the sake of brevity, let us call the duration of the stimulating current the *breadth of stimulus*, the maximum intensity of it the *height of stimulus*, and the maximum electromotive force of the discharge the *height of discharge*.



Oscillogram No. 40 (Plate XVII.), which is the same kind of experiment as No. 37 and in which the breadths of the stimuli are very small, was examined and the constants were calculated as in No. 37 (Plate VIII.).

The following is the table of the constants obtained:—

TABLE III.

Oscillogram No. 40. Left organ, the same preparation as No. 38.

Temperature of the organ: 11.5° C.

No.	M. L. P. obs. in $10^{-4}$ sec.	Mean of $\sqrt{x_1 x_2}$ .	$b^2$ .	$A$ in mm.
1	121	121.6	20.0	44.5
2	119	119.6	20.8	41.0
3	120	120.4	20.6	40.0
4	120	120.2	20.4	38.0
5	122	122.2	21.8	39.0
6	122	122.8	23.2	33.5
7	122	122.0	22.2	35.6
8	122	123.4	22.9	39.5

The data and the details of the observed and the computed numbers are given in the Appendix.

Here the modal latent period is constant again, and  $b^2$  seems to increase with the decrease of the height of the discharge. The agreement between the calculated and the observed curves is shown in Plate VIII. The values of  $b^2$  in No. 37 and No. 40 are equal to 20 in order of magnitude.

Thus having proved the close agreement of the theoretical formula with the experimental curves, we shall next seek the source of the discrepancy between the constants of No. 54 and those of No. 37 and No. 40. In the foregoing considerations, we did not take into account the effect of the stimulus due to the break of the current

at all. The stimulus used in these experiments consisted of the closing and the opening-stimulus.\* The stimulus on the break of the current must be due to the recovery from some sort of polarisation, though not limited to electrical polarisation, caused by the current. It is not therefore unreasonable to suppose that, the closer the opening-stimulus is to the closing-stimulus, the smaller is the effect of the former. Moreover, when we consider the existence of the refractory period, we may suppose the effect of the opening-stimulus neglected when the breadth of the stimulus is sufficiently small. Comparing Oscillograms No. 37 and No. 40 with No. 54, we find that the breadths of the stimuli in No. 54 are greater than those in No. 37 and in No. 40. Examining many other oscillograms, we see that, where the breadth of the stimulus is great, the unsymmetry of the curve is manifest. Hence we may conclude that the anomaly in No. 54 must be due to the superposition of the effect of the opening-stimulus.

In No. 54 we see that, when we take the magnitude of the latent period into consideration, the actual commencement of the discharge by the opening-stimulus must be a little later than the culmination of the curve. Hence assuming that the discharges caused by the closing-stimuli had their origins at the beginning of the stimuli and the ascending branches of the curves were wholly due to them, we calculated  $b^2$  from their respective co-ordinates  $x_1$  and  $y_1$ . These values of  $b^2$  corresponding to each curve in No. 54 are represented in the following table. Let us denote such  $b^2$  by  $b_0^2$ .

TABLE IV.

No.	$x_0$ in $10^{-4}$ sec.	$b_0^2$ .	No.	$x_0$ in $10^{-4}$ sec.	$b_0^2$ .
1	107.5	—	5	109.6	18.8
2	106.4	—	6	108.5	19.8
3	107.8	20.8	7	106.6	24.3
4	107.1	21.1	8	109.9	26.5

\* In this paper, the stimulus on the growth of the stimulating current is called the *closing-stimulus*, and the stimulus on the decay of the current is called the *opening-stimulus*, whether the current is derived directly from the battery or is induced by an induction coil.

Here we see that the values of  $b_0^2$  thus obtained agree in order of magnitude with those of No. 37 and No. 40. To prove that our consideration was correct, we took Curve No. 7 in No. 54, and using the new constants we calculated the values of  $y$  for every  $1/1000$  sec. Plotting the calculated values on the experimental curve, we see that they fall so very closely on the ascending branch, that even the disagreement previously observed at the beginning of the curve disappears; while the descending branches separate from each other widely. The experimental and the calculated curves are shown in Plate IX. Calculating the differences of the ordinates of points on the descending branches of the two curves for every  $4/10000$  sec., we have drawn a residual curve which would no doubt be caused by the opening-stimulus only. The residual curve thus found is plotted on the same Plate. Having assumed the origin of the residual curve to be at the instant of breaking of the stimulating current and having found the value corresponding to  $x_0$  by the formula  $x_0 = \sqrt{x_1 x_2}$ , we calculated the value of  $b^2$  corresponding to the new curve, and we found that it was equal in order of magnitude to that of the main curve. The constants thus found for the residual curve were  $A=10.0$ ,  $b^2=17.2$  and  $x_0=100.8$ . Calculating the values of  $y$  for every  $1/1000$  sec. by using these constants, and plotting them on the residual curve, we see that the agreement is rather wonderful. The value of  $x_0$  of this curve is a little smaller than that of the main curve, but if we consider that the effective instant of the closing-stimulus is a little later than the beginning of the stimulus, we have reason to suppose that the modal latent periods are equal.

Tables V. and VI. show the constants obtained on Oscillograms No. 62 and No. 63, where broad stimuli are used. Oscillograms No. 62, No. 63 and No. 64 (Plate XVI.) form a set of experiments for finding the relation between the intensity of the stimulus and the magnitude of the discharge. The breadth of the stimulus is greatest in No. 62, medium in No. 63 and smallest in No. 64. The temperature of the organ was  $13.5^\circ\text{C}$ .

TABLE V.

No. 62.

No.	$x_0$ in $10^{-4}$ sec.	M. L. P. in $10^{-4}$ sec.	$b^2$ .	$b_0^2$ .	$A$ in mm.
1	46.5	82.0	2.69	12.8	33.7
2	45.0	83.5	3.76	11.9	26.6
3	55.3	83.5	5.10	11.0	19.7
4	90.5	90.5	5.96	11.3	13.7
5	80.5	88.0	9.48	10.7	8.7
6	64.5	84.1	5.05	12.4	4.6
7	—	—	—	—	2.3

TABLE VI.

No. 63.

No.	$x_0$ in $10^{-4}$ sec.	M. L. P. in $10^{-4}$ sec.	$b^2$ .	$b_0^2$ .	$A$ in mm.
1	45.8	84.1	3.28	14.5	25.3
2	44.1	74.2	3.35	14.0	19.3
3	54.5	84.0	4.96	14.0	14.3
4	44.1	83.5	2.84	13.8	10.4
5	53.8	86.0	4.47	13.8	6.4
6	53.0	83.7	4.93	14.7	3.4
7	89.7	85.5	12.4	14.7	1.5
8	—	—	—	—	—
9	38.8	83.0	2.08	14.1	24.4

In these tables the numbers in the columns denoted by  $b_0^2$  are the values of  $b^2$  calculated on the assumption that the origin of the discharge is at the beginning of the stimulus. Here again the values of  $b^2$  seem to vary with the decrease of the height of the stimulus. But the variation of  $b^2$  in No. 54, No. 62 and No. 63 should be apparent, and it shows that the effect of the opening-

stimulus is small when the closing-stimulus is very great or when the opening-stimulus is very small. The increase of  $b^2$  in No. 37 and No. 40 with the decrease of the breadth of the stimulus would show that the narrower the stimulus the smaller the effect of the opening-stimulus.

The last curve in Plate VIII. shows that the formula may be applied to the discharge caused by an *indirect* stimulus, if a small part of the organ is taken. The figure represents a curve reproduced from Oscillogram No. C. 3. which is not shown in this paper. The constants obtained by the ordinary way are :—

No. C. 3.

$$A = 55.4 \text{ mm.},$$

$$x_0 = 57.6 \times 10^{-4} \text{ sec.},$$

$$b^2 = 5.83,$$

$$M. L. P. = 162.2 \times 10^{-4} \text{ sec.}$$

The temperature of the organ was  $10.5^\circ \text{C}$ . The stimulus was indirect and descending. From the order of magnitude of the constants, we may suppose that the discharge is not simple. It seems to the author that the opening-stimulus had some effect on the response curve.

From the above discussion we find that:—

i.) When the discharge is simple, the time-curve of the electromotive force of it may be represented by the formula  $y = Ae^{-b^2 \log^2 \frac{t}{x_0}}$ , where the origin of the discharge is at the stimulus.

ii.) The departure from the above law, as in No. 54, may be considered to be apparent, the superposition of the discharge by the opening-stimulus changing the values of the constants.

iii.) The modal latent period of a simple discharge remains constant in spite of the change of the magnitude of the stimulus.

iv.) The value of  $b^2$  seems to vary a little with the height of the discharge, but the relation is not clear on account of the overlapping of the errors of the same order of magnitude.

v.) It is very doubtful whether the so-called latent period has a definite meaning. It should be a function of the sensitivity of the instrument by which it is determined.

## V. Relation between the Form of Stimulus and the Discharge Caused by It.

The relation between the form of the electric stimulus and the excitation in a nerve caused by it, has been investigated by many physiologists. Some give a formula representing the relation which contains a function of an unknown form. König's formula is such an example and is expressed by

$$E = \int_0^t F(t) \frac{di}{dt} dt,$$

where  $E$  denotes the excitation evoked, and  $i$  the instantaneous value of the stimulating current at a time  $t$  which is measured from the commencement of the stimulating current. According to him  $F(t)$  is a function of an unknown form that acts as a decrement factor and that has a finite value only when  $t$  is very small.

In 1892 Hoorweg,\* in his experiments on the stimulation of a condenser discharge, found a relation connecting the potential difference, by which the condenser was charged, the resistance of the conductor in the circuit, and the capacity of the condenser that caused minimal shock in a nerve. He deduced from it a general expression representing the relation between the electric stimulus and the excitation caused by it. His formula is expressed by

$$E = a \int_0^t i e^{-\beta t} dt, \dots \dots \dots (7)$$

where  $a$  and  $\beta$  are constants. According to his opinion the elementary excitation evoked in a nerve at an instant is proportional to the strength of the current  $i$  at that instant, in opposition to the prevailing opinion in which it depended on the rate of change of the current *i. e.*  $\frac{di}{dt}$ ; and as a decrement factor he introduced  $e^{-\beta t}$ . Although many authors opposed his formula, it is the only one that is expressed by a definite function. He afterwards tried to deduce

---

\* Plüger Archiv. Bd. 52, S. 87, 1892,

his formula from the hypothesis of Nernst, but his solution of the differential equation does not satisfy the initial condition of uniform concentration. The main defects of his formula are: (1) the definition, explaining how the excitation in a nerve is measured, is very obscure; (2) since his formula is deduced from the experimental data at a point of minimal excitation, it is not possible to extend it into the region of finite excitation.

In 1910 Hill,\* following Nernst's hypothesis and introducing the assumption of Lapicque, found excitation formulae in several cases of electric stimuli. Since his consideration is based on the theory of "all or none" first proposed by Goltz, the formulae have a somewhat different meaning from that of Hoorweg. They represent the progression of a local change which on attaining a definite value causes an actual excitation. At anyrate, in the case of a constant current, his formula contains the exponential function as the term that varies with the duration of stimulating current. According to the "all or none" theory the magnitude of the response depends on the number of elementary portions that receive a stimulus greater than the threshold value to evoke the response. The number may depend on the distribution of the current in a tissue or on the variety of the elementary portions whose minimal stimuli are different from one another. In the former case, the relation between the electric stimulus and its response reduces to a mere physical problem, and as in the latter case to that of some kind of probability.

Since it was considered that the discharge of an electric organ is the best means for the investigation of such problems, many experiments in these subjects were made. Let us here explain the superiority of the discharge as a means for the investigation of the general properties of excitation in tissues. The means ordinarily used are muscular contraction and negative variation in a nerve or in a muscle. In the former case very troublesome factors of elasticity and viscosity (if the latter term may be allowed) in a muscle complicate the phenomena. On the contrary, the negative variation is an ideal means for the purpose, but to obtain its record we are obliged

---

\* The Journal of Physiology, Vol. 40, p. 101, 1910.

at present to use such an instrument as the capillary electrometer or the string galvanometer. As we remarked at the beginning of this paper, such an instrument does not give a true picture of the electromotive force as in this case, unless the change of the electromotive force is very slow as in a cardiogram. Some people try to correct the curve obtained on these instruments by finding the inclination of the tangent to the curve from point to point. But since a small error in the measurement of the inclination may cause a considerably great error in the correction, especially when the inclination approaches  $\frac{\pi}{2}$ , it is dangerous to rely on the result obtained by analysing the curve thus corrected, even if it be allowed that the principle of the correction is right. On the contrary, the electromotive force of the discharge of an electric organ is very large and therefore in this case we may employ such an ingenious instrument as the oscillograph, in which, if used with proper care, correction is unnecessary. Moreover the stimulus must be very strong for exciting the organ so that even a subminimal stimulus may be recorded by the same instrument. It must, however, be admitted that the record due to the abrupt change of current is not so correct as that of the discharge. The only difficulty met with was our local trouble in obtaining fish.

Returning to the problem: we made many experiments regarding the magnitude of the electric stimulus and the same of the corresponding discharge. The experiments were made in the main with direct stimulation, and its form was that described in § III. As it was more convenient to make the picture of the stimulus on the oscillogram on the same side of the zero line as that of the discharge, the direction of the stimulating current was always homodrome. By changing the strength of the current of the primary of the induction coil, or by shifting the position of the circuit-breaker with regard to that of the connection-changer on the stimulation-apparatus, stimuli having different strengths and equal durations, or stimuli having different durations and equal strengths, were given to the organ and the resulting discharges were investigated.



Assuming that the opening-stimulus, when very near to the closing-one, has not an appreciable effect on the discharge curve, its influence was not considered in the first plan of the experiment. But in examining the discharge curve very minutely, as in the preceding section, we found that it may be influenced more or less by the opening-stimulus. If that be the case, in the experiment for the relation between the duration of the current and the magnitude of the corresponding discharge, the maximum electromotive force of a discharge may, for two reasons, diminish with the decrease of the duration on account of the opening-stimulus: (1) since the opening-stimulation would be due to the recovery from some kind of polarisation, the magnitude of its effect may be due to the duration of the current that flowed before; and (2) when a stimulus occurs immediately after another it has a smaller effect, being influenced by the preceding one—a phenomenon to be discussed later. Though I believe, after the result of the analysis of No. 37 and of No. 40 in the preceding section, that the decrease of the maximum electromotive force is due mainly to the decrease of the duration of the current of the closing-stimulus, it is very difficult to know how much the opening-stimulus affects the discharge-height. Therefore without making any assumption, we shall now regard the set of our stimuli to be a single stimulus as a whole and deal with its relation to the corresponding response. In the preceding section we see that a discharge curve has three parameters to characterise its form, *i. e.*  $A$ ,  $b^2$  and  $x_0$ . Since, as we see, the changes of  $b_0^2$  and  $x_0$  with respect to the stimulus are not conspicuous, we shall use  $A$  as the measure of the excitation. The area of the curve, which, if we assume the theory of "all or none," would correspond to the number of the electric plates discharged, may be found by integrating the formula of the discharge curve *i. e.*

$$\text{Area} = \int_0^{\infty} A e^{-b \log \frac{x}{x_0}} dx = \frac{\sqrt{\pi}}{b} A x_0 e^{\frac{1}{4b^2}} \dots \dots \dots (8)$$

Indeed it was tried to use the area as the measure of the excitation in the reduction of some of our experiments, but it did not give a result much differing from that of  $A$  in general. Therefore leaving

this problem to more precise investigations, we shall now confine ourselves to the discussion of the relation of  $A$  to the stimulus.

Tables in regard to many experiments for the stimuli with equal breadths and different heights are given next, and graphs representing the relation between the height of the stimulus and the height of the discharge are drawn in Plate X. Fig. 1, 2, 3. Here we may remark that a small error must be taken into account for the height of the stimulus measured on the oscillogram, because even our oscillograph does not follow such an abrupt increase of current as that observed in our stimulating current.

TABLE VII.

Oscillograms No. 35 and No. 36 (Plate XIV.).

Temperature of the organ:  $11.0^{\circ}\text{C}$ .

Resistance of the organ: 130 ohms.

No.	Height of Stim. in mm.			Height of discharge in mm.		
	No. 35.	No. 36.	Mean.	No. 35.	No. 36.	Mean.
1	34.7	35.4	35.1	17.0	17.3	17.2
2	41.2	41.7	41.5	25.0	24.0	24.5
3	47.0	47.2	47.1	31.0	30.1	30.6
4	52.3	53.3	52.8	37.5	37.0	37.3
5	58.0	58.7	58.4	40.8	40.3	40.6
6	62.0	63.3	62.7	43.3	44.5	43.9
7	68.5	69.0	68.8	48.0	48.0	48.0

TABLE VIII.

Oscillogram No. 38 (Plate XV.).

Temperature of the organ:  $11.5^{\circ}\text{C}$ .

No.	Height of Stim. in mm.	Height of discharge in mm.	No.	Height of Stim. in mm.	Height of discharge in mm.
1	26.8	11.0	4	45.7	41.5
2	33.2	20.8	5	51.5	47.0
3	39.2	32.8	6	64.2	58.5

TABLE IX.

Oscillograms No. 42 and No. 43.

Temperature of the organ:  $11.5^{\circ}$  C.

No.	Height of stimulus. in mm.			Height of discharge in mm.		
	No. 42.	No. 43.	Mean.	No. 42.	No. 43.	Mean.
1	12.5	13.5	13.0	2.5	2.5	2.5
2	19.5	19.5	19.5	3.5	3.5	3.5
3	26.0	26.5	26.3	10.0	8.5	9.3
4	32.0	33.0	32.5	20.5	17.5	19.0
5	39.0	38.5	38.8	29.5	24.5	27.0
6	45.0	46.0	45.5	38.0	33.5	35.8
7	51.0	52.0	51.5	43.7	40.5	42.1
8	58.0	58.5	58.3	48.0	48.8	48.4
9	63.5	63.5	63.5	51.0	55.0	53.0

TABLE X.

Oscillogram No. 54 (Plate XIII.).

Temperature of the organ:  $8.5^{\circ}$ — $7.2^{\circ}$  C.

Resistance of the organ: 240 ohms.

No.	Height of Stim. in mm.	Height of discharge in mm.
1	19.0	1.5
2	25.5	5.0
3	31.5	10.0
4	38.0	17.3
5	44.3	26.5
6	50.2	35.8
7	56.8	45.5
8	64.5	56.0

TABLE XI.

Oscillograms No. 55 and No. 56 (Plate XV.).

Temperature of the organ: 10.4° C.

Resistance of the organ: 240 ohms.

No.	Height of Stim. in mm.			Height of discharge in mm.		
	No. 55.	No. 56.	Mean.	No. 55.	No. 56.	Mean.
1	70.0	67.0	68.5	48.5	46.0	47.3
2	63.0	63.0	63.0	39.0	40.0	39.5
3	58.0	56.8	57.4	32.5	32.5	32.5
4	51.5	50.5	51.0	22.5	23.7	23.1
5	45.0	44.5	44.8	15.5	17.3	16.4
6	38.5	37.5	38.0	9.5	10.5	10.0
7	—	32.0	—	—	6.2	—
8	25.0	25.5	25.3	0.8	2.5	1.8
9	68.0	66.0	67.0	45.5	45.7	45.6

TABLE XII.

Oscillograms No. 62, No. 63 and No. 64 (Plate XVI.).

Temperature of the organ: 13.5° C.

Resistance of the organ: 190 ohms.

No.	No. 62.		No. 63.		No. 64.	
	Stim. in mm.	Discharge in mm.	Stim. in mm.	Discharge in mm.	Stim. in mm.	Discharge in mm.
1	63.7	33.7	62.3	25.3	63.3	24.0
2	57.7	26.6	56.5	19.3	57.4	17.4
3	50.8	19.7	50.3	14.3	50.6	12.5
4	44.3	13.7	44.4	10.4	45.6	9.2
5	38.7	8.7	38.5	6.4	38.2	5.5
6	31.7	4.6	31.4	3.4	31.8	3.2
7	25.6	2.3	25.4	1.5	25.5	1.4
8	—	—	62.6	24.4	63.5	22.5

Here in general we used very broad stimuli to avoid the effect due to the difference of their breadths. In No. 35 and No. 36 the preparation of the organ was the same, and in the former case the stimuli were given in the increasing order of height and in the latter in the decreasing order so as to eliminate the progressive change in the organ. The two curves (Plate X., Fig. 1) representing them run very closely to each other, the latter being somewhat lower than the former. This shows that the progressive change, which might be due to the decay of the organ or slow cooling of the same, was very small during the experiments. The mean curve of No. 35 and No. 36 is shown in Plate X., Fig. 2. This may be considered to be the true course of the curve when there exists no progressive change. Oscillograms No. 42 and No. 43 are of a set of experiments of the same kind as the above. The preparation was the same as that of No. 40 and No. 41, which were a set of experiments for the investigation of the relation between the breadth of a stimulus and the corresponding height of the discharge, and which will be discussed later. The stimuli are in the increasing order of height in No. 42, and in the reverse order in No. 43. Here we see that the curves (Plate X.) representing them do not coincide; showing the existence of a progressive change, so that the discharges became relatively smaller with the course of the experiments. Assuming that the progressive change was uniform, the mean curve may represent the true course of the curve. Oscillograms No. 55 and No. 56 (Plate X.) are of experiments of the same kind. Here we have a check on each film, which shows that the effect of the progressive change was very small. In the figure, the check points are marked with *e*. Oscillograms No. 38 and No. 54 have no check for the progressive change (Plate X., Fig. 3). Oscillograms No. 62, No. 63 and No. 64 (Plate X., Fig. 3) relate to a series of experiments in which stimuli given were in the decreasing order with respect to their heights, having a check on each film. The breadths of the stimuli are different in the three films, broadest in No. 62, and narrowest in No. 64.

Tracing the general course of these several curves we see that they converge to the origin of the co-ordinates. The height of the

discharge increases very slowly from zero. Then comes a steep increase of the height of the discharge, where the curve has an inflexion point and then becomes concave with respect to the axis of the abscissa. By direct stimulations we could not arrive at the upper part of the curve on account of the very large stimulation current required. Nevertheless, it is very probable that the curve approaches an asymptotic value of the ordinate which may easily be attained in the case of indirect stimulation. Thus the curve forms an S-shape analogous to that, found by *Waller*, relating to the negative variation in the nerve. Here we may remark that it is very doubtful whether the words *minimal* and *subminimal stimulus* as customarily used have any definite meaning. By the word *minimal stimulus* or *liminal current*, is certainly meant the stimulus by which the response becomes just sensitive to a certain instrument. Of course, if we acknowledge the truth of the "all or none" theory, there certainly exist the minimal and the maximal stimulus in the literal meaning. But that which is ordinarily obtained by experiment would not be the true *minimal* stimulus, *i. e.* not for the response of *a unit* element. Now, if we take the height of the discharge as a measure of the excitation, the proportionality between the current and the response in Hoorweg's formula does not hold good for the finite range of the discharge. It is not clear whether the inclination of the tangent to the curve at the origin is equal to zero or not. If the latter is the case, the proportionality in the very small portion at the beginning of the curve, in agreement with the formula of Hoorweg, is nothing but the general property of any curve, that a small portion of it may be regarded as a straight line. Many trials were made to formulate the relation extending to the finite region of the stimulus, but the results were not satisfactory. As we remarked before, if we may assume that the magnitude of a discharge is due to the number of elements evoked by the stimulus, and that the number depends on the variety of the elementary portions whose minimal stimuli are different from one another, then the curve representing the relation between the strength of the stimulus and the area of the discharge should be the integral curve of the

category of a probability curve. Since I cannot ascertain the proper method of analysing the curve from the standpoint of this hypothesis, I am not able to give the rigorous proof for it. But it is obvious that, qualitatively, the course of the experimental curve agrees with this view.\* I am now working on this principle; I only refer to it here, and shall leave the problem for a later report.

Next we shall treat the relation between the breadth of the stimulus and the height of the discharge. With reference to the problem, the film first examined was that of No. 37, an analysis of which was made in the preceding section. The organ-preparation was the same as that of No. 35 and No. 36, in which we knew that the effect of the progressive change was very small. Assuming Hoorweg's decrement factor to be true and not taking into consideration the effect of the opening-stimulus separately, which Hoorweg, in his condenser investigation, also ignored, we examined whether his factor held good in our case. According to his formula the excitation  $E$  caused by our stimulus is equal to

$$\int_0^t aie^{-\lambda t} e^{-\beta t} dt = \frac{ai}{\lambda + \beta} \{1 - e^{-(\lambda + \beta)t}\},$$

where  $i$  represents the maximum current in the secondary of the induction coil,  $\lambda$  is a constant determined by the self-induction and the resistance of the secondary circuit, and where  $e^{-\beta t}$  means Hoorweg's decrement factor. Of course, in our stimulus there is a steep rising portion of the current before its maximum, which is not considered here. But in treating of the variation only, the part common to all stimuli has no influence on the result, if we take the origin of the time at a proper instant. Hence measuring the time from a suitable origin the formula becomes

$$E = a \frac{i}{\lambda + \beta} \{1 - e^{-(\lambda + \beta)(t - t_0)}\},$$

which, for the sake of brevity, we write

---

\* A trial examination was made on the curves of Oscillogram No. 54. The curve representing the relation between the height of the stimulus and the area of the resulting discharge curve was graphically differentiated by drawing the tangents to the curve, point by point, and by finding the corresponding rates of increase of the ordinates with respect to the abscissa. Then it was found that the differential curve might be expressed by a formula analogous to that of the discharge curve given in the previous section.

$$E = B \{1 - e^{-\gamma(t-t_0)}\}. \dots\dots\dots(9)$$

After laborious trials  $B$ ,  $\gamma$  and  $t_0$  were found from the plotted curve of No. 37 (Plate XI., Fig. 1). As the breadth of the stimulus, we took the interval between its beginning and the instant of abrupt decrease of the current. Though our oscillograph would not give a true picture for such a quick change of current as our stimulus, it does not influence the value of the stimulation-breadth taken as above. The result of the experiment and the corresponding calculated values are given in the next table, and represented graphically in Plate XI., Fig. 1.

TABLE XIII.

Oscillogram No. 37.

Temperature of the organ: 11.0°C.

Resistance of the organ: 130 ohms.

Formula used in calculation:  $y = 34.0 \times (1 - 10^{-0.0872(t-5.1)})$

No.	M. L. P. in $10^{-4}$ sec.	Breadth of stim. in $10^{-4}$ sec.	Height of discharge obs. in mm.	Height of discharge calc. in mm.	Diff.
1	124.2	18.2	31.5	31.5	0.0
2	122.7	16.1	30.8	30.2	+ 0.6
3	125.4	14.2	28.3	28.4	- 0.1
4	126.7	13.0	27.5	26.9	+ 0.6
5	127.1	11.8	25.0	25.0	0.0
6	126.5	11.3	23.3	24.1	- 0.8
7	127.9	9.1	19.0	18.8	+ 0.2
8	127.7	7.7	12.5	13.9	- 1.4

As we see in the table and in the figure, the agreement of the observed with the calculated values is very satisfactory.

Oscillogram No. 58 (Plate XVII.) is an example in which the breadths of the stimuli were too large, so that the heights of the discharges showed a nearly constant value. In this oscillogram, it may be seen that the height of the discharge never becomes smaller with the increasing stimulation-breadth, even



when the beginning of the opening-discharge appears later than the summit of the discharge curve. This shows that the variation of the discharge-height with respect to the stimulation-breadth is not the effect of the opening-stimulus, but is due to the variation of the duration of the closing-stimulation current.

Next we examined Oscillograms No. 40 and No. 41 (Plate XVII.). These are a series of experiments on the same preparation as No. 42 and No. 43. In No. 40 the stimuli were given in the decreasing order of breadth and in No. 41 in the reverse order. For the breadth of the stimulus in this case, we took the breadth on the bottom of the graph, for the measurement as in No. 37 was very difficult to ascertain accurately. In this case, it was found that the heights of the stimuli differed a little from one another. Since the small differences in the heights of the stimuli exceedingly influence the heights of the discharges, the latter were reduced into those corresponding to their respective stimuli having an equal height 44.5 mm. The proportional constants in these calculations were derived from the mean curve of No. 42 and No. 43. Here the stimulation-apparatus did not work well on account of the contraction of the wooden part, by which the two rails were bent a little. So the breadth of the stimuli did not decrease regularly. Moreover, on plotting the points on a section paper, it became clear that some progressive change had occurred during the experiments, so that the points on the figure arranged themselves in a very complex manner. Therefore we assumed a fatigue factor  $e^{-nt}$ , where  $n$  represents the number of the order of a discharge, the first discharge being regarded as zero. The numbers observed and calculated are given in the next table and the graph is represented in Plate XI., Fig. 2.

TABLE XIV.

Oscillograms No. 40 and No. 41.

Temperature of the organ: 11.5 °C.

Formula used in calculation:

$$\text{No. 40, } y = 48.0 \times 10^{-0.00634n} \{1 - 10^{-0.0429(t-0)}\},$$

$$\text{No. 41, } y = 46.9 \times 10^{-0.00631n} \{1 - 10^{-0.0429(t-0)}\}.$$

## No. 40.

No.	M. L. P. in $10^{-4}$ sec.	Breadth of Stim. in $10^{-4}$ sec.	Height of discharge obs. in mm.	Height of discharge calc. in mm.	Diff.
0	121	28.0	44.5	45.0	-0.5
1	119	18.4	39.9	39.7	+0.2
2	120	19.8	39.1	40.1	-1.0
3	120	17.4	37.6	37.8	-0.2
4	122	19.2	38.2	38.6	-0.4
5	122	15.0	33.5	34.6	-1.1
6	122	14.3	35.0	33.3	+1.7
7	122	11.6	29.7	29.7	0.0

## No. 41.

No.	M. L. P. in $10^{-4}$ sec.	Breadth of Stim. in $10^{-4}$ sec.	Height of discharge obs. in mm.	Height of discharge calc. in mm.	Diff.
0	118	13.9	35.9	35.0	+0.9
1	119	13.1	33.7	33.6	+0.1
2	120	15.7	33.0	35.9	+0.1
3	119	17.0	36.7	36.6	+0.1
4	120	18.8	36.4	37.4	-1.0
5	125	17.5	38.6	36.0	+2.6
6	118	23.0	38.6	38.7	-0.1
7	120	22.4	38.4	37.9	+0.5

The details of the data are given in the Appendix.

Next, Oscillograms No. 59, No. 60 and No. 61 are of a series of experiments of the same kind made on the same organ, in which the heights of the stimuli are different in the three films. In each series, the experiments were in decreasing order with respect to the breadths of the stimuli. On each film, a check was taken at the end of the experiments, and it was found that there were

progressive changes. So, using  $e^{-nt}$  as a fatigue factor, in which  $a$ 's were calculated from the checks, and finding the other constants by laborious trials, the corresponding values of  $A$  were calculated. These results are given in the next tables (Plate XI., Fig. 3):—

TABLE XV.

Oscillograms No. 59, No. 60 and No. 61. (Plate XVIII.).

Temperature of the organ:  $13.5^{\circ}\text{C}$ .

Referring to the accompanying figure,  $AF''$  in No. 59,  $AC'$  in No. 60 and  $AF'$  in No. 61 were taken for the stimulation-breadths.

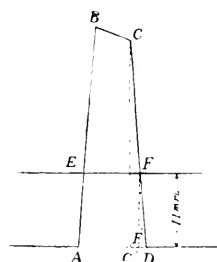


Fig. 6.

Formula used in calculation:

$$\text{in No. 59, } y = 21.3 \times 10^{-0.0372n} \{1 - 10^{-0.0560(t-2)}\},$$

$$\text{in No. 60, } y = 3.1 \times 10^{-0.0121n} \{1 - 10^{-0.0385(t-2)}\},$$

$$\text{in No. 61, } y = 38.8 \times 10^{-0.03319n} \{1 - 10^{-0.062(t-2)}\}.$$

No. 59.

No.	M. L. P. in $10^{-4}$ sec.	Breadth of Stim. in $10^{-4}$ sec.	Height of discharge obs. in mm.	Height of discharge calc. in mm.	Diff.
0	90.0	27.3	20.5	20.5	0.0
1	91.7	19.4	19.5	18.9	+0.6
2	89.5	19.8	19.3	18.8	+0.5
3	91.2	19.3	18.1	18.5	-0.4
4	88.6	16.7	17.4	17.5	-0.1
5	88.1	14.9	17.0	16.5	+0.5
6	83.0	8.1	11.0	11.0	0.0
7	86.9	27.4	19.3	19.3	0.0

## No. 60.

No.	M. L. P. in $10^{-4}$ sec.	Breadth of Stim. in $10^{-4}$ sec.	Height of discharge obs. in mm.	Height of discharge calc. in mm.	Diff.
0	84.5	26.4	32.0	32.0	0.0
1	84.0	22.0	30.8	31.0	-0.2
2	82.9	19.0	29.7	30.0	-0.3
3	80.9	17.3	29.0	29.0	0.0
4	—	—	—	—	—
5	87.4	17.1	27.5	27.4	+0.1
6	78.0	14.8	26.0	26.2	-0.2
7	83.5	27.1	26.3	26.4	-0.1

## No. 61.

No.	M. L. P. in $10^{-4}$ sec.	Breadth of Stim. in $10^{-4}$ sec.	Height of discharge obs. in mm.	Height of discharge calc. in mm.	Diff.
0	83.1	29.4	38.0	38.0	0.0
1	79.5	21.2	36.9	36.1	+0.8
2	84.0	19.9	36.0	35.4	+0.6
3	81.5	18.1	34.6	34.3	+0.3
4	—	—	—	—	—
5	83.0	16.4	32.0	32.8	-0.8
6	85.0	13.8	30.4	30.4	0.0
7	79.2	25.8	36.0	35.6	+0.4

In the calculation, we assumed that the values of  $t_0$  are equal in the three cases. But as we see in the tables, the measurements of the breadths were not ascertained in the same way. Hence the values of  $t_0$  must differ in these three cases. Indeed we attempted to find the more correct values of  $B$ ,  $\gamma$ ,  $t_0$  and  $\alpha$  by applying the method of least squares to the residuals of the approximate values obtained by the trial method, and to compare the values of these constants

for various heights of the stimuli. But the coefficients of the normal equations became very different in order of magnitude, and perhaps for this reason, no significant values could be obtained. Hence we abandoned these calculations, and we shall leave the problem without any presumption upon the variations of the constants with regard to the height of the stimulus, until we shall have had an opportunity of obtaining more trustworthy results free from progressive changes.

In short, except No. 37, the results of the experiments were not perfect: but taking into consideration the difficulty of the measurement of the small duration of the stimulus, and the influence of the troublesome factor of the progressive change, these results rather prove the correctness of the decrement factor of Hoorweg.

Next we shall give an experiment of indirect stimulation, in which momentary stimuli of different heights were given. The relation between the height of the stimulus and the height of the corresponding discharge is given in the next table and in Plate X., Fig. 3.

TABLE XVI.

Oscillogram No. 49 (Plate XXVIII.).

Temperature of the organ: 8.2°C.

Additional resistance inserted in series: 200 ohms.

The stimuli given: Descending.

(The stimulus of Curve No. 1 was ascending by accident.)

No.	L. P. in $10^{-4}$ sec.	M. L. P. in $10^{-4}$ sec.	Height of Stim. in mm.	Height of discharge in mm.
1	142	173	4.0	9.0
2	} Too low for measurement.		6.0	0.5
3			7.0	1.0
4	162	185	9.0	2.3
5	162	188	11.0	8.3
6	159	185	12.5	15.0
7	156	189	13.0	17.0
8	156	189	14.0	18.3

The course of the curve representing the relation between the height of the stimulus and the height of the discharge resembles that of the direct stimulus. Here we may remark that the modal latent periods have very consistent values except in Curves No. 1, No. 2 and No. 3, in which, since the curves are very low, the measurements were very inaccurate.

In closing this section, the results of our experiments are summarised as follows:—

i.) The height of the discharge  $A$  slowly increases with the increasing intensity of the stimulation current from zero.

ii.) Then it increases very steeply, where it passes an inflexion point; and then approaches an asymptotic value.

iii.) With respect to the duration of the stimulating current, Hoorweg's decrement factor seems to be correct, but it is not clear whether the constant  $\beta$  in it does really depend on the strength of the stimulating current or not.

## VI. Discharges by Two Successive Stimuli.

Already in one of the preliminary experiments, we discovered that when two successive stimuli not too far apart in time from each other are given to the nerve, the discharge by the second stimulus shows greater delay compared with the normal. A pair of momentary stimuli which were caused by a contrivance on the shaft of the registering drum were sent periodically, *i.e.* once in each revolution, to the nerve. At first only the preceding one of the pair, then the succeeding, and finally the pair together were sent through the nerve. These were photographed on the same film. The second stimulus was so given that, if the two discharges appeared at the normal delay, the second discharge should appear in a position superposed on the descending branch of the first. But from the film we saw, on the contrary, that the second discharge occurred after the first had been over.

For the precise investigation of the phenomenon, we constructed a special contrivance in our stimulation-apparatus, by means of which two consecutive momentary stimuli separated by a desired

interval of time may be given. The details of the mechanism were explained in § III. and illustrated in Plate V., Fig. 4. As for the strength of the stimuli, care was always taken to obtain the maximal discharges. The sense of the stimulating current was mainly descending, the distance of the two electrodes being about 3 mm. This comes from the consideration that, in a descending stimulus, the excitation in the nerve evoked by the closing-stimulus, occurs at the cathode which is nearer to the organ than the anode and therefore the excitation is evoked in an undisturbed part in the nerve and propagates to the organ without any obstacle, while the excitation caused by the opening-stimulus occurs at the anode and it is arrested by the cathodic block from propagating to the organ. On the contrary, if we use an ascending stimulus, not only it has frequently been observed that the excitation due to the closing stimulus propagates to the organ, though greatly enfeebled in passing the anode; but the excitation by the opening-stimulus must be affected by the stimulating current which flowed before that instant. In short the result in the case of the descending current should be more simple.

Returning to the problem, the influence of the first stimulus to the second consists of two parts: namely (1) the effect on the modal latent period of the second discharge, (2) the effect on the height of the second discharge. The former effect almost disappears when the second stimulus departs from its predecessor about one-hundredth of a second, while the latter remains a little later. These may be the effects of some kind of fatigue that recovers itself in a small fraction of a second. We shall call the phenomena the *temporary fatigue*.

Oscillograms No. 74 and No. 75 (Plate XIX.) are a series of experiments for such phenomena. Two stimuli, separated by various intervals of time, were given at a point on a nerve, and the influences of the first stimulus on the second discharge were measured accurately. The following table shows the numbers deduced from these oscillograms:—

TABLE XVII.

Oscillograms No. 74 and No. 75.

Temperature of the organ: 14.5 °C.

No. 74.

No.	Interval between two Stim. in $10^{-4}$ sec.	Ratio of 2nd M. L. P. to 1st.	Height of 1st discharge in mm.	Height of 2nd discharge in mm.	Ratio of 2nd height to 1st.
1	120.5	1.000	53.0	39.0	0.736
2	110.4	1.015	51.5	41.5	0.806
3	99.5	1.030	48.5	45.5	0.989
4	90.2	1.023	48.0	49.0	1.020
5	79.9	1.063	47.0	48.5	1.030
6	72.5	1.100	46.0	46.7	1.015
7	63.2	1.120	46.0	45.5	0.990
8	55.8	1.175	45.0	42.0	0.935

No. 75.

No.	Interval between two Stim. in $10^{-4}$ sec.	Ratio of 2nd M. L. P. to 1st.	Height of 1st discharge in mm.	Height of 2nd discharge in mm.	Ratio of 2nd height to 1st.
9	43.9	1.301	45.0	24.7	0.550
10	33.6	1.411	43.3	4.5	0.104
11	34.7	1.411	41.5	4.5	0.109
12	27.4	—	42.5	?	—
13	14.9	—	41.8	?	—
14	9.1	—	41.2	—	—
15	3.0	—	42.5	—	—
16	0.0	—	41.5	—	—

*N.B.*:—In this paper, for the sake of brevity, the word *latent period* or *modal latent period* is used to represent the interval between the stimulus and the commencement (observed) of the discharge or between the stimulus and the instant of the maximum electromotive force respectively, whether the stimulus is direct or indirect, *i. e.* the values of them are inclusive of the time for the propagation of the nerve-excitation.



Full details of the data and the computed numbers are given in the Appendix.

The numbers in the table are plotted in Plate XII., Fig. 1. Referring to Curve 1, the abscissa represents the interval between two momentary stimuli in  $10^{-4}$  sec., and the ordinate represents the ratio of the two modal latent periods subtracted by one, *i. e.* the excess of the delay of the second discharge with respect to the first. Here we see that the ordinate decreases exponentially with the increase of the abscissa. We assume the curve to be expressed by exponential function  $y = Me^{-\lambda t}$ , and determine the value of  $M$  and of  $\lambda$ , in which we may find  $M = 1.74$ ,  $\lambda = 409$ . Calculating the values of  $y$  from the formula, and plotting these numbers on the experimental curve, we see that they agree very well within the limits of the experimental errors.

The other curve in the figure is that of the heights of the second discharges. To eliminate the individual errors of each experiment, the ratio of the height of the second discharge to that of the first is taken as ordinate. Referring to the curve we see that, even in  $1/100$  sec. from the first stimulus, the height of the second discharge is smaller than the normal. Proceeding towards the origin from this point it increases even greater than the normal, and then decreases quickly to an almost imperceptible height where the second stimulus enters the so-called refractory period. The refractory period in this experiment is measured to be  $32.0 \times 10^{-4}$  sec. In this experiment it is not certain whether in the refractory period the response does not occur absolutely, or whether some small responses continue to exist up to the origin of the coordinates. Indeed there exist many small discharges that cannot be distinguished from the discharge of the higher order of the preceding experiment. To clear this point further investigations will be necessary.

The increase of the height of the second discharge towards the origin seems to be paradoxical at first sight. But on examining the film, we can find that when the second discharge is great, the second stimulus is at an instant corresponding to a point on the ascending branch of the first discharge, so that the second discharge

overlaps the *secondary discharge* of the first stimulus. Hence we see that the apparent increase of the height may be due to the summation effect of the secondary discharge. To make this fact clearer, we may refer to the following table:—

TABLE XVIII.

Oscillogram No. 74.

From the first set of curves the interval between the first stimulus and the summit of the secondary discharge may be found to be  $193.2 \times 10^{-4}$  sec.

No.	Ratio of two heights.	Interval between first stimulus and summit of second discharge, in $10^{-4}$ sec.
1	0.736	226
2	0.806	214
3	0.989	208
4	1.020	201
5	<u>1.030</u>	<u>193</u>
6	1.015	191
7	0.990	183
8	0.935	185

In this table we see that the maximum ratio between the height of the second discharge and that of the first, occurs when the summit of it just coincides in position with that of the secondary discharge.

Oscillogram No. 65 (Plate XX.) is another series of experiments of the same kind. The corresponding numbers are tabulated in the next table and plotted in Plate XII., Fig. 2.

## TABLE XIX.

Oscillogram No. 65.

Temperature of the organ: 13.5 °C.

No.	Interval between two Stim. in $10^{-4}$ sec.	Ratio of 2nd M. L. P. to 1st.	Height of 1st discharge, in mm.	Height of 2nd discharge, in mm.	Ratio of 2nd height to 1st.
1	133	1.790	24.5	9.0	0.367
2	—	—	22.6	17.8	0.788
3	110	0.970	21.5	19.0	0.885
4	97	1.025	21.0	19.0	0.925
5	88	1.130	20.3	18.0	0.900
6	—	—	20.0	15.0	0.750
7	69	1.230	19.5	16.0	0.820
8	60	1.300	19.9	11.0	0.553
9	49	1.480	18.8	3.9	0.207

The general course of the curve is similar to the preceding. On the right hand side, the arrangement of the points is not so regular as in No. 74—No. 75, especially the position of the last point in the figure deviates exceedingly from the others. But on examining the oscillogram, we see that the second discharge occurs after the secondary discharge of the first. Thus the second stimulus was influenced by the first discharge which acted as a preceding stimulus. Here we may find that  $M = 3.00$ ,  $\lambda = 376$  and the refractory period =  $46.0 \times 10^{-4}$  sec. The values of  $y$  calculated from these constants are plotted on the figure. The interval of time, in which the value of  $y$  becomes one half, may be called the *period of recovery* of the temporary fatigue. In the preceding two experiments the period of recovery is equal to  $17.0 \times 10^{-4}$  sec. in the former and  $18.5 \times 10^{-4}$  sec. in the latter, the temperature being 14.5 °C. and 13.5 °C. respectively.

With respect to the height of the second discharge, we may remark that it decreases with the decreasing interval between the two stimuli. But, if we take the ratio of the height of the second

discharge to that of the first, we can see that it has a maximum value as in No.74—No.75. In this oscillogram the interval between the first stimulus and the summit of the secondary discharge may be measured from the first set of the discharges, and as this value we obtain  $223 \times 10^{-4}$  sec. Here we see again that the maximum of the ratio of the height of the second discharge to that of the first occurs when its summit just coincides with that of the secondary discharge. The relation is shown in the following table:—

TABLE XX.

Oscillogram No. 65.

Interval between the first stimulus and the summit of the secondary discharge:  $223 \times 10^{-4}$  sec.

No.	Ratio of two heights.	Interval between first stimulus and summit of second discharge, in $10^{-4}$ sec.
1	0.367	348
2	0.788	226
3	0.885	229
4	0.925	222
5	0.900	225
6	0.750	222
7	0.820	217
8	0.553	215
9	0.207	220

Now since it was not plain to me whether the seat of the phenomena is in the nerve or in the organ, an experiment was made to determine the question. By giving a pair of stimuli with a fixed interval between them, and by inserting proper resistance in the discharge circuit, we carried out a series of experiments with equal stimuli and different heights of discharges. Changing the magnitude of discharges by varying the resistance, the delay of the second discharge with respect to the first was measured. The following table shows the results.

TABLE XXI.

Oscillogram No. 84 (Plate XX.).

No.	Resistance inserted in ohm.	Interval between two Stim. in $10^{-4}$ sec.	Ratio of two M. L. P.
I. {	0	30.0	1.14
	200	30.6	1.16
	300	30.2	1.17
II. {	0	21.8	1.27
	200	24.6	1.24
	300	24.9	1.25
III. {	0	15.4	1.46
	200	14.6	1.67
	300	23.2	1.36

In each set of the experiments, the ratios of the two modal latent periods were found to be nearly equal. The disagreement in the third set must have occurred in virtue of the differences of the interval between the stimuli as shown in the table. So we have to conclude that the temporary fatigue, so far as it is defined by the prolongation of the modal latent period, is not the result of the discharge.

In December 1909, Lucas \*reported the same phenomenon in a somewhat different way. According to his paper, experiments were made on the negative variation in the sartorius muscle of the frog. The instrument used by him was a capillary electrometer and the curve obtained was corrected by the method of Burch. As the time of reference he always took the latent period *i. e.* the interval between the stimulus and the commencement of its response. Even when he measured the interval between the stimulus and the summit of the response curve in his later paper, he subtracted a constant value in order to obtain the latent period. For my part, to measure on a curve the commencement of the response

\* The Journal of Physiology, Vol. 39, p. 331.

is not only very inaccurate, but it is doubtful whether the so-called latent period measured on a graph has any definite meaning. For example the theoretical curve discussed in § IV., which has its commencement at the stimulus, may give some finite value for the so-called latent period, if it is measured as is usually done on the experimental curve. The response in a muscle or in a nerve may differ in its property from the discharge of an electric organ, though I am inclined to think that the form of the negative variation depends on a similar cause to ours. As a matter of fact, the modal latent period so-called by us, gives more consistent values among themselves than latent periods either in our case, as always observed before, or in the case of the negative variation in a muscle, as was shown in the paper by Lucas. Whatever it may be, he said in his paper: "It is found that the second electric response begins at a constant time after the beginning of the first, whether the stimulus by which it is provoked occurs immediately after the end of the refractory period or considerably later. If the second stimulus occurs immediately after the end of the refractory period the latency of the resulting electric response may be many times the normal. As the second stimulus is made later the latency of the resulting response becomes proportionately less. Only when the second stimulus occurs so late that it would otherwise have a latency less than the normal does the second response depart from its fixed time of occurrence." He also shows that the nearer the second stimulus approaches the end of the refractory period, the smaller the resulting response becomes.

After this paper appeared, Gotch\* reported his analysis of a similar phenomenon on the negative variation in the sciatic nerve of the frog, and concluded that: "I. The electrical response of the excised sciatic nerve of the frog to a second stimulus may show a great increase in delay as compared with the response to the preceding stimulus. II. This increase of delay is augmented in proportion as the second stimulus approaches the end of the period of complete inexcitability (refractory period) which is developed

---

\* The Journal of Physiology, Vol. 40, p. 250, 1910.

during the first response, but becomes imperceptible if the second stimulus occurs at a sufficient interval after the first." He reported the effect of temperature upon the phenomenon and also gave the discussion about the locality of this peculiarity. More recently Lucas \*reported his researches on the locality of the same phenomenon by his ingenious method, and concluded that it is an after effect of the disturbance propagating through a nerve or a muscle. In this paper he plotted many curves which represent the relation between the interval of the two stimuli and the same from the first stimulus to the commencement of the second response, and not only did he accept the behaviour of the delay of the second response agreeing with that of Gotch, so that he modified his first statement, but he found that the interval between the first stimulus and the second response becomes greater in some cases, when the second stimulus is brought very near to the refractory period. Quoting his words: "In the more complex cases with which I have dealt, namely the excitation of nerve and the recording of the consequent electric response in the innervated muscle, it appears that a new phenomenon must be recognised; the electric response becomes still later when the second stimulus is brought very near to the first. This suggests an important difference associated with the passage of the propagated disturbance through successive tissues having unlike time relations." Now we shall reproduce here two figures of such kind given in his paper.

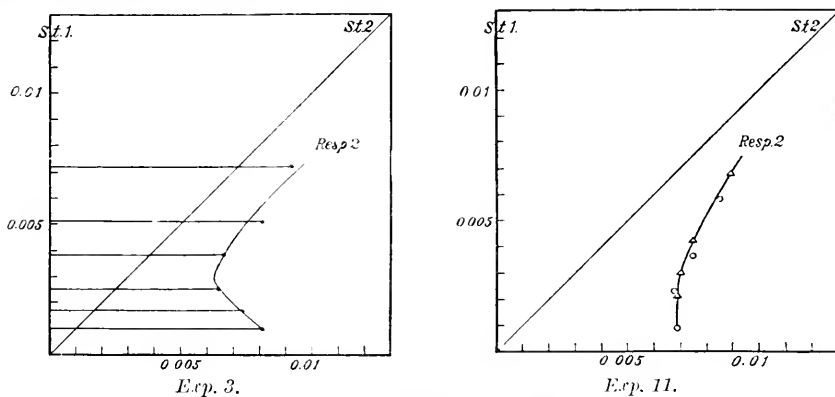


Fig. 7.

\* The Journal of Physiology, Vol. 41, p. 68, 1910.

Here the ordinate represents the interval between the two stimuli, and the abscissa the same between the first stimulus and the commencement of the second response. The length of the abscissa measured from the straight line inclined at  $45^\circ$  to the axis, represents the interval between the second stimulus and the commencement of the second response. The curves have a minimum with respect to the abscissa.

Now from the numbers given in the tables in Lucas's paper, which are reproduced below, I constructed two curves representing the relation between the interval from the second stimulus to the commencement of the second response and the interval between the two stimuli (Plate XII.). Then it was found that the newly reduced curves were simply exponential in agreement with our results. Of course, in this case, the ordinate shows the absolute value of the so-called latent period instead of the ratio of the two modal latent periods. But since the values were obtained by subtracting a constant value which may be considered to be the interval between the beginning of the response and its summit, the nature of the curve must be the same as if it were drawn in our way.

The tables found in the paper of Lucas are given below.

TABLE XXII.

Exp. 3 and Exp. 11 by Lucas. The Journal of Physiology, Vol. 41, p. 337 and p. 399.

Exp. 3. Sciatic-gastrocnemius preparation. Frog. Temp.  $17.5^\circ\text{C}$ .

Obs.	Time first stimulus to second stimulus.	Time first stimulus to second response.	Time second stimulus to second response.
A.	.0010 sec.	.0081 sec.	.0071 sec.
B.	.0017	.0074	.0057
C.	.0025	.0064	.0039
D.	.0038	.0066	.0028
E.	.0051	.0081	.0030
F.	.0072	.0092	.0020



The times of the beginning of the second responses are estimated on the assumption that the response begins always at a fixed time (0.0031) before it attains its maximum P.D.

Ex. 11. Gastrocnimius-sciatic preparation. Frog. Temp. 17.5 °C.

B. Time of commencement of second response calculated from time of its maximum P.D. (as the interval between the commencement of the curve and its summit, .0022 sec. is taken)

I. With second stimulus at same point as first.

Obs.	Time first stimulus to second stimulus.	Time first stimulus to beginning of second response.	Time second stimulus to beginning of second response.
A.	.0021 sec.	.0069 sec.	.0048 sec.
B.	.0030	.0070	.0040
C.	.0042	.0074	.0032
D.	.0067	.0093	.0025

II. With second stimulus 11 mm. nearer to muscle than first.

Obs.	Time first stimulus to second stimulus.	Time first stimulus to beginning of second response.	Time second stimulus to beginning of second response.
E.	.0015 sec.	.0069 sec.	.0054 sec.
F.	.0029	.0067	.0040
G.	.0042	.0074	.0032
H.	.0064	.0084	.0020

Correcting by time of conduction .0006.

Obs.	Time first stimulus to second stimulus.	Time first stimulus to beginning of second response.	Time second stimulus to beginning of second response.
E.	.0009 sec.	.0069 sec.	(.0050) sec.
F.	.0023	.0067	(.0045)
G.	.0036	.0074	(.0038)
H.	.0058	.0084	(.0025)

The numbers enclosed in the brackets are calculated by the present author.

From these data we calculated  $M$  and  $\lambda$ . The values of the normal latent period could not be discovered in his paper and we therefore found them as follows:—

Taking three ordinates  $y_1$ ,  $y_2$  and  $y_3$  on the figure (Plate XII.) with equal intervals in succession, we put

$$\begin{aligned}y_1 &= l + b, \\y_2 &= l + mb, \\y_3 &= l + m^2b,\end{aligned}$$

where  $l$  is the normal latent period and  $m$  a constant to be determined by the period of recovery. So in Exp. 3 we may find  $l=0.0019_s$  and  $m=0.40_s$ , the interval between the successive ordinates being  $0.0024_s$  sec. From these values we obtain  $M=0.0098$ ,  $\lambda=646$ . The numbers calculated from the data are plotted on the curve by the mark  $\bullet$  (Plate XII., Fig. 3 and Fig. 4). In experiment 11 we get  $l=0.0016_s$  and  $m=0.48$ , the interval between the successive ordinates being  $0.0024$  sec. and using these constants, we obtain  $M=0.0058$ ,  $\lambda=300$ . Taking the value of  $0.0031$  in exp. 3 and of  $0.0022$  in Exp. 11 as the interval between the summit and the commencement of the response, we may calculate the values of  $M$  and of  $\lambda$  in the same units as in our case. These constants are given below:—

Exp. 3.	$M = 2.25,$
	$\lambda = 646,$
Exp. 11.	$M = 2.66,$
	$\lambda = 300.$

In Plate XII. we see that the agreement between the experimental and the calculated curves is very good. From these results, we may say that our exponential law for the recovery of the temporary fatigue holds good in the results obtained by Lucas on the gastrocnemius-sciatic preparation of the frog.

Now denoting the interval between the stimuli by  $t$ , and the normal latent period by  $l$ , the interval between the first stimulus

and the commencement of the second response is given by

$$t + lMe^{-\lambda t} + l.$$

This has a minimum with respect to  $t$  at

$$t_m = \frac{1}{\lambda} \log_e \lambda Ml.$$

The values of  $t_m$  at this minimum are evaluated as follows:—

Experiment by Lucas:

No. 3.      0.0029 sec.

No. 11.     0.0020

Experiment by the author:

No. 74—No. 75.    0.0049<sub>5</sub>

No. 65.              0.0069<sub>5</sub>

Thus we see that the existence of the minimum is a consequence of the exponential property of the recovery, and therefore little weight should be placed on this minimum. Since, as we see, the minimum occurs very near to the end of the refractory period, it would sometimes not be discovered in an experimental result. It is very probable then that the so-called irresponsible period reported by Lucas in his first paper was an apparent phenomenon appearing for the reason that the observations were restricted in the vicinity of this minimum, where the variation becomes zero.

The corresponding phenomenon to the supernormal increase of the height of the second discharge was observed by Samojloff\* on the electric response of a muscle indirectly stimulated. Recently Adrian and Lucas† interpreted the phenomenon by the summation of two successive disturbances propagating through a nerve-ending. They considered that a propagated disturbance whose propagation is stopped at the nerve-ending by its decrement, if alone, is successfully transmitted through the block, when the like disturbance passed before. In our case, it seems rather probable that the supernormal magnitude of the second discharge is not the

\* Arch. f. (Anat. u.) Physiol., Suppl., 1908.

† The Journal Physiology, Vol. 44, p. 68, 1912.

direct effect of the disturbance evoked by the first stimulus, but it is the effect of the first discharge acting as a stimulus. In this view we must assume that the maximal disturbance in a nerve-trunk cannot cause the maximal discharge of the organ. The possibility of the fact may be considered in several ways. For instance, some elementary portions of an end-organ, say electric plates or muscle fibres, cannot be excited by the disturbance through a nerve, on account of the enormous decrement of the nerve-endings of those individuals, or else the disturbances in some nerve-fibres are too small to be transmitted to the end-organ for the same cause. In our experiment, when we take a part of an organ with a nerve-trunk attached, there certainly exist electric plates which do not receive the supply of the nerve-fibres from the trunk through which stimuli are given. Such plates cannot be excited by stimulating the nerve-trunk, but can be excited by the discharges of the electric plates belonging to that nerve-trunk. Then, when the discharge of such secondary nature is superposed on the discharge evoked by the second stimulus, the result must be the increase of the magnitude of the second discharge. If we may allow that the electric response of muscle may act as a stimulus, then the same interpretation may be applied in the case of muscle.

Our experiments hitherto described were made in such cases as the discharge evoked by the first stimulus had an asymptotic values in practice. Without presuming the law of "all or none" it is very important to examine the case when the discharge is so-called submaximal. We have three series of such experiments that were obtained accidentally. These are Oscillograms No. 50, No. 47 and No. 51.

In Oscillogram No. 50 (Plate XXI.), when two stimuli separated by an interval  $77.5 \times 10^{-4}$  sec., the response by the second cannot be observed. When they approach  $66.3 \times 10^{-4}$  sec., we see a low discharge scarcely distinguishable from the secondary. Then they approach nearer *i. e.* to  $55.0 \times 10^{-4}$  sec. and the second discharge appears on the descending branch of the first discharge. When they approach each other still nearer *i. e.*  $29.9 \times 10^{-4}$  sec., the second

comes on the ascending branch of the first. At last when the interval between the two becomes  $16.4 \times 10^{-4}$  sec., the discharges coalesce into a single one. Here since the position of the second summit would be displaced on account of its lying on the inclined branch of the first, we cannot measure the modal latent period accurately and therefore we also measured the interval between the stimulus and the commencement of the curve. The next table shows the numbers obtained on the oscillogram.

TABLE XXIII.

Oscillogram No. 50.

Temperature of the organ:  $8.2^{\circ}\text{C}$ .

No.	Interval between Stim. in $10^{-4}$ sec.	L. P. of 1st discharge in mm.	L. P. of 2nd discharge in mm.	Ratio of two L. P.
1	77.5	69.0	No response.	
2	66.3	70.0	71.5	1.02
3	55.0	71.0	70.5	0.99
4	44.2	71.0	65.0	0.92
5	29.9	70.0	65.0	0.93
6	16.4	65.0	Coalesce into a single curve.	
7	5.8	—		

No.	M. L. P. of 1st discharge in mm.	M. L. P. of 2nd discharge in mm.	Ratio of two M. L. P.
1	81.0	—	—
2	82.0	—	—
3	82.0	78.0	0.95
4	79.0	75.5	0.96
5	—	—	—
6	—	—	—
7	—	—	—

As a mere experimental result, it seems that before the so-called refractory period there exists a period in which the response *may occur*. The modal latent period or the latent period of the second discharge seems to decrease even to a smaller value than that of the first for some value of the interval between the two stimuli. Indeed the shortening of the latent period from the normal is equal to 6 mm. in the maximum length on the oscillogram. But in other experiments we know that, while the modal latent period gives very consistent values, the latent periods differ widely according to the height of the curve. It will not therefore be useless to calculate roughly the value of the displacement of the summit of the second discharge curve on account of its lying on the descending branch of the first. Suppose a discharge curve  $y = Ae^{-b^2 \log^2 \frac{x}{x_0}}$  superposed on an inclined straight line

$$y = (p-x)\tan\varphi.$$

Then the resultant curve is expressed by

$$y = (p-x)\tan\varphi + Ae^{-b^2 \log^2 \frac{x}{x_0}}.$$

Differentiating the expression with respect to  $x$ , and equating the result to zero, we have

$$\tan\varphi + 2Ab^2 \log \frac{x}{x_0} \cdot \frac{1}{x} e^{-b^2 \log^2 \frac{x}{x_0}} = 0.$$

A value of  $x$  satisfying the equation must be that for the maximum value of  $y$ .

Let the displacement of the summit be represented by  $\delta$ , which, in the first approximation, may be considered very small when compared with  $x_0$ . Putting  $x = x_0 - \delta$  in the above expression and neglecting the higher orders of  $\frac{\delta}{x_0}$  than the first, we have

$$\delta = \frac{x_0^2 \tan\varphi}{2Ab^2} \dots\dots\dots (10)$$

Taking the third experiment in the oscillogram No. 50, we may put very roughly

$$x_0 = 29 \text{ mm.},$$

$$b^2 = 10.7,$$

$$A = 4 \text{ mm.}$$

and

$$\tan \zeta = \frac{1.5}{10} \text{ at most,}$$

where the value of  $x_0$  and of  $b^2$  are determined from the first experiment. From these data we may get 1.4 mm. as the value of  $\delta$ . Referring to the table, the difference of the two apparent modal latent periods in that experiment is equal to 4.0 mm. So giving full allowance to the effect of  $\delta$ , the difference needs not be smaller than 2.6 mm. The value cannot be considered to be an error of measurement.

Oscillogram No. 47 (Plate XXI.) is another example of the same kind, and the numbers obtained on this film are tabulated in the next table.

TABLE XXIV.

Oscillogram No. 47.

Temperature of the organ:  $8.5^\circ\text{C}$ .

No.	Interval of two Stim. in $10^{-4}$ sec.	M. L. P. of 1st discharge in $10^{-4}$ sec.	M. L. P. of 2nd discharge in $10^{-4}$ sec.	Height of 1st discharge in mm.
1	79.1	174	233	31.0
2	69.4	171	235	31.2
3	58.1	172	248	30.8
4	45.0	175	—	29.0
5	37.6	174	—	29.5
6	28.9	173	188 ?	27.0
7	8.3	176	—	33.2
8	0.0	—	—	33.2

Here the modal latent period of the first discharge is tolerably constant. In the first three, the modal latent period of the second discharge increases a little with the decrease of the interval

between the two stimuli. When the interval becomes  $45.0 \times 10^{-4}$  sec. the second discharge seems to disappear. When it is diminished to  $37.6 \times 10^{-4}$  sec. the second discharge becomes perceptible on the descending branch of the first discharge, but the modal latent period cannot be measured, although it is certain that it is made smaller. When the interval becomes  $28.9 \times 10^{-4}$  sec. the modal latent period of the superposed second discharge may roughly be determined to be  $190 \times 10^{-4}$  sec. Finally, the interval becoming  $8.3 \times 10^{-4}$  sec., the two discharges coalesce into a single one. From this onwards, the height of the first discharge becomes greater than those of the preceding, thus showing the summation of the second discharge.

Oscillogram No. 51 (Plate XX1.) is a series of the experiments of the same type. Here we may find as the ratios of the second modal latent period to the first the values of 1.00, 0.98, 0.95 and 0.93 for 4th, 5th, 6th and 7th curve respectively.

Let us now discuss the results with reference to the theory of "all or none." As the stimulus is submaximal, a part of the nerve fibres is excited by the first stimulus and the other part is not excited, but only receiving the subminimal stimulus. Let us call the former the first part and the latter the second part. When the second stimulus, which is also subminimal to the second part, is in the refractory period and on the outside of the *summation interval*<sup>‡</sup> so-called by Lucas, which must be assumed to be smaller than the refractory period, the second response cannot occur. But when the second stimulus enters into the summation interval it excites the second part in concordance with the first stimulus, while it does not excite the first part. Hence the experimental results can be explained. For the correctness of this interpretation, it must be allowed that the refractory period in this case is greater than  $77.5 \times 10^{-4}$  sec. and the summation interval is greater than  $66.3 \times 10^{-4}$  sec. The latter number is very great compared with the same measured by Lucas on the motor nerve to the gastrocnemius muscle of the frog which was equal to  $5 \times 10^{-4}$  sec. Whether the modal latent

---

\* The Journal of Physiology, Vol. 39, p. 461.



period, measured from the second stimulus, belonging to two subminimal stimuli may take a value smaller than the normal or not is a question which appeared on Oscillograms No. 50 and 51, and worth while investigating hereafter.

Next we shall give an example of summation of two discharges in response to a closing and an opening-stimulus (Plate XXII., Oscillogram No. 70). Stimuli of the same type as those used in the direct stimulation were given to a nerve-trunk with a proper shunt, by which the stimulation current through the nerve remains submaximal and yet the current flowing through the oscillograph was sufficiently large to trace its form. The experiment was made for another purpose *i. e.* for the comparison of the intensity of the stimulating current and the magnitude of the resulting discharge. At first the stimulating current was increased step by step for five successive experiments. Then the duration of the stimulation current was changed, and commencing with the smaller current, it was increased step by step in the five succeeding experiments in an exactly similar way. In the latter half, the forms of stimuli were not good, and we have not therefore used them in the analysis. The following table shows the numbers measured on the oscillogram.

TABLE XXV.

Oscillogram No. 70.

No.	Height of Stim. in mm.	L. P. of 1st discharge in $10^{-4}$ sec.	L. P. of 2nd discharge in $10^{-4}$ sec.	Ratio.	M. L. P. of 1st discharge in $10^{-4}$ sec.	M. L. P. of 2nd discharge in $10^{-4}$ sec.	Ratio.
1	11.0	96.5	101.8	1.055	113.9	119.0	1.045
2	23.3	88.0	101.5	1.150	112.0	115.2	1.030
3	35.5	81.3	103.0	1.270	109.8	111.5	1.015
4	47.0	79.0	100.2	1.270	108.5	108.5	1.000
5	Out of film.	79.5	102.5	1.290	109.0	109.0	1.000

Since the duration of the stimulating current did not exceed  $21 \times 10^{-4}$  sec., it must be allowed that the opening-stimulus had occurred before the end of the refractory period due to the

closing-stimulus, and therefore the response to the opening-stimulus must be due to the nerve-fibres that were not excited by the closing-stimulus. Referring to Oscillogram No. 70, we see that when the intensity of the stimulating current is very weak, the discharge by the opening stimulus is higher than that by closing. When the intensity of the stimulating current is made larger, the discharge due to the closing-stimulus becomes larger while the same due to the opening-stimulus becomes first larger and then smaller. Putting the base for the explanation of this phenomenon upon the theory of "all or none," when the stimulating current is sufficiently strong so that all the plates are discharged by the set of two stimuli, the area of the superposed resultant curve, which corresponds to the number of the plates discharged,\* must be constant. In this view we measured the values proportional to the areas of the curves on the oscillogram by weighing the pictures cut out from bromide paper, and then multiplying each of them by its respective interval corresponding to one-millimetre of the abscissa, we got the values proportional to the number of the plates discharged. These values are given in the next table.

TABLE XXVI.

No	Weight of picture cut out, in mgr.	1 mm. of abscissa corresponds to, in $10^{-4}$ sec.	Product.
1	32.4	3.45	112
2	41.3	3.39	140
3	44.1	3.38	149
4	45.4	3.29	149
5	45.8	3.31	151

\* When we take a small part of the organ as in our experiments, the resistances of all individual columns may be considered to be equal to one another. Let the resistance of one column be denoted by  $r$ , the current flowing through each of the columns at an instant by  $i_1, i_2, \dots, i_n$  respectively, the resistance of the external conductor by  $R$ , and the current flowing through it by  $I$ . Let the electromotive force of an elementary discharge of a plate be  $e$ , and the number of

The above table shows that the area of the discharge curve becomes constant when the stimulus is made strong enough. While the experimental result gives support for the theory of "all or none," it seems to reveal two new facts: (1) the opening-stimulus can evoke its response, which could not be caused on closing the same stimulating current, or, otherwise, the opening-stimulus may be summed up into something that occurred at the anode on closing the current: (2) the delay of the second discharge is longer than the normal. The cause of the second phenomenon is not clear. It may be seen that the modal latent period measured on the oscillogram seems rather to have normal value *i.e.* not prolonged. But since the second summit lies upon the inclined branch of the first discharge curve, the displacement of the apparent summit towards the stimulus is not small. On calculating the displacement by the formula  $\delta = \frac{x_0^2 \tan \epsilon}{2Ab^2}$ , it may be found that the displacement is not smaller than 2 mm. on the film. Therefore the prolongation of the modal latent period of the discharge by opening-stimulus seems certainly to exist.

Before closing this section we have two more oscillograms of allied problem to be explained. Since I thought that the rhythmic response of a nerve or of a muscle to high frequency stimuli, might be the effect of the refractory period, a few experiments were made regarding that subject. Oscillograms No. 67 and No. 85 (Plate XXIII.) represent the results obtained. In No. 67 the make and break of the high frequency of the primary circuit of an induction coil was made by a contrivance like the commutator

---

the plates discharging per second at an instant in each column be  $n_1, n_2, n_3, \dots, n_m$  respectively. Then by Kirchhoff's law, we have

$$\begin{aligned} cn_1e &= RI + ri_1, \\ cn_2e &= RI + ri_2, \\ cn_3e &= RI + ri_3, \\ &\vdots \\ cn_me &= RI + ri_m, \end{aligned}$$

where  $I = i_1 + i_2 + i_3 + \dots + i_m$ , and  $c$  is a proportional constant.

By adding each side of the equations, we have

$$ce \sum_{j=1}^m n_j = (R + r) I,$$

and therefore

$$\int_{t=0}^{t=\infty} \sum_{j=1}^m n_j dt = \frac{R+r}{ce} \int_{t=0}^{t=\infty} I dt,$$

*i.e.* the total number of the plates discharged is proportional to the area of the curve.

of a dynamo, and the nerve-trunk attached to the organ was stimulated by the induced current. For this and the other ends, our shutter was so constructed that, when we made proper connections, the stimulating current could flow only when the shutter opened (Plate IV., *c*). The number of the momentary stimuli given amounts to 885 per sec. In this case the stimuli varied a little in their strength, and hence another experiment No. 85 was made in which the induction coil was not used. Here, as stimulus, a current from eight accumulators was interrupted by the same contrivance as No. 67, no induction coil being used. The stimuli were regular, and their number amounted to 1412 per sec. As may be seen in the oscillograms, the discharges were not so regular as to account for one determinate period, being a series of high and low superposed discharges. This might be the case because the stimuli were not maximal, though in the beginning part it seems to be so. From many other experiments it seems to me, that the liminal value of the stimulus for the maximal response in the nerve increases with the temporary fatigue, and by this assumption the irregularity of the discharges may be easily interpreted. Hence assuming that the stimuli were sufficiently strong at the beginning, we may take as the period of response, the interval between the first and the second discharge, and we get as its value  $117 \times 10^{-4}$  sec. in No. 85, the temperature of the organ being  $15^{\circ}\text{C}$ . For the more advanced discussion the more precise analysis should be necessary, and hence we here allude to this as a mere experimental result.

The summary of this section is :—

i.) When two successive stimuli separated by an interval a little greater than the refractory period are given at a point in a nerve of the electric organ, the modal latent period of the second discharge is prolonged with regard to the normal.

ii.) The recovery of this prolongation follows an exponential law with respect to the interval between the two stimuli.

iii.) The prolongation of the modal latent period of the second discharge is accompanied by the variation of the maximum electromotive force of the second discharge.

iv.) The electromotive force increases probably from zero when the second stimulus separates more and more from the end of the refractory period and when at a certain interval between the two stimuli it becomes even greater than the normal and then decreases again.

v.) The abnormal increase of the electromotive force may be interpreted as the summation effect of the second discharge and the secondary discharge of the first stimulus.

vi.) The second discharge caused by two successive submaximal stimuli given at a point in the nerve may be superposed on the first discharge, and the modal latent period of the second discharge seems to be even smaller than the normal at a certain interval between the two stimuli.

vii.) The discharge by an opening-stimulus given in the nerve may be superposed on that by closing-stimulus.

viii.) Phenomena vi. and vii. may give support for the theory of "all or none," but for this we must assume new subordinate properties of the nerve which is worth while investigating hereafter.

## VII. Fatigue phenomenon.

Fatigue phenomenon was investigated in two different ways.

(1) The registering drum was rotated very slowly by connecting the shaft of it with the clockwork of a kymograph, and successive momentary stimuli about 25 in a second were given to the nerve and the deviation of the strip of the oscillograph was photographed on a film. The periphery speed of the drum being about 1 cm. per sec., a discharge curve reduces to a straight line and the locus of its summit forms the so-called fatigue curve.

(2) The drum was rotated rapidly and two stimuli in each revolution were given to the nerve so that they might be photographed at two fixed places on the film. The stimulus consists of the induced current of an induction coil, which was caused by the make and break of the primary current flowing for a very short interval during which a peg on the shaft makes instantaneous contact with a stationary conductor (Plate IV., Fig. 1). The direc-

tion of the stimulating current was in general descending on closing the primary circuit. But in one case the ascending and the descending stimuli were alternately given to the nerve by a proper contrivance on the shaft of the registering drum (Plate IV., Fig. 3). In another case the stimuli were given directly to the organ. Here, as remarked at the outset of this paper, the induction coil must be excluded from the circuit during the discharge of the organ. This was accomplished by a proper contrivance belonging to the shaft of the registering drum (Plate IV., Fig. 3)

Beginning with the former case, the fatigue curve resembles very closely that of muscle. Oscillograms No. 1, No. 2 (Plate XXIV.), No. 3, No. 4 and No. 5 (Plate XXV.) show such curves. In No. 1, which shows the typical form of the fatigue curve, the electromotive force increases a little during a few discharges at the outset of the fatigue, and passing over a maximum, it decreases almost exponentially. The rate of decrease increases after passing the maximum, then decreases gradually, again increases a little and then decreases again. Thus repeating the same type of variation, in such a way that the locus of the top of the discharge curve forms a mild wave form, the nerve or the organ is tired out. Two low loci on the bottom of the oscillogram are those of the secondary and of the tertiary discharge. The marks of regular intervals on the bottom are those of a second. Here we may remark that the tops of the discharge curves form a smooth curve at the beginning of the fatigue, but when in deep fatigue their heights become very irregular (Oscillogram No. 2).

Oscillograms No. 3, No. 4 and No. 5 (Plate XXV.) form a series of experiments. Oscillogram No. 4 was taken at an interval of one hour after No. 3, and Oscillogram No. 5 at 40 min. after No. 4. The number of stimuli is about 25 per sec. Here we see, that the fatigue may be partially recovered by a repose of the stimulation so that there must be two kinds of fatigue, namely that which can be recovered and that which cannot be recovered. I am of opinion that, that part of the fatigue which can be recovered is the same as the temporary fatigue of the nerve discussed in the

previous section, and that which cannot be recovered is due to the alteration in the organ or in the nerve. Of course, the interval between two consecutive stimuli is very large compared with the period of recovery discussed in the former section, but there is still a fatigue, for not only small residuals of the fatigue may accumulate in such cases, but also a part of the nerve trunk may still be in deep fatigue on account of the stimulation by the discharge of the higher order, when a succeeding stimulus is given. As we remarked in the preceding section, when the fatigue advances, the liminal value for the maximal stimulus increases in nerve, so that the stimulus of the given magnitude, which is sufficiently maximal at the outset of the fatigue, becomes submaximal, and a little variation in its magnitude may cause the discharge of a different magnitude. May not this be the cause of the irregularity of the discharge in the tired state?

In regard to the increase of the contraction at the outset of fatigue in muscle, Fröhlich interprets the phenomenon as the apparent effect of the prolongation of the wave length of the contraction propagating through a muscle. He thinks that, the fact that the same phenomenon could not be observed in negative variation, gives support to his theory. But since a similar interpretation fails to apply in our case, it is probably incorrect. In view of our experimental results, it seems to me that the phenomenon is analogous to the abnormal increase of the electromotive force of the second discharge discussed in the preceding section. In that section, we explained the phenomenon as the effect of the superposition of the second discharge on the secondary discharge. Here, of course, the principal discharge evoked by the succeeding stimulus is very far from the secondary discharge, but it may be superposed with a discharge of one of the higher orders. To express my idea clearly, suppose a discharge followed by a series of higher orders, to be evoked by one of the stimuli separated by a fixed interval of time as in the experiment. When the fatigue advances, the modal latent period is prolonged gradually, as may be observed in the fatigue investigations of the other form, and the secondary, the tertiary discharge *et seq.* delay in propor-

tion to the intervals between these and the stimulus, so that the discharges of the higher orders chase the succeeding stimulus. At the instant at which one of the discharges of the higher orders just comes at the principal discharge due to the succeeding stimulus, the height of the discharge must be increased. By this consideration not only the first maximum of the fatigue curve may be explained, but its wave form may be interpreted also. In the case of muscle, ability for response of the higher order may be observed in the so-called tetanic state which, in my opinion, is caused by a series of responses successively evoked by the preceding electric response acting as a stimulus on the tissue in a highly excitable state. This view may be supported by the fact that the decrease of the proper period with the rise of temperatures follows the same law as that of the increase of the speed of propagation through the nerve.\* Then may not the same interpretation be applied to the case of muscle? Concerning this point further investigation should be necessary. Here we describe this as an interpretation which seems to be true in so far as our experiment goes.

Next we shall explain another form of fatigue oscillogram. Oscillograms No. 6, No. 78 and No. 78' (Plate XXVI.) show such experiments. From these oscillograms we see that, when the fatigue advances, the modal latent period is prolonged and the height of the discharge curve decreases. Oscillogram No. 7 (Plate XXVII.) is an example in which the discharges appeared in a very complex manner. Perhaps the discharge was affected by the tertiary discharge belonging to the preceding set, but no satisfactory explanation has been obtained. The following explanation looks somewhat probable. The discharges due to the opening-stimuli at first appeared, then those due to the closing-stimuli were superposed on their ascending branches, and finally in the advanced stage of the fatigue, only those by the closing-stimuli remained. For the sake of correctness of this consideration, it must be assumed that the modal latent period belonging to the open-

---

\* { Dittler and Tichomirow.      Pflüger Archiv, Bd. 125, S. 117.  
 { Dittler and Oinuma.        Pflüger Archiv, Bd. 139, S. 293.



ing-stimulus was greater than the normal. In these experiments the direction of the stimulating current was generally descending on closing the primary circuit, but in the above case the stimulating current was ascending. If the above phenomenon may be explained by Pflüger's contraction law in the muscle-nerve preparation, it must be recognized that the value of the maximal stimulus with respect to the nerve increases with the progression of the fatigue and hence the same stimulating current will be strong at first, then it will become medial and finally weak with respect to the nerve. If the above explanations be correct, here again we have evidence that the value of the maximal stimulus with respect to the nerve increases with the progression of the fatigue.

Oscillogram No. 8 (Plate XXVI.) shows the case in which the stimulating currents are ascending and descending alternately. This oscillogram shows that the fatigue phenomenon is not the consequence of the polarisation at the electrodes. Oscillograms No. 78 and No. 78' (Plate XXVI.) show the fatigue by the descending and by the ascending stimuli respectively.

Oscillogram No. 9 (Plate XXVII.) is an example of the fatigue phenomenon by the direct stimulations. In this case, it is a remarkable fact that, although the modal latent period is prolonged with the progression of the fatigue, the descending branches of the discharge curves coincide with one another into a line. Since the discharges in the two sets of curves have the very same aspect, notwithstanding the stimuli are different in their breadths, the responses must be due to the closing-stimuli only,—the case when the closing-stimuli are strong enough to evoke the maximal discharges. Therefore the oscillogram shows the fatigue phenomenon in the case when the stimuli are direct and simple.

The principal point of this section is that the increase of the magnitude of the response at the outset of the fatigue exists in the case of the electric organ as well as in muscle. Therefore the explanation by Frölich in the case of muscle cannot be considered correct.

### VIII. Speed of Propagation of Excitation through the Nerve.

Since the time relation can be measured very accurately by our method, some experiments were made regarding the speed of the propagation through the nerve-trunk.

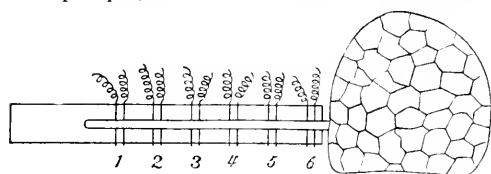


Fig. 8. Nerve-organ preparation with six pairs of the electrodes.

Oscillogram No. C. 5 (Plate XXVIII.) shows an experimental result regarding the uniformity of the speed along the nerve-trunk. On an ebonite plate about 1 cm.

in breadth, six pairs of electrodes were fixed as shown in the accompanying figure. The distance between the electrodes in a pair was 1 mm. and the distances between the corresponding points of such consecutive pairs were 5 mm. A nerve-trunk with a part of an organ was laid on this plate along its length and the momentary stimuli were sent to the points on the nerve in the order of 1, 2, 3, 4, 5, 6 and 2, the last one being for the check. The following numbers were obtained on this oscillogram:—

TABLE XXVII.

Oscillogram No. C. 5.

No additional resistance.

Temperature of the organ : 11.6 °C.

No. of electrodes.	Time stimulus to beginning of discharge in mm.	Number of revolutions of registering drum.	1 mm. corresp. to, in $10^{-4}$ sec.	Time stimulus to beginning of discharge in $10^{-4}$ sec.	5 and 6 of 2nd column interchanged*
1	81.4	13.23	1.515	123.0	
2	66.0	13.04	1.533	101.3	
3	60.9	12.79	1.565	95.5	
4	58.3	13.17	1.520	88.6	
5	50.3	13.27	1.508	76.0	83.0
6	48.7	12.13	1.650	80.4	73.5
2	60.0	11.70	1.710	102.3	

\* In 5 and 6 the electrodes should have been interchanged by accident, therefore for their values we used the numbers in the last column.

The modal latent periods could not be measured, for the summits of the curves were on the outside of the film. Therefore the time between the stimulus and the beginning of the discharge was measured.

In Plate X. a graph representing the time between the stimulus and the beginning of the discharge with regard to the position of the electrodes is drawn. In this figure we see that the check point lies very closely on the curve. This shows that the experiment was not affected by any progressive change. The points 2, 3, 4, 5 and 6 arrange themselves on a straight line, while the point 1 falls on the upward side of the line. This shows that between the points 2 and 6 in the nerve, the speed of propagation was uniform whether the point concerned was near to or far from the stimulated point. As the value of the speed, we obtained 7.31 metres per sec., the temperature of the nerve being 11.6 °C. The discrepancy of the point No. 1 must have its cause in the alteration or decay of the nerve at that portion which occurred near the excised end of the nerve. This becomes very obvious when we examine the oscillogram, for there we see that the discharge curve corresponding to No. 1 is very low compared with the other discharges, while the stimulus is not smaller than the others. The prolongation of the latent period of the discharge evoked by a stimulus given at a point near the excised end of the nerve, may be explained by one of the following assumptions. (1) The speed of propagation in the portion near the excised end of the nerve altered by its injury is smaller than the normal. (2) The local latent period at the nerve-ending or in the organ, *i.e.* the interval between the instant, at which the disturbance arrived at the nerve-ending, and that of the beginning of the discharge is greater when the disturbance in the nerve is smaller. (3) The speed of propagation of the nerve excitations differing in magnitude has different values, the stronger the larger. (4) The local latent period at the point of stimulation is greater when that portion of the nerve is altered. The cases (2) and (3) cannot be considered to be true from the standpoint of

the "all or none" theory. Moreover Oscillogram No. 49 denies these assumptions, for the modal latent periods of the discharges are equal, though the magnitude of the discharges varies very widely. Then the cause of the prolongation must be due either to (1) or to (4). The causes (1) and (4) cannot be separated in our former experiments. I am, however, inclined to believe that the cause would be that of (1).

*N. B.*—Oscillogram No. 49 is an experiment intended to find the relation between the strength of the stimulus and the height of the discharge as shown in § V. The latent periods and the modal latent periods are given again in the following table:—

Table XXVIII.

No.	Height of discharge in mm.	Latent period in $10^{-3}$ sec.	Modal latent period in $10^{-4}$ sec.
1	9.0	142	173
2	0.5	Too low to be measured accurately.	
3	1.0	Too low to be measured accurately.	
4	2.3	162	185
5	8.3	162	188
6	15.0	159	185
7	17.0	156	189
8	18.3	156	189

(The stimulus of No. 1 was ascending by accident.)

Here we see that the latent period decreases with the increase of the height of the discharge and therefore, when our eyes are restricted to L. P., it seems that the speed of the propagation of the excitation increases with the increase of the height of the stimulus. But when our eyes are turned to the modal latent periods, we see that they give tolerably constant value, and show no regular variations with the increasing strengths of the stimuli. This shows that the speed of the propagation through the nerve in the normal state does not depend on the strength of the stimulus or on the magnitude of the excitation. Also this experiment shows that the so-called latent period is not suitable to be used as the time of reference for exact work.

## IX. Miscellaneous problems.

Oscillograms No. 53 and No. 100 (Plate XXIX.) represent photographs of spontaneous discharges of a living fish. At first we tried to open our shutter by the first discharge of the fish and to photograph the motion of the strips of the oscillograph caused by

the succeeding discharges. The shutter could be opened as desired, but the discharge curve could not be obtained. So laying a living fish on a wooden board having a hole of the shape of the organ for an electrode, and applying a pair of electrodes to the dorsal and the ventral side of the organ by my hands, the registering drum was rotated. Judging the proper instant, which could be readily known by the behaviour of the fish before its discharge, the shutter, used as time-shutter, was opened. When the discharges occurred, which were perceived by the shocks felt, the shutter was closed. In the two oscillograms taken under different conditions, we see that a shock always consists of two discharges followed by a very low one, the second discharge being a little smaller than the first. The proper period of the discharges of a living *malapterurus* and its variation by the change of the temperature were investigated by Koike\* with the string galvanometer. In his results a shock consists of many periodic discharges, which Garten and Koike thought to be the effect of rhythmic central excitations. In our experiment, the kind of fish was different from his, and in his experiment the fish was placed in water whereas ours was placed in air. Therefore it is not strange that the results do not agree in the two experiments. But in the face of our experimental results, perhaps the second and the succeeding discharges would be of a secondary nature, for a similar phenomenon *i. e.* two large discharges followed by a very low one was frequently observed in many experiments of the indirect stimulation given to the preparation of the isolated nerve-organ.

We shall next show two experiments regarding the discharge by the stimulating current of long duration in the ascending or in the descending direction. Oscillograms No. 76 and No. 77 (Plate XXX.) are two such experiments. These are the results with different preparations. The original object of these experiments was to test Hoorweg's consideration that the opening stimulus was the effect of the polarisation current flowing through the shunt ordinarily used for the regulation of the stimulation current. The result was of course negative. But on examining the

---

\* Zeitschrift für Biologie, Bd. 54, 1910.

oscillograms precisely, we found that the stimulating current of long duration sent through the nerve influences the strength and the modal latent period of the succeeding discharge in a peculiar way. The experiments were performed by closing the stimulation circuit and by shunting it at the proper instant. These operations can be made by our stimulation apparatus by using two connection changers, one of which is a mercury key of earlier design. The current was directly derived from eight storage cells. The numbers obtained from these oscillograms are tabulated in the following table:—

TABLE XXIX.

Oscillograms No. 76 and No. 77.

Stimulus : Indirect.

Temperature of the organ :  $14.5^{\circ}$

No. 76.

No.	Direction of stimulating current.	Duration of current in $10^{-4}$ sec.	Modal latent period in $10^{-4}$ sec.	Height of discharge in mm.
1	Ascending.	169.9	110.7	20.0
2	Ascending.	304.0	110.0	18.5
3	Descending.	300.0	113.5	8.0
4	Descending.	172.0	120.4	2.0

## No. 77.

No.	Direction of stimulating current.	Duration of current in $10^{-4}$ sec.	Modal latent period in $10^{-4}$ sec.	Height of discharge in mm.
1	Descending.	18.7	129.3	Out of film.
2	Descending.	124.8	133.3	
3	Ascending.	166.0	213.9	47.5
4	Ascending.	43.7	148.2	46.5
5	Ascending.	23.0	138.5	53.5
6	Descending.	21.2	130.5	59.0

The modal latent periods of 1 and 2 in No. 77 were found by the formula  $x_0 = \sqrt{x_1 x_2}$ . Since the stimulus was indirect, it must be allowed that the values of the modal latent period thus found may be somewhat larger than the correct values.

In the descending stimulus, the discharge occurs by the closing-stimulus and in the ascending by the opening-stimulus. The positive direction of the ordinate on the oscillograms shows the descending stimulus.

In No. 77, the modal latent period of the third experiment shows extraordinary prolongation. The discharge was caused by an ascending stimulation current of tolerably long duration and the preceding discharge was that due to the descending current. The succeeding discharges were evoked by the stimulus of the same direction and the result was that, the shorter the duration the shorter the modal latent periods, though it is longer than the normal. The prolongation may be interpreted either as the effect of some local change caused by the ascending stimulating current of long duration, of which the longer the duration, the greater is the prolongation; or as the influence of the preceding stimulus which is recovered by repeating the opposite current. The former is more probable if the observation is limited to this film only, but in the discharge evoked by the stimulus of the same direction in Oscillogram No. 76, it cannot be observed that the modal latent period is prolonged. The number of the series of experiments of the above kind is only two, and therefore we cannot give a definite conclusion.

In Oscillogram No. 71 (Plate XXII.), similar prolongations of the modal latent periods may be observed in the experiments of the ascending-stimulus which were made after a series of experiments of the descending-stimulus. But there is no proof that the prolongation was the influence of the previous descending stimulus.

TABLE XXX.

Oscillogram No. 71.

No.	Height of stimulus in mm.	Height of discharge in mm.	Modal latent period in $10^{-4}$ sec.
1	12.0	26.0	96.5
2	23.0	24.5	92.7
3	34.0	24.0	97.4
4	46.0	24.0	94.0
5	—	23.0	91.5
6	—	18.0	106.3
7	45.0	18.0	110.0
8	34.0	16.0	107.5
9	10.0	20.5	99.0

Here the stimuli of No. 1.—No. 5 and that of No. 9 were descending, and those of No. 6, No. 7 and No. 8 were ascending.

In the oscillograms we may observe that when the modal latent period exhibits its prolongation, it is always accompanied by the decrease of the magnitude of the corresponding discharge, although the converse is not true always. We may remark here that this law applies to all cases whether the cause of prolongation is the temporary fatigue or any other alteration in the nerve, or that of an unknown cause like that above described. On the contrary, when the magnitude of the discharge is small on account of the smallness of the stimulus, the prolongation does not appear. This shows that, when the prolongation appears, the nerve-fibres are changed in its state and in consequence the discharge becomes small, *i. e.* every "all" of an excitation itself in the nerve fibres becomes



small, and perhaps the number of disturbances in the nerves which can pass through the decrement of nerve-endings or of some altered part in the nerve becomes less ; and when the prolongation does not appear, the smallness of the discharge is caused on account of a small part of nerve fibres in a trunk being excited. Thus the phenomenon gives support to the "all or none" theory.

#### Summary.

Since several new phenomena have been brought to light after the analyses of the oscillograms, and since at present we have not an opportunity to confirm them by further experiments, we are obliged to leave many problems as not positively decided. We shall conclude this paper, by summarising the results.

1) A formula expressing the time relation of a simple discharge may be got from the theory of probability and is expressed by

$$y = A e^{-b^2 \log^2 \frac{x}{x_0}},$$

where  $y$  denotes the electromotive force at time  $x$  measured from a certain fixed moment,  $b^2$  and  $x_0$  being constants.

2) In the case of the direct stimulus of short duration, the origin of time in this formula is in agreement with the instant of stimulation.

3) When the direct stimulation is of a longer duration, the discharge in response to it may be analysed into two simple discharges corresponding to the closing and to the opening-stimulus, and each of them may be represented by the above formula, having its origin at the instant of the corresponding stimulus.

4) Taking the value of  $A$  as the measure of the excitation, the relation between the intensity of a stimulating current and the excitation in response forms an S-shaped curve which rises from the zero-stimulus very slowly, then quickly, and after passing an inflexion point on its way, finally approaches asymptotically a constant maximal value.

5) With regard to the relation between the duration of a stimulating current and the excitation in response, Hoorweg's decrement factor seems to hold good.

6) When a stimulation is given to a nerve, there remains a fatigue which recovers in a very short interval and which is called the *temporary fatigue* by the author.

7) The fatigue is characterised by

a) The prolongation of the modal latent period of the discharge in response to a stimulus given in the interval influenced by that fatigue.

b) The decrease in the intensity of the discharge denoted by  $A$  in the discharge formula.

8) The time relation of the recovery of this fatigue measured by the excess of the modal latent period of the second discharge compared with the same of the first may be expressed by an exponential function  $Me^{-\lambda t}$ , and this law of the recovery holds good also in the case of similar results obtained by Lucas in nerve-muscle preparation.

9) The abnormal increase in the intensity of the second of the discharges, evoked by two successive stimuli, may be interpreted by the superposition of the secondary discharge.

10) The behaviour of the discharges in response to the two submaximal indirect stimuli, separated by an interval shorter than the refractory period, gives support to the "all or none" theory.

11) In this case, a new phenomenon is probably involved, *i.e.* the shortening of the modal latent period of the discharge, caused by the summation of the two subminimal stimuli.

12) The discharges in response to submaximal closing and opening-stimulus indirectly given may superpose, and the modal latent period corresponding to the opening-stimulus shows the prolongation in the modal latent period. In this case also, the phenomenon may be explained by the "all or none" theory, together with the assumption that the subminimal stimulus may cause some local change, which is made apparent from the prolongation of the modal latent period of the succeeding discharge and which is not yet otherwise confirmed.

13) The fatigue curve in the case of the electric organ very closely resembles that of the contraction of muscle. In both-

cases, there exist the so-called *staircase* phenomenon and the other details in a similar way, and this fact indicates the failure of Fröhlich's explanation in the case of muscle.

14) The speed of propagation of the excitation is uniform throughout the nerve-trunk whether the point concerned is near to or far from the stimulated point, if the nerve is in the normal state.

15) In the altered part of a nerve, near its periphery end, the speed of propagation becomes smaller and is accompanied by the decrease of the intensity of the corresponding discharge.

16) A spontaneous discharge curve of the living fish *Astrape* consists always of two peaks, sometimes followed by a very low irregular one. The second and the following discharge may be considered to be the secondary discharge, *etc.* evoked by the first.

17) The prolongation of the modal latent period from its normal value, of whatever cause it may be, is necessarily accompanied by the enfeeblement of the discharge, while the feeble discharge evoked by the weak stimulus does not indicate the same prolongation.

---

In closing this paper, I wish to express my best thanks to Prof. K. Osawa, Director of the Physiological Institute, whose liberality enabled me, for such a long period, to carry out in the Institute, these costly experiments. Also cordial thanks are due to Dr. S. Oinuma who was my zealous collaborator at the beginning of these researches, who kindly collected and placed at my disposal the literature relating to the subjects discussed in this paper, and who gave me many valuable advices.

---

## APPENDIX.

### Tables of Experimental Data and Calculated Numbers.

(Table I.—V. are those for the form of the discharge curve.)

TABLE I.

Oscillogram No. 54.

Date of experiment :

Nov. 6, 1909.

Object of experiment:

Relation between the intensity of a stimulating current and the magnitude of the corresponding discharge.

Preparation:

Left organ (whole) of a fish of middle size.

Temperature of the organ:

8.5°–7.2° C.

Resistance of the organ:

240 ohms.

Reading on the stimulation-apparatus:

Circuit-breaker: 64.0 mm.

Connection-changer: 60.0 mm.

No.	Current through primary circuit of induction coil in amp.	Number of revolutions of registering drum per sec.	1 mm. of oscillogram corresponds to, in 10 <sup>-4</sup> sec.	Height of stimulus in mm.	Height of discharge in mm.
1	1.50	6.51	3.07	19.5	1.6
2	2.00	6.38	3.13	25.7	5.0
3	2.50	6.50	3.08	31.8	10.1
4	3.00	6.53	3.06	38.0	17.3
5	3.50	6.40	3.13	44.7	26.7
6	4.00	6.18	3.24	50.0	35.7
7	4.50	6.00	3.33	57.0	44.8
8	4.95	6.36	3.14	65.5	55.6

No.	Latent period		Modal latent period	
	in mm.	in $10^{-4}$ sec.	in mm.	in $10^{-4}$ sec.
1	25.0	76.8	35.0	107.5
2	25.3	79.2	34.0	106.4
3	24.0	73.9	35.0	107.8
4	23.5	71.9	35.0	107.1
5	23.5	73.6	35.0	109.6
6	21.5	69.7	33.5	108.5
7	20.5	68.3	32.0	106.6
8	21.5	67.5	35.0	109.9

Co-ordinates of the points on the discharge curve for every 2 mm. of  $x$  on the oscillogram.

Curve No. 3.		
$x$ in mm.	$x$ in $10^{-4}$ sec.	$y$ in mm.
0.0	0.0	Beginning of stimulus.
24.0	73.9	0.0
5.0	77.0	0.5
7.0	83.2	2.1
9.0	89.3	4.9
31.0	95.5	7.7
3.0	101.6	9.5
5.0	107.8	10.1
7.0	114.0	9.7
9.0	120.1	8.8
41.0	126.3	7.4
3.0	132.4	6.1
5.0	138.6	4.8
7.0	144.8	3.4
9.0	150.9	2.7
51.0	157.1	1.8
3.0	163.2	1.3
5.0	169.4	1.1
7.0	175.6	0.7
9.0	181.7	0.3
Summit of the curve.		
35.0	107.8	10.1

Curve No. 4.		
$x$ in mm.	$x$ in $10^{-4}$ sec.	$y$ in mm.
0.0	0.0	Beginning of stimulus.
23.5	71.9	0.0
25.0	76.5	1.2
7.0	82.6	3.8
9.0	88.7	8.6
31.0	94.9	13.5
3.0	101.0	16.5
5.0	107.1	17.3
7.0	113.2	16.6
9.0	119.3	15.0
41.0	125.5	12.8
3.0	131.6	10.4
5.0	137.7	8.1
7.0	143.8	6.2
9.0	149.9	4.6
51.0	156.1	3.4
3.0	162.2	2.5
5.0	168.3	1.7
7.0	174.4	1.3
9.0	180.5	1.0
Summit of the curve.		
35.0	107.1	17.3

Curve No. 5.		
$x$ in mm.	$x$ in $10^{-4}$ sec.	$y$ in mm.
0 0	0 0	Beginning of stimulus.
23.5	73.6	0 0
25 0	78.3	2.4
7.0	84.5	7.0
9.0	90.8	14.2
31.0	97.0	21.1
3.0	103.3	25.3
5.0	109.6	26.7
7.0	115.8	25.3
9.0	122.1	22.2
41.0	128.3	18.5
3.0	134.6	14.5
5.0	140.9	11.0
7.0	147.1	8.3
9.0	153.4	6.0
51.0	159.6	4.5
3.0	165.9	3.3
5.0	172.2	2.4
7.0	178.4	2.0
9.0	184.7	1.6
Summit of the curve.		
35.0	109.6	26.7

Curve No. 6.		
$x$ in mm.	$x$ in $10^{-4}$ sec.	$y$ in mm.
0.0	0 0	Beginning of stimulus.
21.5	69.7	0 0
23.0	74.5	1.6
5.0	81.0	4.5
7.0	87.5	11.5
9.0	94.0	22.8
31.0	100.4	31.5
3.0	106.9	35.5
5.0	113.4	35.1
7.0	119.9	31.4
9.0	126.4	26.3
41.0	132.8	20.6
3.0	139.3	15.7
5.0	145.8	11.5
7.0	152.3	8.5
9.0	158.8	6.1
51.0	165.2	4.6
3.0	171.7	3.5
5.0	178.2	2.8
7.0	184.7	2.4
9.0	191.2	2.2
Summit of the curve.		
33.5	108.5	35.7

Curve No. 7.		
$x$ in mm.	$x$ in $10^{-4}$ sec.	$y$ in mm.
0.0	0.0	Beginning of stimulus.
20.5	68.3	0.0
3.0	76.6	3.2
5.0	83.3	9.3
7.0	89.9	22.7
9.0	96.6	35.7
31.0	103.2	43.6
3.0	109.9	44.8
5.0	116.6	40.7
7.0	123.2	33.9
9.0	129.9	26.5
41.0	136.5	20.0
3.0	143.2	14.6
5.0	149.9	10.2
7.0	156.5	7.5
9.0	163.2	5.4
51.0	169.8	4.1
3.0	176.5	3.3
5.0	183.2	2.3
7.0	189.8	2.1
Summit of the curve.		
32.0	106.6	45.0

Curve No. 8.		
$x$ in mm.	$x$ in $10^{-4}$ sec.	$y$ in mm.
0.0	0.0	Beginning of stimulus.
21.5	67.5	0.0
23.0	72.2	1.1
5.0	78.5	3.8
7.0	84.8	9.2
9.0	91.1	22.0
31.0	97.3	37.5
3.0	103.6	52.2
5.0	109.9	55.5
7.0	116.2	53.4
9.0	122.5	46.4
41.0	128.7	38.1
3.0	135.0	29.4
5.0	141.3	21.8
7.0	147.6	16.3
9.0	153.9	11.9
51.0	160.1	8.5
3.0	166.4	6.3
5.0	172.7	4.7
7.0	179.0	3.8
9.0	185.3	3.0
Summit of the curve.		
35.0	109.9	55.5

From the values given in the above tables, the curves from No. 3 to No. 8 were reproduced on section papers whose one division is equal to two millimetres. These curves are shown in Plate VI. For the ordinates, one division of the section paper represents one millimetre of the original; and for the abscissa, one division represents  $2 \times 10^{-4}$  sec. On these curves,  $\xi_1$ ,  $\xi_2$  and  $\xi_1'$ ,  $\xi_2'$  were measured; and from these values,  $\delta$ ,  $x_0$  and  $b^2$  were calculated. The following table shows these values. As the unit of  $y$ ,  $\xi_1$ ,  $\xi_2$ ,  $y_1'$ ,  $\xi_1'$  and  $\xi_2'$ , one division of the section paper is taken.

No.	$y$ .	$\xi_1$ .	$\xi_2$ .	$y'$ .	$\xi_1'$ .	$\xi_2'$ .	$\delta$ in $10^{-4}$ sec.	M.L.P. correct. in $10^{-4}$ sec.	$x_0$ in $10^{-4}$ sec.	$b^2$ .
1										
2				Too low to be used.						
3	3.5	10.9	18.5	1.4 <sub>5</sub>	13.4	26.1	+0.6 <sub>8</sub>	108.5	59.2	4.60
4	6.2	10.6	18.4	3.1	12.9	25.1	+1.1 <sub>2</sub>	108.2	59.8	4.69
5	9.8	11.3	17.2	4.3 <sub>5</sub>	14.1	24.8	-0.1 <sub>0</sub>	109.5	64.2	5.63
6	13.0	10.0	17.2	6.5	12.5	24.0	+1.4 <sub>0</sub>	109.9	60.8	5.37
7	16.5	9.8	17.1	8.2	12.1	24.0	+1.0 <sub>6</sub>	107.7	54.8	4.49
8	20.5	9.7	16.4	10.1	12.4	23.4	+1.4 <sub>6</sub>	111.4	61.8	5.95

By using these constants, the ordinates of each curve for every 1/1000 sec. were calculated. These are shown in the next table.



$x$ in $10^{-4}$ sec.	$y$ in mm. (calculated).					
	No. 3.	No. 4.	No. 5.	No. 6.	No. 7.	No. 8.
0.0	Origin of discharge.					
10.0	0.0 <sub>0</sub>	0.0 <sub>0</sub>	0.0 <sub>0</sub>	0.0 <sub>0</sub>	0.0 <sub>0</sub>	0.0 <sub>0</sub>
20.0	0.0 <sub>4</sub>	0.2	0.0 <sub>1</sub>	0.0 <sub>5</sub>	0.5	0.0 <sub>3</sub>
30.0	1.1	1.6	0.9	2.4	8.8	2.5
40.0	5.0	8.2	7.3	13.9	28.8	18.1
50.0	8.9	14.8	18.4	29.1	43.3	42.6
60.0	10.1	17.3	25.9	35.7	43.4	55.3
70.0	8.8	15.4	25.7	32.1	34.4	50.7
80.0	6.5	11.5	20.6	23.8	23.7	37.4
90.0	4.4	7.8	14.4	15.6	14.9	24.0
100.0	2.7	4.8	9.0	9.4	8.9	14.1
110.0	1.6	2.9	5.4	5.4	5.1	7.7
120.0	0.9	1.7	3.1	3.0	2.9	4.1
130.0	0.5	1.0	1.7	1.6	1.6	2.1
140.0	0.3	0.5	0.9	0.9	0.9	1.0
150.0	0.2	0.3	0.5	0.4	0.5	0.1

These values are plotted in Plate VI. by the marks  $\circ$ .

TABLE II.

Oscillogram No. 37.

Date of experiment:

Oct. 23, 1909.

Object of experiment:

Relation between the duration of a stimulating current and the magnitude of the resulting discharge.

Temperature of the organ:

11.0° C.

Resistance of the organ:

130 ohms.

No.	Readings on stimulation-apparatus.		Number of revolutions of registering drum per sec.	1 mm. of oscillogram corresponds to, in 10 <sup>-4</sup> sec.
	Circuit-breaker.	Connection-changer.		
1	64.0 mm.	54.8 mm.	6.60	3.03
2	63.8	„	6.59	3.03
3	63.6	„	6.79	2.95
4	63.4	„	6.94	3.88
5	63.2	„	7.28	2.75
6	63.0	„	7.27	2.75
7	62.8	„	7.66	2.61
8	62.6	„	7.77	2.58

No.	Stimulation breadth		Modal latent period		A.
	in mm.	in 10 <sup>-4</sup> sec.	in mm.	in 10 <sup>-4</sup> sec.	
1	6.0	18.2	40.6	123.0	31.5
2	5.3	16.1	41.0	124.3	30.8
3	4.8	14.2	42.6	125.7	28.3
4	4.5	13.0	44.0	126.7	27.5
5	4.3	11.8	45.6	125.4	25.0
6	4.1	11.3	46.7	128.2	23.3
7	3.5	9.1	49.5	129.5	19.0
8	3.0	7.7	49.5	127.5	12.5

Co-ordinates of the points on the discharge curves for every 2 mm. of  $x$  on the oscillogram.

Curve No. 1.		
$x$ in mm.	$x$ in $10^{-4}$ sec.	$y$ in mm.
0.0	0.0	Beginning of stimulus.
26.0	78.8	0.0
8.0	84.8	1.6
30.0	90.9	4.4
2.0	97.0	9.0
4.0	103.0	15.0
6.0	109.1	22.4
8.0	115.1	29.0
40.0	121.2	31.5
2.0	127.3	30.0
4.0	133.3	25.8
6.0	139.4	20.6
8.0	145.4	15.0
50.0	151.5	10.6
2.0	157.6	7.0
4.0	163.6	4.6
6.0	169.7	2.8
8.0	175.7	2.0
60.0		
Summit of the curve.		
40.6	123.0	31.5

Curve No. 2.		
$x$ in mm.	$x$ in $10^{-4}$ sec.	$y$ in mm.
0.0	0.0	Beginning of stimulus.
27.0	81.8	0.0
8.0	84.8	1.4
30.0	90.9	2.6
2.0	97.0	6.4
4.0	103.0	11.6
6.0	109.1	18.4
8.0	115.1	25.6
40.0	121.2	30.0
2.0	127.3	30.0
4.0	133.3	26.8
6.0	139.4	22.0
8.0	145.4	16.8
50.0	151.5	12.0
2.0	157.6	8.0
4.0	163.6	5.4
6.0	169.7	3.4
8.0	175.7	2.2
60.0	181.8	1.8
Summit of the curve.		
41.0	124.3	30.8

Curve No. 3.		
$x$ in mm.	$x$ in $10^{-4}$ sec.	$y$ in mm.
0.0	0.0	Beginning of stimulus.
28.0	82.6	0.0
30.0	88.5	1.0
2.0	94.4	3.6
4.0	100.3	7.0
6.0	106.2	12.0
8.0	112.1	18.8
40.0	118.0	25.0
2.0	123.9	28.0
4.0	129.8	27.6
6.0	135.7	24.4
8.0	141.6	20.0
50.0	147.5	15.0
2.0	153.4	10.4
4.0	159.3	6.8
6.0	165.2	4.4
8.0	171.1	2.8
60.0	177.0	1.8
Summit of the curve.		
42.6	125.7	28.3

Curve No. 4.		
$x$ in mm.	$x$ in $10^{-4}$ sec.	$y$ in mm.
0.0	0.0	Beginning of stimulus.
29.0	83.5	0.0
32.0	92.2	2.4
4.0	97.9	5.4
6.0	103.7	9.0
8.0	109.4	14.2
40.0	115.2	20.2
2.0	122.0	25.4
4.0	126.7	27.5
6.0	132.5	26.0
8.0	138.2	22.6
50.0	144.0	18.2
2.0	149.8	13.6
4.0	155.5	9.4
6.0	161.3	6.6
8.0	167.0	4.4
60.0	192.8	3.2
2.0	178.6	2.0
Summit of the curve.		
44.0	126.7	27.5

Curve No. 5.		
$x$ in mm.	$x$ in $10^{-4}$ sec.	$y$ in mm.
0.0	0.0	Beginning of stimulus.
30.0	82.3	0.0
2.0	88.0	1.0
4.0	93.5	2.8
6.0	99.0	5.2
8.0	104.5	9.4
40.0	110.0	14.0
2.0	115.5	19.6
4.0	121.0	24.0
6.0	126.5	24.8
8.0	132.0	23.8
50.0	137.5	20.6
2.0	143.0	16.4
4.0	148.5	12.6
6.0	154.0	9.0
8.0	159.5	6.0
60.0	165.0	4.0
2.0	170.5	2.4
4.0	176.0	1.4
Summit of the curve.		
45.6	125.4	25.0

Curve No. 6.		
$x$ in mm.	$x$ in $10^{-4}$ sec.	$y$ in mm.
0.0	0.0	Beginning of stimulus.
30.0	82.3	0.0
2.0	88.0	1.0
4.0	93.5	2.2
6.0	98.0	4.6
8.0	104.5	7.8
40.0	110.0	11.6
2.0	115.5	16.8
4.0	121.0	21.6
6.0	126.5	23.2
8.0	132.0	22.8
50.0	137.5	20.4
2.0	143.0	16.6
4.0	148.5	13.2
6.0	154.0	9.8
8.0	159.5	6.6
60.0	165.0	4.6
2.0	170.5	3.2
4.0	176.0	2.0
Summit of the curve.		
46.7	128.2	23.3

Curve No. 7.		
$x$ in mm.	$x$ in $10^{-4}$ sec.	$y$ in mm.
0 0	0 0	Beginning of stimulus.
33.0	86.1	0.0
4 0	88.7	0.6
6.0	94.0	2.2
8.0	99.2	3.8
40.0	104.4	5.8
2 0	109.6	8.8
4 0	114.8	13.0
6 0	120.1	16.4
8 0	125.3	18.8
50.0	130.5	19.0
2 0	135.7	17.6
4 0	140.9	15.2
6.0	146.2	12.4
8.0	151.4	9.6
60.0	156.6	7.0
2.0	161.8	5.2
4.0	167.0	3.4
6.0	172.3	2.0
Summit of the curve.		
49.5	129.5	19.0

Curve No. 8.		
$x$ in mm.	$x$ in $10^{-4}$ sec.	$y$ in mm.
0 0	0 0	Beginning of stimulus.
35.0	90.3	0.0
6 0	92.9	1.2
8.0	98.0	2.4
40.0	103.2	3.8
2 0	108.4	5.6
4 0	113.5	8.0
6.0	118.7	10.6
8.0	123.0	11.8
50.0	129.0	12.4
2 0	134.2	11.6
4.0	139.3	10.0
6.0	144.5	8.4
8.0	149.6	6.4
60.0	154.8	4.8
2.0	160.0	3.2
4.0	165.1	2.0
Summit of the curve.		
49.5	127.5	12.5

From the values given in the above tables, the curves from No. 1 to No. 8 were reproduced on section papers in the exactly same way as in No. 54. These curves are shown in Plate VII. On these curves  $x_1$  and  $x_2$  for several values of  $y$  were measured. Then the mean of  $\sqrt{x_1 x_2}$  for every curve was found and compared with the value of the modal latent period observed. The units of  $x_1$ ,  $x_2$  and  $y$  are one division of the section paper. Using the mean of  $\sqrt{x_1 x_2}$  as the value of  $x_0$  we calculated  $b^2$ .

No.	$y$ .	$x_1$ .	$x_2$ .	$\sqrt{x_1 x_2}$ .	$y'$ .	$x_1'$ .	$x_2'$ .	$\sqrt{x_1' x_2'}$ .	$y''$ .	$x_1''$ .	$x_2''$ .	$\sqrt{x_1'' x_2''}$ .
1	11.6	50.0	74.9	61.1	6.0	46.6	79.8	61.0	21.0	53.7	69.4	61.0
2	11.4	51.4	75.8	62.4	6.0	48.0	80.7	62.2	20.0	55.2	70.4	62.4
3	10.4	52.4	76.7	63.4	5.0	48.5	81.7	63.0	19.0	56.3	71.3	63.5
4	10.1	52.3	77.1	63.6	5.0	48.8	82.7	63.5	19.0	57.0	71.5	63.9
5	9.2	52.2	76.8	63.4	5.0	49.0	81.0	63.0	17.0	56.3	71.3	63.5
6	8.6	52.7	77.7	64.0	4.0	49.0	83.6	64.0	15.0	56.8	72.8	64.3
7	7.0	53.4	78.5	64.8	4.0	50.0	82.9	64.4	13.0	57.5	72.7	64.6
8	4.6	52.8	77.5	64.0	2.0	48.2	82.5	(63.1)	8.0	56.6	72.6	64.1

The number in the bracket was not taken in the calculation of the mean.

No.	Mean of $\sqrt{x_1 x_2}$ .	$x_0$ thus found, in $10^{-1}$ sec.	$b^2$ .
1	61.0	122.0	23.7
2	62.3	124.6	25.8
3	63.3	126.6	27.1
4	63.7	127.4	27.4
5	63.3	126.6	26.1
6	64.1	128.2	27.0
7	64.6	129.2	26.3
8	64.1	128.2	27.8

By using the constants given in the above tables, the ordinates of the curves for every 1/1000 sec. were calculated. These values are shown in the next table.

$x$ in $10^{-4}$ sec.	$y$ in mm. (calculated).							
	No. 1.	No. 2.	No. 3.	No. 4.	No. 5.	No. 6.	No. 7.	No. 8.
0.0	0.0	0.0	0.0	0.0	0.0	0.0	0.0	0.0
70.0	0.0 <sub>2</sub>	0.0	0.0	0.0	0.0	0.0	0.0	0.0
80.0	0.5	0.2	0.2	0.1	0.1	0.1	0.1	0.0 <sub>3</sub>
90.0	3.5	2.0	1.2	1.0	1.1	0.8	0.7	0.4
100.0	12.5	9.2	6.4	5.6	5.8	4.5	3.5	2.3
110.0	24.5	20.6	16.6	15.3	14.8	12.4	9.6	6.5
120.0	31.3	29.7	26.2	24.3	23.2	20.7	16.4	11.1
130.0	28.6	29.4	27.8	27.2	24.5	23.2	18.8	12.4
140.0	20.1	21.7	21.5	21.5	19.1	18.9	16.0	10.1
150.0	11.5	12.9	13.0	13.2	11.6	12.0	10.6	6.3
160.0	5.5	6.1	6.4	6.8	5.8	6.2	5.7	3.2
170.0	2.3	2.6	2.7	2.8	2.5	2.9	2.6	1.4
180.0	0.8	0.9	1.0	1.0	0.7	1.0	1.1	0.5
190.0	0.2	0.3	0.3	0.3	0.3	0.0 <sub>3</sub>	0.4	0.2
200.0	0.0	0.1	0.1	0.2	0.1	0.0	0.1	0.1



TABLE III.

Oscillogram No. 40.

Date of experiment:

Nov. 24, 1909.

Object of experiment:

The relation between the duration of a stimulating current and the magnitude of the discharge.

Temperature of the organ:

11.5° C

Resistance of the organ:

—

Current of the primary of the induction coil:

3.5 amperes.

No.	Readings on stimulation-apparatus.		Number of revolutions of registering drum per sec.	1 mm. on oscillogram corresponds to, in $10^{-4}$ sec.
	Circuit-breaker.	Connection-changer.		
1	65.0 mm.	54.8 mm.	7.00	2.86
2	64.2	"	6.93	2.88
3	63.8	"	6.77	2.96
4	63.6	"	6.99	2.86
5	63.4	"	6.67	3.00
6	63.2	"	6.67	3.00
7	63.0	"	6.99	2.86
8	62.8	"	7.05	2.84

No.	Stimulation-breadth		Modal latent period		A.
	in mm.	in $10^{-4}$ sec.	in mm.	in $10^{-4}$ sec.	
1	9.8	28.0	42.5	121	44.5
2	6.4	18.4	41.4	119	41.0
3	6.7	19.8	40.7	120	40.0
4	6.1	17.4	42.2	120	39.0
5	6.4	19.2	40.7	122	39.0
6	5.0	15.0	40.8	122	33.5
7	5.0	14.3	42.5	122	35.6
8	4.1	11.6	43.0	122	29.5

Co-ordinates of the points on the discharge curves for every  
2 mm. of  $x$  on the oscillogram.

Curve No. 1.		
$x$ in mm.	$x$ in $10^{-4}$ sec.	$y$ in mm.
0.0	0.0	Beginning of stimulus.
18.7	53.5	0.0
19.7	56.3	0.0
21.7	62.1	0.3
3.7	67.8	1.0
5.7	73.5	1.4
7.7	79.2	2.3
9.7	84.9	4.4
31.7	90.7	8.5
3.7	96.4	16.5
5.7	102.1	25.1
7.7	107.8	34.1
9.7	113.5	41.0
41.7	119.3	44.3
3.7	125.0	43.6
5.7	130.7	49.8
7.7	136.4	34.0
9.7	142.1	27.6
51.7	147.9	21.0
3.7	153.6	15.6
5.7	159.3	11.3
7.7	165.0	8.1
9.7	170.7	5.9
61.7	176.5	4.4
3.7	182.2	3.6
5.7	187.9	3.4
7.7	193.6	3.6
9.7	199.3	4.2
71.7	205.1	4.7
Summit of the curve.		
42.5	121.2	44.5

Curve No. 2.		
$x$ in mm.	$x$ in $10^{-4}$ sec.	$y$ in mm.
0.0	0.0	Beginning of stimulus.
22.0	63.4	0.0
26.0	74.9	0.9
8.0	80.6	3.1
30.0	86.4	6.0
2.0	92.2	10.9
4.0	97.9	18.5
6.0	103.7	26.5
8.0	109.4	35.0
40.0	115.2	39.6
2.0	121.0	40.9
4.0	126.7	38.0
6.0	132.5	32.9
8.0	138.2	26.3
50.0	144.0	20.1
2.0	149.8	14.6
4.0	155.5	10.6
6.0	161.3	7.5
8.0	167.0	5.5
60.0	172.8	4.0
2.0	178.6	3.2
Summit of the curve.		
41.4	119.0	41.0

Curve No. 3.		
$x$ in mm.	$x$ in $10^{-4}$ sec.	$y$ in mm.
0.0	0.0	Beginning of stimulus.
23.5	69.6	0.0
5.5	75.5	1.9
7.5	81.4	2.7
9.5	87.3	6.0
31.5	93.2	11.1
3.5	99.1	18.3
5.5	105.1	27.1
7.5	111.0	35.5
9.5	116.9	39.2
41.5	122.8	39.8
3.5	128.8	36.6
5.5	134.7	31.3
7.5	140.6	24.3
9.5	146.5	17.9
51.5	152.4	12.7
3.5	158.4	8.9
5.5	164.3	6.2
7.5	170.2	4.5
9.5	176.1	3.5
Summit of the curve.		
40.7	120.5	40.0

Curve No. 4.		
$x$ in mm.	$x$ in $10^{-4}$ sec.	$y$ in mm.
0.0	0.0	Beginning of stimulus.
23.9	68.4	0.0
5.9	74.1	1.2
7.9	79.8	2.4
9.9	85.5	4.3
31.9	91.3	8.2
3.9	97.0	14.0
5.9	102.7	21.8
7.9	108.4	29.8
9.9	114.1	36.0
41.9	119.8	39.0
3.9	125.4	37.4
5.9	131.3	33.0
7.9	137.0	27.4
9.9	143.0	21.4
51.9	148.4	15.4
3.9	154.2	11.1
5.9	159.9	7.2
7.9	165.6	5.0
9.9	171.3	3.6
61.9	177.0	2.6
Summit of the curve.		
42.2	120.7	39.0

Curve No. 5.		
$x$ in mm.	$x$ in $10^{-4}$ sec.	$y$ in mm.
0.0	0.0	Beginning of stimulus.
21.1	63.3	0.0
4.1	72.3	0.8
6.1	78.3	1.4
8.1	84.3	2.8
30.1	90.3	6.0
2.1	96.3	11.8
4.1	102.3	18.8
6.1	108.3	27.8
8.1	114.3	34.7
40.1	120.3	38.9
2.1	126.3	38.5
4.1	132.3	34.8
6.1	138.3	28.2
8.1	144.3	21.5
50.1	150.3	15.5
2.1	156.3	10.7
4.1	162.3	6.3
6.1	168.3	4.8
8.1	174.3	3.3
60.1	180.3	3.8
Summit of the curve.		
40.8	122.4	39.0

Curve No. 6.		
$x$ in mm.	$x$ in $10^{-4}$ sec.	$y$ in mm.
0.0	0.0	Beginning of stimulus.
25.0	75.0	0.0
7.0	81.0	1.7
9.0	87.0	3.9
31.0	93.0	6.3
3.0	99.0	11.5
5.0	105.0	17.9
7.0	111.0	25.8
9.0	117.0	31.7
41.0	123.0	33.5
3.0	129.0	31.9
5.0	135.0	27.1
7.0	141.0	21.9
9.0	147.0	15.2
51.0	153.0	11.3
3.0	159.0	7.9
5.0	165.0	5.3
7.0	171.0	3.7
9.0	177.0	2.7
61.0	183.0	2.7
Summit of the curve.		
40.8	122.4	33.5

Curve No. 7.		
$x$ in mm.	$x$ in $10^{-4}$ sec.	$y$ in mm.
0.0	0.0	Beginning of stimulus.
24.1	68.9	0.0
6.1	74.6	0.0
8.1	80.4	1.4
30.1	86.1	4.4
2.1	91.8	6.1
4.1	97.5	11.3
6.1	103.2	18.2
8.1	109.0	26.5
40.1	114.7	32.3
2.1	120.4	35.3
4.1	126.1	34.5
6.1	131.8	31.0
8.1	137.6	25.5
50.1	143.3	19.8
2.1	149.0	14.8
4.1	154.7	10.0
6.1	160.4	6.5
8.1	166.2	4.3
60.1	171.9	3.5
Summit of the curve.		
42.5	122.0	35.6

Curve No. 8.		
$x$ in mm.	$x$ in $10^{-4}$ sec.	$y$ in mm.
0.0	0.0	Beginning of stimulus.
26.5	75.3	0.0
8.5	80.9	1.6
30.5	86.6	2.2
2.5	92.3	4.7
4.5	98.0	8.8
6.5	103.7	14.2
8.5	109.3	20.6
40.5	115.0	26.2
2.5	120.7	29.5
4.5	126.4	28.0
6.5	132.1	25.0
8.5	137.7	20.5
50.5	143.4	16.0
2.5	149.1	12.0
4.5	154.8	8.5
6.5	160.5	6.0
8.5	166.1	4.0
60.5	171.8	2.6
2.5	177.5	1.8
Summit of the curve.		
43.0	122.2	29.5

From the values given in the above tables, the curves No. 1—No. 8 were reproduced on section papers in the same way as in No. 37. These curves are shown in Plate VIII. In these curves,  $x_1, x_2$  for several values of  $y$  were measured. Then the mean of  $\sqrt{x_1x_2}$  for every curve was found and compared with the observed value of the modal latent period. The unit of  $x$  and of  $y$  are one division of the section paper. Using the mean of  $\sqrt{x_1x_2}$  as the value of  $x_0$ , we calculated  $b_2$ .

No.	$y$ .	$x_1$ .	$x_2$ .	$\sqrt{x_1x_2}$ .	$y'$ .	$x_1'$ .	$x_2'$ .	$\sqrt{x_1'x_2'}$ .	Mean of $\sqrt{x_1x_2}$ .	$x_0$ thus found in $10^{-4}$ sec.	$b^2$ .
1	16.3	48.3	76.1	60.6	8.2	45.1	82.5	61.0	60.8	121.6	20.0
2	15.0	47.9	74.5	59.5	7.5	44.4	80.7	59.5	59.5	119.6	20.8
3	14.6	48.3	75.1	60.2	7.3	44.4	81.0	60.2	60.2	120.4	20.6
4	14.2	48.5	75.0	60.3	7.1	44.3	80.8	59.8	60.1	120.2	20.4
5	14.3	49.5	75.7	61.2	7.2	45.9	80.8	60.9	61.1	122.2	21.8
6	12.3	50.0	75.6	61.5	6.2	46.0	81.7	61.3	61.4	122.8	23.2
7	13.0	49.5	75.5	61.1	6.5	46.0	80.4	60.8	61.0	122.0	22.2
8	10.7	49.6	75.4	61.2	5.4	45.8	81.0	61.0	61.1	123.4	22.9

From the constants given in the above tables, the ordinates of the curves for every 1/1000 sec. were calculated. These values are shown in the next table.

$x$ in $10^{-4}$ sec.	$y$ in mm. (calculated).							
	No. 1.	No. 2.	No. 3.	No. 4.	No. 3.	No. 6.	No. 7.	No. 8.
0.0	Beginning of stimulus.							
60.0	0.0	0.0	0.0	0.0	0.0	0.0	0.0	0.0
70.0	0.1	0.1	0.1	0.1	0.0 <sub>4</sub>	0.0 <sub>2</sub>	0.0 <sub>4</sub>	0.0 <sub>2</sub>
80.0	1.4	1.4	1.3	1.3	0.8	0.5	0.7	0.5
90.0	7.3	7.6	7.0	7.0	5.1	3.6	4.6	3.6
100.0	21.0	21.3	19.9	19.6	16.4	12.8	15.0	11.9
110.0	36.4	35.5	33.8	32.9	30.7	25.3	28.1	22.9
120.0	44.4	41.0	40.0	38.6	38.7	33.1	35.4	29.3
130.0	40.7	35.5	35.4	33.7	35.9	31.0	31.8	27.0
140.0	29.9	24.5	25.0	24.0	26.0	22.5	23.4	19.3
150.0	18.5	14.1	14.8	14.2	15.5	13.2	13.8	11.2
160.0	9.9	7.0	7.5	7.3	8.0	6.6	7.0	5.6
170.0	5.3	3.1	3.4	3.3	3.6	2.7	3.1	2.4
180.0	2.1	1.3	1.4	1.4	1.5	1.1	1.2	0.9
190.0	0.8	0.5	0.5	0.5	0.6	0.5	0.5	0.3
200.0	0.3	0.2	0.2	0.2	0.3	0.1	0.2	0.1

TABLE IV.

Oscillogram No. 54, curve No. 7 and its residual curve.

$y=44.8\ e^{-4.49\ log^2\ \frac{x-32.8}{51.8}},$

$y_0=44.8\ e^{-21.3\ log^2\ \frac{x}{106.6}},$

$y=10.0\ e^{-17.2\ log^2\ \frac{x}{100.8}},$

$x$ in $10^{-4}$ sec.	$y$ in mm.	$y_0$ in mm.	$y-y_0$ in mm.
106.0	44.6	44.8	0.2
112.0	43.6	42.2	1.4
6.0	41.0	37.6	3.4
120.0	37.3	31.9	5.4
4.0	33.0	25.8	7.2
8.0	28.6	19.9	8.7
132.0	24.4	14.8	9.6
6.0	20.6	10.7	9.9
140.0	17.1	7.4	9.7
4.0	14.0	5.0	9.0
8.0	11.5	3.3	8.2
152.0	9.3	2.1	7.2
6.0	7.5	1.3	6.2
160.0	6.0	0.8	5.2
4.0	4.8	0.5	4.3
8.0	3.8	0.3	3.5
172.0	3.0	0.2	2.8
6.0	2.4	0.1	2.3
180.0	1.8	0.0 <sub>6</sub>	1.7
4.0	1.5	0.0 <sub>3</sub>	1.5
8.0	1.2	0.0 <sub>1</sub>	1.2
192.0	0.9	0.0 <sub>0</sub>	0.9

$x$ in $10^{-4}$ sec.	$y$ in mm.
0.0	0.0
70.0	0.9
80.0	4.0
90.9	8.1
100.0	10.0
110.0	8.8
120.0	5.9
130.0	3.3
140.0	1.6
150.0	0.7
160.0	0.3

TABLE V.

Oscillogram No. C. 3.

Date of experiment:	May 13, 1910.
Preparation:	About a quarter of the organ with one nerve-trunk.
Temperature of the organ:	10.5° C.
Stimulus:	Indirect momentary stimulus.
One millimetre on the film corresponds to:	1.64×10 <sup>-4</sup> sec.



Co-ordinates of the points on the discharge curve for every 2 mm. of  $x$  on the oscillogram.

$x$ in mm.	$x$ in $10^{-4}$ sec.	$y$ in mm.
0.0	0.0	Beginning of stimulus.
78.0	128.0	0.0
82.0	134.5	2.4
4.0	137.9	5.4
6.0	141.1	10.4
8.0	144.4	19.4
90.0	147.6	29.0
2.0	151.0	39.0
4.0	154.2	47.0
6.0	157.5	52.4
8.0	160.8	55.0
100.0	164.0	55.0
2.0	167.3	53.6
4.0	170.6	50.8
6.0	173.8	47.0
8.0	177.1	42.8
10.0	180.4	38.4
2.0	183.7	33.8
4.0	187.0	29.0
6.0	190.2	24.6
8.0	193.5	20.4
20.0	196.9	16.8
2.0	200.0	13.4
4.0	203.4	11.0
6.0	206.6	8.6
8.0	210.0	6.8
30.0	213.2	5.6
2.0	216.4	4.4
4.0	219.8	3.4
6.0	223.0	2.4
8.0	226.4	2.0
40.0	229.6	1.4
148.0	242.8	0.0
Summit of the curve.		
99.0	162.3	55.4

The values of the ordinates for every  $\frac{1}{1000}$  sec., calculated by the formula

$$y = 55.4 e^{-5.83 \log^2 \frac{x}{57.6 \times 10^{-4}}}$$

$x$ in $10^{-4}$ sec.	$y$ in mm.
0.0	0.0
30.0	4.3
40.0	25.5
50.0	49.3
60.0	54.9
70.0	44.4
80.0	29.5
90.0	17.3
100.0	9.3
110.0	4.8
120.0	2.4
130.0	1.2
140.0	0.6

$$\delta = +0.84.$$

Tables VI.—VIII. are those for the relation between the breadth of the stimulus and the height of the resulting discharge. AC' *et seq.* written on the heads of the columns of the breadth of the stimulus are referred to the accompanying figure.

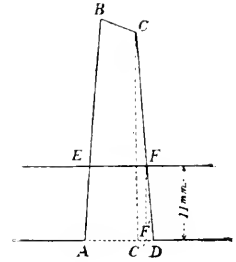


TABLE VI.

Oscillogram No. 37.

Date of experiment:

Oct. 23, 1909.

Preparation:

A whole organ (the same preparation as that of No. 35 and No. 36.).

Temperature of the organ:

11.0° C.

The formula employed in calculation:

$$y = 34.0 \{ 1 - 10^{-(0.1862(x-5.1))} \}.$$

No.	Reading of position of C, B. in mm.	Reading of position of C, Ch. in mm.	Breadth of stimulus (AC') in mm.	Number of revolutions per sec.	1 mm. on film corresponds to, in 10 <sup>-4</sup> sec.
1	64.0	54.8	6.0	6.60	3.03
2	63.8	..	5.3	6.59	3.03
3	63.6	..	4.8	6.79	2.95
4	63.4	..	4.5	6.94	2.88
5	63.2	..	4.3	7.28	2.75
6	63.0	..	4.1	7.27	2.75
7	62.8	..	3.5	7.66	2.61
8	62.6	..	3.0	7.74	2.58

No.	Height of stimulus in mm.	Breadth of stimulus in 10 <sup>-4</sup> sec.	Height of discharge in mm.	Height of discharge calculated by formula.	Difference.
1	45.5	18.2	31.5	31.5	0.0
2	45.5	16.1	30.8	30.2	+0.6
3	46.0	14.2	28.3	28.4	-0.1
4	46.5	13.0	27.5	26.9	+0.6
5	46.3	11.8	25.0	25.0	0.0
6	46.0	11.3	23.3	24.1	-0.8
7	46.3	9.1 <sub>4</sub>	19.0	18.8	+0.2
8	45.6	7.7 <sub>4</sub>	12.5	13.9	-1.4



## No. 41.

No.	Reading of position of C. B. in mm.	Reading of position of C. Ch. in mm.	Breadth of stimulus (AB) in mm.	Number of revolutions per sec.	1 mm. on film corresponds to, in $10^{-4}$ sec.
1	62.8	54.8	4.2	6.05	3.31
2	63.0	„	4.0	6.12	3.27
3	63.2	„	4.8	6.12	3.27
4	63.4	„	5.5	6.47	3.08
5	63.6	„	6.0	6.38	3.14
6	63.8	„	5.3	6.08	3.29
7	64.2	„	7.2	6.25	3.20
8	65.0	„	7.1	6.35	3.16

No.	Height of stimulus in mm.	Breadth of stimulus in $10^{-4}$ sec.	Height of discharge in mm.	Height of discharge reduced to Stn. 44.5, in mm.	Height of discharge calculated, in mm.	Difference.
1	45.0	13.9	36.5	35.9	35.0	+0.9
2	44.5	13.1	33.7	33.7	33.6	+0.1
3	45.0	15.7	36.6	36.0	35.9	+0.1
4	45.5	17.0	38.0	36.7	36.6	+0.1
5	45.0	18.8	37.0	36.4	37.4	-1.0
6	45.0	17.5	39.2	38.6	36.0	+2.6
7	44.8	23.0	39.0	38.6	38.7	-0.1
8	45.0	22.4	39.0	38.4	37.9	+0.5

TABLE VIII.

Oscillograms No. 59, No. 60 and No. 61.

Date of experiment: Nov. 10, 1909.

Preparation: Left organ (whole).

Temperature of the organ: 13.5°

Resistance of the organ: About 200 ohms.

Current in primary:

No. 59: 3 amperes.

No. 60: 4 „ „.

No. 61: 5 „ „.

Formula employed:

No. 59  $y = 21.3 \times 10^{-n \cdot 0.0573} \{1 - 10^{-0.0569(t-2)}\}$ ,No. 60  $y = 32.1 \times 10^{-n \cdot 0.121} \{1 - 10^{-0.0935(t-2)}\}$ ,No. 61  $y = 38.8 \times 10^{-n \cdot 0.0319} \{1 - 10^{-0.0623(t-2)}\}$ .

No. 59.

No.	Reading of position of C. B. in mm.	Reading of position of C. Ch. in mm.	Breadth of stimulus (AF) in mm.	Number of revolutions per sec.	1 mm. on film corresponds to, in 10 <sup>-4</sup> sec.	Height of stimulus in mm.
1	62.0	62.0	8.2	6.00	3.33	38.0
2	61.0	„	6.1	6.28	3.18	37.5
3	60.8	„	5.4	5.46	3.66	37.2
4	60.6	„	5.5	5.70	3.51	37.9
5	60.4	„	4.9	5.87	3.41	38.1
6	60.2	„	4.3	5.77	3.46	37.5
7	60.0	„	2.3	5.67	3.53	32.8
8	62.0	„	8.2	5.98	3.34	37.5

No.	Breadth of stimulus in 10 <sup>-4</sup> sec.	Height of discharge in mm.	Height of discharge reduced to Stm. 37.5, in mm.	Height of discharge calculated, in mm.	Difference.	Height of discharge calculated by neglecting fatigue factor.
1	27.3	21.0	20.5	20.5	0.0	20.5
2	19.4	19.5	19.5	18.9	+0.6	19.0
3	19.8	19.0	19.3	18.8	+0.5	19.1
4	19.3	18.5	18.1	18.5	-0.4	19.0
5	16.7	18.0	17.4	17.5	-0.1	18.1
6	14.9	17.0	17.0	16.5	+0.5	17.3
7	8.1	6.3	11.0	11.0	0.0	11.6
8	27.4	19.3	19.3	19.3	0.0	20.5

## No. 60.

No.	Reading of position of B. C. in mm.	Reading of position of C. Ch. in mm.	Breadth of stimulus (AC) in mm.	Number of revolutions per sec.	1 mm. on film corresponds to, in 10 <sup>-4</sup> sec.	Height of stimulus in mm.
1	62.0	62.0	11.9	9.00	2.22	50.0
2	61.0	,,	9.7	8.83	2.27	50.0
3	60.8	,,	8.5	8.91	2.24	50.5
4	60.6	,,	8.1	9.40	2.13	50.0
5	60.4	,,	—	8.89	2.25	—
6	60.2	,,	8.0	9.33	2.14	50.8
7	60.0	,,	6.4	—	—	50.0
8	62.0	,,	11.7	8.61	2.32	50.0

No.	Breadth of stimulus in 10 <sup>-4</sup> sec.	Height of discharge in mm.	Height of discharge reduced to Stm. 50.0, in mm.	Height of discharge calculated in mm.	Difference.	Height of discharge calculated by neglecting fatigue factor
1	26.4	32.0	32.0	32.0	0.0	32.0
2	22.0	30.8	30.8	31.0	-0.2	31.9
3	19.0	30.2	29.7	30.0	-0.3	31.7
4	17.3	29.0	29.0	29.0	0.0	31.5
5	—	—	—	—	—	—
6	17.1	28.3	27.5	27.4	+0.1	37.4
7	14.8	26.0	26.0	26.2	-0.2	31.0
8	27.1	26.3	26.3	26.4	-0.1	32.0

## No. 61.

No.	Reading of position of C. B. in mm.	Reading of position of C. Ch. in mm.	Breadth of stimulus (AF) in mm.	Number of revolutions per. sec.	1 mm. on film corresponds to, in 10 <sup>-4</sup> sec.	Height of stimulus in mm.
1	62.0	62.0	12.6	8.59	2.33	Could not be measured.
2	61.0	„	9.5	8.96	2.23	
3	60.8	„	8.7	8.74	2.29	
4	60.6	„	8.8	9.73	2.06	
5	60.4	„	—	9.35	2.14	
6	60.2	„	7.9	9.67	2.07	
7	60.0	„	7.1	10.25	1.95	
8	62.0	„	12.7	9.84	2.03	

No.	Breadth of stimulus in 10 <sup>-4</sup> sec.	Height of discharge in mm.	Height of discharge calculated in mm.	Difference.	Height of discharge calculated by neglecting fatigue factor.
1	29.4	38.0	38.0	0.0	38.0
2	21.2	36.9	36.1	+0.8	36.4
3	19.9	36.0	35.4	+0.6	35.9
4	18.1	34.6	34.3	+0.3	35.0
5	—	—	—	—	—
6	16.4	32.0	32.8	-0.8	33.9
7	13.8	30.4	30.4	0.0	32.1
8	25.8	36.0	35.6	+0.4	37.4

TABLE IX.

Oscillograms No. 74—75.

Date of experiment:

Nov. 17, 1909.

Preparation:

A quater of an organ with one nerve-trunk.

Temperature of the organ:

14.5°.

No.	Distance betw. two contacts on stimulation- apparatus in mm.	Number of revolutions per sec.	1 mm. on film corre- sponds to, in 10 <sup>-4</sup> sec.	Interval between two stimuli in mm.	Interval between two stimuli. in 10 <sup>-4</sup> sec.	M. L. P. of first Disch. in mm.	M. L. P. of second Disch. in mm.
1	26.0	5.98	3.35	36.0	120.5	31.5	31.5
2	24.0	6.06	3.30	33.5	110.4	32.0	32.5
3	22.0	6.18	3.24	30.7	99.5	32.5	33.5
4	20.0	6.22	3.22	28.0	90.2	33.5	34.3
5	18.0	5.84	3.43	23.3	79.9	31.0	33.0
6	16.0	6.05	3.31	21.9	72.5	32.5	35.7
7	14.0	6.17	3.24	19.5	63.2	33.0	37.0
8	12.0	6.11	3.28	17.0	55.8	33.5	39.4
9	10.0	6.34	3.16	13.9	43.9	33.0	43.0
10	8.0	6.57	3.05	11.0	33.6	34.0	48.0
11	6.0	6.62	3.02	11.5	34.7	34.0	48.0
12	4.0	6.58	3.04	9.0	27.4	34.0	—
13	2.0	6.71	2.98	5.0	14.9	34.0	—
14	1.0	6.60	3.04	3.0	9.1	34.5	—
15	0.5	6.67	3.00	1.0	3.0	35.0	—
16	0.2	6.92	2.90	Coincide.	0.0	35.5	—

No.	Ratio of two M. L. P.	Interval between first Sum. and second discharge. in mm.	Ditto in 10 <sup>-4</sup> sec.	Height of first Disch. in mm.	Height of second Disch. in mm.	Ratio of two heights.
1	1.000	67.5	226	53.0	39.0	0.736
2	1.015	66.5	214	51.5	41.5	0.806
3	1.030	64.2	208	48.5	45.5	0.989
4	1.023	62.3	201	48.0	49.0	1.020
5	1.063	56.3	193	47.0	48.5	1.030
6	1.100	57.6	191	46.0	46.7	1.015
7	1.120	56.5	183	46.0	45.5	0.990
8	1.175	56.4	185	45.0	42.0	0.935
9	1.301	56.9	180	45.0	24.7	0.550
10	1.411	59.0	180	43.3	4.5	0.104
11	1.411	59.5	180	41.5	4.5	0.109
12	—	—	—	42.5	?	?
13	—	—	—	41.8	?	?
14	—	—	—	41.2	—	—
15	—	—	—	42.5	—	—
16	—	—	—	41.5	—	—



TABLE X.

Oscillogram No. 65.

Date of experiment:

Nov. 10, 1909.

Preparation:

Part of an organ with one nerve-trunk.

Temperature of the organ:

13.5° C.

Stimulus:

Ascending.

No.	Distance betw. two contacts on stimulation-apparatus in mm.	Number of revolutions per sec.	1 mm. on film corresponds to, in 10 <sup>-4</sup> sec.	Interval between two stimuli in mm.	Interval between two stimuli in 10 <sup>-4</sup> sec.	M. L. P. of first Disch. in mm.	M. L. P. of second Disch. in mm.
1	26.0	6.34	3.16	42.0	133	38.0	68.0
2	24.0	6.57	3.04	—	—	39.6	—
3	22.0	6.55	3.05	36.0	110	40.0	39.0
4	20.0	6.20	3.22	30.0	97	38.0	39.0
5	18.0	6.27	3.19	27.6	88	38.0	43.0
6	16.0	6.36	3.14	—	—	37.5	—
7	14.0	6.47	3.09	22.2	69	39.0	48.0
8	12.0	6.55	3.06	19.6	60	39.0	50.8
9	10.0	6.54	3.06	16.0	49	39.0	56.0

No.	Ratio of two M. L. P.	Interval between 1st Stim. and 2nd Disch. in mm.	Ditto in 10 <sup>-4</sup> sec.	Height of first Disch. in mm.	Height of second Disch. in mm.	Ratio of two heights.
1	1.790	110.0	348	24.5	9.0	0.367
2	—	74.4	226	22.6	17.8	0.788
3	0.975	75.0	236	21.5	19.0	0.885
4	1.025	69.0	222	21.0	19.0	0.925
5	1.130	70.6	225	20.3	18.0	0.900
6	—	71.0	222	20.0	15.0	0.750
7	1.230	70.2	217	19.5	16.0	0.820
8	1.300	70.4	215	19.9	11.0	0.553
9	1.480	72.0	220	18.8	3.9	0.207



K. FUJI.

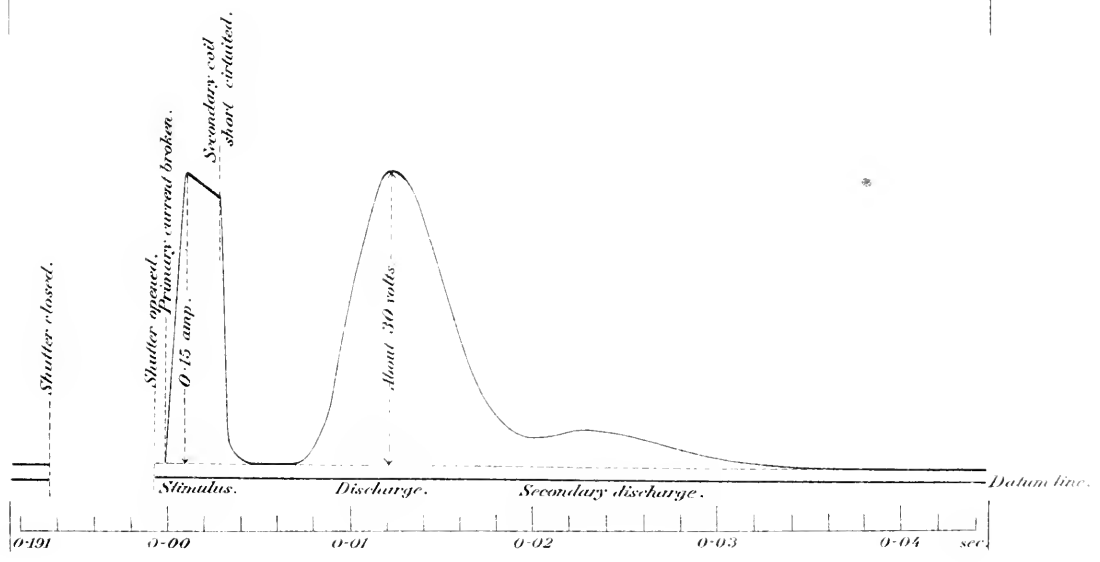
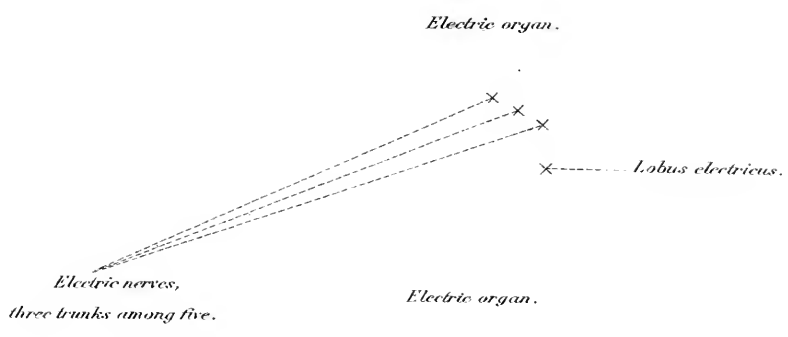
RESEARCHES ON THE ELECTRIC DISCHARGE OF THE ISOLATED ELECTRIC ORGAN  
OF *ASTRAPE* BY MEANS OF OSCILLOGRAPH.

PLATES.

- |       |       |                          |
|-------|-------|--------------------------|
| I.    | III., | Photographs.             |
| IV.   | V.,   | Drawings of instruments. |
| VI.   | XII., | Curves.                  |
| XIII. | XXX., | Oscillograms.            |

### Abbreviations used in Plates.

Stim. or Stim.:	Stimulus.
Resp.:	Response.
C. Stim.:	Closing-stimulus.
O. Stim.:	Opening-stimulus.
E. T.:	Equivalent time <i>i. e.</i> time interval corresponding 1 mm. of abscissa on oscillogram.
$S_{m,1}S_{m,2}S_m$ :	All these abbreviations represent "Stimulus." Figures in suffix show the order of experiment with respect to time. Where two successive stimuli were used, ${}_1S_m$ represents the predecessor in those of the <i>m</i> th experiment, and ${}_2S_m$ the successor in the same set.
$R_{m,1}R_{m,2}R_m$ :	All these abbreviations represent "Response." The numbers in prefix and suffix show the correspondence of the response to the stimulus having the same respective affixes.
2ry D.:	Secondary discharge.
3ry D.:	Tertiary discharge.



Exposition 1889

1889

1889

1889

1889

1889

1889

1889

1889

1889

1889

1889

1889

1889

1889

1889

1889

1889

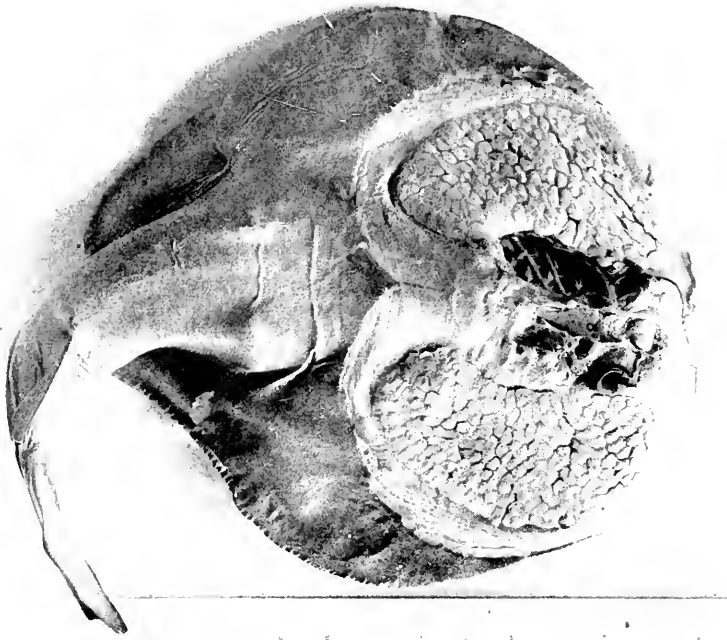
1889

1889

1889

Fig. 1.

*Astrape japonica*.



Anterior part of the skin has been removed to show the electric organs and the electric nerves.

Fig. 2.

A direct stimulus and the resulting discharge.



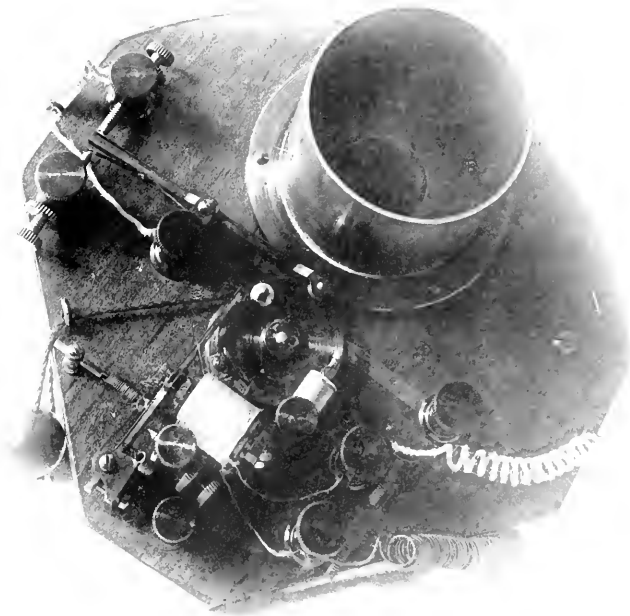




Shutter.

Front view

Fig. 1.



Back view.

Fig. 2.

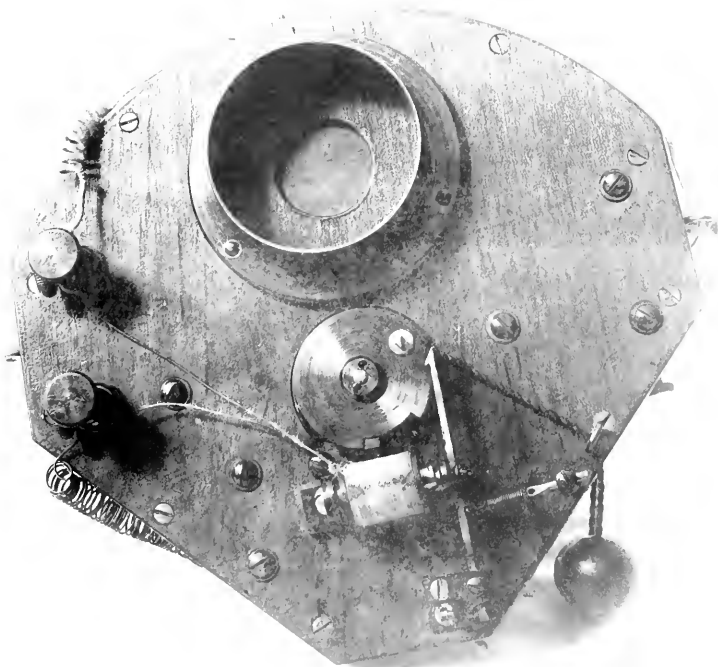




Fig. 1. Registering apparatus (cover removed).

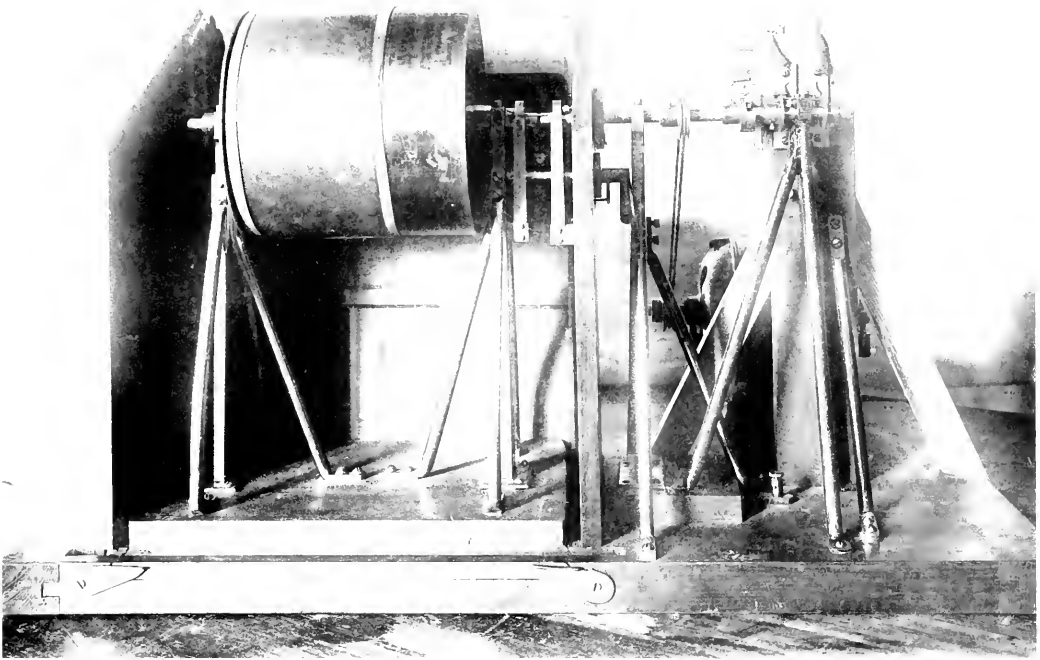
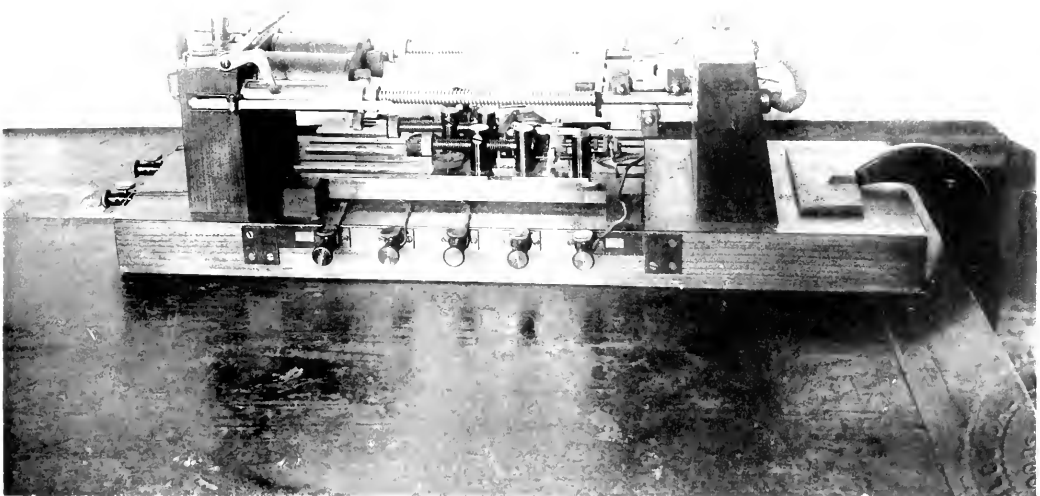


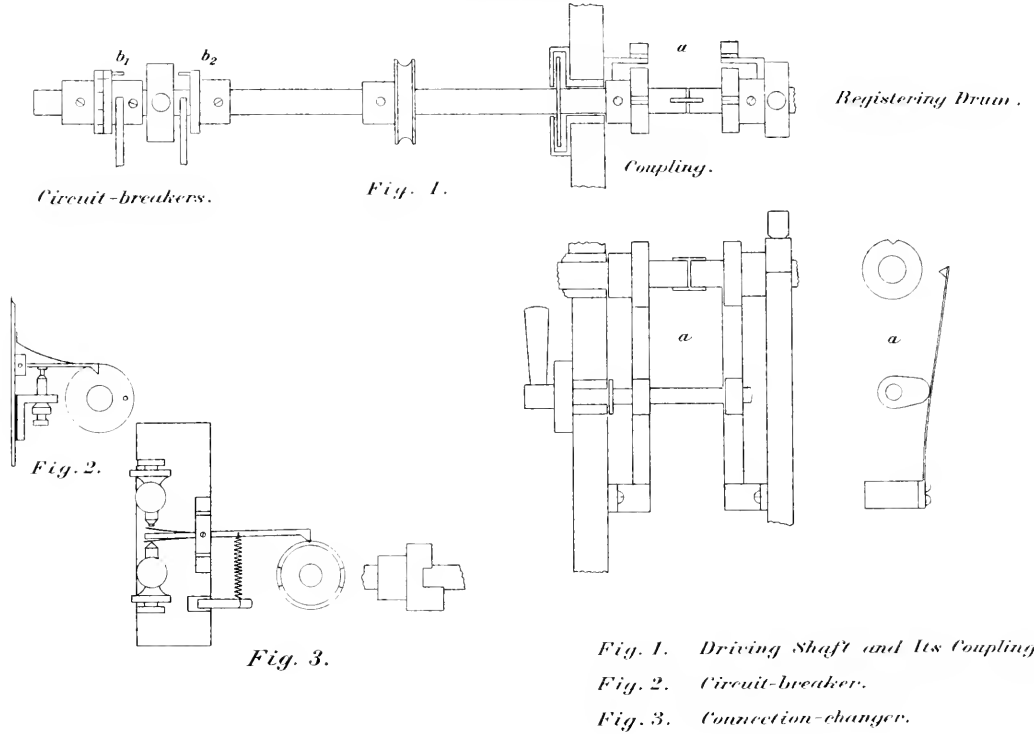
Fig. 2. Stimulation-apparatus clamped to a table.



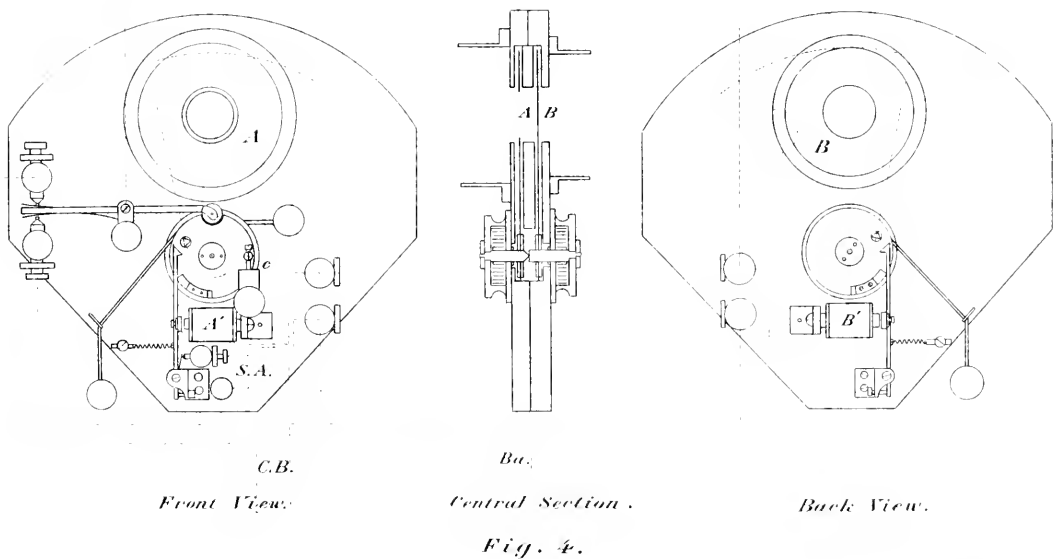


*Driving Shaft of the Registering Drum and Its Accessories.*

( $\frac{2}{5}$  Actual Size.)



*Shutter. ( $\frac{2}{5}$  Actual Size.)*



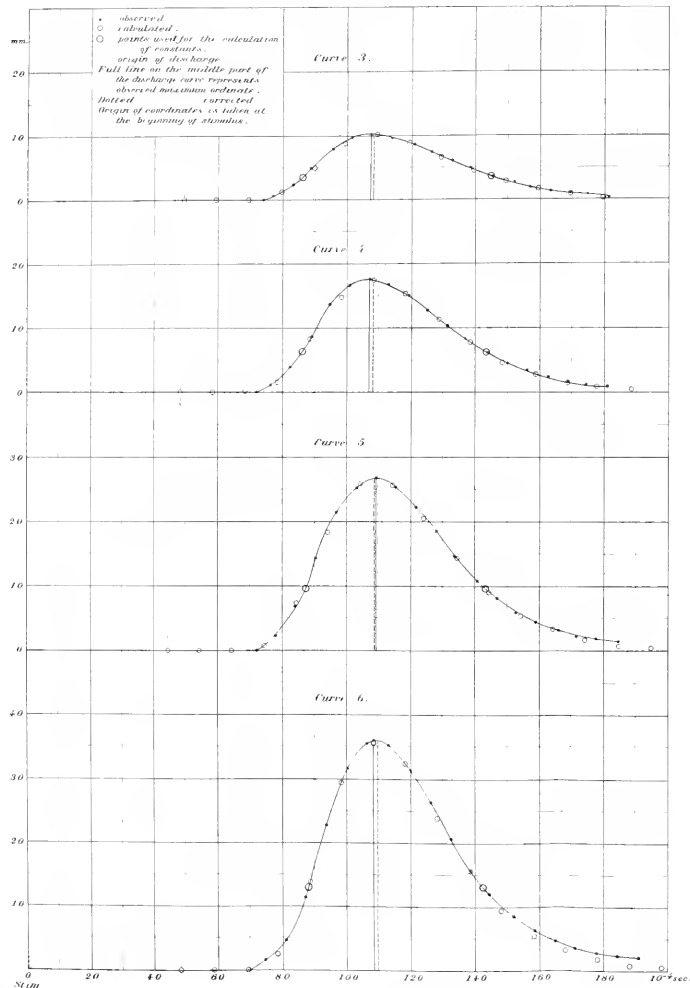




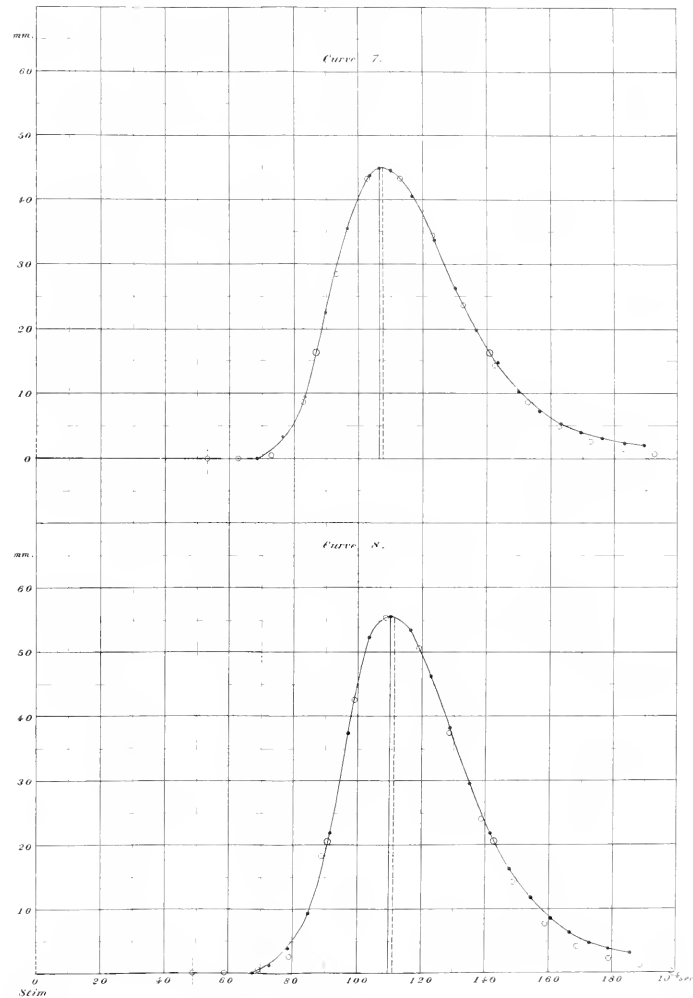




*Oscillogram No. 54.*



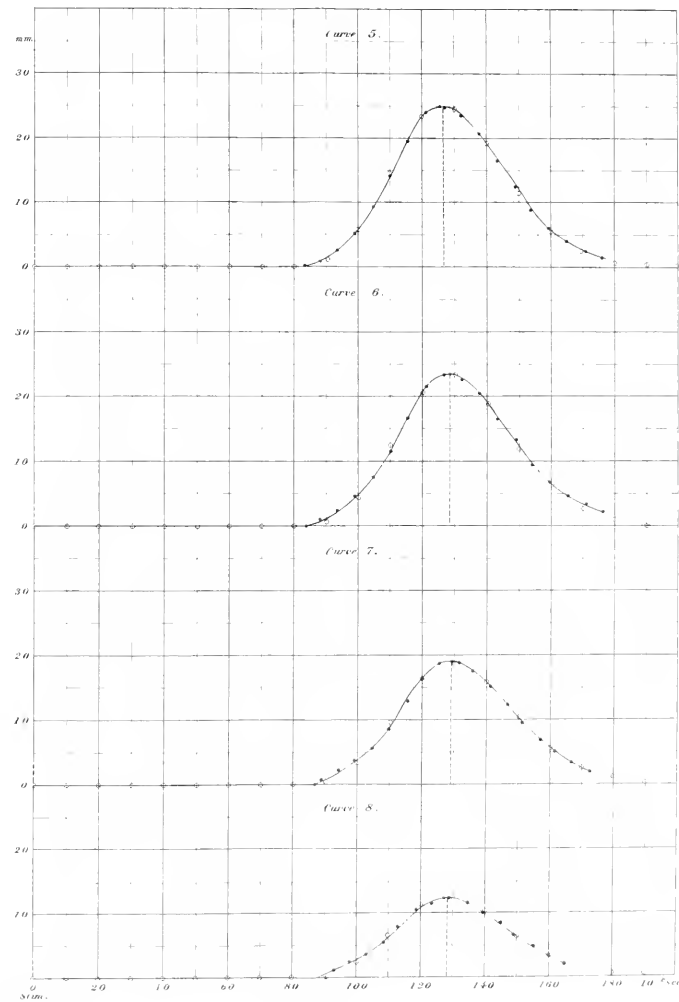
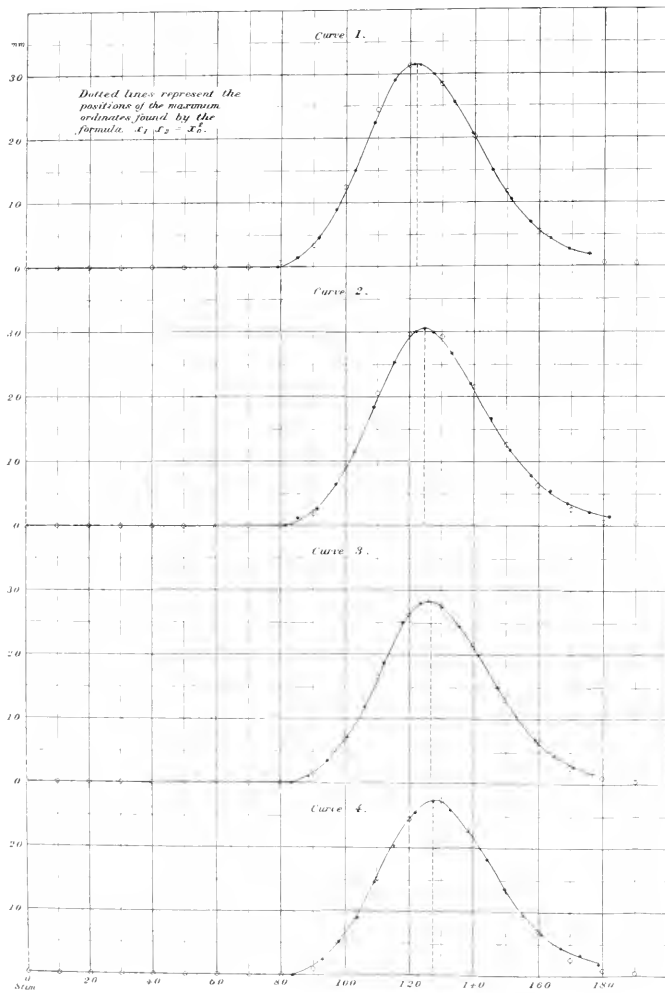
*(Reduced to  $U_{1.5}$  of Actually Used Scale.)*





(Reduced to  $1/15$  of Actually Used Scale.)

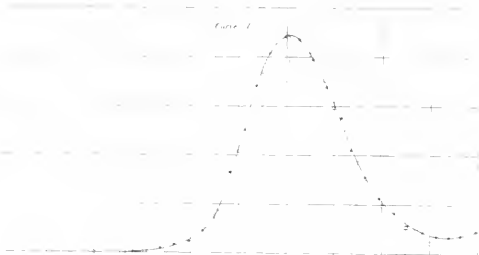
Oscillogram No. 37.



k. Fuji. Researches on the Electric Discharge of the Isolated Electric Organ of *Astron*. (Japanese Electric Ray) by Means of Oscillograph.



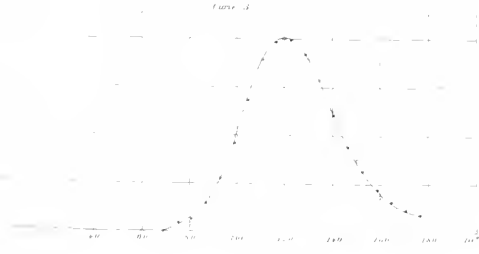
Curve 1



Curve 2



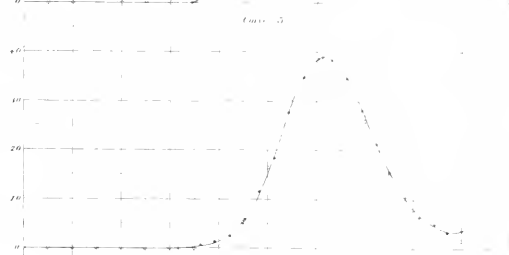
Curve 3



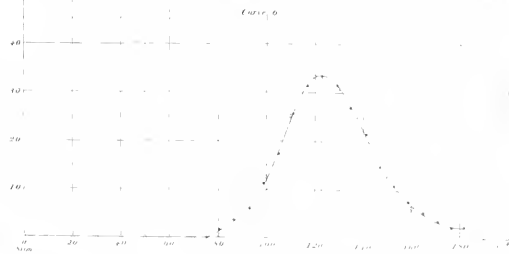
Curve 4



Curve 5



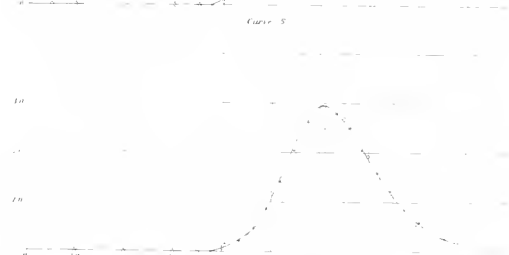
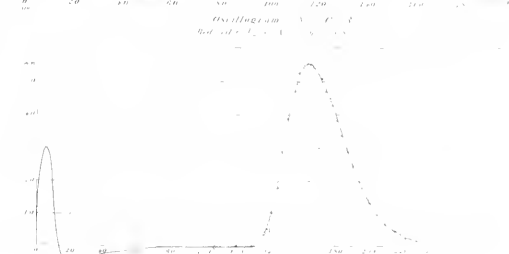
Curve 6



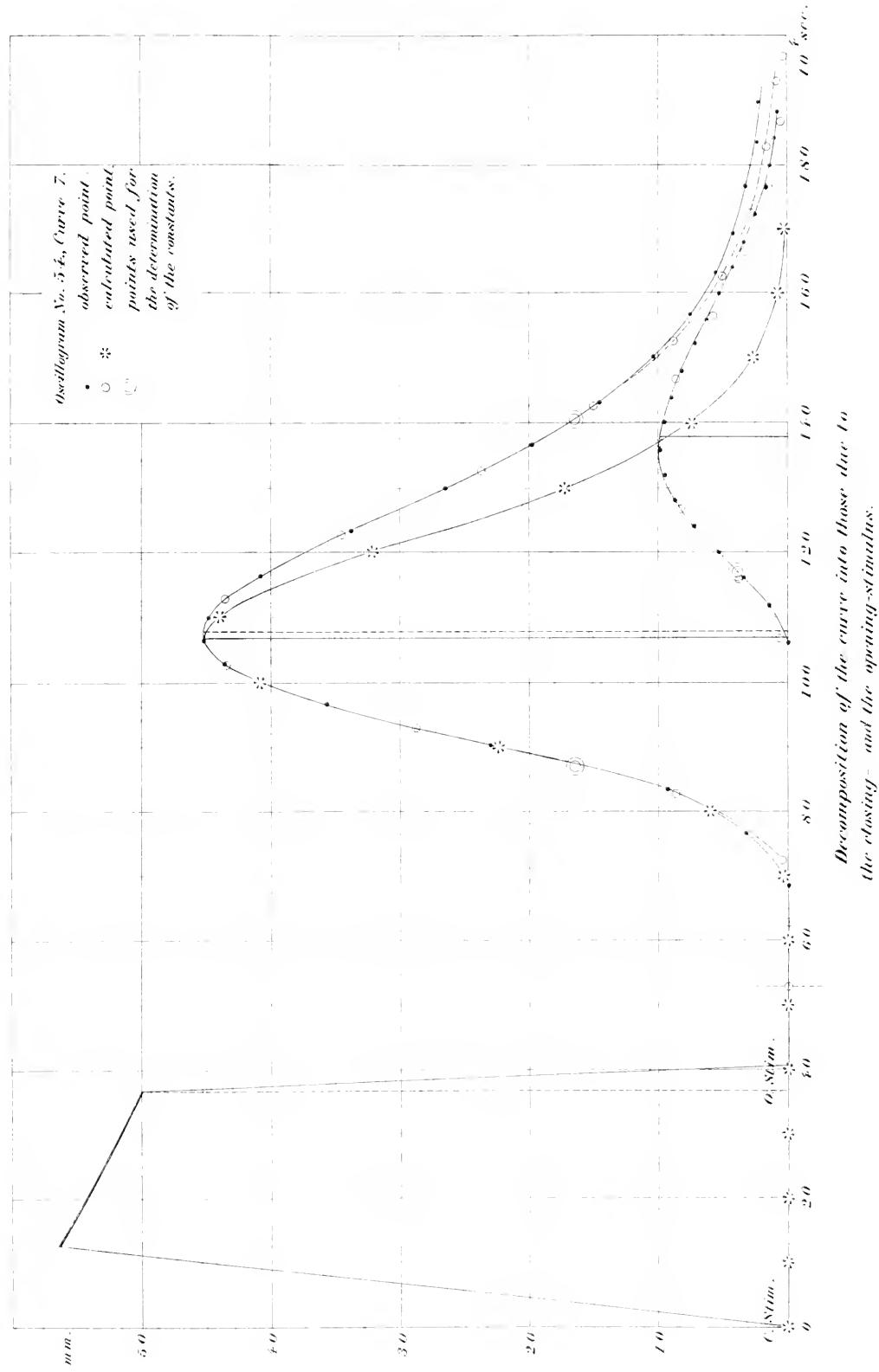
Curve 7



Curve 8

Oscillogram No. 50  
Resonance in the Electric Discharge

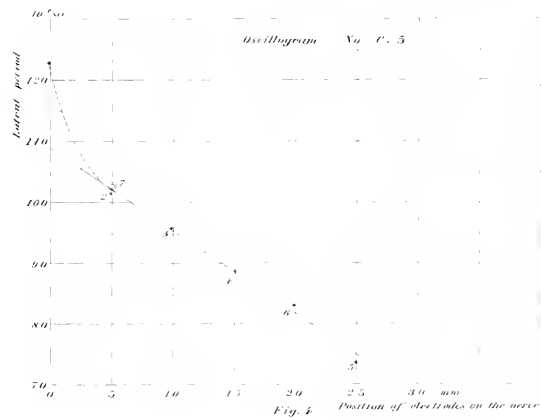
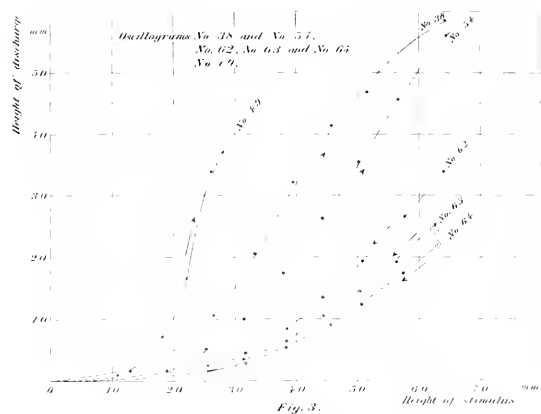
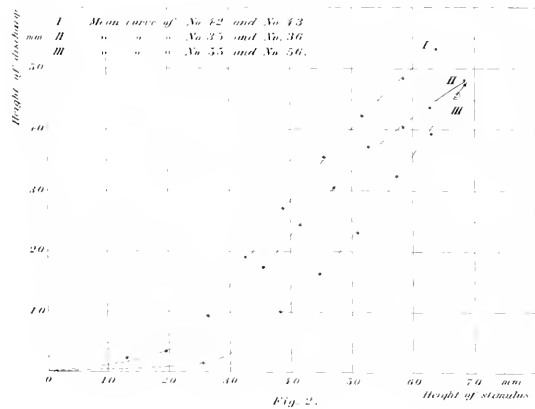
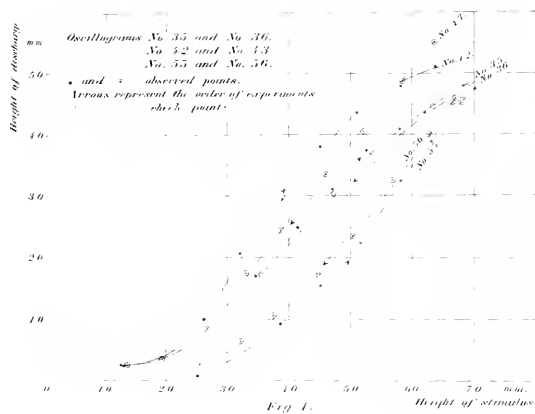




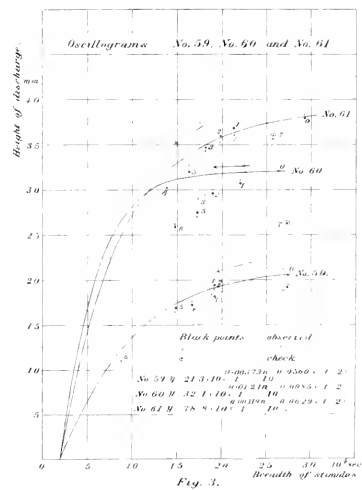
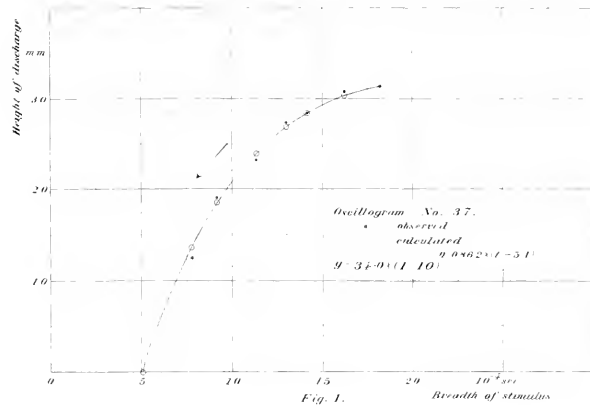
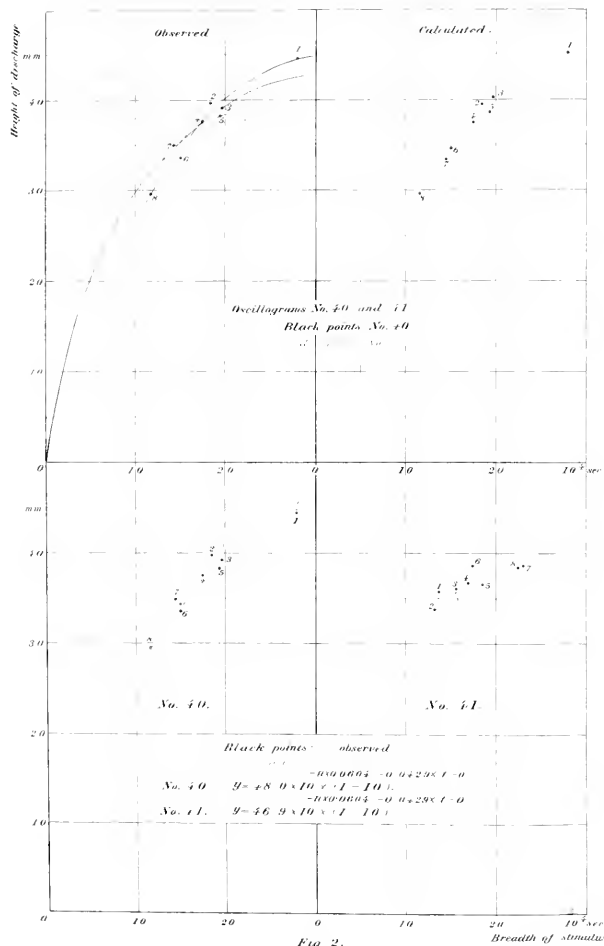
K. Fuji: Researches on the Electric Discharge of the Isolated Electric Organ of *Astrape* (Japanese Electric Ray) by Means of Oscillograph.













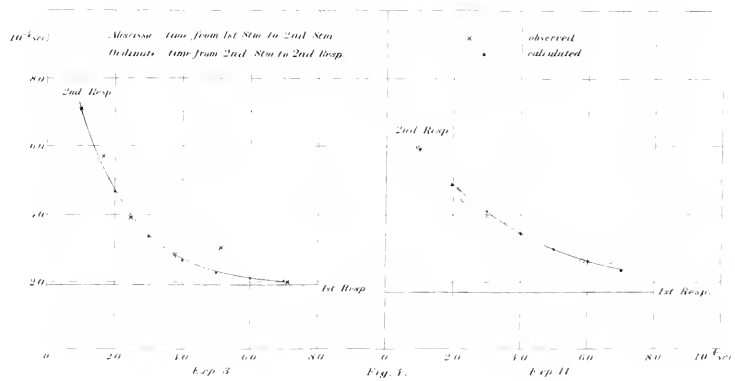
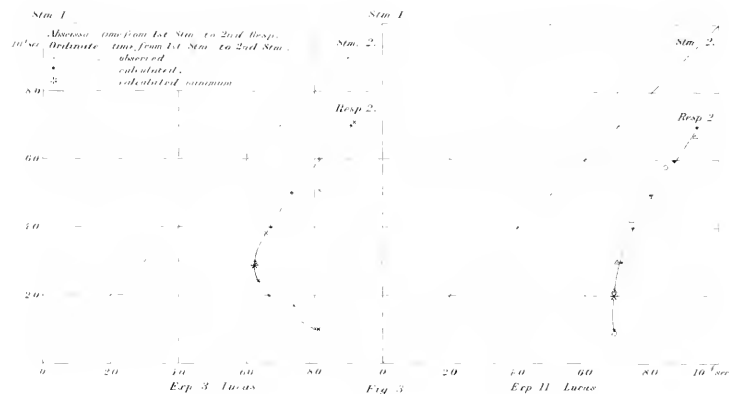
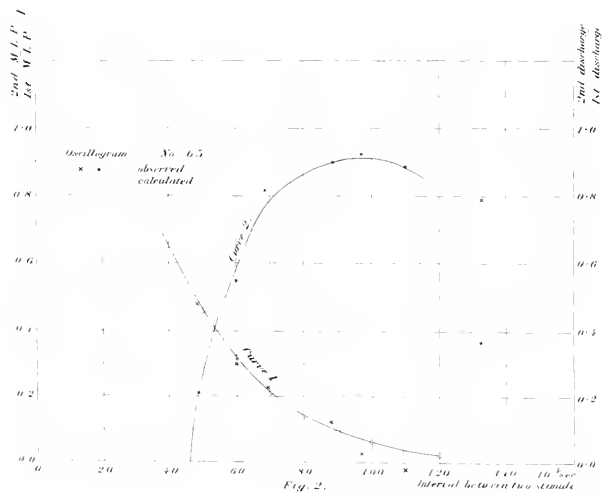
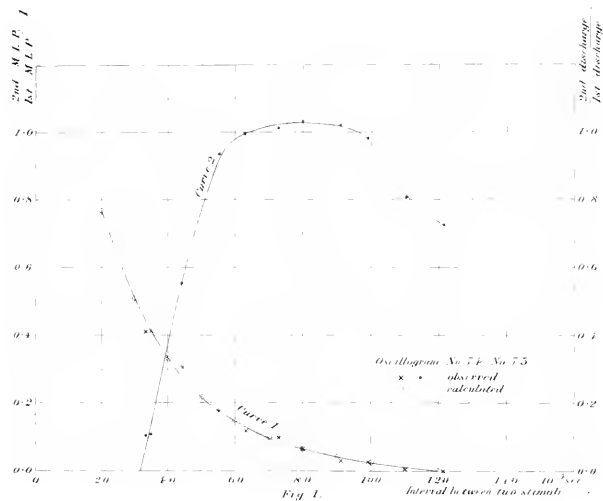










Fig. 1. 0-3 sec. 5.

Temperature of the organ = 44.0 C.

No. of exp.	1	2	3	4	5	6	7	
E.T.	2.80	2.90	2.92	2.92	2.80	3.24	4.00	m. 10 sec.

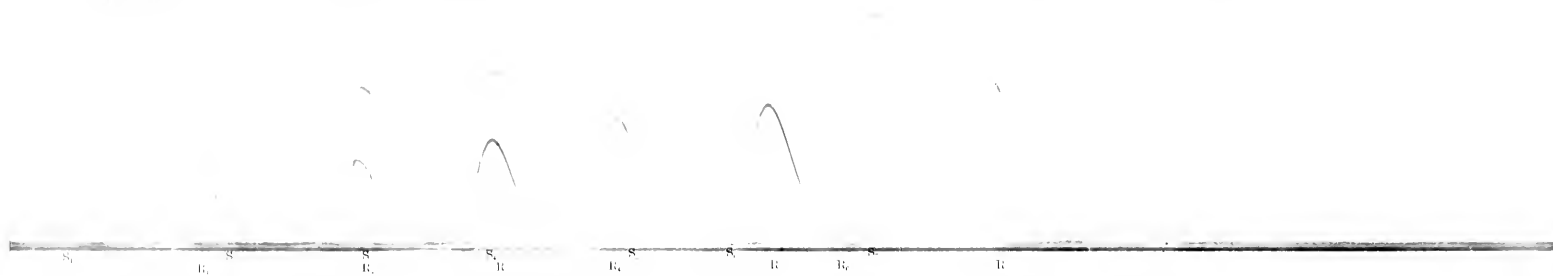


Fig. 2. 0-10 sec. No. 2.

Preparation same as No. 1.

Order of stimuli reversed.

No. of exp.	1	2	3	4	5	6	7	
E.T.	2.90	2.64	2.60	2.70	2.60	2.58	2.76	m. 10 sec.

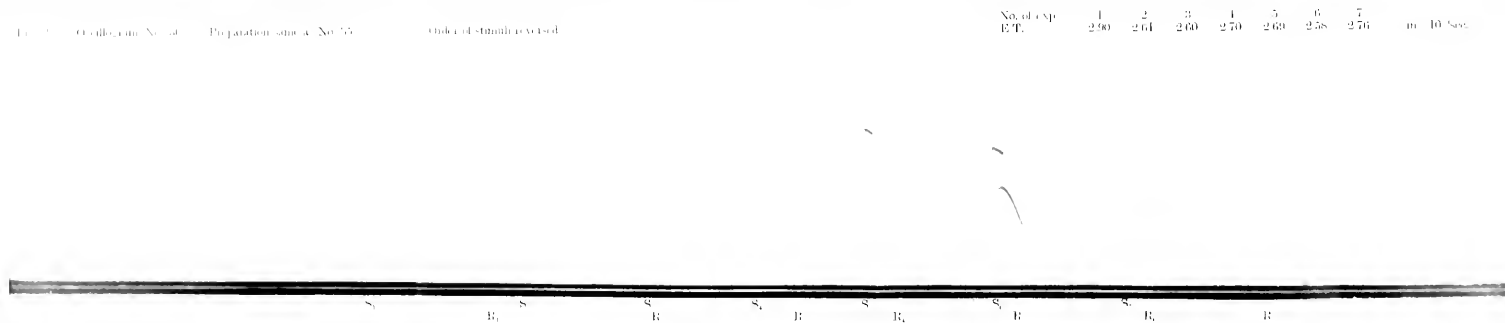


Fig. 3. 0-10 sec. No. 3. Electric Discharge of the Isolated Electro-Organ of *Crangon* (Japan) - Elected by Means of a Graph.



Fig. 1. Oscillogram No. 38.

Temperature of the organ. 11.5° C.

No. of exp	1	2	3	4	5	6	m
E.T., "	2.86	2.78	3.25	3.11	2.96	2.84	10 Sec.

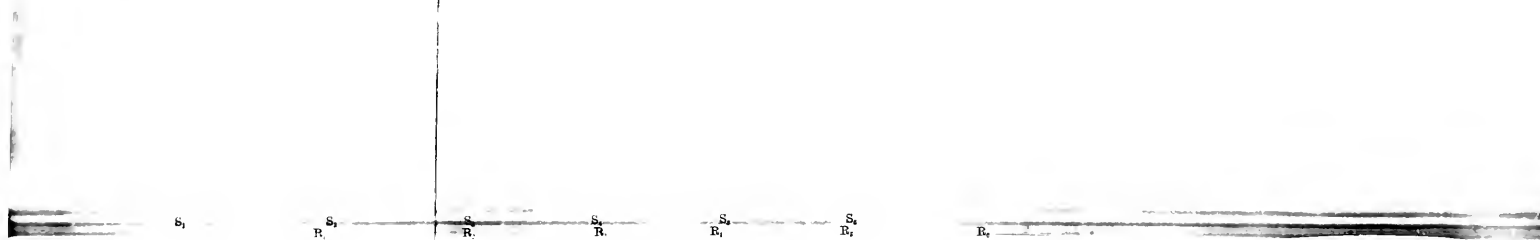


Fig. 2. Oscillogram No. 39.

Temperature of the organ. 10.1° C.

No. of exp	1	2	3	4	5	6	7	8	m
E.T., "	1.06	0.22	1.19	3.11	1.31	1.01	1.54	3.31	10 Sec.

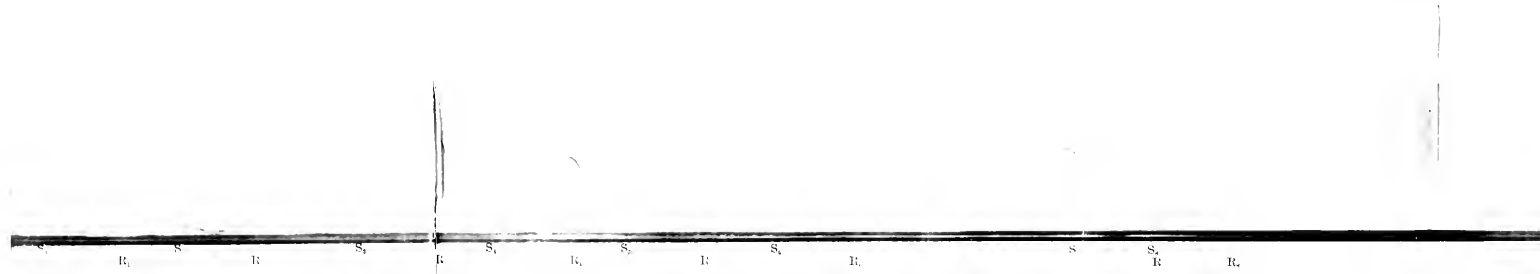


Fig. 3. Oscillogram No. 40.

Temperature of the organ. 10.1° C.

No. of exp	1	2	3	4	5	6	7	8	m
E.T., "	1.06	0.22	1.19	3.11	1.31	1.01	1.54	3.31	10 Sec.





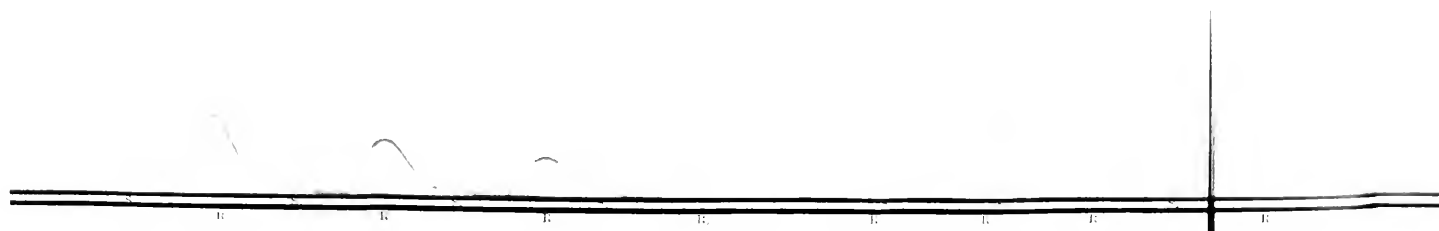
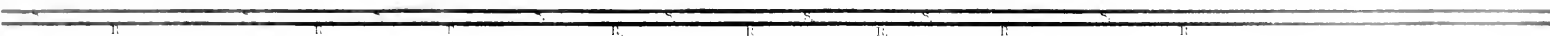
Fig. 1. (Continued)

Top curve of the set

No. of exp. 1 2 3 4 5 6 7  
 E.T. 1.16 2.70 2.88 2.86 2.87 2.78 2.71 in 10<sup>-3</sup> sec



Fig. 2. (Continued)





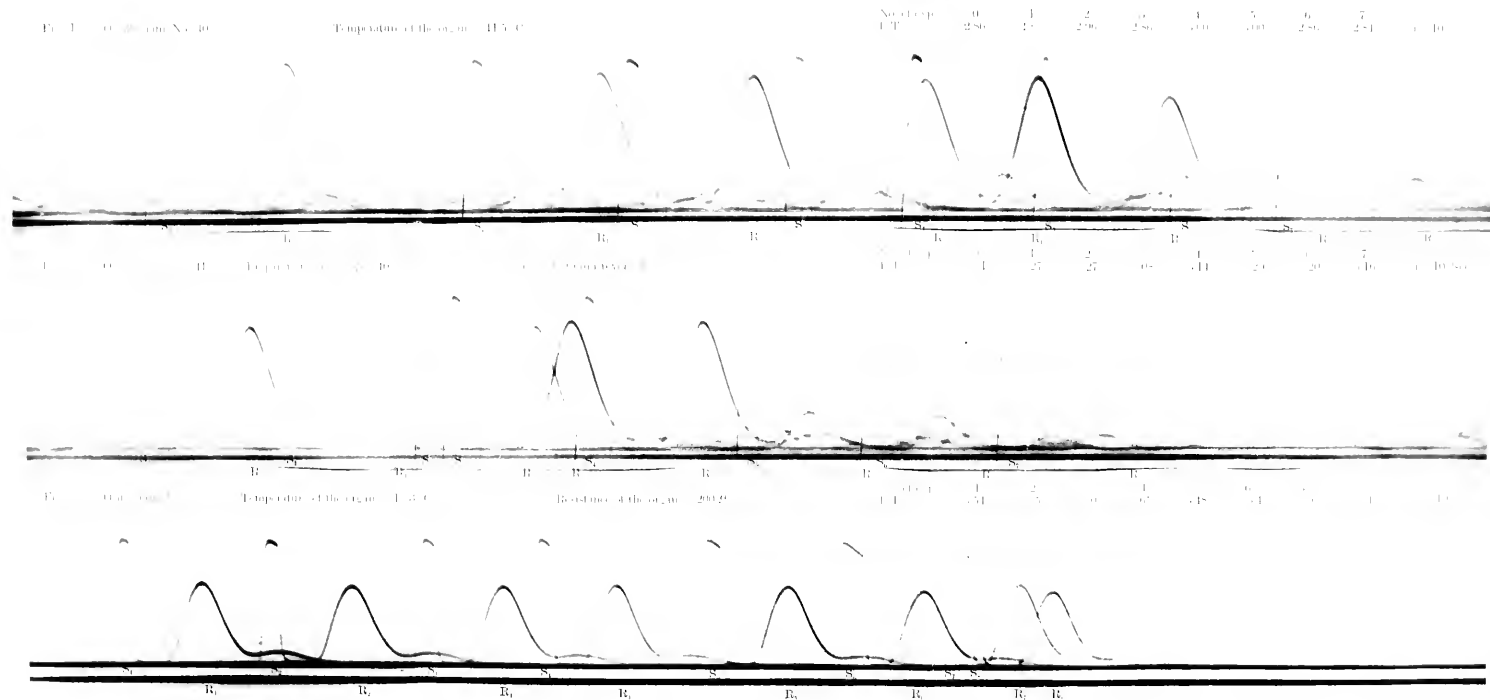


Fig. 1. —  $\text{C}_{10}\text{H}_{16}$  (cont. No. 40). Temperature of the origin =  $41.5^\circ\text{C}$ . Distance of the origin = 200  $\mu$ .





Fig. 1. Oscillogram No. 59.

Temperature of the crystal  $-115^{\circ}\text{C}$ .

No. of exp. 6  
1/T,  $\text{sec}^{-1}$  3.33 3.18 3.66 3.51 3.11 3.46 3.53 3.34 in  $10^{-6}\text{sec}$ .

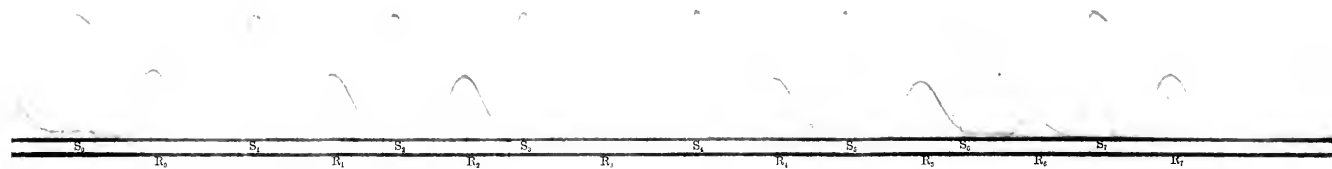


Fig. 2. Oscillogram No. 60.

Preparation time No. 60

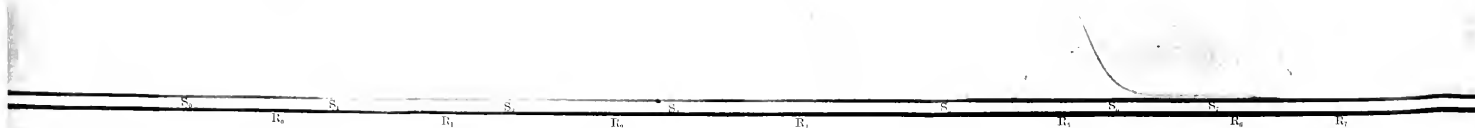
No. of exp. 0  
1/T,  $\text{sec}^{-1}$  2.22 2.27 2.24 2.14 2.25 2.14 — 2.32 in  $10^{-6}\text{sec}$ .



Fig. 3. Oscillogram No. 61.

Preparation time No. 61

No. of exp. 0  
1/T,  $\text{sec}^{-1}$  2.2 2.23 2.29 2.06 2.11 2.07 1.95 2.04 in  $10^{-6}\text{sec}$ .



Oscillograms No. 59, No. 60 and No. 61 are taken with the same preparation time.

R. P. T. — Temperature of the crystal, T. — Time of the experiment, T. — Time of the experiment, T. — Time of the experiment.







Fig. 1. O. diagram No. 65.

Temperature (°C) 100 110 120 130 140 150 160 170 180 190 200 210 220 230 240 250 260 270 280 290 300 310 320 330 340 350 360 370 380 390 400 410 420 430 440 450 460 470 480 490 500 510 520 530 540 550 560 570 580 590 600 610 620 630 640 650 660 670 680 690 700 710 720 730 740 750 760 770 780 790 800 810 820 830 840 850 860 870 880 890 900 910 920 930 940 950 960 970 980 990 1000

No. of copy  
1 2 3 4 5 6 7 8 9 10 11 12 13 14 15 16 17 18 19 20 21 22 23 24 25 26 27 28 29 30 31 32 33 34 35 36 37 38 39 40 41 42 43 44 45 46 47 48 49 50 51 52 53 54 55 56 57 58 59 60 61 62 63 64 65 66 67 68 69 70 71 72 73 74 75 76 77 78 79 80 81 82 83 84 85 86 87 88 89 90 91 92 93 94 95 96 97 98 99 100

1. S. 2. R. S. 3. S. 4. 2ry D. 5. R. 6. S. 7. R. 8. S. 9. S. 10. S. 11. R. 12. S. 13. R. 14. S. 15. R. 16. S. 17. R. 18. S. 19. R. 20. S. 21. R. 22. S. 23. R. 24. S. 25. R. 26. S. 27. R. 28. S. 29. R. 30. S. 31. R. 32. S. 33. R. 34. S. 35. R. 36. S. 37. R. 38. S. 39. R. 40. S. 41. R. 42. S. 43. R. 44. S. 45. R. 46. S. 47. R. 48. S. 49. R. 50. S. 51. R. 52. S. 53. R. 54. S. 55. R. 56. S. 57. R. 58. S. 59. R. 60. S. 61. R. 62. S. 63. R. 64. S. 65. R. 66. S. 67. R. 68. S. 69. R. 70. S. 71. R. 72. S. 73. R. 74. S. 75. R. 76. S. 77. R. 78. S. 79. R. 80. S. 81. R. 82. S. 83. R. 84. S. 85. R. 86. S. 87. R. 88. S. 89. R. 90. S. 91. R. 92. S. 93. R. 94. S. 95. R. 96. S. 97. R. 98. S. 99. R. 100. S.

No. of copy  
1 2 3 4 5 6 7 8 9 10 11 12 13 14 15 16 17 18 19 20 21 22 23 24 25 26 27 28 29 30 31 32 33 34 35 36 37 38 39 40 41 42 43 44 45 46 47 48 49 50 51 52 53 54 55 56 57 58 59 60 61 62 63 64 65 66 67 68 69 70 71 72 73 74 75 76 77 78 79 80 81 82 83 84 85 86 87 88 89 90 91 92 93 94 95 96 97 98 99 100

1. S. 2. R. S. 3. S. 4. 2ry D. 5. R. 6. S. 7. R. 8. S. 9. S. 10. S. 11. R. 12. S. 13. R. 14. S. 15. R. 16. S. 17. R. 18. S. 19. R. 20. S. 21. R. 22. S. 23. R. 24. S. 25. R. 26. S. 27. R. 28. S. 29. R. 30. S. 31. R. 32. S. 33. R. 34. S. 35. R. 36. S. 37. R. 38. S. 39. R. 40. S. 41. R. 42. S. 43. R. 44. S. 45. R. 46. S. 47. R. 48. S. 49. R. 50. S. 51. R. 52. S. 53. R. 54. S. 55. R. 56. S. 57. R. 58. S. 59. R. 60. S. 61. R. 62. S. 63. R. 64. S. 65. R. 66. S. 67. R. 68. S. 69. R. 70. S. 71. R. 72. S. 73. R. 74. S. 75. R. 76. S. 77. R. 78. S. 79. R. 80. S. 81. R. 82. S. 83. R. 84. S. 85. R. 86. S. 87. R. 88. S. 89. R. 90. S. 91. R. 92. S. 93. R. 94. S. 95. R. 96. S. 97. R. 98. S. 99. R. 100. S.



Fig. 1. Oscillogram No. 17. Temperature of the cathode = 52°C. Insulated resistance = 500  $\Omega$ . No. of exp. E.T. 1 2 3 4 5 6 7 m. 10<sup>-5</sup> sec.



Fig. 2. Oscillogram No. 18. Temperature of the cathode = 54°C. Insulated resistance = 300  $\Omega$ . No. of exp. E.T. 1 2 3 4 5 6 7 8 m. 10<sup>-5</sup> sec.

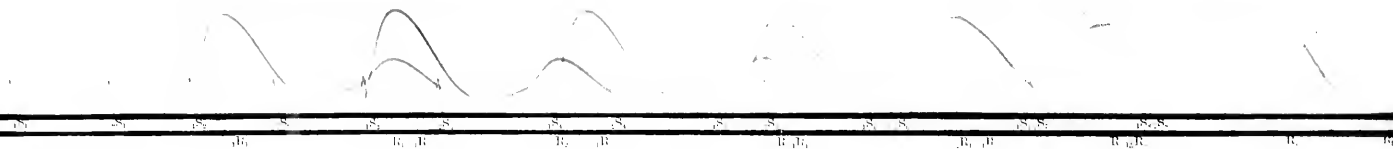


Fig. 3. Oscillogram No. 19. E.T. = 10<sup>-5</sup> sec.

S1 S2 S3 S4 S5 S6 S7 S8 S9 S10 S11 S12 S13 S14 S15 S16 S17 S18 S19 S20 S21 S22 S23 S24 S25 S26 S27 S28 S29 S30 S31 S32 S33 S34 S35 S36 S37 S38 S39 S40 S41 S42 S43 S44 S45 S46 S47 S48 S49 S50 S51 S52 S53 S54 S55 S56 S57 S58 S59 S60 S61 S62 S63 S64 S65 S66 S67 S68 S69 S70 S71 S72 S73 S74 S75 S76 S77 S78 S79 S80 S81 S82 S83 S84 S85 S86 S87 S88 S89 S90 S91 S92 S93 S94 S95 S96 S97 S98 S99 S100

R Top = 10<sup>-5</sup> sec. Electric Discharge of the Isolated Electrode (Group) (applied Electric Ray) by Means of Oscillograph





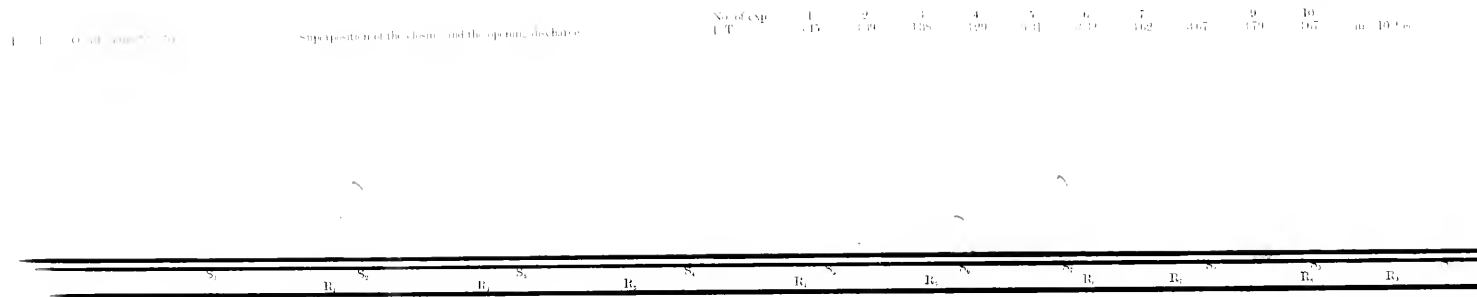
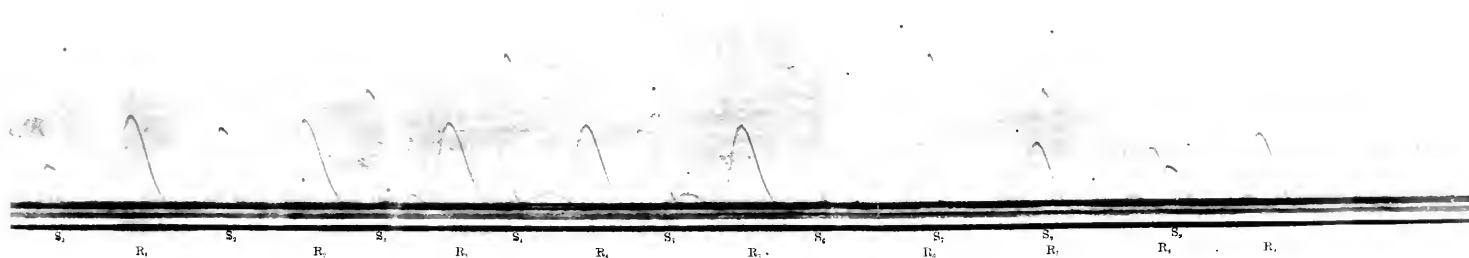


Fig. 2. Oscillogram No. 71. Stimulus: (1) 5 Descending, (2) 5 Ascending, (3) 5 Descending.

No. of exp.	1	2	3	4	5	6	7	8	9	in 10 <sup>-3</sup> sec.
L.T.	3.51	3.51	3.38	1.40	3.51	1.55	1.55	1.55	1.41	



b. Fig. 3. Researches on the Electric Discharge of the Isolated Electric Organ of *Gobius* (Japanese Electric Ray) by Means of Oscillograph.



Fig. 1. Oscillogram No. 67.

Number of stimuli: 885 per sec.

E.T.  $2.86 \times 10^{-6}$  sec.

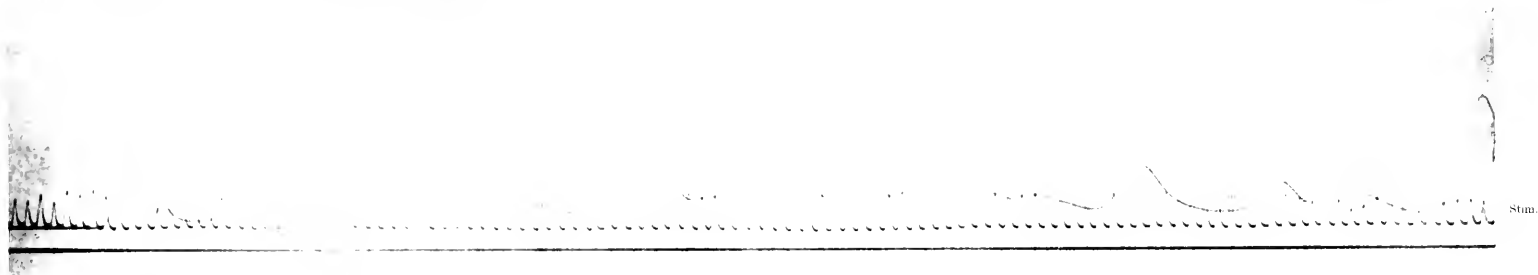


Fig. 2. Oscillogram No. 68.

Number of stimuli: 1412 per sec.

Temperature of the organ:  $15.5^{\circ}\text{C}$

E.T.  $5.08 \times 10^{-6}$  sec.



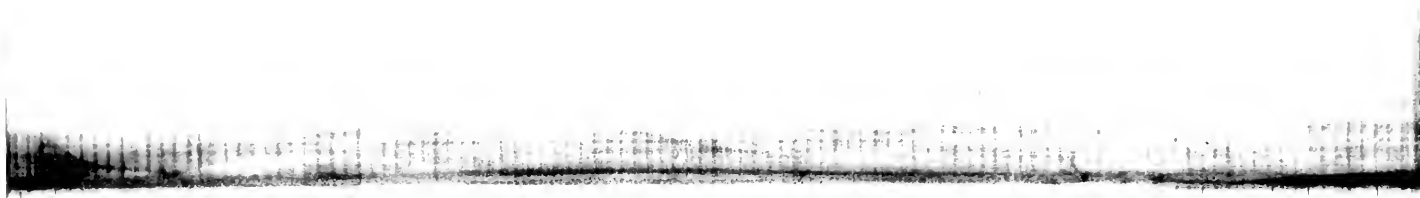
In Figure 1: a) is an act. Electro. Organ of the labeled Electric Organ of the organ. b) is an act. Electro. Ray by Means of an oscillograph.



1911, Vol. 10, No. 1

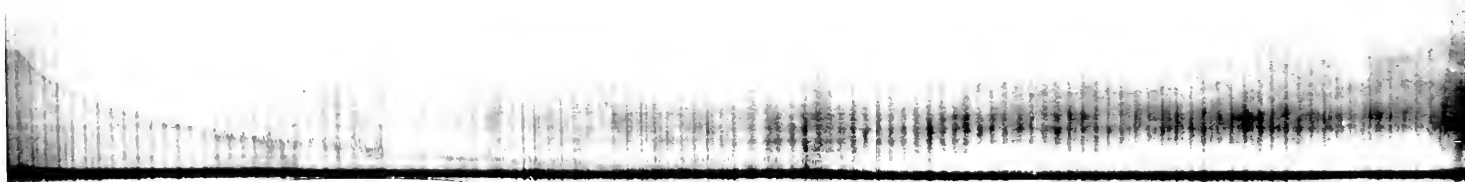
1911, Vol. 10, No. 1

1911, Vol. 10, No. 1



1911, Vol. 10, No. 1, 1911, Vol. 10, No. 1, 1911, Vol. 10, No. 1

1911, Vol. 10, No. 1, 1911, Vol. 10, No. 1, 1911, Vol. 10, No. 1



1911, Vol. 10, No. 1, 1911, Vol. 10, No. 1, 1911, Vol. 10, No. 1

1911, Vol. 10, No. 1, 1911, Vol. 10, No. 1, 1911, Vol. 10, No. 1









Fig. 1. *Ocellular Nerve*

Fig. 1. *Ocellular Nerve*



Fig. 2. *Ocellular Nerve*

Fig. 2. *Ocellular Nerve*



Fig. 3. *Ocellular Nerve*



Fig. 4. *Ocellular Nerve*

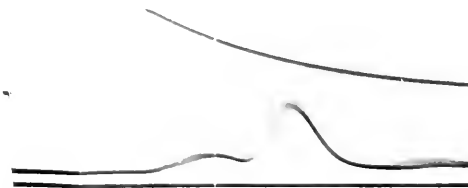




Fig. 1. — *Chamaea* (1000 ft.)

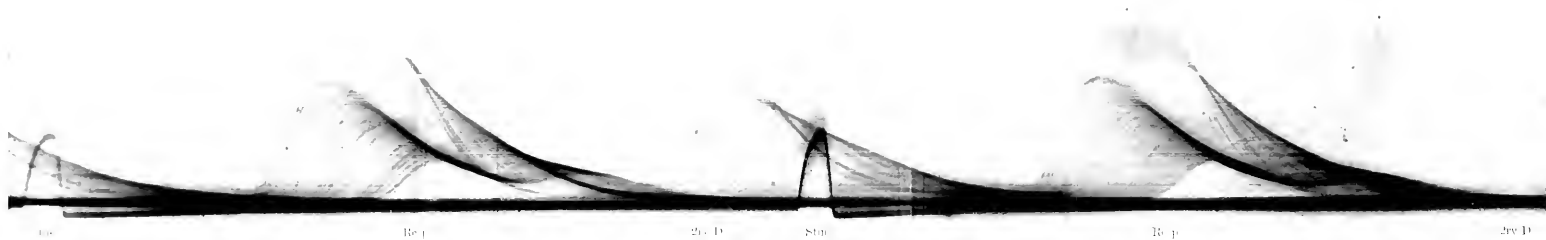


Fig. 2. — *Chamaea* (1000 ft.)

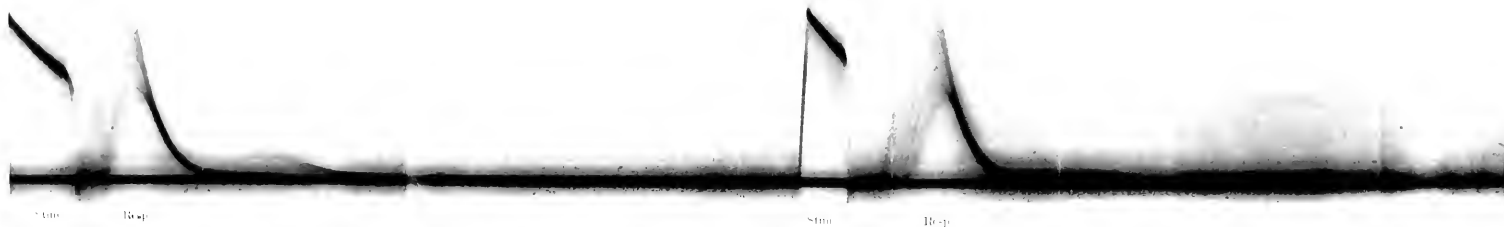








Fig. 1. Oscillogram No. 1



Fig. 2. Oscillogram No. 2

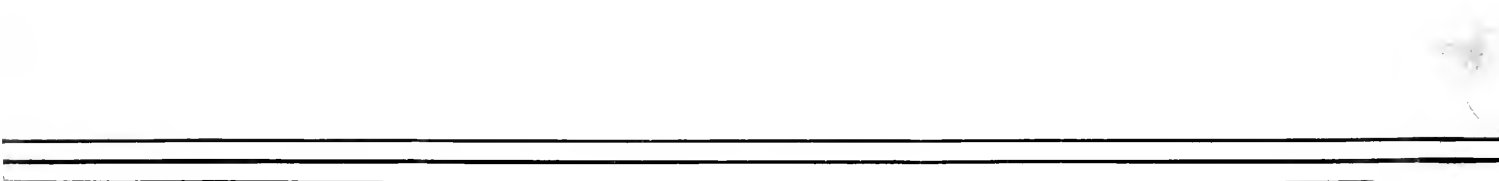


Fig. 3. Origin of waves upon a 100-ohm load. Mean oscillograph





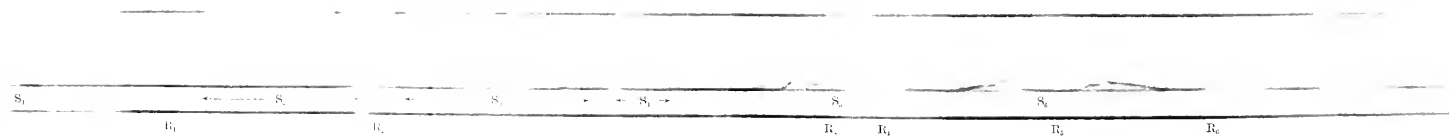
Fig. 1 Oscillogram No. 76 Temperature  $100^{\circ}\text{C}$   $110^{\circ}\text{C}$

No. of exp. 1 2 3 4  
L.T. 2.50 2.20 2.23 2.26 in  $10^{-10}$  sec.



Fig. 2 Oscillogram No. 77 Temperature  $100^{\circ}\text{C}$   $110^{\circ}\text{C}$

No. of exp. 1 2 3 4 5 6  
L.T. 2.50 2.50 2.87 2.43 2.40 2.49 in  $10^{-10}$  sec.





# Recherches sur les spectres d'absorption des ammine-complexes métalliques.

## I

### Les spectres d'absorption des solutions aqueuses des ammine-complexes cobaltiques et leurs constitutions chimiques.<sup>1)</sup>

Par

**Yuji SHIBATA**, *Rigakushi*.

Laboratoire de chimie minérale de l'Université impériale de Tōkiō.

---

*Avec 17 figures.*

---

Quoi que ce soit un fait bien connu et très intéressant que les sels complexes cobaltiques ont toujours les couleurs très diverses et vives, et de plus, que le changement de ces couleurs, d'après les substitutions de quelques restes dans les ions complexes, est très brusque, une étude systématique sur ce sujet, au point de vue de l'optique, n'a pourtant été entreprise que par peu de chimistes. Depuis que j'ai entrepris la présente étude, une notice intitulée "Über die Beziehungen zwischen den Absorptionsspektren und der Konstitution der Komplexenkobaltamminsalze" a été publiée par R. Luter et A. Nikolopoulos.<sup>2)</sup> Mais ce dernier travail bien intéressant, a été exécuté avec un spectrophotomètre et, en conséquence, l'étude n'est pas sortie de l'échelle spectrale visible, tandis que la mienne, parce que j'ai employé un spectrographe de quartz, s'est étendue vers l'extrême ultraviolet. Les matières choisies dans les deux études ne sont pas non plus les mêmes. A

---

1) Une note brève d'une partie de ce travail a été rapportée, sous les noms de G. Urbain et Y. Shibata, dans "Comptes rendus des Séances de l'Académie des Sciences" (Paris), **157**, XV, 593, [Oct. 13, 1913]

2) Zeitschr. physik. Chem. 1913, **82**, 361-378.

part cela, M. A. Werner a consacré un chapitre de son ouvrage aux stéréoisoméries des sels complexes de cobalt.<sup>1)</sup> Mais il n'a traité que de la relation entre les couleurs vues à l'œil nu et des constitutions des sels complexes. Je me suis donc mis à cette étude en employant la méthode d'absorption spectrale des solutions aqueuses des sels complexes cobaltiques les plus divers. Une série de spectrogrammes du visible et de l'ultraviolet que je décris précisément ci-dessous m'a permis de mettre en évidence des relations assez intéressantes entre la constitution de ces complexes et leurs absorptions.

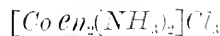
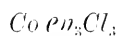
### La méthode et les matières.

Dans ce travail, j'ai employé le spectrographe\* de quartz, construit par M. Adam-Hilger à Londres. Comme la source de rayons, j'ai préféré l'arc de fer à cause de la facilité, avec laquelle on peut connaître la longueur d'onde à l'extrémité d'absorption.

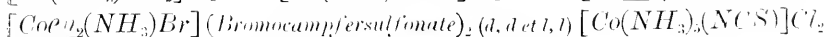
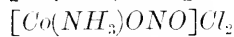
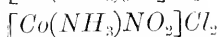
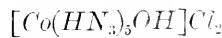
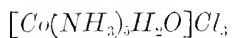
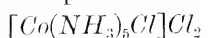
Les solutions des sels complexes ont été prises toujours à la même concentration de  $\frac{N}{100}$  et  $\frac{N}{1000}$ ; seulement pour quelques sels, elles ont été étendues jusqu'à  $\frac{N}{10000}$ . Les mesures ont été traduites par des courbes en portant, suivant deux axes rectangulaires, les logarithmes des épaisseurs des solutions et les fréquences correspondant aux limites de l'absorption, d'après la façon de Baly-Hartely.

Les sels complexes cobaltiques que j'ai pris comme objets de cette étude comprennent les 26 espèces suivantes :

#### Cobaltihéxammines



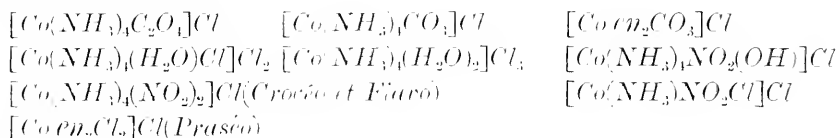
#### Cobaltipentammines



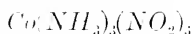
1) A. Werner : Ann. Chem. 1911, **386**, 1-272

\* J'ai commencé ce travail au Laboratoire de chimie minérale de M. le prof. G. Urbain à la Sorbonne de Paris et je l'ai fini à l'Institut de chimie de l'Université impériale de Tôkiô. Comme les deux laboratoires possèdent le même appareil du même fabricant londonien, j'ai pu heureusement achever ce travail, sans interruption ni empêchement, dans les deux laboratoires.

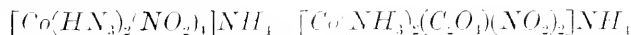
## Cobaltitétrammines



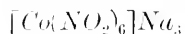
## Cobaltitriammine



## Cobaltidiammines



## Cobaltihexamitrite



Les sels nommés ci-dessus ont été préparés par l'auteur au laboratoire de M. A. Werner à l'Université de Zurich et au laboratoire de chimie minérale de M. G. Urbain à la Sorbonne de Paris. Quant à leur pureté, elle a été assurée par l'analyse et par les formes cristallines.

## Partie théorique

Les diagrammes faits ainsi présentent, dans l'étendue étudiée du spectre, deux ou trois minima des courbes (maxima d'absorption) très nets, dont les fréquences se trouvent toujours respectivement voisines de 2000, 3000 et 4000. Cette troisième absorption n'existe qu'en quelques complexes contenant le groupe de nitro, dont on verra la discussion dans la partie expérimentale. L'absorption qui a lieu à la fréquence de 3000 montre plus de déviation que la première à la fréquence de 2000, selon la constitution des ions complexes.

C'est seulement la première bande d'absorption qui ne manque pas à toutes les solutions des sels cobaltiques, soit les sels d'ammine-complexes, soit les sels ordinaires.<sup>1)</sup> Par conséquent cette première absorption à la fréquence de 2000, nous semble être due à l'atome de cobalt, qui se place au centre des ions complexes,\* tandis que les autres doivent appartenir aux autres atomes métalloïdes qui sont en connexion immédiate avec l'atome de cobalt.

\* D'après l'opinion de M. A. Werner les sels cobaltiques, comme chlorure, nitrate, sulfate etc., en solution aqueuses, font aussi des ions complexes avec l'eau  $[\text{Co}(\text{H}_2\text{O})_6]$ .

1) Comparer A. Hantzsch u. Yuji Shibata: Zeitschr. anorg. chem., 1911, **73**, 309-321.

D'après les recherches des physiciens modernes, les causes de la production des spectres linéaires et de ceux de bandes sont très probablement dues à la vibration respective des électrons positifs et des électrons négatifs.<sup>1)</sup> A la suite de cette théorie fondamentale, J. Stark<sup>2)</sup> a présenté une hypothèse, qui est expérimentalement constatée à certains degrés. Son raisonnement peut être brièvement exposé comme il suit: les valence des atomes chimiques ne sont autre chose que les électrons négatifs qui sont liés avec les lignes de force sur la surface d'un atome, petite particule élémentaire chargée électriquement au signe positif. Ce savant a classifié ces électrons de valence en trois catégories, selon la relation qui existe entre eux et les atomes. L'électron de valence saturé est telle modification qui a lieu entre deux atomes et, en conséquence, leurs lignes de force se terminent à la surface de ces atomes. La deuxième modification, nommée l'électron de valence insaturé, s'attache à un seul atome et, en conséquence, toutes ses lignes de force n'atteignent qu'à la surface de ce même atome, tandis que la troisième, appelée l'électron de valence relâché (gelockert), coexiste nécessairement avec la modification saturée, qui lie deux atomes, et il est caractérisé par ses lignes de force qui ne se terminent qu'à la surface d'un atome. Cette dernière sorte d'électron de valence, se rencontre, par exemple, dans le cas de la double liaison des carbones de combinaisons organiques insaturées.

Or, d'après J. Stark, ce sont ces électrons de valence, qui jouent le rôle du résonateur, dont les oscillations, excitées par une énergie quelconque, soit celle de la chaleur, soit celle des rayons lumineux, produisent des spectres de bandes. Le calcul de J. Stark rend compte du fait que c'est principalement les électrons de valence relâchés, qui donnent les absorptions de bandes dans l'échelle spectrale visible, et ultraviolette; c'est-à-dire l'intérieur de l'enceinte de la longueur d'onde *ca* 7000–1500 Å. C'est donc bien la raison pour laquelle les combinaisons organiques insaturées,

---

1) Voir J. Stark: Die Principien der Atomedynamik, II, Die elementare Strahlung, 1911, S. Hirzel, Leipzig, Paul Ruggli: Die Valenz-Hypothese von J. Stark vom chemischen Standpunkt [1912, Ferdinand Enke, Stuttgart, et G. Urbain: Introduction à l'Etude de la Spectrochimie [1911, A. Hermann et Fils, Paris]

2) loc. cit.

possédant évidemment les électrons de valence relâchés aux points des liaisons doubles ou triples des atomes du carbone, sont vivement colorées, ou donnent des absorptions de bandes bien nettes à la partie ultraviolette.

Comme je l'ai déjà indiqué, les solutions aqueuses des sels cobaltiques montrent deux ou trois bandes d'absorption très nettes dans l'échelle spectrale visible et ultraviolette. L'une d'elles qui est la moins réfrangible, se trouve, sans exception, voisine de la longueur d'onde 5000 Å. et elle est peu influencée par une substitution quelconque dans les ions complexes. En conséquence, cette bande la moins réfrangible est bien probablement causée par l'oscillation des électrons de valence relâchés qui s'attachent à l'atome central de cobalt, tandis que les autres, qui sont plus ou moins sensibles à la substitution, sont caractéristiques des atomes métalloïdes qui se tiennent en directe connexion avec l'atome de cobalt.

Si donc on considère que l'électron de valence joue le rôle d'un petit résonateur qui oscille par l'agitation de l'énergie de rayons avec une certaine longueur d'onde, on peut représenter la relation entre cette énergie et le nombre d'oscillations par la formule fondamentale de M. Planck:  $\varepsilon = h\nu$ , où  $\varepsilon$  représente un quantum de l'énergie d'un résonateur oscillant, et  $\nu$  le nombre d'oscillations, tandis que  $h$  est appelé la constante universelle de Planck, ayant la valeur de  $6.548 \times 10^{-27}$ .

Si l'on replace maintenant le nombre d'oscillations  $\nu$  par les termes de la vitesse des rayons lumineux ( $3 \times 10^{10}$  cm/sec) et de sa longueur d'onde  $\lambda$ , la formule de Planck peut être transformée ainsi.

$$\varepsilon = \frac{6.548 \times 10^{-27} \times 3 \times 10^{10}}{\lambda} = \frac{19.64 \times 10^{-17}}{\lambda}$$

Puisque l'atome de cobalt possède les électrons de valence relâchés qui donnent une bande d'absorption toujours voisine de la longueur d'onde 5000 Å, on pourra alors calculer l'énergie moyenne de ces résonateurs, d'après la formule donnée ci-dessous.

$$\varepsilon = \frac{19.64 \times 10^{-17}}{5 \times 10^{-8}} = 4 \times 10^{-10} (C.G.S.)$$

A présent, il n'y a naturellement aucun moyen direct pour la détermination de la valeur de ce genre-là. Seulement, on pourra examiner cependant, si de pareils sels complexes colorés, par exemple, de chrom. de nickel, de platine etc, donneraient les absorptions caractéristiques aux atomes métalliques. Dans le cas où cela sera possible, la comparaison de la grandeur des énergies d'oscillation des électrons de valence de plusieurs métaux doit être un problème bien intéressant. Je vais continuer davantage mon travail dans ce sens.

## Partie expérimentale

### I. Cobaltihéxammines (Série lutéocobaltique)\*

Les sels complexes de cette série sont toujours colorés très jaune. Ils se cristallisent à aiguilles fines et sont solubles assez facilement dans l'eau.

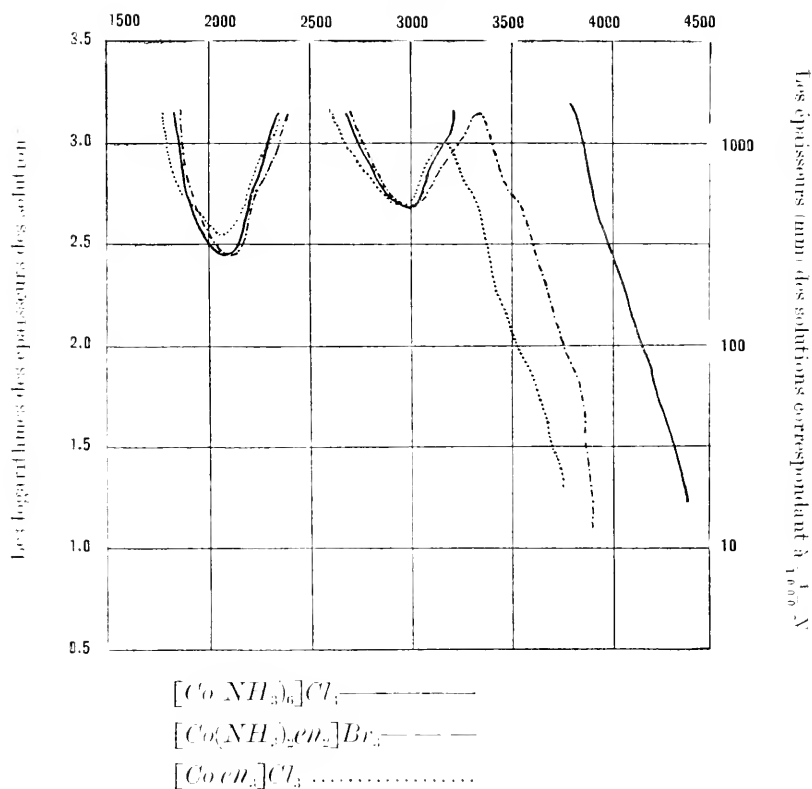
Comme on le voit dans la figure I, ils donnent deux absorptions, dont les minima des courbes (maxima d'absorption) se trouvent à 2100 et 3000 de fréquence. Il est bien intéressant de constater que les absorptions de ces trois corps, chlorure de cobaltihéxammine, bromure de cobaltidiammine-diéthylènediammine et chlorure de cobaltitriéthylènediammine, sont pratiquement égales l'une à l'autre, à propos des positions et des formes des bandes d'absorption. C'est seulement leur absorption à l'extrémité qui n'est pas la même. Ces parties des courbes sont déplacées de plus en plus vers le rouge par la substitution de la molécule d'éthylènediammine à celle d'ammoniac; c'est-à-dire que la courbe de l'absorption d'extrémité du chlorure de cobaltitriéthylènediammine est poussée le plus sensiblement vers le rouge et celle du sel hexammine se trouve à la partie plus réfrangible, tandis que la courbe de l'absorption d'extrémité du sel de diammine-diéthylènediammine se place entre les deux précédentes.

---

\* En ce qui concerne la nomenclature des sels complexes de cobalt, j'ai adopté celle donnée dans un ouvrage de M.G. Urbain "Introduction à la chimie des complexes," [1913; A. Hermann et fils, Paris.]

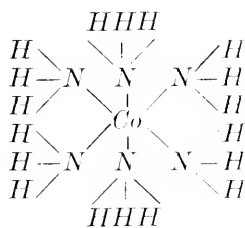


Fig. 1  
Fréquence

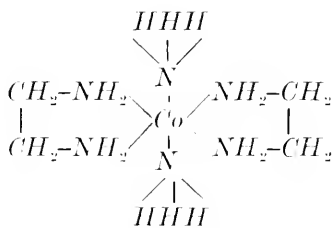


Comme conséquence du fait important que les formes et les positions des deux bandes d'absorption sont presque les mêmes pour ces trois corps, on peut tirer la conclusion suivante: la cause de l'absorption des rayons des sels complexes de cobalt ne réside qu'aux points de connexion de l'atome central du cobalt et des atomes métalloïdes (dans le cas actuel, les atomes d'azote dans les molécules d'ammoniac et d'éthylènediamine) qui sont enclâinés directement avec le premier. Quant à la constitution des molécules ou des groupes, qui forment les ions complexes autour de l'atome du cobalt, elle importe peu à l'égard de l'absorption des rayons.

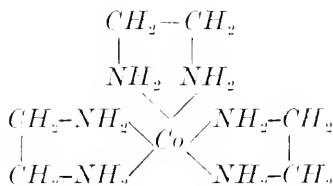
Donc, on doit donner les constitutions suivantes aux ions complexes des trois corps en question:



hexammine



diammine-diéthylènediamine



triéthylènediamine

Il nous semble que l'influence des anions sur l'absorption des rayons est tout-à-fait insignifiante, parce que le chlorure et le bromure montrent peu de différence dans les courbes d'absorption.

Des cas pareils se rencontreront encore souvent dans la suite de ce travail.

## II. Cobaltipentamines (Séries purpurécobaltique et rosécobaltique)

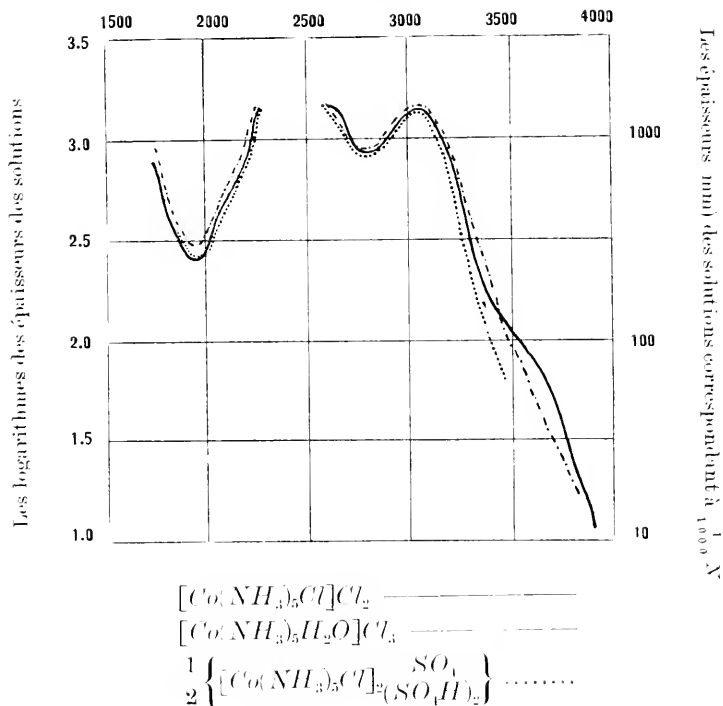
Les sels purpurécobaltiques sont les produits, faits par la substitution d'un atome de chlore à une molécule d'ammoniac des sels lutécobaltiques. Dans cette étude, j'ai choisi deux sels de ce groupe: le chlorure  $[Co(NH_3)_5Cl]Cl_2$  et le sulfate acide  $[Co(NH_3)_5Cl](HSO_4)_2$ .

Les sels rosécobaltiques sont également des corps substitués des séries lutécobaltiques, dont une molécule d'ammoniac est remplacée par une molécule d'eau.

La figure II nous indique que les formes et les positions des bandes d'absorption de ces trois corps ne diffèrent presque pas l'une de l'autre.

Fig. II

Fréquence.



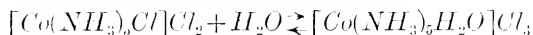
La première bande qui est moins réfrangible montre son maximum d'absorption à 1950 de fréquence, tandis que celle plus réfrangible se trouve à 2800.

En comparant ces figures avec celles des sels lutéocobaltiques, on remarque facilement que les deux bandes, spécialement la deuxième, plus réfrangible, sont sensiblement déplacées vers le rouge: c'est-à-dire que la substitution de l'eau et du chlore à la place d'une molécule d'ammoniac a produit une influence bathochromatique.\* Dans la seconde bande plus réfrangible on voit l'influence hypochromatique en même temps.

\* Comme il est évident que la sensibilité relative des bandes influe autant sur la coloration que la position des bandes dans l'échelle spectrale, nous dirons des groupes auxochromes, qu'ils fonctionnent comme hyperchromes lorsqu'ils augmentent cette sensibilité, et comme hypochromes, lorsqu'ils la diminuent, de même qu'on dit qu'ils fonctionnent comme batho- ou hypsochromes, suivant qu'ils provoquent un déplacement de bandes vers le rouge ou vers l'ultraviolet.

Comme je l'ai déjà indiqué plus haut, il me semble que les secondes bandes plus réfrangibles sont très probablement causées par les oscillations des électrons de valence qui s'attachent aux atomes métalloïdes joints directement à l'atome du cobalt.

Dans le cas actuel, il faut se rappeler que l'atome d'oxygène dans la molécule d'eau (dans le sel roséocobaltique) et l'atome de chlore (dans le sel purpuréocobaltique) produisent la même influence optique : cela est pourtant extraordinaire. Considérons, par conséquent, que les deux sels complexes, purpuréo et roséo, sont en équilibre dans la solution aqueuse :



Mais le sel roséocobaltique est, en général, moins stable que le sel purpuréocobaltique. En effet, le premier est préparé, en faisant précipiter d'une solution ammoniacale du sel purpuréocobaltique par l'addition soigneuse de l'acide chlorhydrique à 0°. Il est alors bien vraisemblable que la réaction montrée par l'équation marche plutôt de droite à gauche dans la solution aqueuse très étendue, et qu'il n'y existe que le sel purpuréocobaltique. Or l'influence optique pauce sur la seconde bande, doit être causée probablement par l'atome du chlore.

On voit ici l'influence insignifiante de l'anion sur l'absorption, parce que les formes des courbes du chlorure et du sulfate acide de chlorpentammine ne diffèrent que peu l'une de l'autre.

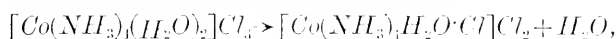
### III. Cobaltidihydratétrammine et Cobaltichlorohydratétrammine (Séries de roséotétrammine et de hydropurpuréotétrammine)

Ces deux sels sont les produits obtenus par la substitution de deux molécules d'ammoniac du sel cobaltihexammine et ont respectivement les formules suivantes :



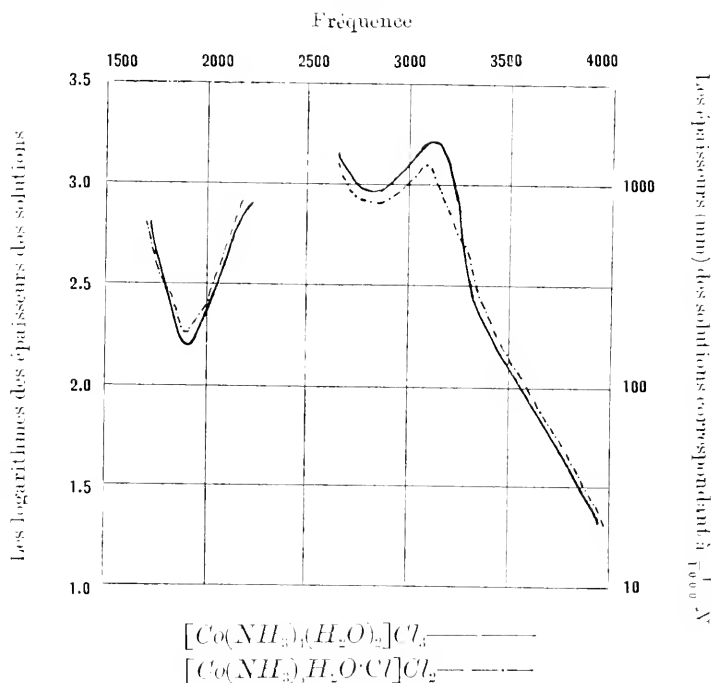
La figure III nous montre que les courbes d'absorption de ces deux corps coïncident à peu près, ayant les maxima d'absorption à 1900 et 2800 de fréquence. Par conséquent, il doit y avoir eu,

comme dans le cas précédent, le changement suivant dans la solution aqueuse de ces deux sels tétrammines



parce que le sel roséotétrammine est assez labile même à l'état solide et incline à se transformer spontanément en sel hydropurpuréotétrammine.

Fig. III



L'influence hyperchromatique de disubstitution pour hexammine est bien remarquable dans la première bande. Quant à l'influence sur la seconde bande, dans l'ultraviolet, elle ne se discerne presque pas de celle qui se produit dans le cas de pentammines.

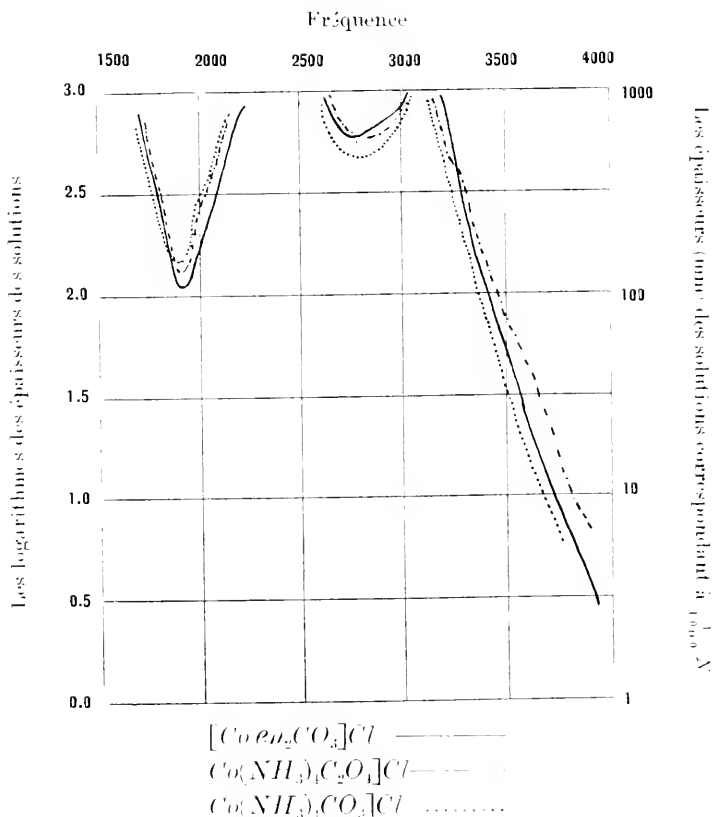
Ce dernier fait, que les courbes d'absorption du sel purpuréopentammine et du sel hydropuréotétrammine possèdent presque les mêmes minima à 2800 de fréquence, est bien compréhensible, si l'on prend la courbe d'absorption du monohydroxypentammine  $[Co(NH_3)_5OH]Cl_2$  en considération. Comme on le verra plus tard,

il manque la deuxième bande dans l'ultraviolet en ce sel complexe, qui contient un groupe d'hydroxyl, dont l'atome d'oxygène se lie directement avec l'atome de cobalt. Un atome d'oxygène étant ainsi indifférent pour la deuxième bande, elle doit donc être due seulement à l'atome de chlore du sel purpuréopentammine et hydropurpuréotétrammine, bien que ce dernier contienne encore en plus une molécule d'eau.

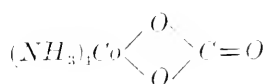
#### IV. Carbonatotétrammine et Oxalatotétrammine

Les sels de cette série se cristallisent bien en aiguilles, quelquefois assez grosses. Le carbonatotétrammine  $[Co(NH_3)_4CO_3]Cl$  et le carbonatodiéthylènediamine  $[Co(en)_2CO_3]Cl$  ont la couleur du carmin foncé, tandis que l'oxalatotétrammine  $[Co(NH_3)_4C_2O_4]Cl$  est rose.

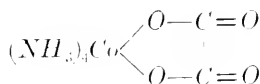
Fig. IV



La figure IV rend compte du fait, que les trois sels absorbent les rayons également. C'est alors encore une preuve que l'absorption n'agit qu'aux points de connexion entre l'atome cobaltique et les atomes métalloïdes, qui sont en coordination avec le premier, et que l'inégalité de structure des groupes de carbonato et d'oxalato importe peu. On peut donc donner les constructions suivantes aux cations complexes de carbonato et oxalatotétrammine



Carbonatotétrammine



Oxalatotétrammine

Les maxima d'absorption de ces deux séries de complexes se trouvent respectivement à 1900 et 2700 de fréquence; par conséquent les deux groupes en question causent une influence bathochromatique sur le sel hexammine. En comparant les absorptions de ces sels tétrammines avec celles du complexe purpurécobaltique, on ne remarque qu'un peu de différence à l'égard de la position de la deuxième bande plus réfrangible, c'est-à-dire une influence un peu bathochromatique. Pourtant l'intensité d'absorption se distingue assez sensiblement l'une de l'autre, comme cela est montré dans la petite table ci-dessous, dont les chiffres rendent compte de l'épaisseur, où les maxima d'absorption de chaque sel commencent de paraître.

	Purpuréo- pentammine	Purpuréo- tétrammine	Carbonato et Oxalatotétrammine
1 <sup>re</sup> bande (1900)	250-300 <sup>mm</sup>	180 <sup>mm</sup>	100-140 <sup>mm</sup>
2 <sup>me</sup> „ (2800-2700)	800 <sup>mm</sup>	800-900 <sup>mm</sup>	500-560 <sup>mm</sup>

Or on y trouve que les groupes de carbonato et d'oxalato sont bien hyperchromatiques.

### V. Combinaisons qui contiennent le groupe des nitros dans les ions complexes.

Les ammine-complexes qui contiennent respectivement un, deux, trois et quatre nitros dans les ions complexes absorbent bien semblablement et mettent en évidence quelques faits fort intéressants.

Il s'agit des dix sels complexes suivants

$[Co(NH_3)_5NO_2]Cl_2$   
chlorure de xanthopentammine

$[Co(NH_3)_5ONO]Cl_2$   
chlorure d'isoxanthopentammine  
ou de nitropentammine

$[Co(NH_3)_4NO_2^{(1)}NO_2^{(2)}]Cl$   
chlorure de flavotétrammine

$[Co(NH_3)_4NO_2^{(1)}NO_2^{(2)}]Cl$   
chlorure de crocéotétrammine

$Co(NH_3)_3(NO_2)_3$   
cobaltitrinitrotriammine

$[Co(NH_3)_2(NO_2)_4]NH_4$   
cobaltidiammonionitrite  
d'ammonium

$[Co(NO_2)_6]Na_3$   
cobaltihéxinitrite de sodium

$[Co(NH_3)_4(NO_2)(OH)]Cl \cdot H_2O$   
chlorure de mononitromono-  
hydroxyltétrammine

$[Co(NH_3)_4(NO_2)Cl]Cl$   
chlorure de monochloromononitro-  
tétrammine

$[Co(NH_3)_2(C_2O_4)(NO_2)_2]NH_4$   
cobaltidiammoniooxalonnitrite  
d'ammonium

Tous les sels de cette série sont colorés jaune ou jaune rougeâtre, spécialement les deux derniers ont la couleur de l'orange rougeâtre.



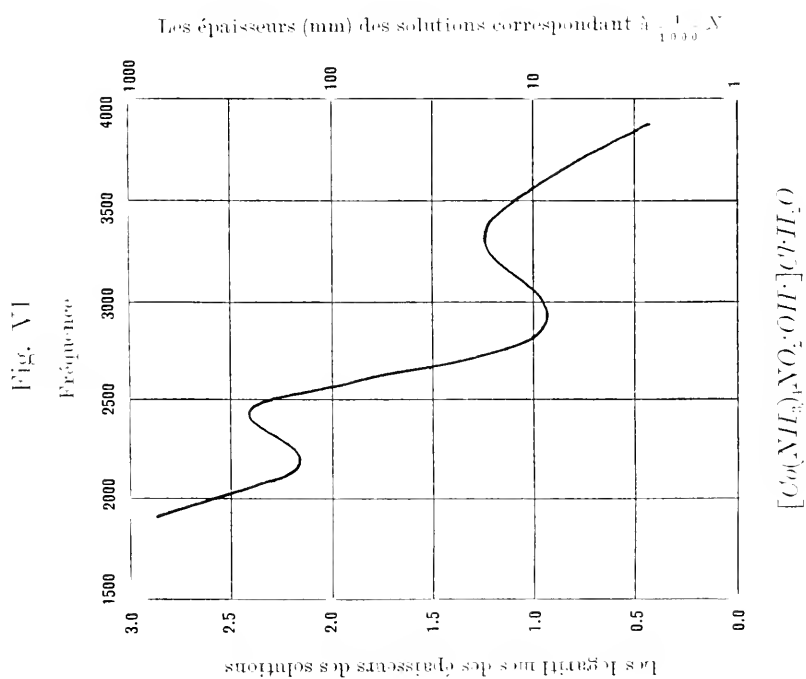
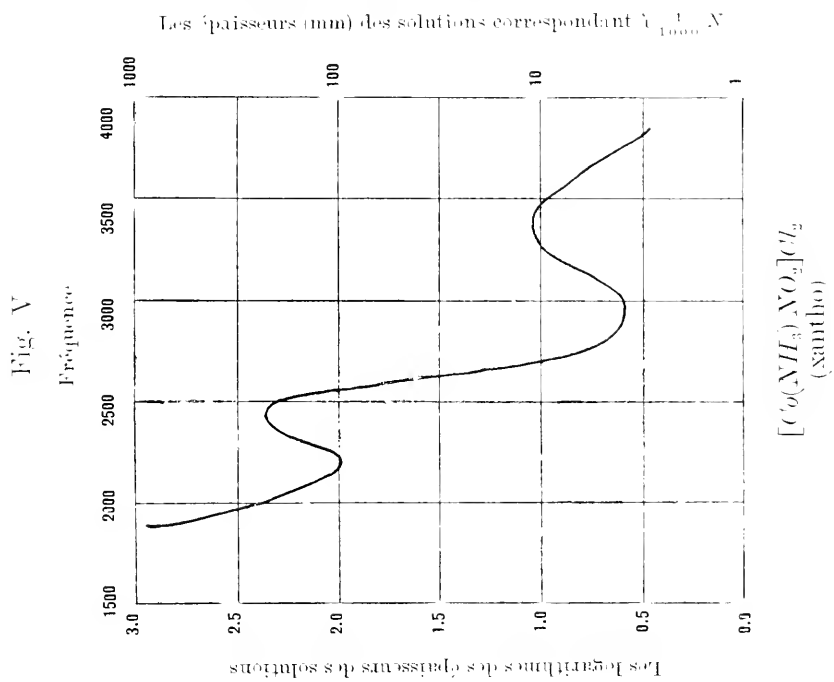


Fig. VII

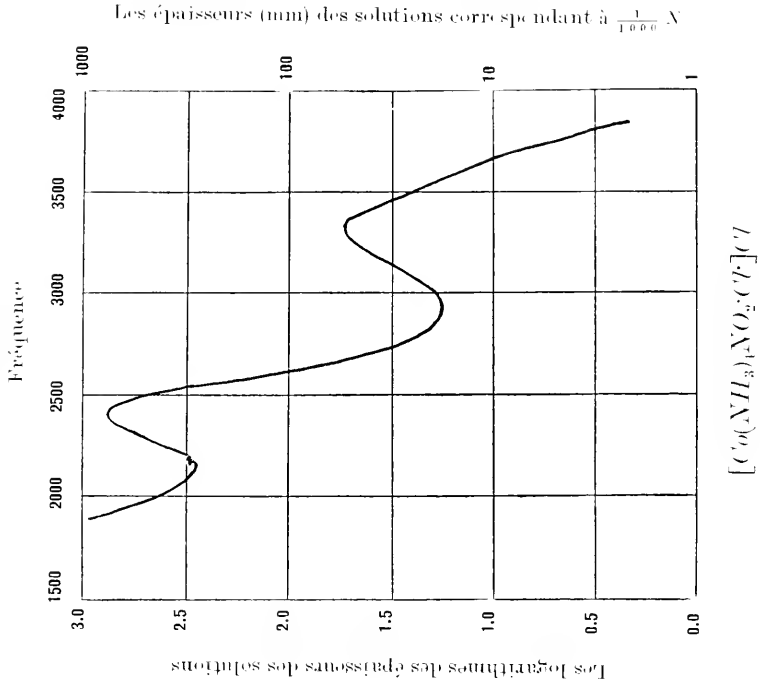


Fig. VIII

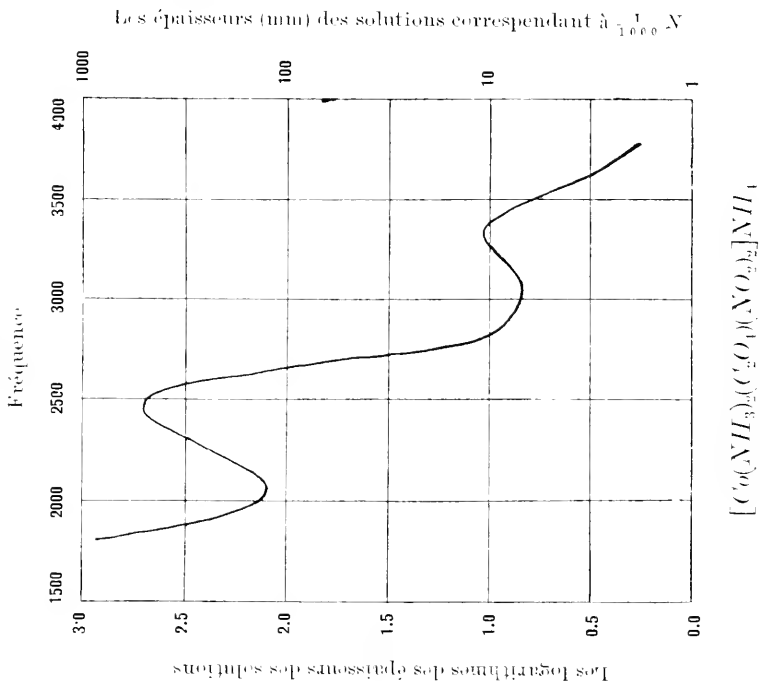


Fig. IX

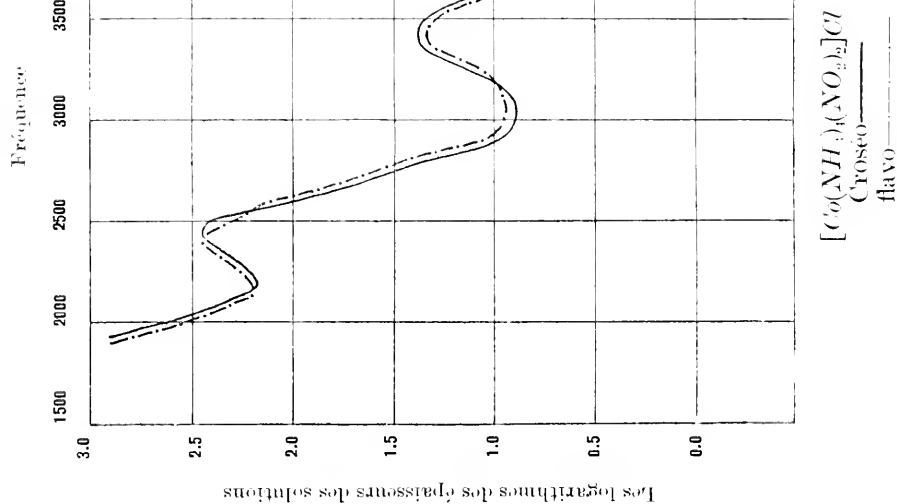
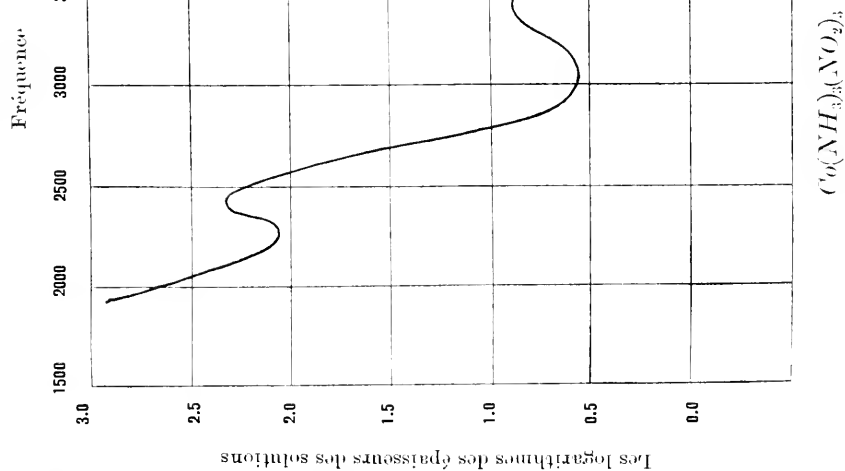
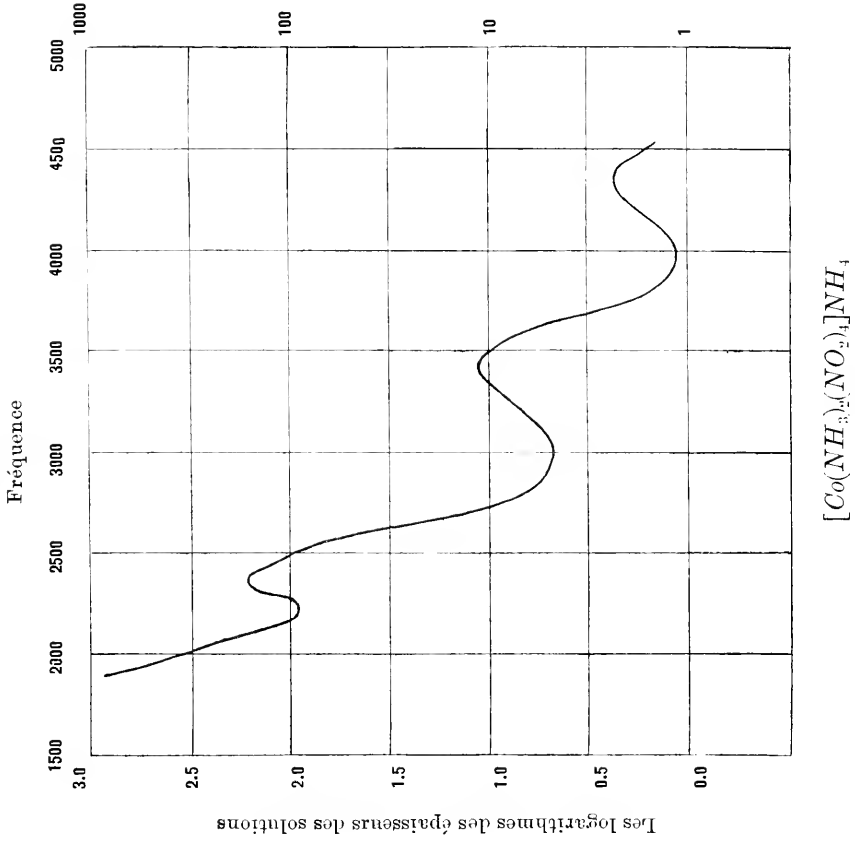


Fig. X



Les épaisseurs (mm) des solutions correspondant à  $\frac{1}{1000} N$

Fig. XI



Les épaisseurs (mm) des solutions correspondant à  $\frac{1}{1000} N$

Fig. XII

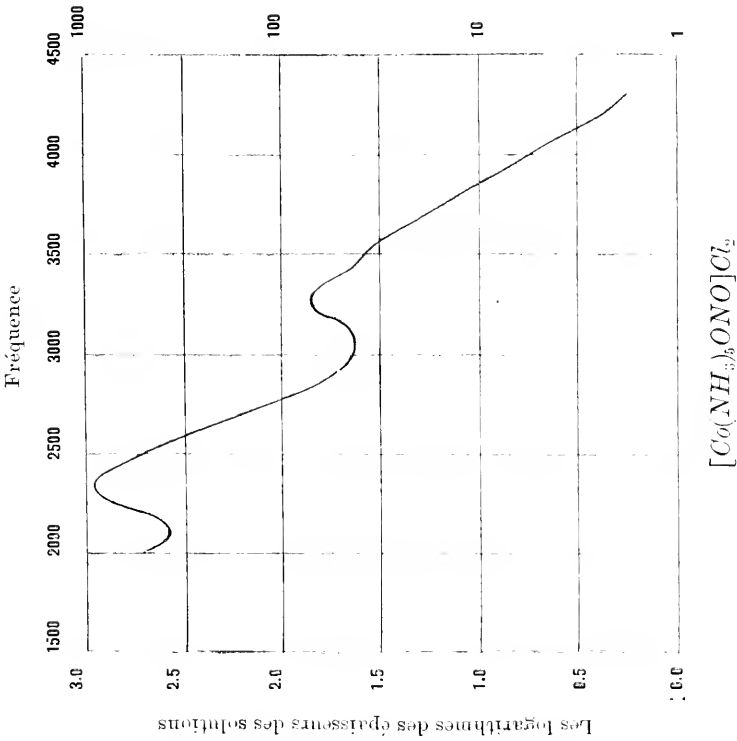
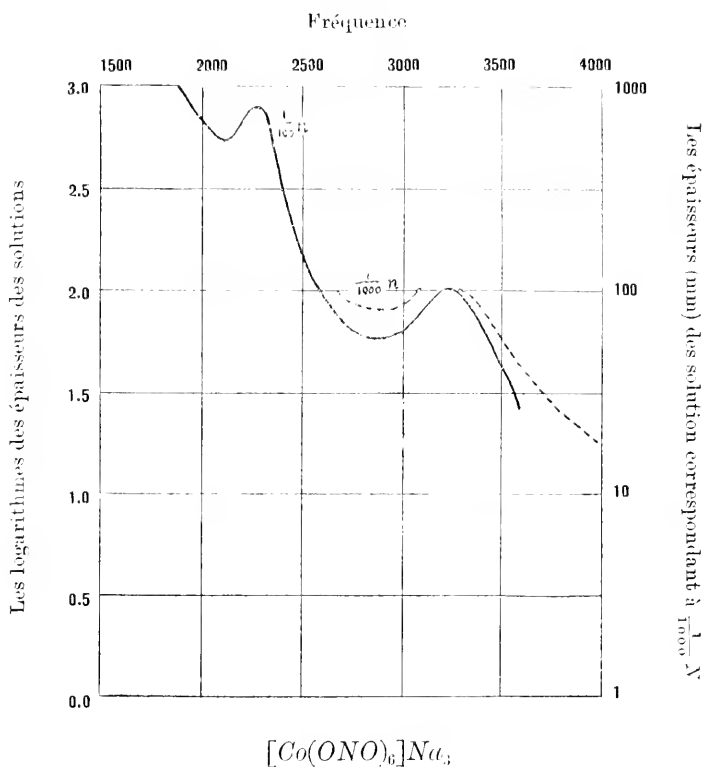


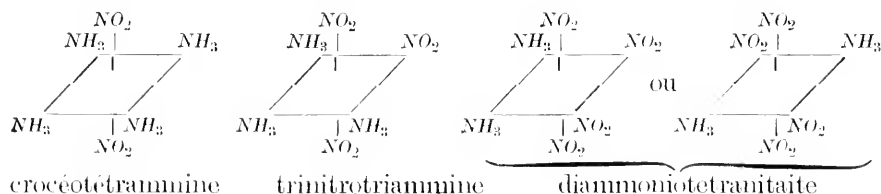
Fig. XIII



Ils se cristallisent en aiguilles fines et sont solubles plus où moins facilement dans l'eau. Les solutions sont bien stables, sauf celle de l'isoxanthopentammine et de l'héxanitrite; il me semble que ce dernier se dissocie en ses composants, c'est-à-dire le nitrite de cobalt et le nitrite de sodium dans la solution par la simple dilution, parce que ses absorptions aux concentrations de  $\frac{1}{100} N$  et de  $\frac{1}{1000} N$  ne s'accordent pas avec la règle de Beer. Quant au sel isoxanthopentammine, il est assez labile même à l'état solide et se transforme en xanthopentammine en quelques jours, tandis que la solution change sa couleur rouge au jaune de son isomère bien rapidement, bien que la solution fraîche satisfasse complètement la règle de Beer.

Comme on voit dans les figures V—XIII, on peut diviser cette

série en deux classes: l'une qui montre deux bandes d'absorption dans l'échelle spectrale et l'autre qui en a trois. Si l'on remarque que seulement trois corps parmi dix donnés ci-dessus, c'est-à-dire le crocétotétrammine, le trinitrotriammine et le diammoniotétranitrite appartiennent à la deuxième classe avec la troisième bande, on comprendra bien que deux nitros à la position de trans (ou 1,6) causent cette troisième absorption à l'extrême ultraviolet (ca 4000 de fréquence), parce que le sel crocétotétrammine a évidemment, d'après A. Werner<sup>1)</sup>, ses deux nitros à la position de trans, et que ceux qui contiennent quatre nitros doivent en avoir deux nécessairement à cette même position. Quant au cobaltitrinitrotriammine, il est théoriquement possible, qu'il apparaisse en deux isoméries stéréochimiques, l'une d'elles ayant deux nitros à la position de trans, et l'autre ses trois nitros à la juxtaposition. A en juger par l'existence de la troisième absorption, il est bien vraisemblable que ce complexe est composé de telle manière que deux de ses trois nitros sont à la position de trans. Alors ces trois sels complexes doivent être représentés par les formules stéréochimiques suivantes



En dehors de cette différence concernant la troisième absorption, toutes les courbes d'absorption des ammine-complexes contenant des nitrose ressemblent fortement l'une l'autre.

En général, les maxima d'absorption de ce groupe se trouvent à 2100 et à 3000 de fréquence; la troisième bande, si elle existe, a son maximum d'absorption à 4000.

En comparant ces absorptions avec celles des hexammine, on aperçoit tout de suite que l'introduction du groupe du nitro dans les ions ammine-complexes cause une influence hyperchromatique

1) loc. cit

qui est très remarquable, spécialement dans les deuxièmes bandes. Seulement, le cobaltihéxanitrite de natrium  $[Co(NO_2)_6]Na_3$  et le chlorure de nitritopentammine (isoxantho)  $[Co(NH_3)_5ONO]Cl_2$  se montrent un peu exceptionnels, c'est-à-dire que leur première bande est assez hypochromatique, comparée avec celle d'héxammine.

Les chiffres suivants rendent compte de ces relations.  $P$ , dans les tables, signifie l'épaisseur des solutions correspondant à  $\frac{1}{1000}$   $N$  où se trouvent les minima des courbes.

### Les premières bandes.

<i>Les sels</i>	<i>p.</i>
Luteohéxammines	280-300 <sup>mm</sup> .
Nitroammines	100-150 „
Héxanitrite	520 „
Nitritopentammine (isoxantho)	340 „

### Les secondes bandes.

Luteohéxammines	470 <sup>mm</sup> .
Héxanitrite	56 „
Nitritopentammine (isoxantho)	45 „
Xanthopentammine	4 „
Crocéo et Flavotétrammines	8 „
Trinitrotriammine	4 „
Tétranitrodiammine	5 „
Monohydroxymononitrotétrammine	9 „
Monochloromononitrotétrammine	18 „
Oxalodinitrodiammine	7 „

La troisième bande à 4000 de fréquence, n'existe que dans les solutions très étendues ( $\frac{1}{10000}$   $N$ ) des sels qui contiennent plus de deux nitros, parmi lesquels deux sont à la position de trans, comme je l'ai indiqué plus haut.

Quant aux épaisseurs des minima ( $p$ ) où commence l'absorption pour la troisième bande, elles ne diffèrent pas beaucoup les unes des autres entre ces trois corps.

<i>Les sels</i>	<i>p</i> (correspondant à la concentration de $\frac{1}{10000} N$ )
Crocéotétrammine	17 <sup>mm</sup> .
Trinitrotriammine	13.5 „
Tétranitrodiammine	11 „

En résumé, on peut tirer de là quelques lois données ci-dessous, à l'égard de l'absorption des sels ammine-complexes qui contiennent des nitros ou de nitrito dans leurs ions complexes.

1°- Les nombres des groupes du nitro dans l'ion complexe influent peu sur la quantité et la qualité d'absorption, parce que le mono-, di-, tri- et tétranitroammines montrent de très semblables courbes d'absorption, si l'on met la troisième bande à part.

2°- L'absorption ne dépend ni du signe, ni des valeurs des ions complexes, parce qu'ils absorbent très semblablement les uns et les autres, sauf la troisième bande, bien que le xanthopentammine, le crocéo- et flavotétrammines et le mononitrohydroxytétrammine soient les cations respectivement de di- et monovalence, et que le tétranitrodiammine et le dinitrooxalodiammine soient les anions de monovalence, tandis que le trinitrotriammine est une molécule sans charge d'électricité.

3°- Les nitros à la position de trans donnent la troisième bande dans les solutions très étendues de  $\frac{1}{10000} N$ , A part ce point, les sels stéréoisomériques, comme crocéo-et flavotétrammine absorbent tous également.

4°- Le cobaltihéxanitrite et le nitritopentammine (isoxantho) absorbent bien semblablement l'un et l'autre. Sans doute, la même construction du groupe du nitrite *ONO* dans les ions complexes a causé cette ressemblance de l'absorption.

## VI. Isosulfocyanopentammine

La courbe d'absorption du chlorure de ce complexe  $[Co(NH_3)_5(NCS)]Cl_2$  a deux bandes très nettes à 1950 et à 3350 de fréquence. La première est un peu bathochrome et la deuxième sensiblement hypsochrome, comparée avec les bandes du lutéohexammine.



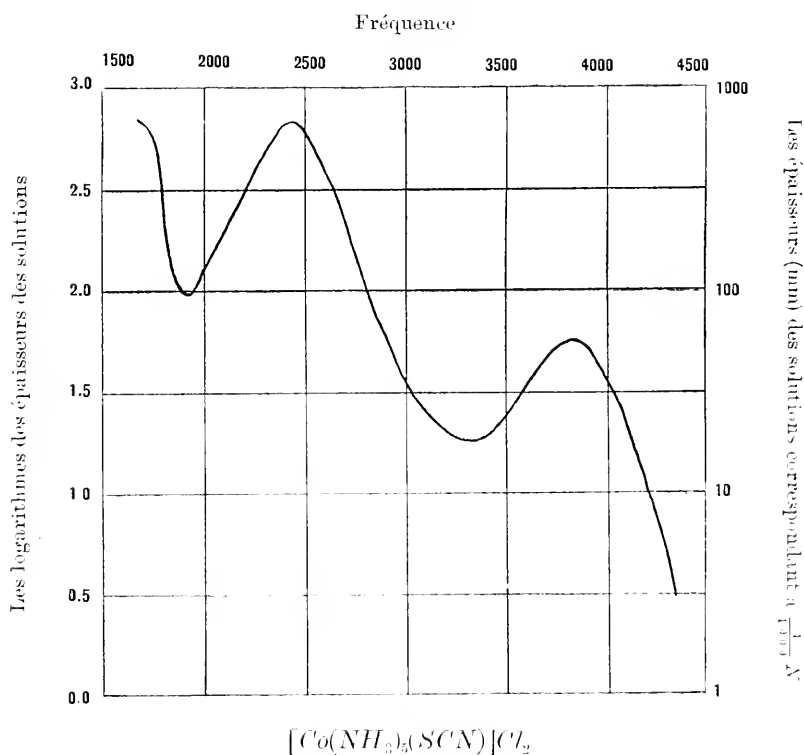
## La première bande

	<i>fréquence</i>	<i><math>\rho</math>.</i>
Lutéohéxammine	2100	300 <sub>mm.</sub>
Isosulfocyanopentammine	1950	100 „

## La deuxième bande

Lutéohéxammine	3000	470 <sub>mm.</sub>
Isosulfocyanopentammine	3350	18 „

Fig. XIV



Il est bien remarquable que la forme et la position des bandes de ce sel complexe sont presque les mêmes que celles de la solution alcoolique du sulfocyanate de cobalt:  $Co(SCy)_2$ <sup>1)</sup>, bien que les couleurs des deux solutions soient très différentes: la solution aqueuse d'isosulfocyanopentammine est brune rougeâtre, tandis que la

1) A. Hantzsch und Y. Shibata: Zeitsch. anorg. Chem., 1911 **73**, 309.

solution alcoolique du sulfocyanate de cobalt a la couleur bleue vive.

Pourtant, si l'on examine d'un peu plus près les deux courbes, on trouve bien facilement que la raison de cette contradiction superficielle réside dans la différence des positions des minima d'absorption (des maxima des courbes). En l'isosulfocyanatopentammine (Fig. XIV), ce point se trouve à 700<sub>mm</sub> de l'épaisseur de la solution correspondant à  $\frac{1}{1000} N$ , tandis que dans le cas du sulfocyanate de cobalt, le minimum d'absorption se place à une épaisseur tellement grande qu'on n'en a pu trouver trace dans la concentration en question.

Or la solution alcoolique du sulfocyanate de cobalt laisse passer les rayons entre le bleu et le violet, tandis que la solution aqueuse assez concentrée (ou assez épaisse) de l'isosulfocyanatopentammine absorbe tous les rayons plus courts que 6000 Å; c'est-à-dire qu'elle est transparente seulement pour le rouge et le jaune.

## VII. Praséotétrammine

La substitution de deux atomes d'halogène à deux molécules d'ammoniac du lutéohexammine produit deux stéréoisomères: le praséotétrammine (trans) et le violéotétrammine (cis). Les deux sels qui sont respectivement colorés en vert et en violet, sont assez stables à l'état solide, cependant leurs solutions aqueuses changent rapidement leurs couleurs et prennent à la fin la même couleur carmine. Seulement le chlorure de chloropraséodithylènediamine  $\left[Co \frac{Cl^{(1)}}{Cl^{(2)}}\right]Cl$  étant un peu plus stable que ses autres dérivés, j'ai préféré ce corps pour l'objet de cette recherche d'absorption.

Comme on le voit dans la figure XV, la forme de la courbe d'absorption montre une anomalie: c'est-à-dire qu'elle ne renferme qu'une seule petite bande à 2100 de fréquence dans l'échelle spectrale mesurable. Cependant, la branche descendante de la courbe au rouge indique qu'il y aurait très probablement une large bande à l'infrarouge.

La courbe qui est indiquée par les lignes brisées est celle de la solution du praséotétrammine qui a été laissée pendant 24 heures pour faire complètement changer la couleur. On y aperçoit facilement la ressemblance entre les formes de cette dernière et

celles du chloropurpuréotétrammine et du roséotétrammine. Alors, le changement de la couleur de la solution du praséotétrammine du vert au rouge s'est passé vraisemblablement dans le sens suivant :

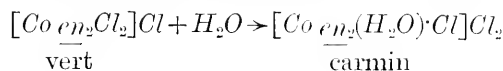
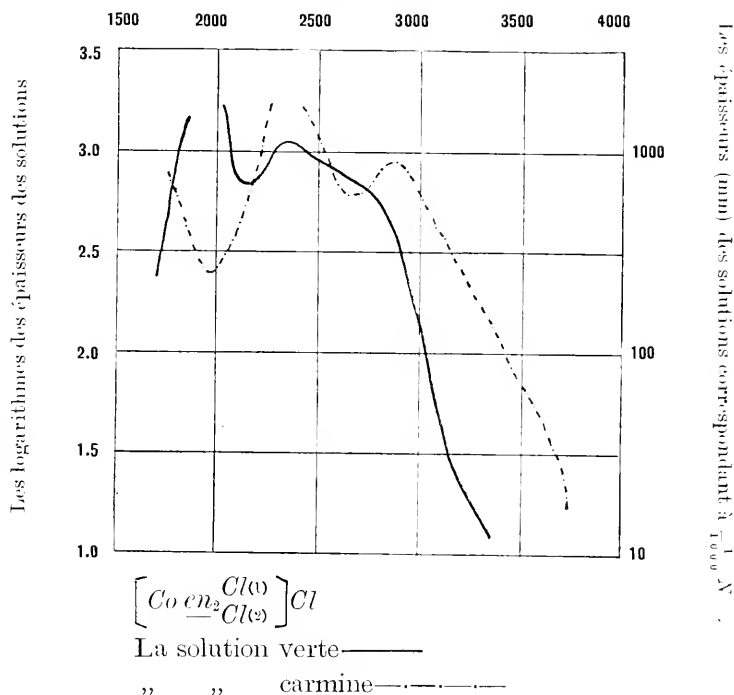


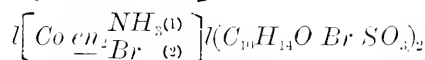
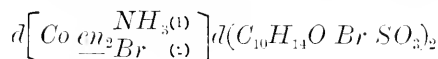
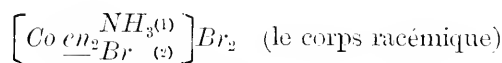
Fig. XV

Fréquence



### VIII. Bromopurpuréopentammine et Mononhydroxypentammine (série du rhodocobalticomplexe.)

Pour la première sorte des complexes, les trois combinaisons suivantes sont choisies :





Tous les sels de cette série ont la couleur violette fade, tandis que leurs solutions sont colorées en carmin. Bien que le bromure et le bromocamphersulfonate fassent des anions d'une grandeur très différente, et de même que deux bromocamphersulfonates soient les antipodes optiques l'un de l'autre, leurs courbes d'absorption (Fig. XVI) coïncident très bien l'une à l'autre. Voilà encore un témoignage pour la conclusion, à laquelle je suis arrivé plus haut en telle sorte que la cause de l'absorption existe seulement aux points de connexion entre l'atome du cobalt et les atomes métalloïdes dans un ion complexe, et que, par conséquent, la grandeur moléculaire des anions importe peu à cet égard, dans le cas où ces anions eux-mêmes ne contiennent aucun chromophore. Pour cette même raison, les antipodes optiques doivent aussi également absorber.

La forme de ces courbes et celle du monohydroxypentammine, qui est un corps rouge et donne une solution de couleur carmine, montrent une exception curieuse, comme on, le voit dans les figures XVI et XVII; c'est-à-dire que chacune des courbes ne renferme qu'une bande à 2000 de fréquence. Cette ressemblance des courbes dans deux séries des complexes avec les atomes de très différents caractères dans les ions complexes, comme  $[(NH_3)_5CoOH]^{++}$  et  $[en_5CoBr^{NH_3}]^{++}$ , est encore inexplicable. Si cela se rencontre seulement par hasard, ou s'il y a quelque raison à cela, je laisse la question à futures recherches.

### Résumé

1°- Lorsque l'atome de cobalt fait un ion complexe en se coordonnant avec les atomes métalloïdes ou avec quelques groupes de ces atomes, la cause de l'absorption des rayons se trouve au point de connexion de l'atome cobaltique avec les atomes métalloïdes. L'absorption caractéristique à l'atome du cobalt, qui est causée probablement par l'électron relâché de ce dernier élément métallique, est très peu influencée par des substitutions quelconques dans l'ion complexe.

2°- La cause de l'absorption existe également dans les atomes métalloïdes qui sont liés directement avec l'atome du cobalt.

Mais, dans ce cas, la bande d'absorption sera plus ou moins sensiblement déplacée par les substitutions dans l'ion complexe.

3°— Si les constitutions chimiques des ions complexes cobaltiques sont semblables entre elles, leur absorption est aussi semblable, et de même, si les atomes métalloïdes dans un groupe de pareil caractère, sont égaux, la complexité et la grandeur moléculaire de ce groupe import peu à l'égard de l'absorption. Par exemple, l'éthylènediamine-complexe et l'ammine-complexe correspondant absorbent bien semblablement, tandis qu'il n'en est pas de même dans le cas de nitroammines et du nitritoammine.

4°— Les différences des signes et des valeurs des ions complexes cobaltiques n'influent presque pas sur l'absorption, si les ions sont pareillement construits. Les antipodes optiques et le corps racémique ne montrent aucune différence d'absorption non plus.

5°— En général, les isomères stéréochimiques absorbent différemment. Dans le cas du praséotétrammine (trans) et du violéotétrammine (cis), par exemple, leurs couleurs à l'oeil nu sont déjà très différentes, tandis que le flavotétrammine (cis) et le crocéotétrammine (trans) absorbent également jusqu'à la concentration de  $\frac{1}{1000} N$ ; mais dans une dilution plus grande ( $\frac{1}{10000} N$ ), le crocéotétrammine montre encore une bande à 4000 de fréquence.

Je me fais un devoir d'adresser ici à Mr. le Professeur G. Urbain à la Sorbonne, qui m'a aidé de conseils bienveillants et a eu l'amabilité de me procurer les appareils nécessaires à ces expériences, lorsque je me trouvais à Paris, mes remerciements les plus sincères et les plus empressés.

Je suis aussi bien reconnaissant à mon préparateur privé Mr. T. Kato qui m'a donné ses aides vigilantes pour ce travail au Laboratoire de Chimie de l'Université impériale de Tōkiō.

Yuji Shibata

Juillet 1915.

## Considerations on the Problem of Latitude Variation.

By

**Kiyofusa SOTOME**, *Rikakushi*,

Assistant Professor of Astronomy, Tokyo Imperial University.

---

### Introduction.

This paper covers some studies on the zenith telescope as an astronomical instrument extensively used in observing the variation of latitude. Herein the writer intends to call attention to the fact that there are, according to his experience, some remarkable phenomena in the behaviour of the zenith telescope, and further, to show the possibility of finding a method of explaining the z-term and closing sum (schlussfehler) in the variation of latitude in connection with these phenomena. The development is made in the following three sections.

#### 1. Singular behaviour of the zenith telescope.

During the years 1906–1911, the writer was in charge of the observations of latitude variation in the Tokyo Astronomical Observatory, under the auspices of the Geodetic Committee. This was in continuation of the series of observations made successively by Professors H. Kimura and K. Hirayama. The instrument used was a zenith telescope of the usual form, made by Wanschaff in Berlin, No. 800, aperture 81<sup>mm</sup> and focal length 100<sup>mm</sup>.

In order to determine the value of one turn of the micrometer

screw. I made observations of polar stars at their greatest elongations every summer and winter. The total number of determinations during the period amounted to 58. When observing the polar stars in their eastern and western elongations, I found a remarkable fact, viz. that the bubbles of the two levels attached to the zenith telescope moved gradually towards the south, both in the eastern and the western positions of the telescope. Moreover, the magnitude of displacement was larger in winter than in summer, and it varied generally with the length of the observation. This can be seen from the following table, in which the first column is the date of observation, the second and third columns the bubble displacements of the first and second levels in units of division, the fourth the observed stars, the fifth the interval of observation, and the sixth the temperature of the observing room.

TABLE I.  
Telescope West.  
(+ increase, — decrease)

Date		Level I.	Level II.	Star	Interval	Temperature
		d	d		m	°
1906 August	4	+ 0.20	+ 0.05	Polaris	33	22.0
„ Sept.	5	0.00	+ 0.25	„	27	21.8
1907 August	17	+ 0.20	+ 0.10	51 H. Cephei	22	23.8
„ „	18	+ 0.15	+ 0.10	„	22	23.4
„ „	19	0.00	— 0.05	„	23	24.7
1908 August	21	+ 0.15	+ 0.05	„	22	23.0
„ „	22	+ 0.05	+ 0.25	„	23	25.5
„ „	26	+ 0.10	+ 0.05	„	25	22.6
„ „	27	+ 0.15	+ 0.50	„	23	22.6
1909 August	8	+ 0.15	+ 0.25	„	23	22.8
„ „	9	+ 0.35	+ 0.55	„	23	22.2
1911 Sept.	2	+ 0.20	+ 0.30	„	23	19.8
„ „	3	+ 0.15	+ 0.45	„	23	21.8
Mean		(+ 0.13)	(+ 0.18)			



Date		Level I.	Level II.	Star	Interval	Temperature
		d	d		m	°
1909 January	23	+ 0.15	+ 0.20	1 H. Draconis	8	1.0
" "	29	+ 0.45	+ 0.25	"	8	99.8
" "	30	+ 0.35	+ 0.25	"	8	99.9
" "	31	+ 0.25	+ 0.50	"	8	2.6
1910 February	2	+ 0.50	+ 0.30	"	8	0.4
" "	7	+ 0.05	+ 0.05	"	8	5.0
" March	5	+ 0.70	+ 0.85	2 Ursae Min.	19	98.1
" "	7	+ 0.75	+ 0.70	"	19	0.8
" "	10	+ 0.85	+ 0.75	"	19	99.9
" "	13	+ 0.40	+ 0.55	"	19	0.3
1911 January	25	+ 0.85	+ 0.40	1 H. Draconis	8	2.2
Mean		(+ 0.42)	(+ 0.44)			

## Telescope East.

Date		Level I.	Level II.	Star	Interval	Temperature
		d	d		m	°
1909 July	24	+ 0.10	0.00	2 Ursae Min.	19	24.0
" "	25	0.00	+ 0.10	"	20	24.6
" "	28	- 0.20	- 0.25	"	20	24.1
" August	2	0.00	0.00	"	20	23.4
1910 October	26	- 0.25	- 0.25	76 Draconis	9	41.9
Mean		(- 0.07)	(- 0.08)			
1907 February	2	- 0.25	- 0.25	Gr. 750	14	96.8
" "	5	- 1.00	- 0.75	"	14	99.7
" "	9	- 0.20	- 0.35	"	14	99.2
" "	14	- 0.25	- 0.25	"	14	99.8
1908 January	12	- 0.59	- 0.65	Polaris	10	2.7
" "	16	- 0.60	- 0.65	"	50	2.6
" "	17	- 0.45	- 0.30	"	15	0.0
" February	22	- 0.10	- 0.15	Gr. 750	14	7.8

Date	Level I.	Level II.	Star	Interval	Temperature
	d	d		m	°
1909 January 16	- 0.10	- 0.20	Polaris	53	99.2
" " 17	- 0.55	- 0.45	"	56	98.6
1910 February 3	- 0.45	- 0.50	Gr. 750	14	0.8
" " 7	- 0.10	- 0.10	"	14	2.8
" " 9	- 0.35	- 0.45	"	14	2.0
" " 12	- 0.50	- 0.65	"	14	98.5
" " 15	- 0.45	- 0.45	"	14	0.7
" March 5	- 0.70	- 0.35	51 H. Cephei	23	98.0
" " 7	- 0.20	- 0.35	"	23	0.2
" " 10	- 0.60	- 0.60	"	23	99.4
" " 13	- 0.45	- 0.50	"	23	0.6
1911 February 3	- 0.30	- 0.10	Gr. 750	14	0.6
" " 4	- 0.10	0.00	43 H. Cephei	8	2.2
" " 7	- 0.60	- 0.60	Gr. 750	14	0.0
" " 9	- 0.30	- 0.45	"	14	99.7
" " 10	- 0.50	- 0.35	43 H. Cephei	16	3.3
" " 11	- 0.15	- 0.45	"	16	6.6
" " 12	- 0.50	- 0.45	"	16	2.5
" " 21	- 0.30	- 0.45	"	7	3.8
" " 22	- 0.45	- 0.30	"	16	5.4
" March 2	- 0.55	- 0.50	"	16	7.8
Mean	(- 0.40)	(- 0.41)			

1<sup>d</sup> of I=1."151<sup>d</sup> of II=1."15

From this table we see the fact that the displacement in the winter is about four times as large as that in the summer, when reduced to the same interval.

Under such circumstances, the question suggested itself, in making the reduction of observations, "Does the bubble displacement correspond exactly to the change of inclination of the telescope?"

Thereupon I made tentative reductions from two extreme standpoints:

- I. The displacement of bubbles is entirely due to some cause in the level itself, and is not due to the variation of inclination of the telescope. The telescope did not move during the observation.
- II. The displacement corresponds exactly to the change of inclination of the telescope. This is the assumption usually adopted. In the reduction, the change between two readings was considered to be proportional to the time interval.

With the first assumption, western elongation gave a greater value of the micrometer than eastern elongation; with the second assumption, on the contrary, eastern elongation gave a greater value than western elongation.<sup>1</sup> This fact is easily seen from the series of observations during February-March 1910, in the following table, in which the first column is the date, the second the polar stars, the third the elongations, the fourth the micrometer value with the first assumption, and the fifth the same with the second assumption.

TABLE II.

Date			Star	Elongation	Micrometer Values with the Assumption	
					I.	II.
1906	August	4	Polaris	E	51.7682	51.7701
"	September	5	"	E	579	583
1907	February	2	Gr. 750	W	619	595
"	"	5	"	W	712	651
"	"	9	"	W	698	682
"	"	14	"	W	638	622
"	August	17	51 H. Cephei	E	623	634
"	"	18	"	E	645	653
"	"	19	"	E	654	659
1908	January	12	Polaris	W	706	654
"	"	16	"	W	723	637
"	"	17	"	W	732	698
"	February	22	Gr. 750	W	638	634

<sup>1</sup> Western elongation was observed in the eastern position of the telescope and eastern elongation in the western position.

Date			Star	Elongation	Micrometer Values with the Assumption	
					I.	II.
1908	August	21	51 H. Cephei	E	51"597	51"603
"	"	22	"	E	658	665
"	"	26	"	E	625	630
"	"	27	"	E	651	654
1909	January	16	Polaris	W	687	678
"	"	17	"	W	681	661
"	"	23	1 H. Draconis	E	668	678
"	"	29	"	E	656	675
"	"	30	"	E	692	708
"	"	31	"	E	669	690
"	July	24	2 Ursae Min.	W	662	665
"	"	25	"	W	659	662
"	"	28	"	W	645	630
"	August	2	"	W	643	643
"	"	8	51 H. Cephei	E	667	679
"	"	9	"	E	619	644
1910	February	2	1 H. Draconis	E	637	660
"	"	3	Gr. 750	W	708	683
"	"	7	1 H. Draconis	E	675	678
"	"	7	Gr. 750	W	689	684
"	"	9	"	W	747	724
"	"	12	"	W	667	651
"	"	15	"	W	687	662
"	March	5	2 Ursae Min.	E	664	708
"	"	5	51 H. Cephei	W	639	629
"	"	7	2 Ursae Min.	E	662	705
"	"	7	51 H. Cephei	W	658	642
"	"	10	2 Ursae Min.	E	692	741
"	"	10	51 H. Cephei	W	721	693
"	"	13	2 Ursae Min.	E	630	655
"	"	13	51 H. Cephei	W	689	664

Date			Star	Elongation	Micrometer Values with the Assumption	
					I.	II.
1910	October	26	76 Draconis	W	51.5620	51.5606
1911	January	25	1 H. Draconis	E	631	698
..	February	3	Gr. 759	W	652	634
..	..	4	43 H. Cephei	W	707	704
..	..	7	Gr. 759	W	734	700
..	..	9	..	W	663	641
..	..	10	43 H. Cephei	W	717	693
..	..	11	..	W	646	629
..	..	12	..	W	716	683
..	..	21	..	W	674	652
..	..	22	..	W	705	683
..	March	2	..	W	629	598
..	September	2	51 H. Cephei	E	595	609
..	..	3	..	E	583	619

Although systematically different values are obtained from the different elongations on the different assumptions, the mean value from both elongations on the first assumption is nearly equal to that from both elongations on the second assumption. So these mean values may be looked upon as giving approximately the real value of the micrometer.

An assumption, to hold good, must be of such a nature as to yield theoretically the same value from both elongations. From this point of view both of the above assumptions are to be rejected, and we must find an intermediate one which will bring both elongations into conformity.

It is manifest that such a reduction, provided its validity be definitely granted, will need a diminishing factor less than unity. In order to determine the diminishing factor I made a complete reduction of my series of elongation observations, forming the equations of condition in the following form,—

$$A + Bt + C\theta = a + Db$$

where A.....unknown constant  
 B.....yearly change of the micrometer value  
 C.....temperature coefficient  
 D.....diminishing factor  
 t.....time  
 $\theta$  .....temperature  
 a.....value of micrometer corresponding to the first assumption.  
 b.....excess of the micrometer value on the second assumption over that on the first assumption.

For the sake of convenience, I took the year 1910.0 and  $7^{\circ}.0$  for the origin of the time and temperature respectively.

Assigning equal weights to all the equations of condition, I treated them by the method of least squares. The solution of the normal equations gave, among others, as the most probable value of the diminishing factor D,

$$D = 0.54 \pm 0.17 \quad \text{mean error.}$$

This result shows that the regular displacement of the level bubbles is due to two different causes :

- I.....A southward displacement of the bubbles due to some cause in the level, independent of the motion of the telescope. This accounts for about half of the total motion.
- II.....A regular northward depression of the telescope, corresponding to nearly half of the total displacement of the bubbles.

Owing to these phenomena we should obtain for the micrometer too large a value from western elongation and too small a value from eastern elongation on the first assumption; conversely, too large a value from eastern elongation and too small a value from western elongation on the second assumption.

The first phenomenon may possibly be a disturbance due to the heat of the observer and of the reading lamp. When observing latitude by the Talcott-Horrebaw method, the proximity of the observer to the instrument is of short duration; so that the effect would

not appear, owing to a reason to be discussed later. And, even if the effect of this were considerable, it would be eliminated from the final result, as the relative position of the observer and the levels does not change in the two positions of the telescope. Therefore I did not try to make any further investigation on this point.

As to the second phenomenon, we can take into consideration the following three causes. —

- i. Flexure of the telescope.
- ii. Differential change of the telescope stand.
- iii. Gradual tilting of the pier and the ground.

A gradual change of the flexure of the telescope tube may be probable, according to K. Hirayama<sup>1)</sup>, although it does not seem to be very effective, considering the structure of our zenith telescope. And this cannot be the sole cause; for if it were, the displacement of the bubble must be wholly attributed to a cause in the level itself, as the flexure of the telescope would by no means appear on the level. As this consequence is of course unnatural and also improbable, we are led to seek some other causes. At any rate, as the effect of flexure on latitude from the observation of a star pair, when we begin with the southerly star, has the tendency to cancel that from a star pair, when we begin with the northerly star, the final effect will tend to vanish, if these distinct pairs are impartially contained in a group. Moreover, even if there be a residual, it would be eliminated by the chain method reduction, as it can be looked upon as persistent with the star pairs. So I shall not attempt any further discussion of this subject.

As to the disturbance of the telescope mounting, I can first of all take into consideration the thermal effect of the observer's body and the unsymmetry of the meteorological conditions with respect to the instrument. In winter the wind blows mostly from the north, producing a draught of cold air; in summer, the south wind prevails, forming a warm air current. These disturbances, combined together, may cause a certain unsymmetrical distribution of heat in the telescope mounting in some way, and therefore a certain change in the inclination of the telescope. As the heating

---

1) *Astronomische Nachrichten*, Nr. 4332.

effect varies with the difference of temperature between the body and the instrument, the disturbance would vary inversely with the temperature, i.e., it would be greater in winter than in summer. This sequence agrees well with the observed phenomenon, and we may take this thermal effect as one cause of the behaviour of the zenith telescope.

With respect to the third cause, I may notice the fact that the horizontal pendulum observers in several parts of the world have revealed a remarkable unsteadiness of the ground. The most conspicuous of the regular movements has a period of one solar day, being due to the effect of the solar radiation on the earth's surface.

E. von Rebeur-Paschwitz did pioneer work with the horizontal pendulum of his original form at Karlsruhe (1887), Strassburg (1892-94), and Nicolaiew (1892), to the effect that the pendulum swinging in the prime vertical showed a regular movement in the period of one solar day, and took the southernmost position in the evening and the northernmost position in the morning, as is here shown, —<sup>1)</sup>

TABLE III.

Component in the meridian (pendulum swinging in the prime vertical) North +, South -.

Local Mean Time	Karlsruhe	Strassburg	Nicolaiew
0	+0.083	+0.017	+0.040
2	-0.035	-0.015	+0.024
4	-0.151	-0.057	+0.033
6	-0.200	-0.079	-0.016
8	-0.184	-0.034	-0.030
10	-0.192	-0.034	-0.037
12	-0.108	-0.011	-0.037
14	-0.016	+0.015	-0.029
16	+0.135	+0.050	-0.010

1) Astronomische Nachrichten, Nr. 3148.



Local Mean Time	Karlsruhe	Strassburg	Nicolaiew
$18^h$	+0. 225	+0. 073	+0. 013
20	+0. 237	+0. 065	+0. 035
22	+0. 204	+0. 041	+0. 045

His result at Strassburg (1892-94) was expressed in the following résumé :<sup>1)</sup>

The epoch of daily minimum or southern elongation of the pendulum lies generally between  $5^h$  and  $6^h$ . The daily maximum or northern elongation comes always in the morning between  $18^h$ - $20^h$ , or slightly later in winter. The amplitude varies between 0."1 and 0."2.

After the early death of von Rebeur, Ehlert took charge of the observations at Strassburg (1895-96). His result was quite similar to that of his predecessor, as may be seen from the table below.<sup>2)</sup>

TABLE IV.

Date	Southern elongation	Northern elongation	Amplitude
Jan. 15	3. 0	$20^h$ 5	0. 039
Feb. 15	3. 5	20. 0	0. 067
March 15	5. 5	20. 8	0. 138
May 1	6. 0	18. 0	0. 201
May 23	5. 9	18. 0	0. 138
June 15	5. 7	17. 9	0. 124
July 15	5. 3	17. 9	0. 135
Aug. 15	6. 0	19. 2	0. 187
Sept. 15	5. 5	20. 2	0. 208
Oct. 15	4. 5	20. 5	0. 053
	November and December, indeterminate		
Mean	$5^h$ 1	$18^h$ 9	

1) Gerlands Beiträge zur Geophysik, B.I. II.

2) Ditto B.I. IV.

He concludes :

Die „tägliche Periode“ besteht in einer Schwankung des Erdbodens, welche im Mittel 0."112 beträgt : in der Tiefe von 5 m findet das Maximum der Nordablenkung im Mittel um 18<sup>b</sup>.9, derjenigen nach Süd um 5.<sup>b</sup>1 statt. Die Ursache liegt in der Ausdehnung der von der Sonne erwärmten Erdoberfläche, welche sich auch nach der Tiefe hin unter Abschwächung und Verzögerung geltend macht.....Klarer Himmel und grosse Temperaturoscillation verstärken das Phenomen.....

According to Hecker's long series of observations at Potsdam in an underground room at the depth of 25 metres (1902–1909)<sup>1)</sup>, the pendulum occupied the extreme southern position in the evening and northern in the morning, just as in the preceding cases.

	Southern elongation	Northern elongation
March, April, May	6 <sup>b</sup>	17 <sup>b</sup>
June, July, August	6 <sup>b</sup>	18
September, October, November	6 <sup>b</sup>	15 <sup>b</sup>
December, January, February	6 <sup>b</sup>	15 <sup>b</sup>

The horizontal pendulum observations at Kyoto (1910–1911) by Shida<sup>2)</sup> gave a similar result, showing a solar daily variation mainly in a SW and NE direction: the pendulum took the extreme south-west position in the evening and the extreme north-east position in the morning. The elongations in the meridian run as follows: —

1) Veröffentlichung des Königl. Preussischen Geodatischen Institutes, Neue Folge Nr. 32, 49.

2) Memoirs of the College of Science and Engineering, Kyoto Imperial University, Vol. IV.

	Southern elongation	Northern elongation
April - June	8 <sup>h</sup>	21 <sup>h</sup>
July - September	10 <sup>h</sup>	21 <sup>h</sup>
October - December	6 <sup>h</sup>	20 <sup>h</sup>
January - March	6 <sup>h</sup>	20 <sup>h</sup>

Observations at Freiburg i. S. made by Hecker at a depth of 190 metres below the surface of the ground (1910-1911) scarcely showed the solar effect. It was almost insensible or negligible, the amplitude not exceeding 0."001. From these facts we can infer that the solar thermal effect is the more pronounced the shallower the ground work, as might also be guessed from mere conjecture.

While most horizontal pendulum rooms are deep and are kept in as invariable a temperature as possible, our astronomical telescope piers are, on the contrary, rather shallowly founded and are subjected to the diurnal change of temperature in its full range, from their exposure to the free air. Moreover, astronomical observations are naturally only practicable in clear weather, when the change of temperature of the environment of the pier is great and rapid. Under these circumstances we are led to conclude that the ground and pier, on which the telescope is set up, are undergoing a continuous tilting whilst it is being used in the night, the meridian component of which is in the direction, north downward or south upward, and the magnitude of which is far greater than that experienced in the horizontal pendulum observations. There is, however, a contradiction between the European and Japanese observations. In Europe the amplitude is at its maximum in summer and its minimum in winter; in Japan<sup>1)</sup>, on the contrary, it is at its maximum in winter and its minimum in summer. This difference may be due to some meteorological causes, depending on the latitude. For low latitudes the latter variation may hold good. It is also

1) Shida, loc. cit.

to be noticed that the rate of the tilting motion increases from evening until midnight.

In this way we are led to the conclusion that the observed phenomenon is to be understood as principally due to the second and third of the above causes, whose effects can be looked upon as generally varying inversely with the temperature during the time of our observations.

The above cited singular behaviour of the zenith telescope was deduced from the regular shift of the level bubbles, as experienced by myself. In order to ascertain whether the same phenomenon is noticed in other observatories, I made enquiry of several latitude observers in various parts of the world respecting this subject. Fortunately, almost all the specialists were kind enough to favour me with detailed answers, for which the writer tenders his most sincere thanks.

Prof. H. Kimura and Dr. M. Hashimoto of the Mizusawa Latitude Observatory recognized the phenomenon in the zenith telescope there used. We can also see the tendency from the results of their elongation observations, as given in "Resultate des Internationalen Breitendienstes," Bd. I., pp. 19-20. In the determination of the value of the micrometer during the period 1899 Dec. 27-1900 March 11, eastern elongations constantly give larger values than western. This corresponds to the case when the reduction was made on assumption II. (*supra*).

I could hear nothing from Tschardui observers. But the series of determinations given in "Resultate," Bd. IV., page 74, makes me suppose that there is also the same tendency there. In the observations during the period 1906 January 19—February 28, the mean value from western elongations (60."268) is decidedly larger than that from eastern elongations (60."148). This may be caused by the method of reduction on assumption I. If such is really the case at Tschardui, we can fairly well account for the fact that the temperature coefficient of the Tschardui micrometer comes out notably larger than those of the other stations. This is because winter observations are principally of western elongation while summer observations are mostly of eastern elongation; so that the

winter value comes out too large, but the summer value too small, giving finally too large a temperature coefficient.

Dr. G. Bemporad of the International Latitude Station at Carloforte reported that his instrument showed variations during elongation observations, but that the sense was not systematic. However, Dr. V. Fontana, the director of the station, wrote me afterwards that he had begun some researches on the problem of the systematic shift of the level bubbles, and desired to know my results.

Dr. F. E. Ross of the Gaithersburg Latitude Observatory informed me that he experienced a similar phenomenon, and considered it to be principally due to a temperature effect in the ground, which usually shows a progressive change one way or the other.

Dr. E. I. Yowell of Cincinnati Observatory favoured me with a letter, stating that his telescope shows a similar tendency. He ascribes that effect to the heat radiation from the observer and the reading lamp.

Dr. W. F. Meyer of the Latitude Observatory at Ukiah kindly reported that his own experience was limited, but that his predecessor, Dr. Schlesinger, had observed the same tendency. The following was extracted from the record book, which gives Dr. Schlesinger's opinion in the matter: "there is reason to believe, from an inspection of the results, that these changes in the levels are not wholly due to a real change of inclination of the telescope. No doubt the presence of the observer for so long a period at one side of the levels has an injurious effect upon the levels."

At Union Observatory, Johannesburg (Astronomer, Prof. R. I. Innes), the method of polar star elongations was not employed.

At Kasan Observatory (Dr. M. A. Gratschew) the instrument and method were different.

The following astronomers have kindly let me know that they experienced no systematic movement of the level bubbles.

Prof. E. Doolittle of Flower Astronomical Observatory, University of Pennsylvania. (Warner & Swasey's zenith telescope).

Prof. J. Bonsdorff of Pulkovo Observatory.

Dr. E. Schoenberg of the University Observatory at Jurjew (Dorpat): (transit instrument of broken type made by Repsold).

After all, it may be concluded that the majority of the most careful latitude observers (especially the international observers) experience a systematic shift of the level bubbles, in the same manner as I have already described.

Thus I have reached the position of being able to make the following résumé, in so far as I have obtained results from the above investigations:—

In most cases the level bubbles of the zenith telescope make a southward shift systematically, when the observer has been near the telescope for a tolerably long time, the magnitude of which varies inversely with the temperature.

This movement may be considered as due, partly to the observer's direct effect on the level, and partly to the tilting of the telescope mounting, owing to the observer's heat disturbance, in conjunction with some meteorological conditions. The regular change in the ground from the solar radiation may also contribute to the latter, although to a comparatively slight degree.

It may not be out of place to remark that we may expect the counter effect to the above phenomenon; that is, when the observer recedes from the instrument after a tolerably long stay near it, the bubble would move back in a northerly direction towards its original position, being freed from the thermal disturbance. This was often experienced by some observers. It seems also to be very desirable from my standpoint that hereafter the elongation observations of polar stars should be more frequently and regularly made and the reduction performed more exhaustively, so as to throw further light upon the subject.

## 2. A theory of the motion of the level Bubbles.

In using a screw micrometer we are accustomed to eliminate

the so-called "dead motion" of the screw by turning it always in the same direction. The same principle is applied in determining the value of a division of the spirit level, always making the bubble come to rest from the same direction. This precaution implicitly recognizes the existence of a failure in the function of the level. It seems to me rather curious that in the practical work of star observation the level is taken as a perfect instrument and the precaution needed in the above case is utterly neglected. Here I intend in the following lines to show that there actually exists such a failure in the function of the spirit level. I will first proceed from the theoretical standpoint and then give an experimental proof.

The motion of a level bubble can be looked upon as analogous to a damped oscillation of a simple pendulum; the equation of motion accordingly takes the following form, —

$$\frac{d^2\theta}{dt^2} + 2p \frac{d\theta}{dt} + n^2\theta = 0$$

where  $p$  and  $n$  are constants and  $\theta$  is the deviation of the bubble from the position of equilibrium. The applicability of this equation was experimentally tested by Bonsdorff<sup>1)</sup> and further discussed by Orloff.<sup>2)</sup>

The integral of this differential equation comes out in the following three forms, according to the cases,  $n > p$ ,  $n = p$ ,  $n < p$  respectively, —

$$(i) \quad n > p, \quad \theta = e^{-pt} \{a_1 \cos pt + a_2 \sin pt\}$$

$$(ii) \quad n = p, \quad \theta = e^{-pt} \{a_3 t + a_4\}$$

$$(iii) \quad n < p, \quad \theta = b_1 e^{-a_5 t} + b_2 e^{-a_6 t}$$

$$\text{where} \begin{cases} p^2 = n^2 - p^2 \\ a_5 = p \left\{ 1 - \sqrt{1 - \frac{n^2}{p^2}} \right\} \\ a_6 = p \left\{ 1 + \sqrt{1 - \frac{n^2}{p^2}} \right\} \end{cases}$$

Here the quantity  $n$  depends on the radius of curvature of the level, and the quantity  $p$  is a function of the bubble length and of the viscosity of the liquid.

1) Mitteilungen der Nikolai-Hauptsternwarte zu Pulkowo, Bd. II, p. 43.

2) Ditto

Bd. II, p. 137.

When the radius of curvature is small, and the bubble length fairly long, the case (i) occurs, exhibiting a periodic motion. But in the sensitive level, the radius of curvature is necessarily long, but the bubble length cannot be proportionately long. This class of instrument corresponds to the cases (ii) or (iii), which represent an aperiodic motion. In these two cases the bubble comes to rest asymptotically, that is, after the lapse of an infinite time. In other words, the bubble of our sensitive level does not come to its destination theoretically in a finite time. In practice, however, to wait even a pretty long time is useless, as some other disturbing cause may interfere with it in the meanwhile.

Let  $t_1$  be the time interval, during which we wait for the resting of the bubble (practically, a minute or two), and  $\theta_1$  the corresponding value of  $\theta$ . Thus, —

$$\theta_1 = e^{-\rho t_1} (a_3 t_1 + a_4) \quad \text{or} \quad \theta_1 = b_1 e^{-a_5 t_1} + b_2 e^{-a_6 t_1}$$

Then we are referring to  $\theta_1$  instead of 0 as the resting point of the bubble. As this discrepancy can be looked upon as caused by internal friction or viscosity of the liquid, the sense of  $\theta_1$  will be naturally opposed, when the direction of motion is opposite, giving  $-\theta_1$ . Therefore, when the bubble has moved from opposite directions the resting points would differ by the quantity  $2\theta_1$ . This property would afford a method of determining the magnitude of  $\theta_1$ , which we may call the resistance of the level.

The occasional lack of parallelism in the two level bubbles of the zenith telescope, commonly experienced by latitude observers, can partly be explained by the above phenomenon, as the parallelism would change by the sum of the resistances of the two levels, when the two bubbles come to rest from opposite directions.

Having thus examined the existence of a defect of the level from the theoretical standpoint, I proceed now to ascertain the order of magnitude of the resistance  $\theta_1$  from the experimental side, depending on the principle cited above.

The instrument I made use of in my experiments was a level trier made by Hildebrand in Freiburg, and the levels subjected to the examination were the following nine pieces : —



- No. 1.        The hanging level of the transit instrument,  
                 Bamberg No. 7958.
- Nos. 2, 3.    The latitude levels of the above.
- No. 4.        The hanging level of the transit instrument,  
                 Bamberg No. 7959.
- Nos. 5, 6.    The latitude levels of the above.
- No. 7.        The hanging level of the transit instrument,  
                 Bamberg No. 11508.
- Nos. 8, 9.    The latitude levels of the above.

First the level was fitted to the trier in such a way that the bubble moved in increasing sense of division in accordance with the increase of the micrometer reading of the trier. Then the micrometer was turned in increasing sense and set, say, to a reading  $\alpha$ . The bubble would move increasingly and come to rest at  $\beta - \theta_1$ , where  $\theta_1$  is the resistance. Next, the micrometer was further turned slowly up to, say, division  $\alpha + 10$ . Hereupon it is turned back to  $\alpha - 1$ ; then again it is set at the reading  $\alpha$ , theoretically bringing the level back to the original position. To this operation the bubble conforms with considerable lag of time, owing to its inertness, and would come to rest in decreasing sense at the point  $\beta + \theta_1$ . Let the reading of the bubble centre for the first position be  $S_1$  and for the second position be  $S_2$ , then we have

$$\theta_1 = \frac{1}{2} (S_2 - S_1).$$

This process was applied to two such points alternately; for the first point, the motion was in the order increasing-decreasing, for the second point in the order decreasing-increasing. This will eliminate the effect of the gradual change of the pier, not to speak of determining the value of one division of the level. The result of my experiments is given in the following table V, in which the resistance  $\theta_1$  is expressed in terms of the unit of division of the levels.

TABLE V.

Level	Date		Bubble Length	Resistance $\theta$	No. of Observations
No. 1.	1915 Feb.	17	$d$ 24	$d$ 0.031	58
	" "	18	24	0.012	30

1 division = 1."32

No. 2.	1913 Dec.	31	$d$ 24	$d$ 0.022	52
	1914 Jan.	8	24	0.026	42
	"	10	24	0.035	44
	"	12	24	0.042	24
	"	13	24	0.047	32
	"	15	23	0.029	28
	"	31	20	0.049	50
	Feb.	7	20	0.031	26
	"	12	21	0.029	54
	"	28	20	0.029	24

1 division = 1."32

No. 3.	1913 Dec.	31	$d$ 26	$d$ 0.020	52
	1914 Jan.	8	26	0.012	52
	"	10	26	0.023	44
	"	12	27	0.016	24
	"	13	26	0.024	32
	"	15	26	0.050	28
	"	31	20	0.030	50
	Feb.	7	21	0.031	26
	"	12	21	0.060	54
	"	28	20	0.027	24

1 division = 1."33

Level	Date		Bubble Length	Resistance $\theta_1$	No. of Observations
No. 4	1915 Jan.	6	<sup>d</sup> 25	<sup>d</sup> 0.069	24
	"	16	27	0.025	18
	"	18	26	0.057	30
	"	19	26	0.062	34
	"	21	28	0.043	14
	Feb.	13	37	0.072	21

1 division = 1."22

No. 5	1914 Oct.	2	<sup>d</sup> 26	<sup>d</sup> 0.587	32
	"	4	26	0.464	28
	"	9	25	0.522	32
	1915 Feb.	14	26	0.479	52
	"	15	27	0.462	16
	"	16	27	0.441	28

(This level is not fit for use.) 1 division = 1."04

No. 6	1914 Oct.	2	<sup>d</sup> 26	<sup>d</sup> 0.053	32
	"	4	26	0.202	28
	"	9	25	0.080	32
	1915 Feb.	14	26	0.055	52
	"	15	27	0.047	16
	"	16	27	0.084	28

1 division = 1."06

No. 7.	1915 Feb.	20	<sup>d</sup> 24	<sup>d</sup> 0.045	42
	"	22	24	0.042	68

1 division = 1."06

No. 8	1915 Jan.	20	<sup>d</sup> 20	<sup>d</sup> 0.059	24
	"	21	20	0.073	20
	"	21	32	0.039	10

Level	Date	Bubble Length	Resistance $\theta_1$	No. of observations
No. 8	1915 Jan. 26	$d$ 33	$d$ 0.006	42
	„ 27	26	0.040	20
	„ 28	26	0.033	48
	„ 29	26	0.029	52
1 division = 1."26				
No. 9	1915 Jan. 20	$d$ 19	$d$ 0.079	24
	„ 21	19	0.060	20
	„ 21	33	0.020	10
	„ 26	34	0.010	42
	„ 27	25	0.040	20
	„ 28	25	0.022	48
	„ 29	25	0.021	52
1 division = 1."28				

These results show that the resistance  $\theta_1$  of the level is not of a negligible magnitude, so far as the degree of accuracy required in the zenith telescope observations is concerned, and we can take it as established that this defect is a common property of the spirit level, as we have confirmed its existence both from the theoretical and the experimental standpoints.

Hitherto we have been considering the motion of the bubble in case the level itself is at rest. But as the motion is purely of a relative nature, we can convert the above obtained result to the case when the bubble is at rest and the level moves.

Thus, when the level is put into slight movement from rest, the bubble will accompany it, and will fail to show the real movement of the level. If the movement of the level is less than or equal to the resistance  $\theta_1$ , as above obtained, the bubble would show no displacement relative to the level.

Moreover, when the level continues to move further, the bubble will follow it to a certain degree. The equation of motion

takes then the following form, taking the origin at the highest point of the level,—

$$-\frac{d^2\theta}{dt^2} + 2p\frac{d\theta}{dt} + n^2\theta = A$$

where the quantity  $A$  depends on the quality and movement of the level. Under the same conditions as before, in the case of our sensitive level, we have

$$\theta_{t_1} = \frac{A}{n^2} + \theta_1$$

This equation shows that another perturbing term interferes in this case. Thus it is to be concluded that the indication of the level bubble has an error greater than the resistance  $\theta_1$ , when the level itself is in motion.

Now I showed in the foregoing part of this essay that there are reasons to believe in an unsteadiness of the telescope and pier, not to speak of the seismic movement of the ground. From the above investigations, we see that the level cannot indicate instantaneously the varying position of the telescope in presence of these disturbances. So it is manifest that the spirit level which we now use is not suited to fulfilling our requirements with the degree of accuracy demanded in modern astronomical measurements. We are faced with the necessity of using some other means in order to realize the present expectations of practical astronomy.

### 3. Application to the Talcott-Horrebrow observations and deduction of effect on the variation of latitude.

In the first section of this essay I discussed certain systematic motions of the levels and zenith telescope, which can be looked upon as due, firstly, to the disturbance from the observer, and secondly, to a terrestrial cause. In the second section I investigated the failure of the function of the level which can be taken as a common defect of the level. Conversely, I can now conjecture how the telescope and level behave under such circumstances. When the observer approaches the telescope, the stand would first suffer a thermal disturbance, and cause the said effect, owing to the unsymmetry of meteorological conditions. To this the level bubble

will not respond immediately, because of the defect discussed above. When the disturbance has exceeded a certain limit, the level begins to indicate it to a certain degree. The thermal effect on the level would appear later, as the levels are more distant and better protected. After a fairly long time, the resulting effect would be the observed systematic shift of the level bubbles, in which the regular tilting of the ground partakes to some extent.

Now the observation of latitude variation is based on the cyclical system of star groups, consisting of pairs of stars selected for the Talcott observations. This method is the so-called chain method. As the result of this procedure, we obtained the polar motion and Kimura's  $z$  term. The closing sum is also a product of the chain method. The  $z$  term and closing sum form the principal enigmas of present-day practical astronomy.

Now for the first subject numerous causes have been proposed, among which we may mention the following, —

1. Yearly atmospheric refraction.
2. Yearly cosmic refraction.
3. Improper value of the parallax and proper motion of the observed stars.
4. Ditto of nutation and aberration.
5. Actual change in the earth's centre of gravity.
6. Result of computation.
7. Latitude variation of short period.

All these hypotheses may be in a greater or less degree probable, and at the same time no one of them has yet such a firm basis of proof, as to secure our universal assent.

The same may be said of the closing sum, for which the following hypotheses may be mentioned, —

1. Erroneous value of aberration constant.
2. Diurnal atmospheric refraction.
3. Latitude variation of short period.

The first explanation has been universally accepted. But the usually adopted value  $20''.47$  is quite consistent with the recently determined value of the solar parallax, and does not permit so

much increase as to account for the whole closing sum. The second and third are nothing more than conjectures.

Under these circumstances, it does not seem utterly superfluous to make new suggestions, to be further discussed and investigated by a wider circle. With this intention, I venture to declare that the above puzzling subjects may possibly be explained by the phenomenon above discussed, in connection with the defect of the spirit level.

Now, provided that the considerations in the earlier part of this essay on the disturbance of the zenith telescope are applicable to the case when the Talcott-Horrebaw observation is made, in which the proximity of the observer is of short duration, the first part of the disturbing effect only may come into play, so that the change of inclination of the telescope, due to the thermal disturbance, would not appear in the position of the level bubbles. Therefore, the level bubbles will be situated too far north of their due position. The result of this is that the corrections depending on the level reading are positively too large or negatively too small, giving finally too large a value of latitude. The principal part of this error varies inversely with the temperature. So the correction to be applied to the latitude is of negative sign and of varying magnitude, depending on the seasons and the hour of the day.

Let the star groups selected for the chain method be from I to XII, as is adopted in the International Latitude Service. And further distinguish these groups by suffixes according to combinations; suffix 1 when combined with the preceding group and suffix 2 when combined with the following group. The period of observation and the corresponding group are as follows, —

Date.	Corresponding Group.
Nov. 2 — Dec. 6	I <sub>2</sub> & II <sub>1</sub>
Dec. 7 — Jan. 4	II <sub>2</sub> & III <sub>1</sub>
Jan. 5 — Jan. 30	III <sub>2</sub> & IV <sub>1</sub>
Jan. 31 — Febr. 24	IV <sub>2</sub> & V <sub>1</sub>

Date.	Corresponding Group.
Febr. 25 — March 21	V <sub>2</sub> & VI <sub>1</sub>
March 22 — April 15	VI <sub>2</sub> & VII <sub>1</sub>
April 16 — May 11	VII <sub>2</sub> & VIII <sub>1</sub>
May 12 — June 8	VIII <sub>2</sub> & IX <sub>1</sub>
June 9 — July 9	IX <sub>2</sub> & X <sub>1</sub>
July 10 — Aug. 13	X <sub>2</sub> & XI <sub>1</sub>
Aug. 14 — Sept. 22	XI <sub>2</sub> & XII <sub>1</sub>
Sept. 23 — Nov. 1	XII <sub>2</sub> & I <sub>1</sub>

As the temperature continues to fall during the latitude observation in one night, we may tentatively but reasonably assign the following mean corrections to the latitude corresponding to each of the groups, —

I <sub>1</sub>	−0.05	I <sub>2</sub>	−0.05
II <sub>1</sub>	−0.07	II <sub>2</sub>	−0.07
III <sub>1</sub>	−0.08	III <sub>2</sub>	−0.07
IV <sub>1</sub>	−0.08	IV <sub>2</sub>	−0.06
V <sub>1</sub>	−0.08	V <sub>2</sub>	−0.05
VI <sub>1</sub>	−0.07	VI <sub>2</sub>	−0.04
VII <sub>1</sub>	−0.06	VII <sub>2</sub>	−0.03
VIII <sub>1</sub>	−0.04	VIII <sub>2</sub>	−0.02
IX <sub>1</sub>	−0.03	IX <sub>2</sub>	−0.01
X <sub>1</sub>	−0.02	X <sub>2</sub>	−0.00
XI <sub>1</sub>	−0.01	XI <sub>2</sub>	−0.01
XII <sub>1</sub>	−0.03	XII <sub>2</sub>	−0.03

Now in the reduction of the chain method it is assumed that the latitude is constant during the observation of two groups in one night, and under this supposition the star places are reduced to the mean of the whole system. But when the apparent latitude obtained from observation requires the said correction, the reduction



to the mean would consequently need a corresponding revision. Thus in order to find how the above corrections enter into the reduction by chain method, i. e., how to reduce them to a true homogeneous system, we must treat these corrections in a manner exactly identical with the chain method reductions.

I form, therefore,—

Correction to	III-IV =	Difference of corrections to	III <sub>2</sub> &	IV <sub>1</sub> =	+0.01
	IV-V =	„	IV <sub>2</sub> &	V <sub>1</sub> =	+0.02
	V-VI =	„	V <sub>2</sub> &	VI <sub>1</sub> =	+0.02
	VI-VII =	„	VI <sub>2</sub> &	VII <sub>1</sub> =	+0.02
	VII-VIII =	„	VII <sub>2</sub> &	VIII <sub>1</sub> =	+0.01
	VIII-IX =	„	VIII <sub>2</sub> &	IX <sub>1</sub> =	+0.01
	IX-X =	„	IX <sub>2</sub> &	X <sub>1</sub> =	+0.01
	X-XI =	„	X <sub>2</sub> &	XI <sub>1</sub> =	+0.01
	XI-XII =	„	XI <sub>2</sub> &	XII <sub>1</sub> =	+0.02
	XII-I =	„	XII <sub>2</sub> &	I <sub>1</sub> =	+0.02
	I-II =	„	I <sub>2</sub> &	II <sub>1</sub> =	+0.02
	II-III =	„	II <sub>2</sub> &	III <sub>1</sub> =	+0.01

Hence,

the correction to the closing sum, in the usual sense, = +0.18

Further, in order to find the corrections to the reductions to the mean system, I form,—

for the group III ; correction to	IV-III =	-0.01
„	V-III =	-0.03
„	VI-III =	-0.05
„	VII-III =	-0.07
„	VIII-III =	-0.08
„	IX-III =	-0.09
„	X-III =	-0.10
„	XI-III =	-0.11
„	XII-III =	-0.13
„	I-III =	-0.15
„	II-III =	-0.17
	Sum =	-0.99

I apply similar treatment to the other groups and divide the sums by 12.

The correction to the closing sum is to be distributed equally among the groups, so that the quantity,—

$$\frac{0.18}{12} \times 11 \div 2 = 0.083$$

is to be added to the above. The resulting quantities constitute the reductions of the star places to a true homogeneous system,—

I	II	III	IV	V	VI	VII	VIII	IX	X	XI	XII
0.000	+0.005	0.000	-0.005	0.000	+0.005	+0.010	+0.005	0.000	-0.005	-0.010	-0.005

Combining these with the said corrections to the latitude observation, we apply the usual process of reduction and form differences with the mean of all of them. Arranging them with respect to seasons, we have, —

Mean Date	Corrections	Mean	Resulting Corrections
Jan. 18	-0.070, -0.085	-0.078	-0.033
Febr. 12	-0.065, -0.080	-0.073	-0.028
Mar. 10	-0.050, -0.065	-0.053	-0.013
Apr. 4	-0.035, -0.050	-0.043	+0.002
Apr. 29	-0.020, -0.035	-0.028	+0.017
May 26	-0.015, -0.030	-0.023	+0.022
June 25	-0.010, -0.025	-0.018	+0.027
July 27	-0.005, -0.020	-0.013	+0.032
Sept. 3	-0.020, -0.035	-0.028	+0.017
Oct. 13	-0.035, -0.050	-0.043	+0.002
Nov. 19	-0.050, -0.065	-0.053	-0.013
Dec. 21	-0.065, -0.080	-0.073	-0.028
		Mean -0.045	

These are the corrections to the latitude variation which may be looked upon as common to all stations. Therefore naturally

it is the correction to that term of latitude variation which is independent of polar motion, or  $z$  term.

Now, according to Ross<sup>1)</sup>, the mean value of  $z$  term during the years 1900–1905, can be put in the following analytical form, —

$$+ 0.''027 \sin (\odot + 170^\circ) \quad (\odot = \text{sun's longitude})$$

when the effects of stellar parallax, Oppolzer's term in latitude variation and nutation are taken into account and excluded. Hence it follows that the result obtained through my argument is practically sufficient to account for the closing sum and  $z$  term.

Now, as the phenomenon discussed by me is considered to arise from some unsymmetry of the meteorological conditions and also from the solar radiation on the ground, its sense should be inverted for the southern hemisphere and is to be considered as an odd function of latitude, vanishing at the equator. So it can be looked upon as varying with  $\sin \varphi$ . Under such a conception, the effect on the southern observations should be opposite to that on the northern, the correction to the latitude being of positive sign and the correction to the closing sum negative.

The correction to be applied to the latitude variation independent of longitude would be

positively small for January, and  
positively large for July.

Therefore, the correction to be applied to the yearly term in the variation of latitude, or  $z$  term, is

negative for January, and  
positive for July.

The sign is the same as that of the northern observations, and is sufficient to interpret the result obtained from the southern observations.

As to the amplitude of the  $z$  term, it depends jointly on the said phenomenon and the seasonal variation, both of which can be looked upon as varying with  $\sin \varphi$ ; so we can consider the amplitude of the correction of  $z$  term as dependent on  $\sin^2 \varphi$ . This signifies that the amplitude of the  $z$  term increases from the value

---

1) *Astronomische Nachrichten*, Nr. 4593.

zero at the equator, towards north and south latitudes symmetrically. To ascertain whether this is actually the case or not, observations at the equatorial zone are very desirable.

The numerical results so far obtained I do not intend to regard as definitive. But they may serve as a clue for the yet unsolved problems, or an indication of the direction in which we must proceed in order to account for them.

Now, as my argument has been advanced from two causes, viz.

1. some regular movements of the zenith telescope;
2. a defect of the spirit level,

I may also state with diffidence the results to which my considerations have led me, as follows:—

If we assume a regular change of inclination of the zenith telescope, varying with the seasons and the hour of the day, the three phenomena, that is,  $z$  term, closing sum, and the regular shift of the spirit level, can all become explicable together. Therein the defect of the level makes the error enter into the latitude value and gives rise to the  $z$  term and closing sum.

My idea, therefore, leads to the conclusion that these enigmatic subjects in the latitude problems would disappear, if the level were really a perfect instrument, or if we were to use another and an ideal means instead of this insufficient instrument.

The photographic observations made with the Cookson floating zenith telescope at the Greenwich Observatory by Mr. Jones<sup>1</sup> are very important in regard to the present problem. The latitude variation obtained from this series was compared with the results of the International Latitude Service. Herein the agreements was particularly improved, when the  $z$  term was subtracted from the latter series. As to the aberration constant, the value

$$20.''467 \pm 0.''006$$

was obtained. In other words, this novel series of observations was practically free from the  $z$  term and closing sum. Arguing from

---

1) Monthly Notices of the R.A.S., Vol. LXXV, No. 7.

my standpoint, this is to be looked upon as a natural and necessary consequence.

The notion that the level is not suited to the most delicate measurements is not novel. Already as early as in the year 1893, E. von Rebeur-Paschwitz<sup>1)</sup> insisted on the inadequacy of the spirit level to meet the disturbance in precise astronomical measurements from pulsatory or microseismic movements of the ground. Also G. H. Darwin is said to have declared to the same effect,—“I venture to predict that at some future time practical astronomers will no longer be content to eliminate variations of level merely by taking means of results, but will regard corrections derived from a special instrument as necessary to each astronomical observation.”

Although the motive of my idea is not strictly the same as that of these authorities, our resulting conceptions are convergent, and I am pleased to conclude my paper with the expectation that Darwin's prediction will be promptly actualized in order to meet the degree of accuracy required in up-to-date astronomical observation.

Lastly, the writer desires to express his sincere thanks to the several astronomers and observers referred to above, by whose efforts and information he has been enabled to accomplish this work.

The Tokyo Astronomical Observatory, September 1915.

---

Published Nov. 30th, 1915.

---

---

1) *Astronomische Nachrichten*, Nr. 3177.



# On the Distribution of Cyclonic Precipitation in Japan.

(Contribution I. from the Geophysical Seminary in the  
Physical Institute, College of Science).

By

**Torahiko TERADA,**

*Rigakuhakushi,*

**Takezô YOKOTA,**

*Rigakushi,*

and

**Syôhu OTUKI.**

*Rigakushi.*

The distribution of cyclonic precipitations has been investigated by many meteorologists for different localities. H. Hildebrandsson<sup>1)</sup> found that in Upsala, the precipitation is most abundant on the W side of a depression. Åkerblom<sup>2)</sup> found the heaviest rainfall in Thorshavn on the front right quadrant of a centre, whereas in Vienna it was on the opposite side. Since these classical investigations, it seems to have been a favourite problem to inquire on which side of a depression the precipitation is most frequent or abundant. Krankenhagen<sup>3)</sup> found greatest precipitation in Swinemünde on the rear side of a cyclone and attributed the fact to the influence of seawind prevailing on that side. V. Drapezyanski<sup>4)</sup> came to the conclusion that the precipitation in St. Louis, U.S.A., is most frequent on the rear side, but the average amount of rain on rainy days most abundant on the S side. H. R. Mill<sup>5)</sup> investigated the trace or "smear" swept by the rain area accompanying a number of remarkable depressions passing over Great Britain, and came to the result that "the belt of cyclonic rains is much wider on the left

1.) H. Hildebrandsson, Sur la distribution des éléments mét. autour des minima et des maxima barométriques, Upsala 1883; v. Belber, Met. ZS., 1884.

2.) Ph. Åkerblom, Sur la distribution à Vienne et à Thorshavn des éléments etc.

3.) Krankenhagen, Met. ZS. 1885. See also Polis, Met. ZS., 1904.

4.) Drapezyanski, Met. ZS. 1903.

5.) H. R. Mill, Symon's Met. Mag. **39**, 1904; Quart. Journ. R. Met. Soc. **36**, 1908.

of the path than on the right, and the heaviest falls occur in advance of the centre" regardless of the direction of progression of the depression. He also remarks that the distribution of cyclonic rains seems to have no apparent relation to the physical feature of the country, though data were wanting to decide the point. J. A. Udden<sup>1)</sup> who attacked the problem for Davonport, Rock Island, Ill., U.S.A. and also for a number of other districts, found that the position of the area of the greatest rainfall-frequency relative to the depression, varies largely for different localities; he suggested that the relation may vary with the hours, the seasons and the courses taken by the depression. W. G. Reed<sup>2)</sup>, following the method adopted by Mill, made an extensive investigation of the "smear" for a number of cyclones passing over the U.S.A. His results are not so simple as that of Mill. He notes rightly the considerable influence of large water bodies, such as the Atlantic Ocean and the Great Lakes and also the fact that the rain area forms a series of patches, the heavier ones being connected by lighter ones or rainless areas. The latter fact is also attributed to the influence of important water bodies, though he concludes: "every relation expected occurs, but there seems to be as yet no classification which will reduce the relation to a system." Hann<sup>3)</sup> discusses these results in his *Lehrbuch* and emphasizes the influence of the districts over which the wind comes.

One of the authors<sup>4)</sup> has discussed the influence of the distribution of land and water in modifying the meteorological feature of a region and proposed a simple theory which may explain many regional irregularities of barometric distribution. As an illustration of this theory, he drew attention to the difference of the Pacific and Japan Sea Coasts, with regard to the relative position of the rain area and the centre of barometric depression. The present paper may be regarded on one hand as the continuation of the above cited one, in so far as the results of the statistical investigation are reviewed under the light of the theory, but on the other hand as a contribution to the literature on the general precipitation problem.

---

1.) J. A. Udden, *Symon's Met. Mag.* **41**, 1906.

2.) W. G. Reed, *Monthly Weather Review*, Oct. 1911.

3.) Hann, *Lehrbuch d. Met.* 3te Auf. S. 524, 552.

4.) Terada, *Proc. Tōkyō Math.-Phys. Soc.* **7**, 1914.



### Method of Investigation.

The "smear" method adopted by Mill and Reed, though very useful and convincing for its proper purpose, is not convenient for revealing the influence of the physical nature of land, since this effect essentially lies in the peculiar distribution of precipitation determined by the momentary position of the given configuration of land and water, or of flat land and mountain range, relative to the centre of depression, and may be quite obliterated if only the smear is compared with the track of the centre. To make the effect apparent, it is necessary to find the probability or the amount of precipitation at different districts for different positions of the depression. If these statistical data be at hand, we may construct the isohyets for the different positions of the depression, or draw for each district a diagram showing the distribution of the probability or the amount for the different positions of the centre relative to the district in question.

As material for the present statistical investigations the daily weather charts and "Kisyôyôran" (a brief monthly weather review) of the Central Meteorological Observatory, from January 1905 to December 1915 were used. The different districts of which the precipitations were to be investigated were at first classified into three groups: Pacific, Japan Sea and middle regions. Each group was again divided into six subgroups including the meteorological stations mentioned below:

- P<sub>1</sub> Kagosima, Satazaki, Toizaki, Miyazaki.
- P<sub>2</sub> Asizuri, Kôti, Hinomisaki, Siomisaki.
- P<sub>3</sub> Namikiri, Tu, Nagoya, Hamamatu.
- P<sub>4</sub> Numadu, Nagaturo, Yokosuka, Yokohama, Tôkyô, Mera, Tyôsi, Mito, Tukuha.
- P<sub>5</sub> Kanayama, Kinkwazan, Isinomaki, Miyako.
- P<sub>6</sub> Tokati, Kusiro, Nemuro, Abasiri.
- M<sub>1</sub> Ôita, Matuyama, Hirosima, Kure.
- M<sub>2</sub> Okayama, Tadotu, Tokusima, Wakayama, Kôbe, Ôsaka, Yagi.

- M<sub>3</sub> Gilu, Iida, Kôhu, Takayama, Matumoto, Nagano.
- M<sub>4</sub> Kumagaya, Maebasi, Asio, Utunomiya.
- M<sub>5</sub> Hukusima, Yamagata, Midusawa.
- M<sub>6</sub> Aomori, Tappi, Hakodate.
- J Kumamoto, Nagasaki, Sascho, Saga, Hukuoka, Simono-seki.
- J Hamada, Sakai.
- J Kyôgasaki, Maiduru, Kyôto, Hikone, Hukui.
- J Kanazawa, Husiki, Minatuki, Niigata.
- J Kamo, Akita.
- J Suttu, Sapporo, Kamikawa, Sôya.

The above order of grouping may appear somewhat arbitrary and be liable to the objection that it takes no account of the peculiar local climatic or physical features. This may, however, be justified if we consider that the principal aim of the present investigation is to sort out the general influence of the configuration of land and water with respect to the centre of depression. Korea, Saghaline and Formosa were excluded, since these regions may obviously stand under the influence of depressions existing beyond the limit of the weather chart.

The position of the centre of depression was determined not only by the daily chart, but also by consulting the chart of the track of depressions given in "Ki-yô-yôran." The chart area was divided into 2.5° square meshes and the position of the centre was fixed within one of these meshes.

Our first procedure was to examine the daily charts one by one and for each position of the centre to note down the districts with or without precipitation. Here we met of course with a difficulty. In many cases more than one centre appeared in the chart, to say nothing of the supposed shallow depressions appearing side by side, especially in days with generally small barometric gradient all over the chart area. In such a case, we are liable to an arbitrary prejudice in discriminating whether the precipitation in a given district was due to the one or the other of the coexisting depressions. Again, when an extensive depression is bifurcated, as is often the case when it is crossing over the main island, we cannot fix the

position of the "effective" centre, without making more or less uncertain assumptions. Since it was our immediate purpose to investigate the distribution for an isolated simple depression and discuss the results from the theoretical standpoint, all these ambiguous cases were excluded, confining our attention only to the simplest cases where only one conspicuous depression is shown in the chart.\* It must be admitted that in adopting this selection, we are taking only those precipitations in consideration which correspond to a quite limited weather type, and hence that the whole subsequent discussion has no reference to the cases of precipitations of noncyclonic type. Again, since each district includes a number of stations, it occurs as a rule that for each position of the centre, many districts have only partial rain or snow. Those cases with precipitation in only one station, but with none in the others, were counted as "no precipitation," otherwise as "precipitation" for that district. It must be remarked that the hours to which the weather charts refer are limited to 6a, 2p, 10p, while the distribution of precipitation in other hours may often vary widely. But for the present investigation, the three observations in a day seem to be more than sufficient. Finally it must be remarked that the cases in which there exists a centre of depression in the chart, but with no precipitation in either station, were excluded. Such a case, which is only met with when the centre is near the margin of the chart, is rather rare and the corresponding position of the centre more or less doubtful. At any rate, the weight of these extreme positions for the result is small and must be taken into consideration, if at all, with precaution.

The statistical part of the investigations was chiefly carried out by Yokota and Otuki. The number of times  $n$  in which the "precipitation" occurred in a given district, say  $P_1$ , corresponding to a given position of the depression, say  $A$ , divided by the number of times  $N$  in which the centre was found in the area  $A$ , expressed in percent, was called the "expectation" of precipitation for the pair  $(P_1, A)$ . The result of the statistical part is shown in Table I. The first column gives the positions of the centre of

---

\* In such cases, the position of the centre could be determined with a fair degree of certainty.

depression ; all those positions of which the total number  $N$  was less than 5 were excluded. The second column gives the number  $N$ . The remaining columns give the percentage expectation  $n/N\%$ , for each district named at the head.

TABLE I.

Position of Centre.		$N$	$P_1$	$P_2$	$P_3$	$P_4$	$P_5$	$P_6$	$M_1$	$M_2$	$M_3$	$M_4$	$M_5$	$M_6$	$J_1$	$J_2$	$J_3$	$J_4$	$J_5$	$J_6$
22.5° - 25° 122.5-125	N E	10	70	40	0	30	0	0	60	0	20	20	0	0	40	20	10	0	0	0
125    "    " 125 -127.5	N E	7	67	71	30	33	0	0	33	40	14	14	0	0	50	33	0	0	0	0
127.5-130	N E	9	33	44	33	22	0	0	33	29	0	0	0	0	33	11	0	0	0	0
25    - 27.5 125 -127.5	N E	18	0	39	0	28	0	0	39	28	22	11	17	0	56	33	28	11	6	0
127.5-130	N E	18	56	44	28	45	0	0	17	7	28	22	11	0	44	17	11	22	6	0
130    "    " 130 -132.5	N E	9	56	78	28	33	0	0	44	17	45	22	0	11	22	55	55	33	11	0
27.5- 30 125 -127.5	N E	13	0	23	15	15	0	0	38	15	8	8	4	0	46	23	15	15	0	0
127.5-130	N E	28	62	43	14	11	0	0	43	36	14	4	11	0	57	36	14	11	0	0
130    "    " 130 -132.5	N E	19	64	47	47	47	5	0	63	52	37	42	8	0	53	47	41	26	0	0
132.5-135	N E	12	58	50	25	42	8	0	42	33	17	25	0	0	33	33	8	14	0	0
30    - 32.5 122.5-125	N E	5	0	0	0	0	0	0	0	0	0	0	0	0	80	0	0	0	0	0
125    "    " 125 -127.5	N E	19	60	32	5	5	0	0	42	26	0	0	0	0	74	26	10	5	0	0
127.5-130	N E	24	37	75	21	17	4	0	67	50	17	8	0	0	71	54	21	16	7	4
130    "    " 130 -132.5	N E	30	71	76	54	27	3	0	73	70	32	19	0	0	78	65	38	24	3	0
132.5-135	N E	37	76	87	73	43	16	5	62	81	68	32	14	3	49	70	73	41	14	0
135    "    " 135 -137.5	N E	37	22	48	87	84	24	8	24	49	65	62	27	11	16	22	49	49	11	3
137.5-140	N E	22	11	18	59	77	37	0	13	23	55	59	32	14	23	23	32	32	9	0
140    "    " 140 -142.5	N E	12	5	0	25	84	25	0	0	18	42	50	33	17	8	42	42	42	25	8
32.5- 35 122.5-125	N E	8	75	50	38	0	0	0	38	0	0	0	0	0	75	25	0	0	0	0
125    "    " 125 -127.5	N E	12	66	58	25	8	0	0	67	58	9	0	0	0	92	75	17	8	0	0
127.5-130	N E	24	50	67	35	8	0	0	62	54	38	13	4	0	83	71	50	21	0	0

Position of Centre		N	P <sub>1</sub>	P <sub>2</sub>	P <sub>3</sub>	P <sub>4</sub>	P <sub>5</sub>	P <sub>6</sub>	M <sub>1</sub>	M <sub>2</sub>	M <sub>3</sub>	M <sub>4</sub>	M <sub>5</sub>	M <sub>6</sub>	J <sub>1</sub>	J <sub>2</sub>	J <sub>3</sub>	J <sub>4</sub>	J <sub>5</sub>	J <sub>6</sub>
32.5°-35° 130 -132.5	N E	21	62	76	48	43	5	0	41	59	57	38	14	0	67	67	62	43	0	0
" " " 132.5-135	N E	24	13	72	63	58	38	0	54	79	71	58	29	13	58	75	75	54	21	4
" " " 135 -137.5	N E	24	8	50	79	79	46	8	25	58	83	67	33	12	25	59	75	67	42	13
" " " 137.5-140	N E	28	4	25	47	90	39	7	71	25	50	68	25	14	14	14	57	39	11	36
" " " 140 -142.5	N E	27	4	0	15	74	56	11	0	7	37	44	29	7	7	19	33	51	15	7
35 - 37.5 125 -127.5	N E	16	31	50	13	6	6	0	50	50	19	12	6	0	62	31	25	19	13	0
" " " 127.5-130	N E	7	35	57	43	43	14	0	72	43	43	19	11	0	86	86	43	57	0	0
" " " 130 -132.5	N E	20	35	75	50	40	15	5	75	75	50	35	10	5	66	55	60	65	15	
" " " 132.5-135	N E	10	10	40	10	80	50	0	40	60	90	80	30	10	50	80	70	90	30	0
" " " 135 -137.5	N E	19	0	0	32	58	52	21	5	19	53	63	53	47	21	26	48	47	26	16
" " " 137.5-140	N E	12	0	0	25	67	58	8	0	9	42	67	58	25	0	8	58	75	42	0
" " " 140 -142.5	N E	20	0	0	5	45	80	35	5	0	20	40	55	10	0	10	26	55	50	20
" " " 142.5-145	N E	14	0	7	4	14	50	22	0	0	21	29	29	36	14	14	36	36	29	14
37.5- 40 130 -132.5	N E	9	11	11	0	0	11	0	22	0	0	0	0	11	14	22	11	11	0	0
" " " 132.5-135	N E	12	42	67	50	42	42	8	50	92	58	33	50	33	33	33	33	25	33	33
" " " 135 -137.5	N E	22	14	41	27	39	45	9	32	41	50	32	22	36	23	36	69	68	50	14
" " " 137.5-140	N E	20	10	5	5	30	75	40	1	10	2	40	45	55	10	15	25	45	50	25
" " " 140 -142.5	N E	9	0	0	11	11	33	44	0	0	11	22	44	78	0	11	22	33	55	56
" " " 142.5-145	N E	17	6	0	6	0	41	70	6	0	6	0	29	59	0	12	29	29	41	47
40 - 42.5 130 -132.5	N E	6	0	60	33	0	17	0	16	17	0	0	0	0	17	17	59	17	0	33
" " " 132.5-135	N E	14	7	2	29	29	36	25	14	14	36	21	29	29	14	33	29	50	29	43
" " " 135 -137.5	N E	12	17	16	50	33	8	25	8	33	67	42	8	42	33	20	42	50	42	25
" " " 137.5-140	N E	8	0	13	13	25	38	62	0	0	43	0	0	25	12	0	0	25	50	50
" " " 140 -142.5	N E	12	0	8	8	8	17	50	0	0	27	8	8	8	0	17	25	50	42	67
" " " 142.5-145	N E	16	0	6	6	12	12	56	0	6	19	12	6	38	0	13	19	31	50	63

Position of Centre	N	P <sub>1</sub>	P <sub>2</sub>	P <sub>3</sub>	P <sub>4</sub>	P <sub>5</sub>	P <sub>6</sub>	M <sub>1</sub>	M <sub>2</sub>	M <sub>3</sub>	M <sub>4</sub>	M <sub>5</sub>	M <sub>6</sub>	J <sub>1</sub>	J <sub>2</sub>	J <sub>3</sub>	J <sub>4</sub>	J <sub>5</sub>	J <sub>6</sub>	
40° - 42.5° 145 - 147.5	N E	10	10	0	0	0	10	60	10	10	20	0	10	50	0	30	30	10	40	50
42.5 - 45 135 - 137.5	N E	7	0	14	0	17	0	16	33	0	16	0	0	0	33	0	33	17	50	50
42.5 - 45 137.5 - 140	N E	12	0	0	0	8	0	82	0	0	0	0	8	33	0	0	0	17	25	67
40 - 42.5 140 - 142.5	N E	15	7	7	7	7	7	40	0	7	7	0	7	47	0	0	7	20	0	73
42.5 - 45 142.5 - 145	N E	9	0	0	0	0	0	56	11	0	0	11	11	22	0	0	22	33	0	55
45 - 47.5 145 - 147.5	N E	7	0	0	0	0	0	42	0	0	14	0	14	0	0	0	0	28	14	43
45 - 47.5 145 - 147.5	N E	7	0	0	0	0	29	14	0	0	14	0	29	57	0	0	57	13	29	100
47.5 - 50 147.5 - 150	N E	7	0	0	0	0	0	42	0	0	14	0	14	100	0	14	13	28	29	86
47.5 - 50 145 - 147.5	N E	5	0	0	0	0	60	20	0	0	40	0	20	40	20	0	40	60	20	60
47.5 - 50 147.5 - 150	N E	10	0	0	0	0	20	0	0	0	0	10	50	70	10	10	30	40	60	40

From this table, we may easily trace the curves of equal expectation corresponding to each given position of the centre, or the locus of the positions of the centre bringing equal expectation for each given district. For the sake of simplicity call the former curves "the isohyets" for the given position of the centre, though here, instead of the amount of the precipitation, the expectation is meant; the latter sets of curves may be called "the centre loci" for the given district. To smooth down local irregularities, the average was taken of the expectations of four adjoining  $2.5^\circ$  meshes and the mean value was attributed to the centre of the four meshes. Those sets of four meshes of which any one had the number of occurrences of depression, i.e.  $N$  less than 5, were excluded. In this way, the uncertainty due to the defect of data in the marginal regions was avoided. From these averaged expectations we constructed the two sets of diagrams mentioned above.

Figs. 1 to 20 show the isohyets for different positions of the depression which is marked with \* in each diagram. Figs. 21 to 38 gives the centre loci for each district, the middle point of which is marked with ●.

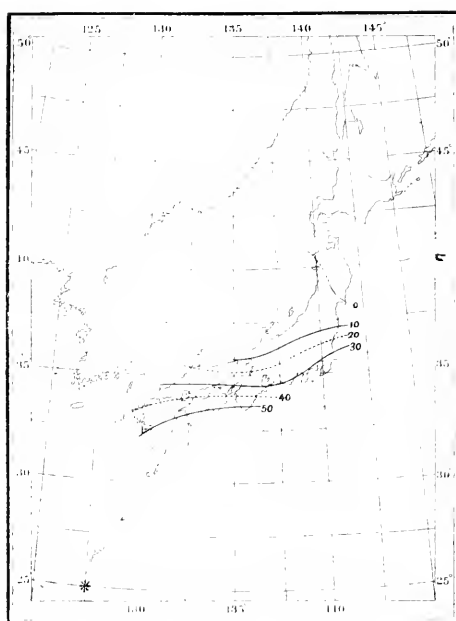


Fig. 1.

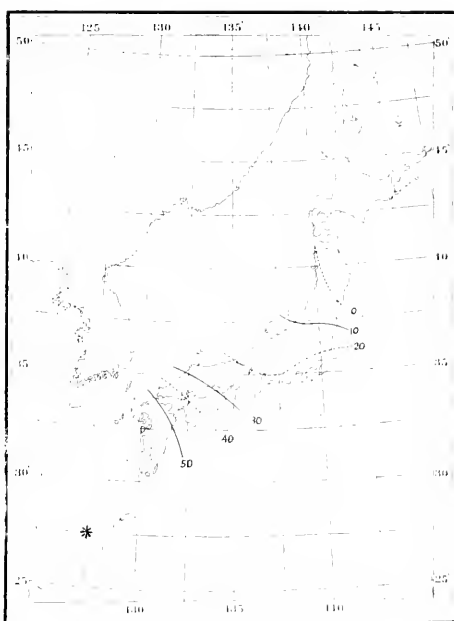


Fig. 2.

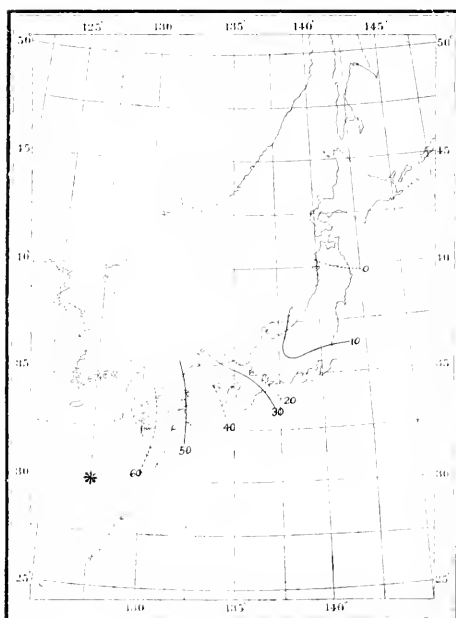


Fig. 3.

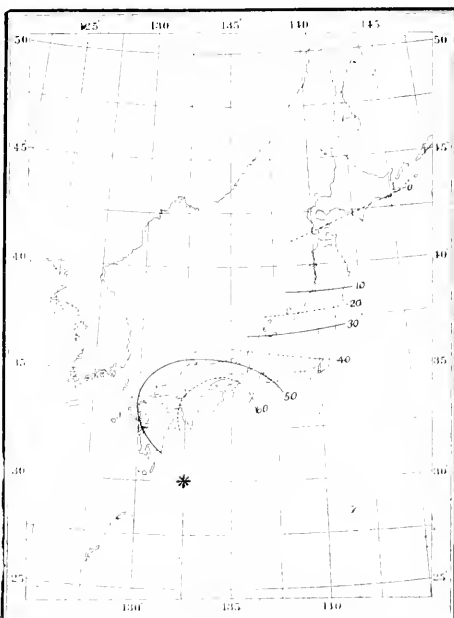
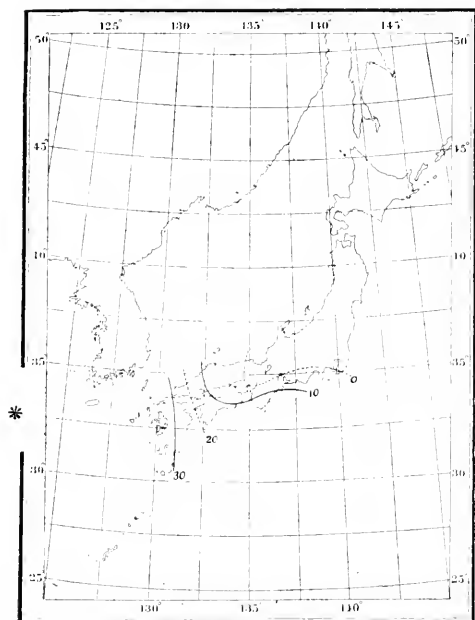
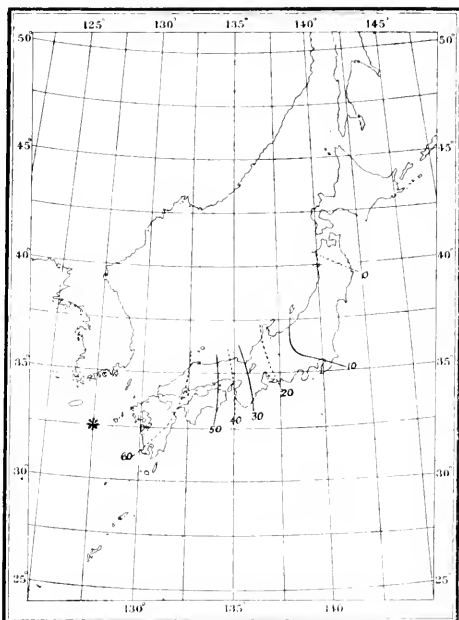
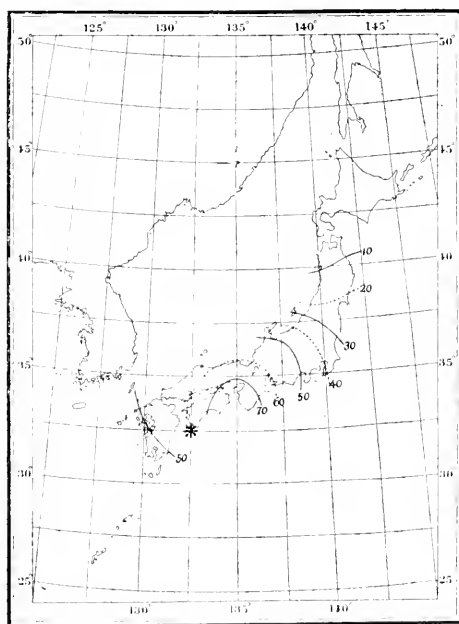
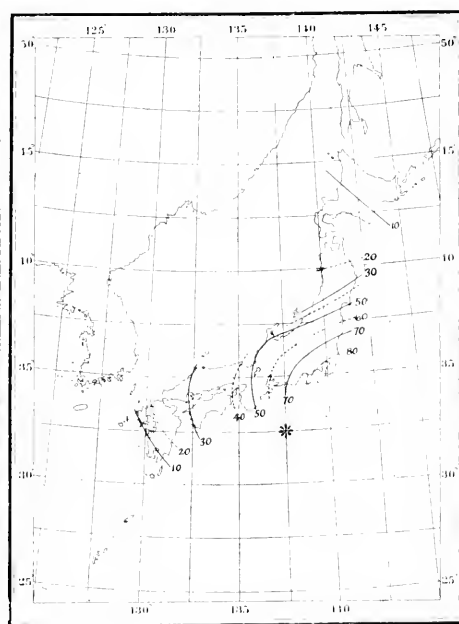


Fig. 4.

*Fig. 5.**Fig. 6.**Fig. 7.**Fig. 8.*



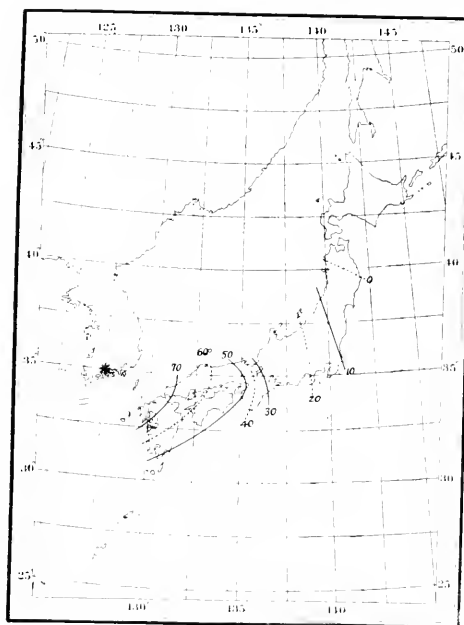


Fig. 9.

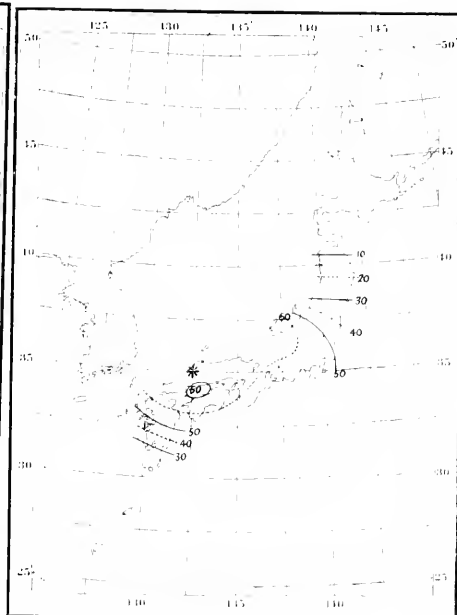


Fig. 10.

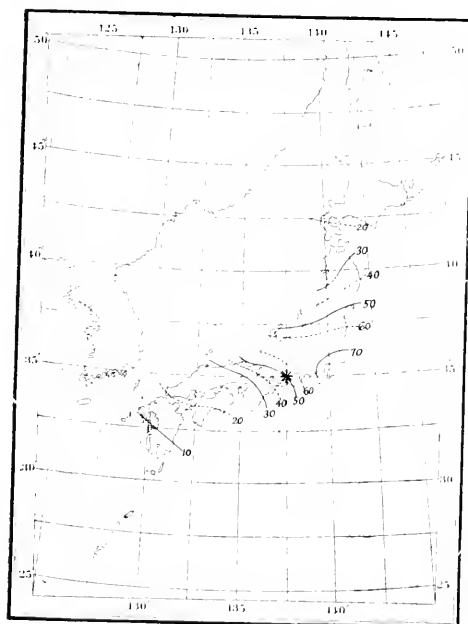


Fig. 11.

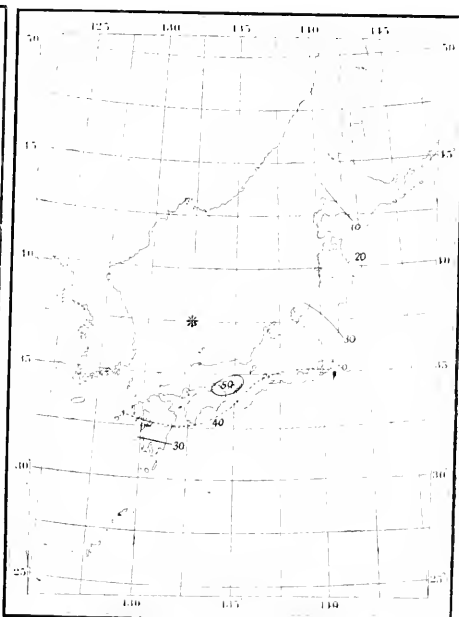


Fig. 12.

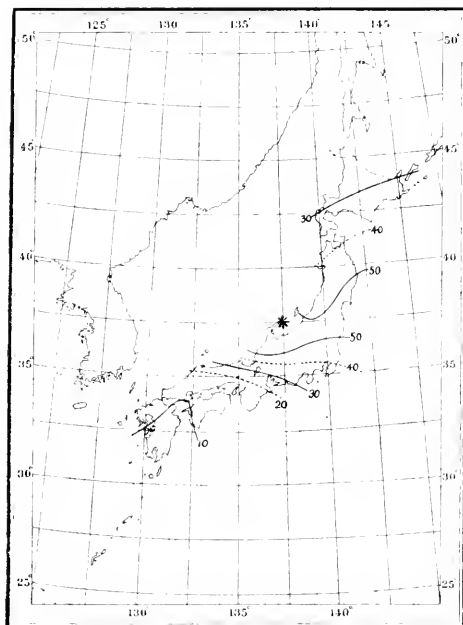


Fig. 13.

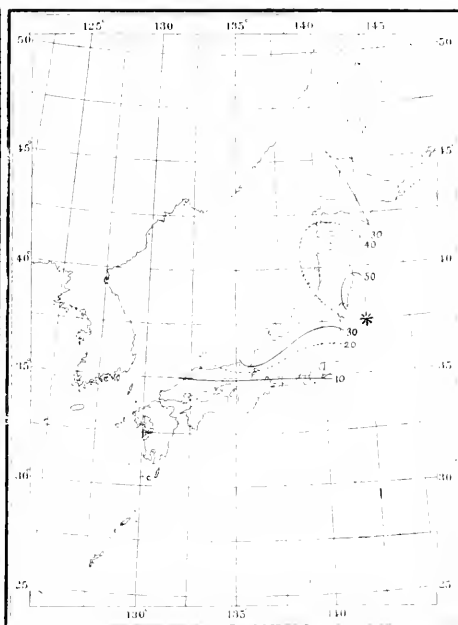


Fig. 14.

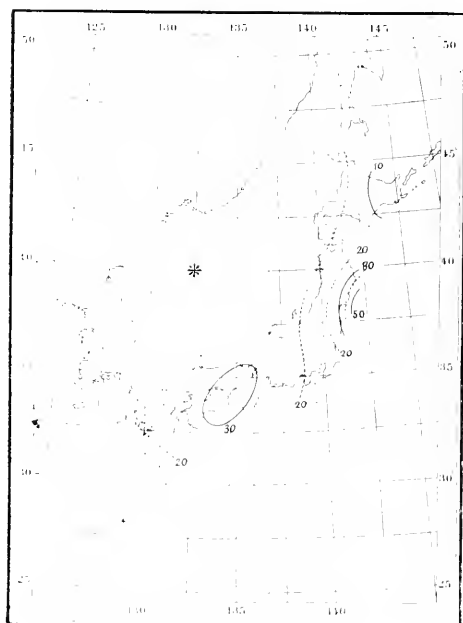


Fig. 15.

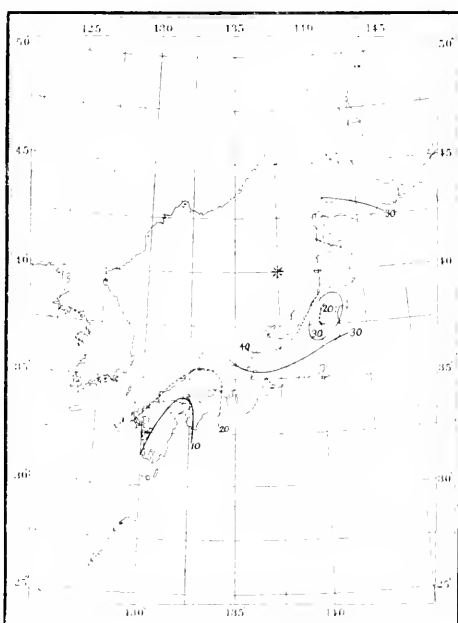


Fig. 16.

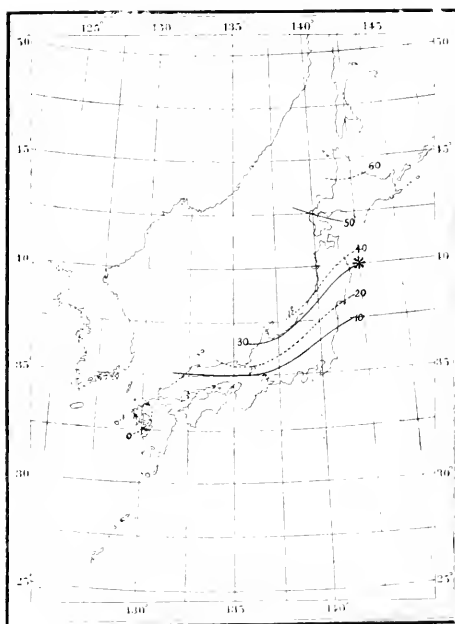


Fig. 17.

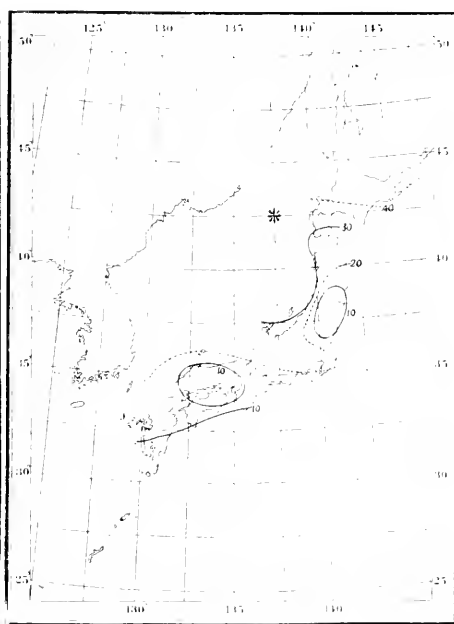


Fig. 18.

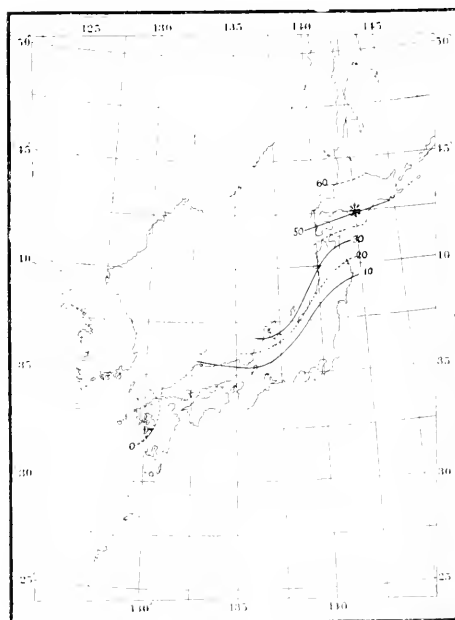


Fig. 19.

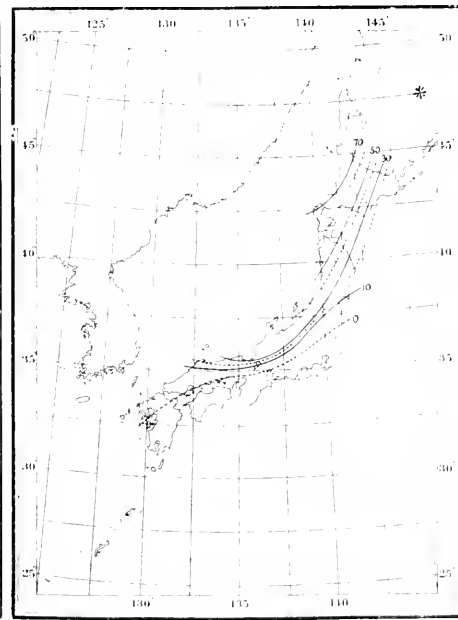
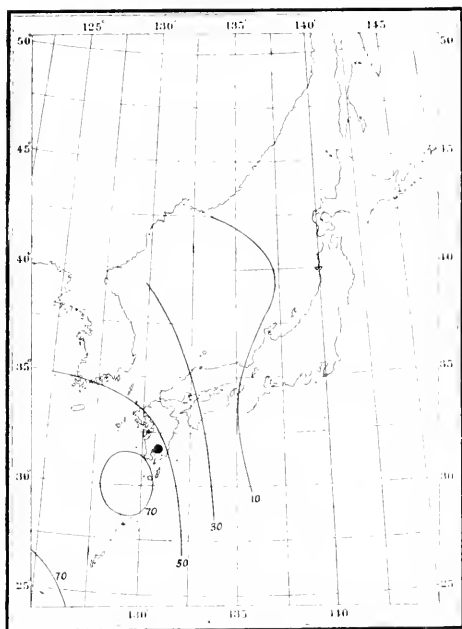
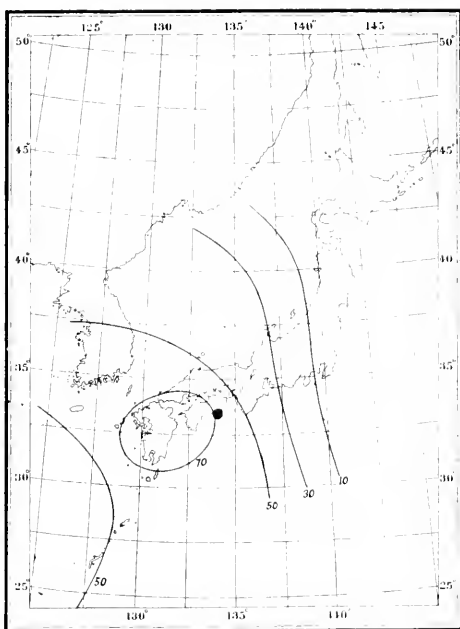
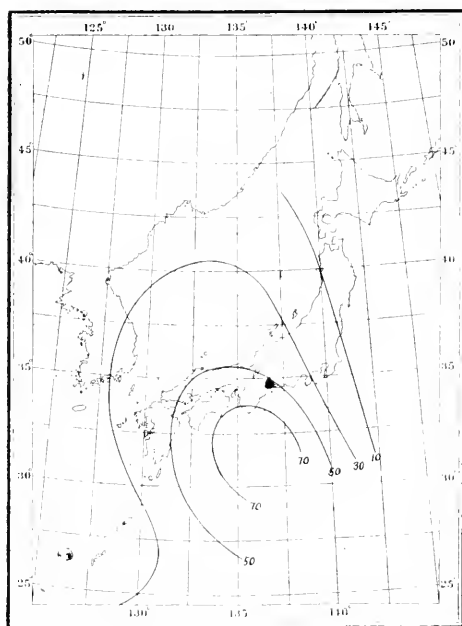
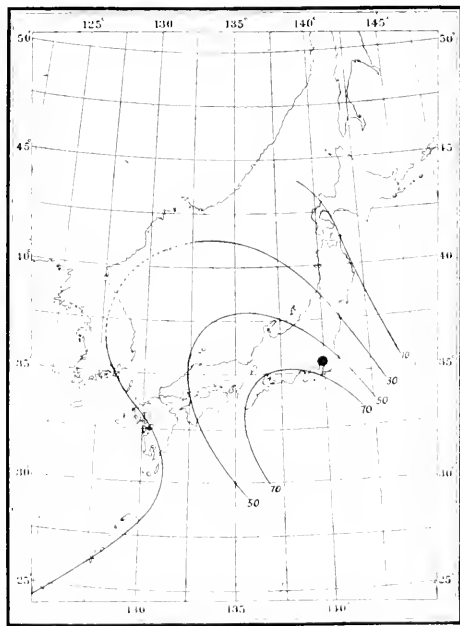


Fig. 20.

*Fig. 21.  $P_1$ .**Fig. 22.  $P_2$ .**Fig. 23.  $P_3$ .**Fig. 24.  $P_4$ .*

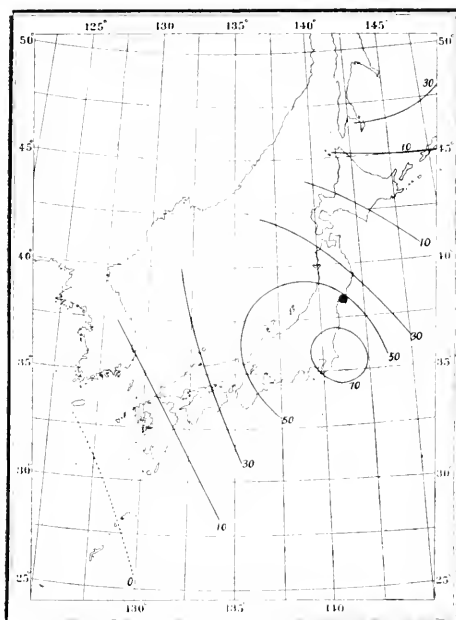


Fig. 25.  $P_5$ .

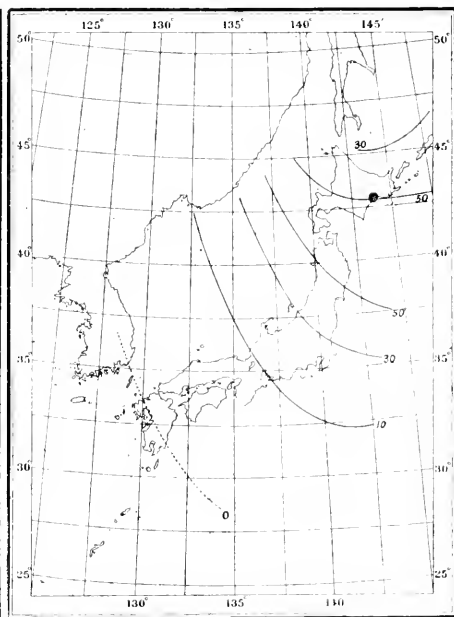


Fig. 26.  $P_6$ .

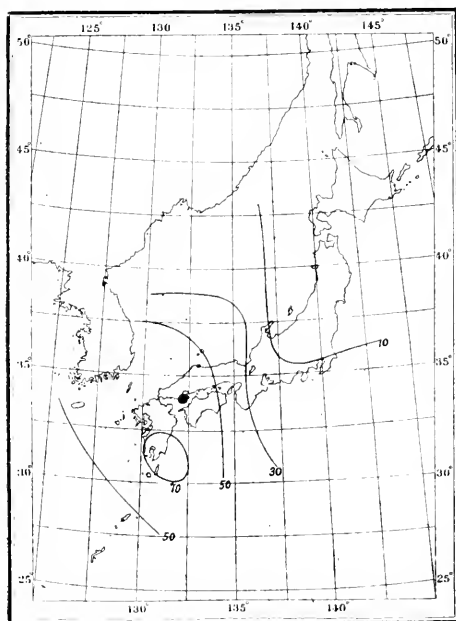


Fig. 27.  $M_1$ .

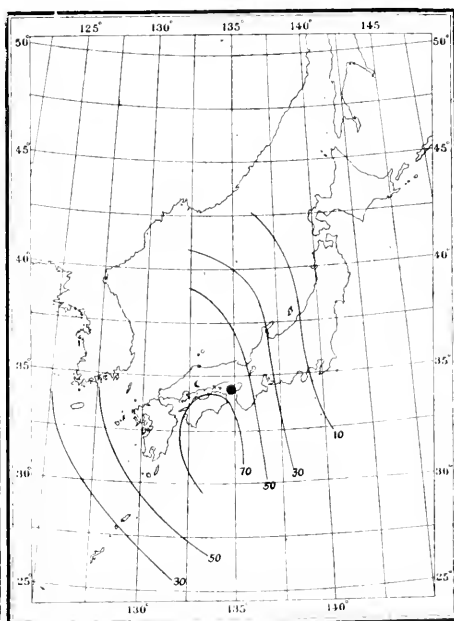
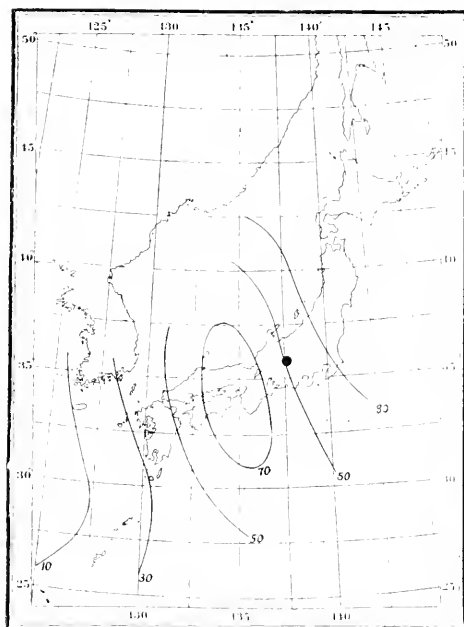
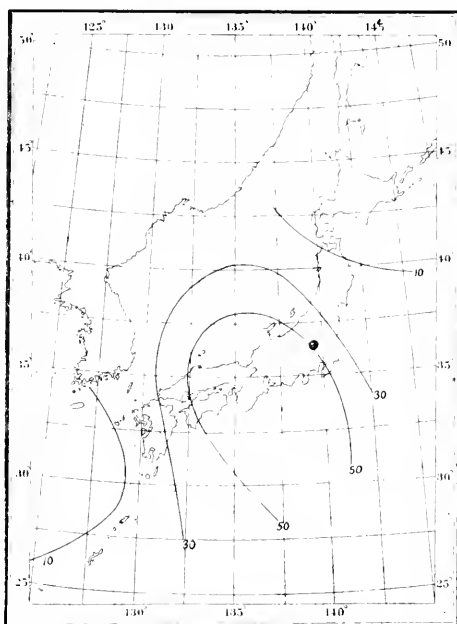
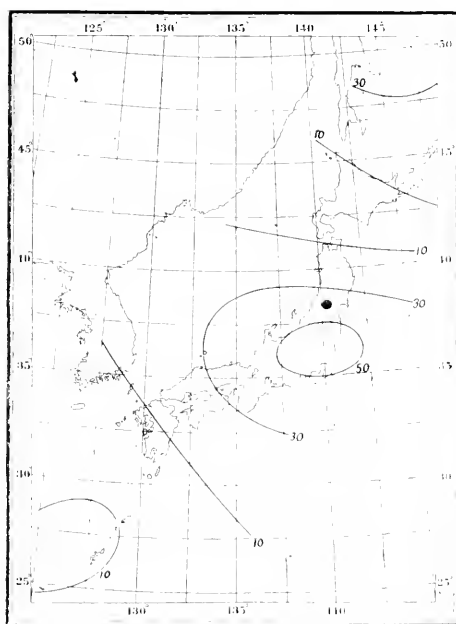
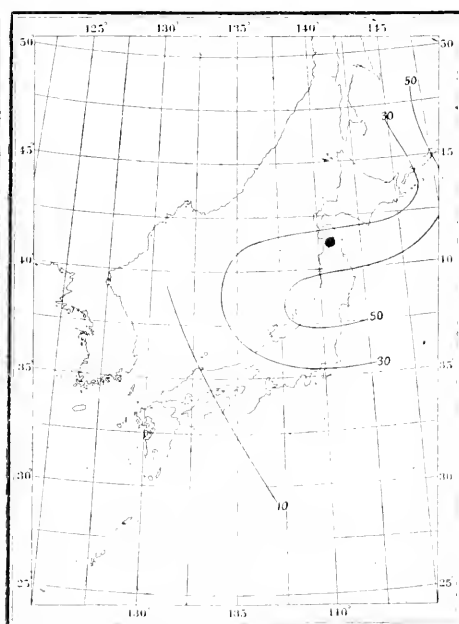


Fig. 28.  $M_2$ .

Fig. 29.  $M_3$ .Fig. 30.  $M_4$ .Fig. 31.  $M_5$ .Fig. 32.  $M_6$ .

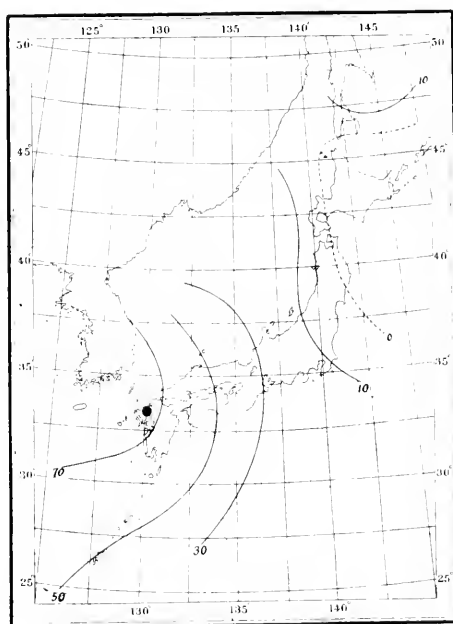


Fig. 33.  $J_1$ .

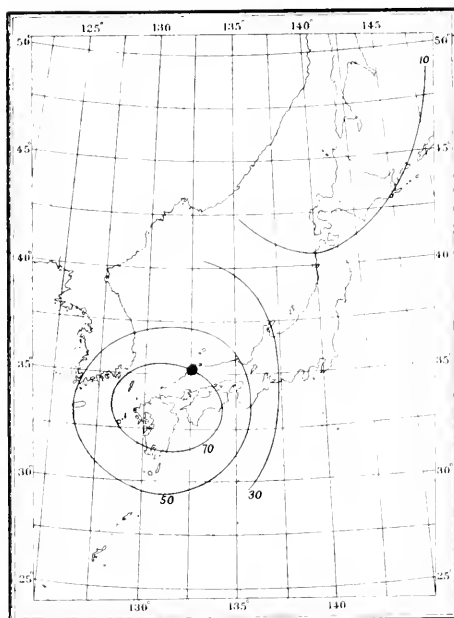


Fig. 34.  $J_2$ .

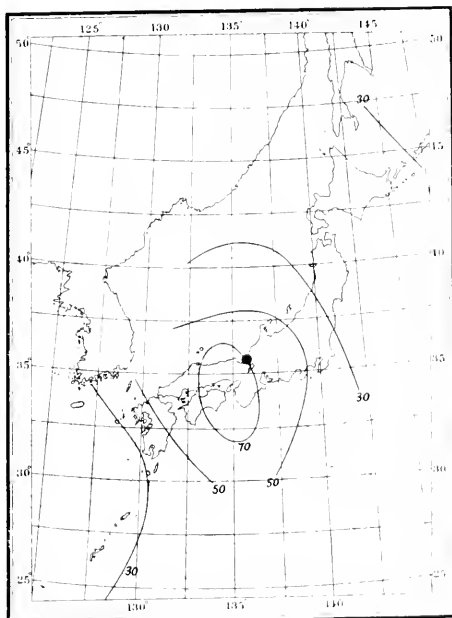
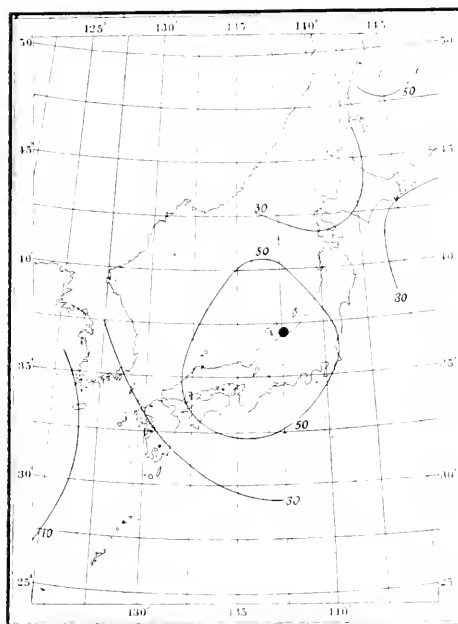
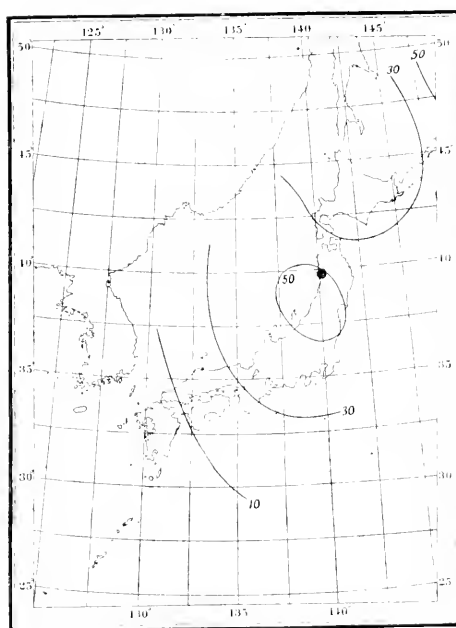
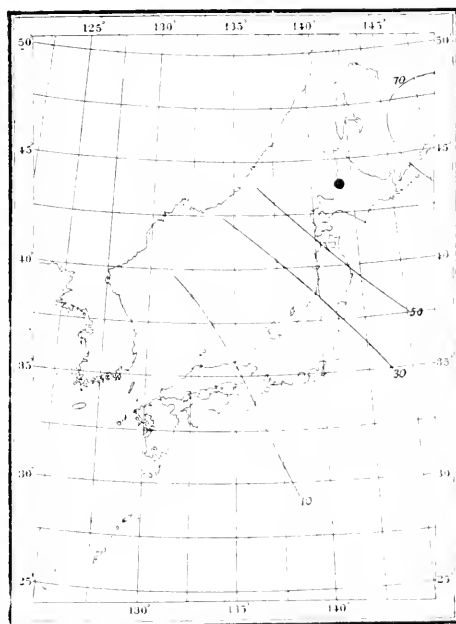


Fig. 35.  $J_3$ .

*Fig. 36.  $J_4$ .**Fig. 37.  $J_5$ .**Fig. 38.  $J_6$ .*



## Discussion of the Results.

### 1.) Isohyets.

A passing glance at the isohyets will reveal the undeniable influence of the land and water. Referring to Figs. 1, 2, 5, 14, 17, 19 and 20, we see that in front of a distant cyclone, the Pacific coast has decidedly greater expectation than the Japan Sea coast, whereas on the rear side the reverse is the case. This fact has already been noticed and explained by one of us in the above cited paper. This relation is not so conspicuous as in the above example when the cyclone approaches the main island, though the same tendency is still suggested by the shape of some isohyets, as in Figs. 3, 4, 6, 7, 8, 11, 13, 16 and 18, especially in the regions remote from the centre of depression. In the immediate neighbourhood of the centre, the difference between the Pacific and the Japan Sea coast is not conspicuous, as may be seen from Figs. 3, 4, 6, 7 etc. It is quite evident that the above cited theory requires a modification in the inner region of a cyclone where the curvature of the isobars and the variation of the gradient could no more be neglected, and the ascending air current proper to this region is more conspicuous, so that the effect of the topography does not appear so pronounced as in the external region.

Comparing Figs. 5, 12, and 15, it may be seen that the district  $M_2$  and probably also  $J_3$  shows some local irregularities, which may probably be attributed to the peculiar configuration of land and water in this region. Next, referring to Figs. 15, 16 and 18, a tendency is suggested that when the centre lies in the Japan Sea, M districts often show smaller expectations than the neighbouring P or J districts. This peculiarity is most pronounced in the isohyets for the position of the centre,  $132.5^\circ$  E,  $42.5^\circ$  N which were omitted in the above diagrams, since the number of occurrence  $N$  in two of the four meshes surrounding this point were less than 5. If we nevertheless calculate the corresponding expectations, we obtain

$M_1$	$M_2$	$M_3$	$M_4$	$M_5$	$M_6$	$P_1$	$P_2$	$P_3$	$P_4$	$P_5$	$P_6$	$J_1$	$J_2$	$J_3$	$J_4$	$J_5$	$J_6$
8	8	9	5	7	7	2	16	16	7	13	6	8	13	32	29	20	32

Thus the corresponding isohyets show a "valley" along the central axis of the main island. If this tendency is any thing real, the explanation must be sought in the draining influence of the Pacific mountain range lying on the wind side of this district, enhancing the ascending air current and condensing abundant moisture on the Pacific side. Moreover, it is interesting to notice that this particular position of the centre lies nearly at the centre of curvature of the circular axial line of Honsiu, and hence the geometrical relation of the different parts of the land with respect to the centre are similar to each other. This may at least explain why the isohyets in this case run nearly parallel to the land. On the contrary, when the centre of depression lies on the Pacific as in Fig. 8, not only the distance of, but the angle made by the coast line, with the radius vector drawn from the centre varies widely for different regions. This explains why the expectation in this case varies rapidly along the coast line. Nevertheless some peculiarities of the M districts similar to the above are suggested by the isohyets corresponding to some more remote positions of the centre than those shown in the above figures. These cases were, however, omitted on account of their small weight, and may better be postponed for a future research.

Again, comparing the Pacific and the Japan Sea coasts, for examples Figs. 7, 8 with 10, 13, or 4 with 16, the expectation seems to be generally greater for the Pacific districts than for the Japan Sea side, when the centre lies on the sea not far from the district in question. This may probably be attributed to the difference of temperature of the extended water bodies over which the wind comes.

Thus far we have considered only the average distribution of precipitation for different positions of the centre of depression. For the actual cases, the influences of an accidental nature, i.e. of the trivial local irregularities in topography, meteorological conditions, etc., may give rise to various discrepancies compared with the average relations. Still it is not difficult to find a number of typical examples among the daily charts, which may well illustrate the above general inference. A few of these examples are shown in Figs 39 to 42.

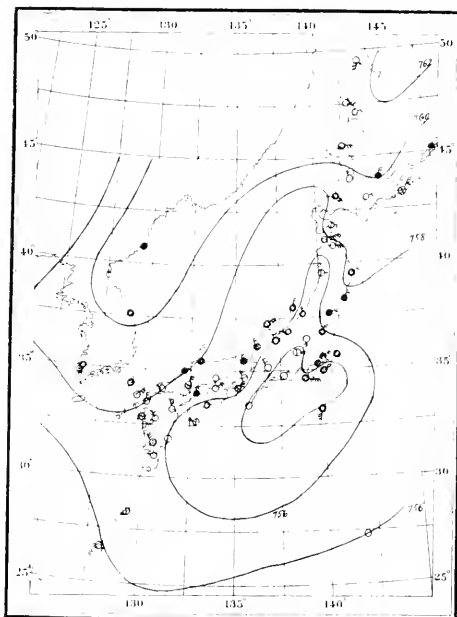


Fig. 39. 10<sup>h</sup> p.m., July 30, 1913 ;  
compare with Figs. 11 and 14.

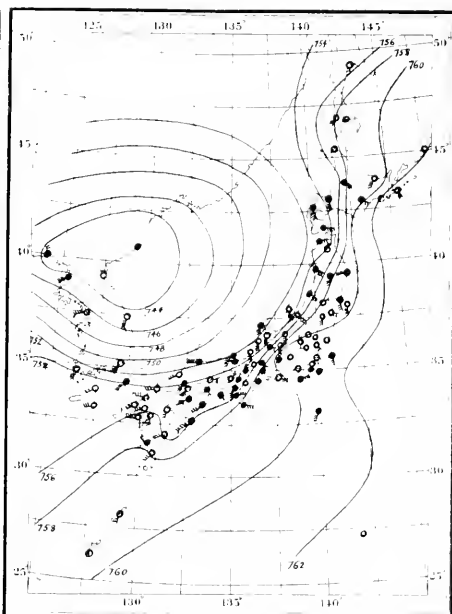


Fig. 40. 6<sup>h</sup> a.m., April 23, 1913 ;  
compare with Fig. 15.

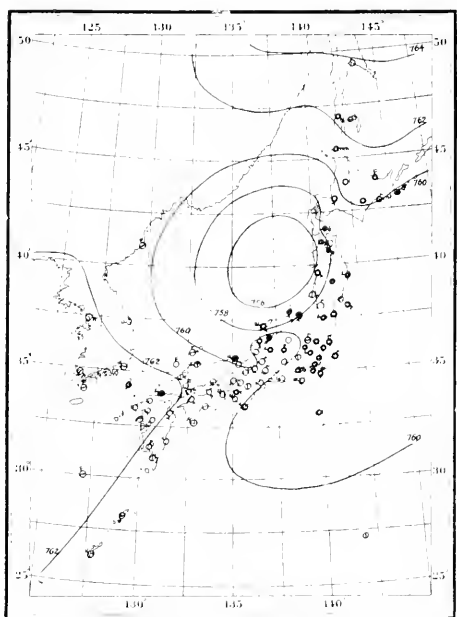


Fig. 41. 6<sup>h</sup> a.m., October 19, 1913 ;  
compare with Figs. 13, 16 and 18.

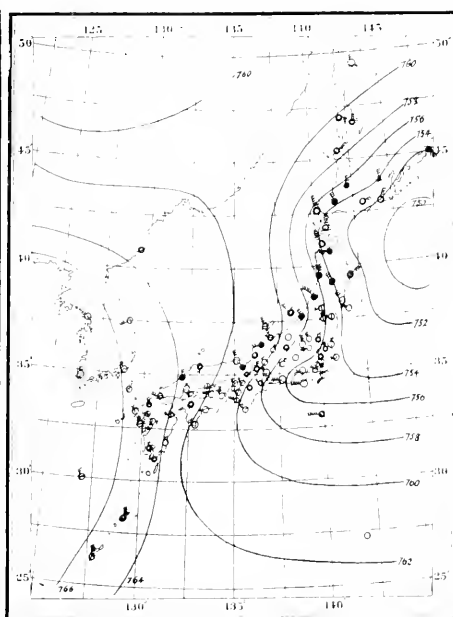


Fig. 42. 6<sup>h</sup> a.m., November 23, 1913 ;  
compare with Figs. 17 and 19.

## 2.) Centre Loci.

As already explained, Figs. 21 to 38 show for each of the 18 districts, the percentage expectation brought about by all possible different positions of the barometric depression. For example, in Fig. 21 the curve marked with 50 shows the trace of the positions of the centre which may bring precipitation to the district  $P_1$  in 50 cases out of 100 on an average.

From these figures, it will be at once seen that the area with the greatest expectation lies mostly on W, SW or S side of the district in question. This implies that the expectation is generally greatest on E, NE or N side of a cyclone. On a closer examination, however, we may easily discern the characteristic difference between the Pacific and the Japan Sea coasts. For the P districts, the 50% curves generally pass along the immediate neighbourhoods of the middle point of the districts concerned and the areas with the greater expectations lie entirely on the W to S sides of the districts. For the J group, however, the districts in question lie decidedly apart from the 50% lines and nearer to the point with the maximum expectation; moreover, the extent of the belt with 10 to 50% expectations in front of the district, is decidedly greater than that in the case of the P districts. Besides,  $J_2$ ,  $J_4$  and  $J_5$  show a belt with the lesser expectation projecting far in advance of the district, while  $J_3$ ,  $J_4$ ,  $J_5$  also suggest another maximum near Saghalien. For  $J_6$  the district in question apparently lies on the rear side of the area with the maximum expectation. For the M districts, the relations are intermediate between P and J as may be expected.

One interesting relation revealed by this way of graphical representation may be worth a special description. Referring to Figs. 22 to 26, suppose a line drawn along the longer axis of the elongated area with expectations above 30 or 50 %, for each of  $P_1$ ,  $P_2$ ,  $P_3$ , ...,  $P_6$ . The lines seem to turn round clockwise as we proceed successively from  $P_1$  to  $P_6$ . The same tendency is more apparent for  $M_3$  to  $M_6$ . The interpretation of this peculiar relation may probably be sought in the influence of the Japan Sea depressions.

We have already shown that when a centre lies far in the Japan Sea, the entire Pacific coast stands under nearly equal conditions, as far as the effect of the position of the coast line relative to the centre is concerned. Hence the influence of these depressions remains persistent when we proceed along the different districts. For the Pacific depressions, the case is quite different; the isohyets cross the land more or less transversally, the expectation varying rapidly along the coast line. In other words, the part of the centre loci on the Pacific side moves *with* the centre, while on the Japan Sea side, it remains comparatively stationary.

### General Theoretical Considerations.

Though we are afraid that we may be drawing our inference rather too far on the basis of too scanty materials, it will not be quite out of place to attempt here a discussion on the general theoretical aspect of the problem at hand.

Among the numerous factors determining the unsymmetrical distribution of precipitation due to a cyclone, we may conveniently distinguish the following three as the most essential:

(1) The first may be called "thermal and planetary" for the sake of simplicity. It consists in the difference of temperature with the latitude and may be considered always present regardless of the distribution of land and water. This influence would predominate if the earth were completely covered with ocean or land only, and would bring, according to the usual simple theory, more abundant rain on the eastern side of a depression.

(2) The second may conveniently be called "thermal and geographical" and consists in the difference of thermal conditions governed by the distribution of land and water, especially of continents and oceans. If this influence predominates, we may expect in the northern hemisphere the following: In summer when the land is generally warmer than the water, the area with the heaviest precipitation will lie in that direction which, viewed from the centre, has the land on the right side, provided of course that the land is sufficiently humid and the air kept nearly in saturation. But if the land be very arid, the reverse may occur, if

we can expect any precipitation at all. In winter, the relation will be different ; we may generally expect heavier rain or snow on that side of the depression which viewed from the centre has the ocean on the right side.

(3) While the above two factor are essentially thermal or thermodynamical, there remains the third one to be considered, which may conveniently be called "hydrodynamical and topographical." This consists in the effect of the forced ascending air current brought about by the discontinuity of the horizontal flow of air across the coast, due to the difference of "friction"\* over land and water, or flat land and mountains. This effect has been discussed in the previously cited paper and may be summarized as follows :

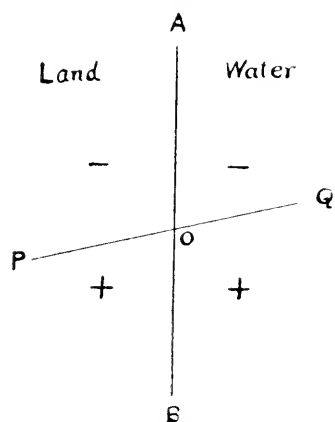


Fig. 43.

In the annexed figure, AB is the coast line bordering the land on its left side. PQ makes with AB a certain angle depending on the coefficient of friction on land and water. The ascending air current is induced when the gradient of the barometric pressure is directed toward the B side of PQ, while the descending current occurs when the gradient points to the A side. The absolute intensity of the current is maximum when the gradient is perpendicular to PQ, while it is zero when the gradient

coincides with OP or OQ. This influence will appear most conspicuous where the land is in the shape of a narrow strip having a large extent of water bodies on both sides, provided the temperature and humidity on the two sides are not very different. Along the coast of a continent, however, the thermal and geographical influence mentioned under the previous paragraph will generally combine with the hydrodynamical influence, so that the relation may vary widely according to season or the physical conditions of the continent.

\* In the sense of Guldberg and Mohn's theory.

In actual cases, these three influences are generally superposed, the resultant effect varying largely according to the degree of relative importance of each factor. For example, in the case of a deep depression of small extent, the first factor plays no greater part than slightly shifting the area with the heaviest precipitation toward E, while the second and the third factors may be important not only for determining the precipitation, but also the subsequent course of progression. It will be especially interesting to investigate the relation with respect to the cases of thunderstorms of the cyclonic type, i.e. those with circular depression in the centres.

The mathematical discussion of these different influences will not be easy, till we have at hand a more or less complete theory of cyclones in general. In the following, however, an attempt is made to illustrate the essential influences of the above mentioned factors for very simple ideal cases, and to found the starting point for analysing the actual complicated phenomena into their essential elements. It must be emphasized that the whole is nothing more than qualitative considerations expressed in mathematical forms.

(1) Planetary thermal influences : Referring to the annexed figure consider a centre of cyclone at O and draw two concentric

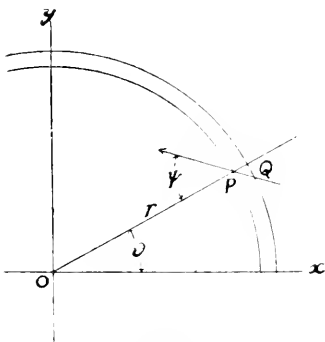


Fig. 44.

isobars with the radii  $r$  and  $r+dr$ , in the inner region, i.e. the region where the ascending current proper to the cyclone is taking place. Suppose now all the isotherms are artificially maintained parallel to the  $x$ -axis. Assume the angle of deflection of the wind  $\phi$ , i.e. the angle between the barometric gradient and the wind, everywhere constant—an assumption apparently contradicting the idea of varying latitude, but since here we are

only considering the effect of the thermal gradient, the small difference of  $\phi$  is evidently not essential. Then we may put

$$\tan \phi = \frac{2\omega \sin \phi_m}{\kappa}$$

where  $\varphi_m$  is the mean latitude and  $\kappa$  the coefficient of friction in Guldberg and Mohn's sense. The flux across the circle with the radius  $r$  is  $2\pi r v \cos \phi$  where  $v$  is the resultant velocity of wind at P, given by

$$v = \frac{G \cos \phi}{\kappa}$$

in which  $G$  is the gradient acceleration :

$$G = K \frac{dB}{dr}$$

where  $B$  is the barometric pressure and  $K$  a constant.\* The excess of the flux across the circle with the radius  $r + dr$  is

$$2\pi \cos \phi \frac{d(rv)}{dr} dr = 2\pi \frac{\cos^2 \phi}{\kappa} (G + r \frac{dG}{dr}) dr.$$

Hence the total amount of the ascending current per unit length of the circular belt with the breadth  $dr$  is

$$\frac{\cos^2 \phi}{r \kappa} (G + r \frac{dG}{dr}) dr.$$

If the air is kept artificially always in saturation corresponding to the momentary temperature as assigned by the given temperature distribution, the condensation of water vapor due to the ascending current will be proportional to the mean absolute humidity or nearly to the mean maximum vapor tension  $E$  between P and Q. The latter is well known as the function of temperature

$$E = f(T) \quad \text{say.}$$

Hence the condensation per unit horizontal area at P will be proportional to

$$R = \frac{f(T)}{\kappa r} (G + r \frac{dG}{dr}) \cos^2 \phi. \quad (1)$$

$$\text{If for example, } G = \text{const.} = G_0, \quad R = \frac{f(T) \cos^2 \phi (G_0)}{\kappa r}, \quad (2)$$

$$\text{or if } G = br, \quad R = \frac{2f(T) b \cos^2 \phi}{\kappa}, \quad (3)$$

in which  $f(T)$  may always be regarded as the function of the space coordinates of  $P$ , since  $T$  is given as such. This holds indeed

---

\* Though of course, in actual cases,  $K$  involves the temperature of the air column, the above assumption may be allowed for the present purpose.



for any distribution of temperature, provided it is maintained stationary by any cause. In the present particular case, the curve of equal  $R$  will be parallel to the isotherms and be straight, if  $G=br$ , and  $R$  will increase toward the direction of the increasing  $T$ . When  $G=const.$  and for example  $T=T_o-Cy$ , the curves will be given by  $f(T_o-Cy)\sqrt{x^2+y^2}=const.$  in Cartesian coordinates, which are generally concave toward the direction of increasing  $T$ . This will hold within the limit of the inner region and the effect will in any case tend to shift the centre of precipitation area toward the direction of the increasing temperature.

The quantity  $R$  is, however, not the only one in determining the precipitation. When the air proceeds from  $Q$  to  $P$ , the temperature must vary, due to the assumption that the isotherms are stationary. It will be easily seen from the figure that the temperature decrease is given by

$$dT=C \frac{\sin(\phi-\theta)}{\cos\phi} dr,$$

when  $T=T_o-Cy$ . Hence the unit volume of air, in proceeding unit distance along  $r$ , condenses out an amount of water given by

$$\frac{dE}{dT} \cdot \frac{dT}{dr} = \frac{d\dot{f}(T)}{dT} \cdot C \frac{\sin(\phi-\theta)}{\cos\phi} = R'. \quad (4)$$

This will be zero for  $\theta=\phi$ , positive for  $\theta=\pi+\phi$  to  $2\pi+\phi$ , and negative (i.e. evaporation instead of condensation) for  $\theta=\phi$  to  $\pi+\phi$ .

The total precipitation will then be proportional to  $R+R'$  in which the effect of  $R'$  is in any case to shift the centre of the heaviest precipitation toward the direction  $\theta=\frac{3\pi}{2}+\phi$ . In the above, it has been assumed that  $R$  at any place is merely due to the condensation caused by the vertical current at that very spot. In the actual case, however, the ascending air is transported leewards by the horizontal current to an extent depending on the ratio of the horizontal velocity to the vertical, and also to the height of the cloud layer. This effect will result in deforming and twisting the isohyets as a whole in counterclockwise sense.

Moreover, even if the isotherms were originally parallel to the latitude, they will be distorted counterclockwise as is well known, since the artificial assumption does not hold that the earth's surface as a sensitive heat reservoir keeps the air always in the temperature prescribed for the latitude. These effects taken altogether, will tend to drive the area of the maximum precipitation toward the eastern side of the depression.

(2) Geographical thermal influences. When the coast line is straight and the air is everywhere saturated, the reasonings of the preceding paragraph exactly apply to this case, only that the temperature gradient is here everywhere small, except in vicinity of the coast line. The part of the precipitation due to the term  $R$  of the preceding paragraph will be abundant on the warmer half-plane. The influence of the term  $R'$  will be only sensible in a narrow zone along the coast line if the variation of temperature across the coast be abrupt or discontinuous. If in the land area the air is not saturated, the case may differ, according as the absolute humidity is greater or less than on the sea. In the special case when in summer the absolute humidity on a very arid land is small compared with that on the colder sea, the result will be reverse to that in the above case, so far as we take no account

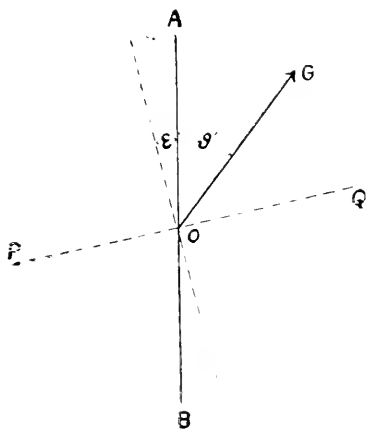


Fig. 45.

of the horizontal transport. The ascending current must, however, in either case be carried leeward as already remarked. Hence we can expect precipitation on the coast of a dry land where the wind comes from the sea. In the normal case, when the air is everywhere saturated, the isohyets will simply be twisted clockwise, so as to increase the precipitation on the coast lying on that side of the centre, which viewed from the centre have the warmer half plane on the right side.

(3) Hydrodynamical topographical influence. Suppose AB is a portion of the coast line bordering the sea on its right

side. OG shows the direction of the barometric gradient which makes an angle  $\theta'$  with OA. Here the essential difference of land and sea is assumed to consist in the difference of the coefficients of friction,  $\kappa$  and  $\kappa'$  respectively; the other thermal behaviours are supposed to be equal on both sides. It has been shown in the above cited paper that the intensity of the ascending current due to the discontinuity of the horizontal flux across AB is given by

$$\delta = D \cos(\theta' + \varepsilon)$$

where

$$D \cos \varepsilon = \frac{1}{2}(\cos 2\phi - \cos 2\phi'), \quad \operatorname{tg} \phi = \frac{c}{\kappa},$$

$$D \sin \varepsilon = \frac{1}{2}(\sin 2\phi - \sin 2\phi'), \quad \operatorname{tg} \phi' = \frac{c}{\kappa'}.$$

If  $\phi = 61^\circ$ ,  $\phi' = 42^\circ$ , then  $D = -0.3255$ ,  $\varepsilon = 13^\circ$ .

Since  $D$  is usually negative, the ascending current at O will be maximum when  $\theta' = \pi - \varepsilon$ , and zero when  $\theta' = -\left(\frac{\pi}{2} + \varepsilon\right)$  or  $\frac{\pi}{2} - \varepsilon$ .

For  $\theta' = -\left(\frac{\pi}{2} + \varepsilon\right)$  to  $\frac{\pi}{2} - \varepsilon$ , the vertical current will be directed downwards; hence the expectation of precipitation at O will be none for these directions if there is no general ascending current proper to the depression. In the case when O lies within the inner region of a cyclone, the ascending current at this point proper to the cyclone will be enhanced when the centre lies on the B side of PQ, but weakened when it lies on the opposite side. If there exists no such hydrodynamical influence, the trace of the cyclonic centre bringing equal expectation to O, will evidently be a circle with O as the centre. In the special case, when the gradient is proportional to the distance from the centre, or  $G = br$ ,  $R$  will be independent of  $r$ , as may be seen from (3) since here the temperature is assumed constant. In general cases, however  $R + R'$  will be a function of  $r$  and  $\theta'$  as may be seen from (2). Denote this by

$$R + R' = F(r\theta').$$

Taking the hydrodynamical influence in account, the centre loci will be given by

$$F(r\theta') + D \cos(\theta' + \varepsilon) = \text{const.}$$

where  $r$  and  $\theta'$  are the polar coordinates, with  $O$  as the origin and  $OA$  as the prime vector. It will be seen, that whatever may be the form of  $E(r\theta')$ , the effect of the second term will be to shift the centre of area of the loci loci toward the direction  $d=\pi-\epsilon$ .

From the above, it will be seen that the first and the second factors are essentially not very different, and there would have been no special need at all to distinguish them, if we are everywhere concerned with humid land only. In the latter case, the essential factor is only the distribution of the isotherms, and the results of the above considerations in the paragraphs under (1) and (2), may be summarized as follows : The maximum precipitation will be expected on the right front quadrant when we look out from the centre of depression toward a direction having the warmer half plane on the right side, provided the isotherms are maintained nearly stationary regardless of the cyclone. The latter condition will be nearly fulfilled when the general temperature distribution is determined by an extensive "centre of action."

When we consider the three factors as separate, it will be seen that the second and third generally conspire in winter, but tend to cancel each other in summer, provided the land and water are of sufficient extent. For a narrow strip of land such as Japan, the second factor will play no important part when a cyclone of considerable dimensions is concerned, since in such a case the assumption does not apply that the land behaves as a reservoir of heat determining the stationary isotherms, regardless of the disturbance due to the cyclone itself. Meanwhile the third influence remains, since it will be independent of the latter disturbance.

Next the first and the third influences conspire when a coast line running more or less in west-easterly direction, face to the water on its southern side, but tend to cancel each other when the water is on the northern side. The resultant effect is well illustrated by comparing the centre loci diagrams for P and J districts. That the first influence predominates in these cases, is shown by the fact that the district in question lies generally on the eastern side of the point of maximum expectation, though yet the eccentricity is more decided in the case of the Pacific coast than in the

Japan Sea districts. The latter fact still shows the unerring effect of the third factor.

Hann remarks that on the northern side of the Alps, the rain fall is most abundant on the rear side of a barometric minimum. This fact may probably be explained by the predominating influence of the hydrodynamical factor, since the effect of a great mountain range is equivalent to the increase of the coefficient of friction. That northern Germany, including Swinemünde and Breslau, has maximum rain fall on the rear side of a depression, may be understood by the combined effect of the second and the third factors. The case of Great Britain investigated by Mill, seems at first sight irreconcilable with the above considerations, since the heaviest rainfall area occurs on the left side of the track of the centre, contradicting in most cases the influence of the third factor. But it must be remembered that Mill's results refer to the "smear" in which the rainfall on the front and rear sides of the centre are supesposed. He states, indeed, that the heaviest rainfall occurs in advance of the centre. The influence of the third factor combined with that of the first one may in some cases shift the centre of the smear to the left side of the track ; the front rain falling on the eastern side of land or mountain is abundant on the northern side of the track, due to the third influence, while the rear rain is abundant on the southern side of the track, on the western side of the land, or any orographic irregularity ; hence if due to the first factor, the rear rain is less abundant than the front rain, the centre of the smear will lie on the northern side of the track. This seems to explain most cases given by Mill where the depressions proceed toward E. In order to explain different cases in which the relation is apparently not so simple as considered above, exact knowledge is of course necessary of the thermal and topographical conditions of the district concerned for each particular case.

Finally, it must be remarked, to avoid misunderstanding, that the present discussions involve no essential novelty as a theory of cyclonic rainfall, except emphasizing the importance of the hydrodynamical influence due to the difference of the coefficient of friction. The above may only be regarded as suggesting a way toward

the better understanding of the complicated rain problem. The discussions refer to different ideal cases, underlying several artificial simplifying conditions. Above all, the assumption is made that the thermal conditions are prescribed independent of the cyclone, and the secondary disturbances both thermal and topographical due to the cyclone itself, are entirely put out of account. The latter disturbances may in some cases modify the resultant effect of the other primary factors in no small degree. Still, we are inclined to believe that the above way of analysing the complicated influences in these principal factors may in many cases facilitate a better understanding of the phenomena of cyclonic rainfall, and if properly understood and applied may be utilized for the purpose of weather prediction.

In conclusion, we wish to express our best thanks to Prof. T. Okada of the Central Meteorological Observatory for many valuable informations.

## On the Relatively Abelian Corpora with respect to the Corpus defined by a Primitive Cube Root of Unity.

By

**Tanzo Takenouchi**, *Rigakushi*.

Professor of Mathematics in the Eighth High School.

It was conjectured by Kronecker that all the relatively Abelian corpora (*Körper*) with respect to an imaginary quadratic corpus are probably exhausted by those which arise from the equations of transformation of elliptic functions with singular moduli. Prof. T. Takagi<sup>1)</sup> investigated this problem in the remarkably interesting special case, in which the fundamental corpus is defined by the imaginary unit  $i$ , and proved that the relatively Abelian corpora with respect to  $k(i)$  are completely exhausted by the division-corpora (*Teilungskörper*) of the function  $\text{sn}$  with the singular modulus  $\kappa=i$ . Following his example, I am going to treat of another interesting special case in which the fundamental corpus is  $k(\rho)$ ,  $\rho$  denoting a primitive cube root of unity.

The present paper consists of two parts. In the first part it will be proved that the relatively Abelian corpora with respect to  $k(\rho)$  are completely exhausted by the division-corpora of the function  $\text{sn}$  with the singular modulus  $\kappa=i\rho$ .

Now, if  $\omega$  be a quadratic number whose imaginary part is positive, and  $m$  a natural number, then the invariant  $j(m\omega)$  is called a class-invariant. By adjoining the class-invariant  $j(m\omega)$  and a primitive  $m$ th root of unity to the quadratic corpus  $k(\omega)$ , we obtain a corpus, to which I shall (§. 16) give the name *strahl-corpus*. It is known that the *strahl*-corpus is relatively Abelian

---

1) Takagi: Journal of the College of Science, Tokyo Imperial University, Vol. XIX, Art. 5; Proceedings of the Tokyo Mathematico-Physical Society, 2nd Ser., Vol. VII, No. 21.

with respect to  $k(\omega)$ . But the relatively Abelian corpora with respect to  $k(\omega)$  are not completely exhausted by *strahl*-corpora.

The chief object of the second part of the present paper is to make these points clear in the special case in which the fundamental quadratic corpus is  $k(\rho)$ .

## PART I.

### §. 1.

Consider the function  $\wp(u)$ , whose periods  $\omega, \omega'$  are in the ratio

$$\frac{\omega'}{\omega} = \rho, \quad \rho = \frac{-1 + \sqrt{-3}}{2}.$$

For such  $\wp$ -function, we have

$$g_2 = 0,$$

and consequently

$$\wp'(u)^2 = 4\wp(u)^3 - g_3.$$

This  $\wp$ -function admits of complex multiplication. Namely, if we denote by  $\mu$  any integer in the quadratic corpus  $k(\rho)$ , then

$$\wp(\mu u) = \frac{R}{P}, \quad (1)$$

where  $P$  and  $R$  are rational integral functions of  $\wp(u)$  of degrees  $m-1$  and  $m$  respectively,  $m$  being the norm of  $\mu$ . Let us suppose, once for all, that the coefficient of the highest power of  $\wp(u)$  in  $P$  is equal to  $\mu^2$ . Then, putting  $u=0$  in (1), we find that the coefficient of the highest term in  $R$  must be equal to unity.

Let us now introduce a function  $\phi_\mu$ , such that

$$\begin{aligned} \phi_\mu &= \mu, & \text{when } m &= 0 \text{ or } 1, \\ \phi_\mu^2 &= \mu^2 P \left\{ \wp(u) - \wp\left(\frac{\omega}{\mu}\right) \right\}, & \text{when } m &> 1, \end{aligned}$$

where the product is to be taken for all such incongruent residues  $\nu$  with respect to the modulus  $\mu$ , that are not divisible by  $\mu$ . Then we get

$$P = \phi_\mu^2$$



and we may put<sup>1)</sup>

$$\begin{aligned}\zeta_\mu &= S_\mu, & \text{if } m \text{ be odd,} \\ \zeta_\mu &= \xi'(u)S_\mu, & \text{if } m \text{ be even,}\end{aligned}$$

where  $S_\mu$  is a rational integral function of  $\xi(u)$  whose highest term is

$$\mu \xi(u)^{\frac{m-1}{2}} \quad \text{or} \quad -\frac{\mu}{2} \xi(u)^{\frac{m-1}{2}},$$

according as  $m$  is odd or even. The sign of  $\zeta_\mu$  is thus completely defined. And it can be seen that, if we expand  $\zeta_\mu$  in an ascending power series of  $u$ , the first term is always equal to

$$\frac{\mu}{u^{m-1}}.$$

Now, by (1),

$$\xi(\mu u) - \xi(u) = \frac{R - \xi(u)P}{P}.$$

Since the expression on the left-hand side vanishes only when

$$\mu u \equiv \pm u \pmod{\omega, \omega'},$$

it follows that the numerator on the right-hand side can differ from  $\zeta_{\mu+1} \zeta_{\mu-1}$  only by a constant factor. Putting  $u=0$ , we find that this constant factor is equal to  $-1$ . Therefore

$$\xi(\mu u) - \xi(u) = -\frac{\zeta_{\mu+1} \zeta_{\mu-1}}{\zeta_\mu^2}.$$

If we assume that

$$\mu = a + b\epsilon,$$

$a$  and  $b$  being rational integers, we get

$$\left. \begin{aligned}\xi(\mu u) - \xi(u) &= -\frac{S_{\mu+1} S_{\mu-1}}{\xi'(u)^2 S_\mu^2}, & \text{when } (a, b) &\equiv (0, 0) \\ &= -\frac{\xi'(u)^2 S_{\mu+1} S_{\mu-1}}{S_\mu^2}, & \text{when } (a, b) &\equiv (1, 0) \\ &= -\frac{S_{\mu+1} S_{\mu-1}}{S_\mu^2}, & \text{when } (a, b) &\equiv (0, 1), (1, 1)\end{aligned} \right\} \pmod{2}.$$

1) Cf. Weber: Lehrbuch der Algebra, Vol. III, §. 58 and §. 152.

## §. 2.

Let  $\nu$  and  $\mu$  be two integers in  $k(\rho)$ . It can be shewn exactly as in the case of ordinary (not complex) multiplication<sup>1)</sup>, that

$$\zeta_{\nu+\mu} \zeta_{\nu-\mu} = \zeta_{\nu+1} \zeta_{\nu-1} \zeta_{\mu}^2 - \zeta_{\nu-1} \zeta_{\nu+1} \zeta_{\mu}^2.$$

Replacing  $(\nu, \mu)$  in this relation by  $(\mu+1, \mu-1)$ ,  $(\mu+1, \mu)$ ,  $(\mu+\rho, \mu)$ ,  $(\mu+1+\rho, \mu)$  respectively, we get

$$\begin{aligned} -\zeta'(u) \zeta_{2\mu} &= \zeta_{\mu+2} \zeta_{\mu} \zeta_{\mu-1}^2 - \zeta_{\mu} \zeta_{\mu-2} \zeta_{\mu+1}^2, \\ \zeta_{2\mu+1} &= \zeta_{\mu+2} \zeta_{\mu}^3 - \zeta_{\mu-1}^3 \zeta_{\mu-1}, \\ \rho \zeta_{2\mu+\rho} &= \zeta_{\mu+1+\rho} \zeta_{\mu-1+\rho} \zeta_{\mu}^2 - \zeta_{\mu-1} \zeta_{\mu-1} \zeta_{\mu+\rho}^2, \\ -\rho^2 \zeta_{2\mu+1+\rho} &= \zeta_{\mu+2+\rho} \zeta_{\mu+\rho} \zeta_{\mu}^2 - \zeta_{\mu-1} \zeta_{\mu-1} \zeta_{\mu+1+\rho}^2. \end{aligned}$$

If we express these formulae in terms of  $S$ , we obtain the following recursion-formulae for  $S: (\mu=a+b\rho)$

(i) when  $(a, b) \equiv (0, 0) \pmod{2}$ ,

$$\begin{aligned} -S_{2\mu} &= S_{\mu+2} S_{\mu} S_{\mu-1}^2 - S_{\mu} S_{\mu-2} S_{\mu+1}^2, \\ S_{2\mu+1} &= \zeta'(u)^4 S_{\mu+2} S_{\mu}^3 - S_{\mu-1}^3 S_{\mu-1}, \\ \rho S_{2\mu+\rho} &= \zeta'(u)^2 S_{\mu+1+\rho} S_{\mu-1+\rho} S_{\mu}^2 - S_{\mu+1} S_{\mu-1} S_{\mu+\rho}^2, \\ -\rho^2 S_{2\mu+1+\rho} &= \zeta'(u)^2 S_{\mu+2+\rho} S_{\mu+\rho} S_{\mu}^2 - S_{\mu-1} S_{\mu-1} S_{\mu+1+\rho}^2; \end{aligned}$$

(ii) when  $(a, b) \equiv (1, 0) \pmod{2}$ ,

$$\begin{aligned} -S_{2\mu} &= S_{\mu-2} S_{\mu} S_{\mu-1}^2 - S_{\mu} S_{\mu-2} S_{\mu-1}^2, \\ S_{2\mu+1} &= S_{\mu+2} S_{\mu}^3 - \zeta'(u)^4 S_{\mu-1}^3 S_{\mu-1}, \\ \rho S_{2\mu+\rho} &= S_{\mu-1+\rho} S_{\mu-1+\rho} S_{\mu}^2 - \zeta'(u)^2 S_{\mu+1} S_{\mu-1} S_{\mu+\rho}^2, \\ -\rho^2 S_{2\mu-1+\rho} &= S_{\mu+2+\rho} S_{\mu+\rho} S_{\mu}^2 - \zeta'(u)^2 S_{\mu-1} S_{\mu-1} S_{\mu+1+\rho}^2; \end{aligned}$$

(iii) when  $(a, b) \equiv (0, 1) \pmod{2}$ ,

$$\begin{aligned} -\zeta'(u)^2 S_{2\mu} &= S_{\mu+2} S_{\mu} S_{\mu-1}^2 - S_{\mu} S_{\mu-2} S_{\mu+1}^2, \\ S_{2\mu+1} &= S_{\mu-2} S_{\mu}^3 - S_{\mu-1}^3 S_{\mu-1}, \\ \rho S_{2\mu+\rho} &= S_{\mu-1+\rho} S_{\mu-1+\rho} S_{\mu}^2 - \zeta'(u)^2 S_{\mu+1} S_{\mu-1} S_{\mu+\rho}^2, \\ -\rho^2 S_{2\mu-1+\rho} &= \zeta'(u)^2 S_{\mu+2+\rho} S_{\mu+\rho} S_{\mu}^2 - S_{\mu+1} S_{\mu-1} S_{\mu+1+\rho}^2; \end{aligned}$$

---

1) Weber: Algebra III, §. 58.

$$\begin{aligned}
\text{(iv) when } (a, b) &\equiv (1, 1) \pmod{2}, \\
-\wp'(u)^2 S_{2a} &= S_{a+2} S_a S_{a-1}^2 - S_a S_{a-2} S_{a-1}^2, \\
S_{2a+1} &= S_{a+2} S_a^3 - S_{a+1}^3 S_{a-1}, \\
\rho S_{2a+\rho} &= \wp'(u)^2 S_{a+1-\rho} S_{a-1-\rho} S_a^2 - S_{a-1} S_{a-1} S_{a+\rho}^2, \\
-\rho^2 S_{2a+1+\rho} &= S_{a+2+\rho} S_{a+\rho} S_a^2 - \wp'(u)^2 S_{a+1} S_{a-1} S_{a+1+\rho}^2.
\end{aligned}$$

The expressions of  $S_n$  for small values of  $a$  and  $b$  can easily be found by direct calculation. They are

$$\begin{aligned}
S_1 &= 0, & S_\rho &= \rho, & S_{-\rho} &= -\rho, \\
S_1 &= 1, & S_{1+\rho} &= 1+\rho, & S_{1-\rho} &= (1-\rho)p, \\
S_2 &= -1, & S_{2+\rho} &= (2+\rho)p, & S_{2-\rho} &= (2-\rho)p^3 - \rho^2 g_3, \\
S_3 &= 3p^4 - 3\rho g_3 p, & S_{3+\rho} &= (3+\rho)p^3 - \rho g_3, & S_{3-\rho} &= (3-\rho)p^6 \\
& & & & & + (3-\rho)(1+3\rho)g_3 p^3 - \rho g_3^2, \\
S_4 &= -2\rho^6 + 10g_3 p^3 + g_3^2,
\end{aligned}$$

where  $p$  stands for  $\wp(u)$ . All the other  $S$  can be found by the recursion-formulae.

The general form of  $S_n$  is as follows<sup>1)</sup>:

$$\left. \begin{aligned}
S_n &= -\frac{n}{2} p^{\frac{n-1}{2}} + c_1 g_3 p^{\frac{n-10}{2}} + \dots - \rho g_3^{\frac{n-6}{6}} p, & \text{when } m \equiv 0 \\
S_n &= \rho p^{\frac{n-1}{2}} + c_1 g_3 p^{\frac{n-7}{2}} + \dots + \begin{cases} (-1)^{\frac{b}{2}} \left(\frac{a+b}{3}\right) \rho^{b(a+b)} g_3^{\frac{n-1}{6}}, \\ (b \text{ being even}) \\ (-1)^{\frac{a(a+3b)}{2}} \left(\frac{a+b}{3}\right) \rho^{b(a+b)} g_3^{\frac{n-1}{6}}, \\ (b \text{ being odd}) \end{cases} & \text{when } m \equiv 1 \\
S_n &= \rho p^{\frac{n-1}{2}} + c_1 g_3 p^{\frac{n-7}{2}} + \dots - (-1)^{\frac{a(a+b)}{2}} \rho g_3^{\frac{n-3}{6}} p, & \text{when } m \equiv 3 \\
S_n &= -\frac{n}{2} p^{\frac{n-4}{2}} + c_1 g_3 p^{\frac{n-10}{2}} + \dots + \left(\frac{a+b}{3}\right) \rho^{b(a+b)} g_3^{\frac{n-4}{6}}, & \text{when } m \equiv 4
\end{aligned} \right\} \pmod{6},$$

where  $c_1, c_2, \dots$  are integers in  $k(\rho)$ , and  $\left(\frac{a+b}{3}\right)$  means Legendre-Jacobi's symbol for quadratic character.

1) T. Takenouchi: Tohoku Mathematical Journal, Vol. VII, Nos. 1, 2.

## §. 3.

Let us now introduce a new function :

$$\tau(u) = \frac{\wp(u)}{\sqrt[3]{g_3}};$$

the ambiguity arising from the cube root of  $g_3$  will be removed afterwards. If we suppose that  $\mu$  is relatively prime to 3, then

$$\tau(\mu u) = \frac{R_\mu(x)}{P_\mu(x)}, \quad x = \tau(u),$$

where  $R_\mu(x)$  and  $P_\mu(x)$  denote rational integral functions of the forms

$$R_\mu(x) = x^m + a_1 x^{m-3} + \dots + a_2 x^{m-3k} + \dots + a_{\frac{m-1}{3}} x,$$

$$P_\mu(x) = \mu^2 x^{m-1} + b_1 x^{m-4} + \dots + b_k x^{m-3k-1} + \dots + (-1)^{m-1} \mu^{2(m-1)}, \quad m = n(\mu),$$

with integral coefficients in  $k(\rho)$ .

Hence, if we regard  $\tau(u)$  as an unknown quantity, the equation

$$R_\mu - \tau(\mu u) P_\mu = 0$$

is of the  $m$ th degree, and its absolute term is associated with  $\tau(\mu u)$ . All the roots of this equation are given by

$$\tau\left(u + \frac{\nu\omega}{\mu}\right),$$

where  $\nu$  is to take all the values of the complete system of residues with respect to the modulus  $\mu$ . Hence we obtain the relation

$$\tau(\mu u) \simeq \prod_{\nu=0}^{\mu-1} \tau\left(u + \frac{\nu\omega}{\mu}\right).$$

$$\text{or} \quad \frac{\tau(\mu u)}{\tau(u)} \simeq \prod_{\nu=0}^{\mu-1} \tau\left(u + \frac{\nu\omega}{\mu}\right);$$

the symbol  $\simeq$  meaning "is associated with."

Now, this last relation exactly corresponds to that of the same form, which presents itself in the complex multiplication of the function  $\text{sn}$ .<sup>1)</sup> Hence, starting from this relation, we can deduce the following results:<sup>2)</sup>

1) Weber: Algebra III, §. 157-22.

2) Weber: Algebra III, §. 157.

If  $a$  be an integer in  $k(\rho)$  and relatively prime to 3, and if  $\mu$  be relatively prime to  $a$ , then the numbers

$$\tau\left(\frac{\mu\omega}{a}\right)$$

are all associated with one another.

If  $\mu$  be a power of a prime, then the reciprocals of the numbers

$$\tau\left(\frac{\nu\omega}{\mu}\right)$$

are divisors of  $\mu$ .

If  $\mu$  consists of more than one distinct prime factor, then the numbers

$$\tau\left(\frac{\nu\omega}{\mu}\right)$$

are algebraic unities.

Next let us consider the case where  $\mu$  is not relatively prime to 3. In this case,  $\mu$  is necessarily divisible by  $1+2\rho$ , for

$$3 = -(1+2\rho)^2.$$

Since

$$R_{1+2\rho}(x) = x^3 - 1,$$

$$P_{1+2\rho}(x) = -3x^2,$$

we get

$$x^3 + 3yx^2 - 1 = 0, \quad (2)$$

$$\text{where } x = \tau(u), \quad y = \tau\{(1+2\rho)u\}.$$

This equation shews that  $x$  is an algebraic unity, provided that  $y$  is an algebraic integer.

Now it can easily be seen that

$$\tau\left(\frac{\omega}{1+2\rho}\right) = 0.$$

Hence, by the repeated application of (2), we conclude that

$$\tau\left(\frac{\nu\omega}{(1+2\rho)^k}\right), \quad k \geq 1,$$

are all algebraic unities.

By the same reasoning, since

$$\tau\left(\frac{\nu\omega}{\mu}\right)$$

is an algebraic unity, when  $\mu$  contains more than one distinct prime, so must also be

$$\tau\left(\frac{\nu\omega}{(1+2\rho)^k\mu}\right), \quad k \geq 1.$$

Lastly, to determine the nature of

$$\tau\left(\frac{\nu\omega}{(1+2\rho)^k\mu}\right), \quad k \geq 1,$$

when  $\mu$  is a power of a single prime, observe that the three roots of the equation (2) are

$$x_1 = \tau(u), \quad x_2 = \tau\left(u + \frac{\omega}{1+2\rho}\right), \quad x_3 = \tau\left(u - \frac{\omega}{1+2\rho}\right),$$

which are so related that

$$x_1 x_2 x_3 = 1,$$

$$x_1 x_2 + x_2 x_3 + x_3 x_1 = 0.$$

Therefore we get

$$\tau\left(u + \frac{\omega}{1+2\rho}\right) \tau\left(u - \frac{\omega}{1+2\rho}\right) = \frac{1}{\tau(u)},$$

$$\tau\left(u + \frac{\omega}{1+2\rho}\right) + \tau\left(u - \frac{\omega}{1+2\rho}\right) = -\frac{1}{\tau(u)^2}.$$

Putting for  $u$  in these relations a fraction in  $k(\rho)$ , whose denominator is a power of a single prime relatively prime to  $1+2\rho$ , we see that

$$\tau\left(\frac{\nu\omega}{(1+2\rho)\mu}\right)$$

is a divisor of  $\mu$ , and its square is associated with the reciprocal of

$$\tau\left(\frac{\nu\omega}{\mu}\right).$$

Thus, the number

$$\tau\left(\frac{\nu\omega}{(1+2\rho)\mu}\right)$$

being an algebraic integer, it follows as before, that

$$\tau\left(\frac{\nu\omega}{(1+2\rho)^k\mu}\right) \quad (k > 1)$$

are algebraic unities.

We shall now sum up the results obtained in the present section.

*Let  $\pi, \pi', \dots$  denote distinct primes in  $k(\rho)$ , not associated with  $1+2\rho$ , then*

$$\tau\left(\frac{\nu\omega}{1+2\rho}\right) = 0,$$

$$\tau\left(\frac{\nu\omega}{(1+2\rho)^k}\right) \simeq 1, \quad k > 1,$$

$$\tau\left(\frac{\nu\omega}{\pi^t}\right) = \frac{1}{x}, \quad \pi \equiv 0 \pmod{x},$$

$$\tau\left(\frac{\nu\omega}{\pi^t\pi'^b\dots}\right) \simeq 1,$$

$$\tau\left(\frac{\nu\omega}{(1+2\rho)\pi^t}\right) = y, \quad y^2 \simeq x,$$

$$\tau\left(\frac{\nu\omega}{(1+2\rho)^k\pi^t}\right) \simeq 1, \quad k > 1,$$

$$\tau\left(\frac{\nu\omega}{(1+2\rho)^k\pi^t\pi'^b\dots}\right) \simeq 1, \quad k \geq 1,$$

where  $\nu$  is any integer in  $k(\rho)$  relatively prime to the denominator in each case.

In particular, when  $\mu$  is a prime in  $k(\rho)$ , not associated with  $1+2\rho$ , all the roots of the equation

$$x^{m-1}P_\rho\left(\frac{1}{x}\right) = \mu^2 + b_1x^1 + \dots + b_nx^{2n} + \dots + (-1)^{m-1}\rho^{2(\iota+b)}x^{m-1} = 0$$

are divisors of  $\mu$ , and are associated with one another. Since the coefficients in this equation, except the last one, are associated with the elementary symmetric functions of the roots, and also since these coefficients all belong to the corpus  $k(\rho)$ , we infer that they are all divisible by  $\mu$ .

When  $\mu = 1+2\rho$ , we have

$$P_{1+2\rho}(x) = -3x^2.$$

Hence, when  $\mu$  is any prime in  $k(\rho)$ , the coefficients of  $P_\rho(x)$ , except the constant term, are all divisible by  $\mu$ .

The same property holds also for  $S_\rho^{(1)}$ ; whence follows, by Eisenstein's theorem, that  $S_\rho$  is irreducible in  $k(\rho)$ .

#### §. 4.

The only thing we have hitherto assumed concerning the function  $\mathfrak{E}(u)$  is the relation

$$\frac{\omega'}{\omega} = \rho,$$

which gives

$$g_2 = 0.$$

Here, as well as hereafter, we shall completely specialise the function by the additional conditions:

$$\left. \begin{aligned} c_1 &= \mathfrak{E}\left(\frac{\omega}{2}\right) = \frac{\rho}{\rho-1}, \\ c_2 &= \mathfrak{E}\left(\frac{\omega'}{2}\right) = \frac{\rho^2}{\rho-1}, \\ c_3 &= \mathfrak{E}\left(\frac{\omega+\omega'}{2}\right) = \frac{1}{\rho-1}, \end{aligned} \right\} \quad (3)$$

and consequently

$$\begin{aligned} g_3 &= 4c_1c_2c_3 = \frac{4}{(\rho-1)^3}, \\ \mathfrak{E}'(u)^2 &= 4\left\{\mathfrak{E}(u)^3 + \frac{1}{(1-\rho)^3}\right\}. \end{aligned}$$

Then, let us put

$$\tau(u) = \frac{\mathfrak{E}(u)}{\sqrt[3]{g_3}}, \quad \sqrt[3]{g_3} = \frac{\sqrt[3]{4}}{\rho-1}.$$

The ambiguity in the former definition of  $\tau(u)$  is thus removed.

Now, let  $O, A, B, C$  be the vertices of the parallelogram in the Gaussian plane, corresponding respectively to the values

$$u = 0, \omega, \omega + \omega', \omega';$$

and let  $OE, OF$  be drawn perpendicular to  $AB, BC$  respectively, and  $BG, BH$  perpendicular to  $CO, CA$  respectively. Since

1) Takenouchi: loc. cit.



$$u = \int_z^{\mathfrak{z}} \frac{d\mathfrak{z}}{2\sqrt{\mathfrak{z}^3 + \frac{1}{(1-\rho)^2}}},$$

we get

$$\frac{u}{\sqrt{\rho-1}} = \frac{1}{\sqrt[3]{2}} \int_{\infty}^{\tau} \frac{d\tau}{\sqrt{4\tau^3-1}}.$$

This shews that, in the parallelogram  $OACU$ , the locus of the point  $u$ , for which  $\tau(u)$  is real, consists of two straight lines, on which

$$\frac{u}{\sqrt{\rho-1}} \quad \text{or} \quad \frac{i u}{\sqrt{\rho-1}}$$

is always real. Taking into account the values (3) and the relation

$$\rho\tau(\rho^2 u) = \rho^2\tau(\rho u) = \tau(u), \quad (4)$$

we arrive at the following conclusion :

$$\begin{array}{llll} \tau(u) & \text{is real along the straight lines} & OB, & AC, \\ \rho\tau(u) & \dots\dots\dots & \dots & OC, AB, OE, BG, \\ \rho^2\tau(u) & \dots\dots\dots & \dots & OA, BC, OF, BH. \end{array}$$

The direction of  $OB$ , along which  $\tau(u)$  is real and positive, makes with the real axis of the Gaussian plane an angle, which is equal to the phase of the number  $\sqrt{\rho-1}$ , i.e. the angle of  $75^\circ$ .

In our specialised  $\mathfrak{z}$ -function, since  $g_2=0$ , we have  $j(\omega)=0$ . Hence

$$1-x^2\kappa'^2=0,$$

which gives

$$x = \pm i\rho \quad \text{or} \quad \pm i\rho^2.$$

Between our  $\mathfrak{z}$ -function and the function  $\text{sn}$  with the singular modulus  $x = i\rho$ , there exists the relation

$$\mathfrak{z}(u) = \frac{1}{\text{sn}^2 u} - \frac{1}{1-\rho}, \quad (5)$$

and

$$2K = \omega, \quad 2iK' = \omega + \omega'.$$

If we combine (4) with (5), the following formulæ can easily be deduced:

$$\left. \begin{aligned} \operatorname{sn} \rho u &= \rho \frac{\operatorname{sn} u}{\operatorname{dn} u}, & \operatorname{sn} \rho^2 u &= \rho^2 \frac{\operatorname{sn} u}{\operatorname{cn} u}, \\ \operatorname{cn} \rho u &= \frac{1}{\operatorname{dn} u}, & \operatorname{cn} \rho^2 u &= \frac{\operatorname{dn} u}{\operatorname{cn} u}, \\ \operatorname{dn} \rho u &= \frac{\operatorname{cn} u}{\operatorname{dn} u}, & \operatorname{dn} \rho^2 u &= \frac{1}{\operatorname{cn} u}, \end{aligned} \right\} \quad (6)$$

Also, differentiating (5) with respect to  $u$ , we get

$$\left. \begin{aligned} \wp'(u) &= -\frac{2 \operatorname{cn} u \operatorname{dn} u}{\operatorname{sn}^3 u} \\ &= -\frac{2}{\operatorname{sn} u \operatorname{sn} \rho u \operatorname{sn} \rho^2 u}. \end{aligned} \right\} \quad (7)$$

Assume that

$$\left. \begin{aligned} \rho &= a + b\rho, \\ a &\equiv 1 \pmod{4}, & b &\equiv 0 \pmod{2}, \end{aligned} \right\} \quad (8)$$

$a$  and  $b$  being rational integers. Then we know that<sup>1)</sup>

$$\operatorname{sn} \rho u = \frac{x A_\rho(x)}{D_\rho(x)}, \quad x = \operatorname{sn} u,$$

where

$$\begin{aligned} \varepsilon A_\rho(x) &= \varepsilon \rho + A_3 x^2 + \cdots + A_{m-2} x^{m-3} + \sqrt{x^{m-1}} x^{n-1}, \\ D_\rho(x) &= 1 + D_{m-2} x^2 + \cdots + D_3 x^{m-3} + \varepsilon \rho \sqrt{x^{m-1}} x^{m-1}, \\ m &= n(\rho), \quad x = i\rho, \quad \varepsilon^2 = 1, \end{aligned}$$

the coefficients  $A$ 's and  $D$ 's being integers in  $k(\rho, i)^{2)}$ , such that

$$A_i \sqrt{x^{m-2i+1}} = D_i, \quad i = 3, 4, \dots, m-2.$$

To find the exact value of  $\varepsilon$ , observe that

$$\begin{aligned} \frac{1}{\operatorname{sn}^2 \rho u} - \frac{1}{\operatorname{sn}^2 u} &= \wp'(\rho u) - \wp'(u) \\ &= -\frac{\wp'(u)^2 S_{\rho+1}' S_{\rho-1}'}{S_\rho'^2}, \end{aligned}$$

1) Weber: Algebra III, §. 157.

2) It follows from (9) on the next page, that the coefficients of  $A_\rho(x)$ , i.e.,

$$\frac{A_i}{\varepsilon}, \quad i = 3, 4, \dots, m-2,$$

are integers in  $k(\rho)$ .

consequently

$$\operatorname{sn}^2 u = \frac{\operatorname{sn}^2 u S_\rho^2}{S_\rho^2 - \operatorname{sn}^2 u \operatorname{sn}'(u)^2 S_{\rho-1} S_{\rho+1}}.$$

Hence, if we regard  $S_\rho$  as a function of  $x = \operatorname{sn} u$ , and express it by  $S_\rho\left(\frac{1}{x^2} - \frac{1}{1-\rho}\right)$ , we get

$$\frac{1}{x^{m-1}} A_\rho(x) = S_\rho\left(\frac{1}{x^2} - \frac{1}{1-\rho}\right). \quad (9)$$

In the limit when  $x = \infty$ , we get

$$\frac{1}{\varepsilon} \sqrt{\kappa^{m-1}} = S_\rho\left(\frac{1}{\rho-1}\right).$$

The value of the right-hand side can be calculated successively by means of the recursion-formulae of  $S$  given in §. 2. (The supposition that  $b$  is even is essential in this calculation.) The general form of it is

$$S_\rho\left(\frac{1}{\rho-1}\right) = (-1)^{\frac{a+b-1}{2}} \rho^{1-m} = (-1)^{\frac{b}{2}} \rho^{1-m}.$$

Therefore

$$\varepsilon = (-1)^{\frac{b}{2}} \rho^{m-1} \sqrt{\kappa^{m-1}} = i^{-\frac{b}{2}},$$

and the product of all the roots of the equation

$$A_\rho(x) = 0$$

is equal to

$$(-1)^{\frac{b}{2}} \rho^{m-1} \mu.$$

Now, it is well-known that, if  $\operatorname{sn} u$  be any one of the roots of this equation, then both  $\operatorname{cn} u$  and  $\operatorname{dn} u$  can be rationally expressed by  $\operatorname{sn} u$  in the corpus  $k(\rho)$ . Therefore, it follows from (6) that the corpus obtained by adjoining  $\operatorname{sn} u$  to  $k(\rho)$  must remain unaltered, if we change  $\rho$  into another integer associated with  $\rho$ . On the other hand, it is certain that, if there be given any integer with the odd norm in  $k(\rho)$ , then among the integers associated with it we can always find one, and only one, possessing the form (8). Hence, in treating the nature of the corpus  $k(\rho, \operatorname{sn} u)$ , we may entirely confine ourselves to the case where  $\rho$  is of the form (8), provided that the norm  $m$  be odd.

Hereafter we shall call prime integers of the form (8) simply *primary integers*.

### §. 5.

Let  $\mu$  be a primary integer relatively prime to 3, and  $m$  its norm, then

$$m \equiv 1 \pmod{6};$$

and the equation of the  $(m-1)$ th degree

$$A_{\mu}(x) = 0$$

is irreducible in  $k(\rho)$ . The roots of this equation are

$$x_{\lambda} = \operatorname{sn}\left(\rho^{\lambda} \frac{\omega}{\mu}\right), \quad \lambda = 0, 1, 2, \dots, m-2,$$

$\rho$  denoting a primitive root of  $\mu$ .

Now, to find the discriminant of this equation, we make use of the equality:

$$\begin{aligned} & (\operatorname{sn} u - \operatorname{sn} v)(\operatorname{sn} u + \operatorname{sn} v) \{ \operatorname{sn}(u+v) - \operatorname{sn}(u-v) \} \\ &= 2 \operatorname{sn} v \operatorname{cn} u \operatorname{dn} u \operatorname{sn}(u+v) \operatorname{sn}(u-v) \\ &= \frac{2 \operatorname{sn}^2 u \operatorname{sn} v \operatorname{sn}(u+v) \operatorname{sn}(u-v)}{\operatorname{sn} \rho u \operatorname{sn} \rho^2 u}, \end{aligned} \quad (10)$$

which can immediately be verified by the addition-theorem of the function  $\operatorname{sn}$  and the relation (6). If we put

$$u = \rho^{\lambda} \frac{\omega}{\mu}, \quad v = \rho^{\lambda'} \frac{\omega}{\mu},$$

$$\lambda, \lambda' = 0, 1, 2, \dots, m-2, \quad \lambda \not\equiv \lambda' \pmod{\frac{m-1}{2}},$$

then, corresponding to each of the  $(m-1)(m-3)$  different combinations of values of  $\lambda$  and  $\lambda'$ , we obtain an equation of the form (10). Multiplying all these equations side by side, we get

$$\begin{aligned} \prod_{(\lambda, \lambda')} (x_{\lambda} - x_{\lambda'})^2 &= 2^{(m-1)(m-3)} \prod_{\lambda} x_{\lambda}^{2(m-3)} \\ &= 2^{(m-1)(m-3)} \rho^{(m-3)}. \end{aligned}$$

Hence, putting

$$\delta = \prod_{(\lambda, \lambda')} (x_{\lambda} - x_{\lambda'})^2,$$

we get

$$\delta = \varepsilon 2^{\frac{(m-1)(m-3)}{3}} \mu^{m-3},$$

where  $\varepsilon$  is a certain cube root of unity. If we denote the required discriminant by  $D$ , then

$$\begin{aligned} D &= (-1)^{\frac{(m-1)(m-3)}{2}} \delta (-1)^{\frac{m-1}{2}} H(2x_\lambda) \\ &= \delta 2^{m-1} \mu. \end{aligned}$$

On the other hand, let  $D_1$  be the discriminant of the equation

$$S_\rho(y) = 0,$$

which is of degree  $\frac{m-1}{2}$ , and whose roots are

$$y_\lambda = \wp\left(\lambda \frac{\omega}{\mu}\right), \quad \lambda = 0, 1, 2, \dots, \frac{m-3}{2}.$$

Then, on account of the relation

$$\wp(u) - \wp(v) = \frac{1}{\operatorname{sn}^2 u} - \frac{1}{\operatorname{sn}^2 v} = \frac{(\operatorname{sn} v - \operatorname{sn} u)(\operatorname{sn} v + \operatorname{sn} u)}{\operatorname{sn}^2 u \operatorname{sn}^2 v},$$

we obtain

$$D_1^4 = \frac{\delta^2}{\mu^{(m-3)}} = \frac{\varepsilon^2 2^{\frac{(m-1)(m-3)}{3}}}{\mu^{(m-3)}}. \quad (11)$$

It was shewn in §. 2, that  $S_\rho(y)$  is an integral function of  $y^3$ . Hence, if we regard  $y^3$  as an unknown quantity, the above equation is of degree  $\frac{m-1}{6}$ , and its discriminant  $D_2$  must satisfy the relation

$$\begin{aligned} D_1 &= D_2^3 (-3)^{\frac{m-1}{2}} H y_\lambda^2 \\ &= D_2^3 (-3)^{\frac{m-1}{2}} \rho^{2(a+b)} g^{\frac{m-1}{3}} \\ &= D_2^3 \rho^{2b(a+b)} \frac{2^{\frac{(m-1)}{3}}}{\mu^2}. \end{aligned}$$

Therefore

$$D_1^4 = D_2^{12} \rho^{2(a+b)} \frac{2^{\frac{8(m-1)}{3}}}{\mu^4}.$$

Comparing this result with (11), and remembering that  $\varepsilon$  must be a cube root of unity, we find that

$$\varepsilon = \rho^{l(a+b)}.$$

Thus we obtain

$$D = \rho^{b(a+b)} 2^{\frac{m(m-1)}{3}} \mu^{m-2},$$

$$D_1 = \pm \rho^{2l(a+b)} \frac{2^{\frac{(m-1)(m-3)}{6}}}{\mu^2},$$

$$D_2^3 = \pm \frac{2^{\frac{(m-1)(m-7)}{6}}}{\mu^2}.$$

Lastly, let  $D_3$  be the discriminant of the equation  $S_\rho(y)=0$  regarded as an equation for

$$\frac{y_3}{y_\lambda^3}.$$

Then we can shew without any difficulty that

$$D_3 = D_2 \frac{y_3^{\frac{m-1}{6}} y_\lambda^{\frac{m-7}{6}}}{H y_\lambda^{\frac{m-7}{3}}};$$

whence follows

$$D_3^3 = \pm 3^{\frac{(m-1)(m-7)}{8}} \mu^{\frac{m-7}{2}}.$$


---

Hitherto we have supposed that  $\mu$  is a primary integer. But, the same method of calculating the discriminants can also be applied to the case where  $\mu$  is a composite integer, provided that it is odd. The result is exactly the same as in the above case. But, it must be observed that the equation  $A_\rho(x)=0$  in this case is not irreducible. The corpus of  $\mu$ -division is determined by a root of the equation of the  $\zeta(\mu)$ th degree

$$A'_\rho(x) = 0,$$

where  $A'_\rho(x)$  is an irreducible factor of  $A_\rho(x)$ . The above method cannot give the discriminant of this latter equation. For, if  $\mu$  be not a prime, then in the form

$$u \pm v = \frac{(\gamma^k \pm \gamma^{k'})\omega}{\mu},$$

the numerator may have a common divisor with  $\mu$ , without being divisible by  $\mu$ ; and consequently  $\sin(u \pm v)$  is not necessarily a root of  $A'_\rho(x) = 0$ .

Since it is evident, however, that the discriminant of the latter equation must be a divisor of that of the equation  $A_\mu(x) = 0$ , the following conclusion is valid:

*The discriminant of the equation of  $\mu$ -division of periods of sn cannot contain an odd prime, which is relatively prime to  $\mu$ ,  $\mu$  being an odd integer in  $k(\rho)$ .*

Hence it follows, exactly as in the case of primary  $\mu$ , that

*the discriminant of the corresponding division-equation for the function  $\frac{1}{z^3}$  cannot contain a prime, which is relatively prime to 3 and  $\mu$ .*

## §. 6.

Again, let  $\mu$  be a primary integer relatively prime to 3, and  $m$  its norm. By adjoining a root  $x$  of the equation

$$A_\mu(x) = 0$$

to  $k(\rho)$ , a corpus is determined, which we shall denote by  $K(x)$ , instead of  $k(\rho, x)$ , for the sake of simplicity. This corpus is of the  $(m-1)$ th relative degree and relatively cyclic, when we take  $k(\rho)$  as the fundamental corpus. In the following, when the fundamental corpus is not explicitly mentioned, it should always be understood to be  $k(\rho)$ .

Since the discriminant  $D$  of the above equation contains only two distinct primes, viz. 2 and  $\mu$ , the relative discriminant of the corpus  $K(x)$  contains no other prime than these two.

It is well-known that all the roots

$$\operatorname{sn}\left(\gamma^{\lambda} \frac{\omega}{\mu}\right), \quad \lambda = 0, 1, 2, \dots, m-2,$$

are associated with one another, and

$$\mu = \left(\operatorname{sn} \frac{\omega}{\mu}\right)^{m-1}.$$

Hence  $\left(\operatorname{sn} \frac{\omega}{\mu}\right)$  is a prime principal ideal (*Hauptideal*) in  $K(x)$ , and  $\mu$  is associated with its  $(m-1)$ th power. Therefore the relative discriminant of  $K(x)$  contains  $\mu$  to the  $(m-2)$ th power.

As for the prime 2, we proceed as follows:

Since  $A_\mu(x)$  contains only even powers of  $x$ , the corpus  $K(x)$  must be relatively quadratic with respect to  $K(x^2)$ . But, this latter corpus is identical with the corpus  $K(y)$  defined by adjoining to  $k(\rho)$  the number

$$y = \wp\left(\frac{\omega}{\mu}\right),$$

which is a root of the equation

$$S_\mu(y) = 0. \quad (12)$$

This equation can also be regarded as an equation for  $y^3$  of degree  $\frac{m-1}{6}$ . Hence the corpus  $K(y)$  is relatively cubic with respect to  $K(y^3)$ . Consequently,  $K(x)$  is relatively sextic with respect to  $K(y^3)$ .

The corpus  $K(y^3)$  can be defined by the number

$$\frac{g_3}{y^3}$$

as well as by  $y^3$ . The former is an algebraic integer as shewn in §. 3, while it is not the case with the latter. But, as we have found in the preceding section, the discriminant  $D_3$  of the equation (12), considered as an equation for  $\frac{g_3}{y^3}$ , does not contain the prime factor 2. Hence the relative discriminant of  $K(y^3)$  cannot contain the factor 2.

Next, let us consider the relative discriminant of  $K(y)$ , i.e. of  $K(x^2)$ , with respect to  $K(y^3)$ .

Let

$$y_1 = \wp(u), \quad y'_1 = \wp(v)$$

be two roots of (12), such that  $y_1 \neq y'_1$ , then

$$y_2 = \wp(u+v), \quad y'_2 = \wp(u-v)$$

are also two roots of (12), and  $y_2 \neq y'_2$ . From the relation (7), we get

$$\wp'(u) \simeq \wp'(v),$$

and then, from the identity

$$\{\wp(u) - \wp(v)\}^2 \{\wp(u+v) - \wp(u-v)\} = -\wp'(u)\wp'(v),$$

we see that

$$(y_1 - y'_1)^2 (y_2 - y'_2) \simeq \wp'(u)^2.$$



Changing  $u, v$  into  $u+v, u-v$  respectively, we get

$$(y_2 - y_2')(y_3 - y_3') \approx \mathfrak{E}'(u+v)^2 \approx \mathfrak{E}'(u)^2;$$

$$\text{where} \quad y_3 = \mathfrak{E}(2u), \quad y_3' = \mathfrak{E}'(2v).$$

Let us repeat the same process successively, until we arrive at the relation

$$(y_h - y_h')(y_1 - y_1') \approx \mathfrak{E}'(u)^2,$$

where  $y_h, y_h'$  are derived from  $y_{h-1}, y_{h-1}'$  by changing  $u, v$  into  $u+v, u-v$  respectively. From these  $h$  relations, it can be concluded that

$$(y - y_1')^2 \approx \mathfrak{E}'(u)^2. \quad (13)$$

From the multiplication-formula

$$\mathfrak{E}\{(1-\rho)u\} = \frac{\mathfrak{E}(u)^2 - y_3}{(1-\rho)^2 \mathfrak{E}(u)^2},$$

we get

$$\mathfrak{E}\{(1-\rho)u\} - \mathfrak{E}(\rho^2 u) = \frac{\mathfrak{E}'(u)^2}{(1-\rho)^2 \mathfrak{E}(u)^2}.$$

If  $\mathfrak{E}(u)$  be a root of (12), so must also be  $\mathfrak{E}\{(1-\rho)u\}$  and  $\mathfrak{E}(\rho^2 u)$ , and they are evidently unequal. Hence, putting

$$y_1 = \mathfrak{E}\{(1-\rho)u\}, \quad y_1' = \mathfrak{E}(\rho^2 u)$$

in (13), we get

$$\mathfrak{E}'(u)^2 \approx (1-\rho)^2 \mathfrak{E}(u)^2.$$

Therefore, by (7),

$$(1-\rho)^3 \mathfrak{E}(u)^3 \approx \frac{4}{\sin^2 u \sin^2 \rho u \sin^2 \rho^2 u}.$$

If we put

$$\begin{aligned} \alpha &= (1-\rho) \mathfrak{E}(u) \sin^2 u, \\ \beta &= (1-\rho) \mathfrak{E}(u) \sin^2 \rho u, \\ \gamma &= (1-\rho) \mathfrak{E}(u) \sin^2 \rho^2 u, \end{aligned}$$

then  $\alpha, \beta, \gamma$  are all algebraic integers in  $K(x^2)$ , such that

$$\alpha^3 + \beta^3 + \gamma^3 = 4.$$

Hence, in the corpus  $K(x^2)$ , the principal ideal (2) must be equal to the cube of some ideal, say

$$(2) = (\mathfrak{p}_1 \mathfrak{p}_2 \cdots \mathfrak{p}_r)^3.$$

Now, the number  $a$  breaks up into two factors in  $K(x^2)$ , as follows :

$$\begin{aligned} a &= (1-\rho)\wp(u)\operatorname{sn}^2u \\ &= (1-\rho)-\operatorname{sn}^2u \\ &= (\operatorname{cn}u+\rho^2)(\operatorname{cn}u-\rho^2). \end{aligned}$$

Since the difference between these two factors is  $2\rho^2$ , both of them must be divisible by the same power of  $\mathfrak{p}_1 \mathfrak{p}_2 \dots\dots$ . Hence we find that

$$(\operatorname{cn}u+\rho^2) = \mathfrak{p}_1 \mathfrak{p}_2 \dots\dots.$$

Consequently the relative *different* of  $K(x^2)$ , i.e. of  $K(y)$ , with respect to the corpus  $K(y^3)$ , must contain the same power of  $\mathfrak{p}_1 \mathfrak{p}_2 \dots$  as the relative *different* of the number  $\operatorname{cn}u+\rho^2$  with respect to the corpus  $K(y^3)$  does.<sup>1)</sup>

Under our present supposition that  $\mu$  is primary, the following relation holds for a variable  $u$  :

$$\operatorname{cn}\mu u = \operatorname{cn}u R(\operatorname{sn}^2u),$$

where  $R(\operatorname{sn}^2u)$  denotes a certain rational function of  $\operatorname{sn}^2u$ .<sup>2)</sup> From this relation, putting

$$u = \frac{\omega}{\mu} = \frac{2K}{\mu},$$

we obtain

$$\begin{aligned} \operatorname{cn}u &= -\frac{1}{R(\operatorname{sn}^2u)}, \\ \operatorname{cn}\rho u &= \frac{1}{R(\operatorname{sn}^2\rho u)}, \\ \operatorname{cn}\rho^2u &= -\frac{1}{R(\operatorname{sn}^2\rho^2u)}. \end{aligned}$$

Hence, if we put

$$\begin{aligned} \xi &= \operatorname{cn}u + \rho^2, \\ \xi' &= -\operatorname{cn}\rho u + \rho^2, \\ \xi'' &= \operatorname{cn}\rho^2u + \rho^2, \end{aligned}$$

1) Hilbert: Theorie der algebraischen Zahlkörper (Jahresbericht der Deutschen Mathematiker-Vereinigung, IV), §. 126.

2) Weber: Elliptische Funktionen und algebraische Zahlen (1st edition), §. 117.

then these three numbers are conjugate to one another with respect to  $K(y^3)$ ; and

$$\xi^3 + \xi'^3 + \xi''^3 = 2,$$

consequently

$$(\xi) = (\xi') = (\xi'') = \mathfrak{p}_1 \mathfrak{p}_2 \dots.$$

Now, the relative *different* of  $\xi$  with respect to  $K(y^3)$  is

$$\begin{aligned} (\xi - \xi')(\xi - \xi'') &= (\text{en } u + \text{en } \rho u)(\text{en } u - \text{en } \rho^2 u) \\ &= \frac{(\text{en } u \, \text{dn } u + 1)(\text{en}^2 u - \text{dn } u)}{\text{en } u \, \text{dn } u}. \end{aligned}$$

Hence, observing that both  $\text{en } u$  and  $\text{dn } u$  are algebraic unities, and also that

$$\begin{aligned} \text{en } u \, \text{dn } u + 1 &= \xi'' \text{en}^2 u - \rho^2 \xi^2 + 2\rho \xi, \\ \text{en}^2 u - \text{dn } u &= \rho \xi' \text{dn } u + \xi^2 - 2\rho^2 \text{en } u - 2 \text{dn } u, \end{aligned}$$

we see that the *different* in question contains  $\mathfrak{p}_1 \mathfrak{p}_2 \dots$  to the second power.

Next, to investigate the relative *different* of  $K(x)$  with respect to  $K(x^2)$ , put

$$\eta = \frac{1 + \text{en } u + \text{sn } u}{\rho^2 + \text{en } u},$$

and let  $\eta'$  be conjugate to  $\eta$  with respect to  $K(x^2)$ , then

$$\eta' = \frac{1 + \text{en } u - \text{sn } u}{\rho^2 + \text{en } u};$$

and

$$\begin{aligned} \eta + \eta' &= \frac{2(1 + \text{en } u)}{\rho^2 + \text{en } u}, \\ \eta \eta' &= \frac{2 \text{en } u (1 + \text{en } u)}{(\rho^2 + \text{en } u)^2}, \end{aligned}$$

which shew that  $\eta$  and  $\eta'$  are integers in  $K(x)$ . Also, since

$$1 + \text{en } u = 2 + \rho + (\rho^2 + \text{en } u),$$

the number  $1 + \text{en } u$  is relatively prime to 2. We conclude therefore that each of the ideals  $\mathfrak{p}_1, \mathfrak{p}_2, \dots$  must break up into two equal prime ideals in  $K(x)$ . Let us put

$$\mathfrak{p}_1 \mathfrak{p}_2 \dots = (\mathfrak{P}_1 \mathfrak{P}_2 \dots)^2,$$

then the integers  $\eta$  and  $\eta'$  are both divisible by  $\mathfrak{P}_1 \mathfrak{P}_2 \dots$ , but by

no higher power of it. Hence the relative *different* of the corpus  $K(x)$  and of the number  $\eta$ , with respect to  $K(x^2)$ , must contain  $\mathfrak{P}_1, \mathfrak{P}_2, \dots$  to the same power. But, since

$$\eta - \eta' = \frac{2 \sin u}{\rho^2 + \cos u},$$

we conclude that the power in question must be the fourth.

Therefore the relative *different* of  $K(x)$  with respect to  $K(x^2)$ , as well as to  $k(\rho)$ , contains  $\mathfrak{P}_1, \mathfrak{P}_2, \dots$  to the eighth power. Thus, we find that the relative discriminant of  $K(x)$  with respect to  $k(\rho)$  is equal to

$$2^{\frac{4(m-1)}{3}} \mu^{m-2}.$$

### §. 7.

The corpus  $K(x)$  is a relatively cyclic corpus of relative degree  $m-1$ . Hence, if  $d$  be a divisor of  $m-1$ , there exists certainly a divisor (*Unterkörper*) of  $K(x)$ , which is of relative degree  $d$ , and of course also relatively cyclic. We shall denote it by  $C_d$ .

Let

$$m-1 = 2^{h+1} 3^{h'+1} p_1^{h_1} p_2^{h_2} \dots,$$

where  $p_1, p_2, \dots$  are distinct natural primes, different from 2 and 3. Then the corpus  $K(x)$  can be looked upon as the result of composition of the relatively cyclic corpora  $C_{2^{h+1}}, C_{3^{h'+1}}, C_{p_1^{h_1}}, C_{p_2^{h_2}}, \dots$ , taken all together.

Let us now determine the relative discriminant of each of these corpora.

In  $C_{2^{h+1}}$ , the number  $\mu$  breaks up into  $2^{h+1}$  equal prime ideals. Therefore the relative discriminant of  $C_{2^{h+1}}$  contains  $\mu$  to the power  $2^{h+1}-1$ . The same reasoning applies also to other corpora  $C_{3^{h'+1}}, C_{p_1^{h_1}}, \dots$ .

On the other hand, it can be shewn generally that the relative discriminant of a relatively cyclic corpus  $C'$  of relative degree  $p^h$ ,  $p$  being a natural prime, cannot contain the factor 2, unless  $p=2$  or 3. For, if  $p \neq 2$  and 2 enter into the relative discriminant of  $C'$ , then, since 2 is relatively prime to the relative degree  $p^h$ , the corpus of ramification (*Verzweigungskörper*) of 2 in  $C'$  must be the

corpus  $\mathcal{C}'$  itself, while the corpus of inertia (*Trägheitskörper*), whose relative discriminant cannot contain 2, must necessarily be a proper divisor of  $\mathcal{C}'$ . Hence the relative degree of the corpus of ramification with respect to the corpus of inertia must be  $p^k$ ,  $h \geq k \geq 1$ . Then, if  $f$  be the degree of a prime ideal contained in 2 in the corpus  $\mathcal{C}'$ , we get<sup>1)</sup>

$$4^f - 1 \equiv 0 \pmod{p^k}.$$

But, since  $f$  must be a power of  $p$ , it follows from this congruence that

$$4^f - 1 \equiv 4 - 1 \equiv 0 \pmod{p},$$

which is impossible, unless  $p=3$ .

Therefore, among the corpora we are considering, only the two, viz.  $\mathcal{C}_{2^{h+1}}$  and  $\mathcal{C}_{3^{h+1}}$ , may contain 2 in their relative discriminants. The relative discriminants of other corpora  $\mathcal{C}'_{p_1^{h_1}}$ ,  $\mathcal{C}'_{p_2^{h_2}}$ , ..... are equal to  $\mu^{p_1^{h_1}-1}$ ,  $\mu^{p_2^{h_2}-1}$ , ..... respectively.

The corpus  $K(y^{\frac{1}{6}})$ , i.e.  $\mathcal{C}_{\frac{6}{6}-1}$ , has the relative discriminant relatively prime to 2. Hence the corpora  $\mathcal{C}_{2^h}$  and  $\mathcal{C}_{3^h}$ , both being divisors of  $\mathcal{C}_{\frac{6}{6}-1}$ , must also have the relative discriminants relatively prime to 2. Their relative discriminants are therefore  $\mu^{2^h-1}$  and  $\mu^{3^h-1}$  respectively.

As for the exceptional corpora  $\mathcal{C}_{2^{h+1}}$  and  $\mathcal{C}_{3^{h+1}}$ , we have to consider them a little further. If we put

$$m' = 2^h p_1^{h_1} p_2^{h_2} \dots,$$

the relative discriminant of the corpus  $\mathcal{C}_{m'}$  is relatively prime to 2. Composing  $\mathcal{C}_{m'}$  with  $\mathcal{C}_{3^h}$  or  $\mathcal{C}_{3^{h+1}}$ , we obtain  $K(y^{\frac{1}{3}})$  or  $K(y)$  respectively. Hence, the relative *different* of  $\mathcal{C}_{3^{h+1}}$  with respect to  $\mathcal{C}_{3^h}$  must contain as many ideal factors of 2 as the relative *different* of  $K(y)$  with respect to  $K(y^{\frac{1}{3}})$  does. Therefore the relative discriminant of  $\mathcal{C}_{3^{h+1}}$  is  $2^{2 \cdot 3^h} \mu^{3^{h+1}-1}$ .

Next, to investigate the relative discriminant of  $\mathcal{C}_{2^{h+1}}$ , let us consider the corpus  $K(z)$ , where

$$z = \wp \left( \frac{\omega}{\mu} \right).$$

1) Weber: Algebra II, §. 181.

Hilbert: loc. cit., §. 11.

Since

$$z^2 = 4y^3 - g_3,$$

the corpus  $K(z)$  must either be relatively quadratic with respect to  $K(y^3)$  or coincide with it. But, if  $K(z)$  coincide with  $K(y^3)$ , the corpus  $K(y)$ , i.e.  $K(x^2)$ , must contain both  $z$  and  $\operatorname{sn}^2 u$ . Then, by the relation

$$z = -\frac{2 \operatorname{cn} u \operatorname{dn} u}{\operatorname{sn}^3 u},$$

$K(y)$  must also contain  $\operatorname{sn} u$ ; which is of course impossible. Hence  $K(z)$  must be relatively quadratic with respect to  $K(y^3)$ , and consequently  $K(x)$  is relatively cubic with respect to  $K(z)$ .

The principal ideal (2) is equal to the sixth power of an ideal in  $K(x)$ . Hence, in  $K(z)$ , (2) is equal to the square of an ideal, say

$$(2) = (q_1 q_2 \cdots)^2.$$

If we regard  $q_1 q_2 \cdots$  as an ideal in  $K(x)$ , it follows that

$$q_1 q_2 \cdots = (\mathfrak{P}_1 \mathfrak{P}_2 \cdots)^3.$$

Now, in general, if a prime ideal  $\mathfrak{p}$  in a certain corpus  $k$  is equal to the  $e$ th power of an ideal  $\mathfrak{P}$  in another corpus  $K$ , which contains  $k$  as a divisor, and if  $e$  be divisible by  $\mathfrak{p}$ , then the relative *different* of  $K$  with respect to  $k$  contain  $\mathfrak{P}$  at least to the  $e$ th power.<sup>1)</sup> Hence, in the present case, the relative *different* of  $K(z)$  with respect to  $K(y^3)$  must contain at least  $(q_1 q_2 \cdots)^2$ . On the other hand, if the *different* in question contain  $(q_1 q_2 \cdots)^3$ , the relative *different* of  $K(x)$  with respect to  $K(y^3)$  must be divisible at least by  $(\mathfrak{P}_1 \mathfrak{P}_2 \cdots)^3$ , which is contradictory to the result obtained in the preceding section. Therefore the relative *different* of  $K(z)$  contains  $q_1 q_2 \cdots$  exactly to the second power.

Composing  $C'_{2^{i+1}}$  or  $C'_{2^i}$  with  $C'_{m'}$ , where

$$m' = 3^k p_1^{h_1} p_2^{h_2} \cdots,$$

we obtain  $K(z)$  or  $K(y^3)$  respectively. Thus, here the corpus  $K(z)$  playing the part of  $K(y)$ , we can shew just as in the case of  $C'_{3^{i+1}}$ , that the relative discriminant of  $C'_{2^{i+1}}$  is equal to  $2^{2^{i+1}} \mu^{2^{i+1}-1}$ .

1) Hilbert: loc. cit., §. 12.

Weber: Algebra II, §. 174.

We close the present section with the following list of the divisors of  $K(c)$ .

Divisors		Relative Discriminants
$C_{p_1^{\lambda_1}},$	$\lambda_1 = 1, 2, \dots, h_1$	$\mu^{p_1^{\lambda_1}-1}$
$C_{p_2^{\lambda_2}},$	$\lambda_2 = 1, 2, \dots, h_2$	$\mu^{p_2^{\lambda_2}-1}$
.....		.....
$C_{3^{\lambda'}},$	$\lambda' = 1, 2, \dots, h'$	$\mu^{3^{\lambda'}-1}$
$C_{3^{h'+1}}$		$2^{2 \cdot 3^{h'}} \mu^{3^{h'+1}-1}$
$C_{2^{\lambda}},$	$\lambda = 1, 2, \dots, h$	$\mu^{2^{\lambda}-1}$
$C_{2^{h+1}}$		$2^{2^{h+1}} \mu^{2^{h+1}-1}$

## §. 8.

Before proceeding to the discussion of the division of periods of sn by powers of  $\mu$ , let us insert here a digression on the classes of congruent integers in an algebraic corpus.

Let  $\mathfrak{p}^a$  be a power of a prime ideal in an algebraic corpus. The integers in the corpus can be classified into classes of congruent integers with respect to the modulus  $\mathfrak{p}^a$ . These classes can be composed with one another by multiplication. They form an Abelian group of order  $p^{f(a-1)}(p^f-1)$ , where  $p$  is a natural prime divisible by  $\mathfrak{p}$ , and  $f$  the degree of  $\mathfrak{p}$ .

The problem of determining the rank and the invariants of this group has already been solved to some extent by G. Wolff<sup>1)</sup> and by the present author.<sup>2)</sup> The result obtained by the latter is as follows.

The Abelian group in question can be decomposed into two component subgroups  $\mathfrak{A}$  and  $\mathfrak{B}$  of orders  $p^{f(a-1)}$  and  $p^f-1$  respectively.

1) Wolff: Ueber Gruppen der Reste eines beliebigen Moduls im algebraischen Zahlkörper (Dissertation; Giessen, 1905).

2) Takemouchi: Journal of the College of Science, Tokyo Imperial University, Vol. XXXVI, Art. 1.

$\mathfrak{B}$  is a cyclic group. If

$$p^d - 1 = p_1^{n_1} p_2^{n_2} \dots,$$

where  $p_1, p_2, \dots$  are distinct primes, the invariants of  $\mathfrak{B}$  are  $p_1^{n_1}, p_2^{n_2}, \dots$ .

$\mathfrak{U}$  is an Abelian group, whose invariants consist of powers of  $p$ . If  $\mathfrak{p}^d$  be the highest power of  $\mathfrak{p}$  contained in  $p$ , then the rank  $r$  of  $\mathfrak{U}$  is

$$r = fd + 1 \quad \text{or} \quad fd, \quad \text{if} \quad n > d + k, \quad k = \left[ \frac{d}{p-1} \right],$$

according as the congruence

$$p + x^{p-1} \equiv 0 \pmod{\mathfrak{p}^{d+1}}$$

has a solution or not.

$$\begin{aligned} r &= fd, & \text{if} \quad n = d + k, \\ r &= f \left( n - \left[ \frac{n}{p} \right] \right), & \text{if} \quad d + k > n > 1, \\ r &= 1, & \text{if} \quad n = 1; \end{aligned}$$

where the symbol  $[x]$  denotes the natural number, such that

$$x + 1 > [x] \geq x.$$

In the case where  $d$  is not divisible by  $p-1$ , we can find not only the rank, but also a system of bases as follows.

Let  $\pi$  be such an integer in the given corpus, that is divisible by  $\mathfrak{p}$ , but not by  $\mathfrak{p}^2$ , and  $\xi_i$  ( $i = 1, 2, \dots, f$ ) such integers in the same corpus that

$$c_1 \xi_1 + c_2 \xi_2 + \dots + c_f \xi_f \not\equiv 0 \pmod{\mathfrak{p}},$$

for all rational integral values of  $c_i$  ( $i = 1, 2, \dots, f$ ), except when

$$c_1 \equiv c_2 \equiv \dots \equiv c_f \equiv 0 \pmod{p}.$$

Then, the following  $fd$  numbers represent a system of bases:

$$1 + \xi_i \pi^i, \quad \begin{array}{l} a = 1, 2, 3, \dots, d + k - 1, \quad \text{excluding multiples of } p, \\ i = 1, 2, 3, \dots, f. \end{array}$$

Even if  $d$  be divisible by  $p-1$ , we obtain similar results, provided that  $n \leq d + k$ . But, if  $n > d + k$ , we cannot determine a



system of bases in general. Supposing that  $k$  is not divisible by  $p$ , the only thing we can conclude is as follows:

Determine an integer  $\rho$  from

$$\rho \equiv \pi^d \rho \pmod{p^{d+1}}.$$

Then we distinguish two cases according as the congruence

$$\rho + x^{p-1} \equiv 0 \pmod{p}$$

has a solution or not.

If it has no solution, the  $fd$  numbers given above represent a system of bases.

If it has a solution, say  $x \equiv x_0$ , then  $f$  rational integers  $a_i$  ( $i = 1, 2, \dots, f$ ), such that

$$x_0 \equiv a_1 \tilde{\pi}_1 + a_2 \tilde{\pi}_2 + \dots + a_f \tilde{\pi}_f \pmod{p}$$

can be uniquely determined with respect to mod.  $p$ . Hereby, without losing generality, we may suppose  $a_1 \not\equiv 0 \pmod{p}$ . Then determine an integer  $\tilde{\pi}_0$ , such that

$$\rho \left( \sum_{i=1}^f c_i \tilde{\pi}_i \right) + \left( \sum_{i=1}^f c_i \tilde{\pi}_i \right)^p + c_0 \tilde{\pi}_0 \not\equiv 0 \pmod{p},$$

for all rational integral values of  $c$ 's, except when

$$c_0 \equiv c_2 \equiv c_3 \equiv \dots \equiv c_f \equiv 0 \pmod{p}.$$

Now, it can be shewn that all the elements of  $\mathfrak{A}$  can be represented by means of the  $fd+1$  numbers:

$$1 + \tilde{\pi}_i \pi^i, \quad a = 1, 2, \dots, d+k-1, \quad \text{excluding multiples of } p, \\ i = 1, 2, \dots, f,$$

$$\text{and } 1 + \tilde{\pi}_0 \pi^{l+k}.$$

But, these  $fd+1$  numbers do not in general represent a system of bases. In fact, they represent a system of bases only when  $e_k \equiv p$ , where  $e_k$  denotes the exponent to which the number  $1 + \tilde{\pi}_0 \pi^k$  belongs with respect to mod.  $p^n$ .

Let us now confine ourselves to the corpus  $k(\rho)$ ,  $\rho$  denoting a primitive cube root of unity:

$$\rho = \frac{-1 + \sqrt{-3}}{2}.$$

(i) When  $p \equiv 1 \pmod{6}$ ,  $p$  can be decomposed into two different prime factors of the first degree in  $k(\rho)$ . Hence

$$d = 1, \quad f = 1, \quad k = 1,$$

and consequently  $r=1$ . There exist primitive roots of  $\mathfrak{p}^n$ .

(ii) When  $p \equiv -1 \pmod{6}$ ,  $p$  is itself a prime number of the second degree in  $k(\rho)$ , and

$$d = 1, \quad f = 2, \quad k = 1.$$

If  $n=1$ , then  $r=1$ . There exist primitive roots of  $p$ .

If  $n>1$ , then  $r=2$ . The invariants of  $\mathfrak{A}$  are  $p^{n-1}$ ,  $p^{n-1}$ .

Putting

$$\pi = p, \quad \xi_1 = 1, \quad \xi_2 = \xi,$$

$\xi$  being a primitive root of  $p$ , we obtain a system of bases of  $\mathfrak{A}$ ; viz.,

$$1+p, \quad 1+\xi p.$$

As for the root of  $\mathfrak{B}$ , we may take such a power of  $\xi$  as prescribed in §. 1 of my paper just cited.

(iii) The natural prime 3 is associated with the square of a prime in  $k(\rho)$ , viz.

$$3 = -(1+2\rho)^2.$$

Hence

$$d = 2, \quad f = 1, \quad k = 1,$$

and thus we meet with a case where  $d$  is divisible by  $p-1$ .

If  $n=1$  or 2, then  $r=1$ . Consequently there exist primitive roots of  $1+2\rho$  and  $(1+2\rho)^2$ , e.g.  $-1$  and  $-\rho$  respectively.

If  $n=3$ , then  $r=2$ ; the invariants of  $\mathfrak{A}$  being 3, 3. Putting

$$\pi = \rho-1, \quad \xi_1 = 1,$$

we obtain a system of bases of  $\mathfrak{A}$ :

$$\rho, \quad 1-3\rho.$$

If  $n>3$ , then  $r=3$ . If we put

$$\pi = -(1+2\rho), \quad \xi_1 = \rho^2, \quad \xi_2 = \rho^2,$$

---

1) Strictly speaking, we obtain a system of numbers representing a system of bases of  $\mathfrak{A}$ ; for, the elements of  $\mathfrak{A}$  are not numbers, but the classes of numbers. But, for the sake of simplicity, we shall hereafter use this abridged term.

we obtain the three numbers

$$1 + \xi_1 \pi = \rho, \quad 1 + \xi_1 \pi^2 = 4 + 3\rho, \quad 1 + \xi_0 \pi^2 = 4 - 3\rho,$$

which belong (mod.  $(1+2\rho)^n$ ) to the exponents

$$3, \quad 3\left[\frac{n-2}{2}\right], \quad 3\left[\frac{n-3}{2}\right]$$

respectively. Thus  $e_{11}=3$ , whence we conclude that the above three numbers form a system of bases of  $\mathfrak{A}$ . The exponents to which they belong are the invariants of  $\mathfrak{A}$  in this case.

As for  $\mathfrak{B}$ , the invariant being 2, we may take  $-1$  as its base.

(iv) The natural prime 2 is itself a prime number in  $k(\rho)$ , and

$$d = 1, \quad f = 2, \quad k = 1.$$

Thus we have another case where  $d$  is divisible by  $p-1$ .

If  $n=1$ , then there exist primitive roots of 2, e.g.  $\rho$ .

If  $n=2$ , then  $r=2$ ; the invariants of  $\mathfrak{A}$  being 2, 2. Putting

$$\pi = -2, \quad \xi_1 = 1, \quad \xi_2 = \rho,$$

we obtain a system of bases of  $\mathfrak{A}$ :

$$-1, \quad 1-2\rho.$$

If  $n>2$ , then  $r=3$ . Putting

$$\pi = -2, \quad \xi_1 = 1, \quad \xi_2 = \rho, \quad \xi_0 = -\rho^2,$$

we obtain the three numbers

$$1 + \xi_1 \pi = -1, \quad 1 + \xi_2 \pi = 1 - 2\rho, \quad 1 + \xi_0 \pi^2 = 1 - 4\rho^2,$$

That these numbers form a system of bases of  $\mathfrak{A}$  can be shewn as in (iii). The invariants of  $\mathfrak{A}$  in this case are

$$2, \quad 2^{n-1}, \quad 2^{n-2}.$$

Since the last one  $(1-4\rho^2)$  of the above bases can be decomposed into  $1-2\rho$  and  $1+2\rho$ , we can represent all the elements of the group also by means of

$$-1, \quad 1-2\rho, \quad 1+2\rho.$$

But these three do not form a system of bases.

As for  $\mathfrak{B}$ , the invariant being 3, we may take  $\rho$  as its base.

## §. 9.

Let us again assume that  $\mu$  is a primary integer relatively prime to 3, and  $m$  its norm. It was shewn in §. 4 that

$$\operatorname{sn} \mu u = \frac{x\phi_1}{Z_1}, \quad x = \operatorname{sn} u,$$

$$\text{where} \quad \phi_1 = A_\mu(x), \quad Z_1 = D_\mu(x).$$

Substituting  $x\frac{\phi_1}{x_1}$  in place of  $x$ , we get

$$\operatorname{sn} \mu^2 u = x \frac{Y_2}{X_2},$$

where  $Y_2$  is a rational integral function of  $x$  of degree  $m^2-1$ , which must be divisible by  $\phi_1$ . If we put

$$Y_2 = \phi_1 \phi_2,$$

then  $\phi_2$  is necessarily of the form

$$\phi_2 = \varepsilon x^n + a_2 x^{n-2} + \dots + a_{2k} x^{n-2k} + \dots + \mu,$$

$$n = m(m-1),$$

where  $\varepsilon$  is an algebraic unity and  $a_2, \dots, a_{2k}, \dots$  are all integers in  $k(\rho)$  divisible by  $\mu$ .

It can be shewn by mathematical induction, that in general

$$\operatorname{sn} \mu^h u = x \frac{Y_h}{X_h},$$

$$Y_h = \phi_1 \phi_2 \dots \phi_h,$$

where  $\phi_h$  is of degree  $m^{h-1}(m-1)$ , and its coefficients possess the same property as those of  $\phi_2$ .

Hence, if we put

$$\phi_h = 0,$$

this equation is irreducible, and gives as its roots the values of  $\operatorname{sn} u$  corresponding to the  $\mu^h$ -division of periods. That the discriminant of this equation can contain only two distinct prime factors 2 and  $\mu$  has already been remarked at the end of §. 5.

To find the Galois' group of this equation, we have to distinguish the following two cases.

(i) When  $\mu$  is not real, put  $\mu=\pi$ ,  $m=p$ . Then

$$p \equiv 1 \pmod{6},$$

hence there exist primitive roots for  $\pi^h$ . The roots of the above equation are

$$\text{sn}\left(r^\lambda \frac{\omega}{\pi^h}\right), \quad \lambda = 0, 1, 2, \dots, p^{h-1}(p-1)-1,$$

$r$  being a primitive root of  $\pi^h$ .

The corpus obtained by adjoining these roots to  $k(\rho)$  is relatively cyclic, the relative degree being  $p^{h-1}(p-1)$ . There are two divisors of this corpus, of relative degrees  $p-1$  and  $p^{h-1}$ . The first, of relative degree  $p-1$ , is nothing else but the corpus discussed in §. 6 and §. 7. The second, of relative degree  $p^{h-1}$ , is also relatively cyclic, and its relative discriminant is a power of  $\pi$ .

(ii) When  $\mu$  is real, put  $\mu=q$ . Then

$$q \equiv -1 \pmod{6}$$

and  $m=q^2$ . In this case we have to use two integers, say  $r$  and  $r'$ , which belong to the exponents  $q^{h-1}(q^2-1)$  and  $q^{h-1}$  respectively, in order to obtain all the roots in the form

$$\text{sn}\left(r^\lambda r'^{\lambda'} \frac{\omega}{q^h}\right), \quad \begin{aligned} \lambda &= 0, 1, 2, \dots, q^{h-1}(q^2-1)-1, \\ \lambda' &= 0, 1, 2, \dots, q^{h-1}-1. \end{aligned}$$

The corpus obtained by adjoining these roots to  $k(\rho)$  is relatively Abelian, the relative degree being  $q^{2(h-1)}(q^2-1)$ . The divisor of this corpus of relative degree  $q^2-1$  is nothing else but the corpus discussed in §. 6 and §. 7. The other divisor of relative degree  $q^{2(h-1)}$  is relatively Abelian, and its relative discriminant contains no other prime than  $q$ . Since the Galois' group of this latter divisor is of the form

$$s^a t^b, \quad a, b = 0, 1, 2, \dots, q^{h-1}-1,$$

it contains  $q^{h-2}(q+1)$  different cyclic subgroups of relative degree  $q^{h-1}$ . Namely, if we use the notation  $(x)$  to denote a cyclic group consisting of all the powers of a substitution  $x$ , then these subgroups are

$$\begin{aligned} (s), (st), (st^2), \dots, (st^{q^{h-1}-1}), \\ (t), (s^2t), (s^{2^2}t), \dots, (s^{q^{h-2}-1}t). \end{aligned}$$

Corresponding to these subgroups, there are as many relatively cyclic corpora of relative degree  $q^{h-1}$ , whose relative discriminants contain no other prime than  $q$ .

### §. 10.

The primary integer  $\mu$  has hitherto been supposed to be relatively prime to 3. In the present section, let us consider the case where  $\mu$  is a primary divisor of 3:

$$\mu = 1 + 2^{\rho}.$$

If we put

$$x_h = \operatorname{sn} v_h, \quad v_h = \frac{\omega}{(1+2^{\rho})^h},$$

then, on account of the relations (5) and (7), it follows that the corpus  $K(x_h)$  can be composed of two corpora  $K(\wp(v_h))$  and  $K(\wp'(v_h))$ .

From the multiplication-formula

$$\wp\{(1+2^{\rho})u\} = \frac{\wp(u)^3 - g_3}{-3\wp(u)^2}, \quad (14)$$

we find that

$$\wp(v_1) = 0 \quad \text{and} \quad \wp(v_2)^3 = g_3.$$

Hence, if we put

$$y_h = \frac{\wp(v_h)}{\sqrt[3]{g_3}}, \quad \text{where} \quad \sqrt[3]{g_3} = \frac{\sqrt[3]{4}}{\rho-1},$$

then, since the corpus  $K(\wp(v_h))$ ,  $h > 1$ , must necessarily contain the number  $\wp(v_2)$ , we get

$$K(\wp(v_h)) = K(y_h, \sqrt[3]{g_3}) = K(y_h, \sqrt[3]{2}), \quad h > 1.$$

The relation (14) gives

$$y_h^3 + 3y_{h-1}y_h^2 - 1 = 0. \quad (15)$$

Differentiating (14) with respect to  $u$ , we obtain

$$(1+2^{\rho})\wp'\{(1+2^{\rho})u\} = \frac{\wp(u)^3 + 2g_3}{-3\wp(u)^3}\wp'(u),$$

which gives

$$-3(1+2^{\rho})\wp'\{(1+2^{\rho})u\} = \frac{\wp(u)^3 + 9g_3}{\wp(u)^3 + g_3}\wp'(u). \quad (16)$$

Hence, putting

$$z_h = \frac{\mathfrak{E}'(r_h)}{\sqrt{-g_3}},$$

we get

$$z_h^3 + 3(1+2\rho)z_{h-1}z_h^2 - 9z_h - 3(1+2\rho)z_{h-1} = 0. \quad (17)$$

Since, by (16), the number  $\mathfrak{E}'(r_h) = \pm\sqrt{-g_3}$  can always be rationally expressed by  $\mathfrak{E}'(r_h)$ , we see that the corpus  $K(\mathfrak{E}'(r_h))$  is identical with  $K(z_h, \sqrt{-g_3})$ , i.e.  $K(z_h, \sqrt{1-\rho})$ . Thus we conclude that

$$K(x_h) = K(\mathfrak{E}(r_h), \mathfrak{E}'(r_h)) = K(y_h, z_h, \sqrt[3]{2}, \sqrt{1-\rho}), \quad h \geq 1,$$

$$K(x_1) = K(\mathfrak{E}(r_1), \mathfrak{E}'(r_1)) = K(\sqrt{1-\rho}).$$

Now, if we put as before

$$\tau(u) = \frac{\mathfrak{E}(u)}{\sqrt[3]{g_3}}, \quad \sqrt[3]{g_3} = \frac{\sqrt[3]{4}}{\rho-1},$$

the relation (14) becomes

$$\tau\{(1+2\rho)u\} = \frac{f_1}{g_1},$$

$$\text{where } f_1 = \tau(u)^3 - 1, \quad g_1 = -3\tau(u)^2.$$

Therefore, by successive iteration, we get

$$\tau\{(1+2\rho)^{h-1}u\} = \frac{f_{h-1}}{g_{h-1}},$$

where  $f_{h-1}$  and  $g_{h-1}$  are integral functions of  $\tau(u)$ , of degrees  $3^{h-1}$  and  $3^{h-1}-1$  respectively. The recursion-formulae for  $f_{h-1}$  and  $g_{h-1}$  are

$$f_{h-1} = f_{h-2}^3 - g_{h-2}^3,$$

$$g_{h-1} = -3f_{h-2}^2 g_{h-2}.$$

All the values of  $y_h$  are the roots of the equation

$$f_{h-1} = (f_{h-2} - g_{h-2})(f_{h-2} - \rho g_{h-2})(f_{h-2} - \rho^2 g_{h-2}) = 0.$$

Since each factor in this equation is of the  $3^{h-2}$ th. degree, the relative degree of the corpus  $K(y_h)$  cannot be greater than  $3^{h-2}$ .

But, on the other hand, since  $1+2\rho$  is a primary integer, it can be shewn exactly as in the preceding section, that the corpus  $K(\text{sn}^2 r_h)$ , i.e.  $K(\mathfrak{E}(r_h))$ , is of relative degree  $3^{h-1}$ . Therefore, since the equation of degree  $3^{h-1}$  for determining  $\mathfrak{E}(r_h)$  can be looked upon as an equation for  $\mathfrak{E}(r_h)^3$  of degree  $3^{h-2}$ , the corpus  $K(\mathfrak{E}(r_h)^3)$ ,

i.e.  $K(y_h^3)$ , is of relative degree  $3^{h-2}$ . Consequently,  $K(y_h)$  must be at least of the  $3^{h-2}$ th relative degree.

It follows therefore that the relative degree of  $K(y_h)$  must be exactly equal to  $3^{h-2}$ ; and consequently the equation (15) is irreducible in  $K(y_{h-1})$ . At the same time, it follows that

$$K(y_h) = K(y_h^3). \quad (18)$$

Now, since

$$\begin{aligned} y_1 &= 0, & z_1 &= \pm 1, \\ y_2 &= 1, \rho, \rho^2, & z_2 &= \pm(1+2\rho), \end{aligned}$$

we find that

$$K(y_1) = K(z_1) \quad \text{and} \quad K(y_2) = K(z_2).$$

More generally, it can be shewn by mathematical induction, that

$$K(y_h) = K(z_h)$$

for all values of  $h$ . For, if we suppose that

$$K(y_{h-1}) = K(z_{h-1}),$$

then, by (17),  $K(z_h)$  must be at most relatively cubic with respect to  $K(y_{h-1})$ . On the other hand, however, since

$$z_h^2 = 1 - 4y_h^3,$$

the same corpus  $K(z_h)$  contains  $K(y_h^3)$ . Hence, by (18), it contains  $K(y_h)$ ; consequently it must be at least relatively cubic with respect to  $K(y_{h-1})$ . We conclude, therefore, that  $K(z_h)$  must coincide with  $K(y_h)$ .

Thus we find that the corpus  $K(x_h)$  can be decomposed into the following three divisors:

$$K(y_h), \quad K(\sqrt[3]{2}), \quad K(\sqrt{1-\rho}).$$

## §. 11.

Let us now investigate the nature of  $K(y_h)$ . But, since this corpus for a certain value of  $h$  is contained in another corpus of the same type having a greater value of  $h$ , we may confine ourselves to the case

$$h = 2n+2 > 3.$$



It follows from §. 8 (iii), that the roots of the equation

$$f_{2n+1} = (f_{2n} - g_{2n})(f_{2n} - \rho g_{2n})(f_{2n} - \rho^2 g_{2n}) = 0 \quad (19)$$

are the values of  $\tau(u)$ , where

$$u = \frac{\rho^c (4 + 3\rho)^a (4 - 3\rho)^b}{(1 + 2\rho)^{2a+2}} \omega, \quad \begin{aligned} c &= 0, 1, 2, \\ a &= 0, 1, 2, \dots, 3^a - 1, \\ b &= 0, 1, 2, \dots, 3^a - 1; \end{aligned}$$

or, in other words,

$$u = \frac{\rho^{\xi} (\xi + \eta \rho)}{(1 + 2\rho)^{2a+2}} \omega, \quad \begin{aligned} \xi &= 1, 4, \dots, 3(3^a - 1) + 1, \\ \eta &= 0, 3, \dots, 3(3^a - 1). \end{aligned}$$

It is evident that, of all the roots of equation (19), those which arise from one and the same factor on the right-hand side must correspond to the same value of  $c$  in the above expressions for  $u$ . But, the consideration of the parallelogram of periods of  $\tau(u)$ , as shewn in §. 4, gives

$$\tau\left(\frac{\omega}{3}\right) = \rho, \quad \tau\left(\frac{\omega + \omega'}{3}\right) = 1, \quad \tau\left(\frac{\omega'}{3}\right) = \rho^2;$$

whence we infer that the roots of the equations

$$f_{2n} - g_{2n} = 0, \quad f_{2n} - \rho g_{2n} = 0, \quad f_{2n} - \rho^2 g_{2n} = 0$$

correspond respectively to the values

$$c = 2, 0, 1.$$

Since these three equations define one and the same relative corpus with respect to  $k(\rho)$ , we may confine ourselves to the one

$$f_{2n} - g_{2n} = 0.$$

This equation can be reduced to the following series of cubic equations:

$$y_k^3 + 3y_{k-1}y_k^2 - 1 = 0, \quad (20)$$

$$k = 3, 4, \dots, 2n+2, \quad y_2 = 1.$$

If we consider (20) as an equation for  $\frac{1}{y_k}$ , its discriminant is

$$D = 3^3(4y_{k-1}^3 - 1) = -3^3\epsilon_{k-1}^2.$$

But it follows from (17) that  $z_{k-1}$  cannot contain any ideal factor relatively prime to 3. Hence it must also be the case with  $D$ , and consequently also with the relative discriminant of the corpus  $K(y_k)$ . Therefore the relative discriminants of the corpus of decomposition (*Zerlegungskörper*) and of the corpus of inertia of the number  $1+2\rho$  in  $K(y_k)$  must be an algebraic unity. Hence both of these corpora coincide with  $k(\rho)$ . It follows therefore that  $1+2\rho$  is equal to the  $3^{2n}$ th. power of a prime ideal of the first degree in  $K(y_k)$ .

That this prime ideal is a principal ideal can be shewn as follows.

Put 
$$\zeta_k = \frac{1+2\rho}{y_k - y_{k-1}}, \quad k = 3, 4, \dots, 2n+2,$$

and let its conjugate numbers with respect to  $K(y_{k-1})$  be denoted by  $\zeta'_k$  and  $\zeta''_k$ . Then, observing that, if  $y_k, y'_k, y''_k$  denote the three roots of (20),

$$(y_k - y_{k-1})(y'_k - y_{k-1})(y''_k - y_{k-1}) = -3y_{k-1}^2(y_{k-1} - y_{k-2}),$$

we obtain

$$\begin{aligned} \zeta_k + \zeta'_k + \zeta''_k &= -3\zeta_{k-1}, \\ \zeta_k \zeta'_k + \zeta'_k \zeta''_k + \zeta''_k \zeta_k &= \frac{2(1+2\rho)}{y_{k-1}} \zeta_{k-1}, \\ \zeta_k \zeta'_k \zeta''_k &= \frac{1}{y_{k-1}^2} \zeta_{k-1}. \end{aligned}$$

Since  $y_{k-1}$  is an algebraic unity,  $\zeta_k$  must be an integer, provided that  $\zeta_{k-1}$  is an integer. But, this is really the case with

$$\zeta_3 = \frac{1+2\rho}{y_3-1},$$

for

$$\begin{aligned} \zeta_3 + \zeta'_3 + \zeta''_3 &= (1+2\rho)^3, \\ \zeta_3 \zeta'_3 + \zeta'_3 \zeta''_3 + \zeta''_3 \zeta_3 &= 2(1+2\rho)^2, \\ \zeta_3 \zeta'_3 \zeta''_3 &= 1+2\rho. \end{aligned}$$

Hence  $\zeta_k$  is certainly an integer. Its relative norm taken with respect to  $K(y_{k-1})$  is, as shewn above, associated with  $\zeta_{k-1}$ . Hence we infer that the relative norm of  $\zeta_k$  taken with respect to  $k(\rho)$  must be associated with that of  $\zeta_3$ . Thus we get

$$(1+2\rho) = (\zeta_{2n+2})^{3^{2n}}.$$

The relative *different* of  $\zeta_k$  with respect to  $K(y_{k-1})$  is

$$\begin{aligned} (\zeta_k - \zeta_k')(\zeta_k - \zeta_k'') &= \frac{(y_k' - y_k)(y_k'' - y_k)}{y_{k-1}^2(y_{k-1} - y_{k-2})(y_k - y_{k-1})} \\ &= \frac{3y_k^2 + 6y_{k-1}y_k}{y_{k-1}^2(y_{k-1} - y_{k-2})(y_k - y_{k-1})} \\ &= (1+2\rho)\zeta_{k-1}\{(1+2\rho)y_{k-1}\zeta_k - 1\} \frac{y_k}{y_{k-1}^2}. \end{aligned}$$

Therefore the relative *different* of  $K(y_k)$  with respect to  $K(y_{k-1})$  must be equal to  $(1+2\rho)\zeta_{k-1}$ . Consequently, that of  $K(y_{2n+2})$  with respect to  $k(\rho)$  is

$$(1+2\rho)^{2n}\zeta_{2n+1}\zeta_{2n}\cdots\cdots\zeta_3\zeta_2, \quad \zeta_2 = 1+2\rho;$$

whence we conclude that the relative discriminant of  $K(y_{2n+2})$  is equal to

$$\begin{aligned} &(1+2\rho)^{2n}3^{2^1+3+3^2+\cdots+3^{2n}} \\ &= (1+2\rho)^{2n} \frac{(4n+3)3^{2^n}-3}{2}. \end{aligned}$$

As in case (ii) of §. 9, it can be shewn that the corpus  $K(y_{2n+2})$  contains as its divisors  $4 \cdot 3^{n-1}$  different relatively cyclic corpora of relative degree  $3^n$ , whose relative discriminants are powers of  $1+2\rho$ .

Next, let us consider the corpus

$$C = k(\rho, \sqrt[3]{2}),$$

which is relatively cubic with respect to  $k(\rho)$ . Since the discriminant of the equation

$$x^3 - 2 = 0$$

is  $-2^2 \cdot 3^3$ , the relative discriminant of  $C$  cannot contain any other prime than 2 and  $1+2\rho$ . If we put

$$x = \sqrt[3]{2}, \quad y = \frac{1+2\rho}{1+x},$$

then

$$1+2\rho = \frac{y^3}{1-x}.$$

Therefore, since  $1-x$  is an algebraic unity, we get

$$\begin{aligned} 2 &= x^3, \\ 1+2\rho &= y^3, \quad y^2 = 1+x. \end{aligned}$$

The relative *different*e of  $y$  with respect to  $k(\rho)$  is

$$(1+2\rho)^2 \left( \frac{1}{1+x} - \frac{1}{1+\rho x} \right) \left( \frac{1}{1+x} - \frac{1}{1+\rho^2 x} \right) = x^2(1-x)(1+x)^2 \simeq x^2 y^4.$$

Hence the relative *different*e of  $C$  with respect to  $k(\rho)$  contains  $y$  to the fourth power. The relative discriminant of  $C$  is therefore equal to  $2^2 3^2$ ,

In the relatively quadratic corpus

$$Q = k(\sqrt{1-\rho}) = k(\sqrt{1+2\rho}),$$

all the integers can be represented in the form

$$\frac{\alpha + \beta \sqrt{1+2\rho}}{2},$$

where  $\alpha$  and  $\beta$  are integers in  $k(\rho)$ , such that

$$\alpha^2 - (1+2\rho)\beta^2 \equiv 0 \pmod{4}.$$

From this congruence, it follows that

$$\alpha^2 - \beta^2 = (\alpha + \beta)(\alpha - \beta) \equiv 0 \pmod{2}.$$

Hence  $\alpha^2 - \beta^2$  must be divisible by 4. Therefore, from the original congruence, we see that  $\beta$ , and consequently also  $\alpha$ , must be divisible by 2.

Thus the numbers 1 and  $\sqrt{1+2\rho}$  form a system of bases (*Minimalbasis*) of  $Q$ , so that the relative discriminant of  $Q$  is  $2^2(1+2\rho)$ .

## §. 12.

In this section we consider the division of periods of  $\operatorname{sn}$  by a power of 2.

Put

$$p(u) = (\rho - 1)\operatorname{K}(u),$$

then the duplication-formula for  $p(u)$  is

$$p(2u) = \frac{p(u)^4 + 8p(u)}{4\{p(u)^3 - 1\}}. \quad (21)$$

Differentiating (21) with respect to  $u$ , and making use of the relation

$$(\rho-1)^3 \mathfrak{k}'(u)^2 = 4(p(u)^3-1),$$

we obtain

$$\mathfrak{k}'(2u) = \frac{\mathfrak{k}'(u)^4 + 8(1+2\rho)\mathfrak{k}'(u)^2 + 16}{8\mathfrak{k}'(u)^3}.$$

Hence, if we put

$$q(u) = \frac{\mathfrak{k}'(u)}{2},$$

then

$$q(2u) = \frac{q(u)^4 + 2(1+2\rho)q(u)^2 + 1}{8q(u)^3}. \quad (22)$$

Let  $y_h$  and  $z_h$  denote the values of  $p(u)$  and  $q(u)$  respectively, when

$$u = \frac{\omega}{2^n}.$$

Then, from (21) and (22), we find that

$$y_1^3 = 1 \quad \text{and} \quad z_1 = 0;$$

therefore

$$K(y_1) = K(z_1) = k(\rho).$$

To find  $y_2$  and  $z_2$ , we have to solve the equations

$$y_2^4 - 4y_1y_2^3 + 8y_2 + 4y_1 = 0$$

$$\text{and} \quad z_2^4 + 2(1+2\rho)z_2^2 + 1 = 0$$

respectively. Both of these equations are reducible. In fact, they break up into factors as follows:

$$(y_2^2 - 2y_1y_2 - 2y_1^2)^2 = 0,$$

$$(z_2^2 + 2\rho z_2 - 1)(z_2^2 - 2\rho z_2 - 1) = 0.$$

Therefore

$$y_2 = (1 \pm \sqrt{3})y_1,$$

$$z_2 = \pm \rho(1 \pm \rho i).$$

Thus we see that

$$K(y_2) = K(z_2) = k(\rho, i).$$

Now, from (21), we can derive by iteration the formula

$$p(2^h u) = \frac{f_h}{g_h},$$

where  $f_h$  and  $g_h$  are defined by the recursion-formulae

$$\begin{aligned} f_h &= f_{h-1}(f_{h-1}^3 + 8g_{h-1}^3), \\ g_h &= 4g_{h-1}(f_{h-1}^3 - g_{h-1}^3), \end{aligned}$$

with the initial values

$$\begin{aligned} f_1 &= p(u)(p(u)^3 + 8), \\ g_1 &= 4(p(u)^3 - 1). \end{aligned}$$

By similar reasoning as in the preceding section, it can be shewn that the roots of the equation of the  $2^{2h-3}$ th degree

$$f_{h-1} - \rho^c g_{h-1} = 0, \quad c = 0, 1, 2, \quad h \geq 2, \quad (23)$$

are the values of  $\rho(u)$ , where

$$u = \frac{\rho^{c-1}(1+2\rho)^a(1-2\rho)^b}{2^c} \omega, \quad \begin{aligned} a &= 0, 1, 2, \dots, 2^{h-1}-1, \\ b &= 0, 1, 2, \dots, 2^{h-2}-1; \end{aligned}$$

or, in other words,

$$u = \frac{\rho^{c-1}(\xi + \eta\rho)}{2^c} \omega, \quad \begin{aligned} \xi &= 1, 5, \dots, 4(2^{h-2}-1)+1, \\ \eta &= 0, 2, \dots, 2(2^{h-1}-1). \end{aligned}$$

As will be shewn hereafter (§. 17), the corpus  $K(y_h)$  is the class-corpus (*Klassenkörper*) corresponding to the group of numbers  $\alpha$  in  $k(\rho)$ , such that

$$\alpha \equiv 1 \pmod{2^h}.$$

Therefore the relative degree of  $K(y_h)$  cannot be less than<sup>1)</sup>

$$\frac{\varphi(2^h)}{6}, \quad \text{i.e., } 2^{2h-3}.$$

Hence, of course, the relative degree of  $K(y_h)$  cannot be less than  $2^{2h-3}$ . Thus we see that the equation (23) must be irreducible in  $k(\rho)$ . And it follows, at the same time, that

$$K(y_h^3) = K(y_h);$$

whence it can be proved, as in the preceding section, that

$$K(y_h) = K(z_h),$$

for all values of  $h$ .

1) Weber: Algebra III, §. 167.

In virtue of the relations:

$$\operatorname{sn} 2u = \frac{2 \operatorname{sn} u \operatorname{cn} u \operatorname{dn} u}{1 + \rho^2 \operatorname{sn}^4 u},$$

$$p(u) = \frac{\rho - 1}{\operatorname{sn}^2 u} + 1,$$

$$q(u) = -\frac{\operatorname{cn} u \operatorname{dn} u}{\operatorname{sn}^3 u},$$

it can be concluded that  $\operatorname{sn} 2u$  can be rationally expressed by  $p(u)$  and  $q(u)$  in the corpus  $k(\rho)$ . Therefore, if we put

$$x_h = \operatorname{sn} \frac{\omega}{2^h},$$

then the corpus  $K(x_{h-1})$  must a divisor of  $K(y_h, z_h)$ , i.e. of  $K(y_h)$ . But, on the other hand, this latter corpus  $K(y_h)$  is evidently a divisor of  $K(x_h)$ . Thus we find that the two kinds of corpora

$$K(x_i) \quad \text{and} \quad K(y_i), \quad i = 1, 2, \dots,$$

can be arranged in such a series

$$K(y_1), K(x_1), K(y_2), K(x_2), \dots, K(y_h), K(x_h), \dots,$$

that each corpus is a divisor of the next one. It will also be proved presently that none of these corpora coincide with the neighboring ones, except

$$K(y_1) = K(x_1) = k(\rho).$$

Hence, in the following, we shall consider  $K(y_k)$  instead of  $K(x_k)$ , where  $y_h$  is a root of the equation of the  $2^{h-1}$ th degree:

$$f_{h-1} - y_{h-1} = 0.$$

By (21), this equation can be reduced to a series of the following biquadratic equations:

$$y_k^4 - 4y_{k-1}y_k^2 + 8y_k + 4y_{k-1} = 0, \quad (24)$$

$$k = 2, 3, \dots, h, \quad y_1 = 1.$$

The irreducibility of (24), excepting the case  $k=2$ , follows at once from that of (23). It is, however, imprimitive; for, any one root of it can be rationally expressed in  $k(\rho)$  in terms of any other root

of the same equation. In fact, if

$$y_k = p(r)$$

be a root of (24), then evidently the other three roots are

$$y'_k = p\left(r + \frac{\omega}{2}\right) = \rho \frac{y_k + 2\rho}{y_k - \rho},$$

$$y''_k = p\left(r + \frac{\omega'}{2}\right) = \rho^2 \frac{y_k + 2\rho^2}{y_k - \rho^2},$$

$$y'''_k = p\left(r + \frac{\omega + \omega'}{2}\right) = \frac{y_k + 2}{y_k - 1}.$$

Putting

$$y_k + y'''_k = Y_k, \quad y'_k + y''_k = Y'_k,$$

we get

$$Y_k + Y'_k = 4y_{k-1},$$

$$Y_k Y'_k = -4(y_{k-1} + 1),$$

$$Y_k + 2 = y_k y'''_k.$$

Thus the solution of the biquadratic equation (24) can be reduced to those of the following two quadratic equations :

$$Y_k^2 - 4y_{k-1} Y_k - 4(y_{k-1} + 1) = 0,$$

$$y_k^2 - Y_k y_k + (Y_k + 2) = 0.$$

The discriminants of these equations are respectively

$$D_k = 16(y_{k-1}^2 + y_{k-1} + 1),$$

$$d_k = Y_k^2 - 4(Y_k + 2).$$

$D_k$  can be transformed as follows.

$$\begin{aligned} D_k &= 16 \frac{y_{k-1}^2 - 1}{y_{k-1} - 1} = 16 \frac{(\rho - 1)^2 x_{k-1}^2 - 1}{y_{k-1} - 1} \\ &= 16(\rho - 1)^2 x_{k-1}^2 x_{k-1}^2. \end{aligned}$$

This shews that the corpus  $K(Y_k)$  can be derived from  $K(y_{k-1})$  by adjoining  $x_{k-1}$  to it; in other words,  $K(Y_k)$  is identical with  $K(x_{k-1})$ . It follows therefore that  $K(x_{k-1})$  cannot coincide with  $K(y_{k-1})$ , if  $k > 2$ .



Next, since

$$Y_k^2 = 4(y_{k-1}Y_k + y_{k-1} + 1),$$

$d_k$  can be transformed as follows:

$$d_k = 4(y_{k-1} - 1)(Y_k + 1).$$

Now, from the relation

$$y_k - 1 = \frac{\rho - 1}{x_k^2} = \rho - 1,$$

we conclude that both  $y_k - \rho$  and  $y_k - \rho^2$  are divisible by  $\rho - 1$ . Consequently both

$$\begin{aligned} \frac{Y_k + 1}{\rho - 1} &= \frac{y_k - \rho}{\rho - 1} + \frac{y_k''' - \rho^2}{\rho - 1} \\ \text{and} \quad \frac{Y_k' + 1}{\rho - 1} &= \frac{y_k' - \rho}{\rho - 1} + \frac{y_k'' - \rho^2}{\rho - 1} \end{aligned}$$

must be algebraic integers. But, since

$$\frac{Y_k + 1}{\rho - 1} = \rho^2 \frac{\rho - 1}{Y_k' + 1},$$

it follows that

$$Y_k + 1 = Y_k' + 1 = \rho - 1.$$

The corpus  $K(Y_k)$  can be defined by an integer

$$\frac{Y_k + 1}{\rho - 1}.$$

But, the relative discriminant of this integer with respect to  $K(y_{k-1})$  is

$$\frac{D_k}{(\rho - 1)^2} = 16z_{k-1}^2x_{k-1}^2 = 16,$$

since it can easily be inferred from (22) that  $z_{k-1}$  is an algebraic unity. Hence we see that the relative discriminant of  $K(Y_k)$  with respect to  $K(y_{k-1})$  can contain no ideal factor relatively prime to 2.

The corpus  $K(y_k)$  can be defined by an integer

$$\frac{y_k - 1}{\rho - 1},$$

whose relative discriminant with respect to  $K(Y_k)$  is

$$\frac{d_k}{(\rho - 1)^2} = 4.$$

Hence the relative discriminant of  $K(y_k)$  must consist of ideals, which are all divisors of 2.

It follows therefore that the relative discriminant of  $K(y_h)$  with respect to  $k(\rho)$  cannot contain any other prime than 2. Hence the principal ideal (2) must be equal to the  $2^{2h-3}$ th power of a prime ideal of the first degree in  $K(y_h)$ .

That this is a principal ideal can be shewn as follows. Put

$$\frac{1}{\zeta_h} = \frac{y_h^3}{4} = \tau \left( \frac{\omega}{2^h} \right),$$

then, as shewn in §. 3,  $\zeta_h$  is a divisor of 2. The norm of  $\zeta_h$  taken with respect to  $K(y_{h-1})$  is, by (24),

$$n(\zeta_h) = \frac{4^3}{(4y_{h-1})^3} = \zeta_{h-1}, \quad h > 2,$$

$$n(\zeta_2) = \frac{4^2}{(-2y_1)^2} = -2;$$

whence we conclude that

$$(2) = (\zeta_h)^{2^{2h-3}}, \quad \text{Q. E. D.}$$

Let us next consider the relative *different* of  $\zeta_h$  with respect to  $K(y_{h-1})$ , supposing that  $h > 2$ . If we indicate the conjugates of any number by placing accents upon it, the *different* of  $\zeta_h$  is

$$\begin{aligned} & (\zeta_h - \zeta_h')(\zeta_h - \zeta_h'')(\zeta_h - \zeta_h''') \\ &= 4^3 \left( \frac{1}{y_h^3} - \frac{1}{y_h'^3} \right) \left( \frac{1}{y_h^3} - \frac{1}{y_h''^3} \right) \left( \frac{1}{y_h^3} - \frac{1}{y_h'''^3} \right) \\ &= 4^3 - (y_h^3 + 2)^3 + 3^3 y_{h-1}^3 y_h^6 \\ &= -2^6 - \frac{\zeta_{h-1}}{\zeta_h} - 3 \cdot 2^3 \zeta_{h-1} - 3 \cdot 2^3 \zeta_{h-1} \zeta_h - 2^3 \zeta_{h-1} \zeta_h^2 + 3^3 \cdot 2^6, \end{aligned}$$

Therefore the *different* is divisible by  $2^3 \zeta_h^2$ , but by no higher power of  $\zeta_h$ .

In the corpus  $K(y_2)$ , i.e.  $K(i)$ , the number (2) is decomposed as follows:

$$2 = (\sqrt{3}+1)(\sqrt{3}-1) \equiv (\sqrt{3}+1)^2.$$

Hence the relative *different* of  $K(y_2)$  is equal to 2.

The relative *different* of  $K(y_h)$  is therefore

$$2^{3(h-2)+1}(\frac{y}{y_h} \frac{y}{y_{h-1}} \dots \frac{y}{y_3})^6.$$

Accordingly the relative discriminant of  $K(y_h)$  is

$$2^{(3h-4)2^{h-3}-2}.$$

Now, the corpus  $K(y_h)$ ,  $h > 2$ , is relatively Abelian, and its Galois' group is of the form

$$\begin{aligned} s^a t^b, \quad & a = 0, 1, 2, \dots, 2^{h-1}-1, \\ & b = 0, 1, 2, \dots, 2^{h-2}-1. \end{aligned}$$

In this Galois' group, there are  $2^{h-2}$  cyclic subgroups of order  $2^{h-1}$ , viz.

$$(s), (st), (st^2), \dots, (st^{2^{h-2}-1}).$$

Besides them, there are also  $2^{h-2}$  cyclic subgroups of order  $2^{h-2}$ , viz.

$$(t), (s^2t), (s^4t), \dots, (s^{2^{h-2}-1}t).$$

Therefore the corpus  $K(y_h)$  contains as its divisors  $2^{h-2}$  relatively cyclic corpora (we shall call them  $A$ ) of relative degree  $2^{h-2}$ , and also  $2^{h-2}$  relatively cyclic corpora ( $B$ ) of relative degree  $2^{h-1}$ .

Similarly, the corpus  $K(y_{h+1})$  will contain  $2^{h-1}$  relatively cyclic divisors ( $C$ ) of relative degree  $2^{h-1}$ , and  $2^{h-1}$  ( $D$ ) of relative degree  $2^h$ . The relation between  $C$  and  $A$  is such that each one of  $C$  contains a certain one of  $A$ , and conversely, each one of  $A$  is contained in certain two of  $C$ . Similar relation exists between  $D$  and  $B$ .

Hence we see that, by the division of periods by powers of 2, we obtain

$$2^{h-2} + 2^{h-1} = 3 \cdot 2^{h-2}$$

different relatively cyclic corpora in all, whose relative degrees are all  $2^{h-1}$ , and whose relative discriminants are powers of 2.

### §. 13.

We have considered all the division-corpora arising from the division of periods of  $\text{sn}$  with the singular modulus  $x=i\rho$  by powers of primes in  $k(\rho)$ ; and analysed them into relatively cyclic components. Let us here tabulate these component corpora.

In the following table,  $\mu$  denotes an odd prime in  $k(\rho)$  relatively prime to 3, and  $m$  the norm of  $\mu$ . The decomposition of  $m-1$  into distinct natural primes is supposed to be

$$m-1 = 2^{h+1} 3^{h'+1} p^k \dots\dots.$$

	Relative Degree	Distinct Primes in Relative Discriminant	Number of Corpora of the same Relative Degree
I	$\rho^\lambda, \lambda = 1, 2, \dots\dots, h$	$\mu$	1
II	$3^\lambda, \lambda = 1, 2, \dots\dots, h'$	$\mu$	1
III	$3^{h'+1}$	$\mu$ and 2	1
IV	$2^\lambda, \lambda = 1, 2, \dots\dots, h$	$\mu$	1
V	$2^{h+1}$	$\mu$ and 2	1
VI	3	$1+2\rho$ and 2	1
VII	2	$1+2\rho$ and 2	1
VIII	$m^n, n$ being any natural number	$\mu$	$\begin{cases} (m+1)m^{n-1}, & \text{when } \mu \text{ is real} \\ 1, & \text{when } \mu \text{ is not real} \end{cases}$
IX	$3^n, n$ being any natural number	$1+2\rho$	$4 \cdot 3^{n-1}$
X	$2^n, n$ being any natural number	2	$3 \cdot 2^{n-1}$

Hereafter we shall call these corpora simply *elementary corpora*.

If we analyse the division-corpus for a composite divisor  $\mu$ , no other corpus will be found than the elementary corpora. For, if  $\mu$  contains more than one distinct prime factor, we can decompose  $\mu$  into two factors relatively prime to each other, say  $\mu = \alpha\beta$ . Then two integers  $\xi$  and  $\eta$  can be found, such that

$$\frac{1}{\mu} = \frac{\xi}{\alpha} + \frac{\eta}{\beta};$$

and, putting

$$w = \frac{\omega}{\mu}, \quad u = \frac{\xi\omega}{\alpha}, \quad v = \frac{\eta\omega}{\beta},$$

we get

$$\operatorname{sn} w = \frac{\operatorname{sn} u \operatorname{cn} v \operatorname{dn} v + \operatorname{sn} v \operatorname{cn} u \operatorname{dn} u}{1 + \rho^2 \operatorname{sn}^2 u \operatorname{sn}^2 v}.$$

But, since  $\text{en } u \cdot \text{dn } u$  and  $\text{en } v \cdot \text{dn } v$  can be rationally expressed by  $\text{sn } u$  and  $\text{sn } v$  respectively, even in the case where  $u$  or  $v$  is a power of 2 (§. 12), we conclude that

$$K(\text{sn } w) = K(\text{sn } u, \text{sn } v), \quad \text{Q. E. D.}$$

## §. 14.

We are now in a position to prove the following important theorem.

*There can be no other relatively Abelian corpora with respect to  $k(\rho)$  than those contained in the division-corpora of the elliptic function  $\text{sn}$  with the singular modulus  $\kappa=i\rho$ .*

The same thing may also be put in another way as follows:

*given any relatively Abelian corpus with respect to  $k(\rho)$ , we can always find such a corpus which is composed of elementary corpora only and contains the given corpus as a divisor of it.*

It is well known that every Abelian corpus can be decomposed into cyclic ones, whose degrees are powers of primes. This is true not only for absolutely Abelian corpora, but also for relatively Abelian corpora with respect to  $k(\rho)$ . Hence we shall prove our theorem only for such relatively cyclic corpora.

Let  $C_h$  be a relatively cyclic corpus of relative degree  $p^h$ ,  $p$  being a natural prime, and  $C_1$  its divisor of relative degree  $p$ . If the relative discriminant of  $C_1$  contain a prime factor in  $k(\rho)$  relatively prime to  $p$ , let it be denoted by  $\mu$ . Now, consider the corpus of inertia of  $\mu$  in  $C_h$ . Since the relative discriminant of it must be relatively prime to  $\mu$ , this corpus of inertia cannot contain  $C_1$  in it; consequently it must coincide with  $k(\rho)$ . On the other hand, the corpus of ramification of  $\mu$  is  $C_h$  itself, since  $\mu$  is relatively prime to the relative degree  $p^h$  of  $C_h$ . Therefore the number  $\mu$  is equal to the  $p^h$ th power of a prime ideal of the first degree in  $C_h$ . If the norm of  $\mu$  be denoted by  $m$ , we get<sup>1)</sup>

$$m-1 \equiv 0 \pmod{p^h}.$$

1) Weber; Algebra II, §. 181.  
Hilbert: loc. cit., §. 41.

Hence, if  $p$  be not equal to 2 or 3, we can always find an elementary corpus  $E$ , whose relative degree is  $p^h$  and whose relative discriminant is a power of  $\mu$ . Let it be called  $E$ . Composing  $E$  with  $C_h$ , we obtain a corpus of relative degree  $p^n$ , where  $h \leq n \leq 2h$ . In this corpus  $EC_h$ , the principal ideal  $(\mu)$  will be equal to the  $p^{n'}$ th power of an ideal, where  $h \leq n' \leq 2h$ . Then, since  $EC_h$  is itself the corpus of ramification of  $\mu$  in  $EC_h$ , it follows that this corpus must be at least of relative degree  $p^h$ , and relatively cyclic, with respect to the corpus of inertia  $C'$  of  $\mu$ . But, since it is evident that the Galois' group of  $EC_h$  cannot contain a cyclic subgroup whose degree is higher than the  $p^h$ th, the relative degree of  $EC_h$  with respect to  $C'$  must be exactly equal to  $p^h$ ; whence follows that the relative degree of  $C'$  is  $p^{n-h}$ .

The two corpora  $E$  and  $C'$  have no other common divisor than  $k(\rho)$ , for their relative discriminants are relatively prime to each other. Hence we get

$$CE = C'E. \quad (25)$$

If  $p=2$  or 3, the same reasoning can be applied, provided that  $p^h$  be not the highest power of 2 or 3 contained in  $m-1$ .

If  $p^h$  be the highest power of 2 or 3 contained in  $m-1$ , we must take an elementary corpus V, VII or III, VI in place of  $E$ , according as  $p=2$  or 3. Then the relative discriminant of  $E$  contains the factor 2. It may happen, therefore, that the relative discriminant of  $C'$  is not relatively prime to that of  $E$ . Nevertheless, it is still valid that  $C'$  and  $E$  cannot have a common divisor other than  $k(\rho)$ . For, if there be a common divisor, it must be a relatively cyclic corpus, whose relative discriminant is a power of 2. But, it is evident that none of the corpora V, VII, III, VI contains such a divisor. Thus again we arrive at (25).

The relative discriminant of  $C'$  contains all or a part of the prime factors in the relative discriminant of  $C_h$ , with the exception of  $\mu$ .

If the divisor  $C'_1$ , of relative degree  $p$ , of  $C'$  still contain a prime  $\mu'$  relatively prime to  $p$ , then apply the above process once more to  $C'$  to get rid of this factor  $\mu'$ . In this way, repeating

this process a number of times, we shall arrive at a corpus  $C_h$  of relative degree  $p^h$  ( $h \leq h$ ), the relative discriminant of whose divisor  $\bar{C}_1$ , of relative degree  $p$ , does no longer contain a prime relatively prime to  $p$ .

### §. 15.

It was proved by Hilbert<sup>1)</sup> that every cyclic corpus, whose degree is an odd prime  $u$ , and whose discriminant does not contain any other prime than  $u$ , must necessarily be a *Kreiskörper*. Following his example, we can now prove that the corpus  $\bar{C}_1$  of relative degree  $p$  is nothing else but an elementary corpus VIII, IX or X, according as  $p > 3$ ,  $p = 3$  or  $p = 2$ .

In the case  $p > 3$ , the proof can be effected without any difficulty by Hilbert's method<sup>2)</sup>. As for the method, the reader is referred to his original work, as it will occupy too much space to reproduce it here.

Next we have to prove that the relatively cyclic corpora of relative degree 3, whose relative discriminants are powers of  $1 + 2\rho$ , are exhausted by the four relatively cubic ones of the elementary corpus IX.

From what has been shewn in §. 10 and §. 11, it follows that the relatively cyclic corpus obtained by adjoining

$$\sqrt[3]{\frac{\omega}{(1+2\rho)^4}}$$

to  $k(\rho)$  is of relative degree 9, and that this corpus contains four different relatively cubic divisors, whose relative discriminants are powers of  $1 + 2\rho$ .

But, on the other hand, it can be shewn that there are no more relatively cubic corpora, whose relative discriminants are powers of  $1 + 2\rho$ , than the above four corpora. For, since the fundamental corpus  $k(\rho)$  contains the primitive cube roots of unity, every relatively cyclic corpus of the third degree can be obtained from  $k(\rho)$  by adjoining to it a cube root of a certain integer, say  $\alpha$ .

1) Hilbert: loc. cit., §. 103.

2) Also cf. Takagi: loc. cit., §. 13 and §. 14.

properly chosen in  $k(\rho)'$ . Without losing generality, we may suppose that this integer  $a$  does not contain such factors that are perfect cubes in  $k(\rho)$ . Then, any prime factor in  $a$ , since it becomes a cube in  $K(\sqrt[3]{a})$ , must necessarily enter into the relative discriminant of this corpus. Hence there can be no other relatively cubic corpora, whose relative discriminants are powers of  $1+2\rho$ , than the following ones:

$$K(\sqrt[3]{\rho^a(1+2\rho)^b}), \quad a, b \equiv 0, 1, 2 \pmod{3}.$$

Here the combination  $a \equiv b \equiv 0$  should of course be avoided; also it is to be observed that the two pairs of values  $(a, b)$  and  $(-a, -b)$  give rise to one and the same corpus. It follows therefore that there can be at most four different corpora of this kind, Q. E. D.

Lastly, let us consider the case  $p=2$ . From §. 12 we see that the relative corpus defined by  $p\left(\frac{\omega}{8}\right)$  is of relative degree 8, and contains three different relatively quadratic divisors, whose relative discriminants are powers of 2. On the other hand, it is evident that there can be only three relatively quadratic corpora, whose relative discriminants are powers of 2; viz.  $K(i)$ ,  $K(\sqrt{2})$ ,  $K(\sqrt{2}i)$ . Our proposition is thus proved.

The case  $h=1$  having been finished, we can now prove, by mathematical induction, that  $\bar{C}_n$ ,  $\bar{h}>1$ , is a divisor of a corpus composed of elementary corpora only.

The theorem is true in the case  $\bar{h}=1$ . Suppose that it is true for all  $\bar{C}_n$ ,  $\bar{h}<n$ ,  $n$  being a certain natural number; and consequently that it is also true for all relatively cyclic corpora of relative degree  $p^{\bar{h}}$ , not necessarily of the kind  $C$ .

Now, let  $E_h$  denote an elementary corpus VIII, IX or X of relative degree  $p^{\bar{h}}$ , according as  $p>3$ ,  $p=3$  or  $p=2$ . Since the divisor  $\bar{C}_1$  of  $\bar{C}_n$  must be identical with a certain  $E_1$  contained in  $E_n$ , we can find such a relatively cyclic corpus  $D$  that

$$\bar{C}_n E_n = D E_n,$$

1) Hilbert: loc. cit., §. 101.



and such that its relative degree is less than  $p^n$ .<sup>1)</sup> Therefore  $D$ , and consequently also  $\bar{C}_n$ , must be contained in a corpus composed of elementary corpora only.

## PART II.

### §. 16.

Let  $j(m\rho)$  be a class invariant,  $m$  being a natural number. By adjoining  $j(m\rho)$  to  $k(\rho)$ , we obtain a relative corpus called *order-corpus* (*Ordnungs-körper*). Order-corpora are often called *class-corpora* (*Klassenkörper*). But, to avoid confusion, we shall never use the word *class-corpus* in this sense. As for the definition of *class-corpus* used in the following, the reader is referred to Weber's *Lehrbuch der Algebra*, Vol. III, §. 164.

The order-corpus  $K(j(m\rho))$  is relatively Abelian with respect to  $k(\rho)$ , and its relative degree is equal to the number of classes of the order  $[m]$  (*Ordnung mit dem Führer  $m$* ). Hence, if the decomposition of  $m$  into distinct natural primes be

$$m = p_1^{h_1} p_2^{h_2} \cdots p_i^{h_i} \cdots,$$

the relative degree is

$$h = \frac{1}{3} H p_i^{h_i-1} \left( p_i - \left( \frac{p_i}{3} \right) \right).$$

It is known that the irreducible equation of the  $h$ th degree, which gives  $j(m\rho)$  as a root, becomes reducible, when we adjoin

$$\begin{aligned} \sqrt[p_i-1]{(-1)^{\frac{p_i-1}{2}} p_i}, & \quad i = 1, 2, \cdots, \text{ supposing that } p_i \neq 2, \\ \sqrt{-1}, & \quad \text{if } m \equiv 0 \pmod{4}, \\ \sqrt{-1}, \sqrt{2}, & \quad \text{if } m \equiv 0 \pmod{8}, \end{aligned}$$

to the fundamental corpus  $k(\rho)$ .<sup>2)</sup> But, no further reduction of the equation can take place, whatever roots of unity may be adjoined

1) Takagi: loc. cit., §. 9.

Hilbert: loc. cit., §. 103.

2) Fueter: Der Klassenkörper der quadratischen Körper etc. (Dissertation; Göttingen, 1903).

Weber: Algebra III., §. 138.

to the fundamental corpus<sup>1)</sup>. Hence, if a primitive  $m$ th root of unity, in terms of which all the square roots above given can be rationally expressed, be adjoined to the order-corpus  $K(j(m, \rho))$ , then the resultant corpus must be of relative degree

$$\begin{aligned} H &= \frac{1}{2^{r+s}} h H_i^{h_i-1} (p_i-1) \\ &= \frac{1}{3 \cdot 2^{r+s}} H_i^{2(h_i-1)} (p_i-1) \left( p_i - \left( \frac{p_i}{3} \right) \right), \end{aligned}$$

where  $r$  denotes the number of distinct odd primes in  $m$ , and

$$s = 0, \quad \text{if } m \not\equiv 0 \pmod{4},$$

$$s = 1, \quad \text{if } m \equiv 4 \pmod{8},$$

$$s = 2, \quad \text{if } m \equiv 0 \pmod{8}.$$

This corpus of the  $H$ th relative degree is relatively Abelian with respect to  $k(\rho)$ . We shall denote it by the symbol  $K[m]$ .

It is known that the corpus  $K[m]$  is the class-corpus corresponding to the group of numbers  $a$ , which belong to the order  $[m]$ , and satisfy the condition

$$a \equiv 1 \pmod{m},$$

all the prime factors of  $m$  being taken in the *excludent*.<sup>2)</sup> Such a group of numbers is called a *strahl* by R. Fueter<sup>3)</sup>. Hence the corpus  $K[m]$  may well be called a *strahl-corpus*.

Weber concluded that his so-called division-corpus, i.e. the corpus obtained by adjoining to  $k(\rho)$  the numbers  $\kappa$  and  $S\left(\frac{\omega}{\mu}\right)^2$ , where

$$S\left(\frac{\omega}{\mu}\right) = \sqrt{\kappa} \operatorname{sn} \frac{\omega}{\mu},$$

$\mu$  being an integer in  $k(\rho)$ , can always be looked upon as a divisor of a certain *strahl*-corpus<sup>4)</sup>.

It seems to me, however, that there are two defects in his proof. The one is the misconception that his division-corpus for

1) Weber : Algebra III, §. 168.

2) Weber : Algebra III, §. 168.

3) Fueter : Crelle's Journal, Vols. 130, 132 : Math. Ann., Vol. 75.

4) Weber : Algebra III, §. 169.

any composite value of  $\mu$  can always be composed of those for which  $\mu$ 's are powers of single primes<sup>1)</sup>. The other is the confusion of terminology. His proof that the division-corpus is the class-corpus corresponding to the group of numbers  $a$ , such that

$$a \equiv 1 \pmod{\mu},$$

is correct only when the word *division-corpus* means

$$K\left(\wp\left(\frac{\omega}{\mu}\right)^{\frac{1}{\mu}}\right);$$

while he used the word to mean his so-called division-corpus mentioned above<sup>2)</sup>.

Recently Fueter has given a simple example<sup>3)</sup>, which denies Weber's conclusion. However, as for the relation between *strahl*-corpora and division-corpora, there still remains a great deal of obscurity.

Let us now begin our own investigation upon this point.

## §. 17.

Let  $\pi$  be an odd prime of the first degree in  $k(\rho)$ , which is relatively prime to 3, and such that

$$\pi = a + b\rho, \quad b \equiv 0 \pmod{2},$$

$a$  and  $b$  being rational integers. Then as we have seen in §. 4,

$$\varepsilon \sin \pi u = \frac{\sqrt{\kappa^{p-1}}x^p + A_{p-2}x^{p-2} + \dots + A_3x^3 + \varepsilon \pi x}{\varepsilon \pi \sqrt{\kappa^{p-1}}x^{p-1} + D_3x^{p-3} + \dots + D_{p-2}x^2 + 1},$$

where

$$\begin{aligned} x &= \sin u, & \rho &= n(\pi), \\ \kappa &= i\rho, & \varepsilon &= (-1)^{\frac{a+b-1}{2}} \sqrt{\kappa^{p-1}}. \end{aligned}$$

The coefficients  $A$ 's and  $D$ 's are all integers in  $k(\rho, i)$ , and divisible by  $\pi$ . Squaring both sides of this formula, we obtain

$$\sin^2 \pi u = \frac{x^{2p} + B_{p-1}x^{2(p-1)} + \dots + B_2x^4 + \pi^2 x^2}{\pi^2 x^{2(p-1)} + C_{p-2}x^{2(p-2)} + \dots + C_1x^2 + 1},$$

1) Weber: Algebra III, §. 158.

2) Weber: Algebra III, §. 167. In his original paper (Math. Ann., Vol. 50, p. 22), we find a necessary precaution against this point.

3) Fueter: Math. Ann., Vol. 75.

where  $B$ 's and  $C$ 's are integers in  $k(\rho)$ , and divisible by  $\pi$ . Introducing the relation

$$\mathfrak{k}(u) = \frac{1}{\sin^2 u} + \frac{1}{\rho-1},$$

and also remembering that

$$(\rho-1)^{\rho-1} \equiv 1 \pmod{\pi},$$

we find, after a few steps of transformation, that

$$(\rho-1)\mathfrak{k}(\pi u) = \frac{(\rho-1)^{\rho}\mathfrak{k}(u)^{\rho} + Q}{R+1}, \quad (26)$$

where  $Q$  and  $R$  are rational integral functions of  $\mathfrak{k}(u)$ , the coefficients being all integers in  $k(\rho)$  and divisible by  $\pi$ .

On the other hand, if we put

$$\tau(u) = \frac{(\rho-1)\mathfrak{k}(u)}{\sqrt[\rho]{4}},$$

we get, from §. 1 and §. 2, the formula of the form

$$\tau(\pi u) = \frac{y^{\rho} + a_3 y^{\rho-3} + \dots + a_{\rho-1} y}{\pi^2 y^{\rho-1} + b_4 y^{\rho-4} + \dots + \rho^{2b(a-b)}}, \quad y = \tau(u), \quad (27)$$

the coefficients  $a$ 's and the  $b$ 's being integers in  $k(\rho)$ .

We have already shewn (§. 3) that the  $b$ 's are all divisible by  $\pi$ . Now, comparing (27) with (26), we see that the  $a$ 's must also be divisible by  $\pi$ . It follows therefore that

$$\tau(\pi u)^{\rho} \equiv \tau(u)^{\rho\rho} \pmod{\pi}. \quad (28)$$

Hitherto we have supposed that  $b$  is even. But, if it be odd, we may use  $\rho\pi$  or  $\rho^2\pi$  instead of  $\pi$ : for

$$\begin{aligned} \rho\pi &= -b + (a-b)\rho, \\ \rho^2\pi &= -a + b - a\rho, \end{aligned}$$

and either  $a-b$  or  $a$  must certainly be even. Therefore the relation (28) holds good, even if  $b$  be odd.

This premised, we are going to shew that, if  $\mu$  be an integer in  $k(\rho)$ , and

$$u = \frac{\omega}{\mu},$$

then the relative corpus determined by  $\tau(u)^3$ , i.e. by  $\mathfrak{K}(u)^3$ , is the class-corpus corresponding to the group  $A$  of numbers  $a$ , such that

$$a \equiv \pm 1, \pm \rho, \pm \rho^2 \pmod{\mu},$$

where the *excludent* consists of all the prime factors of  $\mu$ .

The relative degree of  $K(\tau(u)^3)$  is not higher than  $\frac{m-1}{6}$ , where  $m$  is the norm of  $\mu$ . Hence, in proving the above statement, no generality will be lost, if we suppose that  $m > 7$ . Under this supposition it can easily be verified that the group  $A$  does not contain a divisor of 3.

As shewn in §. 3, if

$$\mu \simeq \pi'^a \quad \text{or} \quad (1+2\rho)\pi'^a,$$

$\pi'$  being a prime in  $k(\rho)$ , then the reciprocal of  $\tau(u)$  is an algebraic integer. In all other cases  $\tau(u)$  is itself an algebraic integer. At any rate, it follows from (27) or (28) that, if  $t$  be a primitive integer of the corpus  $K(\tau(u)^3)$ , and  $\mathfrak{p}$  any prime ideal factor of  $\pi$  in the same corpus, we get

$$t \equiv t' \pmod{\mathfrak{p}}, \quad (29)$$

supposing that  $\pi$  belongs to the group  $A$ . If  $\pi$  be a prime, which is relatively prime to the *excludent*, but does not belong to  $A$ , then the congruence (29) does not hold. For, since the discriminant of the equation for  $\tau(u)^3$  is not divisible by  $\mathfrak{p}$  (§. 5), we get

$$\tau(u)^{3p} \equiv \tau(\pi u)^3 \not\equiv \tau(u)^3 \pmod{\mathfrak{p}}.$$

Hence we see that the congruence (29) holds good, when and only when  $\mathfrak{p}$  is a prime ideal factor of  $\pi$ , where  $\pi$  is a prime integer of the first degree in  $k(\rho)$  belonging to the group  $A$ . But, this is the very condition, necessary and sufficient, in order that the corpus  $K(\tau(u)^3)$  may be the class-corpus corresponding to the group  $A$ . Our statement is thus proved.

Now, in general, if  $G$  be any group of numbers in an imaginary quadratic corpus, and  $E$  the group of algebraic unities in the same corpus, then the class-corpus corresponding to  $G$  is identical with that which corresponds to  $EG^{(1)}$ . Hence, for the sake of

simplicity, we shall hereafter characterise the group  $A$ , to which the class-corpus  $K(\tau(u)^3)$  corresponds, by the congruence

$$a \equiv 1 \pmod{\mu}.$$

It is also known<sup>1)</sup>, that the relative degree of the class-corpus corresponding to the group  $G$  is not lower than

$$d = \frac{(O, G)}{(EG, G)},$$

where  $O$  is the group of all the numbers in  $k(\rho)$  (of course, taking the *excludent* into consideration), and  $(O, G)$  and  $(EG, G)$  denote the indices of  $G$  with respect to  $O$  and  $EG$  respectively. If we put  $G=A$ , then

$$d = \frac{\varphi(\mu)}{6},$$

supposing that  $\mu$  is associated neither with 2 nor with  $1+2\rho$ . This value of  $d$  coincides with the degree of the equation for  $\tau(u)^3$ . Therefore the relative degree of  $K(\tau(u)^3)$  must be exactly equal to  $\frac{1}{6}\varphi(\mu)$ . When  $\mu$  is associated with 2 or  $1+2\rho$ , the relative degree reduces itself to unity.

---

Not only  $K(\tau(u)^3)$ , but also other division-corpora, e.g.  $K(\wp(u))$ ,  $K(\sin u)$ , etc., can be looked upon as class-corpora corresponding to some groups of numbers. But, as it is not at all necessary for our subsequent investigations, and moreover, as it will occupy too much space, we shall not here enter into a detailed discussion of them. However, it will not be out of place to give here the results I have arrived at.

---

1) Weber: Algebra III, §. 167.

Class-corpus	Group of Numbers	Ex- cludent	Relative Degree
$\left(u = \frac{\omega}{\mu}\right)$	$(a = a + b\rho)$		
$K(\tau(u)^3) = K(\wp(u)^3)$	$a \equiv 1 \pmod{\mu}$	$\mu$	$\frac{1}{6}\varphi(\mu)$
$K(\tau(u))$	$a \equiv 1 \pmod{\mu}, \quad b \equiv 0 \pmod{3}$	$3\mu$	$\begin{cases} \frac{1}{2}\varphi(\mu), & \text{when } \mu \not\equiv 0 \pmod{3} \\ \frac{1}{6}\varphi(\mu), & \text{when } \mu \equiv 0 \pmod{3} \end{cases}$
$K(\wp(u)) = K(\text{sn}^2 u)$	$a \equiv 1 \pmod{\mu}, \quad b \equiv 0 \pmod{2}$	$2\mu$	$\begin{cases} \frac{1}{2}\varphi(\mu), & \text{when } \mu \not\equiv 0 \pmod{2} \\ \frac{1}{6}\varphi(\mu), & \text{when } \mu \equiv 0 \pmod{2} \end{cases}$
$K(\kappa, \text{sn}^2 u)$ (Weber's division-corpus)	$a \equiv 1 \pmod{\mu}, \quad b \equiv 0 \pmod{4}$	$2\mu$	$\begin{cases} \varphi(\mu), & \text{when } \mu \not\equiv 0 \pmod{2} \\ \frac{1}{3}\varphi(\mu), & \text{when } \mu \equiv 2 \pmod{4} \\ \frac{1}{6}\varphi(\mu), & \text{when } \mu \equiv 0 \pmod{4} \end{cases}$
$K(\text{sn } u)$	$a \equiv 1 \pmod{\mu}, \quad b \equiv 0 \pmod{2},$ $a + b \equiv 1 \pmod{4}$	$2\mu$	$\varphi(\mu)$

## §. 18.

Hereafter, for the sake of simplicity, we shall denote the corpora  $K\left(\text{sn } \frac{\omega}{\mu}\right)$ ,  $K\left(\wp\left(\frac{\omega}{\mu}\right)\right)$ ,  $K\left(\wp\left(\frac{\omega}{\mu}\right)^3\right)$  by  $S(\mu)$ ,  $P(\mu)$ ,  $P^3(\mu)$  respectively.

As shewn in the preceding section,  $P^3(m)$  is the class-corpus corresponding to the group  $A$  of numbers  $a$ , such that

$$a \equiv 1 \pmod{m}.$$

On the other hand,  $K[m]$  is the class-corpus corresponding to the group  $B$  of numbers  $\beta$ , such that all these numbers  $\beta$  belong to the order  $[m]$  and satisfy the condition

$$n(\beta) \equiv 1 \pmod{m}.$$

Now, if we suppose that

$$a = a + b\rho \equiv 1 \pmod{m},$$

$a$  and  $b$  being rational integers, then taking the conjugate number, we get

$$a' = a + b\rho^2 \equiv 1 \pmod{m}.$$

Therefore

$$\left. \begin{aligned} n(a) = aa' &\equiv 1 \\ a - a' = b(\rho - \rho^2) &\equiv 0 \end{aligned} \right\} \pmod{m}.$$

From the latter congruence, it follows that  $b$  must be divisible by  $m$ . Hence we see that all the numbers of  $A$  are included in  $B$ ; symbolically we may write

$$B \supseteq A,$$

the sign  $\supseteq$  standing for “includes, as a proper divisor.” Therefore it follows that

$$P^2(m) \supseteq K[m].$$

Let  $H'$  be the relative degree of  $P^2(m)$  with respect to  $k(\rho)$ . In general,  $H'$  is equal to  $\frac{1}{6}\zeta(m)^{11}$ ,  $m$  being regarded as an integer in  $k(\rho)$ , not as a natural number. Hence, if

$$m = p_1^{h_1} p_2^{h_2} \cdots p_i^{h_i} \cdots,$$

where  $p_1, p_2, \dots, p_i, \dots$  are distinct natural primes, then

$$H' = \frac{1}{6} H p_i^{2(h_i-1)} (p_i-1) \left( p_i - \left( \frac{p_i}{3} \right) \right) = 2^{r+s-1} H;$$

the meanings of  $r$  and  $s$  are as in §. 16. The only exceptional case is when  $m=2$ , in which case we have

$$H' = H = 1.$$

Hence the equality

$$P^2(m) = K[m]$$

holds only in the following cases:

- (i)  $r=1, s=0$ ; i.e.  $m=p^k$ ,  $p$  being an odd prime,
- (ii)  $r=0, s=1$ ; i.e.  $m=4$ ,
- (iii)  $m=2$ .

Now, since the class-invariant  $j(\omega)$  can always be rationally



expressed by  $j(n\omega)$ ,  $n$  being any natural number, we get

$$P^3(m) \cong K[m] \cong K[p_1^{h_1}] K[p_2^{h_2}] \cdots K[p_i^{h_i}] \cdots, \quad (30)$$

where  $K[p_i^{h_i}] = P^3(p_i^{h_i})$ , in general,  
the only exception being

$$P^3(2^h) > K[2^h], \quad h > 2.$$

### §. 19.

Before proceeding further, let us insert here a few preliminary considerations.

1. Let  $C_1, C_2, \dots, C_h$  be absolutely or relatively cyclic corpora of degrees  $p^{a_1}, p^{a_2}, \dots, p^{a_h}$  respectively,  $p$  being a prime. We suppose that these corpora are independent of one another, i.e., we suppose that none of these corpora has common divisors with the corpus composed of all the others.

If we compose these cyclic corpora all together, we get an Abelian corpus of degree  $p^{a_1+a_2+\dots+a_h}$ , which we shall call  $A$ . The Galois' group of  $A$  must be of the form

$$S_1^{e_1} S_2^{e_2} \cdots S_i^{e_i} \cdots S_h^{e_h}, \quad \begin{matrix} e_i = 0, 1, 2, \dots, p^{a_i}-1. \\ (i = 1, 2, \dots, h) \end{matrix}$$

Here  $S_i$  denotes a substitution, by which all the numbers in  $C_i$  are changed into their conjugate numbers, while those of other  $C$ 's remain unchanged. We may express this fact by saying that the corpus

$$C_1 C_2 \cdots C_{i-1} C_{i+1} \cdots C_h$$

*belongs to* the cyclic group

$$S_i^{e_i}, \quad e_i = 0, 1, 2, \dots, p^{a_i}-1.$$

Now, let  $C'_i$  be the divisor of  $C_i$  of degree  $p^{a_i-1}$ , then the Abelian corpus

$$C'_1 C'_2 \cdots C'_i \cdots C'_h$$

belongs to the group of the form

$$S_1^{c_1} S_2^{c_2} \cdots S_i^{c_i} \cdots S_h^{c_h}, \quad \begin{matrix} S'_i = S_i^{p^{a_i-1}} \\ c_i = 0, 1, 2, \dots, p-1, \end{matrix} \quad (i = 1, 2, \dots, h).$$

All the cyclic subgroups of this Abelian group are of the form

$$(S_1^{a_1} S_2^{a_2} \dots S_i^{a_i} \dots S_h^{a_h})^e, \quad e = 0, 1, 2, \dots, p-1,$$

where  $a_1, a_2, \dots, a_i, \dots, a_h$  are some fixed integers for each subgroup. Each of these  $a$ 's can take  $p$  values:  $0, 1, 2, \dots, p-1$ . Hence there are  $(p-1)^{h-1}$  special cyclic subgroups, in which all of these  $a$ 's are different from zero. If we denote by  $B$  a divisor of  $A$  belonging to one of these special cyclic subgroups, then  $B$  must possess the following properties:

- (i)  $A > B \cong C'_1 C'_2 \dots C'_h$ ,
- (ii)  $A$  is of the  $p$ th relative degree with respect to  $B$ .
- (iii) none of the original cyclic corpora  $C_1, C_2, \dots, C_h$  is contained in  $B$  completely.

It can easily be seen that these three properties are characteristic of  $B$ .

Let us call  $B$  a *derived corpus* of  $C'_1, C'_2, \dots, C'_h$ . There are in all  $(p-1)^{h-1}$  different derived corpora. In particular, when  $p=2$ , the derived corpus is uniquely determinate.

II. Let there be systems of cyclic corpora

$$\left. \begin{array}{l} C_1, C_2, \dots, \\ D_1, D_2, \dots, \\ \dots\dots\dots \\ E_1, E_2, \dots, \\ S_1, S_2, \dots, \\ T_1, T_2, \dots, \\ \dots\dots\dots \end{array} \right\} \text{of degrees} \left\{ \begin{array}{l} p^{c_1}, p^{c_2}, \dots, \\ q^{d_1}, q^{d_2}, \dots, \\ \dots\dots\dots \\ r^{e_1}, r^{e_2}, \dots, \\ u^{s_1}, u^{s_2}, \dots, \\ v^{t_1}, v^{t_2}, \dots, \\ \dots\dots\dots \end{array} \right.$$

respectively, where  $p, q, \dots, r, u, v, \dots$  are all primes. Suppose that these corpora are independent of one another, and that  $p, q, \dots, r$  are all different from one another, but not necessarily all different from  $u, v, \dots$ . Composing these corpora all together, we obtain an Abelian corpus, which we shall call  $A$ .

Now, let

$$C'_1, C'_2, \dots, D'_1, D'_2, \dots, E'_1, E'_2, \dots$$

be the divisors of

$$C_1, C_2, \dots, D_1, D_2, \dots, E_1, E_2, \dots,$$

of degrees

$$p^{c_1-1}, p^{c_2-1}, \dots, q^{d_1-1}, q^{d_2-1}, \dots, \dots, r^{e_1-1}, r^{e_2-1}, \dots$$

respectively; and let  $B$  be a divisor of  $A$ , such that

- (i)  $A > B > C'_1 C'_2 \dots D'_1 D'_2 \dots E'_1 E'_2 \dots S_1 S_2 \dots T_1 T_2 \dots$ ,
- (ii) the relative degree of  $A$  with respect to  $B$  is  $p q \dots r$ ,
- (iii)  $B$  does not contain any one of  $C_1, C_2, \dots, D_1, D_2, \dots, \dots, E_1, E_2, \dots$  completely.

Then it can easily be seen that this corpus  $B$  must be composed of the following corpora:

a derived corpus of  $C_1, C_2, \dots$ ,

a derived corpus of  $D_1, D_2, \dots$ ,

.....

a derived corpus of  $E_1, E_2, \dots$ ,

$S_1, S_2, \dots$ ,

$T_1, T_2, \dots$ ,

.....

## §. 20.

Let  $m$  be a natural number, such that

$$m = \pi_1^{a_1} \pi_2^{a_2} \dots,$$

where  $\pi_1, \pi_2, \dots$  are distinct primes in the corpus  $k(\rho)$ . Then

$$S(m) = S(\pi_1^{a_1}) S(\pi_2^{a_2}) \dots.$$

The relative degree of  $S(\pi_i^{a_i})$ ,  $i = 1, 2, \dots$ , is

$$\zeta(\pi_i^{a_i}), \quad \text{when } \pi_i \text{ is odd,}$$

$$\frac{1}{3}\zeta(\pi_i^{a_i}), \quad \text{when } \pi_i = 2.$$

Therefore the relative degree of  $S(m)$  is

$$\zeta(m), \quad \text{when } m \text{ is odd,}$$

$$\frac{1}{3}\zeta(m), \quad \text{when } m \text{ is even.}$$

Now, it is evident that

$$S(m) \cong P(m) \cong P^3(m),$$

and  $S(m)$  is at most relatively quadratic with respect to  $P(m)$ , and  $P(m)$  at most relatively cubic with respect to  $P^3(m)$ . But the relative degree of  $P^3(m)$  is in general  $\frac{1}{6}\varphi(m)$ , the only exceptional case being when  $m=2$ . Hence, when  $m$  is odd, the relative degree of  $P(m)$  must be  $\frac{1}{2}\varphi(m)$ . When  $m$  is even, the relative degree of  $P(m)$  must be either  $\frac{1}{3}\varphi(m)$  or  $\frac{1}{6}\varphi(m)$ . But, since  $P(m)$  cannot be relatively quadratic with respect to  $P^3(m)$ , the value  $\frac{1}{3}\varphi(m)$  is inadmissible. Hence  $P(m)$  is of relative degree  $\frac{1}{6}\varphi(m)$ , and consequently coincides with  $P^3(m)$ , provided that  $m$  be even.

Between the three kinds of division-corpora  $S$ ,  $P$ ,  $P^3$ , there exist the relations:

$$\left. \begin{aligned} S(m) &= S(\pi_1^{a_1}) S(\pi_2^{a_2}) \cdots, \\ S(m) &\cong P(m) \cong P(\pi_1^{a_1}) P(\pi_2^{a_2}) \cdots, \\ P(m) &\cong P^3(m) \cong P^3(\pi_1^{a_1}) P^3(\pi_2^{a_2}) \cdots, \end{aligned} \right\} \quad (31)$$

If we decompose  $S(\pi_i^{a_i})$ ,  $i=1, 2, \cdots$ , into elementary corpora, we get the components of the following types:

$$\left. \begin{aligned} \text{(i)} \quad & \text{I}_i, \text{II}_i, \text{III}_i, \text{IV}_i, \text{V}_i, & \text{when } \pi_i \neq 1+2\rho, \pi_i \neq 2, a_i \geq 1, \\ & \text{VIII}_i, & a_i = 1, \\ \text{(ii)} \quad & \text{VII}_i, & \text{when } \pi_i = 1+2\rho, a_i \geq 1, \\ & \text{VI}_i, & a_i = 1, \\ & \text{IX}_i, & a_i \geq 2, \\ \text{(iii)} \quad & \text{X}_i, & \text{when } \pi_i = 2, a_i \geq 1. \end{aligned} \right\} \quad (32)$$

The suffix  $i$  is attached to the components in (i) to make clear their dependency upon  $\pi_i$ .

The corpus  $P(\pi_i^{a_i})$ ,  $\pi_i$  being an odd prime, can be decomposed into two components (cf. §. 9.). The one is of relative degree  $\frac{1}{2}\varphi(\pi_i)$ , and is no other than  $P(\pi_i)$ ; the other is of relative degree  $\pi_i(\pi_i)^{a_i-1}$ , and its relative discriminant is a power of  $\pi_i$ . The former is a divisor of  $S(\pi_i)$ ; and the latter is a corpus composed of  $\text{VIII}_i$  or  $\text{IX}$  or  $\text{X}$ . Hence, if we decompose  $P(\pi_i^{a_i})$  into elementary corpora, we get:

$$\left. \begin{array}{ll} \text{(i)} & \text{I}_\rho, \text{ II}_\rho, \text{ III}_\rho, \text{ IV}_\rho, \quad \text{when } \pi_i \neq 1+2\rho, \pi_i \neq 2, a_i \geq 1, \\ & \text{VIII}_\rho, \quad a_i > 1, \\ \text{(ii)} & \text{VI}, \quad \text{when } \pi_i = 1+2\rho, \quad a_i > 1, \\ & \text{IX}, \quad a_i > 2, \\ \text{(iii)} & \text{X}, \quad \text{when } \pi_i = 2, \quad a_i > 1, \end{array} \right\} (33)$$

These premised, let us now consider the relation between  $P(m)$  and the elementary corpora. In virtue of (31), we see that the elementary corpora given in (33) are certainly contained in  $P(m)$ . But, as for the corpora  $V_i$  and VII, which are contained in (32), but not in (33), we have to make a further investigation.

To begin with, suppose that  $m$  is odd. In this case, both  $V_i$  and VII can never be contained in  $P(m)$ . For, if  $V_1$  be contained in  $P(m)$ , the number  $\text{sn}\left(\frac{\omega}{\pi_1}\right)$ , and consequently also  $\wp'\left(\frac{\omega}{\pi_1}\right)$ , must be contained in  $P(m)$ . Then, from the formula

$$\wp(u+v) - \wp(u-v) = - \frac{\wp'(u)\wp'(v)}{\{\wp(u) - \wp(v)\}^2},$$

it follows that  $P(m)$  must contain the number  $\wp'\left(\frac{\omega}{\pi_2, \dots, \dots}\right)$ , and consequently also  $\text{sn}\left(\frac{\omega}{\pi_2, \dots, \dots}\right)$ . But, in terms of this last number,

all the numbers  $\text{sn}\left(\frac{\omega}{\pi_i}\right)$ ,  $i = 2, 3, \dots$ , can be rationally expressed.

It follows, therefore, that  $P(m)$  contains all the corpora  $V_i$ ,  $i = 1, 2, \dots$ , and VII. Then  $P(m)$  would coincide with  $S(m)$ ; which is impossible. Similar reasoning applies also to  $V_2, V_3, \dots$  and VII.

Hence, making use of the lemma given in the last section, we see that the corpus  $P(m)$  must be composed of the following components:

$$\left. \begin{array}{ll} \text{(i)} & \text{I}_\rho, \text{ II}_\rho, \text{ III}_\rho, \text{ IV}_\rho, \quad i = 1, 2, \dots, \text{ excepting the value,} \\ & \quad \text{for which } \pi_i = 1+2\rho, \\ & \text{VIII}_\rho, \quad \text{when } m \equiv 0 \pmod{\pi_i^2}, \\ \text{(ii)} & \text{VI}, \quad \text{when } m \equiv 0 \pmod{3}, \\ & \text{IX}, \quad \text{when } m \equiv 0 \pmod{3^2}, \\ \text{(iii)} & \text{the derived corpus of } V_i (i = 1, 2, \dots; V_i = \text{VII, if } \pi_i = 1+2\rho). \end{array} \right\} (34)$$

If  $m$  be even, but not divisible by 4, the relative degree of  $P(m)$  is equal to that of  $P\left(\frac{m}{2}\right)$ . Hence

$$P(m) = P\left(\frac{m}{2}\right),$$

all the components of which are given in (34).

Next, let  $m$  be divisible by 4. In this case, one or more  $X$ 's may be contained in  $P(m)$ . Composing these  $X$ 's all together, we obtain a relatively Abelian corpus, which we shall call  $X_p$ . Similarly, composing all the  $X$ 's contained in  $S(m)$ , we obtain an Abelian corpus  $X_s$ . It is evident that  $X_p$  is a divisor of  $X_s$ . But,  $X_p$  can never coincide with  $X_s$ . For, if  $X_p = X_s$ , then  $P(m)$  must contain  $sn\left(\frac{m}{2^a}\right)$ , where  $2^a$  is the highest power of 2 contained in  $m$ . That this is impossible can be shown by exactly the same reasoning as we have done for  $V_i$  and VII in the above.

It must be remarked, however, that the same proof does no longer hold for  $V_i$  and VII in the present case, since the assumption that  $\pi_2, \pi_3, \dots$  are all odd is essential in that proof. In fact, both  $V_i$  and VII are completely contained in  $P(m)$ . For, since  $X_p < X_s$ , the relative degree of  $X_p$  is at most half that of  $X_s$ . But, since  $S(m)$  is relatively quadratic with respect to  $P(m)$ , it follows that the relative degree of  $X_p$  must be exactly half that of  $X_s$ , and all the other elementary corpora in  $S(m)$  must be completely contained in  $P(m)$ . Thus we see that  $P(m)$  is composed of

$$\left. \begin{array}{ll} \text{(i)} & \text{I, II, III, IV, V, } i=1, 2, \dots, \text{ excepting the values,} \\ & \text{for which } \pi_i = 1 + 2\rho \text{ or } 2, \\ & \text{VIII,} \\ & \text{when } m \equiv 0 \pmod{\pi_i^2}, \\ \text{(ii)} & \text{VI, VII,} \\ & \text{when } m \equiv 0 \pmod{3}, \\ & \text{IX,} \\ & \text{when } m \equiv 0 \pmod{3^2}, \\ \text{(iii)} & \text{X.} \end{array} \right\} \quad (35)$$

Now, from (34) and (35), the following conclusions can be deduced.

*All the elementary corpora are included in the division-corpora  $P(m)$ , if  $m$  be made to assume all the positive integral values, or at*

least all the integers of the form  $4p^h$ , where  $p$  is a natural prime (the case  $p=2$  being included).

Therefore all the relatively Abelian corpora with respect to  $k(p)$  are exhausted by the division-corpora  $P^3(m)$ , and consequently also by Weber's division-corpora.

When  $m$  is odd, the relative discriminant of  $P^3(m)$  does not contain the factor 2 (§. 5). Therefore  $P^3(m)$  cannot contain the elementary corpora III, V, VI, VII. Hence we see that  $P^3(m)$ ,  $m$  being odd, is composed of

- (i)  $I_i, II_i, IV_i, \dots, \text{excepting the value,}$   
 $VIII_i, \text{for which } \pi_i = 1+2\rho,$   
 $\text{when } m \equiv 0 \pmod{\pi_i^2},$
- (ii)  $IX, \text{when } m \equiv 0 \pmod{3^2},$
- (iii) a derived corpus of  $III_i$  ( $i=1, 2, \dots$ ;  $III_i=VI$ , if  $\pi_i = 1+2\rho$ ),
- (iv) the derived corpus of  $V_i$  ( $i=1, 2, \dots$ ;  $V_i=VII$ , if  $\pi_i = 1+2\rho$ ).

But, as we have remarked before, the corpus  $P^3(m)$ , when  $m$  is even, coincides with  $P(m)$ , whose constitution is given in (34) and (35).

Therefore we conclude that

*the relatively Abelian corpora with respect to  $k(p)$  are exhausted also by the division-corpora  $P^3(m)$ .*

## §. 21.

Let us now proceed a step further and consider the constitution of the *strahl*-corpus  $K[m]$ .

As we have shewn in §. 18,

$$K[p^h] = P^3(p^h),$$

when  $p$  is an odd prime, or when  $p=2$ ,  $h=1, 2$ . In other cases, in which  $p=2$ ,  $h>2$ , the corpus  $P^3(2^h)$  is relatively quadratic with respect to  $K[2^h]$ .

Hence, if we remember the relation (30) and the value of the relative degree  $H$ , the decomposition of  $K[m]$  into elementary corpora can be effected by §. 19 without any difficulty.

When  $m$  is odd, the components are

- (i)  $I, II, IV_i, \quad i=1, 2, \dots, \text{ excepting the value,}$   
 $\quad \quad \quad \quad \quad \quad \quad \quad \text{for which } \pi_j = 1+2\rho,$   
 $\quad \quad \quad \quad \quad \quad \quad \quad \text{when } m \equiv 0 \pmod{\pi_i^2},$
- (ii)  $IX, \quad \quad \quad \text{when } m \equiv 0 \pmod{3^2},$
- (iii) a derived corpus of  $III_i$  ( $i=1, 2, \dots$ ;  $III_i=VI$ , if  $\pi_i = 1+2\rho$ ).

When  $m$  is even, but not divisible by 4, we get

- (i) (ii)  $\quad \quad \quad \text{as above,}$
- (iii)  $III_i, \quad i=1, 2, \dots, \text{ excepting the values,}$   
 $\quad \quad \quad \text{for which } \pi_i = 2 \text{ or } 1+2\rho,$   
 $\quad \quad \quad VI, \quad \quad \quad \text{when } m \equiv 0 \pmod{3}.$

When  $m$  divisible by 4, we get

- (i) (ii) (iii)  $\quad \text{as above,}$
- (iv)  $X.$

Observe that, in these lists, we miss two kinds of elementary corpora, viz. V and VII.

But, is it not possible that the corpus V or VII is contained in the whole corpus  $K[m]$ ? We are now going to shew that it is impossible. We shall, however, confine ourselves to the proof that  $V_1$  is not contained in  $K(m)$ . The same reasoning also applies to other V's and VII.

Decompose  $K[m]$  into elementary corpora as above. Then, reject  $IV_1$  from the components thus obtained, and recompose all the rest. We obtain a relatively Abelian corpus, which we shall call  $K'$ . Now, after the rejection of  $IV_1$  from the components of  $K[m]$ , there may be still some elementary corpora, whose relative degrees are powers of 2; viz.  $IV_i$ ,  $i=2, 3, \dots$ , or some X's, if  $m$  be even. Composing these elementary corpora all together, we obtain a divisor of  $K'$ . We shall call it  $K''$ . Then, every divisor of  $K'$  having a power of 2 as its relative degree must necessarily be a divisor of  $K''$ ; consequently its relative discriminant cannot contain the factor  $\pi_1$ . It follows therefore that  $K'$  is relatively prime to  $V_1$ . Hence, if we compose  $V_1$  with  $K'$ , we obtain a relatively



Abelian corpus, whose relative degree is evidently twice that of  $K[m]$ . Therefore

$$V_1 K[m] = V_1 K' \supset K[m],$$

which shews that  $V_1$  is not a divisor of  $K[m]$ .

Thus we are led to the following important conclusions:

*Relatively Abelian corpora with respect to  $k(p)$  are not exhausted by strahl-corpora.*

*If  $p$  be an odd prime in  $k(p)$ ,  $m$  its norm, and if  $2^h$  be the highest power of 2 contained in  $m-1$ , then the relatively cyclic corpus of relative degree  $2^h$  contained in the division-corpus  $S(p)$  can never be contained in a strahl-corpus.*

Now, in §. 14 and §. 15, we have given a method of finding a corpus composed of elementary corpora only, such that any given relatively Abelian corpus may be a divisor of it. In that method, V and VII are used only in the case when the relative degree of the given corpus is even. Hence we see that

*relatively Abelian corpora of odd relative degree with respect to  $k(p)$  are exhausted by strahl-corpora.*

## §. 22.

According to Fueter,<sup>1)</sup> all the prime factors of the relative discriminant of  $K[m]$  must be contained in  $m$ ; and conversely, all the prime factors of  $m$  must, in general, be contained in the relative discriminant of  $K[m]$ . The only exceptional case is when  $m$  is divisible by 3, but not by  $3^2$ ; in this case, the relative discriminant of  $K[m]$  does not contain the factor 3.

But, I think, this is not quite correct. In the first place, the most obvious exceptional case  $m=2$  is not noticed in the above statement. Secondly, his so-called exceptional case is not necessarily exceptional. For example, take the value  $m=6$ , then

$$j(6\rho) = j(-3+3\sqrt{-3}) = j(\sqrt{-27}).$$

But, we know that

$$j(\sqrt{-27})^3 = 2x,$$

where  $x^3 - 3x^2 - 3x - 1 = 0$ ,<sup>2)</sup> i.e.  $x = 1 + \sqrt[3]{2} + \sqrt[3]{4}$ .

1) Fueter: Math. Ann., Vol. 75.

2) Weber: Algebra III, p. 722.

Hence  $K[6]$  is nothing else but the elementary corpus VI, whose relative discriminant is divisible by 3.

Let us now determine the nature of the relative discriminant of  $K[m]$ , as a sequel to our preceding investigations.

If we assume, as in §. 18, that

$$m = p_1^{h_1} p_2^{h_2} \cdots p_i^{h_i} \cdots,$$

then we have

$$K[m] \cong K[p_1^{h_1}] K[p_2^{h_2}] \cdots K[p_i^{h_i}] \cdots,$$

$$\text{where} \quad K[p_i^{h_i}] = P^3(p_i^{h_i}), \quad \text{if } p_i \neq 2 \text{ or } p_i = 2, h_i = 1, 2,$$

$$\text{and} \quad P^3(2^{h_i}) > K[2^{h_i}] > P^3(2^{h_i-1}), \quad \text{if } h_i > 2.$$

But, the relative discriminant of  $P^3(p_i^{h_i})$  is a power of  $p_i$ , except when  $p_i^{h_i} = 2$  or 3. Hence the relative discriminant of  $K[m]$  must contain all the prime factors of  $m$ , except in the following cases :

$$(i) \quad m \equiv 0 \pmod{2}, \text{ but } \not\equiv 0 \pmod{2^2},$$

$$(ii) \quad m \equiv 0 \pmod{3}, \text{ but } \not\equiv 0 \pmod{3^2}.$$

On the other hand, since

$$P^3(m) \cong K[m],$$

we see that the relative discriminant of  $K[m]$  does not contain prime factors relatively prime to  $m$ . Thus, if we exclude the above two cases (i) and (ii), we may conclude that the relative discriminant of  $K[m]$  contains all the prime factors of  $m$ , but no other.

In case (i), since  $m$  is divisible by 2, the corpus  $K[m]$  contains the elementary corpus III or VI (§. 21), except when  $m=2$ . Therefore its relative discriminant must contain the factor 2. Thus we see that this case (i) need not be excluded from the above statement, provided that  $m \neq 2$ .

Next, consider the case (ii), and suppose that  $m \neq 3$ . If  $m$  be even, then  $K[m]$  contains VI, and consequently its relative discriminant is divisible by 3.

If, on the contrary,  $m$  be odd, then  $K[m]$  does not contain VI itself, but a derived corpus of III<sub>*i*</sub> ( $i=1, 2, \dots, p_i \neq 3$ ) and VI. Hence we have to inquire, whether the relative discriminant of

this derived corpus is divisible by 3 or not.

Without losing generality, we may suppose  $p_1 \neq 3$ . Let  $C$  be a relatively cubic divisor of  $\text{III}_1$ . There are two different derived corpora of  $C$  and VI. At least one of these derived corpora is certainly a divisor of  $K[m]$ . Let us call it  $D$ . If the relative discriminant of  $K[m]$  were relatively prime to 3, so would also be that of  $D$ . Moreover, since  $m$  is odd, this relative discriminant cannot contain the factor 2. Hence  $D$  would be a relatively cyclic, cubic corpus different from  $C$ , with the relative discriminant, a power of  $p_1$ , provided that the relative discriminant of  $K[m]$  is relatively prime to 3.

But, this is evidently impossible, if  $C$  be a proper divisor of  $\text{III}_1$ . For, if  $C$  does not coincide with  $\text{III}_1$ , then the relative discriminant of  $C$  must be a power of  $p_1$ , without containing the factor 2, and consequently it can be proved that  $D$  cannot be different from  $C$ .<sup>1)</sup>

If  $C = \text{III}_1$ , then the relative discriminant of  $C$  is divisible by 2. Compose  $C$  with  $D$ , and consider the corpus of inertia of a prime ideal contained in  $p_1$ . This corpus of inertia must be relatively cyclic, and its relative discriminant must be a power of 2. Also, since  $D$  is not identical with  $C$ , this corpus of inertia cannot reduce itself to  $k(\rho)$  (cf. §. 14). Therefore it must be relatively cubic. But, we can shew, as follows, that this is again impossible.

We know that every relatively cyclic, cubic corpus, with respect to  $k(\rho)$ , can be obtained by adjoining to  $k(\rho)$  a cube root of a certain integer in  $k(\rho)$ . Hence, if there be a relatively cyclic corpus of the third relative degree, whose relative discriminant does not contain any other prime than 2, it must be one of the forms

$$\begin{aligned} (a) \quad & K(\sqrt[3]{2\varepsilon}), \\ (b) \quad & K(\sqrt[3]{\varepsilon}), \end{aligned} \quad \varepsilon = 1, \rho, \rho^2.$$

In the corpus (a), however, the following decomposition holds:

$$\begin{aligned} 1+2\varepsilon &= (1+\sqrt[3]{2\varepsilon})(\rho+\sqrt[3]{2\varepsilon})(\rho^2+\sqrt[3]{2\varepsilon}) \\ &\simeq (1+\sqrt[3]{2\varepsilon})^3. \end{aligned}$$

---

1) Takagi: loc. cit., §. 10.

Hence the relative discriminant of this corpus must contain the factor  $1+2\epsilon$ . The relative discriminant of the corpus ( $b$ ) does not contain the factor 2, since the discriminant of the equation

$$x^3 - \epsilon = 0$$

is  $-27\epsilon^2$ . Thus we see that there can be no relatively cyclic, cubic corpus, whose relative discriminant is a power of 2, Q. E. D.

The relative discriminant of  $K[m]$  must therefore be divisible by 3, when  $m$  is divisible by 3, provided that  $m \neq 3$ .

Thus we arrive at the following conclusion.

*All the prime factors of the relative discriminant of  $K[m]$  are contained in  $m$ ; and conversely, all the prime factors of  $m$  enter into the relative discriminant of  $K[m]$ , except when  $m=2$  or 3.*

In the two exceptional cases,  $K[m]$  coincides with the fundamental corpus  $k(\rho)$ .

Nagoya, November 1915.

## Numerical Calculation of the Jacobian Ellipsoids.

By

**Ryosuke KAIBARA**, *Rigakushi*.

*Professor of Physics, Imperial Peers' College, Tokyo.*

1. The Jacobian ellipsoid, or the ellipsoidal figure of equilibrium of a rotating mass of homogeneous fluid, was first calculated numerically by Darwin<sup>1)</sup> for the whole range of the ratios of axes and angular velocity. In a previous paper,<sup>2)</sup> I solved the same problem by a different method of treatment, and then interpolated values which I intended to compare with those given in Darwin's table. In his *Scientific Papers*,<sup>3)</sup> Darwin has recomputed a part of his table, and pointed out the discrepancy between his results and mine; he has also given an evidence for the incorrectness of some of the interpolated values. The discrepancy is, in general, very small, but in a few of the results, it amounts to several units of the third decimal place. These considerable discrepancies occur in those values, for which, by the nature of the method I adopted, the calculation was the most tedious, and an inaccuracy in the interpolations of the order mentioned was therefore unavoidable. It may be remarked, however, that a majority of my results agree better with Darwin's corrected values than with his original ones.

More accurate results on this subject being desirable, I have greatly modified the method so as to remove its imperfection in the previous paper as far as possible, and have repeated the whole calculation.<sup>4)</sup> In the following paragraphs, this improved method will be explained and tables of numerical results added.

---

1) G. H. Darwin, *Proc. Roy. Soc. London*, 41 (1887), p. 319.

2) R. Kaibara, *Proc. Tokyo Math.-Phys. Soc.*, 4 (1907), p. 98.

3) G. H. Darwin, *Scientific Papers*, 3 (1910), p. 130.

4) Some of my notations in the former paper are also altered to conform to those usually adopted.

2. Let  $a, b, c$  ( $a > b > c$ ) be the semi-axes of the ellipsoid,  $\sigma$ , its density, and  $\omega$ , the angular velocity (about the axis  $c$ ); then, if we write

$$P = abc \int_0^\infty \frac{ds}{(a^2+s)J} ,$$

$$Q = abc \int_0^\infty \frac{ds}{(b^2+s)J} ,$$

$$R = abc \int_0^\infty \frac{ds}{(c^2+s)J} ,$$

where

$$J = \sqrt{(a^2+s)(b^2+s)(c^2+s)},$$

the condition for the equilibrium of the ellipsoid is expressed by the well-known equations:

$$a^2(P-Q) = b^2(Q-R) = c^2R, \quad (1)$$

where

$$Q = -\frac{\omega^2}{2\pi\sigma}.$$

From these equations, we get

$$P-Q + \left( \frac{c^2}{b^2} - \frac{c^2}{a^2} \right) R = 0; \quad (2)$$

this represents the relation to be fulfilled by the axes  $a, b, c$ .

For the sake of brevity, we shall denote the ratios of axes and eccentricities of the principal sections thus:—

$$\left. \begin{aligned} \rho_1 &= \frac{c}{a}, & \varepsilon_1 &= \frac{\sqrt{a^2-c^2}}{a}, \\ \rho_2 &= \frac{c}{b}, & \varepsilon_2 &= \frac{\sqrt{b^2-c^2}}{b}, \\ \rho_3 &= \frac{b}{a}, & \varepsilon_3 &= \frac{\sqrt{a^2-b^2}}{a}. \end{aligned} \right\} \quad (3)$$

It can be easily proved that  $P, Q, R$  satisfy the identities:

$$\left. \begin{aligned} P+Q+R &= 2, \\ a^2P+b^2Q+c^2R &= S. \end{aligned} \right\} \quad (4)$$

where

$$S = abc \int_0^\infty \frac{ds}{J}.$$

By combining (4) with (1), various forms of expression can be

obtained for the angular velocity, of which the following two will be utilised hereafter:<sup>1)</sup>

$$\Omega = \frac{(1 + \rho_1^2 + \rho_2^2)Sa^{-2} - 6\rho_1^2}{1 + \rho_2^2 + \rho_3^2 + \rho_1^2\rho_3^2 - 4\rho_1^2}, \quad (5)$$

and 
$$\Omega = \frac{(1 + \rho_1^2 + \rho_2^2)P - 2\rho_1^2}{1 - \rho_1^2 + \rho_2^2}. \quad (6)$$

Let  $\mu$ ,  $e$ ,  $i$  be the quantities which measure the moment of momentum  $M$ , the kinetic energy  $E$ , and the intrinsic energy  $I$  respectively of the ellipsoid, and which are defined according to Darwin thus:—

Writing  $m$  for the whole mass of the ellipsoid, we have

$$M = \frac{1}{5} m(a^2 + b^2)\omega;$$

this we put equal to

$$m^{\frac{3}{2}}(abc)^{\frac{1}{6}}\mu,$$

so that

$$\mu = \frac{\sqrt{6}}{10}(\rho_1\rho_3)^{-\frac{3}{2}}(1 + \rho_3^2)\sqrt{\Omega}. \quad (7)$$

Again,

$$E = \frac{1}{2}\omega M = m^2(abc)^{-\frac{1}{2}}e,$$

where

$$e = \frac{\sqrt{6}}{4}\mu\sqrt{\Omega}. \quad (8)$$

Lastly, if  $V$  be the potential of the ellipsoid at an internal point, and  $dv$ , an element of its volume, then

$$\begin{aligned} I &= -\frac{1}{2}\int V\sigma dv \\ &= -\frac{1}{2}\pi\sigma^2 \left[ S\int dv - P\int x^2 dv - Q\int y^2 dv - R\int z^2 dv \right], \end{aligned}$$

or, evaluating the integrals and introducing (4), we find

$$I = -\frac{2}{5}\pi\sigma m S = m^2(abc)^{-\frac{1}{2}}.(i-1),$$

1) In the previous paper,  $\Omega$  was calculated from an equation deduced from

$$\Omega = 1 - \frac{1}{2}(1 + \rho_1^2 + \rho_2^2)R.$$

But I have found that the two forms in the text, though less simple, are more suitable for obtaining accurate numerical results.

where 
$$i = 1 - \frac{3}{10}(\rho_1 \rho_3)^{-\frac{2}{3}} S a^{-2}. \quad (9)$$

The problem now is to reduce equation (2) into a form which is numerically soluble, and with its solutions, to determine systems of values for  $\rho$ 's,  $\varepsilon$ 's,  $Q$ ,  $\mu$ ,  $e$ , and  $i$ .

3. First, the integrals  $P$ ,  $Q$ ,  $R$ ,  $S$  must be evaluated. Put

$$a^2 + s = \lambda^2(\xi w - e_3),$$

$$b^2 + s = \lambda^2(\xi w - e_2),$$

$$c^2 + s = \lambda^2(\xi w - e_1),$$

and let  $s = 0$  correspond to  $w = u$ , so that

$$\left. \begin{aligned} a^2 &= \lambda^2(\xi u - e_3), \\ b^2 &= \lambda^2(\xi u - e_2), \\ c^2 &= \lambda^2(\xi u - e_1); \end{aligned} \right\} \quad (10)$$

then we have

$$P = -\xi' u \int_0^u \frac{dw}{\xi w - e_3} = \frac{\xi' u}{(e_1 - e_3)(e_2 - e_3)} \left\{ \frac{\sigma_3' u}{\sigma_3 u} + e_3 u \right\}.$$

This result may be expressed in terms of  $\vartheta$ -functions<sup>1)</sup> with argument  $v = u/2\omega$ , and modulus  $\tau = \omega'/\omega$ , thus:

$$\left. \begin{aligned} P &= \frac{\vartheta_1(2v)}{\vartheta_1' \vartheta_1^3(v)} \vartheta_0^4 \left\{ \frac{\vartheta_0''}{\vartheta_0} \cdot v - \frac{\vartheta_0'(v)}{\vartheta_0(v)} \right\}, \\ Q &= -\frac{\vartheta_1(2v)}{\vartheta_1' \vartheta_1^3(v)} \vartheta_3^4 \left\{ \frac{\vartheta_3''}{\vartheta_3} \cdot v - \frac{\vartheta_3'(v)}{\vartheta_3(v)} \right\}, \\ R &= \frac{\vartheta_1(2v)}{\vartheta_1' \vartheta_1^3(v)} \vartheta_2^4 \left\{ \frac{\vartheta_2''}{\vartheta_2} \cdot v - \frac{\vartheta_2'(v)}{\vartheta_2(v)} \right\}; \end{aligned} \right\} \quad (11)$$

and 
$$S a^{-2} = \frac{\vartheta_0^2 \vartheta_2(v) \vartheta_3(v)}{\vartheta_0(v) \vartheta_1(v)} \cdot 2\pi v. \quad (12)$$

By means of (10), the ratios of axes and eccentricities may be written

$$\rho_1 = \frac{\sigma_1 u}{\sigma_3 u} = \frac{\vartheta_0 \vartheta_2(v)}{\vartheta_2 \vartheta_0(v)}, \quad \varepsilon_1 = \sqrt{e_1 - e_3} \frac{\sigma u}{\sigma_3 u} = \frac{\vartheta_3 \vartheta_1(v)}{\vartheta_2 \vartheta_0(v)}, \quad (13)$$

1) The notation here adopted for the functions is in accordance with that given in Weierstrass-Schwarz, Formeln u. Lehrsätze zum Gebrauche d. ellip. Funktionen. Formule in that book are used throughout this paper.



$$\left. \begin{aligned} \rho_2 &= \frac{\sigma_2 u}{\sigma_2 u} = \frac{\partial_2 \partial_2(r)}{\partial_2 \partial_2(r)}, & \varepsilon_2 &= \sqrt{e_1 - e_2} \frac{\sigma u}{\sigma_2 u} = \frac{\partial_0 \partial_1(r)}{\partial_2 \partial_3(r)}, \\ \rho_3 &= \frac{\sigma_3 u}{\sigma_3 u} = \frac{\partial_0 \partial_3(r)}{\partial_3 \partial_0(r)}, & \varepsilon_3 &= \sqrt{e_2 - e_3} \frac{\sigma u}{\sigma_3 u} = \frac{\partial_2 \partial_1(r)}{\partial_3 \partial_0(r)}. \end{aligned} \right\} (13)$$

4. In bringing (2) into a form suitable for our purpose, the same method as in the previous paper is adopted, which may be briefly sketched as follows:—

Substituting from (11) and (13), equation (2) becomes, after reduction

$$\left[ \partial_3^4 \partial_3'' \partial_0(2r) + \partial_0^4 \partial_0'' \partial_3(2r) \right] 2r = \partial_3^5 \partial_0'(2r) + \partial_0^5 \partial_3'(2r) - \pi \partial_2^7 \partial_1(2r). \quad (14)$$

On replacing the  $\partial$ -functions by their expressions in  $h$ -series, it is immediately seen that each member of the above equation is divisible by  $h^2$ ; hence a solution of this equation is  $h=0$ , from which it follows that  $e_2=e_3$  or  $a=b$ . This solution determines the well-known series of Maclaurin's spheroids, the consideration of which, however, is not an aim of this paper.

Dividing out the factor  $h^2$  on both sides of (14), arranging the quotients in powers of  $h$ , and transposing, we obtain

$$A_0 + A_1 h^2 + A_2 h^4 + \dots + A_6 h^{12} + \dots = 0, \quad (15)$$

where  $A$ 's are known functions of  $r$  alone.

If, in the last equation, we put  $h=0$ , then

$$A_0 \equiv (4 - \cos 2z)2z - 16 \sin z + 5 \sin 2z = 0, \quad (16)$$

where

$$z = 2\pi r.$$

The value of  $z$ , say  $z_0$ , which satisfies (16) corresponds to the starting point of the Jacobian from the revolutionary series, and can be found, as will be given below, by the method of successive approximation.

Now,  $z_0$  being known, the general value of  $z$ , which is defined by (15) as a function of  $h$ , can be expanded in the neighbourhood of  $h=0$ , thus:—

$$z = z_0 + a_1 h^2 + a_2 h^4 + \dots + a_6 h^{12} + \dots \quad (17)$$

The numerical coefficients  $z_0, a_1, a_2, \dots, a_5$  were recomputed and  $a_6$  was newly found for the present paper, the result being

$$\begin{aligned}
z_0 &= +1.8974390607 \\
a_1 &= -0.16732092 \\
a_2 &= -0.4747820 \\
a_3 &= +0.380062 \\
a_4 &= +0.40908 \\
a_5 &= -0.3475 \\
a_6 &= -0.894.
\end{aligned}$$

By means of the equation just obtained, the value of  $z$  can be determined for an assigned value of  $h$ , provided the latter is not near unity.

5. Formulæ for  $\rho$ 's and  $\varepsilon$ 's given in (13) and thence those for  $\vartheta$  and  $i$  given in (5), (6) and (9) can be adapted to numerical calculation, by quadratic transformation of the  $\vartheta$ -functions and by introducing auxiliary angles.

With a pair of corresponding values of  $h$  and  $z$ , let the following four functions be computed:

$$\left. \begin{aligned}
\theta_2 &= 2\sqrt{h}(1+h^4+h^{12}+\dots), \\
\theta_3 &= 1+2h^2+2h^8+\dots, \\
\theta_2(2r) &= 2\sqrt{h}(\cos z+h^4\cos 3z+h^{12}\cos 5z+\dots), \\
\theta_3(2r) &= 1+2h^2\cos 2z+2h^8\cos 4z+\dots,
\end{aligned} \right\} \quad (18)$$

where the symbol  $\theta$  signifies that the modulus of the function is  $2\tau$ , *i. e.*,

$$\theta_i = \vartheta_i(0|2\tau), \quad \theta_i(2r) = \vartheta_i(2r|2\tau), \quad (i = 2, 3).$$

All these series converge very rapidly; in most cases, the first two terms of each series will give a sufficiently accurate value of the function. Next, let angles  $\alpha$ ,  $\beta$  be determined by the equations

$$\left. \begin{aligned}
\tan \alpha &= \frac{\theta_2}{\theta_3}, \\
\tan \beta &= -\frac{\theta_2(2r)}{\theta_3(2r)};
\end{aligned} \right\} \quad (19)$$

then, we have the formulæ:

$$\left. \begin{aligned}
\vartheta_2^2 &= 2\theta_2\theta_3 = \lambda^2 \sin 2\alpha, \\
\vartheta_3^2 &= \theta_3^2 + \theta_2^2 = \lambda^2, \\
\vartheta_0^2 &= \theta_3^2 - \theta_2^2 = \lambda^2 \cos 2\alpha,
\end{aligned} \right\} \quad (20)$$

$$\left. \begin{aligned} \theta_1^2(r) &= \theta_2\theta_3(2r) - \theta_1\theta_2(2r) = \lambda\mu \sin(a+i\beta), \\ \theta_2^2(r) &= \theta_2\theta_3(2r) + \theta_3\theta_2(2r) = \lambda\mu \sin(a-i\beta), \\ \theta_3^2(r) &= \theta_3\theta_3(2r) + \theta_2\theta_2(2r) = \lambda\mu \cos(a+i\beta), \\ \theta_0^2(r) &= \theta_3\theta_3(2r) - \theta_2\theta_2(2r) = \lambda\mu \cos(a-i\beta), \end{aligned} \right\} \quad (20)$$

where  $\lambda = \frac{\theta_3}{\cos a}, \quad \mu = \frac{\theta_3(2r)}{\cos i\beta}.$

Hence (13) becomes

$$\left. \begin{aligned} \rho_1^2 &= \frac{\tan(a-i\beta)}{\tan 2a}, & \epsilon_1^2 &= \frac{\sin(a+i\beta)}{\sin 2a \cos(a-i\beta)}, \\ \rho_2^2 &= \frac{\sin(a-i\beta)}{\sin 2a \cos(a+i\beta)}, & \epsilon_2^2 &= \frac{\tan(a+i\beta)}{\tan 2a}, \\ \rho_3^2 &= \frac{\cos 2a \cos(a+i\beta)}{\cos(a-i\beta)}, & \epsilon_3^2 &= \frac{\sin 2a \sin(a+i\beta)}{\cos(a-i\beta)}. \end{aligned} \right\} \quad (21)$$

From the definition of  $\rho$ 's and  $\epsilon$ 's, it follows that

$$\rho_i^2 + \epsilon_i^2 = 1, \quad (i = 1, 2, 3);$$

hence  $\epsilon_i$  can be found from  $\rho_i$ , or vice versa. But, actually, these six quantities were all calculated independently from (21), using the above identities as a means of verification.

6. Substituting in (5) the value of  $S$  given in (12), and using (20), (21), we get

$$\Omega = -\frac{2\theta_2\theta_3z\rho_2}{\epsilon_3} \left\{ 1 + 2 \left( \frac{\rho_2 \cos(a+i\beta)}{\rho_3} \right)^2 \right\} - 6 \left( \frac{\rho_2 \cos(a+i\beta)}{\rho_3} \right)^2 \epsilon_2^2 \left( 1 + \frac{\cos 2\beta}{\cos^3 2a} \right).$$

If, herein, we put

$$\left. \begin{aligned} \tan \varphi &= \frac{\rho_3}{\sqrt{2\rho_2 \cos(a+i\beta)}}, \\ \tan \psi &= \left( \frac{\cos^3 2a}{\cos 2\beta} \right)^{\frac{1}{2}}, \\ \sin \chi &= \left( \frac{3\epsilon_3}{2\theta_2\theta_3z\rho_2} \right)^{\frac{1}{2}} \cos \varphi, \end{aligned} \right\} \quad (22)$$

then 
$$\Omega = 3 \left( \frac{\sin \psi}{\epsilon_2 \tan \varphi \tan \chi} \right)^2. \quad (23)$$

The second form of expression for  $\Omega$ , viz. (6), can be treated in the same manner: putting

$$\left. \begin{aligned} t_0'' &= \frac{1}{8\pi^2 h} \partial_0'' = 1 - 4h^3 + 9h^8 - \dots, \\ t_0'(r) &= \frac{1}{4\pi h} \partial_0'(r) = \sin z - 2h^3 \sin 2z + 3h^8 \sin 3z - \dots, \end{aligned} \right\} \quad (24)$$

and defining an angle  $\omega$  by

$$\sin \omega = \left( \frac{t_0'(r)}{t_0'' z} \right)^{\frac{1}{2}} \left( \frac{2\theta_2 \cos \alpha \cos \beta}{\theta_3(2r) \tan 2\alpha \cos(\alpha - \beta)} \right)^{\frac{1}{2}}, \quad (25)$$

it can be proved that (6) becomes

$$\Omega = \frac{4h t_0'' z \rho_2}{\theta_2 \theta_3 \sqrt{2\theta_2 \theta_3} \rho_3 \varepsilon_2 \varepsilon_3} \left( \frac{\tan \zeta' \cos \omega}{\varepsilon_2 \sin \zeta'} \right)^2 - \left( \frac{\varepsilon_1 \tan \zeta'}{\varepsilon_2 \tan \zeta'} \right)^2. \quad (26)$$

The values of  $\Omega$  were always found from both (23) and (26). Since these two equations lead to identical results under the condition that (17) is satisfied, the comparison of the two values for  $\Omega$  thus obtainable, enables us to verify the calculation and confirm the accuracy of the values of  $z$  found from (17).

Lastly, the quantities  $\mu$ ,  $e$ , and  $i$  are determined by

$$\left. \begin{aligned} \mu &= \frac{\sqrt{6}}{10} (\rho_1 \rho_3)^{-\frac{2}{3}} (1 + \rho_3^2) \sqrt{\Omega}, \\ e &= \frac{\sqrt{6}}{4} \mu \sqrt{\Omega}, \\ i &= 1 - \frac{3}{5} (\rho_1 \rho_3)^{\frac{1}{3}} \frac{\theta_2 \theta_3 z}{\varepsilon_3}. \end{aligned} \right\} \quad (27)$$

By the method hitherto explained, the calculation was carried out with values of  $h$  taken in the range from 0 to 0.24 at equal intervals of 0.02. The result is shown in the first 13 rows of Table I at the end of this paper. Following the scheme of Darwin's table, the quantities

$$\left. \begin{aligned} \delta_1 &= \frac{a}{(abc)^{\frac{1}{3}}} = \left( \frac{\rho_1}{\rho_3 \rho_2} \right)^{\frac{1}{3}}, \\ \delta_2 &= \frac{b}{(abc)^{\frac{1}{3}}} = \left( \frac{\rho_2}{\rho_3} \right)^{\frac{1}{3}}, \\ \delta_3 &= \frac{c}{(abc)^{\frac{1}{3}}} = (\rho_1 \rho_2)^{\frac{1}{3}} \end{aligned} \right\} \quad (28)$$

are tabulated instead of  $\rho_1$ ,  $\rho_2$ ,  $\rho_3$ .

7. As  $h$  tends to unity, the foregoing equations become gradually inconvenient. In this case, the  $\vartheta$ -functions with modulus  $\tau$  may be transformed into those with modulus  $\tau_1 = -\tau^{-1}$ , according to the formulæ

$$\left. \begin{aligned} \vartheta_1(r) &= -i\sqrt{-i\tau_1} e^{\pi i \tau_1 r} \vartheta_1(\tau_1 r), \\ \vartheta_2(r) &= \sqrt{-i\tau_1} e^{\pi i \tau_1 r^2} \bar{\vartheta}_0(\tau_1 r), \\ \vartheta_3(r) &= \sqrt{-i\tau_1} e^{\pi i \tau_1 r^2} \vartheta_3(\tau_1 r), \\ \vartheta_0(r) &= \sqrt{-i\tau_1} e^{\pi i \tau_1 r^2} \vartheta_2(\tau_1 r), \end{aligned} \right\} \quad (29)$$

where  $\bar{\vartheta}$  denotes that the modulus of the function is  $\tau_1$ . By this transformation,  $h$  goes over to  $h_1$ , where

$$\operatorname{lognat} h \cdot \operatorname{lognat} h_1 = \pi^2. \quad (30)$$

It must be borne in mind that the values of  $h$ , with which we shall be concerned hereafter, are exceedingly small, being less than 0.0000920 which corresponds to the extreme value 0.24 of  $h$  referred to above.

By the modular transformation, (14) becomes

$$\left[ \bar{\vartheta}_2' \bar{\vartheta}_2'' \bar{\vartheta}_3(2\tau_1 r) + \bar{\vartheta}_3' \bar{\vartheta}_3'' \bar{\vartheta}_2(2\tau_1 r) \right] 2\tau_1 r = \bar{\vartheta}_2' \bar{\vartheta}_3'(2\tau_1 r) + \vartheta_3' \bar{\vartheta}_2'(2\tau_1 r) + \pi \bar{\vartheta}_0' \bar{\vartheta}_1(2\tau_1 r). \quad (31)$$

In this case, an equation analogous to (17) cannot be obtained, for the argument  $\tau_1 r$  increases without limit as  $h$  approaches zero. We may, however, proceed thus:—

$$\text{Writing} \quad \tau_1 = -2\pi i \tau_1 r = \frac{z}{\pi} - 4 \operatorname{lognat} \frac{1}{h_1}, \quad (32)$$

and substituting for the functions in (31) their respective  $h_1$ -series, this equation may be put into the form

$$(AU + BV)\tau_1 = CX + Y, \quad (33)$$

$$\left. \begin{aligned} U &= \cosh z_1 + h_1^2 \cosh 3z_1 + h_1^6 \cosh 5z_1 + \dots, \\ V &= 1 + 2h_1 \cosh 2z_1 + 2h_1^4 \cosh 4z_1 + \dots, \\ X &= h_1 \sinh 2z_1 + 2h_1^4 \sinh 4z_1 + \dots, \\ Y &= D \sinh z_1 + D_1 h_1 \sinh 3z_1 + D_2 h_1^5 \sinh 5z_1 + \dots \end{aligned} \right\} \quad (34)$$

$$\left. \begin{aligned} A &= -\bar{\theta}_3^4 \bar{\theta}_3'' / (8\pi^2 h_1) = 1 + 8h_1 + 24h_1^2 + 36h_1^3 + 56h_1^4 + \dots, \\ B &= -\bar{\theta}_2^4 \bar{\theta}_2'' / (16\pi^2 h_1^5) = 2(1 + 13h_1^2 + 42h_1^4 + \dots), \\ C &= \bar{\theta}_2^5 / (4h_1^5) = 8(1 + 5h_1^2 + 10h_1^4 + \dots), \\ D &= (\bar{\theta}_3^5 - \bar{\theta}_0^5) / 8h_1 = \frac{1}{2}(6 - 11h_1 + 90h_1^2 - 121h_1^3 + 238h_1^4 - \dots), \\ D_1 &= (3\bar{\theta}_3^5 + \bar{\theta}_0^5) / 8 = \frac{1}{2}(1 + 4h_1 + 51h_1^2 - 10h_1^3 + 211h_1^4 - \dots), \\ D_2 &= (5\bar{\theta}_3^5 - \bar{\theta}_0^5) / 8 = \frac{1}{2}(1 + 16h_1 + 29h_1^2 + 170h_1^3 - 31h_1^4 + \dots). \end{aligned} \right\} (35)$$

Here, the values of  $A, B, C, D, \dots$  can be determined for a given value of  $h_1$  either by calculating  $\bar{\theta}_2, \bar{\theta}_3, \bar{\theta}_0, \bar{\theta}_2'', \bar{\theta}_3''$ , or preferably by direct evaluation from the series in (35). Then the corresponding value of  $z_1$  is found from (33) by the method of successive approximation.

For convenience of subsequent interpolations, values were first assigned to  $h$  at the intervals previously chosen, and then the corresponding values of  $h_1$  were accurately determined from (30). A further advantage of this procedure is that equation (17) is still available, for, from the value of  $z$  furnished by this equation, we can calculate that of  $z_1$  by (32), which serves as a first approximation. If  $h$  be not very near to unity, this approximate value of  $z_1$  is fairly close to the true one, so that by applying (33) once or twice, a final approximation of sufficient accuracy is arrived at. When  $h$  is close to unity, the extreme smallness of  $h_1$  facilitates the work with (33), and thus the trouble arising from the roughness of the first approximation is compensated.

8. For the calculation of  $\rho$ 's,  $\epsilon$ 's,  $\Omega$ , etc., the process is the same as before. Let

$$\left. \begin{aligned} \bar{\theta}_2 &= 2\sqrt{h_1}(1 + h_1^4 + \dots), \\ \bar{\theta}_3 &= 1 + 2h_1^2 + 2h_1^8 + \dots, \\ \bar{\theta}_2(2\tau_1 v) &= 2\sqrt{h_1}(\cosh z_1 + h_1^4 \cosh 3z_1 + \dots), \\ \bar{\theta}_3(2\tau_1 v) &= 1 + 2h_1^2 \cosh 2z_1 + 2h_1^8 \cosh 4z_1 + \dots; \end{aligned} \right\} (36)$$

then the angles  $\alpha$  and  $\beta$  introduced in § 5 are now given by

$$\left. \begin{aligned} \tan(45^\circ - \alpha) &= \frac{\bar{\theta}_2}{\bar{\theta}_3}, \\ \tan(45^\circ + \beta) &= \frac{\bar{\theta}_2(2\tau_1 v)}{\bar{\theta}_3(2\tau_1 v)}. \end{aligned} \right\} (37)$$

Formulae similar to (20) can be easily written down for  $\bar{\theta}$ 's; then by means of them and (29), it may be verified that exactly the same expressions as (21) hold good for  $\rho_1, \rho_2, \rho_3, \epsilon_1, \epsilon_2, \epsilon_3$ .

Again, the angles  $\varphi$  and  $\psi$  are determined by the same equations as in (22), but the equation giving  $\chi$  now transforms into

$$\sin \chi = \left( \frac{3\epsilon_2\rho_3}{2\theta_2\theta_3z_1\rho_2} \right)^{\frac{1}{2}} \cos \varphi. \quad (38)$$

Then, expression (23) for  $\Omega$  also applies in this case.

As to the second expression for  $\Omega$ , put

$$\left. \begin{aligned} \bar{t}_2'' &= -\frac{\bar{\theta}_2''}{2\pi^2 h_1^4} = 1 + 9h_1^2 + 25h_1^6 + \dots, \\ \bar{t}_2'(\tau_1 v) &= -\frac{\bar{\theta}_2'(\tau_1 v)}{2\pi i h_1^4} = \sinh \frac{z_1}{2} + 3h_1^2 \sinh \frac{3z_1}{2} + 5h_1^6 \sinh \frac{5z_1}{2} + \dots, \end{aligned} \right\} \quad (39)$$

and let a new angle  $\omega_1$  be defined by

$$\sin \omega_1 = \left( \frac{2\bar{t}_2'(\tau_1 v)}{\bar{t}_2'' z_1} \right)^{\frac{1}{2}} \left( \frac{2\theta_2 \cos(45^\circ - \alpha) \cos(45^\circ - \beta)}{\theta_2(2\tau_1 v) \cos(\alpha - \beta)} \right)^{\frac{1}{2}} \quad (40)$$

then we have

$$\Omega = \frac{h_1^4 \bar{t}_2'' z_1 \rho_1}{\theta_2 \theta_3 \epsilon_2 \sqrt{2\theta_2 \bar{\theta}_3}} \left( \frac{\tan \psi \cos \omega_1}{\epsilon_3 \sin \varphi} \right)^2 - \left( \frac{\epsilon_1 \tan \psi}{\epsilon_2 \tan \varphi} \right)^2. \quad (41)$$

Lastly, the expressions for  $\mu$  and  $c$  given in (27) remain unchanged, while that for  $i$  becomes

$$i = 1 - \frac{3}{5} \left( \frac{\rho_2}{\rho_3} \right)^{\frac{1}{2}} \frac{\theta_2 \theta_3 z_1}{\epsilon_2}. \quad (42)$$

The method of §§ 7, 8 was applied for  $h=0.24-0.6$  at intervals of 0.04; the last 11 rows of Table I show the result.

9. As an example, let  $h=0$ . Here, we may conveniently proceed from the original equations (5), (6) and (13), which simplify in this case thus:

$$\begin{aligned} \rho_1 &= \rho_2 = \cos \frac{z_0}{2}, & \rho_3 &= 1, \\ \epsilon_1 &= \epsilon_2 = \sin \frac{z_0}{2}, & \epsilon_3 &= 0, \end{aligned}$$

and 
$$\varrho = \frac{(2 + \cos z_0)z_0 - 3 \sin z_0}{(1 - \cos z_0) \tan \frac{z_0}{2}} = \frac{\sin^2 z_0}{5 - 2 \cos^2 z_0},$$

where, as was already given,

$$z_0 = 1.89743906 = 108^\circ 42' 54''.900.$$

Hence we find

$$\begin{aligned} \rho_1 &= \rho_2 = 0.5827242, & \rho_3 &= 1, \\ \varepsilon_1 &= \varepsilon_2 = 0.8126700, & \varepsilon_3 &= 0, \\ \varrho &= 0.1871148. \end{aligned}$$

This set of values determines the ellipsoid of transition referred to in § 4. Of course, the same result can be obtained from (21), (23), (26) by the use of the auxiliary angles  $\alpha$ ,  $\beta$ ,  $\zeta$ , etc.

Next, take  $h=0.24$ . From (17) we get

$$z = 1.88630305 = 108^\circ 4' 37''.934;$$

hence, from (18),

$$\begin{aligned} \log \theta_2 &= 1.9925741, & \log \theta_2(2r) &= 1.4791308, \\ \log \theta_3 &= 0.0473614, & \log \theta_3(2r) &= 1.9576028, \end{aligned}$$

and therefore by (19),

$$\alpha = 41^\circ 23' 44''.00, \quad \beta = 18^\circ 22' 53''.59.$$

Then from (21) we obtain

$$\begin{aligned} \rho_1^2 &= 0.0537271, & \rho_2^2 &= 0.7828731, & \rho_3^2 &= 0.0686280, \\ \varepsilon_1^2 &= 0.9462730, & \varepsilon_2^2 &= 0.2171269, & \varepsilon_3^2 &= 0.9313719. \end{aligned}$$

Also, we find

$$\begin{aligned} \zeta &= 22^\circ 34' 59''.76, & \psi &= 2^\circ 50' 35''.75, \\ \chi &= 55^\circ 12' 41''.96, & \omega &= 29^\circ 59' 24''.59. \end{aligned}$$

Hence from (23),  $\varrho = 0.09485037$ ,

and from (26),  $\varrho = 0.09485084$ .

Corresponding to  $h=0.24$ , we get from (30),

$$h_1 = 0.0009920201;$$

whence by (32),  $z_1 = 4.1524265$ .



By applying (33), it can be proved that this value of  $z_1$  is correct to the seventh decimal figure, so that the approximation is sufficient, if the accuracy required for  $\rho$ 's,  $\varepsilon$ 's,  $\Omega$ , etc. be that attainable by the use of seven-figure logarithms. Now (37) gives the same values of  $\alpha$  and  $\beta$  as shown above, and (41) gives

$$\Omega = 0.09485085.$$

As the last example, take  $h=0.6$ , to which corresponds

$$h_1 = 0.000000004064856.$$

The first approximation for  $z_1$  as given by (17) is

$$z_1 = 11.047.$$

By means of (33), we find that the second approximation is

$$z_1 = 11.0505,$$

and that the third is

$$z_1 = 11.0505035,$$

which can be proved to be correct to the sixth decimal.

From (23) and (41), we find respectively

$$\Omega = 0.0005114177,$$

and

$$\Omega = 0.0005114175.$$

**10.** To compare the result with that obtained by Darwin<sup>1)</sup>, Table II was calculated thus:—

In Darwin's method, the auxiliary quantity to which arbitrary values are attributed is an angle  $\gamma$  which is defined in our notation by

$$\cos \gamma = \rho_1,$$

or

$$\cos \gamma = \frac{\partial_0 \partial_2(r)}{\partial_2 \partial_0(r)} = \frac{\partial_2 \partial_0(\tau_1 r)}{\partial_0 \partial_2(\tau_1 r)}. \quad (43)$$

From the computed values of  $\rho_1 = \cos \gamma$ , the value of  $h$  corresponding to an assigned value of  $\gamma$  was first interpolated, a correction was added, when necessary, to this value of  $h$  so as to satisfy (43) accurately, and then, by the usual method, the corresponding values of  $\partial_1$ ,  $\partial_2$ ,  $\partial_3$  and  $\frac{1}{2} \Omega$  were interpolated from Table I. The

---

1) G. H. Darwin, *l. c.*

results are shown in Table II with Darwin's values side by side. From this table, it will be noticed that the results are in good agreement, excepting the values of  $\delta_1$  and  $\delta_2$  for  $\gamma=60^\circ$  and

TABLE 1.

Auxiliary Quantities			Axes			Ang. Vel.
$h$	$h_1$	$z$ or $z_1$	$\delta_1 = \frac{a}{(abc)^{\frac{1}{2}}}$	$\delta_2 = \frac{b}{(abc)^{\frac{1}{2}}}$	$\delta_3 = \frac{c}{(abc)^{\frac{1}{2}}}$	$\Omega = \frac{\omega^2}{2\pi\sigma}$
0	—	$z=1.89743906$	1.19723	1.197234	0.697657	0.187115
0.02	—	1.89737206	1.26294	1.136253	0.696854	0.186278
0.04	—	1.89717013	1.33395	1.079494	0.694449	0.183786
0.06	—	1.89683057	1.41091	1.026513	0.690458	0.179694
0.08	—	1.89634886	1.49456	0.976915	0.684903	0.174096
0.1	—	1.89571876	1.58578	0.930348	0.677818	0.167115
0.12	—	1.89493234	1.68554	0.886497	0.669244	0.158905
0.14	—	1.89398010	1.79500	0.845082	0.659229	0.149615
0.16	—	1.89285104	1.91551	0.805849	0.647831	0.139533
0.18	—	1.89153282	2.04864	0.768571	0.635111	0.128780
0.2	—	1.89001190	2.19626	0.733042	0.621137	0.117604
0.22	—	1.88827376	2.36057	0.699075	0.605982	0.106223
0.24	$0.99202015.10^{-3}$	1.88630305	2.54420	0.666502	0.589722	0.0948509
0.28	$0.42935054.10^{-3}$	$z_1=1.6436612$	2.98276	0.604938	0.554205	0.0729128
0.32	$0.17306452.10^{-3}$	5.1717957	3.54635	0.547279	0.515239	0.0531468
0.36	$0.63756224.10^{-4}$	5.7462979	4.28736	0.492629	0.473467	0.0344823
0.4	$0.20994321.10^{-4}$	6.3781799	5.28644	0.440321	0.429603	0.0233988
0.44	$0.60121544.10^{-5}$	7.0899845	6.67793	0.389744	0.384220	0.0138533
0.48	$0.14457357.10^{-5}$	7.8720639	8.69008	0.340513	0.337942	0.0074594
0.52	$0.27878215.10^{-6}$	8.7743890	11.73766	0.292410	0.291358	0.0035774
0.56	$0.40503148.10^{-7}$	9.8192530	16.62132	0.245465	0.245105	0.0014860
0.6	$0.40348561.10^{-8}$	11.0535035	25.06353	0.199798	0.199695	0.0005114
1	0	$\infty$	$\infty$	0	0	0

those of  $\frac{1}{2}Q$  for  $\gamma=80^\circ$  where the discrepancies are still sensible.

In writing this paper, I owe very much to Prof. H. Nagaoka for his kind advice.

TABLE I<sub>2</sub>.

$h$	Eccentricities of Sections			Mom. of Mom.	Energy		
	$\varepsilon = \frac{1}{a} \sqrt{a^2 - c^2}$	$\varepsilon_1 = \frac{1}{b} \sqrt{b^2 - c^2}$	$\varepsilon_2 = \frac{1}{a} \sqrt{a^2 - b^2}$	$g$	Kinetic $e$	Intrinsic $i$	Total $E$
0	0.812670	0.812670	0	0.30375	0.080461	0.41495	0.49541
0.02	0.833996	0.789857	0.436535	0.30512	0.080642	0.41549	0.49613
0.04	0.853803	0.765606	0.587468	0.30923	0.081180	0.41712	0.49830
0.06	0.872075	0.739984	0.686048	0.31611	0.082059	0.41983	0.50189
0.08	0.888817	0.713075	0.756800	0.32584	0.083255	0.42364	0.50690
0.1	0.904046	0.684978	0.809817	0.33848	0.084733	0.42856	0.51329
0.12	0.917797	0.655805	0.850520	0.35415	0.086450	0.43459	0.52104
0.14	0.930119	0.625383	0.882241	0.37298	0.088355	0.44174	0.53010
0.16	0.941073	0.594750	0.907201	0.39514	0.090388	0.45003	0.54012
0.18	0.950732	0.563153	0.926960	0.42084	0.092483	0.45946	0.55194
0.2	0.959174	0.531048	0.942655	0.45032	0.094570	0.47004	0.56461
0.22	0.966488	0.498597	0.955142	0.48387	0.096573	0.48177	0.57834
0.24	0.972766	0.465969	0.965076	0.52182	0.098415	0.49466	0.59307
0.28	0.982537	0.400857	0.979218	0.61266	0.101307	0.52386	0.62516
0.32	0.989390	0.337135	0.988021	0.72711	0.102649	0.55750	0.66015
0.36	0.993883	0.276195	0.993377	0.87135	0.101918	0.59534	0.69725
0.4	0.996692	0.219295	0.996525	1.05439	0.098767	0.63681	0.73558
0.44	0.998343	0.167767	0.998295	1.29009	0.092987	0.68136	0.77434
0.48	0.999244	0.122649	0.999232	1.60008	0.084628	0.72803	0.81266
0.52	0.999692	0.084752	0.999690	2.01974	0.073977	0.77567	0.84965
0.56	0.999891	0.054504	0.999891	2.60922	0.061594	0.82275	0.88435
0.6	0.999968	0.031990	0.999968	3.47997	0.048192	0.86773	0.91592
1	1	0	1	$\infty$	0	1	1

TABLE II.

$\gamma$	$h$	$\delta_1$		$\delta_2$		$\delta_3$		$\frac{1}{2}Q$	
		Darwin	Kailara	Darwin	Kailara	Darwin	Kailara	Darwin	Kailara
55°	0·0059319	1·216	1·2162	1·179	1·1787	0·698	0·6976	0·0935	0·09352
57°	0·0245838	1·279	1·2787	1·123	1·1229	0·696	0·6964	0·093	0·09293
60°	0·0531895	1·3831	1·3840	1·0454	1·0442	0·6916	0·6920	0·09060	0·09063
65°	0·103149	1·6007	1·6009	0·9235	0·9233	0·6765	0·6766	0·08295	0·08295
70°	0·157310	1·859	1·8988	0·8111	0·8110	0·6494	0·6494	0·07047	0·07046
75°	0·218351	2·346	2·3463	0·7019	0·7018	0·6072	0·6073	0·0536	0·05358
80°	0·291436	3·1294	3·1293	0·5881	0·5881	0·5434	0·5434	0·03307	0·03350
85°	0·391275	5·0406	5·0407	0·4516	0·4516	0·4393	0·4393	0·01293	0·01297

---

Published July, 20th, 1916

---

## On the Elastic Equilibrium of a Semi-Infinite Solid under given Boundary Conditions, with some Applications.

By

Kwan-ichi TERAZAWA, *Riyakushi*,

### I. Introduction.

§1. The statical problem concerning an infinite elastic solid bounded by a plane subjected to a given distribution of traction or deformation has attracted the attention of numerous eminent elasticians. The first solution for the case of a purely normal load was given by LAMÉ AND CLAPEYRON<sup>1)</sup> by means of FOURIER's theorem, through which an assigned function of two variables is expressed as a quadruple integral. The credit of first improvement on this subject may well be claimed by J. BOUSSINESQ,<sup>2)</sup> who introduced several kinds of potentials—direct, inverse and logarithmic with three variables—into the theory of elasticity, and opened a new field of treatment in it. Almost all conceivable cases have been solved by him, especially in relation to what takes place at the boundary surface. Besides Boussinesq, many other authors have touched on this problem, employing the method of integration by Green's functions. Not long ago, Prof. H. LAMB<sup>3)</sup> solved a special case of this problem, viz. that in which the boundary condition is a normal pressure symmetrically distributed about a point on the surface, by making use of the integral theorem of Fourier's type concerning Bessel function of the zeroth order; and thus, Lamé and Clapeyron's method, which was considered to

---

1) CRELLE's Journal, vol. 7 (1831) p.p. 400-404.

2) Application des Potentiels, Paris, (1885).

3) Lond. Math. Soc. Proc. vol. 34 (1902) p. 276.

be extremely unsuited for obtaining physical results, seems now to have gained practical importance.

§2. The present paper deals with the problem in the case in which the boundary is subjected to any given normal pressure, by generalizing the method adopted by LAMB.<sup>1)</sup> In the first two sections the general solution of the problem is obtained in the type of the Bessel-Fourier expansion of a function. The third section discusses several examples in the case of symmetry about an axis normal to the boundary, and forms the main part of this communication. Most of these special examples have been investigated by the authors above cited: the behaviour at the surface especially; and yet it may be worth while to discuss them again more closely, referring especially to the behaviour inside the boundary.

The last section is added as an appendix, supplying the general solutions corresponding to several boundary conditions, excepting that of normal pressure, in the case of symmetry about a normal to the boundary.

§3. The results of these special examples applied to find the limit of rupture of a foundation over which a heavy load is distributed. Strictly speaking, by applying the mathematical theory of elasticity, we can treat of rupture only, for some kinds of brittle solids like cast iron, in which the linear relation of stress and strain holds and, moreover, the strains are so small that their squares are negligible up to the point where rupture takes place. For a ductile material, such as mild steel, and for an imperfectly elastic material, like cement or sandstone, we must bear in mind that the theoretical results indicate only roughly the state of stress when, in the first case, it begins to take permanent set, and, in the second case, when it breaks.

§4. Another application will be found in a problem of geophysics. In his elaborate observations on the lunar deflection of gravity, Dr. O. HECKER has pointed out that the force acting on the pendulum at Pot-dam is a large fraction of the moon's force when it acts towards the east or west than when it acts towards the

---

1) Though the writer had not read his paper until the work was almost finished.

north or south.<sup>1)</sup> Various explanations of this anomaly have been proposed, among them one, suggested by Prof. A.E.H. Love,<sup>2)</sup> is that a possible cause may perhaps be found in the effect of the tide wave in the North Atlantic. Recently Prof. A.A. MICHELSON<sup>3)</sup> has found a similar result in his arduous task of measuring the lunar perturbation of a very long water-level at Chicago. Prof. Sir J. LARMOR kindly suggested to me a query whether the excess-pressure of the tide in the North Atlantic would affect much the measurement of the water-level at Chicago, owing to the depression of the solid earth that it would produce. A calculation is undertaken in order to ascertain to what extent the consideration of the tilting of the ground is important for the explanation of this geodynamical discrepancy; we may in a first estimation neglect the curvature of the earth.<sup>4)</sup>

## II. Solution of Equation of Equilibrium.

§5. The equation of equilibrium of an isotropic elastic body free from the action of a body force is

$$\text{curl curl } u = \frac{\lambda + 2\mu}{\mu} \text{ grad } J, \quad (1)$$

where  $u$  denotes the displacement,  $\lambda$  and  $\mu$  Lamé's constants which specify the elastic nature of the body concerned, and  $J$  is the amount of dilatation defined by the equation

$$J = \text{div } u. \quad (2)$$

Our first object is to find the solution of the equation of equilibrium, which is appropriate for the discussion of the problem concerning a semi-infinite elastic body.

Since  $\text{div. curl}$  of any vector quantity vanishes, if we perform the operation  $\text{div}$  on both sides of equation (1) we have simply

$$\text{div grad } J = 0, \quad (3)$$

---

1) A similar result has been found by A. ORLOFF at Dorpat and T. SHIDA at Kyoto.

2) Some Problems of Geodynamics, Cambridge, (1911) p. 88.

3) The Astrophysical Journal, vol. 39 (1914) p. 105.

4) The geodynamical application will appear shortly in the Trans. Roy. Soc. London.

which determines the dilatation  $\mathcal{J}$ . If  $\mathcal{J}$  is found from this equation, the displacement  $u$  can be determined by solving the equation

$$\text{grad div } u - \text{curl curl } u = -\frac{\lambda + \mu}{\mu} \text{grad } \mathcal{J}. \quad (4)$$

The elastic body which we deal with is supposed to be bounded by an infinite (say) horizontal plane in its natural state and to extend without limit both horizontally and downwards. Take the cylindrical coordinates  $(r, \theta, z)$  such that the axis of  $z$  coincides with an inward normal to the boundary and the origin lies on the boundary surface of the body in its natural state, then we have, for  $z > 0$ , the equations

$$\frac{\partial^2 \mathcal{J}}{\partial r^2} + \frac{1}{r} \cdot \frac{\partial \mathcal{J}}{\partial r} + \frac{1}{r^2} \frac{\partial^2 \mathcal{J}}{\partial \theta^2} + \frac{\partial^2 \mathcal{J}}{\partial z^2} = 0 \quad (5)$$

to determine  $\mathcal{J}$ , and

$$\left. \begin{aligned} \frac{\partial^2 u_r}{\partial r^2} + \frac{1}{r} \cdot \frac{\partial u_r}{\partial r} + \frac{\partial^2 u_r}{\partial z^2} - \frac{1}{r^2} \left( u_r - \frac{\partial^2 u_r}{\partial \theta^2} \right) - \frac{2}{r^2} \cdot \frac{\partial u_\theta}{\partial \theta} &= -\frac{\lambda + \mu}{\mu} \cdot \frac{\partial \mathcal{J}}{\partial r}, \\ \frac{\partial^2 u_\theta}{\partial r^2} + \frac{1}{r} \cdot \frac{\partial u_\theta}{\partial r} + \frac{\partial^2 u_\theta}{\partial z^2} - \frac{1}{r^2} \left( u_\theta - \frac{\partial^2 u_\theta}{\partial \theta^2} \right) + \frac{2}{r^2} \cdot \frac{\partial u_r}{\partial \theta} &= -\frac{\lambda + \mu}{\mu} \cdot \frac{1}{r} \cdot \frac{\partial \mathcal{J}}{\partial \theta}, \\ \frac{\partial^2 u_z}{\partial r^2} + \frac{1}{r} \cdot \frac{\partial u_z}{\partial r} + \frac{\partial^2 u_z}{\partial z^2} + \frac{1}{r^2} \cdot \frac{\partial^2 u_z}{\partial \theta^2} &= -\frac{\lambda + \mu}{\mu} \cdot \frac{\partial \mathcal{J}}{\partial z}, \end{aligned} \right\} \quad (6)$$

where  $u_r, u_\theta, u_z$  are the components of the vector  $u$ . The equation (5) follows from (3), and (6) from (4).

§6. To solve these equations, assume

$$\mathcal{J} = \delta(r) \cdot e^{-kz} \frac{\cos}{\sin} \Big\} m\theta,$$

where  $k$  is a positive constant so that there may be no dilatation at  $z = \infty$ , and  $m$  is an integer, positive or negative, or zero so that the solution may be unique round the origin, then the equation (5) gives

$$\frac{r^2 \delta}{dr^2} + \frac{1}{r} \cdot \frac{d\delta}{dr} + \left( k^2 - \frac{m^2}{r^2} \right) \delta = 0,$$

of which the solution is

$$\delta = C_m J_m(kr)^{1)}$$

---

1) The second solution is rejected for the reason of its singularity at the origin which we exclude from our present investigation.



where  $J_m(r)$  is the Bessel coefficient of order  $m$ , and  $C_m$  is a constant of integration. Thus we obtain

$$J = C_m e^{-kz} J_m(kr) \left\{ \begin{matrix} \cos \\ \sin \end{matrix} \right\} m\theta. \quad (7)$$

§7. To find  $u$  corresponding to

$$J = C_m e^{-kz} J_m(kr) \cos m\theta,$$

assume that

$$u_r = U_r \cos m\theta,$$

$$u_\theta = U_\theta \sin m\theta,$$

$$u_z = U_z \cos m\theta,$$

$U_r, U_\theta, U_z$ , being functions of  $r$  and  $z$ . Then equations (6) transform into

$$\frac{\partial^2 U_r}{\partial r^2} + \frac{1}{r} \frac{\partial U_r}{\partial r} + \frac{\partial^2 U_r}{\partial z^2} - \frac{m^2 + 1}{r^2} U_r - \frac{2m}{r^2} U_\theta = -\frac{\lambda + \mu}{\mu} k C_m e^{-kz} J_m(kr), \quad (8)$$

$$\frac{\partial^2 U_\theta}{\partial r^2} + \frac{1}{r} \frac{\partial U_\theta}{\partial r} + \frac{\partial^2 U_\theta}{\partial z^2} - \frac{m^2 + 1}{r^2} U_\theta - \frac{2m}{r^2} U_r = \frac{\lambda + \mu}{\mu} \cdot \frac{m}{r} C_m e^{-kz} J_m(kr), \quad (9)$$

$$\frac{\partial^2 U_z}{\partial r^2} + \frac{1}{r} \frac{\partial U_z}{\partial r} + \frac{\partial^2 U_z}{\partial z^2} - \frac{m^2}{r^2} U_z = \frac{\lambda + \mu}{\mu} k C_m e^{-kz} J_m(kr) \quad (10)$$

in which  $J_m'(x)$  means  $dJ_m(x)/dx$  as usual.

The last equation suggests that  $U_z$  has the form  $V J_m(kr)$ , where  $V$  is a function of  $z$  only and satisfies the equation

$$\frac{d^2 V}{dz^2} - k^2 V = \frac{\lambda + \mu}{\mu} k C_m e^{-kz}.$$

The solution of this equation is

$$V = \left( -\frac{\lambda + \mu}{2\mu} C_m z + D_m \right) e^{-kz},$$

$D_m$  being an arbitrary constant. Thus

$$u_z = -\left( \frac{\lambda + \mu}{2\mu} C_m z - D_m \right) e^{-kz} J_m(kr) \cos m\theta. \quad (11)$$

To find  $U_r$  and  $U_\theta$ , write

$$U_r + U_\theta = X,$$

$$U_r - U_\theta = Y,$$

then combining the equations (8) and (9) we have

$$\frac{\partial^2 X}{\partial r^2} + \frac{1}{r} \cdot \frac{\partial X}{\partial r} + \frac{\partial^2 X}{\partial z^2} - \frac{(m+1)^2}{r^2} X = \frac{\lambda + \mu}{\mu} k C_m e^{-kz} J_{m+1}(kr),$$

$$\frac{\partial^2 Y}{\partial r^2} + \frac{1}{r} \cdot \frac{\partial Y}{\partial r} + \frac{\partial^2 Y}{\partial z^2} - \frac{(m-1)^2}{r^2} Y = -\frac{\lambda + \mu}{\mu} k C_m e^{-kz} J_{m-1}(kr).$$

These equations suggest that  $X$  and  $Y$  vary as  $J_{m+1}(kr)$  and  $J_{m-1}(kr)$  respectively with regard to  $r$ , and they can be solved in a manner similar to the equation (10). The result is

$$X = \left( -\frac{\lambda + \mu}{2\mu} C_m z + E_m \right) e^{-kz} J_{m+1}(kr),$$

$$Y = \left( \frac{\lambda + \mu}{2\mu} C_m z + F_m \right) e^{-kz} J_{m-1}(kr),$$

$E_m$  and  $F_m$  being arbitrary constants. Writing

$$E_m + F_m = 2A_m,$$

$$E_m - F_m = 2B_m,$$

and simplifying, we have

$$\left. \begin{aligned} U_r &= \frac{\lambda + \mu}{2\mu} C_m z J'_m(kr) + \left[ A_m \frac{m}{kr} J_m(kr) - B_m J'_m(kr) \right] \\ U_\theta &= -\frac{\lambda + \mu}{2\mu} C_m z \frac{m}{kr} J_m(kr) + \left[ B_m \frac{m}{kr} J_m(kr) - A_m J'_m(kr) \right] \end{aligned} \right\} e^{-kz}.$$

Thus we have a system of solutions: —

$$\left. \begin{aligned} \mathcal{A} &= C_m J_m(kr) e^{-kz} \cos m\theta, \\ u_r &= \left\{ \left[ \frac{\lambda + \mu}{2\mu} C_m z - B_m \right] J_m(kr) + A_m \frac{m}{kr} J_m(kr) \right\} e^{-kz} \cos m\theta, \\ u_\theta &= -\left\{ \left[ -\frac{\lambda + \mu}{2\mu} C_m z - B_m \right] \frac{m}{kr} J_m(kr) + A_m J'_m(kr) \right\} e^{-kz} \sin m\theta, \\ u_z &= -\left\{ \frac{\lambda + \mu}{2\mu} C_m z - D_m \right\} J_m(kr) e^{-kz} \cos m\theta. \end{aligned} \right\} \quad (12)$$

The constants  $B_m, C_m$  and  $D_m$  are not independent of one another, but are connected by the relation

$$k(B_m - D_m) = \frac{\lambda + 3\mu}{2\mu} C_m, \quad (13)$$

which follows from the definition of  $J$ .

§8. Next, the solutions corresponding to  $J$  which has  $\sin m\theta$  in its factor can be found in a similar way. They are distinguished from the above by placing a bar on every quantity.

$$\left. \begin{aligned} J &= C_m J_m(kr) e^{-kz} \sin m\theta, \\ u_r &= \left\{ \left[ \frac{\lambda + \mu}{2\mu} C_m z - B_m \right] J'_m(kr) + A_m \frac{m}{kr} J_m(kr) \right\} e^{-kz} \sin m\theta, \\ u_\theta &= \left\{ \left[ \frac{\lambda + \mu}{2\mu} C_m z - B_m \right] \frac{m}{kr} J_m(kr) + A_m J'_m(kr) \right\} e^{-kz} \cos m\theta, \\ u &= - \left\{ \frac{\lambda + \mu}{2\mu} C_m z - D_m \right\} J_m(kr) e^{-kz} \sin m\theta; \end{aligned} \right\} \quad (14)$$

with

$$k(B_m - D_m) = \frac{\lambda + 3\mu}{2\mu} C_m. \quad (15)$$

§9. The stress can be calculated by using the formulae

$$\left. \begin{aligned} \widehat{zz} &= \lambda J + 2\mu \frac{\partial u_z}{\partial z}, \\ \widehat{rz} &= \mu \left\{ \frac{\partial u_r}{\partial z} + \frac{\partial u_z}{\partial r} \right\}, \\ \widehat{z\theta} &= \mu \left\{ \frac{1}{r} \frac{\partial u_z}{\partial \theta} + \frac{\partial u_\theta}{\partial z} \right\}, \\ \widehat{rr} &= \lambda J + 2\mu \frac{\partial u_r}{\partial r}, \\ \widehat{\theta\theta} &= \lambda J + 2\mu \left\{ \frac{1}{r} \frac{\partial u_\theta}{\partial \theta} + \frac{u_r}{r} \right\}, \\ \widehat{r\theta} &= \mu \left\{ \frac{\partial u_\theta}{\partial r} - \frac{u_\theta}{r} + \frac{1}{r} \frac{\partial u_r}{\partial \theta} \right\}. \end{aligned} \right\} \quad (16)$$

Thus corresponding to the first solution (12), we obtain

$$\left. \begin{aligned}
 \widehat{zz} &= \left\{ (\lambda + \mu)kC_m z - \mu C_m - 2\mu kD_m \right\} J_m(kr) e^{-kz} \cos m\theta, \\
 \widehat{zr} &= - \left\{ \left[ (\lambda + \mu)kC_m z - \frac{\lambda + \mu}{2} C_m - \mu k(B_m + D_m) \right] J'_m(kr) \right. \\
 &\quad \left. + \frac{\mu m}{r} A_m J_m(kr) \right\} e^{-kz} \cos m\theta, \\
 \widehat{z\theta} &= \left\{ \left[ (\lambda + \mu)kC_m z - \frac{\lambda + \mu}{2} C_m - \mu k(B_m + D_m) \right] \frac{m}{kr} J_m(kr) \right. \\
 &\quad \left. + \mu k A_m J'_m(kr) \right\} e^{-kz} \sin m\theta, \\
 &\text{etc. ;}
 \end{aligned} \right\} \quad (17)$$

and corresponding to the second solution (14),

$$\left. \begin{aligned}
 \widehat{zz} &= \left\{ (\lambda + \mu)k\bar{C}_m z - \mu \bar{C}_m - 2\mu k\bar{D}_m \right\} J_m(kr) e^{-kz} \sin m\theta, \\
 \widehat{zr} &= - \left\{ \left[ (\lambda + \mu)k\bar{C}_m z - \frac{\lambda + \mu}{2} \bar{C}_m - \mu k(\bar{B}_m + \bar{D}_m) \right] J'_m(kr) \right. \\
 &\quad \left. + \frac{\mu m}{r} A_m J_m(kr) \right\} e^{-kz} \sin m\theta, \\
 \widehat{z\theta} &= - \left\{ \left[ (\lambda + \mu)k\bar{C}_m z - \frac{\lambda + \mu}{2} \bar{C}_m - \mu k(\bar{B}_m + \bar{D}_m) \right] \frac{m}{kr} J_m(kr) \right. \\
 &\quad \left. + \mu k A_m J'_m(kr) \right\} e^{-kz} \cos m\theta, \\
 &\text{etc.}
 \end{aligned} \right\} \quad (18)$$

### III. Lamé and Clapeyron's Problem.

§10. We will apply the solution obtained in the last article to discuss the effect caused by a given normal pressure applied locally on the boundary. Suppose as a preliminary that a system of stress of the form

$$\left. \begin{aligned}
 \widehat{zz} &= \left\{ Z \cos m\theta + Z \sin m\theta \right\} J_m(kr), \\
 \widehat{zr} &= 0, \quad \widehat{z\theta} = 0
 \end{aligned} \right\} \quad (19)$$

is given at the surface  $z=0$ . Then we must have the following relations between the arbitrary constants:—

$$\begin{aligned}
-\mu C_m - 2\mu k D_m &= Z, \\
\frac{\lambda + \mu}{2} C_m + \mu k (B_m + D_m) &= 0, \\
A_m &= 0; \\
-\mu \bar{C}_m - 2\mu k \bar{D}_m &= \bar{Z}, \\
\frac{\lambda + \mu}{2} \bar{C}_m + \mu k (\bar{B}_m + \bar{D}_m) &= 0, \\
\bar{A}_m &= 0.
\end{aligned}$$

From these equations, combining (13) and (15), we have

$$\begin{aligned}
C_m &= \frac{Z}{\lambda + \mu}, & \bar{C}_m &= \frac{\bar{Z}}{\lambda + \mu}, \\
B_m &= \frac{Z}{2k(\lambda + \mu)}, & \bar{B}_m &= \frac{\bar{Z}}{2k(\lambda + \mu)}, \\
D_m &= -\frac{(\lambda + 2\mu)Z}{2\mu k(\lambda + \mu)}, & \bar{D}_m &= -\frac{(\lambda + 2\mu)\bar{Z}}{2\mu k(\lambda + \mu)}, \\
A_m &= 0, & \bar{A}_m &= 0,
\end{aligned}$$

Putting these values in the formulæ (12) and (14) and adding them together, we have an exact solution of the form

$$\left. \begin{aligned}
u_r &= \left\{ \frac{z}{2\mu} - \frac{1}{2(\lambda + \mu)k} \right\} \left\{ Z \cos m\theta + \bar{Z} \sin m\theta \right\} J'_m(kr) e^{-kz}, \\
u_\theta &= \left\{ \frac{z}{2\mu} - \frac{1}{2(\lambda + \mu)k} \right\} \left\{ \bar{Z} \cos m\theta - Z \sin m\theta \right\} \frac{m}{kr} J_m(kr) e^{-kz}, \\
u_z &= -\left\{ \frac{z}{2\mu} + \frac{\lambda + 2\mu}{2\mu(\lambda + \mu)k} \right\} \left\{ Z \cos m\theta + \bar{Z} \sin m\theta \right\} J_m(kr) e^{-kz} \end{aligned} \right\} \quad (20)$$

corresponding to the boundary conditions (19). The formulæ for stress are

$$\left. \begin{aligned}
\widehat{zz} &= (1 + kz) \left\{ Z \cos m\theta + \bar{Z} \sin m\theta \right\} J_m(kr) e^{-kz}, \\
\widehat{zr} &= -kz \left\{ Z \cos m\theta + \bar{Z} \sin m\theta \right\} J'_m(kr) e^{-kz} \\
\widehat{z\theta} &= -kz \left\{ \bar{Z} \cos m\theta - Z \sin m\theta \right\} \frac{m}{kr} J_m(kr) e^{-kz}, \\
&\text{etc.} \end{aligned} \right\} \quad (21)$$

§11. To generalize the above so that the solution may be suitable to discuss the effect of any given normal pressure at the boundary surface, suppose that  $Z$  and  $\bar{Z}$  are functions of  $k$  of the form  $Z_m(k)dk$  and  $\bar{Z}_m(k)dk$  respectively, and superpose the corresponding solutions for all positive values of  $k$ , then add them together for all integral values of  $m$ . Thus, corresponding to the boundary conditions

$$\left. \begin{aligned} \widehat{z}z &= \sum_{m=0}^{\infty} \int_0^{\infty} \left\{ Z_m(kr) \cos m\theta + \bar{Z}_m(k) \sin m\theta \right\} J_m(kr) dk, \\ \widehat{z}r &= 0, \quad \widehat{z}\theta = 0 \end{aligned} \right\} \quad (22)$$

at  $z=0$ , we have

$$\left. \begin{aligned} u_r &= \sum_{m=0}^{\infty} \frac{Z}{2\mu} \int_0^{\infty} \left\{ Z_m(k) \cos m\theta + \bar{Z}_m(k) \sin m\theta \right\} e^{-kz} J'_m(kr) dk \\ &\quad - \sum_{m=0}^{\infty} \frac{1}{2(\lambda + \mu)} \int_0^{\infty} \left\{ Z_m(k) \cos m\theta + \bar{Z}_m(k) \sin m\theta \right\} e^{-kz} J'_m(kr) \frac{dk}{k}, \\ u_\theta &= \sum_{m=0}^{\infty} \frac{mz}{2\mu r} \int_0^{\infty} \left\{ Z_m(k) \cos m\theta - \bar{Z}_m(k) \sin m\theta \right\} e^{-kz} J_m(kr) \frac{dk}{k} \\ &\quad - \sum_{m=0}^{\infty} \frac{m}{2(\lambda + \mu)r} \int_0^{\infty} \left\{ Z_m(k) \cos m\theta - \bar{Z}_m(k) \sin m\theta \right\} e^{-kz} J_m(kr) \frac{dk}{k^2}, \\ u_z &= - \sum_{m=0}^{\infty} \frac{Z}{2\mu} \int_0^{\infty} \left\{ Z_m(k) \cos m\theta + \bar{Z}_m(k) \sin m\theta \right\} e^{-kz} J_m(kr) dk \\ &\quad - \sum_{m=0}^{\infty} \frac{\lambda + 2\mu}{2\mu(\lambda + \mu)} \int_0^{\infty} \left\{ Z_m(k) \cos m\theta + \bar{Z}_m(k) \sin m\theta \right\} e^{-kz} J_m(kr) \frac{dk}{k}; \end{aligned} \right\} \quad (23)$$

and

$$\left. \begin{aligned} \widehat{z}z &= \sum_{m=0}^{\infty} \int_0^{\infty} (1 + kz) \left\{ Z_m(k) \cos m\theta + \bar{Z}_m(k) \sin m\theta \right\} e^{-kz} J_m(kr) dk, \\ \widehat{z}r &= - \sum_{m=0}^{\infty} z \int_0^{\infty} k \left\{ Z_m(k) \cos m\theta + \bar{Z}_m(k) \sin m\theta \right\} e^{-kz} J'_m(kr) dk, \\ \widehat{z}\theta &= - \sum_{m=0}^{\infty} \frac{mz}{r} \int_0^{\infty} \left\{ Z_m(k) \cos m\theta - \bar{Z}_m(k) \sin m\theta \right\} e^{-kz} J_m(kr) dk, \\ &\quad \text{etc.} \end{aligned} \right\} \quad (24)$$

More generally, if the boundary conditions are given in the form of an arbitrary function, e.g.

$$\left. \begin{aligned} \widehat{zz} &= f(r, \theta), \\ \widehat{zr} &= 0, \quad \widehat{z\theta} = 0 \end{aligned} \right\} \quad (25)$$

at  $z=0$ , the general solution can be obtained by making use of the integral theorem

$$F(r) = \int_0^\infty \widehat{J}_m(kr) k dk \int_0^\infty F(a) J_m(ka) a da, \quad (26)$$

provided the function  $f(r, \theta)$  can be expanded into a trigonometrical series of the form

$$f(r, \theta) = \sum_{m=0}^\infty \left\{ f_m(r) \cos m\theta + \bar{f}_m(r) \sin m\theta \right\}, \quad (27)$$

where  $f_m(r)$  and  $\bar{f}_m(r)$  are supposed to satisfy the above integral theorem.

Comparing the expansion (27) with  $(\widehat{zz})_0$  which follows from the first formula of (24) by putting  $z=0$ , we see that the functions  $Z_m(k)$  and  $\bar{Z}_m(k)$  which correspond to the boundary conditions (25) or (27) are the solutions of the integral equations

$$\begin{aligned} f_m(r) &= \int_0^\infty Z_m(k) J_m(kr) dk, \\ \bar{f}_m(r) &= \int_0^\infty \bar{Z}_m(k) J_m(kr) dk. \end{aligned}$$

Looking at the integral theorem (26), the solutions of these integral equations appear easily to be

$$\left. \begin{aligned} Z_m(k) &= k \int_0^\infty f_m(a) J_m(ka) a da, \\ \bar{Z}_m(k) &= k \int_0^\infty \bar{f}_m(a) J_m(ka) a da. \end{aligned} \right\} \quad (28)$$

Thus, substituting these values of  $Z_m(k)$  and  $\bar{Z}_m(k)$  in the formulæ (23) and (24) we get the solution answering to the

boundary condition (25). In his book of differential equations, H. WEBER<sup>1)</sup> solves the same problem by using the Cartesian coordinates. But it seems that his mode of using Fourier's theorem was anticipated by Lamé and Clapeyron.

#### IV. Examples in the Case of Symmetry.

§12. The solution for the case of symmetry round the origin, which is discussed by BOUSSINESQ with numerous examples, has been afterwards obtained by Prof. LAMB in the same way as adopted here. This case is implied, of course, in our solution. Suppose

$$\left. \begin{aligned} \widehat{zz} &= f(r), \\ \widehat{zr} &= 0, \quad \widehat{z\theta} = 0 \end{aligned} \right\} \quad (29)$$

are given at the surface  $z=0$ . The corresponding solution will then be obtained from (23) and (24), by taking only the first term ( $m=0$ ) in the summation. Thus

$$\left. \begin{aligned} u_r &= -\frac{z}{2\mu} \int_0^\infty Z(k) e^{-kz} J_1(kr) dk \\ &\quad + \frac{1}{2(\lambda+\mu)} \int_0^\infty Z(k) e^{-kz} J_1(kr) \frac{dk}{k}, \\ u_\theta &= 0, \\ u_z &= -\frac{z}{2\mu} \int_0^\infty Z(k) e^{-kz} J_0(kr) dk \\ &\quad - \frac{\lambda+2\mu}{2\mu(\lambda+\mu)} \int_0^\infty Z(k) e^{-kz} J_0(kr) \frac{dk}{k}; \end{aligned} \right\} \quad (30)$$

and

$$\left. \begin{aligned} \widehat{rr} &= -z \int_0^\infty Z(k) e^{-kz} J_0(kr) k dk + \frac{z}{r} \int_0^\infty Z(k) e^{-kz} J_1(kr) dk \\ &\quad + \int_0^\infty Z(k) e^{-kz} J_0(kr) dk - \frac{\mu}{(\lambda+\mu)r} \int_0^\infty Z(k) e^{-kz} J_1(kr) \frac{dk}{k}, \end{aligned} \right\}$$

1) Part. Diff. Gleichungen, vol. 2 (1912) §76—.



$$\left. \begin{aligned}
 \widehat{\theta\theta} &= -\frac{\lambda}{r} \int_0^\infty Z(k) e^{-kz} J_1(k) dk + \frac{\mu}{(\lambda + \mu)r} \int_0^\infty Z(k) e^{-kz} J_1(kr) \frac{dk}{k} \\
 &\quad + \frac{\lambda}{\lambda + \mu} \int_0^\infty Z(k) e^{-kz} J_0(kr) dk, \\
 \widehat{zz} &= z \int_0^\infty Z(k) e^{-kz} J_0(kr) k dk + \int_0^\infty Z(k) e^{-kz} J_0(kr) dk, \\
 \widehat{\theta z} &= 0, \\
 \widehat{zr} &= z \int_0^\infty Z(k) e^{-kz} J_1(kr) k dk, \\
 \widehat{r\theta} &= 0;
 \end{aligned} \right\} \quad (31)$$

where the auxiliary function  $Z$  is connected with the prescribed condition by

$$Z(k) = k \int_0^\infty f(a) J_0(ka) a da. \quad (32)$$

We shall now apply the general theorem to a few special examples.

### Example I.

§13. The first example, which is discussed by Prof. LAMB, is to find the effect of a given normal pressure concentrated at a point on the boundary, on the supposition that  $f(r)$  is zero for all values of  $r$  except those in the immediate neighbourhood of the origin, where it becomes infinitely great in such a manner that

$$\int_0^\infty f(r) \cdot 2\pi r \cdot dr = -H, \quad (33)$$

in which  $H$  is the total amount of the pressure applied and is finite. The function  $Z(k)$  now is

$$Z(k) = -\frac{H}{2\pi} k.$$

Putting this in (30) and (31), and then integrating we get

$$\left. \begin{aligned} u_r &= \frac{H}{4\pi\mu} \left\{ \frac{zr}{(r^2+z^2)^{3/2}} - \frac{\mu}{\lambda+\mu} \left[ \frac{1}{r} - \frac{z}{r(r^2+z^2)^{1/2}} \right] \right\} \\ u_z &= \frac{H}{4\pi\mu} \left\{ \frac{z^2}{(r^2+z^2)^{3/2}} + \frac{\lambda+2\mu}{\lambda+\mu} \cdot \frac{1}{(r^2+z^2)^{1/2}} \right\}; \end{aligned} \right\}^{(1)} \quad (34)$$

and

$$\left. \begin{aligned} \widehat{rr} &= -\frac{H}{2\pi} \left\{ \frac{3zr^2}{(r^2+z^2)^{3/2}} - \frac{\mu}{\lambda+\mu} \left[ -\frac{1}{r^2} - \frac{z}{r^2(r^2+z^2)^{1/2}} \right] \right\}, \\ \widehat{\theta\theta} &= \frac{H}{2\pi} \cdot \frac{\mu}{\lambda+\mu} \left\{ \frac{z(2r^2+z^2)}{r^2(r^2+z^2)^{3/2}} - \frac{1}{r^2} \right\}, \\ \widehat{rz} &= -\frac{H}{2\pi} \cdot \frac{3z^2}{(r^2+z^2)^{3/2}}, \\ \widehat{r\theta} &= -\frac{H}{2\pi} \cdot \frac{3z^2r}{(r^2+z^2)^{3/2}}, \\ \widehat{r\theta} &= 0, \quad \widehat{\theta z} = 0. \end{aligned} \right\} \quad (35)$$

At the surface ( $z=0$ ) they reduce simply to

$$\left. \begin{aligned} (u_r)_0 &= -\frac{H}{4\pi(\lambda+\mu)} \cdot \frac{1}{r}, \\ (u_z)_0 &= \frac{H(\lambda+2\mu)}{4\pi\mu(\lambda+\mu)} \cdot \frac{1}{r}; \end{aligned} \right\} \quad (36)$$

$$\left. \begin{aligned} (\widehat{rr})_0 &= \frac{H\mu}{2\pi(\lambda+\mu)} \cdot \frac{1}{r^2}, \\ (\widehat{\theta\theta})_0 &= -\frac{H\mu}{2\pi(\lambda+\mu)} \cdot \frac{1}{r^2}, \\ (\widehat{rz})_0 &= 0. \end{aligned} \right\} \quad (37)$$

§14. It is interesting to show by graph the state of deformation at different depths from the surface. For the sake of simplicity we assume that the material satisfies the Poisson's relation  $\lambda=\mu$ , and we take only one component of the displacement  $u_z$  for reference, which is now written in the simple form

$$u_z = \frac{H}{4\pi\mu} \left\{ \frac{z^2}{(r^2+z^2)^{3/2}} + \frac{3}{2} \cdot \frac{1}{(r^2+z^2)^{1/2}} \right\}.$$

The attached diagram is drawn on the supposition that  $H=4\pi\mu$

(1) The integrations have been carried out by Lamb, and so it is unnecessary to recapitulate them here.

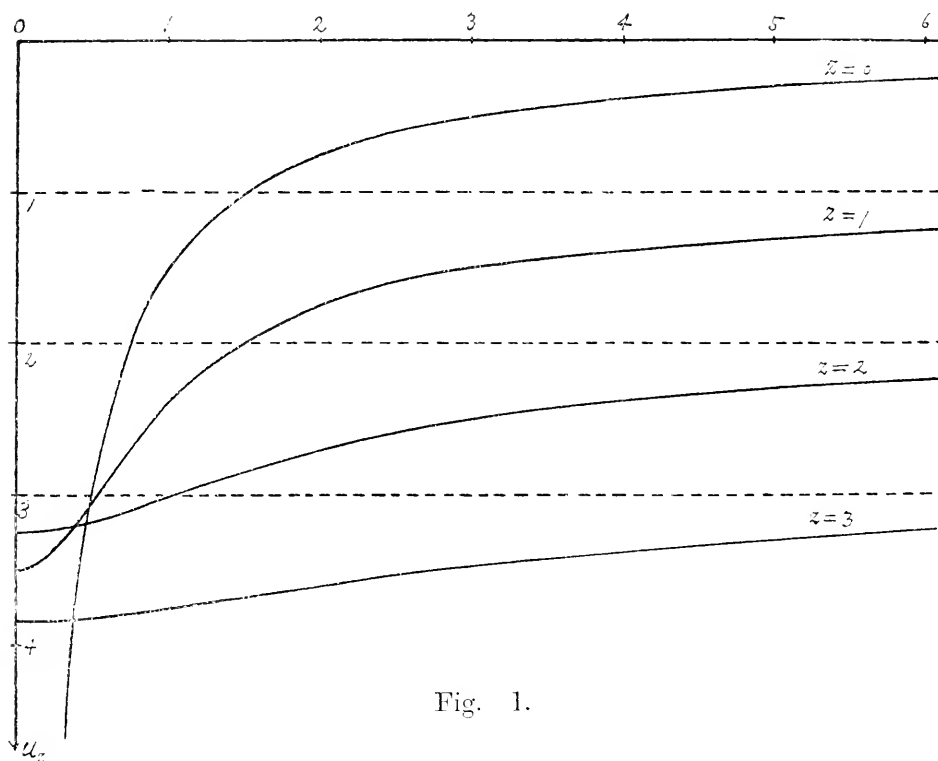


Fig. 1.

As seen from the diagram the state of affairs in the neighbourhood of the origin and even at a finite distance from it is an impossible one, and the mathematical theory of elasticity does not apply to such a case. The above argument must, if possible, be amended by a suitable process of analysis. The general solution found above is restricted to a special class of functions  $f(r)$  which satisfy the integral theorem (26). The hypothesis of point concentration of given pressure does not, in a strictly mathematical sense, satisfy this important condition, and the solution deduced from it may not be looked upon as a legitimate one, at least in the vicinity of the origin.<sup>1)</sup> What follows from the assumption of point-concentration of given pressure may, however, be considered, except locally, as the limiting case of the effect of a pressure which

1) A quite similar failure of the solution will occur in the problem of the deep-sea water-wave and allied problems which can be solved by the aid of Fourier's Integral Theorem.

acts on a slightly extended area of the boundary, which will be discussed in the next example.

### Example II.

§15. Suppose the normal pressure at  $z=0$  is given in the form

$$f(r) = -\frac{H}{2\pi} \cdot \frac{a}{(a^2 + r^2)^{3/2}}, \quad a > 0, \quad (38)$$

$H$  being its total amount. The function  $Z(k)$  is

$$Z(k) = -\frac{H}{2\pi} \cdot k \int_0^\infty \frac{a J_0(ka) a da}{(a^2 + a^2)^{3/2}} = -\frac{H}{2\pi} k e^{-ak} \quad (39)$$

Thus the solution corresponding to the boundary condition (38) will be given by

$$\left. \begin{aligned} u_r &= -\frac{Hz}{4\pi\mu} \int_0^\infty e^{-(z+a)\gamma} J_1(kr) k dk \\ &\quad - \frac{H}{4\pi(\lambda + \mu)} \int_0^\infty e^{-(z+a)\gamma} J_1(kr) dk, \\ u_z &= \frac{Hz}{4\pi\mu} \int_0^\infty e^{-(z+a)\gamma} J_0(kr) k dk \\ &\quad + \frac{H(\lambda + 2\mu)}{4\pi\mu(\lambda + \mu)} \int_0^\infty e^{-(z+a)\gamma} J_0(kr) dk; \end{aligned} \right\} \quad (40)$$

and

$$\left. \begin{aligned} \widehat{rr} &= -\frac{Hz}{2\pi} \int_0^\infty e^{-(z+a)\gamma} J_0(kr) k^2 dk - \frac{Hz}{2\pi r} \int_0^\infty e^{-(z+a)\gamma} J_1(kr) k dk \\ &\quad - \frac{H}{2\pi} \int_0^\infty e^{-(z+a)\gamma} J_1(kr) k dk + \frac{H\mu}{2\pi(\lambda + \mu)r} \int_0^\infty e^{-(z+a)\gamma} J_1(kr) dk, \\ \widehat{\theta\theta} &= \frac{Hz}{2\pi r} \int_0^\infty e^{-(z+a)\gamma} J_1(kr) k dk - \frac{H\mu}{2\pi(\lambda + \mu)r} \int_0^\infty e^{-(z+a)\gamma} J_1(kr) dk \\ &\quad - \frac{H\lambda}{2\pi(\lambda + \mu)} \int_0^\infty e^{-(z+a)\gamma} J_0(kr) k dk, \end{aligned} \right\} \quad (41)$$

$$\left. \begin{aligned} \widehat{\sigma_z} &= -\frac{H}{2\pi} \int_0^\infty e^{-(z+a)k} J_0(kr) k^2 dk - \frac{H}{2\pi} \int_0^\infty e^{-(z+a)k} J_0(kr) k dk, \\ \widehat{\sigma_r} &= -\frac{H}{2\pi} \int_0^\infty e^{-(z+a)k} J_1(kr) k^2 dk, \\ \widehat{r\theta} &= 0, \quad \widehat{\theta z} = 0. \end{aligned} \right\}$$

These integrals can be expressed in terms of zonal harmonics and the associated functions. If  $P_n(x)$  denotes the zonal harmonic of  $n$ th order and

$$P_n^{(m)}(x) = (1-x^2)^{-\frac{m}{2}} \int_x^1 \int_x^1 \dots P_n(x) dx^m,$$

$$P_n^{(m)}(x) = (1-x^2)^{-\frac{m}{2}} \frac{d^m P_n(x)}{dx^m},$$

then

$$\left. \begin{aligned} \int_0^\infty k^n e^{-kz} J_m(kr) dk &= \frac{(n+m)!}{(r^2+z^2)^{n+1/2}} \cdot P_n^{(m)}\left(\frac{z}{\sqrt{r^2+z^2}}\right), \\ \int_0^\infty k^n e^{-kz} J_m(kr) dk &= \frac{(n-m)!}{(r^2+z^2)^{n+1/2}} \cdot P_n^{(m)}\left(\frac{z}{\sqrt{r^2+z^2}}\right), \quad (m \leq n). \end{aligned} \right\} \quad (42)$$

By making use of these formulae, we have

$$\left. \begin{aligned} u_r &= \frac{H}{4\pi\mu} \left\{ \frac{zr}{(r^2+(z+a)^2)^{3/2}} - \frac{\mu}{\lambda+\mu} \left[ \frac{1}{r} - \frac{z+a}{r(r^2+(z+a)^2)^{1/2}} \right] \right\}, \\ u_z &= -\frac{H}{4\pi\mu} \left\{ \frac{z(z+a)}{(r^2+(z+a)^2)^{3/2}} + \frac{\lambda+2\mu}{\lambda+\mu} \cdot \frac{1}{(r^2+(z+a)^2)^{1/2}} \right\}; \end{aligned} \right\} \quad (43)$$

and

$$\left. \begin{aligned} \widehat{r r} &= -\frac{H}{2\pi} \left\{ \frac{a(r^2+(z+a)^2)+3zr^2}{(r^2+(z+a)^2)^{3/2}} - \frac{\mu}{\lambda+\mu} \left[ \frac{1}{r^2} - \frac{z+a}{r^2(r^2+(z+a)^2)^{1/2}} \right] \right\}, \\ \widehat{\theta \theta} &= \frac{H}{2\pi} \left\{ \frac{z}{(r^2+(z+a)^2)^{3/2}} - \frac{\mu}{\lambda+\mu} \left[ \frac{1}{r^2} - \frac{z+a}{r^2(r^2+(z+a)^2)^{1/2}} \right] \right. \\ &\quad \left. - \frac{\lambda}{\lambda+\mu} \cdot \frac{z+a}{(r^2+(z+a)^2)^{3/2}} \right\}, \\ \widehat{z z} &= -\frac{H}{2\pi} \cdot \frac{(3z+a)(z+a)^2+ar^2}{(r^2+(z+a)^2)^{3/2}}, \end{aligned} \right\} \quad (44)$$

$$\left. \begin{aligned} \widehat{zr} &= -\frac{H}{2\pi} \cdot \frac{3zr(z+a)}{(r^2+(z+a)^2)^{3/2}}, \\ r\theta &= 0, \quad \widehat{\theta z} = 0. \end{aligned} \right\}$$

If we proceed to the limit  $a \rightarrow 0$ , we have the same result as that due to the pressure of point concentration. But this limiting process is, in general, not permissible. A little examination of the value of  $\frac{\partial u_z}{\partial z}$  shows that the quantity  $a$  has a lower limit, such that

$$27a^2 > \frac{H(2\lambda+3\mu)^3}{4\pi\mu(\lambda+\mu)^3}, \quad (45)$$

in order to avoid the impossible state of affairs near the  $z$ -axis. At a distance from the origin great compared with  $a$ , these solutions reduce, in a first approximation, to those in Ex. I., so that the solution which follows from the assumption of point concentration of given pressure may be valid at a great distance from the origin, though only approximately.

§16. It is desirable here also to see how the displacement varies with the depth. On the same hypothesis as before, that  $\lambda = \mu$ , the variation of  $U_z$  is shown in the attached diagram, in which the upper curve represents the distribution of applied pressure (38) and the lower ones represent  $u_z$  on a proper scale.  $a$  is put equal to unity for the sake of simplicity.

§17. At the surface, the expressions for displacement and stress become

$$\left. \begin{aligned} (u_r)_0 &= -\frac{H}{4\pi(\lambda+\mu)} \left\{ \frac{1}{r} - \frac{a}{r(r^2+a^2)^{1/2}} \right\}, \\ (u_z)_0 &= \frac{H(\lambda+2\mu)}{4\pi\mu(\lambda+\mu)} \cdot \frac{1}{(r^2+a^2)^{1/2}}; \\ (\widehat{rr})_0 &= -\frac{H}{2\pi} \left\{ \frac{a}{(r^2+a^2)^{3/2}} - \frac{\mu}{\lambda+\mu} \left[ \frac{1}{r^2} - \frac{a}{r^2(r^2+a^2)^{1/2}} \right] \right\}, \\ (\theta\theta)_0 &= -\frac{H}{2\pi} \left\{ \frac{\mu}{\lambda+\mu} \left[ \frac{1}{r^2} - \frac{a}{r^2(r^2+a^2)^{1/2}} \right] + \frac{\lambda}{\lambda+\mu} \cdot \frac{a}{(r^2+a^2)^{3/2}} \right\}, \\ (zz)_0 &= -\frac{H}{2\pi} \cdot \frac{a}{(r^2+a^2)^{3/2}}, \\ (\widehat{rz})_0 &= 0, \end{aligned} \right\} \quad (47)$$

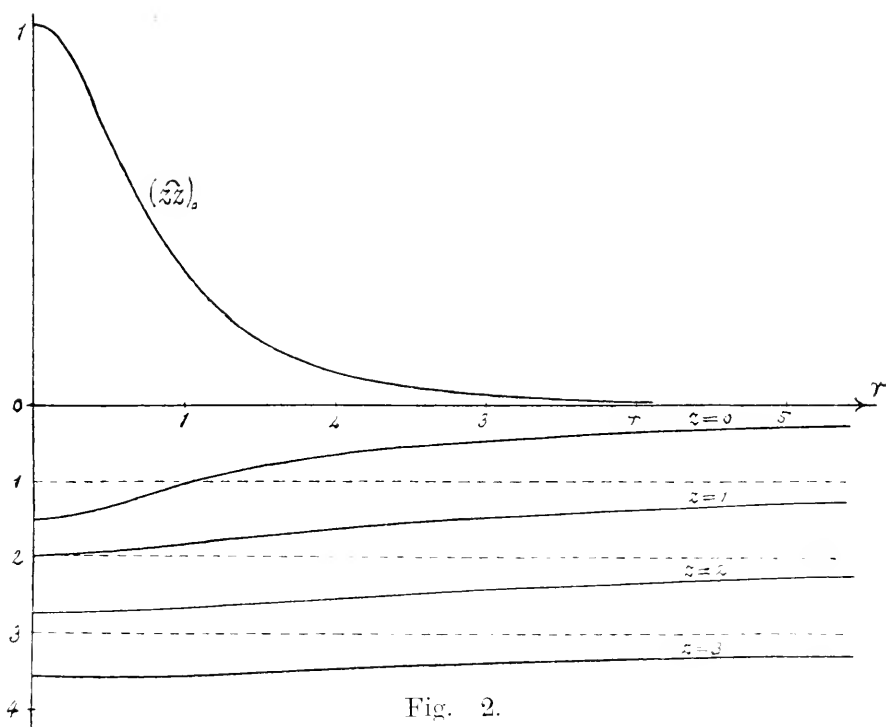


Fig. 2.

By integrating  $(u_z)_0$  over the surface, it may be easily seen that the total depression of the surface appears to be infinitely great, though it is caused by a finite normal pressure of total amount  $H$ . This seems again to be paradoxical, but that is not the case; if we calculate the work done by the given pressure, instead of total depression, it will appear to be finite, equal to  $\frac{H}{8\pi a} \cdot \frac{\lambda+2\mu}{\mu(\lambda+\mu)}$ , inversely as  $a$ .

§18. Let us now proceed to apply the results of this example to the theory of rupture of a foundation over which a heavy load is spread. There have been proposed several hypotheses concerning the conditions under which an elastic body is ruptured or nearly so. Among those hypotheses usually adopted there are two in which a limitation on stress is taken as the measure of tendency to rupture: the one which was introduced by LAMÉ is that the greatest tension should be less than a certain limit which is

different for different materials; the other which was recommended by G. H. DARWIN asserts that, as mere hydrostatic pressure can hardly affect the case, the maximum difference of the greatest and the least principal stresses should be less than a certain limit.<sup>1)</sup> These two hypotheses lead, in general, to different results. Either of them will give warning that danger is being approached, and in any case a certain factor of safety must, in practice, be adopted. Here we shall calculate the limits following from these two hypotheses and compare corresponding results.

For this purpose we have, in the first place, to find the distribution of principal stresses throughout the body concerned. Let  $N_1, N_2, N_3$  denote the values of principal stresses at the point  $(r, \theta, z)$ . Owing to the hypothesis of symmetry round the axis of  $z$ , the component  $\bar{\theta}\theta$  is one of the principal stresses, say  $N_2$ , as is to be seen from the formulae (31); and any plane passing through the  $z$ -axis is one of the principal planes of stress. The other two principal stresses will be found by

$$\left. \begin{aligned} N_1 &= \frac{1}{2} (\bar{r}r + \bar{z}z) + \frac{1}{2} \sqrt{(\bar{r}r - \bar{z}z)^2 + 4\bar{r}z^2}, \\ N_3 &= \frac{1}{2} (\bar{r}r + \bar{z}z) - \frac{1}{2} \sqrt{(\bar{r}r - \bar{z}z)^2 + 4\bar{r}z^2}. \end{aligned} \right\} \quad (48)$$

At the surface, since  $\bar{r}z = 0$ , the stress components  $\bar{r}r, \bar{\theta}\theta, \bar{z}z$  themselves are the principal stresses.

§19. Now, to apply these formulae to this example, let us assume<sup>2)</sup> that the pressure modulus  $\lambda$  is so great compared with the rigidity  $\mu$  that the material may be considered to be incompressible. Thus, substituting the values of the stress-components found in (44) in the formulae (48) and making  $\lambda = \infty$ , we have simply

$$\left. \begin{aligned} N_1 &= -\frac{H}{2\pi} \cdot \frac{3z+a}{(r^2+(z+a)^2)^{3/2}}, \\ N_3 = N_2 &= -\frac{H}{2\pi} \cdot \frac{a}{(r^2+(z+a)^2)^{3/2}}. \end{aligned} \right\} \quad (49)$$

1) There is another view often adopted, in which a limitation on strain is taken as the measure.

2) This supposition is not at all necessary, but it makes the calculation extraordinarily simple.



$N_1$  being greater than  $N_2$  and  $N_3$  which are equal. Thus the stress quadric at any point in the interior is a spheroid, of which the axis of rotation lies in a plane passing through the  $z$ -axis.

If we denote by  $D$  the difference of the greatest and the least principal stresses, then

$$D = N_1 - N_3 = -\frac{H}{2\pi} \cdot \frac{3z}{(r^2 + (z+a)^2)^{3/2}}. \quad (50)$$

$D$  is a maximum at the point  $(r=0, z=\frac{a}{2})$  and its value is

$$D_{max} = -\frac{2H}{9\pi a^2}, \quad (51)$$

while  $N_1$ , the greatest principal stress, is a maximum at the point  $(r=0, z=0)$  and

$$N_{1max} = -\frac{H}{2\pi a^2}. \quad (52)$$

Thus the latter maximum is greater than the former, and, moreover, the position where the rupture might occur is quite different for the two hypotheses: it is at a certain distance below the surface in the former, while it is at the surface in the latter.

In Fig. 3 it is shown how the greatest principal stress and the greatest difference of principal stresses along the  $z$ -axis vary with the depth from the surface.

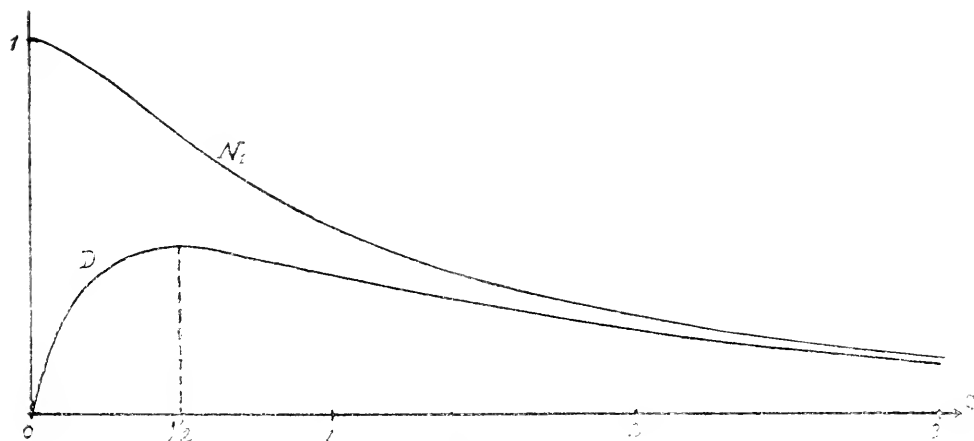


Fig. 3.

§20. To fix matters, suppose an isolated mountain or a high tower of uniform density with a circular base standing on the ground; the surface of the mountain or the other being given by the other by the equation

$$-z = \frac{m^3 h^4}{(m^2 h^2 + (n^3 - 1)r^2)^{3/2}}. \quad (53)$$

This equation is so adjusted that the height at the centre is  $h$  and that at the point  $r=mh$  is  $h/n$ . We shall make the rough assumption that each point on the surface of the ground is pressed normally downwards with a pressure given by the product of the specific gravity and the height of the mountain at that point. The quantity  $a$ , used in the above, is now

$$a = \frac{mh}{\sqrt{n^3 - 1}}.$$

In the annexed diagram, the upper curves are supposed to represent the profiles of mountains and the inner ones those of columnar buildings such as chimneys or monuments, the height being taken as unity, and  $m$  and  $n$  chosen properly.

Curve	$n$	$m$	$a/2$
$C_1$	1·837	1	0·7071
$C_2$	1·837	1·2	0·3536
$C_3$	2·828	1/3	0·1667
$C_4$	5·196	1/5	0·0707
$C_5$	11·180	1/10	0·0250

If we denote the specific gravity of the mountains or other bodies by  $w$ , then the total amount of pressure will be

$$H = \frac{2\pi w n^2 h^3}{n^3 - 1}.$$

The maximum of the greatest principal stress becomes

$$N_{1\text{ } aa} = -wh, \quad (54)$$

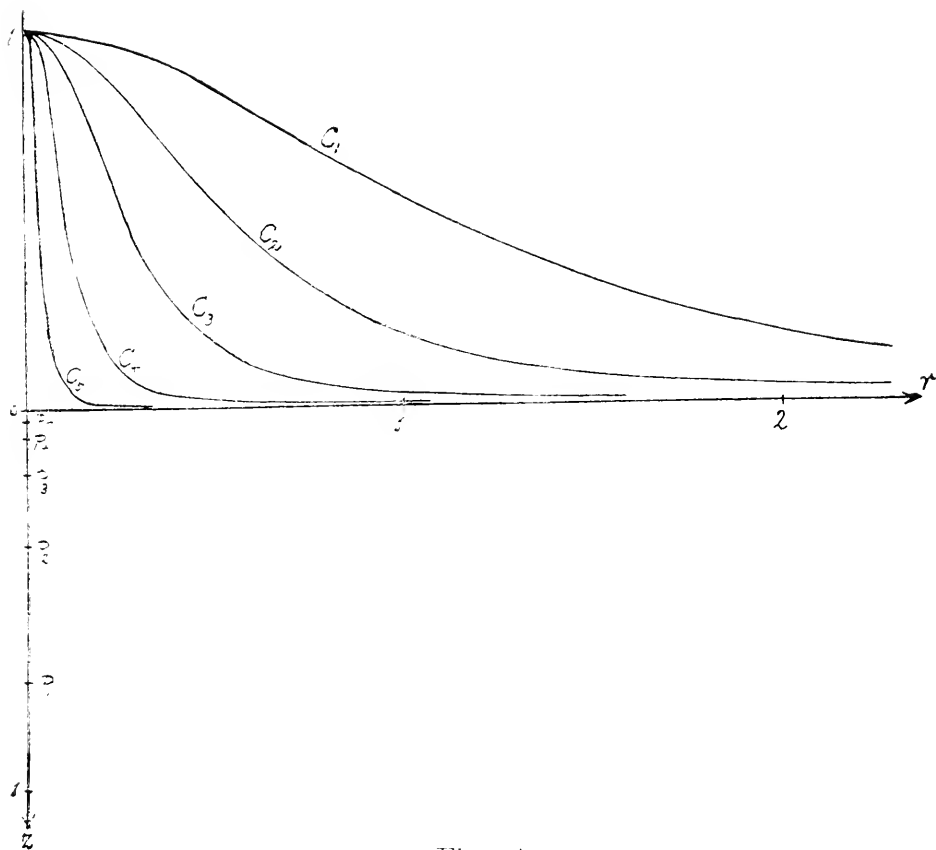


Fig. 4.

acting at the origin; and the maximum of the difference between the greatest and the least principal stress is

$$D_{\max} = -\frac{4}{9} wh, \quad (55)$$

acting at the point  $\left(r=0, z=\frac{a}{2}\right)$ . The values of  $a/2$  corresponding to the curves are calculated in the last column of the above table, and the positions of the critical points corresponding to them are shown also in the figure by the points  $P_1, P_2, \dots$ .

It will be interesting to find the limiting height of mountains, which stand on bases of several kinds of materials without crushing the latter. In the following table a few examples are given: the third column contains the greatest heights of a mountain given by

the formula (54), and in the fourth column are given those calculated by means of the formula (55); the value of  $w$  being taken as 3 grammes weight per cubic centimetre.

Material in the base	Strength to resist crushing in kg. per cm. <sup>2</sup>	Max. height in km. by (54)	Max. height in km. by (55)
Cement . . . . .	320	1.07	2.40
Strong sand stone . . . . .	800	2.67	6.00
Strong granite . . . . .	1600	5.33	12.00
Strong glass . . . . .	2400	8.00	18.00
Wrought iron . . . . .	3200	10.67	24.00

### Example III.

§21. Next we will consider the case in which a uniform normal pressure acts on the surface within a circular area of radius  $a$ , outside of which the surface is free from traction.

Suppose

$$f(r) = \begin{cases} -\frac{H}{\pi a^2}, & \text{for } a \geq r, \\ 0 & \text{,, } a < r \end{cases} \quad (56)$$

$H$  being again the total amount of the given pressure. The function  $Z(k)$  will be

$$Z(k) = -\frac{H}{\pi a^2} k \int_0^a J_0(ka) a da = -\frac{H}{\pi a} J_1(ka), \quad (57)$$

and the components of displacement can be computed from the formulæ

$$u_r = \begin{cases} \frac{Hz}{2\pi a \mu} \int_0^\infty e^{-kz} J_1(kr) J_1(ka) dk \\ - \frac{H}{2\pi a(\lambda + \mu)} \int_0^\infty e^{-kz} J_1(kr) J_1(ka) \frac{dk}{k}, \end{cases} \quad (58)$$

$$u_z = \left. \begin{aligned} & \frac{Hz}{2\pi a\mu} \int_0^\infty e^{-lz} J_0(kr) J_1(ka) dk \\ & + \frac{H(\lambda+2\mu)}{2\pi a\mu(\lambda+\mu)} \int_0^\infty e^{-lz} J_0(kr) J_1(ka) \frac{dk}{k} \end{aligned} \right\}$$

and those of stress are given by

$$\left. \begin{aligned} \widehat{rr} &= \frac{Hz}{\pi a} \int_0^\infty e^{-lz} J_0(kr) J_1(ka) k dk - \frac{Hz}{\pi a r} \int_0^\infty e^{-lz} J_1(kr) J_1(ka) dk \\ &\quad - \frac{H}{\pi a} \int_0^\infty e^{-lz} J_0(kr) J_1(ka) dk + \frac{H\mu}{\pi(\lambda+\mu)ar} \int_0^\infty e^{-lz} J_1(kr) J_1(ka) \frac{dk}{k}, \\ \widehat{\theta\theta} &= \frac{Hz}{\pi ar} \int_0^\infty e^{-lz} J_1(kr) J_1(ka) dk - \frac{H\mu}{\pi(\lambda+\mu)ar} \int_0^\infty e^{-lz} J_1(kr) J_1(ka) \frac{dk}{k} \\ &\quad - \frac{H\lambda}{\pi(\lambda+\mu)a} \int_0^\infty e^{-lz} J_0(kr) J_1(ka) dk, \\ \widehat{zz} &= -\frac{Hz}{\pi a} \int_0^\infty e^{-lz} J_0(kr) J_1(ka) k dk - \frac{H}{\pi a} \int_0^\infty e^{-lz} J_0(kr) J_1(ka) dk, \\ \widehat{zr} &= -\frac{Hz}{\pi a} \int_0^\infty e^{-lz} J_1(kr) J_1(ka) k dk, \\ \widehat{r\theta} &= 0, \quad \widehat{\theta z} = 0. \end{aligned} \right\} \quad (59)$$

§22. The integrals required here cannot be evaluated in a very simple way. Some of them are closely connected to the magnetic potential due to a circular current, or to the velocity-potential and stream function of a circular vortex and have been discussed by various authors. In his paper on the inductance of circular coils,<sup>1)</sup> Prof. H. NAGAOKA has devised a comparatively simple method which may be applied to evaluate all the integrals needed here. Let us follow his method and describe it briefly.

Put

$$R = \sqrt{a^2 - 2ar \cos \theta + r^2}, \quad (60)$$

then we have

$$\left. \begin{aligned} J_0(kr) J_1(ka) &= \frac{1}{\pi} \int_0^\pi J_0(kR) \cos \theta d\theta, \\ J_0(kr) J_1(ka) &= \frac{1}{\pi} \int_0^\pi J_1(kR) \frac{a-r \cos \theta}{R} d\theta, \end{aligned} \right\} \quad (61)$$

1) Phil. Mag., VI, 6 (1903), p. 19.

$$J_1(kr)J_1(ka) = \frac{kar}{\pi} \int_0^\pi \frac{J_1(kR) \sin^2 \theta}{R} d\theta \quad (61)$$

which follow from Neumann's addition theorem for the Bessel function. Making use of these formulæ and on referring to the formulæ (42), we obtain

$$\left. \begin{aligned} \int_0^\infty e^{-\lambda z} J_1(kr) J_1(ka) dk &= \frac{1}{\pi} \int_0^\pi \frac{\cos \theta}{\sqrt{R^2 + z^2}} d\theta, \\ \int_0^\infty e^{-\lambda z} J_0(kr) J_1(ka) dk &= \frac{1}{\pi} \int_0^\pi \frac{a - r \cos \theta}{R^2} d\theta - \frac{z}{\pi} \int_0^\pi \frac{a - r \cos \theta}{R^2 \sqrt{R^2 + z^2}} d\theta, \\ \int_0^\infty e^{-\lambda z} J_1(kr) J_1(ka) \frac{dk}{k} &= \frac{ar}{\pi} \int_0^\pi \frac{\sin^2 \theta}{R^2} d\theta - \frac{arz}{\pi} \int_0^\pi \frac{\sin^2 \theta}{R^2 \sqrt{R^2 + z^2}} d\theta, \\ \int_0^\infty e^{-\lambda z} J_0(kr) J_1(ka) \frac{dk}{k} &= \frac{1}{\pi} \int_0^\pi \frac{\sqrt{R^2 + z^2}}{R^2} (a - r \cos \theta) d\theta \\ &\quad - \frac{z}{\pi} \int_0^\pi \frac{a - r \cos \theta}{R^2} d\theta \end{aligned} \right\} \quad (62)$$

To find these integrals, put

$$\left. \begin{aligned} a &= \left( \frac{2}{ar} \right)^{\frac{1}{2}}, & \beta &= \frac{a^2 + r^2 + z^2}{6ar}, \\ c_1 &= \frac{2\beta}{a} = \frac{a^2 + r^2 + z^2}{3ara}, \\ c_2 &= \frac{1 - \beta}{a} = -\frac{a^2 + r^2 + z^2 - 6ar}{6ara}, \\ c_3 &= -\frac{1 + \beta}{a} = -\frac{a^2 + r^2 + z^2 + 6ar}{6ara} \end{aligned} \right\} \quad (63)$$

so that

$$\begin{aligned} c_3 &< c_2 < c_1, \\ c_1 + c_2 + c_3 &= 0, \end{aligned}$$

and change the integration variable from  $\theta$  to  $s$  by putting

$$\cos \theta = as + \beta,$$

then we have

$$\int_0^\pi \frac{\cos \theta}{\sqrt{R^2 + z^2}} d\theta = a^2 \int_{e_3}^{e_2} \frac{(s + \frac{1}{2}e_1)ds}{\sqrt{4(s-e_1)(s-e_2)(s-e_3)}},$$

similarly for the others.

Put again

$$s = \wp(u)$$

and denote by  $\omega_1$  and  $\omega_3$  the real and imaginary half-period respectively and  $\omega_2 = \omega_1 + \omega_3$ , then, since  $s$  or  $\wp(u)$  is real and lies between  $e_3$  and  $e_2$ ,  $s=e_3$  and  $s=e_2$  correspond to  $u=\omega_3$  and  $u=\omega_2$  respectively, if we take the sign of  $\wp'(u)$  to be positive.<sup>1)</sup> Thus

$$\begin{aligned} \int_0^\pi \frac{\cos \theta}{\sqrt{R^2 + z^2}} d\theta &= a^2 \int_{\omega_3}^{\omega_2} \left\{ \frac{1}{2}e_1 + \wp(u) \right\} du \\ &= a^2 \left( \frac{1}{2}e_1\omega_1 - \eta_1 \right). \end{aligned} \quad (64)$$

For the evaluation of the other integral, write

$$\wp(v) = \frac{a^2 + r^2 - 2ar\wp}{2ara} = \frac{2(a^2 + r^2) - z^2}{6ara}, \quad (65)$$

then we have

$$\int_0^\pi \frac{a - r \cos \theta}{R^2 \sqrt{R^2 + z^2}} d\theta = \frac{a}{2a} \omega_1 - \frac{r^2 - a^2}{4a^2 r} \int_{\omega_3}^{\omega_2} \frac{du}{\wp(v) - \wp(u)},$$

etc.

Now

$$\left. \begin{aligned} \int_{\omega_3}^{\omega_2} \frac{\wp'(v) du}{\wp(v) - \wp(u)} &= \left[ \log \frac{\sigma_3 u + v}{\sigma_3(u - v)} - 2u\zeta(v) \right]_{\omega_3}^{\omega_2} \\ &= 2 \left\{ v\eta_1 - \omega_1 \zeta(v) + m\pi i \right\} \end{aligned} \right\} \quad (66)$$

in which the term  $m\pi i$  enters because of the many-valued property of a logarithm. The actual value of  $m$  and  $\wp'(v)$  will be determined by the following consideration.

1 If we assume  $\wp'(u)$  to be negative, then  $s=e_1$  and  $s=e_2$  correspond to  $u=\omega_2$  and  $u=2\omega_1 + \omega_3$  respectively. But the same result will, as a matter of course, be obtained after integration.

From the definition of  $\mathfrak{F}(v)$  and  $e_1, e_2, e_3$ , it follows immediately that

$$\begin{aligned}\mathfrak{F}(v)-e_1 &= -\frac{v^2}{2ar\alpha}, \\ \mathfrak{F}(v)-e_2 &= -\frac{(a-r)^2}{2ar\alpha}, \\ \mathfrak{F}(v)-e_3 &= -\frac{(a+r)^2}{2ar\alpha},\end{aligned}$$

accordingly

$$e_2 < \mathfrak{F}(v) < e_1.$$

The last inequality shows that the value of  $v$  must be one of the following:

$$\left. \begin{aligned} \text{(i)} \quad v &= (2n+1)\omega_1 + (2n'+\theta)\omega_3, \\ \text{(ii)} \quad v &= (2n+1)\omega_1 + (2n'+2-\theta)\omega_3 \end{aligned} \right\} \quad (67)$$

where  $n$  and  $n'$  denote any integers, positive or negative, or zero and  $\theta$  a positive number less than unity.

To determine the value of  $m$  in the formula (66) for the value of  $v$  given in (i) of (67), observe that the integral on the left hand side of (66) and the function  $v\zeta_1 - \omega_3\zeta(v)$  change their values continuously as  $\theta$  varies from 0 to 1, while  $m$  remains unchanged during this variation. In the limit as  $\theta \rightarrow 0$ , the value of the integral is nil and

$$2v\zeta_1 - 2\omega_3\zeta(v) \rightarrow 2n\pi i,$$

and therefore we have

$$\text{(i)} \quad m = -n'.$$

Similarly for the value of  $v$  given in (ii) of (67), proceeding to the limit  $\theta \rightarrow 0$ , we find

$$\text{(ii)} \quad m = -(n'+1).$$

The value of  $\mathfrak{F}'(v)$  will be obtained from

$$\mathfrak{F}'(v) = 4\{\mathfrak{F}(v-e_1)\}\{\mathfrak{F}(v)-e_2\}\{\mathfrak{F}(v)-e_3\}.$$



In the present case, we get

$$\mathfrak{F}'(r) = \pm i \frac{(a^2 - r^2)}{2ar}.$$

It may easily be shown that the value of  $\mathfrak{F}'(r)$  is a pure imaginary quantity for the values of  $r$  given in (67), with positive sign for (i) and with negative sign for (ii). Therefore we have to take

$$\left. \begin{aligned} \mathfrak{F}'(r) &= +i \frac{(a^2 - r^2)}{2ar}, \\ m &= -n', \\ r &= (2n+1)\omega_1 + (2n'+\theta)\omega_2; \end{aligned} \right\}$$

for

$$\left. \begin{aligned} \mathfrak{F}'(r) &= -i \frac{(a^2 - r^2)}{2ar}, \\ m &= -(n'+1), \\ r &= (2n+1)\omega_1 + (2n'+2-\theta)\omega_2 \end{aligned} \right\}$$

for

in which  $0 < \theta < 1$ .

Hereafter we shall, for the sake of simplicity, take into account only the value of  $r$  which will be obtained by putting  $n=0$ ,  $n'=0$  in (i) of (67) viz.

$$r = \omega_1 + \theta\omega_2.$$

By this convention the term  $m\pi i$  disappears and the value of  $\mathfrak{F}'(r)$  is to be taken as

$$\mathfrak{F}'(r) = +i \frac{(a^2 - r^2)}{2ar}. \quad (68)$$

Thus

$$\int_0^\pi \frac{a - r \cos \theta}{R^2 \sqrt{R^2 + z^2}} d\theta = \frac{a}{2a} \left( \omega - \frac{r^2 - a^2}{2ar} \right) + \frac{1}{\mathfrak{F}'(r)} \left\{ rz_1 - \omega_1 z(r) \right\}. \quad (69)$$

Similarly we have

$$\begin{aligned} \int_0^\pi \frac{\sin^2 \theta}{R^2 \sqrt{R^2 + z^2}} d\theta &= \frac{a^2}{2ar} \left\{ \omega, \left[ \mathfrak{F}(r) + c_1 \right] - z_1 \right. \\ &\quad \left. - \frac{2[\mathfrak{F}(r) - c_1][\mathfrak{F}(r) - c_2]}{\mathfrak{F}'(r)} [rz_1 - \omega_1 z(r)] \right\}, \end{aligned} \quad (70)$$

$$\int_0^\pi \frac{\sqrt{R^2+z^2}}{R^2} (a-r\cos\theta) d\theta = \frac{2}{a\pi} (\eta_1 + e_1 \omega_1) - \frac{r^2-a^2}{a^2 r a^2} \omega_1 \\ + \frac{2(r^2-a^2)}{a^2 r a^2} \cdot \frac{\wp(v) - e_1}{\wp'(v)} \left\{ v \eta_1 - \omega_1 \zeta(v) \right\}. \quad (71)$$

The other integrals in (62) are found without the knowledge of elliptic functions.

$$\left. \begin{aligned} \int_0^\pi \frac{a-r\cos\theta}{R^2} d\theta &= \frac{\pi}{a} \text{ for } r < a, \\ &= 0 \quad ,, \quad r > a; \end{aligned} \right\} \quad (72)$$

$$\left. \begin{aligned} \int_0^\pi \frac{\sin^2\theta}{R^2} d\theta &= \frac{\pi}{2a^2} \quad ,, \quad r < a, \\ &= \frac{\pi}{2r^2} \quad ,, \quad r > a, \end{aligned} \right\} \quad (73)$$

§23. Substituting these values of integrals in (58) we obtain the following expressions for the displacement:

$$u_r = \frac{H a^2 z}{2 a \pi^2 \mu} \left\{ \frac{1}{2} e_1 \omega_1 - \eta_1 \right\} \\ - \frac{H}{2 a \pi (\lambda + \mu)} \left\{ \begin{aligned} &\frac{r}{2a} (r < a) \\ &\frac{a}{2r} (r > a) \end{aligned} \right\} + \frac{a^2 z}{2 \pi} [\eta_1 - \omega_1 (\wp(v) + e_1)] \\ + \frac{a^2 z}{\pi} [\wp(v) - e_2] \cdot [\wp(v) - e_3] \frac{v \eta_1 - \omega_1 \zeta(v)}{\wp'(v)} \left\{ \right. , \quad (74)$$

$$u_z = \frac{H z}{2 a \pi \mu} \left\{ \begin{aligned} &\frac{1}{a} (r < a) \\ &0 \quad (r > a) \end{aligned} \right\} - \frac{a z \omega_1}{2 a \pi} + \frac{z(r^2-a^2)}{2 a^2 r \pi} \cdot \frac{v \eta_1 - \omega_1 \zeta(v)}{\wp'(v)} \left\{ \right. \\ + \frac{H(\lambda+2\mu)}{2 a \pi \mu (\lambda + \mu)} \left\{ \begin{aligned} &\frac{z}{a} (r < a) \\ &0 \quad (r > a) \end{aligned} \right\} + \frac{2}{a a \pi} (\eta_1 + e_1 \omega_1) - \frac{r^2-a^2}{\pi a^2 r a^2} \omega_1 \\ + \frac{2(r^2-a^2)}{\pi a^2 r a^2} [\wp(v) - e_1] \frac{v \eta_1 - \omega_1 \zeta(v)}{\wp'(v)} \left\{ \right. . \quad (75)$$

§24. For purposes of calculation, it will be very convenient to have the formulæ expressed in terms of JACOBI'S  $q$ -series.  $q$  is defined by

$$q = e^{i\pi\tau}, \quad \tau = \frac{\omega_3}{\omega_1}.$$

After WEIERSTRASS, if we put

$$l = \frac{(e_1 - e_3)^i - (e_1 - e_2)^i}{(e_1 - e_3)^i + (e_1 - e_2)^i},$$

then  $q$  can be computed from

$$q = \frac{l}{2} + 2\left(\frac{l}{2}\right)^5 + 15\left(\frac{l}{2}\right)^9 + 150\left(\frac{l}{2}\right)^{13} + O(l^{17}),$$

of which the first two or three terms are usually sufficient. The  $q$ -series of the functions needed here are as follows:—

$$\begin{aligned} \omega_1 &= \frac{\pi}{2} \left(\frac{a}{2}\right)^{\frac{1}{2}} \vartheta_2^2(o), \\ \eta_1 &= -\frac{1}{12\omega_1} \cdot \frac{\vartheta_1''(o)}{\vartheta_1'(o)}, \\ \frac{1}{2} e_1 \omega_1 - \eta_1 &= \frac{1}{8\omega_1} \left\{ \frac{\vartheta_1''(o)}{\vartheta_1'(o)} - \frac{\vartheta_2''(o)}{\vartheta_2'(o)} \right\}, \\ \eta_1 + e_1 \omega_1 &= \frac{\pi^2}{\omega_1} \left\{ \frac{1}{4} + 2 \sum_{n=1}^{\infty} \frac{q^n}{(1+q^{2n})^2} \right\}; \end{aligned}$$

and

$$\begin{aligned} \vartheta_2(o) &= 2q^{\frac{1}{2}}(1+q^2+q^6+q^{12}+\dots), \\ \vartheta_1'''(o) &= -2\pi^3 q^{\frac{1}{2}}(1-3^3q^2+5^3q^6-7^3q^{12}+\dots), \\ \vartheta_1'(o) &= 2\pi q^{\frac{1}{2}}(1-3q^2+5q^6-7q^{12}+\dots), \\ \vartheta_2'(o) &= -2\pi^3 q^{\frac{1}{2}}(1+3^2q^2+5^2q^6+7^2q^{12}+\dots). \end{aligned}$$

§25. The calculation of the term  $v\eta_1 - \omega_1 \zeta(v)$  requires a little explanation. By the formula

$$e^{-\frac{1}{2} \cdot \frac{\eta_1}{\omega_1} v^2} \cdot \sigma(v) = 2\omega_1 \frac{\vartheta_1\left(\frac{v}{2\omega_1}\right)}{\vartheta_1'(o)},$$

we have

$$v\eta - \omega_1 \zeta(v) = -\frac{1}{2} \cdot \frac{\vartheta_1' \left( \frac{v}{2\omega_1} \right)}{\vartheta_1 \left( \frac{v}{2\omega_1} \right)}.$$

Making use of the expansion formula of the right member, we get

$$v\eta - \omega_1 \zeta(v) = -\frac{\pi}{2} \left\{ \cot \frac{\pi v}{2\omega_1} + 4 \sum_{n=1}^{\infty} \frac{q^{2n}}{1-q^{2n}} \cdot \sin \frac{n\pi v}{\omega_1} \right\}. \quad (76)$$

The quantity  $v$  may be calculated by utilizing the WEIERSTRASS' formula to any degree of accuracy,<sup>1)</sup> and therefore the value of the function  $v\eta - \omega_1 \zeta(v)$ . The approximate value of this function can, however, be found in the following way:

Put

$$\frac{1}{2} \cdot \frac{(e_1 - e_2)^4 (\wp(v) - e_3)^4 - (e_1 - e_3)^4 (\wp(v) - e_2)^4}{(e_1 - e_2)^4 (\wp(v) - e_3)^4 + (e_1 - e_3)^4 (\wp(v) - e_2)^4} = t,$$

and

$$\begin{aligned} & \frac{1}{2} \cdot \frac{(e_1 - e_3)^4 \sigma_2(v) - (e_1 - e_2)^4 \sigma_3(v)}{(e_1 - e_3)^4 \sigma_2(v) + (e_1 - e_2)^4 \sigma_3(v)} \\ &= \frac{q \cos \frac{v\pi}{\omega_1} + q^9 \cos \frac{3v\pi}{\omega_1} + \dots}{1 + 2q^4 \cos \frac{2v\pi}{\omega_1} + 2q^{16} \cos \frac{4v\pi}{\omega_1} + \dots} = Q(v), \end{aligned}$$

then, since  $e_2 < \wp(v) < e_1$ , we shall have

$$Q(v - \omega_1) = t.^{2)}$$

As  $q^4$  is usually a very small quantity, we may take

$$\cos \frac{\pi(v - \omega_1)}{\omega_1} = \frac{t}{q} = s \text{ say}$$

with a close approximation. Since  $v - \omega_1 = \theta \omega_1$  purely imaginary, we may put

$$\frac{\pi(v - \omega_1)}{\omega_1} = ix.$$

1) This method has been adopted by Prof. NAGAOKA, loc. cit.

2) HALPHEN, Traité des Fonctions Elliptiques, I, p. 274.

$x$  being a real quantity, then

$$\cosh x = s,$$

and we have

$$\cot \frac{\pi c}{2\omega_c} = -i \tanh \frac{x}{2} = -i \left( \frac{s-1}{s+1} \right)^{\frac{1}{2}},$$

$$\sin \frac{\pi c}{\omega_c} = -i \sinh x = -i(s^2-1)^{\frac{1}{2}},$$

$$\sin \frac{2\pi c}{\omega_c} = i \sinh 2x = 2is(s^2-1)^{\frac{1}{2}},$$

.....

Substituting these values in the equation (76), we have

$$v\zeta_1 + \omega_c \zeta(v) = \frac{i\pi}{2} \left\{ \left( \frac{s-1}{s+1} \right)^{\frac{1}{2}} + 4q^2(s^2-1)[1-q^2(2s-1)] \right\}.$$

This approximation formula is recommended for the case in which  $\theta < \frac{1}{2}$ .

For the case  $\theta > \frac{1}{2}$ , if we put

$$\frac{(c_1 - c_2)^{\frac{1}{2}}(c_1 - c - c_2 - \xi(v))^{\frac{1}{2}}}{(c_1 - c_2)^{\frac{1}{2}}(c_1 - c)^{\frac{1}{2}} + c_2 - \xi(v)} = t',$$

then we shall have

$$Q(v - \omega_c) = t',$$

and making use of this formula, we shall obtain an approximation formula which is convenient for the case  $\theta > \frac{1}{2}$ .

§26. The expressions obtained in §23 are rather complicated, and the state of deformation can hardly be grasped at a glance. The formula for the displacement at the surface is, however, comparatively simple and can be calculated with any accuracy.

Putting  $z=0$  in the general formulae, we obtain

$$(u_r)_0 = - \frac{H}{4\pi\mu(\lambda + \mu)} \begin{cases} \frac{r}{a} & (r < a) \\ a & (r > a) \end{cases} \quad (77)$$

and

$$(u_z)_0 = \frac{H}{\pi a^2} \cdot \frac{\lambda + 2\mu}{2(\lambda + \mu)\mu} \cdot \frac{1}{\pi} \left\{ \frac{2}{a} (z_1 + e_1 \omega_1) - \frac{r^2 - a^2}{ar a^2} \omega_1 \right\} \quad (78)$$

where

$$a = \left( \frac{2}{ar} \right)^{\frac{1}{3}},$$

$$e_1 = \frac{a^2 + r^2}{3ara}, \quad e_2 = -\frac{a^2 + r^2 - 6ar}{6ara}, \quad e_3 = -\frac{a^2 + r^2 + 6ar}{6ara}.$$

At the surface the value of  $l$  becomes simply

$$l = \frac{(r+a)^{\frac{1}{3}} - |r-a|^{\frac{1}{3}}}{(r+a)^{\frac{1}{3}} + |r-a|^{\frac{1}{3}}},$$

so that the use of the  $q$ -series is very advantageous for the calculation, especially at the points near the origin or at a distance from it. For example, at the point  $r = 3a$ , we have

$$\frac{l}{2} = 0.085786, \quad q = 0.085796;$$

thus, even for the value  $r = 3a$ , we may neglect the terms after  $l^4$  and  $q^4$  in the series. For larger values of  $r$  the  $q$ -series converge of course very rapidly.<sup>1)</sup>

§27. The formula for  $(u_z)_0$  can be transformed into the form which is convenient for the use of LEGENDRE's table of elliptic integrals. If we remember that

$$z_1 + e_1 \omega_1 = \sqrt{e_1 - e_3} E,$$

$$\omega_1 = \frac{K}{\sqrt{e_1 - e_3}},$$

$K$  and  $E$  being the first and the second complete elliptic integrals with the moduli  $k$  and  $k'$ , and

$$k^2 = \frac{4ar}{(r+a)^2}, \quad k'^2 = \left( \frac{r-a}{r+a} \right)^2,$$

the expression for  $(u_z)_0$  becomes

1) For the point near the edge of the circle, the calculation may be undertaken by using similar series, specified by  $q_1$  and  $l_1$ . See below.

$$(u_z)_0 = \frac{H}{\pi a^2} \cdot \frac{\lambda+2\mu}{2(\lambda+\mu)\mu} \cdot \frac{1}{\pi} \left\{ (r+a)E - (r-a)K \right\}. \quad (79)$$

At the centre of the loaded circle, since

$$k = 0, \quad K = E = \frac{\pi}{2},$$

we get

$$(u_z)_0 = \frac{H}{\pi a} \cdot \frac{\lambda+2\mu}{2(\lambda+\mu)\mu}, \quad (80)$$

and at the periphery of the circle ( $r=a$ ), since

$$k = 1, \quad E = 1, \quad K \rightarrow \log \frac{4}{k'}, \quad (r-a)K \rightarrow 0,$$

we have

$$(u_z)_0 = \frac{H}{\pi a} \cdot \frac{\lambda+2\mu}{2(\lambda+\mu)\mu} \cdot \frac{2}{\pi}. \quad (81)$$

The values of  $(u_z)$ , at the centre and at the periphery of the circle bear the constant ratio  $\pi/2$ , and this is independent of the elastic constants and radius.

At the centre, as will be seen from the formula (80), the vertical displacement varies inversely as the radius, when the same amount of total pressure is applied to different circular areas, while it varies directly as the radius when the pressure of the same intensity is applied to different areas. The same relation holds at the edge of the circle, with regard to both the components, radial and vertical, of the displacement.

By the aid of the LEGENDRE table of  $K$  and  $E$ , we can trace by a graph the general march of  $(u_z)_0$ . The next diagram is drawn in this way, where the radius  $a$  is taken as unity and the pressure  $H$  is taken equal to  $2\pi a\mu(\lambda+\mu)/(\lambda+2\mu)$

§28. To find the formulæ for stress we need two more integrals which can be also carried out by the same method as before. We have, from (61), that

1) This result may be obtained from (58) directly by using the formula  $\int_0^\infty J_0(ka) \frac{dk}{k} = 1$ . The result (80) and (81) agree with those given by BOUSSINESQ, p. 140, i.e.

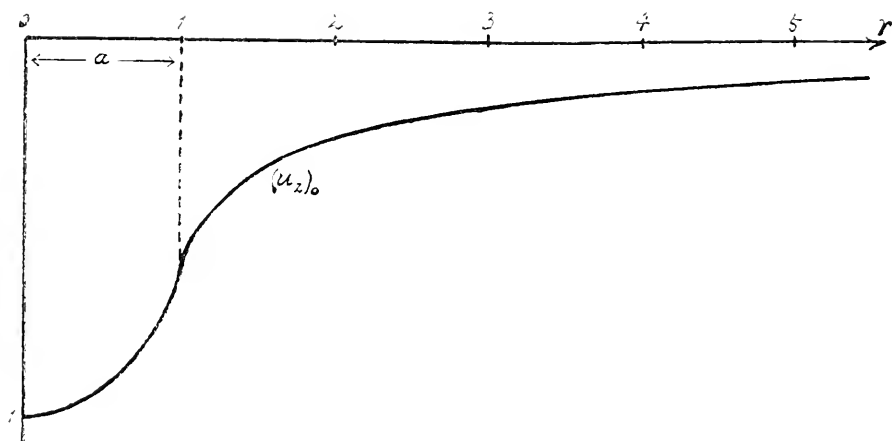


Fig. 5.

$$\left. \begin{aligned} \int_0^{\infty} e^{-kz} J_1(kr) J_1(ka) k dk &= \frac{z}{\pi} \int_0^{\pi} \frac{\cos \theta}{(R^2 + z^2)^{3/2}} d\theta, \\ \int_0^{\infty} e^{-kz} J_0(kr) J_1(ka) k dk &= \frac{1}{\pi} \int_0^{\pi} \frac{a - r \cos \theta}{(R^2 + z^2)^{3/2}} d\theta \end{aligned} \right\} \quad (82)$$

$R$  being defined by (60). Of course we may find their values by differentiation of the integrals already found with respect to  $z$ , but, owing to the complexity of the elliptic functions, it will be seen that the direct method of integration is much easier. By the same transformation of variables as before, we have

$$\int_0^{\pi} \frac{\cos \theta}{(R^2 + z^2)^{3/2}} d\theta = \frac{a^4}{4} \int_{\omega_3}^{\omega_2} \frac{3e_1/2}{e_1 - \wp(u)} du - \frac{a^4}{4} \omega_1,$$

and by the aid of the formula

$$\frac{1}{\wp(u) - e_1} = \frac{\wp(u + \omega_1) - e_1}{(e_1 - e_2)(e_1 - e_3)},$$

the integral can be found to be

$$\int_0^{\pi} \frac{\cos \theta}{(R^2 + z^2)^{3/2}} d\theta = \frac{a}{2ar} \left\{ \frac{3e_1(\gamma_1 + e_1\omega_1)}{2(e_1 - e_2)(e_1 - e_3)} - \omega_1 \right\} \quad (83)$$



Similarly the second integral in (82) is

$$\int_0^\pi \frac{a-r \cos \theta}{(R^2+z^2)^{3/2}} d\theta = \frac{1}{2ar} \left\{ \frac{(2a-3e_1ra)(\gamma_1+e_1\omega_1)}{2(e_1-e_2)(e_1-e_3)} + ar\omega_1 \right\} \quad (84)$$

Substituting these values and those found before in the formulæ (59), we have for the stress

$$\begin{aligned} \widehat{rr} = & \frac{Hz a}{2\pi^2 a^2 r} \left\{ \frac{(2a-3arc_1)(\gamma_1+e_1\omega_1)}{2a(e_1-e_2)(e_1-e_3)} + 2r\omega_1 - a\omega(e_1\omega_1-2\gamma_1) \right. \\ & - \frac{r^2-a^2}{a\omega} \cdot \frac{v\gamma_1-\omega_1\zeta(r)}{\wp'(r)} + \frac{a\mu}{\lambda+\mu} \left[ \gamma_1-e_1\omega_1-\omega \wp(r) \right. \\ & \left. \left. + 2[\wp(r)-e_2] \cdot [\wp(r)-e_3] \cdot \frac{v\gamma_1-\omega_1\zeta(r)}{\wp'(r)} \right] \right\} \\ & - \frac{H}{\pi a} \left\{ \frac{1}{a} (r < a) + \frac{\mu}{(\lambda+\mu)r} \cdot \frac{r}{2a} (r < a) \right. \\ & \left. \frac{0}{a} (r > a) + \frac{a}{2r} (r > a) \right\}, \quad (85) \end{aligned}$$

$$\begin{aligned} \widehat{\theta\theta} = & \frac{Hz a^2}{2\pi^2 ar} \left\{ e_1\omega_1-2\gamma_1 + \frac{\lambda}{(\lambda+\mu)a\omega} \left[ r\omega_1 - \frac{r^2-a^2}{a\omega} \cdot \frac{v\gamma_1-\omega_1\zeta(r)}{\wp'(r)} \right] \right. \\ & \left. - \frac{\mu}{\lambda+\mu} \left[ \gamma_1-e_1\omega_1-\omega \wp(r) + 2[\wp(r)-e_2] \cdot [\wp(r)-e_3] \cdot \frac{v\gamma_1-\omega_1\zeta(r)}{\wp'(r)} \right] \right\} \\ & - \frac{H}{\pi(\lambda+\mu)ar} \left\{ \mu \left[ \frac{r}{2a} (r < a) + \frac{a}{2r} (r > a) \right] + \lambda \left[ \frac{r}{a} (r < a) \right. \right. \\ & \left. \left. \frac{0}{a} (r > a) \right] \right\}, \quad (86) \end{aligned}$$

$$\begin{aligned} \widehat{zz} = & -\frac{Hz}{2\pi^2 a^2 r} \left\{ \frac{(2a-3arc_1)(\gamma_1+e_1\omega_1)}{2(e_1-e_2)(e_1-e_3)} + \frac{r^2-a^2}{a} \cdot \frac{v\gamma_1-\omega_1\zeta(r)}{\wp'(r)} \right\} \\ & - \frac{H}{\pi a} \left\{ \frac{1}{a} (r < a) \right\}, \quad (87) \end{aligned}$$

$$\widehat{zr} = -\frac{Hz^2 a}{2\pi^2 a^2 r} \left\{ \frac{3e_1(\gamma_1+e_1\omega_1)}{2(e_1-e_2)(e_2-e_3)} - \omega \right\}, \quad (88)$$

$$\widehat{r\theta} = 0, \quad \widehat{\theta z} = 0.$$

§29. At the surface these expressions for the stress reduce to simpler ones.

$$\left. \begin{aligned} (\widehat{rr})_0 &= -\frac{2\lambda+\mu}{2(\lambda+\mu)} \cdot \frac{H}{\pi a^2} \quad (r < a), \\ &= -\frac{\mu}{2(\lambda+\mu)} \cdot \frac{H}{\pi r^2} \quad (r > a); \\ (\widehat{\theta\theta})_0 &= -\frac{2\lambda+\mu}{2(\lambda+\mu)} \cdot \frac{H}{\pi a^2} \quad (r < a); \\ &= -\frac{\mu}{2(\lambda+\mu)} \cdot \frac{H}{\pi r^2} \quad (r < a). \\ (\widehat{rz})_0 &= -\frac{H}{\pi a^2} \quad (r < a), \\ &= 0 \quad (r > a); \\ (\widehat{zr})_0 &= 0, \end{aligned} \right\} \quad (89)$$

All the tractions acting on the boundary vanish, as they ought to, under the conditions of our problem, except a uniform pressure on the circle of radius  $a$ . The state of stress just below the surface is made up of a simple and beautiful scheme of the pressure system with a radial tension equal to  $-\frac{2\lambda+\mu}{2(\lambda+\mu)} \cdot \frac{H}{\pi a^2}$  inside the circle, and  $-\frac{\mu}{2(\lambda+\mu)} \cdot \frac{H}{\pi r^2}$  outside it; and a transverse tension equal to  $-\frac{2\lambda+\mu}{2(\lambda+\mu)} \cdot \frac{H}{\pi a^2}$  inside the circle, and  $-\frac{\mu}{2(\lambda+\mu)} \cdot \frac{H}{\pi r^2}$  outside it.

§30. Along the edge of the loaded circle there occurs a singularity of stress. We have seen already that as a rule the component stress  $\widehat{rz}$  vanishes at the boundary surface. But this is not always the case. If we put  $r=a$  in (88) and then proceed to the limit  $z \rightarrow 0$ , we shall have

$$(\widehat{rz})_0 = -\frac{1}{\pi} \cdot \frac{H}{\pi a^2}, \quad (r = a). \quad (90)$$

Thus the tangential traction  $(\widehat{rz})_0$  does not vanish at the periphery of the loaded area, which is contradictory to our assumed boundary

condition. It appears that along the circumference of the loaded circle a radial shearing stress of magnitude equal to the given normal pressure, divided by  $\pi$ , should be applied. This was also pointed out by BOUSSINESQ.<sup>1)</sup> But the area on the boundary over which this shearing stress applies is infinitely small, so that it is practically of no account at all. This singularity possibly means that the region in the interior of the body in which the stress component  $\widehat{r\theta}$  exists has a cuspidal edge, which touches the boundary surface at the periphery of the circle. To avoid the above difficulty, BOUSSINESQ supposed that at the edge of the loaded area the pressure decreases more or less rapidly to zero, instead of vanishing abruptly.<sup>2)</sup> If, in the actual problem, there were no singularity, this consideration might lead to legitimate results.

§31. In this example, it is not easy to calculate the maximum of the greatest principal stress or that of the difference between the greatest and the least principal stresses, even when the material is incompressible, consequently we shall abandon the general discussion concerning the conditions of rupture. But if we confine our attention only to the condition which determines how much load the body can sustain without breaking at the surface, the problem becomes tractable.

The equation (89) gives

$$\begin{aligned} (\widehat{rr})_0 = (\widehat{\theta\theta})_0 &= -\frac{E-\mu}{2\mu} \cdot \frac{H}{\pi a^2}, \\ (\widehat{rz})_0 &= -\frac{H}{\pi a^2} \end{aligned}$$

for  $r < a$ , in which the elastic constants  $\lambda$  and  $\mu$  are replaced by Young's modulus  $E$  and rigidity  $\mu$ . Since  $3\mu > E$  in ordinary materials the component  $(\widehat{rz})_0$  is the greatest. The difference between the greatest and the least principal stresses at the surface is

1) BOUSSINESQ p. 148. l.c.

2) For example, we might take  $f(r) = \frac{A}{1+r^{10}}$  or a similar relation. But the analysis might be very complicated.

$$D_0 = - \frac{3\mu - E}{2\mu} \cdot \frac{H}{\pi a^2}.$$

The values of  $(\bar{z}\bar{z})_0$  and  $D_0$  might give the condition of rupture of the surface.

§32. Now we shall apply this solution to the geophysical phenomena mentioned in the introduction. Dr. C. CHREE<sup>1)</sup> followed by Prof. NAGAOKA<sup>2)</sup> finds a formula, by using the solution obtained by BOUSSINESQ, to calculate the deviation of the direction of gravity due to the attraction of a material loading on the surface of the earth. The same result will be attained of course from our solution. The expression of the vertical displacement at a point on the surface

$$(u_z)_0 = \frac{\lambda + 2\mu}{2\mu(\lambda + \mu)} \int_0^{\pi} \int_0^{\pi} k r \, dk \int_0^{\pi} p(r') J_0(kr') r' dr' d\epsilon$$

where  $p(r')$  is the pressure produced by the material load, can be transformed into

$$(u_z)_0 = \frac{1}{2\pi} \cdot \frac{\lambda + 2\mu}{2\mu(\lambda + \mu)} \int_0^{2\pi} \int_0^{\pi} \frac{p(r')}{R'} r' dr' d\epsilon$$

by making use of NEUMANN'S addition theorem for the BESSEL function, where  $R'$  stands for

$$R' = \sqrt{r^2 - 2rr' \cos \epsilon + r'^2}$$

On the other hand, if we denote the attraction constant by  $\gamma$ , and gravity, prior to the application of the load, by  $g$ , then the gravitation-potential at a point on the surface due to the load can be expressed by

$$V = \frac{\gamma}{g} \int_0^{2\pi} \int_0^{\pi} \frac{p(r')}{R'} r' dr' d\epsilon,$$

provided the height of the material load is negligibly small compared with the distance of the point under consideration from

1) Phil. Mag. (V) vol. 43 (1897) p. 177.

2) Tokyo, Sug. But. Kizi (VI) (1912) p. 28.

any point in the loaded area. Comparing the above two expressions we have

$$V = \frac{2\pi r}{g} \cdot \frac{2\mu(\lambda + \mu)}{\lambda + 2\mu} (u_z),$$

Thus the direction of gravity becomes, in consequence of the attraction of the load, inclined to the vertical at the angle  $\zeta'$  which will be determined by

$$\tan \zeta' = \frac{2\pi r}{g^2} \cdot \frac{2\mu(\lambda + \mu)}{\lambda + 2\mu} \left( \frac{\partial u_z}{\partial r} \right), \quad (91)$$

while its tilting effect is expressed by

$$\tan \zeta = \left( \frac{\partial u_z}{\partial r} \right)_0. \quad (92)$$

§33. In the present example, in which a uniform material loading is confined in the circle of radius  $a$ , we have, from the formula (58),

$$\left( \frac{\partial u_z}{\partial r} \right)_0 = - \frac{H}{\pi a} \cdot \frac{\lambda + 2\mu}{2\mu(\lambda + \mu)} \left[ \int_0^{\infty} e^{-\omega_1 z} J_1(kr) J_1(ka) dk \right]_{z=0}.$$

Referring to the formulæ (61), (62) and (64), we obtain

$$\tan \zeta = - \frac{H}{\pi a^2} \cdot \frac{\lambda + 2\mu}{2\mu(\lambda + \mu)\pi} \cdot aa^2 \left( \frac{1}{2} e_1 \omega_1 - \gamma_1 \right)_{z=0}, \quad (93)$$

$$\tan \zeta' = - \frac{H}{\pi a^2} \cdot \frac{2r}{g^2} \cdot aa^2 \left( \frac{1}{2} e_1 \omega_1 - \gamma_1 \right)_{z=0}. \quad (94)$$

The function  $\frac{1}{2}e_1\omega_1 - \gamma_1$  has been discussed already and the expression which is suitable for the calculation of its value at a point not near to the edge of the circle has been established in terms of  $q$ . Using the  $q$ -series in §24 we shall have

$$aa^2 \left( \frac{1}{2} e_1 \omega_1 - \gamma_1 \right) = 2\pi \sqrt{\frac{a}{r}} \cdot q^{3/2} (1 + 3q^4 - 4q^6 - 9q^8 + 22q^{12} + \dots), \quad (95)$$

It is equally interesting and important to find the value of  $\zeta$  at the point near the edge of the loaded area. This will be

accomplished by using the quantity  $q_1$ , instead of  $q$ , which is defined by

$$q_1 = e^{i\pi\tau_1}, \quad \tau_1 = -\frac{\omega_1}{\omega_3} = -\frac{1}{\tau}.$$

Now, by the aid of the relation

$$\frac{\partial_1''(o)}{\partial_1'(o)} = \frac{\partial_0''}{\partial_0'} + \frac{\partial_2'}{\partial_2} + \frac{\partial_3''}{\partial_3'}$$

the expression of  $\frac{1}{2}e_1\omega_1 - \tau_1$  found in §24 may be transformed into

$$4\pi\sqrt{-\frac{a}{2}}\left(\frac{1}{2}e_1\omega_1 - \tau_1\right) = \frac{1}{\partial_2^2(o/\tau)} \cdot \left\{ \frac{\partial_0''(o/\tau)}{\partial_0'(o/\tau)} + \frac{\partial_1'(o/\tau)}{\partial_3(o/\tau)} \right\}.$$

Making use of the transformation formulæ of Theta-functions it will be easily shown that

$$\begin{aligned} \frac{\partial_0''(o/\tau)}{\partial_0'(o/\tau)} &= 2i\pi\tau_1 + \tau_1^2 \cdot \frac{\partial_2''(o/\tau_1)}{\partial_2'(o/\tau_1)}, \\ \frac{\partial_3''(o/\tau)}{\partial_3'(o/\tau)} &= 2i\pi\tau_1 + \tau_1^2 \cdot \frac{\partial_3''(o/\tau_1)}{\partial_3'(o/\tau_1)}, \\ \partial_2^2(o/\tau) &= -i\tau_1\partial_0^2(o/\tau_1), \end{aligned}$$

consequently we have

$$\begin{aligned} 4\pi^2\left(\frac{1}{2}e_1\omega_1 - \tau_1\right) &= \frac{1}{2}\sqrt{-\frac{a}{r}} \cdot \frac{1}{\partial_0^2(o/\tau_1)} \left\{ -4 \right. \\ &\quad \left. + \frac{1}{\pi^2} \log q_1 \left[ \frac{\partial_2''(o/\tau_1)}{\partial_2'(o/\tau_1)} + \frac{\partial_3''(o/\tau_1)}{\partial_3'(o/\tau_1)} \right] \right\}. \quad (96) \end{aligned}$$

The  $q$ -series for the functions needed here are as follows:

$$\begin{aligned} \partial_0'' &= -2\pi^2 q^i (1 + 3^2 q_1^2 + 5^2 q_1^6 + 7^2 q_1^{12} + \dots), \\ \partial_2 &= -3q^i (1 + q_1^2 + q_1^6 + q_1^{12} + \dots), \\ \partial_3'' &= -8\pi^2 (q_1 + 2^2 q_1^3 + 3^2 q_1^9 + \dots), \\ \partial_3 &= 1 + 2q_1 + 2q_1^4 + 2q_1^9 + \dots, \\ \partial_1 &= 1 - 2q_1 + 2q_1^3 - 2q_1^9 + \dots. \end{aligned}$$

The quantity  $q_1$  will be found from

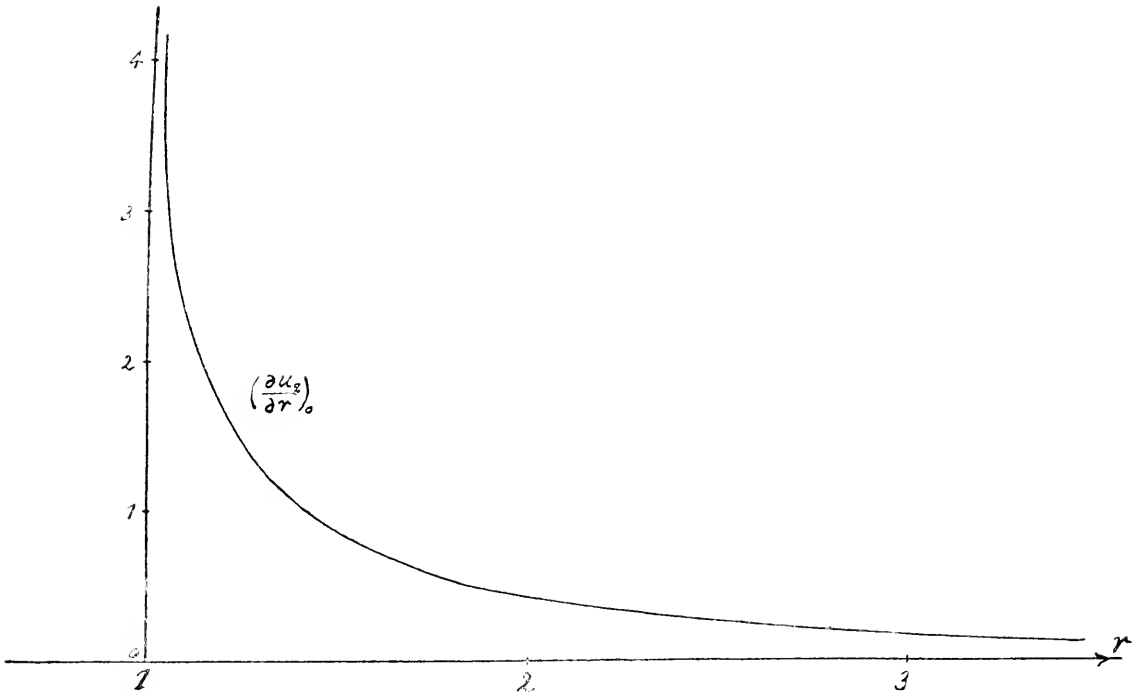


Fig. 6.

$$g_1 = -\frac{l_1}{2} + 2\left(\frac{l_1}{2}\right)^5 + 17\left(\frac{l_1}{2}\right)^9 + 156\left(\frac{l_1}{2}\right)^{13} + O(l_1^{17}),$$

$$l_1 = \frac{1 - \sqrt{k}}{1 + \sqrt{k}} = \frac{\sqrt{(r+a)} - \sqrt{(2\sqrt{ar})}}{\sqrt{(r+a)} + \sqrt{(2\sqrt{ar})}}.$$

Thus the deviation of the direction of gravity at any point can be calculated with any accuracy.

In the next diagram the approximate course of  $ax^2(\frac{1}{2}c\omega_1 - z_1)$  is exhibited as a function of the distance of the point of observation from the centre of the loaded circle, the radius of which is taken as unity.

§34. If we liken the North Atlantic to a circular basin of a large radius and determine the relative position of Potsdam or Chicago referring to the centre of it, the attraction effect of the periodic filling and emptying of tide, which might assist in producing the extra east-west force in observations of the lunar

disturbance of gravity, may be computed by our formula. If we suppose the place of the observation not to be very near to the circular basin, the effect, as we see from the above diagram, is of course small, but it increases repidly as the edge is approached.

For the water-level measurement, the effect of a material loading will appear in the form  $\varphi + \phi$ , instead of  $\phi$  only, where  $\phi$  is due to the attraction exerted by the material loading and  $\varphi$  to the deformation caused by its weight.

For example, suppose the radius of the North Atlantic basin to be 2000 km, the position of Chicago to be 3000 km from the centre, and the level of the water in this area to be raised *one metre*, then

$$\frac{r}{a} = 1.5, \quad q_1 = 0.00255.$$

$$aa^2 \left( \frac{e, \omega_1}{2} - q_1 \right) = 0.8639.$$

Further assume that the density of sea water is unity and in c.g.s.

$$\begin{aligned} \gamma &= 6.65 \times 10^{-8}, & g &= 980, \\ \frac{\lambda + 2\mu}{2(\lambda + \mu)} &= \frac{3}{4}, & \mu &= 6 \times 10^{11}, \end{aligned}$$

then we shall have

$$\begin{aligned} \phi &= 1.17 \times 10^{-8} = 0''.0024, \\ \varphi &= 3.37 \times 10^{-8} = 0''.0069, \end{aligned}$$

accordingly the total effect amounts to

$$\phi + \varphi = 4.54 \times 10^{-8} = 0''.009.$$

It will be noticed that the effect of tilting is about three times as great as that of the attraction, so far as the material constants are assumed as above. According to Lord KELVIN,<sup>1)</sup> who initiated these investigations, the direct lunar effect on the deviation of a plumbline is a maximum when the moon is at the

---

1) Natural Philosophy, Part II, p. 383.



altitude  $45^\circ$  and amounts to 0."017 nearly. The total effect of a tide of amplitude one metre (which is possibly two or three times the actual amount) found here is not small enough to be neglected compared with the direct effect of the moon. As the tilting effect and the attraction effect of the tide wave are directly proportional to the height of the tide, the total effect oscillates in time in accordance with the law which the tide obeys. There is, in general, a difference in phase between the lunar effect and tidal effect, which is worthy of closer investigation. But we must bear in mind that the calculation adopted here is nothing but a rough estimation of order of magnitude, since the north Atlantic is far from circular, the tidal loading in it is never uniform. Nevertheless the above analysis shows that the tidal effect on the water-level measurement, even at a point as far from the coast as Chicago, plays an important role and cannot be regarded as a small correction.

#### Example IV.

§35. Let us take another example by assuming the normal pressure of the form

$$\left. \begin{aligned} f(r) &= -\frac{3H}{2\pi a^3} \sqrt{a^2 - r^2} \quad \text{for } r < a \\ &= 0 \quad \text{for } r > a \end{aligned} \right\} \quad (97)$$

to be given at  $z=0$ ,  $H$  being its total amount. In this case the function  $Z(k)$  becomes

$$\begin{aligned} Z(k) &= -\frac{3H}{2\pi a^3} k \int_0^a \sqrt{a^2 - a'^2} J_0(ka') a' da' \\ &= -\frac{3H}{2\pi a} \left\{ \frac{\sin ka - ka \cos ka}{k^2 a^2} \right\}. \end{aligned} \quad (98)$$

Therefore the components of displacement are given by

$$\left. \begin{aligned} u_r &= \frac{3H\lambda}{4\pi a\mu} \int_0^\infty e^{-kz} \left\{ \frac{\sin ka - ka \cos ka}{k^2 a^2} \right\} J_1(kr) dk \\ &\quad - \frac{3H}{4\pi(\lambda + \mu)} \int_0^\infty e^{-kz} \left\{ \frac{\sin ka - ka \cos ka}{k^3 a^3} \right\} J_2(kr) dk, \\ u_z &= \frac{3H\lambda}{4\pi a\mu} \int_0^\infty e^{-kz} \left\{ \frac{\sin ka - ka \cos ka}{k^2 a^2} \right\} J_0(kr) dk \\ &\quad + \frac{3H(\lambda + 2\mu)}{4\pi\mu(\lambda + \mu)} \int_0^\infty e^{-kz} \left\{ \frac{\sin ka - ka \cos ka}{k^3 a^3} \right\} J_1(kr) dk. \end{aligned} \right\} \quad (99)$$

The integrals contained in the above can be obtained by expanding the trigonometric functions into power series of  $k$  and making use of the formulæ (42). In this way we have

$$\left. \begin{aligned} u_r &= \frac{3H}{2\pi a\mu} \cdot \frac{z}{\sqrt{r^2 + z^2}} \sum_{n=1}^\infty (-1)^{n-1} \frac{n(2n-2)!}{(2n+1)!} \left( \frac{a}{\sqrt{r^2 + z^2}} \right)^{2n-1} P_{2n-1}^1(\nu) \\ &\quad - \frac{3H}{2\pi(\lambda + \mu)} \cdot \frac{1}{\sqrt{r^2 + z^2}} \sum_{n=1}^\infty (-1)^{n-1} \frac{n(2n-3)!}{(2n+1)!} \left( \frac{a}{\sqrt{r^2 + z^2}} \right)^{2n-1} P_{2n-2}^1(\nu),^{1)} \\ u_z &= \frac{3H}{2\pi a\mu} \cdot \frac{z}{\sqrt{r^2 + z^2}} \sum_{n=1}^\infty (-1)^{n-1} \frac{n(2n-1)!}{(2n+1)!} \left( \frac{a}{\sqrt{r^2 + z^2}} \right)^{2n-1} P_{2n-1}(\nu) \\ &\quad + \frac{3H(\lambda + 2\mu)}{2\pi\mu(\lambda + \mu)} \cdot \frac{1}{\sqrt{r^2 + z^2}} \sum_{n=1}^\infty (-1)^{n-1} \frac{n(2n-2)!}{(2n+1)!} \left( \frac{a}{\sqrt{r^2 + z^2}} \right)^{2n-2} P_{2n-2}(\nu) \end{aligned} \right\} \quad (100)$$

where

$$\nu = \frac{z}{\sqrt{r^2 + z^2}}.$$

These series converge for  $\sqrt{r^2 + z^2} > a$ , and are applicable in this region.

At the boundary, we have to put  $z=0$  and  $\nu=0$ . Since

$$\begin{aligned} P_0^{-1}(0) &= 1, & P_{2n-1}^1(0) &= 0, \\ P_{2n-2}(0) &= (-1)^{n-1} \frac{1.3 \dots (2n-3)}{2.4 \dots (2n-2)}, \end{aligned}$$

---

1) For the first term ( $n=1$ ) of the second series we have to take  $\frac{1}{3!} P_0^{-1}(\nu)$ .

we have

$$\left. \begin{aligned} \int_0^{\infty} \frac{\sin ka - ka \cos ka}{k^3 a^3} J_1(kr) dk &= \frac{1}{3r}, \\ \int_0^{\infty} \frac{\sin ka - ka \cos ka}{k^3 a^3} J_0(kr) dk &= \frac{1}{3r} F\left(\frac{1}{2}, \frac{1}{2}, \frac{5}{2}, \frac{a^2}{r^2}\right) \\ &= \frac{1}{2a} \left\{ \left(1 - \frac{1}{2} \frac{r^2}{a^2}\right) \sin^{-1} \frac{a}{r} + \frac{r}{2a} \sqrt{1 - \frac{a^2}{r^2}} \right\} \end{aligned} \right\} \quad (101)$$

for  $a \leq r$ . Consequently

$$\left. \begin{aligned} (u_r)_0 &= -\frac{H}{4\pi(\lambda + \mu)} \cdot \frac{1}{r}, \\ (u_z)_0 &= \frac{3H(\lambda + 2\mu)}{4\pi\mu(\lambda + \mu)} \cdot \frac{1}{2a} \left\{ \left(1 - \frac{r^2}{2a^2}\right) \sin^{-1} \frac{a}{r} + \frac{r}{2a} \sqrt{1 - \frac{a^2}{r^2}} \right\} \end{aligned} \right\} \quad (102)$$

for  $a \leq r$ .

§36. To find the expressions for the displacement within the loaded circle, we proceed as follows:

Making use of the power series of the Bessel function, we have

$$\left. \begin{aligned} \int_0^{\infty} e^{-kz} \left\{ \frac{\sin ka - ka \cos ka}{k^3 a^3} \right\} J_1(kr) dk \\ &= \frac{1}{a} \sum_{n=0}^{\infty} \frac{(-1)^n}{n!(n+1)!} \left(\frac{r}{2a}\right)^{2n+1} \mathcal{Q}_{2n+1}\left(\frac{z}{a}\right), \\ \int_0^{\infty} e^{-kz} \left\{ \frac{\sin ka - ka \cos ka}{k^3 a^3} \right\} J_0(kr) dk \\ &= \frac{1}{a} \sum_{n=0}^{\infty} \frac{(-1)^n}{(n!)^2} \left(\frac{r}{2a}\right)^{2n} \mathcal{Q}_{2n}\left(\frac{r}{a}\right) \end{aligned} \right\} \quad (103)$$

where  $\mathcal{Q}$  stands for

$$\mathcal{Q}_m(x) = \int_0^{\infty} e^{-\lambda x} \left\{ \frac{\sin \lambda - \lambda \cos \lambda}{\lambda^3} \right\} \lambda^m d\lambda.$$

By the aid of the formulæ

$$\int_0^{\infty} e^{-\lambda x} \frac{\sin \lambda}{\lambda} d\lambda = \tan^{-1} \frac{1}{x},$$

$$\int_0^{\infty} e^{-\lambda x} \cos \lambda d\lambda = \frac{x}{1+x^2},$$

the evaluation of the function  $\mathcal{Q}_m(x)$  can be undertaken. A little calculation will give us

$$\mathcal{Q}_0(x) = \frac{\pi}{4} - \frac{1}{2} \left\{ x + \tan^{-1} x - x^2 \tan^{-1} \frac{1}{x} \right\},$$

$$\mathcal{Q}_1(x) = 1 - x \tan^{-1} \frac{1}{x},$$

$$\mathcal{Q}_2(x) = \tan^{-1} \frac{1}{x} - \frac{x}{1+x^2},$$

$$\mathcal{Q}_3(x) = \frac{2}{(1+x^2)^2},$$

and in general

$$\mathcal{Q}_m(x) = (-1)^{m-1} \frac{d^{m-1}}{dx^{m-1}} \left\{ \frac{2}{(1+x^2)^3} \right\}, \quad m > 2.$$

Thus the integrals on the left hand side of (103) can be expanded in ascending power series of  $r/a$  which probably converge for limited values of  $r$  if the value of  $z$  is fixed. These series and those found in (100) have a common region in which they are both convergent and therefore they must be congruent to each other in that region. On the proof of this proposition we shall not enter; but we shall find the region of convergency of these latter series at the boundary. Let us take the first series of (103). Expand the function  $\mathcal{Q}_{n+1}\left(-\frac{z}{a}\right)$  for  $n \geq 1$  into a power series of  $z/a$ , supposing  $z/a$  to be sufficiently small, then the first term of it will be  $(-1)^{\frac{n-1}{2}} 2n(2n-2)!$ . Thus if we put  $z=0$  in the first series of (103), its general term will then be

$$\frac{2n(2n-2)!}{n!(n+1)! 2^{2n+1}} \left( \frac{r}{a} \right)^{2n+1}.$$

The series which has this expression as its general term converges obviously for the value of  $r$  smaller than  $a$ . Similarly for the second series.

Since, for  $z = 0$ ,

$$Q_0(0) = \frac{\pi}{4}, \quad Q_1(0) = 1,$$

$$Q_2(0) = \frac{\pi}{2}, \quad Q_3(0) = 2,$$

$$\dots \dots \dots$$

$$Q_{2n}(0) = 0, \quad Q_{2n+1}(0) = (-1)^{n+1} 2n(2n-2)!, \quad n \geq 1,$$

we have, after summation,

$$\left. \begin{aligned} \int_0^\infty \frac{\sin ka - ka \cos ka}{k^3 a^3} J_0(kr) dk &= \frac{1}{3r} \left\{ 1 - \left( 1 - \frac{r^2}{a^2} \right)^{3/2} \right\}, \\ \int_0^\infty \frac{\sin ka - ka \cos ka}{k^3 a^3} J_1(kr) dk &= \frac{\pi}{4a} \left\{ 1 - \frac{r^2}{2a^2} \right\}, \end{aligned} \right\} \quad (104)$$

for  $r \leq a$ .

Consequently we have

$$\left. \begin{aligned} (u_r)_0 &= -\frac{H}{4\pi(\lambda + \mu)} \cdot \frac{1}{r} \left\{ 1 - \left( 1 - \frac{r^2}{a^2} \right)^{3/2} \right\}, \\ (u_z)_0 &= \frac{3(\lambda + 2\mu)}{16(\lambda + \mu)a} \cdot \frac{1}{a} \left\{ 1 - \frac{1}{2} \cdot \frac{r^2}{a^2} \right\}, \end{aligned} \right\} \quad (105)$$

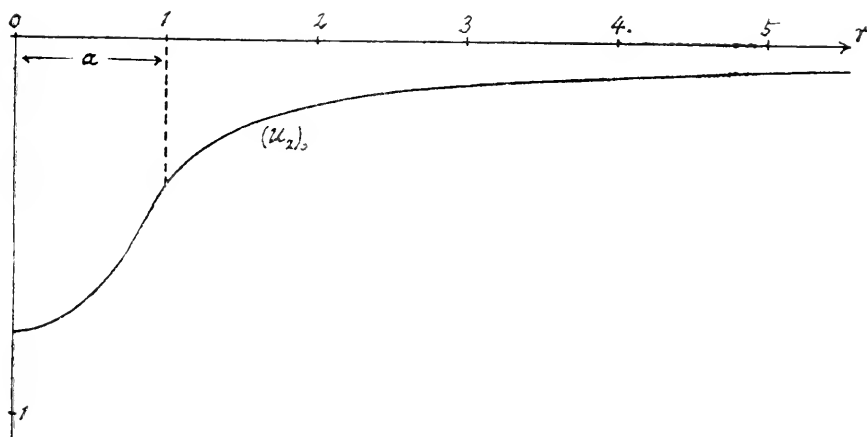


Fig. 7.

for  $r \leq a$ . In the annexed diagram the approximate course of the vertical displacement is shown in proper scale.

§37. By a similar process the distribution of stress can be found. Here we shall calculate the stress at the boundary. It may be shown that

$$\left. \begin{aligned} \int_0^\infty \frac{\sin ka - ka \cos ka}{k^2 a^2} J_0(kr) dk &= 0 && \text{for } r \geq a, \\ &= \frac{1}{a} \sqrt{1 - \frac{r^2}{a^2}} && \text{for } r \leq a, \end{aligned} \right\} \quad (106)$$

and, therefore, as the expressions for the stress-components at the surface we have

$$\left. \begin{aligned} (\widehat{rr})_0 &= \frac{H\mu}{2\pi(\lambda + \mu)} \cdot \frac{1}{r^2}, \\ (\widehat{\theta\theta})_0 &= -\frac{H\mu}{2\pi(\lambda + \mu)} \cdot \frac{1}{r^2}, \\ (\widehat{zz})_0 &= 0, \quad (\widehat{r\theta})_0 = 0 \end{aligned} \right\} \quad (107)$$

for  $r \geq a$ , and

$$\left. \begin{aligned} (\widehat{rr})_0 &= -\frac{3H}{2\pi a^2} \left\{ \left(1 - \frac{r^2}{a^2}\right)^{\frac{1}{2}} - \frac{\mu}{\lambda + \mu} \cdot \frac{a^2}{3r^2} \left[1 - \left(1 - \frac{r^2}{a^2}\right)^{\frac{3}{2}}\right] \right\}, \\ (\widehat{\theta\theta})_0 &= -\frac{3H}{2\pi a^2} \left\{ -\frac{\lambda}{\lambda + \mu} \left(1 - \frac{r^2}{a^2}\right)^{\frac{1}{2}} + \frac{\mu}{\lambda + \mu} \cdot \frac{a^2}{3r^2} \left[1 - \left(1 - \frac{r^2}{a^2}\right)^{\frac{3}{2}}\right] \right\}, \\ (\widehat{zz})_0 &= -\frac{3H}{2\pi a^2} \left(1 - \frac{r^2}{a^2}\right)^{\frac{1}{2}}, \\ (\widehat{r\theta})_0 &= 0, \end{aligned} \right\} \quad (108)$$

for  $r \leq a$ .

The result of this example may be looked upon as a special case of what has been discussed by H. HERTZ in his papers<sup>1)</sup> concerning the contact of two elastic bodies. He assumed the area on which pressure acts to be an ellipse instead of a circle. If we put  $b=a$  in his results, we get exactly the same formulæ for the pressure and for the vertical displacement. And therefore this

1) Gesammelte Werke, I, p. 154—and p. 175.

example may be applied to the discussion of contact of an elastic body upon another with plane-surface.

§38. Another application will be considered here. Suppose we have a material loading of a semi-spheroidal form whose equation is

$$\frac{z^2}{b^2} + \frac{r^2}{a^2} = 1, \quad (z < 0)$$

and of uniform density  $\rho$ . This load may be likened to the tidal inequality in the North Atlantic ocean which affects the gravity measurement. In this case  $H$  will be replaced by  $\frac{2\pi a^2 b g \rho}{3}$ . As before, the deviation of the direction of gravity produced by the attraction of this load is given by

$$\tan \phi = -\frac{3H}{2\pi a^2} \cdot \frac{2\pi r}{g^2} \int_0^\infty \frac{\sin ka - ka \cos ka}{k^2 a} J_1(kr) dk,$$

and the level-change due to the deformation of the ground arisen from the load by

$$\tan \varphi = -\frac{3H}{2\pi a^2} \cdot \frac{\lambda + 2\mu}{2\mu(\lambda + \mu)} \int_0^\infty \frac{\sin ka - ka \cos ka}{k^2 a} J_2(kr) dk.$$

The evaluation of this integral can be undertaken in a manner similar to those of (99) and will appear to be

$$\left. \begin{aligned} & \int_0^\infty \frac{\sin ka - ka \cos ka}{k^2 a} J_1(kr) dk \\ &= \frac{r}{2a} \left\{ \sin^{-1} \frac{a}{r} - \frac{a}{r} \sqrt{1 - \frac{a^2}{r^2}} \right\}, \quad a \leq r \\ &= \frac{\pi r}{4a}, \quad r \leq a \end{aligned} \right\} \quad (100)$$

Thus we have

$$\tan \phi = -\frac{3H}{2\pi a^2} \cdot \frac{\pi r}{g^2} \cdot \frac{r}{a} \left\{ \sin^{-1} \frac{a}{r} - \frac{a}{r} \sqrt{1 - \frac{a^2}{r^2}} \right\}, \quad (110)$$

$$\tan \varphi = -\frac{3H}{2\pi a^2} \cdot \frac{(\lambda + 2\mu)}{4\mu(\lambda + \mu)} \cdot \frac{r}{a} \left\{ \sin^{-1} \frac{a}{r} - \frac{a}{r} \sqrt{1 - \frac{a^2}{r^2}} \right\}, \quad (111)$$

for the point  $r > a$ .

In the next diagram, the general march of the function  $x \sin^{-1} \frac{1}{x} - \sqrt{1 - \frac{1}{x^2}}$  is exhibited, where  $x$  is the ratio of the distance of the point under consideration from the centre of the loaded circle to its radius. The course of the curve is very similar to that of Fig. 6, except at the point very near to the edge of the loaded area, where, in this case, it remains finite.

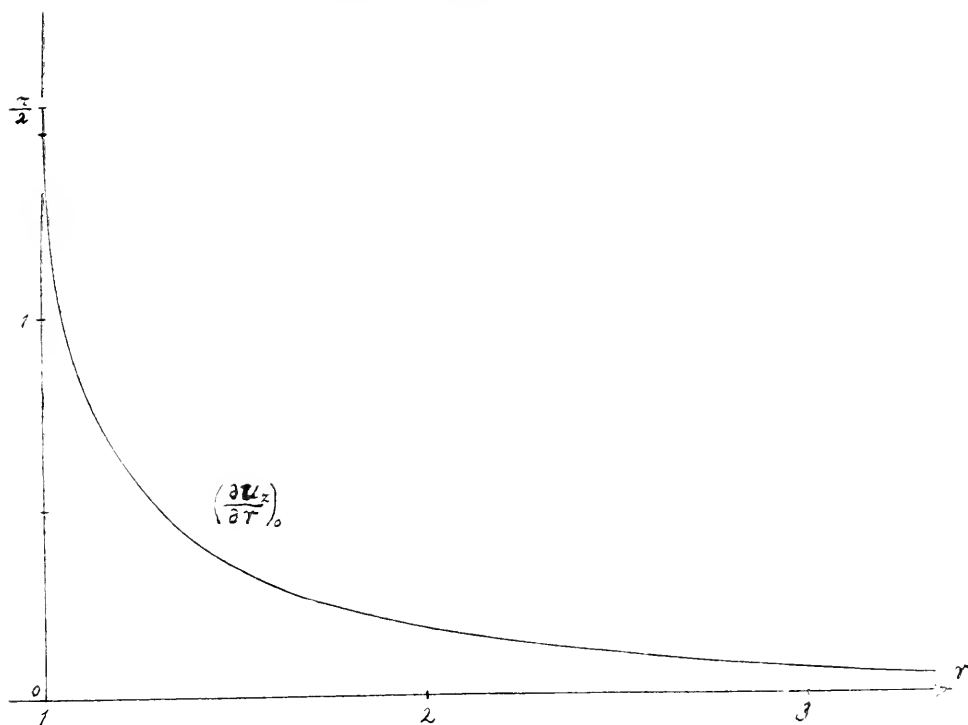


Fig. 8.

For example, with the same assumption regarding the material constants of the earth as in the former example, and supposing that the total amount of the load is the same as before, i.e. the mean height of the tide is one metre, and  $a = 2 \times 10^8$ ,  $r = \times 10^8$  cm. we have



$$\zeta = 1.12 \times 10^{-8} = 0''.0023,$$

$$\zeta = 3.21 \times 10^{-8} = 0''.0066,$$

and

$$\zeta + \zeta = 4.33 \times 10^{-8} = 0''.009$$

nearly the same as the results in the former example.

If we suppose the place of the observation to be very near to the edge of the loaded area, then

$$\zeta = 5.0 \times 10^{-8} = 0''.01,$$

$$\zeta = 14.4 \times 10^{-8} = 0''.03,$$

and

$$\zeta + \zeta = 0''.04$$

greater than the maximum of the direct effect of the moon.

### Example V.

§39. Lastly, we shall take another example in which the normal pressure of the form

$$f(r) = -\frac{H}{2\pi a} \cdot \frac{1}{\sqrt{a^2 - r^2}} \quad (112)$$

is applied to the boundary within a circle of radius  $a$ , which is otherwise left free from traction. This problem has been discussed also by BOUSSINESQ and others, and the expression for the vertical displacement at the boundary has been found. In this case the function  $Z(k)$  becomes

$$Z(k) = -\frac{H}{2\pi a} k \int_0^a \frac{J_0(ka) a da}{\sqrt{a^2 - r^2}} = -\frac{H}{2\pi a} \sin ka. \quad (113)$$

Consequently we have

$$u_r = \left. \begin{aligned} & \frac{H\lambda}{4\pi a\mu} \int_0^\infty e^{-kz} \sin ka J_1(kr) dk \\ & - \frac{H}{4\pi a(\lambda + \mu)} \int_0^\infty e^{-kz} \sin ka J_1(kr) \frac{dk}{k} \end{aligned} \right\} \quad (114)$$

$$u_z = \left. \begin{aligned} & \frac{Hz}{4\pi a\mu} \int_0^a e^{-kz} \sin ka J_0(kr) dk \\ & + \frac{H(\lambda+2\mu)}{4\pi a(\lambda+\mu)\mu} \int_0^\infty e^{-kz} \sin ka J_0(kr) \frac{dk}{k} \end{aligned} \right\} \quad (114)$$

The integration can be carried out by expanding  $\sin ka$  into a power series and making use of the formulæ (42). Thus we obtain

$$\left. \begin{aligned} u_r &= \frac{H}{4\pi a\mu} \cdot \frac{z}{\sqrt{r^2+z^2}} \sum_{n=0}^{\infty} \frac{(-1)^n}{2n+1} \left( \frac{a}{\sqrt{r^2+z^2}} \right)^{2n+1} I_{2n+1}^{(1)}(\nu) \\ &\quad - \frac{H}{4\pi a(\lambda+\mu)} \sum_{n=0}^{\infty} \frac{(-1)^n}{2n(2n+1)} \left( \frac{a}{\sqrt{r^2+z^2}} \right)^{2n+1} P_{2n}^{(1)}(\nu) \\ u_z &= \frac{H}{4\pi a\mu} \cdot \frac{z}{\sqrt{r^2+z^2}} \sum_{n=0}^{\infty} (-1)^n \left( \frac{a}{\sqrt{r^2+z^2}} \right)^{2n+1} P_{2n+1}(\nu) \\ &\quad + \frac{H(\lambda+2\mu)}{4\pi a(\lambda+\mu)\mu} \cdot \sum_{n=0}^{\infty} \frac{(-1)^n}{2n+1} \left( \frac{a}{\sqrt{r^2+z^2}} \right)^{2n+1} P_{2n}(\nu), \end{aligned} \right\} \quad (115)$$

where

$$\nu = \frac{z}{\sqrt{r^2+z^2}}.$$

These series apply for the region  $\sqrt{r^2+z^2} > a$ .

As in the last example, the expressions which may be applied for small values of  $r$  and  $z$  can be found by using the power series of the Bessel function and the formula

$$\int_0^a k^{n-1/2} \sin ka \cdot dk = \frac{n!}{(z^2+a^2)^{\frac{n+1}{2}}} \cdot \sin \left[ (n+1) \tan^{-1} \frac{a}{z} \right].$$

Thus

---

1) For  $a=0$  we have to take  $\frac{a}{\sqrt{r^2+z^2}} P_{2n+1}(\nu)$ .

$$\left. \begin{aligned} u_r &= \frac{H}{4\pi a \mu} \cdot \frac{z}{\sqrt{z^2 + a^2}} \sum_{n=0}^{\infty} \frac{(-1)^n (2n+1)!}{n! (n+1)! 2^{2n+1}} \left( \frac{r}{\sqrt{z^2 + a^2}} \right)^{2n+1} \sin(2n+2)\zeta \\ &\quad - \frac{H}{4\pi a(\lambda + \mu)} \sum_{n=0}^{\infty} \frac{(-1)^n (2n)!}{n! (n+1)! 2^{2n+1}} \left( \frac{r}{\sqrt{z^2 + a^2}} \right)^{2n+1} \sin(2n+1)\zeta, \\ u_z &= \frac{H}{4\pi a \mu} \cdot \frac{z}{\sqrt{z^2 + a^2}} \sum_{n=0}^{\infty} \frac{(-1)^n (2n)!}{(n!)^2 2^{2n}} \left( \frac{r}{\sqrt{z^2 + a^2}} \right)^{2n} \sin(2n+1)\zeta \\ &\quad + \frac{H(\lambda + 2\mu)}{4\pi a(\lambda + \mu) \mu} \sum_{n=0}^{\infty} \frac{(-1)^n (2n-1)!}{(n!)^2 2^{2n}} \left( \frac{r}{\sqrt{z^2 + a^2}} \right)^{2n} \sin 2n\zeta, \end{aligned} \right\} \quad (116)$$

where

$$\zeta = \tan^{-1} \frac{a}{z}.$$

§40. At the surface ( $z=0$ ) they reduce simply to<sup>1)</sup>

$$\left. \begin{aligned} (u_r)_0 &= - \frac{H}{4\pi(\lambda + \mu)a} \cdot \frac{a - \sqrt{a^2 - r^2}}{r}, \\ (u_z)_0 &= \frac{H(\lambda + 2\mu)}{8(\lambda + \mu)\mu a}, \end{aligned} \right\} \quad (117)$$

for  $r \leq a$ ; and

$$\left. \begin{aligned} (u_r)_0 &= - \frac{1}{4\pi(\lambda + \mu)} \cdot \frac{1}{r}, \\ (u_z)_0 &= \frac{H(\lambda + 2\mu)}{4\pi(\lambda + \mu)\mu a} \cdot \sin^{-1} \frac{a}{r}, \end{aligned} \right\} \quad (118)$$

for  $r \geq a$ .

As seen from the formula (117) the vertical displacement is constant over the loaded area, and therefore this solution is applicable when an absolutely rigid body of circular base is pressed normally against an infinite elastic body; the problem has been attacked by various writers from this point of view.

§41. Similarly the expressions for the stresses at the surface will be found to be

- 
- 1) For  $n=0$  we have to take  $\frac{1}{2}$  instead of zero.
  - 2) If we wish to know the expressions for displacement only at the surface, these can be obtained with less calculation. See DAMELÉ.

$$\left. \begin{aligned} (\widehat{rr})_0 &= -\frac{H}{2\pi a} \left\{ \frac{1}{\sqrt{a^2-r^2}} - \frac{\mu}{\lambda+\mu} \cdot \frac{a-\sqrt{a^2-r^2}}{r^2} \right\}, \\ (\widehat{\theta\theta})_0 &= -\frac{H\lambda}{2\pi a(\lambda+\mu)} \left\{ \frac{1}{\sqrt{a^2-r^2}} + \frac{\mu}{\lambda} \cdot \frac{a-\sqrt{a^2-r^2}}{r^2} \right\}, \\ (\widehat{zz})_0 &= -\frac{H}{2\pi a} \cdot \frac{1}{\sqrt{a^2-r^2}}, \end{aligned} \right\} \quad (119)$$

for  $r < a$ ; and

$$\left. \begin{aligned} (\widehat{rr})_0 &= \frac{H\mu}{2\pi(\lambda+\mu)} \cdot \frac{1}{r^2}, \\ (\widehat{\theta\theta})_0 &= -\frac{H\mu}{2\pi(\lambda+\mu)} \cdot \frac{1}{r^2}, \\ (\widehat{zz})_0 &= 0, \end{aligned} \right\} \quad (120)$$

for  $r > a$ .

The stress at the periphery of the loaded area is infinitely great, so that the elastic body would be ruptured at the edge. The present problem may, therefore, throw considerable light upon the explanation of the phenomena of punching.

§42. The expressions for the stress-components in the interior of the body which, so far as I am aware, have not been treated by any one can be found without using any special functions. We shall take here a simple case, for example, in which the material is incompressible.

Since the integral

$$\int_0^{\infty} e^{-kz} J_0(\tilde{z}k) dk = \frac{1}{\sqrt{z^2 + \tilde{z}^2}}$$

is valid for all values of  $z$  and  $\tilde{z}$ , real or complex, provided the real part of  $z$  is not smaller than the absolute value of the imaginary part of  $\tilde{z}$ , putting  $z = -ia$ ,  $\tilde{z} = r$  in this integral and equating the imaginary parts in both members we have

$$\int_0^{\infty} e^{-kz} \sin ka \cdot J_0(kr) dk = \frac{\sqrt{S^2 - (z^2 + r^2 - a^2)}}{\sqrt{2S^2}} \quad (121)$$

where  $S^2$  stands for

$$S^2 = \sqrt{(z^2 + r^2 - a^2)^2 + 4a^2 z^2}. \quad (122)$$

For  $z=0$ , this formula is still applicable, if we take

$$\left. \begin{aligned} S^2 &= r^2 - a^2 && \text{for } r > a, \\ &= a^2 - r^2 && \text{for } r < a. \end{aligned} \right\}$$

Similarly, putting

$$\left. \begin{aligned} P &= \sqrt{S^2 - (z^2 + r^2 - a^2)}, \\ Q &= \sqrt{S^2 + (z^2 + r^2 + a^2)}, \end{aligned} \right\} \quad (123)$$

we have

$$\int_0^\infty e^{-kz} \sin ka \cdot J_0(kr) k dk = \frac{a(z^2 - r^2 + a^2)Q + z(z^2 + r^2 + a^2)P}{\sqrt{2} \cdot S^6}, \quad (124)$$

$$\int_0^\infty e^{-kz} \sin ka \cdot J_1(kr) k dk = \frac{aQ - zP}{\sqrt{2} \cdot rS^2}, \quad (125)$$

$$\int_0^\infty e^{-kz} \sin ka \cdot J_2(kr) k dk = \frac{r\{(z^2 + r^2 - a^2)P + 2azQ\}}{\sqrt{2} \cdot S^6}. \quad (126)$$

Thus, for the case of incompressibility, we have

$$\left. \begin{aligned} \widehat{rr} &= -\frac{H}{2\sqrt{2\pi}a} \left\{ \frac{P}{S^2} + \frac{z(aQ - zP)}{r^2 S^2} - \frac{z[a(z^2 - r^2 + a^2)Q + z(z^2 + r^2 + a^2)P]}{S^6} \right\}, \\ \widehat{\theta\theta} &= -\frac{H}{2\sqrt{2\pi}a} \left\{ \frac{P}{S^2} - \frac{z(aQ - zP)}{r^2 S^2} \right\}, \\ \widehat{zz} &= -\frac{H}{2\sqrt{2\pi}a} \left\{ \frac{P}{S^2} + \frac{z[a(z^2 - r^2 + a^2)Q + z(z^2 + r^2 + a^2)P]}{S^6} \right\}, \\ \widehat{zr} &= -\frac{Hz}{2\sqrt{2\pi}a} \left\{ \frac{r(z^2 + r^2 - a^2)P + 2azQ}{S^6} \right\}, \end{aligned} \right\} \quad (127)$$

for the stress components.

## V. Boussinesq's Problem.

§43. The problem of LAMÉ and CLAPEYRON is a special case of those known as Boussinesq's, which can be stated as follows:

A limited portion of the surface of a large mass of elastic material is subjected to local stress or to local deformation, it is required to find the strain and stress in the body due to these local disturbances.

In the case of symmetry about an axis perpendicular to the surface of the body, this problem may be discussed, in a general way, by applying our method of analysis. We shall sketch the results here as an addendum.

The typical solution of the equilibrium, in this special case, is

$$\left. \begin{aligned} u_r &= -\left\{ \frac{\lambda + \mu}{2\mu} Cz - B \right\} J_1(kr) e^{-kz}, \\ u_\theta &= -AJ_1(kr) e^{-kz}, \\ u_z &= -\left\{ \frac{\lambda + \mu}{2\mu} Cz - D \right\} J_0(kr) e^{-kz}; \end{aligned} \right\} \quad (128)$$

and

$$\left. \begin{aligned} \widehat{z}z &= \{(\lambda + \mu)kCz - \mu C - 2\mu kD\} J_0(kr) e^{-kz}, \\ \widehat{z}\theta &= \mu kAJ_1(kr) e^{-kz}, \\ \widehat{z}r &= \left\{ (\lambda + \mu)kCz - \frac{\lambda + \mu}{2} C - \mu k(B + D) \right\} J_1(kr) e^{-kz}, \\ &\text{etc. ;} \end{aligned} \right\} \quad (129)$$

with the relation

$$k(B + D) = \frac{\lambda + 3\mu}{2\mu} C,$$

in which the components  $u_\theta$  and  $\widehat{z}\theta$  follow from the supposition that  $A$  is nil. Since these do not give very interesting results, we shall not consider them here.

§44. Case in which all the surface tractions are given.

We suppose first of all that

$$\left. \begin{aligned} \widehat{z}z &= ZJ_0(kr), \\ \widehat{z}r &= RJ_1(kr) \end{aligned} \right\} \quad (130)$$

are given at  $z=0$ , then we shall have the following values for the arbitrary constants:

$$\begin{aligned} B &= -\frac{\lambda+2\mu}{2\mu(\lambda+\mu)k}R + \frac{1}{2(\lambda+\mu)k}Z, \\ D &= -\frac{\lambda+2\mu}{2\mu(\lambda+\mu)k}Z + \frac{1}{2(\lambda+\mu)k}R, \\ C &= -\frac{1}{\lambda+\mu}(Z-R). \end{aligned}$$

Putting these in (128) and (129) we have the solution corresponding to the boundary conditions (130).

If the traction over the surface is given in the form

$$\left. \begin{aligned} \widehat{z}z &= p(r), \\ \widehat{r}r &= \tau(r), \end{aligned} \right\} \quad (131)$$

$p$  and  $\tau$  being any prescribed functions of  $r$ , the corresponding solution can be obtained by making use of the integral theorem (26), on the supposition that the functions  $p(r)$  and  $\tau(r)$  do not violate that theorem.

Thus

$$\left. \begin{aligned} u_r &= -\int_0^\infty \left\{ \frac{z}{2\mu} [Z(k) - R(k)] + \frac{\lambda+2\mu}{2\mu(\lambda+\mu)k} \cdot R(k) \right. \\ &\quad \left. - \frac{1}{2(\lambda+\mu)k} \cdot Z(k) \right\} e^{-kz} J_0(kr) dk, \\ u_z &= -\int_0^\infty \left\{ \frac{z}{2\mu} [Z(k) - R(k)] + \frac{\lambda+2\mu}{2\mu(\lambda+\mu)k} \cdot Z(k) \right. \\ &\quad \left. - \frac{1}{2(\lambda+\mu)k} \cdot R(k) \right\} e^{-kz} J_1(kr) dk; \end{aligned} \right\} \quad (132)$$

and

$$\left. \begin{aligned} \widehat{z}z &= \int_0^\infty \{ k z [Z(k) - R(k)] + Z(k) \} e^{-kz} J_0(kr) dk, \\ \widehat{r}r &= \int_0^\infty \{ k z [Z(k) - R(k)] + R(k) \} e^{-kz} J_1(kr) dk, \\ &\text{etc. ;} \end{aligned} \right\} \quad (133)$$

where the functions  $Z$  and  $R$  are determined by

$$\left. \begin{aligned} Z(k) &= k \int_0^{\infty} p(a) J_0(ka) a da, \\ R(k) &= k \int_0^{\infty} z(a) J_1(ka) a da. \end{aligned} \right\} \quad (134)$$

If we put  $\tau(r)=0$  in this solution, we get as a matter of course the solution (30) and (31).

§45. Case in which the normal traction and radial displacement at the surface are given.

If

$$\left. \begin{aligned} u_r &= u(r), \\ \widehat{z}z &= p(r) \end{aligned} \right\} \quad (135)$$

are given at  $z=0$ , the corresponding solution is:

$$\left. \begin{aligned} u_r &= - \int_0^{\infty} \left\{ \frac{z(\lambda+\mu)}{2\mu(\lambda+2\mu)} [Z(k)+2\mu k U(k)] - U(k) \right\} e^{-kz} J_1(kr) dk, \\ u_z &= - \int_0^{\infty} \left\{ \frac{z(\lambda+\mu)}{2\mu(\lambda+2\mu)} [Z(k)+2\mu k U(k)] + \frac{\lambda+3\mu}{2\mu(\lambda+2\mu)k} Z(k) \right. \\ &\quad \left. + \frac{\mu}{\lambda+2\mu} U(k) \right\} e^{-kz} J_0(kr) dk; \end{aligned} \right\} \quad (136)$$

and

$$\left. \begin{aligned} \widehat{z}z &= \int_0^{\infty} \left\{ \frac{z(\lambda+\mu)k}{\lambda+2\mu} [Z(k)+2\mu k U(k)] + Z(k) \right\} e^{-kz} J_0(kr) dk, \\ \widehat{z}r &= \int_0^{\infty} \left\{ \frac{z(\lambda+\mu)k}{\lambda+2\mu} [Z(k)+2\mu k U(k)] - \frac{\mu}{\lambda+2\mu} Z(k) \right. \\ &\quad \left. + \frac{2\mu(\lambda+\mu)k}{\lambda+2\mu} U(k) \right\} e^{-kz} J_1(kr) dk, \\ &\quad \text{etc.;} \end{aligned} \right\} \quad (137)$$

in which  $U$  and  $Z$  are given by



$$\left. \begin{aligned} U(k) &= k \int_0^\infty p(a) J_0(ka) a da, \\ Z(k) &= k \int_0^\infty p(a) J_0(ka) a da. \end{aligned} \right\} \quad (138)$$

46. Case in which the tangential traction and normal displacement at the surface are given.

If

$$\left. \begin{aligned} \widehat{r} &= \tau(r), \\ u_r &= w(r) \end{aligned} \right\} \quad (139)$$

are given at  $z=0$ , then we obtain

$$\left. \begin{aligned} u_r &= - \int_0^\infty \left\{ - \frac{z(\lambda+\mu)}{2\mu(\lambda+2\mu)} [R(k) + 2\mu k W(k)] + \frac{\mu}{\lambda+2\mu} W(k) \right. \\ &\quad \left. + \frac{\lambda+3\mu}{2\mu(\lambda+2\mu)k} R(k) \right\} e^{-kz} J_1(kr) dk, \\ u_z &= - \int_0^\infty \left\{ - \frac{z(\lambda+\mu)}{2\mu(\lambda+2\mu)} [R(k) + 2\mu k W(k)] \right. \\ &\quad \left. + W(k) \right\} e^{-kz} J_0(kr) dk; \end{aligned} \right\} \quad (140)$$

and

$$\left. \begin{aligned} \widehat{\tau} &= - \int_0^\infty \left\{ \frac{z(\lambda+\mu)k}{\lambda+2\mu} [R(k) + 2\mu k W(k)] + \frac{2\mu(\lambda+\mu)k}{\lambda+2\mu} W(k) \right. \\ &\quad \left. - \frac{\mu}{\lambda+2\mu} R(k) \right\} e^{-kz} J_0(kr) dk, \\ \widehat{r} &= - \int_0^\infty \left\{ - \frac{z(\lambda+\mu)k}{\lambda+2\mu} [R(k) + 2\mu k W(k)] \right. \\ &\quad \left. + R(k) \right\} e^{-kz} J_1(kr) dk, \\ &\text{etc. ;} \end{aligned} \right\} \quad (141)$$

where

$$\left. \begin{aligned} R(k) &= k \int_0^z \tau(a) J_1(ka) a da, \\ W(k) &= k \int_0^z w(a) J_0(ka) a da. \end{aligned} \right\} \quad (142)$$

§47. Case in which both the displacement components at the boundary are given.

If

$$\left. \begin{aligned} u_r &= u(r), \\ u_z &= w(r) \end{aligned} \right\} \quad (143)$$

are given at  $z=0$ , we have

$$\left. \begin{aligned} u_r &= \int_0^\infty \left\{ \frac{z(\lambda+\mu)k}{\lambda+3\mu} [W(k)-U(k)] + U(k) \right\} e^{-zJ_0(kr)} dk, \\ u_z &= \int_0^\infty \left\{ \frac{2(\lambda+\mu)k}{\lambda+3\mu} [W(k)-U(k)] + W(k) \right\} e^{-zJ_0(kr)} dk, \end{aligned} \right\} \quad (144)$$

and

$$\left. \begin{aligned} \hat{u}_r &= \int_0^\infty \left\{ \frac{2z\mu(\lambda+\mu)k^2}{\lambda+3\mu} [U(k)-W(k)] - \frac{2\mu^2k}{\lambda+3\mu} U(k) \right. \\ &\quad \left. - \frac{2\mu(\lambda+2\mu)k}{\lambda+3\mu} W(k) \right\} e^{-kz} J_0(kr) dk, \\ \hat{u}_z &= \int_0^\infty \left\{ \frac{2z\mu(\lambda+\mu)k^2}{\lambda+3\mu} [U(k)-W(k)] - \frac{2\mu^2k}{\lambda+3\mu} W(k) \right. \\ &\quad \left. - \frac{2\mu(\lambda+2\mu)k}{\lambda+3\mu} U(k) \right\} e^{-zJ_0(kr)} dk, \\ &\text{etc. ;} \end{aligned} \right\} \quad (145)$$

in which

$$\left. \begin{aligned} U(k) &= k \int_0^\infty u(a) J_1(ka) a da, \\ W(k) &= k \int_0^\infty w(a) J_0(ka) a da, \end{aligned} \right\} \quad (146)$$

## CONTENTS.

### I. Introduction.

§§ 1—4.

### II. Solution of Equation of Equilibrium.

- § 5. Differential equations concerning the equilibrium of a semi-infinite elastic body.  
 §§ 6—8. Solution for displacement.  
 § 9. Solution for stress.

### III. Lamé and Clapeyron's Problem.

- § 10. Statement of the problem and typical solution.  
 § 11. General solution for any given normal pressure at the boundary.

### IV. Examples in the Case of Symmetry.

- § 12. General solution for the case of symmetry.

#### Example I.

- § 13. Normal pressure concentrated at a point.  
 § 14. Failure of the solution.

#### Example II.

- §§ 15—17. Diffused distribution of normal pressure according to the law  $A/(a^2 + r^2)^{3/2}$ .  
 §§ 18—20. Application to the problem of rupture of foundation. Stability of a mountain.

#### Example III.

- § 21. Normal pressure distributed uniformly over a circular area.  
 § 22. Evaluation of certain integrals.  
 §§ 23—27. Expressions for displacement.  
 §§ 28—29. Formulæ for stress  
 § 30. Singularity at the edge of the loaded area.  
 § 31. Application to the rupture of the surface.  
 §§ 32—34. Effect of a material loading on the water-level measurement.

**Example IV.**

- §§35—37. Normal pressure distributed over a circular area according to the law  $A(a^2 - r^2)^{\frac{1}{2}}$ .  
 §38. Application to the water-level measurement.

**Example V.**

- §§39—42. Normal pressure of the form  $A/(a^2 - r^2)^{\frac{1}{2}}$  distributed over a circular area.

**V. Boussinesq's Problem**

- §43. Statement of the problem.  
 §§44—47. Solutions when at the surface all the surface tractions are given ; the normal traction and radial displacement ; the tangential traction and normal displacement ; the radial and normal displacements.

# Recherches sur les spectres d'absorption des ammine-complexes métalliques.

Par

**Yuji SHIBATA**, *Rigakushi*.

Laboratoire de Chimie minérale de l'Université Impériale de Tōkiō.

## II.

### A) Spectres d'absorption et conductibilités électrolytiques des solutions aqueuses des nitro-ammine-complexes cobaltiques, qui sont des coordination-polymères.<sup>1)</sup>

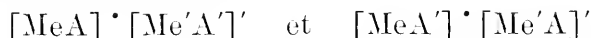
Fait en commun avec K. Matsuno, *Rigakushi*.

---

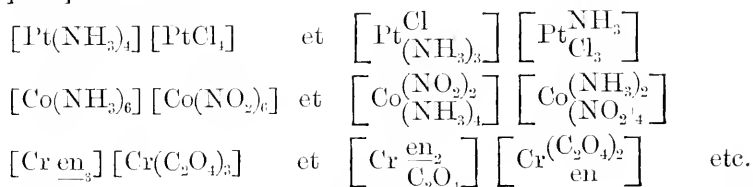
Avec 5 figures.

---

Si un métal Me forme deux ions complexes s'enchainant tantôt avec un groupe atomique A, tantôt avec un autre groupe atomique A' et si, de même, un autre métal Me' se comporte comme le premier, on appelle coordination-isomères les deux sels complexes suivants ainsi formés :



cette catégorie de l'isomérisation est aussi possible, dans le cas où les atomes métalliques centraux dans les ions négatifs et positifs ne sont pas différents. Il y a de nombreux exemples de tels isomères. En voici quelques uns :

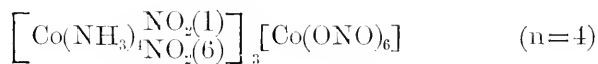
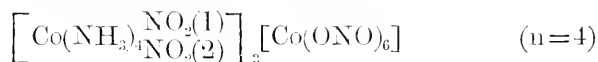
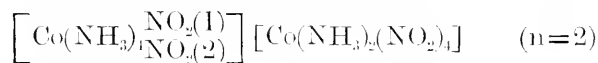
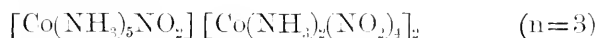



---

1) Comparer „Neuere Anschauungen auf dem Gebiete der anorganischen Chemie“ par M. A. Werner, P. 260. [1909, Friedrig Vieweg u. Sohn, Braunschweig].

De plus, dans le cas où les noyaux des ions négatifs et positifs consistent en un même métal, la polymérie est aussi possible et les complexes, qui sont en une telle relation les uns avec les autres, sont appelés coordination-polymères.

Les six complexes suivants, dont j'étudie ici les spectres d'absorption de leurs solutions aqueuses, appartiennent à cette dernière catégorie de l'isomérisie, et peuvent être représentés par la formule générale  $n[\text{Co}(\text{NH}_3)_3(\text{NO}_2)_3]^{1*}$  :



Dans le travail de l'un de nous<sup>1)</sup>, l'auteur a démontré, que les anions et les cations de ces sels complexes sont chromophores remarquables et, que leurs solutions aqueuses donnent deux ou trois bandes d'absorption très nettes dans l'échelle spectrale entière, quand ils forment des sels complexes ordinaires, en se liant avec les anions ou les cations simples, comme  $\text{Cl}'$ ,  $\text{SO}_4''$ ,  $\text{Na}^+$  ou  $\text{NH}_4^+$  etc., selon leurs signes électrolytiques.

Le but du présent travail est donc d'examiner, quelles propriétés optiques ont les six sels complexes donnés plus haut, dont les anions et les cations sont, à la fois, complexes et chromophores, sous le rapport de l'absorption des rayons, et si les ions complexes et chromatiques exercent quelque influence les uns sur les autres, quand leurs solutions absorbent des rayons.

1) S. M. Jørgensen : Zeitschr. f. anorg. Chem. **5**, 175 (1894).

\* Parmi 8 polymères préparés par Jørgensen, les deux qui contiennent le tétraco-complexe  $[\text{Co}(\text{NH}_3)_6]^{++}$  n'ont pas été étudiés dans ce travail, à cause de leur insolubilité dans l'eau.

2) Yuji Shibata : Journ. of the College of Science, Imp. Univ., Tokyo. Vol. XXXVII, Art. **2** (1915).

Afin de comparer plus facilement, les absorptions de ces sels à celles de leur corps mère, trinitro-triammine cobaltique, nous avons pris  $1/n$  molécule de chaque sel et préparé des solutions de  $\frac{1}{100}$  jusqu'à  $\frac{1}{10000}$  d'équivalent. Les solutions ainsi préparées sont toujours tout à fait stables, et, en conséquence, la loi de Beer sur l'absorption des rayons est complètement satisfaite par elles.

En examinant les courbes d'absorption de ces six polymères complexes, on peut remarquer facilement, qu'ils peuvent être classés en deux catégories: les polymères qui possèdent l'anion complexe, diammine-tétranitro cobaltique  $[\text{Co}(\text{NH}_3)_2(\text{NO}_2)_4]'$ , dans leurs molécules, et les autres, qui contiennent l'héxanitrite cobaltique  $[\text{Co}(\text{ONO})_6]'''$ , comme leur anion.

Ceux qui appartiennent à la première catégorie montrent une bande d'absorption très caractéristique à 2200 de fréquences. Elle ne devrait peut-être pas être appelée „la bande“ dans le sens strict, parce qu'elle est tout à fait plane, et ne montre aucun point étroit du maximum d'absorption, en présentant l'aspect du point d'inflexion de la courbe mathématique. Les spectres d'absorption des solutions des sels de cette catégorie montrent encore une seconde et une troisième bande respectivement à 3000 et à 4000 de fréquences; la seconde de ces bandes est commune à tous les nitro-ammine-complexes cobaltiques, tandis que la troisième est caractéristique de l'anion tétranitro-diammine cobaltique  $[\text{Co}(\text{NO}_2)_4(\text{NH}_3)_2]'$ .

Les polymères complexes de la deuxième catégorie, qui contiennent l'anion complexe, héxanitrite cobaltique, montrent deux ou trois bandes d'absorption très nettes et normales, dans l'état de solution aqueuse.

En résumé, la propriété optique concernant l'absorption des rayons des six polymères complexes, qui sont formés d'anions et de cations à la fois complexes et chromatiques, est généralement additive, sauf seulement le cas de la première bande d'absorption anormale des trois sels déjà nommés.

Pour rechercher d'où provenait cette dernière anomalie, nous avons alors entrepris la mesure de la conductibilité électrolytique des solutions aqueuses des polymères complexes, parce que si l'ano-

malie est causée par un changement quelconque de la constitution chimique de ces sels complexes à l'état de solution, leurs conductibilités électrolytiques, qui rendent compte des nombres des ions, doivent montrer aussi quelques anomalies. Pourtant les résultats de ces mesures, comme on verra dans la partie expérimentale, se sont trouvés être tout à fait normaux. Alors on ne peut plus attribuer la cause de l'anomalie des premières bandes d'absorption des polymères de la première catégorie à la transformation de leur constitution chimique. Nous avons donc essayé d'expliquer cette anomalie par le fait que les oscillations des électrons de valence relâchés,<sup>1.)</sup> s'attachant aux atomes cobaltiques dans les deux ions, cation et anion, des polymères complexes, sont fortement limitées par leurs connexions mutuelles. Nous avons renvoyé la discussion précise sur ce sujet dans la conclusion à la fin.

### Partie expérimentale.

#### 1.) Spectres d'absorption des solutions aqueuses des polymères complexes de la première catégorie.\*

Les trois sels, — $[\text{Co}(\text{NH}_3)_5\text{NO}_2]^{++} [\text{Co}(\text{NH}_3)_2(\text{NO}_2)_4]_2^{-}$ ,  $[\text{Co}(\text{NH}_3)_4\overset{\text{NO}_2(1)}{\text{NO}_2(2)}]^{+} [\text{Co}(\text{NH}_3)_2(\text{NO}_2)_4]^{-}$  et  $[\text{Co}(\text{NH}_3)_4\overset{\text{NO}_2(1)}{\text{NO}_2(6)}]^{+} [\text{Co}(\text{NH}_3)_2(\text{NO}_2)_4]^{-}$ —qui contiennent l'anion monovalent, diammine-tétranitro cobaltique, ont été groupés dans la première catégorie des polymères complexes présentement étudiés. Ils ont été préparés par la méthode de la double décomposition, en mélangeant la solution aqueuse saturée du cobalt-diammine-tétranitrite de potassium,  $[\text{Co}(\text{NH}_3)_2(\text{NO}_2)_4]\text{K}$  respectivement avec celles des chlorures pentammine-mononitro-cobaltique (xantho), cis-dinitro-tétrammine-cobaltique (flavo), et trans-dinitro-tétrammine-cobaltique (crocéo).

Le xantho- et le flavo-diammine-tétranitro-cobalt ont été étudiés dans les concentrations respectivement de 0.0025–0.000025

1.) Comparer le dernier travail de l'un des auteurs, Yuji Shibata ; loc. cit.

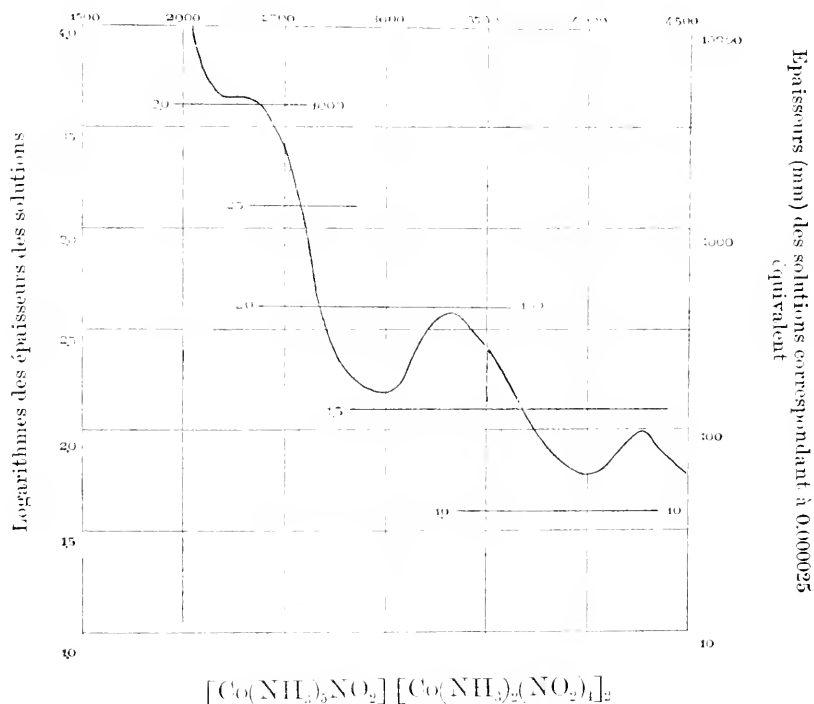
\* Pour ce qui concerne la méthode de l'étude de l'absorption des rayons et des représentations graphiques, l'un des auteurs, Yuji Shibata, l'a décrit dans son dernier travail, loc. cit.



équivalent et de 0.01–0.0001 équivalent, tandis que le crocéo-diammine-tétranitro-cobalt n'a pu être étudié que dans la solution de la concentration de 0.0001 équivalent, à cause de sa faible solubilité dans l'eau.

Fig. I

Fréquence

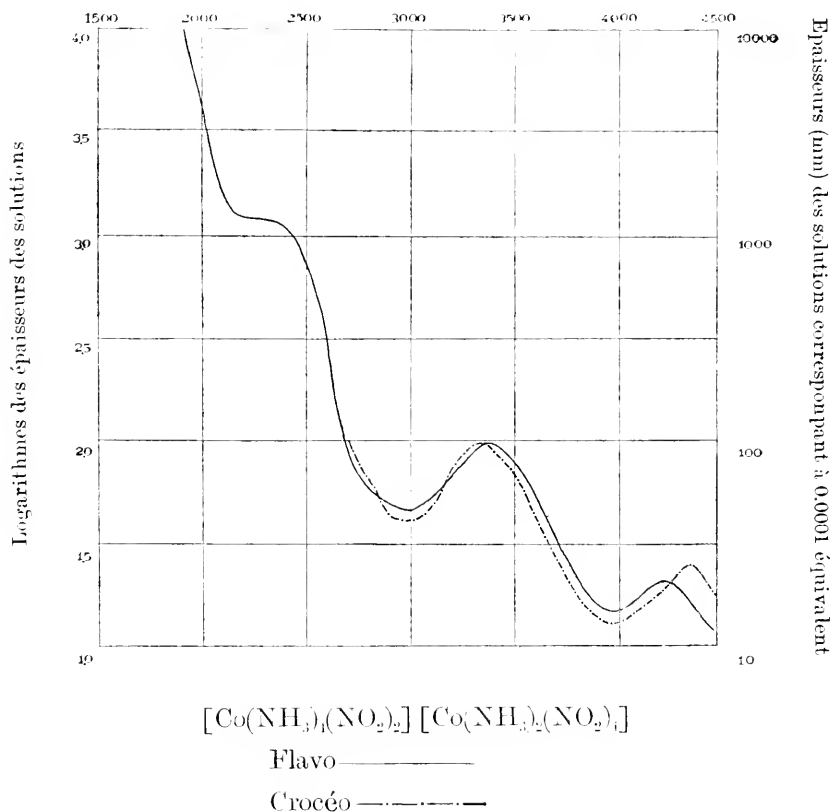


La figure I représente la courbe d'absorption du xantho-diammine-tétranitro-cobalt. Les lignes courtes, tirées horizontalement dans la figure, signifient les épaisseurs recalculées correspondant à 0.0001 équivalent; les chiffres placés aux deux côtés des lignes expriment naturellement les épaisseurs (à droite) et leurs logarithmes (à gauche). Comme nous l'avons déjà indiqué, la bande d'absorption à 2200 de fréquences de ce sel est très caractéristique, ayant presque la forme du point d'inflexion de la courbe mathématique.

Les deux autres bandes sont, au contraire, tout à fait normales dans les nitro-ammine-complexes, dont au moins les deux groupes de nitro se placent aux positions de trans l'un et l'autre. Dans ce cas, en effet, l'anion remplit cette condition.

Fig. II

Fréquence

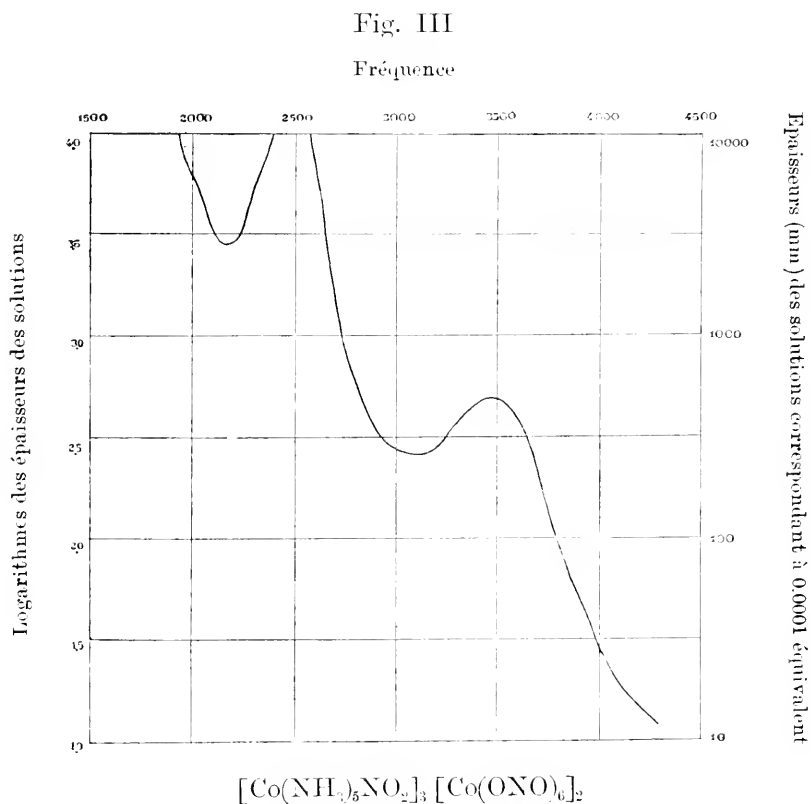


Dans la figure II, on aperçoit les courbes d'absorption des deux sels qui contiennent les cations complexes respectivement du crocéo cobaltique et du flavo cobaltique. La forme de leurs courbes coïncide parfaitement avec celle du complexe précédent.

## 2) Spectres d'absorption des solutions aqueuses des polymères complexes de la deuxième catégorie.

Les trois sels appartenant à cette catégorie—xantho-, flavo- et crocéo-héxanitrite cobaltique—ont été préparés de la même manière que les sels précédents. Cependant les solubilités des produits ultimes étant considérables dans ce cas, il a fallu qu'on fasse refroidir les solutions mélangées avec le mélange réfrigérant, pour les faire se séparer par cristallisation.

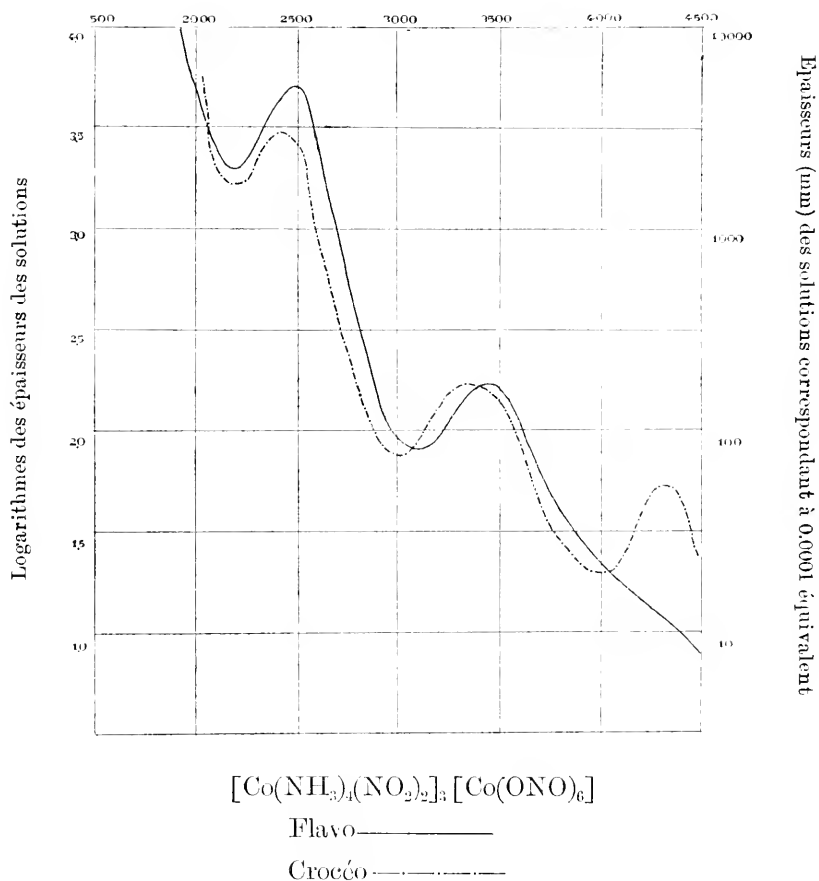
La figure III représente la courbe d'absorption du xantho-héxanitrite cobaltique. Elle a deux bandes d'absorption à 2100 et



à 3000 de fréquences; les deux bandes paraissent aux épaisseurs de solution sensiblement plus grandes que celles des autres nitro-ammine-complexes.

Fig. IV

Fréquence



Les courbes d'absorption de flavo- et de crocéo-héxanitrite cobaltique, qui sont tracées dans la figure IV, sont presque les mêmes, pour leurs formes, que celles des chlorures de flavo et de crocéo; c'est-à-dire que les flavo-complexes ne montrent que deux bandes d'absorption, tandis que les crocéo-complexes en ont trois, dont les deux premières coïncident dans les deux cas pour la position et pour l'épaisseur, où elles paraissent.

En résumé les polymères complexes appartenant à cette catégorie ne montrent aucune anomalie à l'égard de l'absorption des rayons.

### 3) Conductibilités électrolytiques des solutions aqueuses des coordination-polymères cobaltiques.

M. M. Werner, Miolati et leurs élèves ont mesuré les conductibilités électrolytiques des solutions aqueuses des plusieurs ammine-complexes métalliques, dans le but de connaître le nombre de leurs ions dans l'eau, en comparant les valeurs de leurs conductibilités moléculaires.

Nous avons suivi ces exemples de mesure de conductibilités électrolytiques des polymères complexes cobaltiques, pour connaître aussi les nombres de leurs ions dans l'état de solution aqueuse, pour la raison déjà donnée dans l'introduction.

Comme les chiffres, que nous allons donner ci-dessous, l'expliquent bien, les résultats des mesures des conductibilités électrolytiques ont été tout à fait normaux, c'est-à-dire qu'il n'y a eu aucun changement des constitutions chimiques des polymères complexes au moment de leur préparation.

Quant à la méthode de mesure des conductibilités électrolytiques, cette mesure a été exécutée d'après le système d'Ostwald, et les dilutions des solutions observées ont été prises, selon les solubilités des polymères complexes, entre 256 et 16384, les températures d'observation étant toujours 25°.

Les polymères complexes cobaltiques étant des électrolytes assez faibles, leurs conductibilités moléculaires n'atteignent presque pas à la valeur constante, quand même les dilutions des solutions sont suffisamment grandes. De même, la tendance minima de l'hydrolyse des solutions fait monter la valeur de la conductibilité moléculaire de plus en plus, quand on les mesure, pour un sel d'une certaine dilution, à certains intervalles de temps. Par cette raison, il nous a fallu faire la comparaison des valeurs de nos mesures avec celles des auteurs déjà cités, dans la dilution fixée; pour cette dilution de comparaison nous avons choisi la dilution 1024.

Table I.

[Co(NH <sub>3</sub> ) <sub>5</sub> NO <sub>2</sub> ] [Co(NH <sub>3</sub> ) <sub>2</sub> (NO <sub>2</sub> ) <sub>4</sub> ] <sub>2</sub>		
V (Dilution)	k (Conductibilité spécifique)	$\mu$ (Conduct. moléculaire)
1024	22.00 $\times 10^{-5}$	225.2
2048	12.16 "	249.0
4096	6.798 "	278.4
8192	3.740 "	306.3

Table II.

[Co(NH <sub>3</sub> ) <sub>4</sub> (NO <sub>2</sub> ) <sub>2</sub> ] <sub>3</sub> [Co(NH <sub>3</sub> ) <sub>2</sub> (NO <sub>2</sub> ) <sub>4</sub> ]		
V	k	$\mu$
256	36.48 $\times 10^{-5}$	93.35
512	20.21 "	103.5
1024	10.69 "	109.4
2048	5.982 "	122.6
4096	3.399 "	139.2

Table III.

[Co(NH <sub>3</sub> ) <sub>4</sub> (NO <sub>2</sub> ) <sub>2</sub> ] <sub>3</sub> [Co(NH <sub>3</sub> ) <sub>2</sub> (NO <sub>2</sub> ) <sub>4</sub> ]		
V	k	$\mu$
2048	87.98 $\times 10^{-6}$	180.2
4096	49.85 "	204.2
8192	29.33 "	240.3
16384	19.68 "	322.4

Table IV.

[Co(NH <sub>3</sub> ) <sub>5</sub> NO <sub>2</sub> ] <sub>3</sub> [Co(ONO) <sub>6</sub> ] <sub>2</sub>						
V	k <sub>1</sub>	k <sub>2</sub>	$\mu_1$	$\mu_2$		
256	33.99 $\times 10^{-4}$	—	870.2	—		
512	18.24 "	—	934.0	—		
1024	9.84 "	93.48 $\times 10^{-5}$	1008.0	957.2		
2048	5.157 "	49.85 "	1056.0	1021.0		
4096	2.876 "	26.71 "	1178.0	1093.0		
8192	1.558 "	14.33 "	1276.0	1250.0		

Table V.

[Co(NH <sub>3</sub> ) <sub>4</sub> (NO <sub>2</sub> ) <sub>2</sub> ] <sub>3</sub> [Co(ONO) <sub>6</sub> ]		
V	k	$\mu$
1024	37.40 $\times 10^{-5}$	391.8
2048	20.48 "	419.6
4096	10.69 "	437.5
8192	6.503 "	532.7

Table VI.

[Co(NH <sub>3</sub> ) <sub>4</sub> (NO <sub>2</sub> ) <sub>2</sub> ] <sub>3</sub> [Co(ONO) <sub>6</sub> ]		
V	k	$\mu$
256	12.26 $\times 10^{-4}$	313.8
512	6.50 "	333.0
1024	3.32 "	340.3
2048	1.824 "	373.6
4096	9.906 $\times 10^{-5}$	405.5
8192	5.540 "	453.8

Pour permettre la comparaison, nous citons ici les résultats des mesures des conductibilités moléculaires, obtenus par M. M. Werner, Miolati et leurs élèves\* pour les sels complexes de platine et de cobalt dans la dilution 1000.

\*A. Werner et A. Miolati : Zeitschr. f. phys. Chem. **12**, 35 (1894).

A. Werner et Ch. Herty : " " " " **38**, 331 (1901).

V. Kohlshütter : Ber. d. deutsch. Chem. Gesell. **36**, 1151 (1903).

A. Miolati : Zeitschr. f. anorg. Chem. **22**, 445 (1900).

A. Miolati et Pizzighelli : Journ. f. Prakt. Chem. **77** 417 (1908).

## a) Complexes qui consistent en deux ions

$[\text{Pt}(\text{NH}_3)_3\text{Cl}]\text{Cl}$	$\mu=115.8$
$[\text{Pt}(\text{NH}_3)\text{Cl}_5]\text{K}$	108.5
$[\text{Co}(\text{NH}_3)_4\text{CO}_3]\text{Br}$	106.0
$[\text{Co}(\text{NH}_3)_4(\text{NO}_2)_2^{(1)}]\text{Cl}$	100.7
$\left[ \text{Co} \begin{smallmatrix} (\text{NH}_3)_4 \\ (\text{NO}_2)_2^{(1)} \end{smallmatrix} \right] \left[ \text{Co} \begin{smallmatrix} (\text{NO}_2)_4 \\ (\text{NH}_3)_2 \end{smallmatrix} \right]$	61.19

(Temperature d'observation 25°).

Notre valeur pour  $\mu$  (dil. = 1024) du flavo diammine-tétranitrite cobaltique, qui est donnée dans la table II, coïncide alors très bien avec celles des complexes consistant en deux ions de platine et de cobalt, tandis que la valeur donnée par les auteurs cités ci-dessus et celle donnée par nous pour le même complexe du flavo diammine-tétranitrite cobaltique diffèrent plutôt d'une façon considérable. Mais nous croyons que notre valeur est meilleure que celle de M. M. Werner et Miolati, parce que notre conductibilité moléculaire de ce complexe montre une excellente coïncidence avec la majorité des complexes consistant en deux ions de platine et de cobalt.

Alors il est bien sûr que ce sel complexe possède la formule normale de  $\left[ \text{Co}(\text{NH}_3)_4 \begin{smallmatrix} \text{NO}_2^{(1)} \\ \text{NO}_2^{(2)} \end{smallmatrix} \right] \left[ \text{Co}(\text{NH}_3)_2(\text{NO}_2)_4 \right]$  et qu'il n'y a eu aucun changement de sa constitution au moment de la préparation par la double décomposition entre le chlorure de flavo cobaltique et le cobalti-diammine-tétranitrite de potassium.

Quant à la conductibilité électrolytique du crocéo-diammine-tétranitrite cobaltique, isomère stéréochimique du sel précédent, elle n'a été mesurée qu'à partir de la dilution 2048 à cause de sa faible solubilité. Nous n'avons pas, par conséquent, sa valeur de  $\mu$  à la dilution 1024 pour faire la comparaison. Au surplus, on obtient toujours les sensiblement hautes valeurs de  $\mu$  pour ce sel, parce qu'on a besoin d'un peu plus de temps pour sa dissolution complète dans l'eau.

## b) Complexes qui consistent en trois ions

$[\text{Pt}(\text{NH}_3)_4\text{Cl}_2]\text{Cl}_2$	$\mu=228.9$
$[\text{Pt}(\text{NH}_3)_4(\text{NO}_2)_2](\text{NO}_3)_2$	234.4
$[\text{Co}(\text{NH}_3)_5(\text{NO}_2)](\text{NO}_2)_2$	234.4

$[\text{Co}(\text{NH}_3)_5 \text{Br}] \text{Br}_2$	$\mu=257.6$
$[\text{Cr}(\text{NH}_3)_5 \text{Cl}] \text{Cl}_2$	260.2
(dil.=1000 ; temp.=25°)	

Notre valeur  $\mu$  (dil.=1024; temp.=25°) pour le xantho-diammine-tétranitrite cobaltique, qui est donnée dans la table I, est 225.2 et coïncide encore très bien avec les valeurs pour les complexes consistant en trois ions de platine, cobalt et de chrome, dont les chiffres donnés par M. M. Werner et Miolati sont cités ci-dessus.

**c)** Complexes qui consistent en quatre ions

$[\text{Co}(\text{NH}_3)_5 \text{H}_2\text{O}] \text{Br}_3$	$\mu=412.9$
$[\text{Co}(\text{NH}_3)_5 (\text{H}_2\text{O})_3] \text{Cl}_3$	383.8
$[\text{Co}(\text{NH}_3)_4 (\text{H}_2\text{O})_2] \text{Br}_3$	399.5
$[\text{Co}(\text{NH}_3)_6] (\text{NO}_3)_3$	421.9
(dil.=1000 ; temp.=25°)	

Dans les tables V et VI, on voit nos valeurs des conductibilités moléculaires pour le flavo- et le crocéo-héxanitrite cobaltique. Ces valeurs  $\mu_{1024}=391.8$  et  $\mu_{1024}=340.3$  montrent encore une coïncidence satisfaisante avec celles des complexes cobaltiques consistant en quatre ions cités ci-dessus.

**d)** Complexes qui consistent en cinq ions

Comme nous l'avons montré dans la table IV, notre valeur  $\mu_{1024}$  pour le xantho-héxanitrite cobaltique  $[\text{Co}(\text{NH}_3)_5 \text{NO}_2]_3 [\text{Co}(\text{ONO})_6]_2$  est à peu près 1000, tandis que celle mesurée par M. M. Werner et Miolati<sup>1)</sup> pour le même sel est de  $\mu_{2700}=572.2$  et pour  $[\text{Pt}(\text{NH}_3)_6] \text{Cl}_4$ , elle est de  $\mu_{1000}=522.9$ . Par conséquent notre valeur est sûrement trop haute pour le sel de cinq ions, quoique nous ayons exécuté deux séries de mesures aussi attentivement que possible.

Cette haute valeur extraordinaire est causée très probablement par l'hydrolyse partielle de l'anion,  $[\text{Co}(\text{ONO})_6]'''$  dans la solution, parce que cet ion est assez instable dans l'eau, comme l'un des auteurs l'a indiqué dans le cas de l'étude spectroscopique de la solution aqueuse du cobalthéxanite de sodium dans son dernier travail<sup>2)</sup>.

1) loc. cit.

2) Yuji Shibata : loc. cit.



En effet, nous avons obtenu encore les trop hautes valeurs de  $\mu$  pour le cobalthéxanitrite de sodium; nous allons en montrer les chiffres dans la table suivante :

Table VII.

[Co(ONO) <sub>6</sub> ] Na <sub>3</sub>		
V	k	$\mu$
256	$16.62 \times 10^{-4}$	425.4
512	8.798 "	450.5
1024	4.532 "	464.0
2048	2.337 "	478.6
4096	1.268 "	519.0

La valeur de  $\mu_{1024}$  est alors 464.0, tandis que celle d'un complexe de quatre ions compte env. 390, comme nous l'avons dit plus haut à propos des observations de M. M. Werner et Miolati.

Maintenant ce que nous venons d'apprendre des résultats de nos mesures de conductibilités électrolytiques des solutions aqueuses des coordination-polymères, est que les doubles décompositions, dans le cas des préparations des polymères, se font tout à fait régulièrement, et peuvent être représentées par la formule générale suivante:



### Conclusion.

Comme nous l'avons indiqué ça et là plus haut, il ne faut pas attribuer la cause de l'anomalie de la première bande d'absorption des trois polymères complexes, qui contiennent l'anion  $[Co(NH_3)_2 \cdot (NO_2)_4]$ , au changement de leurs constitutions chimiques, mais cette cause doit être attribuer absolument à la restriction de vibrations des électrons de valence relâchés, qui s'attachent aux atomes de cobalt dans les ions complexes.

Avant de rentrer dans la discussion sur cette supposition relative à la restriction des vibrations des électrons, nous voulons exprimer une opinion hypothétique, qui est tenue par l'un de nous depuis long temps, sur l'état des sels dissous dans les solvants, spécialement dans l'eau. L'un de nous pense que les anions et les cations

d'un certain sel dissocié dans un solvant ne se trouvent pas séparé sans ordre, mais qu'ils sont liés encore par couple; l'affinité entre eux est naturellement très affaiblie peut être par l'hydratation des ions respectifs. Maintenant si l'on fait passer un courant d'électricité dans la solution, cette liaison légère entre les ions est coupée, et leurs mouvements vers les électrodes sont ensuite observés.

Cette supposition est aussi appuyée par le fait que les pouvoirs rotatoires des solutions des sels optiquement actifs sont fortement influencés par les anions (ou cations) qui s'accouplent avec ces cations (ou anions) optiquement actifs. Par exemple, dans le cas des ammine-complexes cobaltiques optiquement actifs, dont la plupart ont les cations complexes asymétriquement construits, les pouvoirs rotatoires de leurs solutions aqueuses changent régulièrement d'après la grandeur des anions\*, bien que l'activité optique ne soit causée absolument que par la structure asymétrique des cations, et que les anions n'aient aucune relation avec elle. Si on admettait l'idée que les ions négatifs et positifs se trouvent séparément dans la solution, ce dernier fait serait évidemment improbable. Quant à l'espèce d'électrons de valence, qui sert à lier légèrement les anions et les cations dans la solution, elle ne peut être naturellement déterminée en général. Mais revenant à notre sujet, nous osons dire que, au moins dans notre cas, ce sont les électrons de valence relâchés attachant aux atomes cobaltiques dans les ions complexes, qui les lient dans l'eau.

Prenons d'abord en considération les nombres des valences auxiliaires des atomes cobaltiques dans les anions et les cations, qui forment la molécule de chaque coordination-polymère :

---

*Comparer	A. Werner :	Ber. d. deutsch. chem. Gesell. <b>44</b> 1887 (1911)					
	"	"	"	"	"	"	2445 "
	"	"	"	"	"	"	3272 "
	"	"	"	"	"	"	3279 "
	"	"	"	"	"	"	<b>45</b> 121 (1912)
A. Werner et	McCutcheon :	"	"	"	"	"	3281 "
"	" Y. Shibata :	"	"	"	"	"	3287 "
"	" Tschernoff :	"	"	"	"	"	3294 " etc.

---

Table VIII.

Polymères de la première catégorie.		Nombres des valences auxiliaires.	
$[\text{Co}(\text{NH}_3)_5 \text{NO}_2]_1$	$[\text{Co}(\text{NH}_3)_2(\text{NO}_2)_4]_2$	$\left\{ \begin{array}{l} \text{dans le cation} \\ \text{dans l'anion} \end{array} \right.$	$\left\{ \begin{array}{l} 5 \\ 6 \end{array} \right.$
$[\text{Flavo}]_1$	$[ \quad " \quad ]_1$	$\left\{ \begin{array}{l} \text{dans le cation} \\ " \text{ l'anion} \end{array} \right.$	$\left\{ \begin{array}{l} 4 \\ 3 \end{array} \right.$
$[\text{Crocéo}]_1$	$[ \quad " \quad ]_1$	$" \quad " \quad "$	$"$
Polymères de la deuxième catégorie.			
$[\text{Co}(\text{NH}_3)_5 \text{NO}_2]_1$	$[\text{Co}(\text{ONO})_6]_2$	$\left\{ \begin{array}{l} \text{dans le cation} \\ " \text{ l'anion} \end{array} \right.$	$\left\{ \begin{array}{l} 15 \\ 6 \end{array} \right.$
$[\text{Flavo}]_1$	$[ \quad " \quad ]_1$	$\left\{ \begin{array}{l} " \text{ le cation} \\ " \text{ l'anion} \end{array} \right.$	$\left\{ \begin{array}{l} 12 \\ 3 \end{array} \right.$
$[\text{Crocéo}]_3$	$[ \quad " \quad ]_1$	$" \quad " \quad "$	$"$

D'après l'hypothèse de J. Stark, c'est très probablement l'électron de valence relâché, qui donne la bande d'absorption dans l'échelle spectrale visible ou ultraviolette\*. C'est donc notre avis que dans les composés minéraux, cette espèce d'électrons de valence se trouve toujours aux points de connexion produite par la valence auxiliaire, parce que presque tous les sels minéraux colorés contiennent des ions complexes dans leurs molécules, sauf quelques iodures et sulfures, où les derniers atomes sont les chromophores remarquables. De plus, l'un de nous a constaté autrefois que le changement de nombre de coordination de certains sels complexes cobaltiques provoque la transformation de leurs couleurs.<sup>1)</sup>

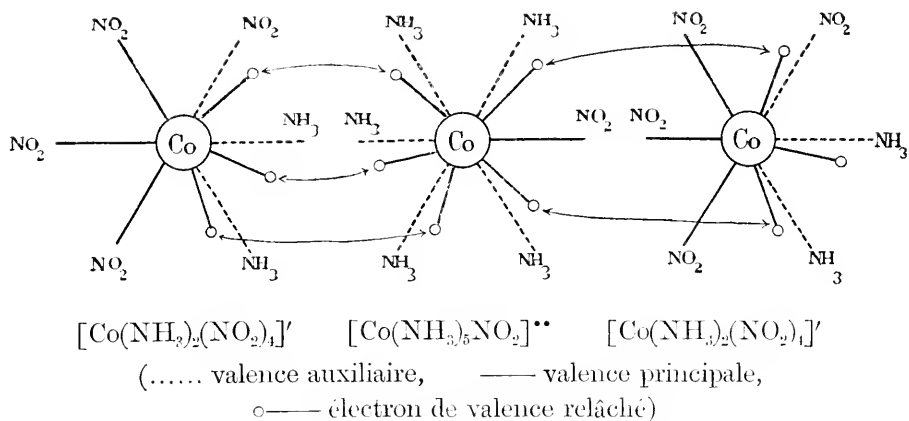
Dans la figure V nous avons représenté la manière de liaison hypothétique des ions d'un polymère complexe, par exemple du xanthodiammine-tétranitrite cobaltique, selon notre opinion que les électrons de valence relâchés se trouvent aux points de connexion produite par la valence auxiliaire et que des électrons de valence de cette espèce servent à lier les ions dans l'eau.

Comme on le voit dans la table et la figure, la différence de nombre des électrons de valence relâchés dans les cations et les anions étant égale à 1, dans les trois polymères de la première catégorie, il n'y en a qu'un qui puisse osciller librement, tandis que

\* Voir le dernier travail de Yuji Shibata : loc. cit.

1) A. Hantzsch et Yuji Shibata : Zeitschr. f. anorg. Chem. **73** 309 (1911)

Fig. V.



les autres sont enchainés les uns aux autres dans les anions et les cations, et leurs vibrations sont, par conséquent, fortement restreintes. Si cette dernière supposition est admise, il sera bien naturel que l'aspect de la première bande d'absorption devienne très plane, ayant un maximum et un minimum d'absorption bien insignifiants, parce que, comme l'un de nous l'a fait remarquer dans son dernier travail<sup>1)</sup>, la première bande à env. 2000 de fréquences des sels cobaltiques est provoquée probablement par les vibrations des électrons de valence relâchés s'attachant aux atomes de cobalt.

Le fait que tous les trois polymères de la seconde classe donnent la première bande d'absorption très nette et normale, est facilement compris, si l'on observe, comme l'indique notre dernière table, que les différences des nombres des valences auxiliaires dans les anions et les cations sont bien considérables c'est-à-dire 9; en d'autres termes, il y a neuf électrons de valence relâchés, s'attachant aux atomes de cobalt, qui peuvent osciller librement.

Parmi les trois polymères de la deuxième catégorie, le xanthohéxanitrite cobaltique  $[\text{Co}(\text{NH}_3)_5\text{NO}_2]_3 [\text{Co}(\text{ONO})_6]_2$  donne les bandes d'absorption sensiblement hypochromatiques, et la forme de sa courbe ressemble beaucoup à celle du cobalthéxanitrite de sodium<sup>2)</sup>  $[\text{Co}(\text{ONO})_6] \text{Na}_3$ , tandis que les deux autres donnent les

1) Voir le dernier travail de Yuji Shibata, loc. cit.

2) loc. cit.

courbes d'absorption caractéristiques dans leurs cations, flavo et crocéo, et ne sont presque pas influencés par l'anion  $[\text{Co}(\text{ONO})_6]'''$ , qui est un hypochrome remarquable. Cette différence des formes des courbes d'absorption de ces trois sels :  $[\text{Co}(\text{NH}_3)_5\text{NO}_2]_3[\text{Co}(\text{ONO})_6]_2$ ,  $\left[ \text{Co}(\text{NH}_3)_4 \begin{smallmatrix} \text{NO}_2^{(1)} \\ \text{NO}_2^{(2)} \end{smallmatrix} \right]_3 [\text{Co}(\text{ONO})_6]$  et  $\left[ \text{Co}(\text{NH}_3)_4 \begin{smallmatrix} \text{NO}_2^{(1)} \\ \text{NO}_2^{(6)} \end{smallmatrix} \right]_3 [\text{Co}(\text{ONO})_6]$  doit être causée par l'inégalité des nombres des groupes de nitro et de nitrito dans chaque molécule des polymères ; en effet, le xantho-cobalthéxanitrite possède 12 nitritos pour 3 nitros dans sa molécule, tandis que la flavo-et le crocéo-cobalthéxanitrite n'ont qu'un nitrito pour 6 nitros.



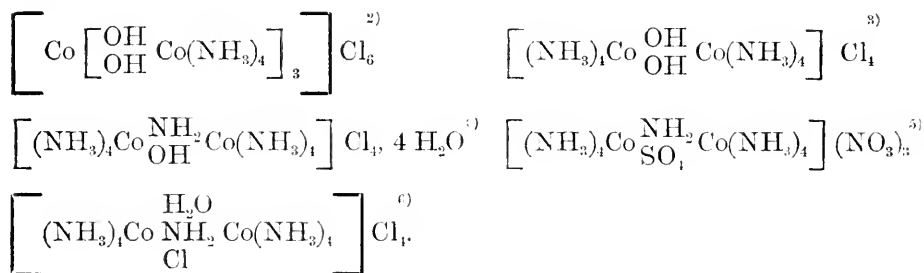
## B.) Spectres d'absorption des solutions aqueuses des ammine-complexes cobaltiques des poly-noyaux<sup>1)</sup>.

*Avec 6 figures.*

On connaît de nombreux ammine-complexes métalliques, dont les cations complexes contiennent plus d'un atome métallique. Nous devons la découverte de la plupart de ces complexes à M. M. Jörgensen, Werner et à leurs élèves. Spécialement M. Werner a fait des travaux très intéressants sur la détermination de leurs constitutions chimiques, au point de vue de sa théorie de coordination.

J'ai étudié les absorptions des solutions aqueuses de quelques sels complexes appartenant à cette catégorie, corps purs dont les préparations sont comparativement faciles et, dont la constitution est bien claire.

Ce sont les cinq sels suivants que j'ai choisis comme objets de la présente étude :



Les concentrations des solutions mesurées ont été, comme toujours, d'un centième normal jusqu'à un dix-millième normal; seulement dans le cas du chlorure de dodécamine-héxol-tétracobalt, la moitié seulement de cette concentration a été prise, parce qu'il contient des atomes de cobalt deux fois plus que les autres, tandis que l'azotate d'octamine- $\mu$ -amino-sulfato-dicobalt a été

1) Comparer "Neuere Auschanungen auf dem Geliete der anorg. Chemie" par M. A. Werner, Page 185. [1909, Vieweg u. sohn, Braunschweig.]

2) A. Werner: Ber. d. deutsch. chem. Gesell. **40** 4426 (1907)

3) " " " " " " " 4434 "

4) " " " " " " " 4605 "

5) A. Werner et Baselli: Zeitschr. f. anorg. chem. **16** 111 (1898)

6) A. Werner: Ber. d. deutsch. chem. Gesell. **40** 4605 (1907)

étudié dans les solutions des concentrations de  $\frac{N}{400}$  et  $\frac{N}{1000}$  à cause de sa faible solubilité.

A mesure que je les ai étudié, j'ai remarqué que ces sels complexes ne sont pas du tout stables à l'état de solution aqueuse : dans tous les cas, elle change rapidement sa couleur originale qui devient d'abord très brune, et puis cette couleur s'assombrit peu à peu jusqu' à ce qu'elle paraisse presque opaque. Par conséquent la loi de Beer sur l'absorption des rayons n'est point satisfaite par ces solutions. De même, on remarque que l'inclination à l'abscisse des courbes d'absorption de ces solutions instables est toujours sensiblement plus faible que dans le cas de la solution acide des complexes, qui est tout à fait stable.

Cette faible inclination des courbes d'absorption des solutions aqueuses fait penser qu'il s'agit, sans doute, de l'absorption de la solution colloïdale de l'hydrate de cobalt, qui est formée par la décomposition hydrolytique. Cette considération a été bien constatée expérimentalement, comme on le verra dans la partie expérimentale.

Comme je l'ai indiqué plus haut, j'ai ajouté ensuite aux solutions des sels complexes un peu de l'acide correspondant à ses anions, pour empêcher la décomposition hydrolytique. Dans ce cas, les solutions étaient bien stables et la loi de Beer a été complètement satisfaite et les résultats des observations de l'absorption m'a permis de mettre en évidence quelques faits bien intéressants que je vais décrire et discuter dans la partie expérimentale et dans la conclusion.

## Partie expérimentale.

### 1) Chlorure dodécammine-héxol-tétracobaltique.

Ce sel complexe bien intéressant a été récemment coupé en des composants optiquement actifs par M. Werner<sup>1)</sup>. La solution aqueuse de ce complexe est assez instable et, si on l'abandonne

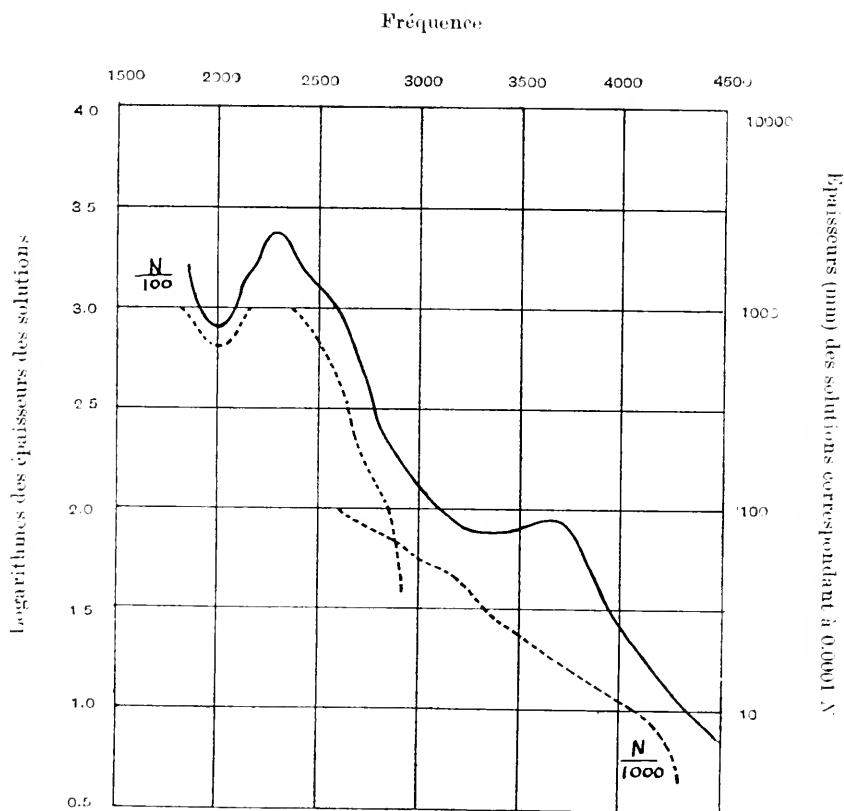
1) A. Werner : Sur l'activité optique de composés chimiques sans carbone ; Comptes rendus des séances de l'Académie des Sciences (Paris), **159**, XVII 423 (1914).



quelque temps, on remarque que la couleur de la solution est complètement perdue et que la coagulation totale de l'hydrate de cobalt, formé par la décomposition hydrolytique, l'accompagne en même temps. En faisant évaporer l'eau mère, on n'obtient que le chlorure d'ammoniaque.

Les courbes d'absorption de la solution aqueuse de ce complexe sont tracées aux lignes ponctuées dans la figure I. Cette solution ne satisfait pas la loi de Beer, et chaque branche des courbes correspondant à plusieurs concentrations ne continue pas ;

Fig. I.



celle de la solution la plus concentrée ( $\frac{N}{200}$ ) montre encore une bande d'absorption, parce que l'hydrolyse de la solution n'était pas encore très sensible au moment de l'observation de cette partie, tandis que l'autre partie de la courbe de la solution dix fois étendue met déjà en évidence le développement de l'hydrolyse par sa faible inclination.

La solution acide, qui a été préparée en dissolvant le complexe dans  $\frac{N}{100}$  l'acide chlorhydrique, est cependant très stable et satisfait la loi de Beer, donnant une courbe d'absorption bien continue dans toutes les concentrations des solutions. Cette courbe, tracée dans la figure I, par une ligne noire, montre les deux bandes d'absorption très nettes, dont la première se place à la fréquence 2000, comme on voit la même bande d'absorption dans tous les sels cobaltiques déjà étudiés, tandis que la seconde se trouve à la fréquence 3400. C'est cette seconde bande nouvelle qu'on n'avait jamais observée dans les sels cobaltiques, soit les simples, soit les complexes. Elle paraît d'une épaisseur assez mince, en effet elle est d'env. 60 mm correspondant à la concentration de  $\frac{1}{2000}$  normal. Il me semble que cette bande d'absorption hyperchromatique est bien caractéristique des sels cobaltiques, dont les ions complexes instables sont construits d'une manière semblable, comme ceux présentement étudiés; c'est-à-dire que chaque atome cobaltique (du noyau) est lié avec quatre molécules d'ammoniaque et deux groupes basiques ou acides.

Ces dernières connexions aux groupes basiques ou acides doivent être bien probablement si faibles que leurs affinités ne peuvent plus être actives dans l'eau, et la décomposition hydrolytique commence, sans doute, aux points de ces connexions faibles.

Je reviendrai encore une fois sur ce sujet plus tard dans la conclusion.

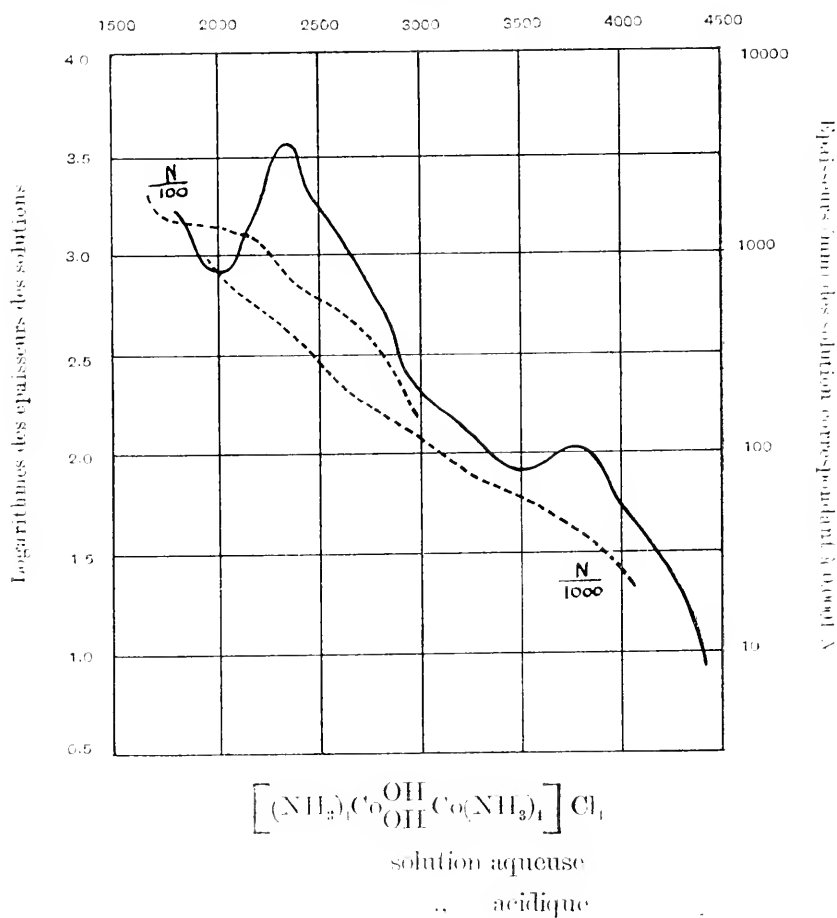
## 2) Chlorure octammine-diol-dicobaltique.

Ce sel violet rougeâtre est bien soluble dans l'eau et la solution est aussi très instable; la précipitation totale de l'hydrate de cobalt et, par conséquent, la décoloration complète de la solution

sont observées en quelques heures. Son eau mère ne donne que le chlorure d'ammoniaque en s'évaporant.

Fig. II.

Fréquence



Les courbes tracées en lignes ponctuées dans la figure II représentent les absorptions des solutions aqueuses de ce complexe. Dans le cas de ce sel, la courbe de la première concentration de  $\frac{N}{100}$  déjà ne montre aucune bande d'absorption et son inclination à l'abscisse est sensiblement plus faible que celle de la solution acide qui est tracée avec la ligne noire dans la même figure.

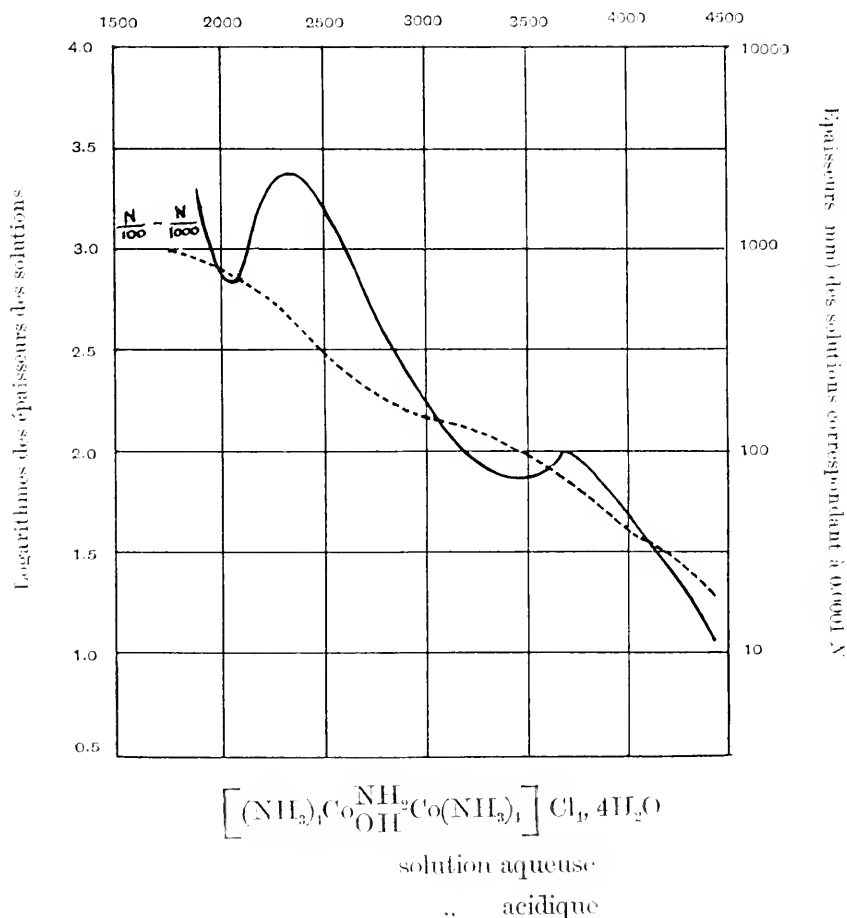
Cette dernière courbe d'absorption de la solution acide

montre encore deux bandes très nettes, comme le sel complexe précédent. De même, les positions des bandes et la forme totale de leurs courbes sont presque les mêmes l'une et l'autre. On verra toujours cette coïncidence curieuse et remarquable des courbes d'absorption entre les différents sels complexes étudiés dans ce travail.

### 3) Chlorure octammine- $\mu$ -amino-ol-dicobaltique.

Fig. III.

Fréquence



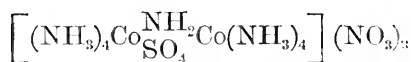
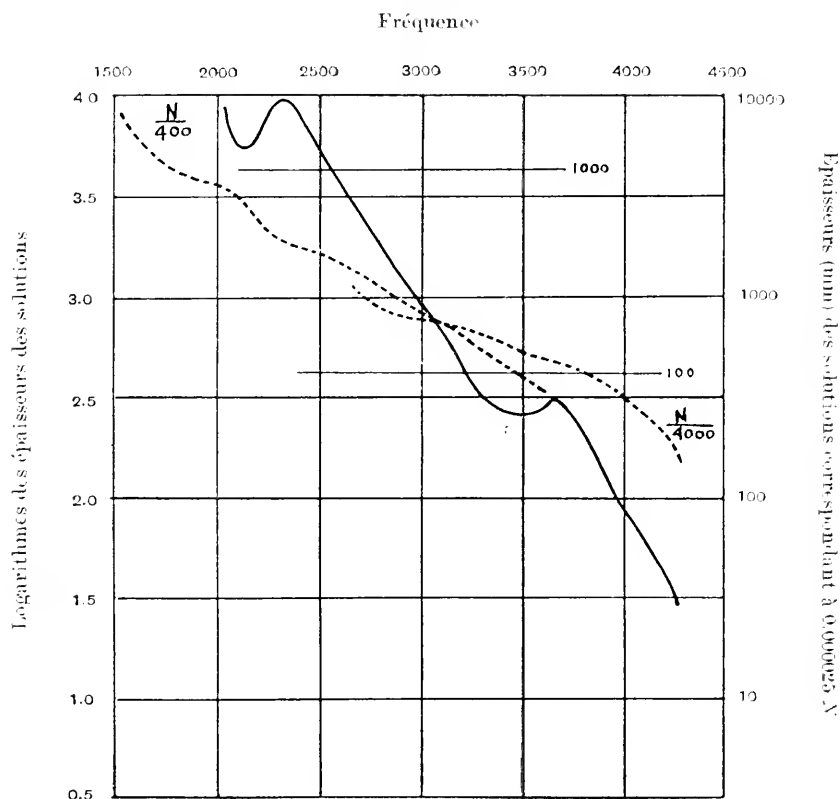
La décomposition hydrolytique de la solution aqueuse et la production de l'hydrosol de l'hydrate de cobalt est peut être la plus

facile en ce sel complexe, parce que, comme on le voit dans la figure III, l'inclinaison des courbes de cette solution ne change plus par les dilutions, et elles continuent assez bien dans chaque concentration, en satisfaisant la loi de Beer.

L'absorption de la solution acide donne deux bandes, dont la position et la forme sont égales à celles des autres, dont nous avons parlé, bien que ce sel complexe contienne un nouveau groupe d'amino.

#### 4) Azotate octammine- $\mu$ -amino-sulfato-dicobaltique.

Fig. IV.



..... solution aqueuse

„ acide

Ce sel complexe, étant moins soluble, nous avons mesuré les absorptions de ses solutions dans les concentrations de  $\frac{N}{400}$  et de  $\frac{N}{1000}$ . Sa solution aqueuse est aussi très instable et les courbes d'absorption donnent une inclination bien caractéristique à la solution colloïdale, tandis que la solution acide est normale et donne une courbe tout à fait semblable aux autres. Le nouveau groupe de sulfato, non plus, n'exerce aucune influence sur la forme de la courbe d'absorption.

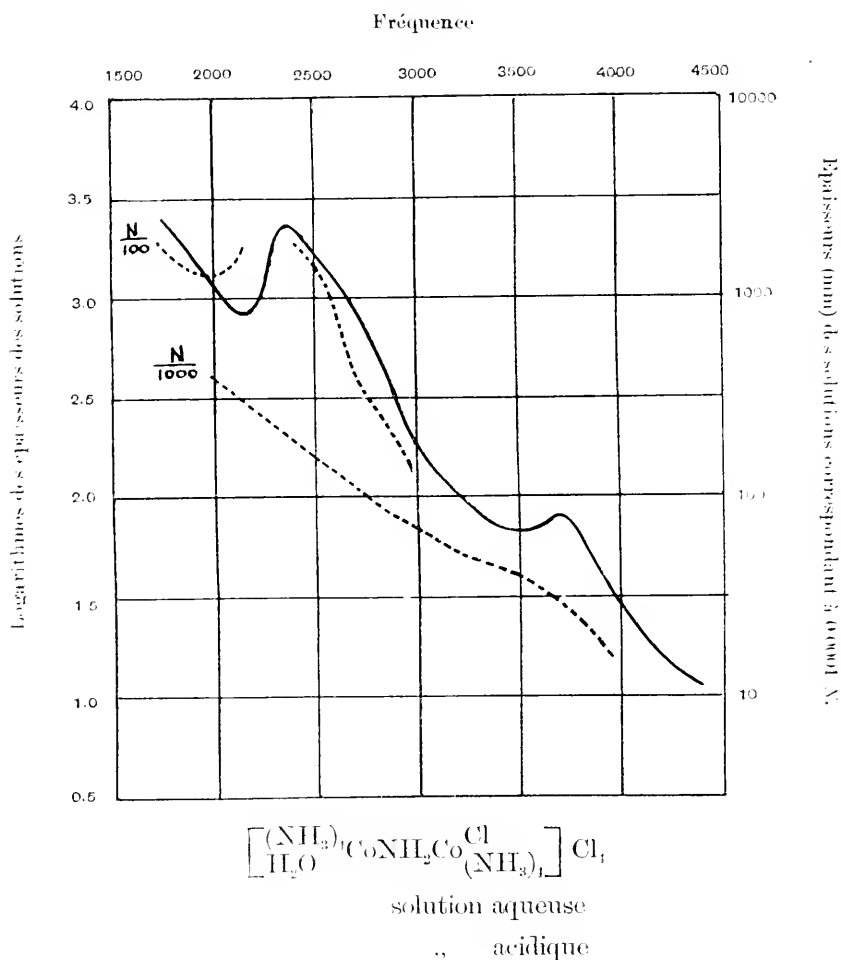
Les deux lignes horizontales dans la figure IV, qui portent les chiffres 1000 et 100 à leur extrémité droite, indiquent les épaisseurs recalculées correspondant à la concentration de 0.0001N.

### 5) Chlorure octammine-monochloro-monoaquo- $\mu$ -amino-dicobaltique.

La solution aqueuse de ce sel est un peu plus stable que celle des autres, parce que sa courbe d'absorption de la solution avec la concentration  $\frac{N}{100}$  donne encore une bande à la fréquence 2000. Dix fois étendue, elle ne satisfait plus la loi de Beer et la courbe de cette partie présente l'inclination faible caractéristique à l'hydrosol de l'hydrate de cobalt.

La solution acide de ce sel aussi donne une courbe d'absorption complètement pareille à celle des autres, quoi qu'il contienne encore deux nouveaux substituants, c'est-à-dire, un atome de chlore et une molécule d'eau, dans son cation complexe.

Fig. V.

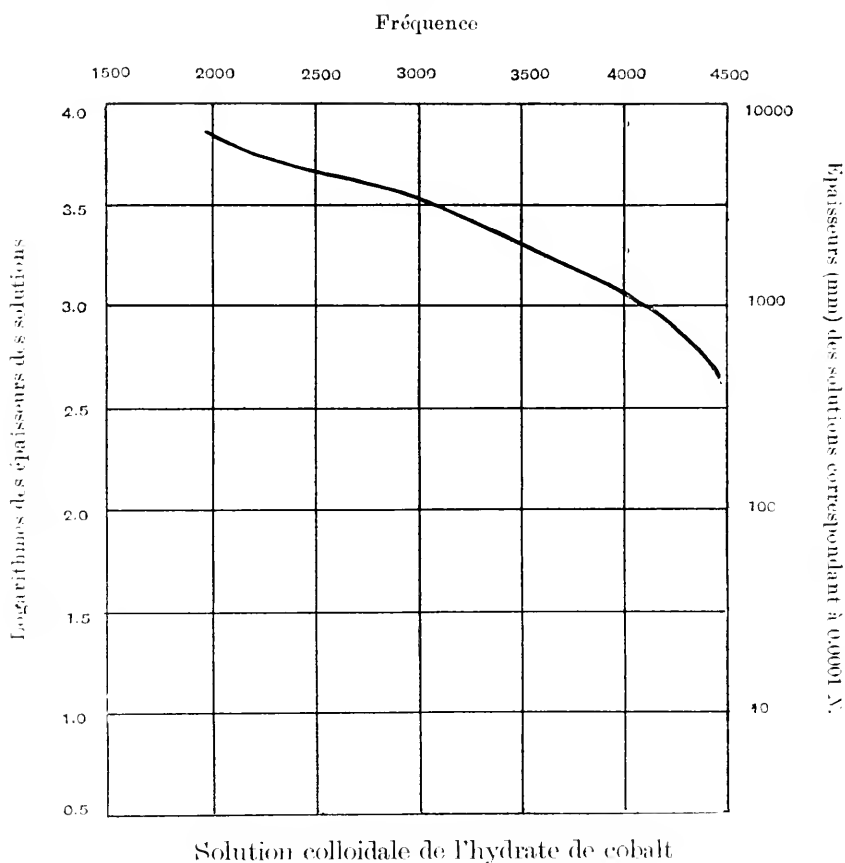


## 6) Hydrosol de l'hydrate de cobalt.

La solution colloïdale de l'hydrate de cobalt a été préparée d'après la méthode donnée par M. Theo Svedberg dans son livre, intitulé "Herstellung colloïdaler Lösungen." Selon cette méthode, la préparation de l'hydrosol de l'hydrate de cobalt a été exécutée de telle sorte qu'on fait précipiter d'abord l'hydrate de cobalt de la solution aqueuse de son azotate, en y ajoutant l'alcalie. Le précipité est donc filtré et parfaitement lavé en grande hâte avec

de l'eau pure. Quand on bouillit ensuite cet hydrate de cobalt filtré avec une solution étendue ( $\frac{1}{20}$  N) d'acide chlorhydrique, on obtient une solution colloïdale de l'hydrate de cobalt d'un brun foncé. La teneur de cobalt dans l'hydrosol ainsi préparé a été dosé et la solution a été donc étendue jusqu'à la concentration de  $\frac{N}{100}$ , pour mesurer son absorption des rayons.

Fig. VI.



La courbe d'absorption de cette solution, comme je l'avais pensé d'avance, montre une inclination faible et donne une forme très semblable aux courbes d'absorption des solutions hydrolysées des sels complexes avec poly-noyaux.

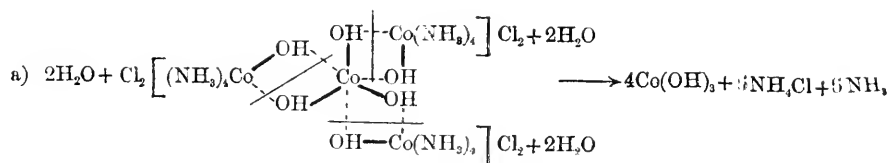


### Conclusion.

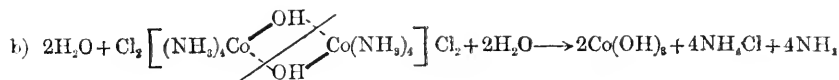
Dans les résultats expérimentaux que je viens de décrire avec précision, on peut apercevoir deux faits bien remarquables—premièrement l'hydrolyse parfaite des solutions aqueuses des complexes étudiés, et deuxièmement la même propriété de leurs solutions acides, relativement à l'absorption des rayons.

La cause de ces deux phénomènes chimique et physique se trouve sûrement dans le fait que les connexions de deux noyaux (les atomes cobaltiques) des ions complexes, qui sont liés indirectement à l'aide des groupes d'amino, d'hydroxyl, de sulfato ou de deux d'entre eux, sont extraordinairement faibles. La décomposition hydrolytique de leurs solutions aqueuses, il me semble, se produit aux points de ces faibles connexions, et enfin la molécule complexe se décompose complètement, donnant l'hydrate de cobalt et le chlorure d'ammoniaque, l'azotate d'ammoniaque ou le sulfate d'ammoniaque.

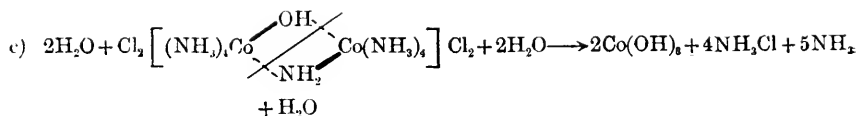
Les modes de ces décompositions hydrolytiques peuvent être bien comprises, si on représente les sels complexes par les formules constitutionnelles:



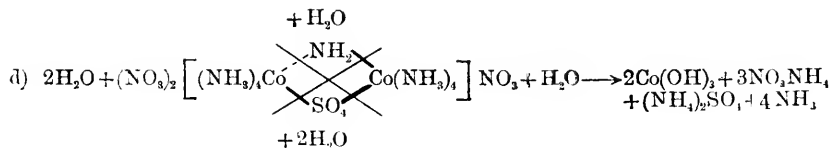
Chlorure dodécamine-hexol-tétracobaltique.



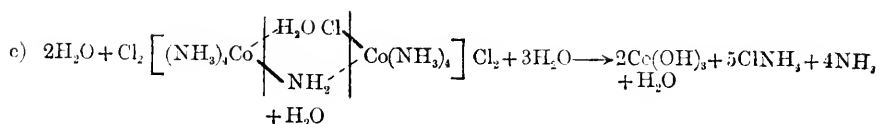
Chlorure octamine-diol-dicobaltique.



Chlorure octamine- $\mu$ -amino-ol-dicobaltique.



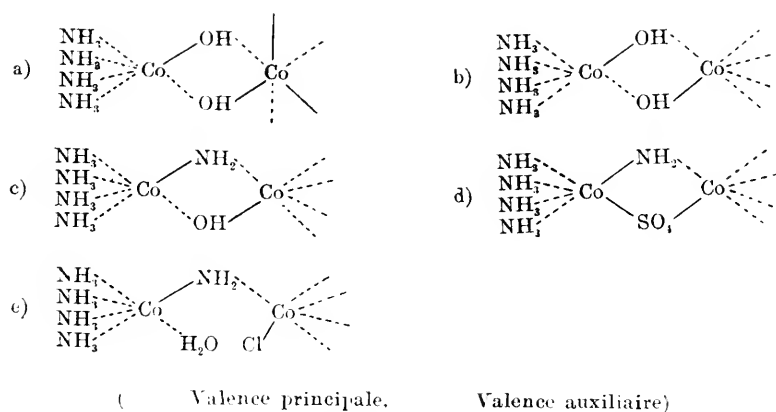
Azotate octamine- $\mu$ -amino-sulfate-dicobaltique.



Chlorure octamine-monochloro-monoquo- $\mu$ -amine-dicobaltique.

Selon la loi d'action de masse, une petite quantité des acides correspondant aux anions, ajoutée à leurs solutions aqueuses, sert à arrêter parfaitement la marche de la décomposition hydrolytique. Dans ce cas même, les affinités entre les atomes cobaltiques et les groupes atomiques, qui lient les noyaux, atomes cobaltiques, doivent être encore beaucoup moins fortes que les autres affinités de coordination, parce que les différences chimiques de ces groupes n'exercent aucune influence sur l'absorption des rayons, comme on l'a vu dans leurs courbes d'absorption, qui sont presque les mêmes les unes et les autres. A la fin, j'ajouterai encore quelques lignes sur la cause de cette égalité remarquable des courbes d'absorption des solutions acidiques.

Considérons encore une fois les formules constitutionnelles des complexes relativement aux distributions des valences principales et auxiliaires autour d'un noyau, atome cobaltique, de chaque sel :



Un coup d'œil suffit pour nous faire comprendre qu'ils sont construits très semblablement les uns et les autres, et que, par conséquent, ils absorbent des rayons de la même manière.



TO PROFESSOR AIKITU TANAKADATE  
ON THE OCCASION COMMEMORATING HIS TWENTY-FIVE YEARS' SERVICE  
DEDICATED BY  
HIS DEVOTED PUPIL, THE AUTHOR.

---

## On Rapid Periodic Variations of Terrestrial Magnetism.

By

Torahiko TERADA, *Rikugunhakushi*.

### PART I.

#### Introduction.

1. Immediately after the organization of the Imperial Earthquake Investigation Committee, regular magnetographic observations were begun, on the proposal of Prof. Tanakadate, at four stations, Kumamoto, Kyôto, Sendai and Nemuro, with the special purpose in view of detecting any magnetic disturbances which might reveal themselves associated with destructive earthquakes. The instruments used were of the ordinary Mascart type. On the other hand, a general magnetic survey of the empire was undertaken, 1893-96, the result of which has been published in the Journal of the College of Science, Vol. XIV. In discussing therein the local disturbing field due to Mt. Huzi, Prof. Tanakadate came to the conclusion that even if the whole mass of the mountain be suddenly removed, the disturbance in the vicinity would

scarcely amount to 1  $\gamma$ . Hence it was considered futile to continue the observations with instruments of such low sensibility, and the regular observations were suspended in 1909. At the same time, he devised and constructed, with the able assistance of Dr. H. Kadooka, now expert to the Military Telegraphic Department, a set of extraordinarily sensitive magnetographs, and laid before the Committee the plan of a provisory magnetic observatory equipped with these instruments. The proposal was approved, and the necessary arrangements were promptly made under his supervision. An underground room was excavated for the purpose, in the vicinity of the Marine Biological Laboratory of the Science College, at Misaki. The regular observations were commenced early in 1910. In the summer of 1911, Dr. Kadooka was appointed to his present position, and the author took charge of the Observatory, until April 1914, when the observations were suspended for an indefinite term.

The observers who were successively resident at Misaki and took charge of the instruments were :

Mr. Hideo Momose, formerly Hitotuyanagi, now teacher in the Nagoya Sôdô-syû Third Middle School,

Mr. Takeo Tatiiri, now Assistant in the Meidi Technical School, Tobata, Hukuoka Prefecture,

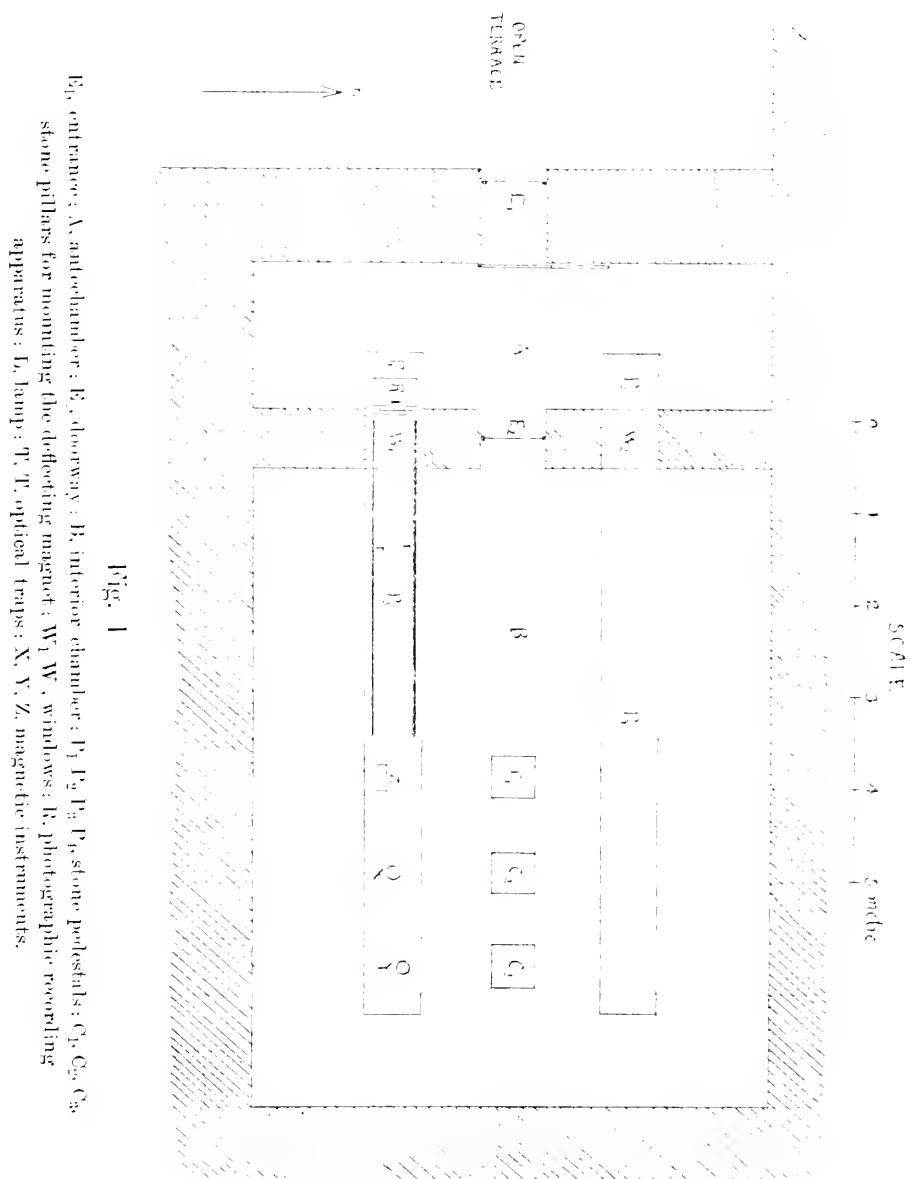
The late Mr. Kisaburô Matui, at the time of his death teacher in the Sibusi Middle School, Kagosima Prefecture,

Mr. Murato Nakata, now teacher in the Hakodate Commercial School,

to whom the author's sincerest thanks are due for their untiring alertness to their duty, which claimed their utmost patience and attention, to say nothing of the inconveniences of living which had to be endured on account of the lonely situation of the Observatory.

The entire task of examining and studying the magnetographic records in detail and drawing up the report thereon, was entrusted to the author. Though the investigations are as yet by no means completed, it seems now to be the proper time to summarize here the principal results hitherto obtained.

2. OBSERVATORY.—The observatory is situated at the foot of the northern slope (139°37'5 E, 35°9'4 N.) bordering the Bay of Aburatubo, Misaki, Province of Sagami, a few minutes walk from the Marine Biological Laboratory belonging to the College of Science, Imperial University of Tôkyô. The station was chosen



on account of its remoteness from any powerful electrical plant<sup>1)</sup> and also for the conveniences which its proximity to the Marine Laboratory afforded. The edge of the terrace overlooking the bay was partly cut off to form a vertical cliff. An underground room was then excavated with a narrow entrance (Fig. 1,  $E_1$ ) opening at the foot of the cliff. Since the rock was entirely of a soft tertiary formation, the excavation was comparatively easy. The approximate size and the arrangements of the room may be seen from Fig. 1. A is the antechamber where the photographic recording apparatus R and the acetylene lamp L used as the source of light, were installed on the pedestal  $P_1$  or  $P_2$ . In the interior chamber B, communicating with A by the narrow entrance  $E_2$  and also by the windows  $W_1$  and  $W_2$ , two long pedestals  $P_3$  and  $P_4$  are laid for mounting the magnetic instruments.  $C_1$ ,  $C_2$  and  $C_2$  are small stone pillars on which were fixed the stands for fitting the magnetic bar used for determining the sensibility or constant of the magnetographs.

In the beginning of the observation, two similar sets of instruments were arranged on  $P_1$   $P_3$  and  $P_2$   $P_4$  respectively and run simultaneously. The results were almost identical, as was to be expected, and the later part of the observations was almost exclusively made on pedestals  $P_1$  and  $P_3$ .

The temperature of the interior chamber was kept tolerably constant, the daily variation amounting to only a fraction of a degree and the annual range scarcely reaching  $3^{\circ}\text{C}$ .

A serious difficulty met with was, however, the extreme dampness of the chamber during the summer months. Not only does the moisture of the external air, saturated at very high temperature, gradually condense in the cooler interior, but humidity is constantly supplied by the percolation of underground water, through numerous fissures in the wall and ceiling, fed by the abundant rain during "*Baiu*," the rainy season on our entire Pacific coast in early summer. This caused so much trouble that during a certain period observations were almost rendered impossible. Though it was not impossible to overcome this difficulty, the funds at our disposal were not sufficient to carry out the

---

1) The nearest tramway line is at Kamakura, nearly 20 km. N. from the station.

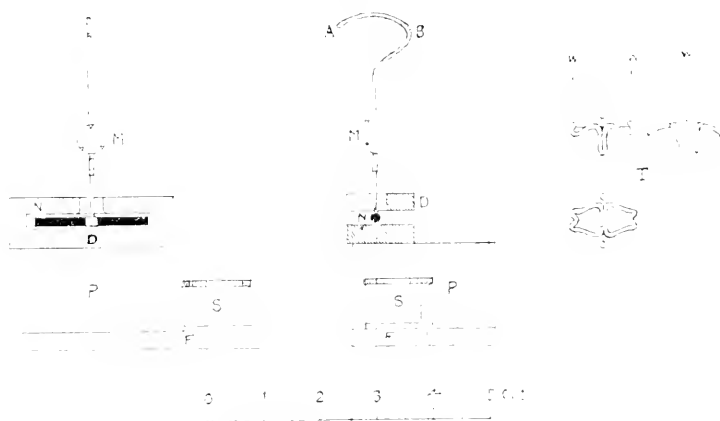


necessary reconstruction of the room. In any future work of the kind, it will be absolutely necessary to provide first of all for the removal of this obnoxious humidity.

3. INSTRUMENTS.—Since it was the immediate purpose of the present investigation to detect the most minute disturbances possible, the sensibility of the usual instruments was far from being sufficient. To meet this need, Prof. Tanakadate and Dr. Kadooka devised a specially sensitive set of instruments which will be separately described in the following paragraphs:

a) *West-East- or Y-Component Instrument* (West taken as positive). Maxwell, in his discussion of the theory of bifilar suspension<sup>1)</sup>, suggested the utility for the measurement of the WE-component, of a suspended magnetic needle twisted nearly  $180^\circ$  from its natural direction, which can be made highly sensitive by properly adjusting the breadth of the bifilar suspension. This principle was adopted in the following manner. The magnetic needle (Fig. 2, N) with a length of 20 mm. and a diameter of 1.5

Fig. 2



mm., was held by a hook AB, made of aluminium wire of 0.7 mm. diameter, bent in the form as shown in the figure. A kind of light stirrup for supporting the hook with the magnetic needle was made with pieces of thin fused quartz rods, welded together

1) Maxwell, Electricity and Magnetism, 3rd. Edition, Vol. II, p. 118.

into shape as shown in Fig. 2, T. This was made to hang on the looped end of the suspension wire  $ww$ , for which fine Wollaston wire of  $5\text{--}10\ \mu$  diameter was used. The upper arc of the aluminium hook is made to ride on the central V-shaped recess  $cc$  of the stirrup. M is a light plane mirror of 5 mm. diameter, attached to the hook. The whole system was hung in the metallic case of Mascart's magnetograph made by Carpentier, Paris, from which the usual attachment in the interior was removed. The regulating screw attached at the top of the case for adjusting the breadth of the suspension was utilized as such. For damping the natural vibration of the suspension, an electromagnetic damper D made of a copper block was introduced. The damper could be rotated on a cylindrical brass block P, which in its turn could be rotated about the screw S, fixed to the bed plate of the case, passing through the groove cut along the projecting arm F at the foot of L. The damping was very effective, making the vibration completely aperiodic.

To set the suspension in working condition, we proceeded as follows. At first, the stirrup only was hung on the wire, making the breadth of the suspension sufficiently large. After hanging the magnetic needle carefully in its natural direction, twist the torsion head slowly till the needle is turned about  $180^\circ$ , and the luminous image of the slit formed by the reflexion of the mirror M appears within its proper range. Then, after bringing the damper in position gradually narrow the breadth of the bifilar suspension, at the same time adjusting the torsion head so as to keep the luminous spot always within the range assigned to it. Proceeding very carefully in this way, the sensibility can be made extremely great, till at last the suspension attains its unstable position. It must be remarked that near this extreme position any minute change in the elastic property of the wire, the breadth of the bifilar suspension or the weight of the suspended system, may sensibly affect the deflection. Nor is the system independent of the slight inclination and the vertical acceleration of the instrument. In one instance, an inclination of about  $4'$  produced a displacement of about 2 cm. on the photographic record. Since

the latter effect seems to be due chiefly to the rigidity of the suspension wire. it is advisable to use as fine a wire as possible. In any future work, a thorough annealing of the wire after hanging the suspended system is very desirable.

The tripod support of the instrument rested on a thick glass plate, which was provided with a hole and a V-groove for receiving the feet of the levelling screw, and was rigidly fixed to the face of the stone pedestal.

The lens in front of the instrument case was replaced with another with a focal length of 5 m.

The deflecting magnetic rod for determining the sensibility, was fixed to a special holder<sup>1)</sup> such as is usually attached to Mascart's magnetograph for a similar purpose, and placed on the support pasted on the pillar C<sub>3</sub> in the same meridian as the instrument. After starting the photographic apparatus, the deflecting magnet was brought in position, *i.e.* horizontally in WE direction, and reversed every 3 or 5 minutes. The magnetic moment of the rod mostly used was  $M=77$  e.g.s. at the room temperature. The distance of the deflecting rod from the needle of the instrument was 123 cm., so that with the rod "side on," the change of the WE-component corresponding to the reversal of the deflector was 8.3  $\gamma$ . The sensibility was so adjusted as to make the corresponding deflection nearly 50 mm.; *i.e.* 1 mm. on the record corresponded to 0.17  $\gamma$ . The sensibility, though fairly constant, showed occasionally a tendency to decrease slightly after running for 24 hours, though not at all so serious as to affect the general aspect of the results obtained. It was therefore considered preferable to test the sensibility at least once every day and redetermine the constant. This gradual decrease of sensibility is probably due to the influence of a slight elastic time-effect of the suspension wire, made apparent on account of the extreme position of the bifilar system. The presence of a sensible time-effect in the wire used, is also made evident on the photographic record, when an abrupt deviation is effected by means of the deflecting magnet. After an immediate deflection, a slow creeping up of the

---

1) Mascart, *Magnétisme Terrestre*, p. 195, Fig. 46 c.

luminous image is always to be traced, which in most cases practically attains the final position after a few minutes (see Pl. I, marked with\*). This effect will of course affect the accuracy of the record, especially in relatively magnifying the disturbances of the longer period compared with the shorter ones. The error may, indeed, amount to several percent in unfavorable cases, if the relative amplitudes of the disturbances with decidedly different periods are to be compared with accuracy. However, the general inferences which will be given in the following communication will not be seriously affected, since here the comparison of amplitudes is either made of the X- and Y-components for waves of the same period, or of the X- and Z-components for waves with the periods usually longer than 1 minute. In the former case, both instruments show after-effects very similar to each other. Even in the latter case, where the Z-instrument is comparatively free from such effect, any serious error will occur only in the case of very short waves. This very disagreeable time-effect could probably be avoided by the use of quartz fibre suspension, directly welded to the quartz stirrup, though in this case we must devise a necessary modification of the suspension head.

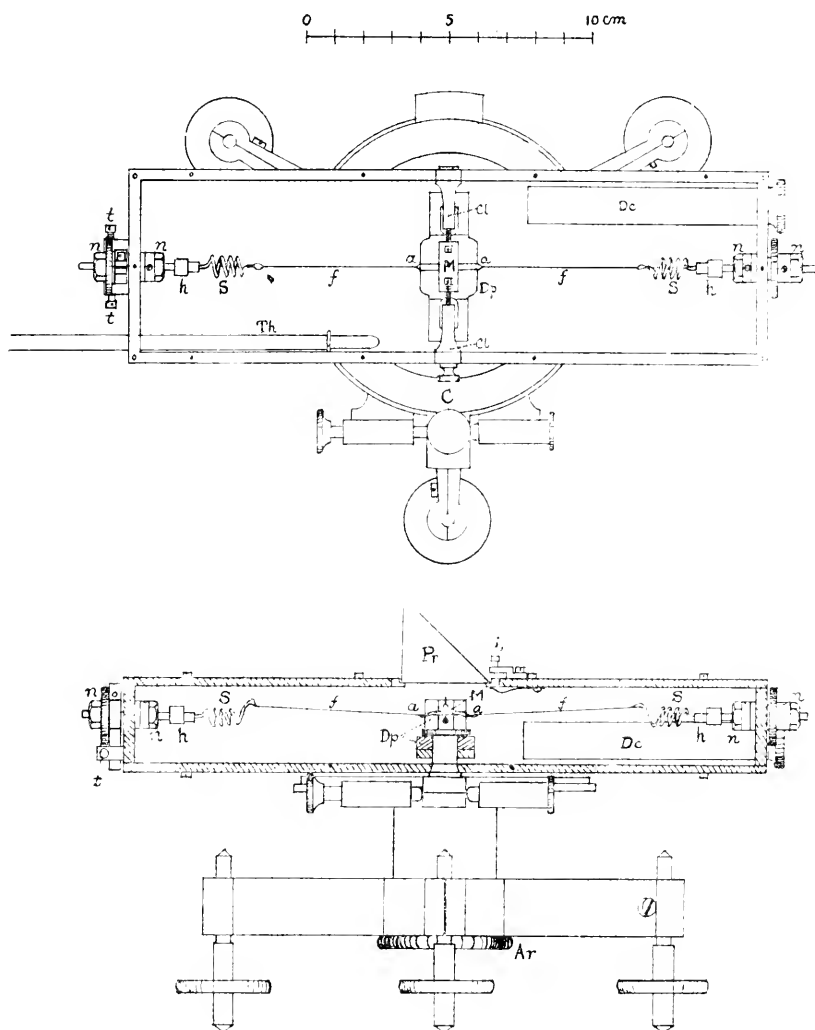
*b) North-South- or X-Component Instrument* (North taken as positive). The NS- instrument is essentially the same as that of Mascart's magnetograph. The suspension system is, however, replaced by one quite similar to that of the WE- instrument above described, except that in the present case the plane of the mirror is perpendicular to the axis of the magnetic needle.

Keeping the breadth of the bifilar suspension at first sufficiently wide, the torsion head is slowly twisted, till the luminous spot appears in the assigned range. Then cautiously turn the torsion head, at the same time regulating the breadth of the bifilar suspension, so as to keep the luminous image always within proper range. The unstable position is attained in a certain azimuth of the torsion head, which may be noted down for subsequent readjustment. The determination of the constant is carried out in a way similar to that in the case of the Y-instrument, with the only difference that in this case the deflecting magnet is

applied "end on," so that for the same distance of the deflector, the deflection must be made twice as large as in the case of the Y-instrument to insure the same sensibility. The distance of the deflecting magnet from the needle of the instrument was 127 cm., so that 1 mm. on the record corresponds to 0.15  $\gamma$ .

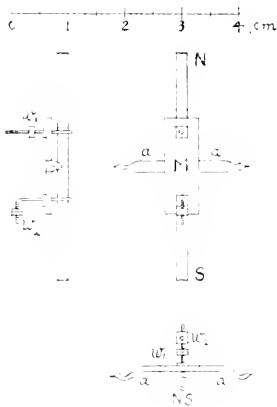
The gradual creeping of the luminous spot is also observed in this case. Hence the same remark applies as to the accuracy of the records.

Fig. 3, A.



c) *Vertical or Z-Component Instrument* (downward taken as positive). Instead of the ordinary Lloyd's balance, a new instrument was designed and constructed by Prof. Tanakadate and Dr. Kadooka, which proved very satisfactory. The magnetic needle (Fig. 3, NS), 4 cm. long and 2 mm. thick, was fixed to the lower face of a rectangular plane mirror M ( $6 \times 17 \times 1$  mm.),

Fig. 3, B.



made of fused quartz plate, platinized on its upper surface by means of cathode discharge. The mirror has a pair of projecting arms *aa* on both sides, to the pointed ends of which are welded quartz fibres *ff* of 0.05–0.08 mm. diameter. The welding may be easily made, after some practice, by pointing the sharp point of a fine oxyhydrogen flame to the spot where the fibre is attached to the arm by slightly wetting the surface. The fibres *ff* are stretched in EW direction by means of helical springs *SS*<sup>1)</sup> made of fused quartz rod, of which the one end is welded to the

fibre and the other is rigidly fixed to the brass holder *hh* by means of solder applied in the cavity for receiving the quartz rod. By means of the nuts *nn*, the tension could be adjusted without twisting the fibre. By turning the screw *t*, a slight torsion could be given to the fibre, in order to adjust the zero position of the mirror. Damping is effected by means of the copper block *Dp*, which serves also for clamping the suspended system when lifted up by means of the screw *Ar* at the lowest part of the instrument. *Pr* is the reflecting prism originally used in Mascart's vertical component instrument for a similar purpose. The inclination of the prism could be adjusted by means of the screw *i*. *De* is the desiccator containing calcium chloride and *Th* a thermometer.

The points of junction of the mirror arm *aa* with the fibre are originally so adjusted that the centre of gravity of the suspended

1) The spring may be dispensed with, provided that the temperature is kept sufficiently constant, without sensibly impairing the reliability of the instrument, though there is the danger of breaking the fibre by accidental shock given to the instrument during manipulation.

system is very near the line connecting them. The sensibility may be then adjusted by means of a small weight  $w_1$  playing on the fine screw projecting on the upper face of the mirror, while the inclination of the mirror can be regulated by means of another pair of small nuts  $w_2$ , running on the horizontal screw as shown in Fig. 3, B.

For determining the sensibility, the same deflecting magnetic rod as used for the preceding two instruments, was placed on the pedestal  $C_1$  in the same meridian as the instrument at a distance of 128.5 cm. In this case the deflector was of course applied and reversed in the vertical position. The sensibility was so adjusted that the reversal of the deflector produces the displacement of about 5 cm. on the record, or 1 mm. corresponds to 0.15 %.

The instrument worked very satisfactorily. Once carefully adjusted, it remained so constant in every respect that it might have run many years without any further trouble, except for the excessive humidity of the room, which caused gradual rusting of the instrument, especially of the magnetic needle, also a gradual deterioration of the platinized mirror, and necessitated the complete rearrangement of the instrument. The great advantage of quartz fibre is very clearly shown in this instrument compared with the others, since here no sensible creeping up of the luminous image after abrupt deviation is observed, as may be seen from Pl. I. An instrument of a similar construction may be replaced with great advantage for Lloyd's balance, for the usual work of lower sensibility.

*d) Illuminating and Photographic Apparatus.* The source of light used for photographic purposes was an ordinary acetylene burner with two orifices facing each other, which was fed by a capacious tank placed outside the room. The burner was fixed in the interior of the metallic case of the lamp originally attached to Mascart's magnetograph, in front of which a suitable vertical slit and a cylindrical lens was inserted. The lamp was hung over the pedestal  $P_1$  of the antechamber, close by the window  $W_1$ , and immediately above the photographic apparatus placed on  $P_1$ . The drum carrying the photographic paper was 24 cm. in diameter and 30 cm. in length, and revolved once every 3.76 hours on an average, by means of a suitable clockwork, so that 1 mm. corres-

ponds nearly to 17.8 sec. Closely in front of the drum a fine horizontal slit and a cylindrical lens are introduced, both of the same length as the drum. During the wet season, a desiccator dish containing calcium chloride was placed under the drum.

For giving time-marks on the record, a clockwork was placed in front of the lamp to interrupt the light for a few minutes at the end of each hour.

The three magnetic instruments are arranged in succession as shown in Fig. 1. For the Z-instrument an auxiliary lens with the focal length of 2 m. was placed in the path of the incident beam of light, by means of a special holder fixed to the pedestal.

To save the considerable breadth of the photographic paper required, owing to the remarkable sensibility of the instruments, the following device was adopted with success. Two long strips of thick plane glass plate (breadth 10 cm., length 3 m.) were placed along both sides of the long pedestal  $P_1$  (Fig. 1, T). These were held firmly by means of special holders, with their reflecting surfaces vertical and parallel to each other, so that when the luminous beam reflected from the magnetic instrument is deviated just beyond the limit of the horizontal slit of the photographic apparatus, it is caught by one of the glass plates, or "optical traps" as we have called them, and reflected back to the slit. For a still greater deviation the opposite glass caught the beam reflected from the first one, and so on. Except in the extremely damp season, even the third reflection produced a luminous spot intense enough to affect the photographic paper. By properly adjusting the position of the three instruments and also the mean direction of the reflected beams produced by them, an uninterrupted record of the three components could be obtained, even in the case of remarkable magnetic storms.

The mutual magnetic influences of the three instruments were tested by mechanically disturbing each instrument, while the photographic record was being taken. No sensible effect was noticed.

Since the drum carrying the photographic paper revolved once per 3.76 hours, paper of a length of about 4.85 m. was



required per day and night. To save the excessive use of paper, it was replaced only twice during 24 hours, *i.e.* usually at 6 o'clock in the morning and evening. Hence the record was run over three times by each component, which caused considerable confusion of the record, on quiet days by the superposition of the trace of the same component, and on disturbed days, by the mutual intersections of the different components either direct or reflected by the traps. The confusion is, however, merely apparent in most cases. The time marks, the difference in the intensity of traces and also slight differences in the optical error of the mirrors of different instruments, causing different shading of the photographic traces, served together as convenient signs for disentangling the intricate record. Ambiguous cases were extremely rare, even if two branches of traces were nearly superposed. After we became familiar in the course of the investigation, with the characteristic behaviours of short period disturbances for different components, the distinction of the different components became still easier.

During the summer months, the pedestal  $P_2$  was covered with large cases of zinc, which consisted of seven pieces and when put together in series, formed a continuous channel extending along the entire length of the pedestal. Five or six dishes with  $\text{CaCl}_2$  were placed inside the channel. These arrangements were, however, far from being efficient for the prevention of the extraordinary dampness of the chamber during a certain period of the warmest season.

The clock for giving the time mark was occasionally compared with that of the Post Office in Misaki and also checked by means of the sundial placed in the yard of the Marine Laboratory, so that the accuracy of the time was only of the order of a minute at the most. A convenient control could be made by the very frequent occurrence of slight local earthquakes which left distinct marks on the photographic records and could be easily identified with the seismographic record obtained in Tôkyô.<sup>1)</sup>

---

1) The distance between the Observatory and the Tokyo Central Meteorological Observatory is about 60 km., so that the time taken by the principal phase of seismic waves will never exceed 18 seconds.

## PART II.

### General Results of the Investigation.

4. The general character of the photographic records obtained by our system of instruments may be seen in Pl.I. and II. The time taken as abscissa increases from left to right. Upward corresponds to the positive direction of each component for the non-reflected trace. Pl.I. is the representative record for a quiet day. The trace of the sensibility determination is to be seen at the beginning of the curves (marked with\*). Pl.III. is one of the typical records for disturbed days, the parts of the curves reflected from the "traps" are marked with the letters  $R_1$ ,  $R_2$ , the suffix giving the number of reflexions.

Even on the most quiet days, the records shows as a rule numerous trains of more or less regular waves or pulsations, the periods of which range from about 20 sec. to several minutes. Allied phenomena seem to have been studied first by Balfour Stewart<sup>1)</sup> who found periods of 30 seconds. Kohlrausch<sup>2)</sup> found by direct eye observations a wave of 12 sec. period. Arendt<sup>3)</sup> investigated waves with periods of several minutes, frequent in night hours, in connection with his researches on the magnetic disturbances associated with the phenomena of thunderstorms. Eschenhagen<sup>4)</sup> found prevalent waves of 30 sec. which appeared most frequently during daytime. Birkeland<sup>5)</sup> studied the phenomena for Haldde as well as for Potsdam, and obtained most frequent groups of waves with periods of 10 and a little longer than 30 sec. More recently, van Bemmeln in Batavia<sup>6)</sup> studied similar waves with 1-4 minutes periods which he called "pulsations".

1) Balfour Stewart, Phil. Trans. 1861, p. 425.

2) F. Kohlrausch, Wied. Ann. **60**, p. 336.

3) Th. Arendt, Das Wetter, 1886, p. 241 and 265.

4) Max Eschenhagen, Sitz. Ber. d. preuss. Akad. d. Wiss., Berlin, **32**, 1897, p. 678; Terr. Mag. and Atm. Elec., **2**, 1897, p. 105.

5) Kr. Birkeland, Expédition Norvégienne de 1899-1900 pur l'étude des aurores boréales. Résultats des recherches magnétiques. Christiania, 1901.

6) W. van Bemmeln, Verslag. Konink. Akad. v. Wet. t. Amsterdam, Proc. of the Sec. of Sc., **2**, 1899-1900, p. 202.

tions" to distinguish them from peculiar disturbances called "spasms," and discovered a remarkable daily period of frequency with a maximum near midnight. Afterwards<sup>2)</sup> he compared the materials from Zi-Ka-Wei and Kew, and found for the former station a similar nightly maximum as in the case of Batavia, while for the latter station, the maximum frequency was found in the day time. Recent authorities seem to agree in the opinion that the magnetic waves in question are chiefly due to some fluctuations of the electric current existing in the upper atmosphere, though the actual modes of fluctuation still remain obscure.

Though the original purpose of our investigation was to detect any abnormal disturbances associated with earthquakes, it was in any case necessary to study the characteristic pulsatory waves in some detail, even if these waves should have no direct connection with earthquakes, in order to be able to distinguish which were the normal and which the abnormal disturbances. The present paper is chiefly confined to the study of these characteristic pulsatory disturbances, since unfortunately no positive results have yet been obtained with regard to earthquakes.

In the following, we shall enumerate the most interesting results obtained by the detailed study of the magnetographic records comprising observations extending over four years.

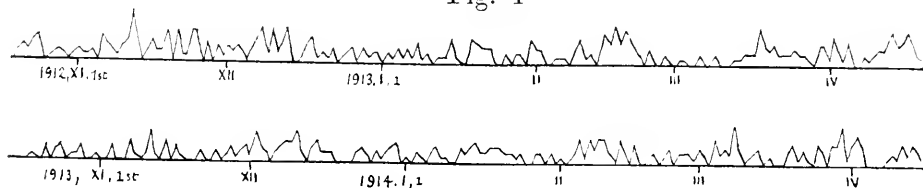
5. *a) Generally speaking*, the magnetic waves in question are decidedly more regular in the night than in day time when waves of different periods seem to be very irregularly superposed. In the great majority of cases remarkably long continuous trains of moderately regular waves with period of 30-60 sec. appear at 5<sup>h</sup>-7<sup>h</sup> in the morning and continue up to 9<sup>h</sup>-11<sup>h</sup>, with occasional interruptions (Pl. II., III., IV. and V). The number of hours, in the course of which such trains occurred, was noted for successive days, quite regardless of the length or the number of the trains. The number shows occasionally an apparent periodicity of 25-30 days, though generally not so regular as to allow us to deduce any

---

2) W. van Bemmeln, *Natuurk. Tijdschr. v. Nederlandsch-Indië*, **62**, 1902, p. 71.

definite period from the scanty material at hand. The general aspect will be seen from the annexed figure (Fig. 4).

Fig. 4



Since it was suspected that the number in question may have some relation with the solar activity, it was compared with the "provisory sun-spot number," published in *Meteorologische Zeitschrift*, but no convincing relation could be found.<sup>1)</sup> It will however, be interesting to compare the present number with the occurrence of sun-spots on a definite central area of the solar disc.<sup>2)</sup>

b) These *short* period waves appearing simultaneously in the X- and Y-components run remarkably parallel to each other during the morning hours, viz. 6<sup>h</sup>—8<sup>h</sup> say, every detail in one component being repeated by the other with marvellous similarity, no noteworthy phase difference being observed between the two components (Pl. V). Moreover, the amplitudes of the two components are generally of nearly the same order of magnitude. It seems as if these waves were due to the fluctuation of an electric current running from NE to SW, making an angle nearly 45° to the meridian. For these *short* waves, Z-component is comparatively insignificant and may be clearly discerned only when the photographic trace is very fine.

In the later afternoon hours, the parallelism between X- and Y-components becomes imperfect. Some waves are present either in

1) W. van Bemmeln compared the frequency of the "pulsations" with the sun-spot number and arrived at a negative result, *loc. cit.*

2) E. W. Maunder noticed a 27 days period of magnetic disturbances and came to the conclusion that the cause of the disturbance is to be sought on a limited portion of the sun's surface, *Monthly Notice of R. Astr. Soc.*, **65**, 1904—05, p. 2, 538. The paper was criticized by A. Schuster, *ibid.*, p. 186. E. Marchand found a connection between the magnetic disturbances and the sun-spots passing the central meridian of the sun's disc. *Congr. intern. de météorolog.*, Paris, 1900, p. 148.

one or the other component only. Even if a train of waves may be traced in both components, the variation of the disturbing field is generally of irregular rotatory character.

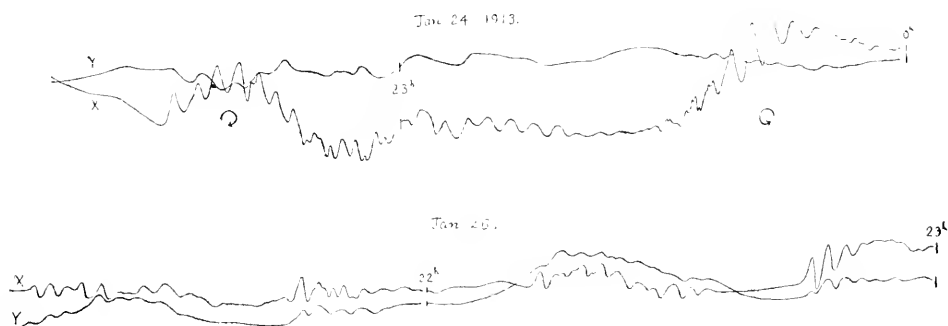
c) Generally, no corresponding regular trains of short waves with such remarkable duration can be seen during the evening hours, nor is the remarkable parallelism between X- and Y-components so conspicuous as in the morning.

d) During the later hours of the evening, the short waves with periods of less than one minute generally disappear, while very regular waves with 2-4 minutes periods appear instead, frequently forming beautiful trains of nearly simple harmonic waves. Another remarkable characteristic of the evening waves is that the Y-component waves are generally inverted with respect to the X-waves, *i.e.* the fluctuation of the horizontal magnetic field is such as could be caused by the periodic variation of a current running from NW to SE. Generally speaking, however, the horizontal components show more or less rotatory character, X- and Y-components showing frequently decided phase difference. This latter point will be fully investigated later.

For these *longer* waves, the Z-component is more conspicuous than for the shorter waves frequent in day time, and runs remarkably similar to the X-component, though lagging behind it by a considerable fraction of the period (see Plates I-IV).

Fig. 5, A (reduced to  $\frac{1}{3}$  original size).

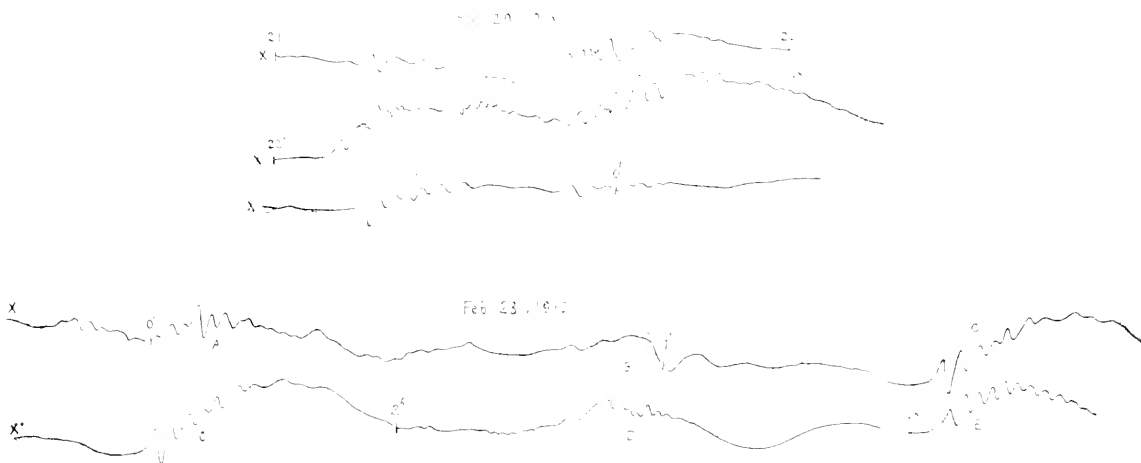
Note the rotatory character of the horizontal component in the upper curves.



e) The beginning of these waves is sometimes gradual, but frequently abrupt, starting quite suddenly after a period of dormant calmness (Fig. 5). The trains with the abrupt beginning

Fig. 5, B ( $\frac{1}{3}$  original size).

Remark the regularity with which similar disturbances are repeated.



are frequently accompanied by an abrupt increase of the average value of the X-component which gradually attains a maximum and then falls slowly (see Figs. 5 and 6). The sudden increase of the X-component is usually accompanied by the simultaneous sudden change of the average value of the Y-component, which is at the outset generally toward E before midnight and toward W after midnight. It seems as if an electric current were suddenly started with rapidly increasing and fluctuating intensity, with its direction NW to SE, or SW to NE according to the hour of occurrence. Disturbances of this kind seem to have been studied by Birkeland who succeeded in tracing a system of whirling currents (*tourbillons de courants*) extending over the N-hemisphere, fixed relative to the sun. The slow change of the horizontal components gradually attains a rotatory character, the sense of which seems to generally confirm the result obtained by R.B. Sangster,<sup>1)</sup> *i.e.* mostly counterclockwise (N-W-S) before, and

1) R. B. Sangster, Proc. Roy. Soc., **84** A. 1911.

clockwise (N-E-S) after a certain hour near midnight. This seems just as if the magnetic disturbing vector, initially inclined to the meridian, rotates in the sense to become parallel to the meridian.

Characteristic disturbances of the above type are met with most frequently just at midnight. In other hours, especially near

Fig. 6, A ( $\frac{1}{3}$  original size).

Note the parallelism between X and Z.

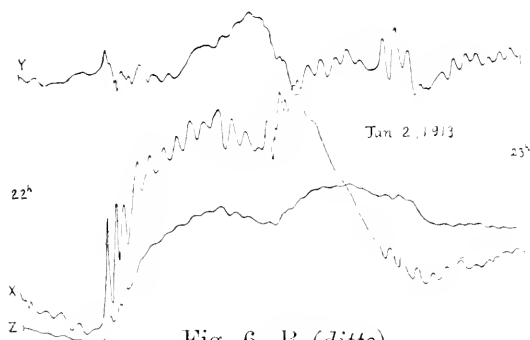


Fig. 6, B (*ditto*).

Remark the apparent "beat" of the waves in the lower curves.

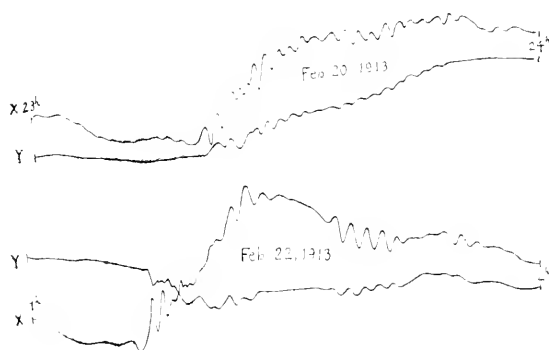
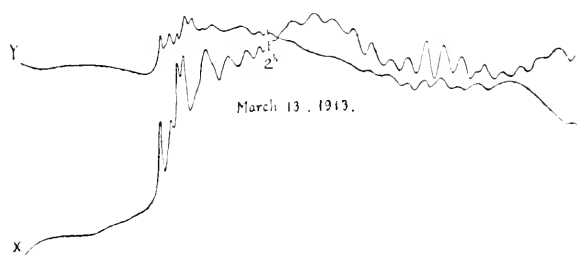


Fig. 6, C (*ditto*).



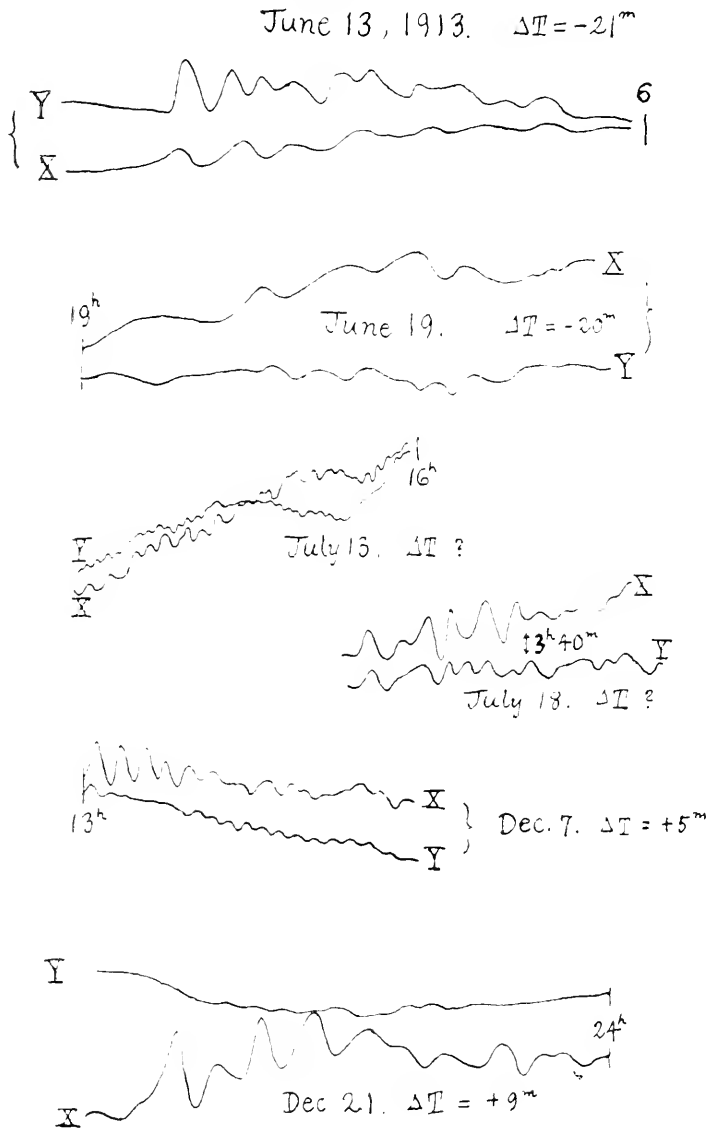
18<sup>h</sup> cases occur not rarely where an abrupt increase of the horizontal component is not accompanied with any conspicuous train of waves.

It is a very remarkable fact that even for these abrupt nonperiodic disturbances of long duration, the Z-component follows the various fluctuations of the X-component with utmost faithfulness, except for a reduced amplitude and a definite retardation. This characteristic behaviour served as a very convenient means for disentangling the chaos of photographic traces in the records of disturbed days.

At the beginning of the abruptly starting train of waves, the amplitude is some-

times very large, in one instance amounting to  $5.47$  with a period of  $1.2$  minute (see Fig. 6, A). The amplitude is generally damped gradually, with a sensibly constant period. On closer examination, cases were also found where the period of the waves changed gradually in an apparently coherent train. Sometimes,

Fig. 7 ( $\frac{3}{4}$  original size).





a very characteristic train is repeated two or three times with nearly equal intervals of  $15^m$   $40^m$  *etc.*, as if the same train of waves were recurring to the point of observation with a definite period (Fig. 5, B).

*f*) It is frequently observed that while a fairly regular train of waves is traced in both the X- and Y-components at the same time, the periods of waves are quite different for the two components (for examples, see Fig. 7). Among 68 conspicuous cases chosen, 42 were those in which the periods were longer in X- than in Y-component. The distribution of such cases in different hours of the day may be seen in the following table:

TABLE I.

Hour.	$T_X > T_Y$	$T_X < T_Y$	Hour.	$T_X > T_Y$	$T_X < T_Y$
0—2	0	2	12—14	8	0
2—4	4	2	14—16	3	1
4—6	7	3	16—18	0	1
6—8	2	2	18—20	2	6
8—10	6	3	20—22	3	0
10—12	4	2	22—24	3	4

A tendency is suspected, though not very apparent, that the cases where the periods of X-waves are greater than those of Y, are most frequent near midnight and noon, while they are comparatively rare in the morning and evening hours.

*g*) Though the most conspicuous regular trains are chiefly observed with periods ranging from  $30^s$  to  $300^s$ , still longer waves are not at all rare, if we take those trains together in account, with only a small number of maxima and minima. The longest wave traced was of a period nearly amounting to one hour, which may of course be detected in the ordinary magnetographic record of low sensibility, when the amplitude is sufficiently large. The intermediate periods are rather evenly represented in our list of

the waves, though there seems to be a maximum of frequency near 15.<sup>1)</sup>

*h)* Slight local earthquakes, which are very frequent, affect the instruments, leaving a trace similar to that of the Milne seismograph (see for example Pl. V). This is in all probability mainly due to the mechanical shock, to which our instruments, especially X- and Y-instruments, are rather sensitive. These traces, however, served as very convenient and trustworthy time-signals, as already mentioned. Besides, remarkable earthquake waves with long periods, originating in distant regions, are beautifully recorded in our magnetographs (Pl. IV). The most conspicuous periods are of the order 10<sup>s</sup>–20<sup>s</sup>, *i.e.* decidedly shorter than the usual magnetic waves. These peculiar waves appear in the vertical component as conspicuous as in the horizontal components,<sup>2)</sup> while in the case of the usual magnetic waves of such a short period the vertical component is almost nil in comparison with the horizontal ones. Since our instruments are neither quite free from the influence of inclination nor of acceleration, even in the case of the Z-instrument, we can not be sure whether these waves are not largely due merely to the mechanical effect, though it seems not altogether improbable that an actual magnetic wave is produced by the earthquake. To decide this point, it will be desirable to carry out simultaneous observations with quite different systems of instruments with the same magnetic sensibility, but with considerably different mechanical sensibilities, though it will be difficult to obtain instruments perfectly free from mechanical disturbances.<sup>2)</sup>

*i)* All slight or conspicuous magnetic disturbances which may serve as premonitory signs preceding earthquakes, were carefully sought, throughout the records in hands. At first, a possible connection was suspected between the earthquakes and the characteristic abrupt occurrence of the regular wave trains,

1) The vertical-force magnetograph as now constructed may be regarded as a sort of seismograph, inasmuch as the line of suspension does not pass through the centre of the mass of the suspend system.

2) The trace of the same earthquake on the X-component record of the Eschenhagen magnetograph at Kakioka Magnetic Observatory, was about 6 mm. in maximum amplitude, while the magnetic sensibility was about 5  $\gamma$  per mm.

described in paragraph *e*). But the trains in question which are most frequent during the night hours, are distributed quite haphazard with respect to the earthquakes, if we either take slight and moderate earthquakes together, or confine our attention to the moderate ones only. In any case, a further study in this direction seems scarcely promising, in so far as the characteristic magnetic waves are of no local phenomena confined within a very limited area of the earth's surface.

On some occasions, slight irregular disturbances of very abnormal type were observed in both components, but usually in one component only, no corresponding simultaneous anomaly being marked in the other. These irregularities are most probably due to some slight accidental shock acting as an impulse to settling down a slight unstable position of the suspended system; for example, a slipping of microscopic magnitude, or the introduction of a minute dust particle at the point where the suspension wire touches the adjusting screw, may cause a quite sensible displacement in such an ultrasensitive state of suspension as adopted in our instruments. To detect premonitory, if any, magnetic disturbances, it will therefore be necessary to protect the instrument more thoroughly from any mechanical shock or other accidental disturbance.

However, during the entire course of the observations, no remarkable *destructive* earthquake occurred in the neighbouring districts, so that we are not yet in a position to draw any definite conclusion as to the value of magnetic observations as a means for predicting strong earthquakes—which was the original purpose of our present installation.

### PART III.

#### Special Statistical Investigations in Detail.

6. In the following, some of the results of the detailed statistical investigations with respect to some of the general results above described, will be given, which are on one hand a confirmation of the qualitative remarks stated in the preceding

paragraphs, and on the other hand constitute the basis of the theoretical considerations to be propounded later on.

It is the pleasant duty of the author to acknowledge here his indebtedness to Messrs. T. Tatiiri, the late H. Suzuki, M. Nakata and S. Hana who successively served as his assistants and computers in examining and making toilsome measurements of the records, and carrying out many tedious calculations, with indefatigable zeal and true scientific candour.

Some parts of the statistical work which necessitated the utmost care in measurements, for example the determination of the phase differences of different components *etc.* were made by the author himself.

7. At first, the photographic record were examined sheet by sheet, the conspicuous waves constituting more or less regular trains were selected and the approximate *mean* periods determined by dividing the time interval by the number of waves contained in the train.<sup>1)</sup> It is indeed difficult to decide which trains to take and which to omit. It was therefore decided to take as many trains as possible with different periods, provided that the trains comprise at least three very regular simple waves with sensible amplitudes. When during the course of an hour a very long continuous regular train with nearly constant period occurred, the period was determined only for one or two portions of the train chosen arbitrarily from the most conspicuous parts.

The case is more difficult when the fundamental waves are superposed with different "overtones." Very complicated waves, liable to ambiguities, were omitted, even if it were possible to analyse them into simple components, and the apparently regular trains only were taken into account. The results of the examination were systematically tabulated, separately for each of the three components, according to the successive hours of day. These tables formed the basis of some of the following investigations.

---

1) Strictly speaking, the periods are sometimes variable even in an apparently regular train of simple waves. The inconstancy is too considerable to be explained by the irregularities of motion of the drum carrying the photographic paper.

8. *Hourly distribution of waves of different periods.* The different periods were classified into the following arbitrary groups:  $30\cdot0^s-49\cdot9^s$ ,  $50\cdot0^s-69\cdot9^s$ ,  $70\cdot0^s-89\cdot9^s$ ,  $90\cdot0^s-129\cdot9^s$ ,  $130^s-200^s$ . The occurrence of waves belonging to the different groups, in different hours of successive days, was plotted down in diagrams similar to those drawn by Bidlingmeier<sup>1)</sup> in his "Uebersicht über die Tätigkeit des Erdmagnetismus."

From these diagrams, it could at once be seen that waves with periods shorter than about  $50^s$  are most frequently met with during the day time, while the longer waves over  $90^s$  periods are generally most frequent during the night. This is naturally true for each of the three components, though in Z-component the shorter waves are generally of almost insignificant amplitudes. To make this remarkable fact more apparent, the following procedure was adopted. Different days of a month, or of a season, were taken together, and the number of those days in the said interval, in which a certain given hour was disturbed by the waves of a certain given period, was counted and then divided by the total number of days in that interval, in which the observation was actually made at the very hour in question; the latter reduction was necessary, since especially in summer, the records were often imperfect. The number thus reduced, multiplied with 100, was called the "frequency" of that given group of waves in that particular hour, for the month or season in question. The following tables give the hourly frequency of the different wave groups in X- and Y-component, for different seasons, all the records available being taken into account. Z-component is omitted, since it is always a reduced facsimile of X-component, as already mentioned.

---

1) Bidlingmeier, Veröffentlichungen d. kais. Observatoriums in Wilhelmshaven

TABLE II.

The numbers give the frequency of the waves of different periods in %.

X.		30°—50°				Y.		30°—50°			
Month.	II III VI	V VI VII	VIII IX X	XI XII I	Year.	II III IV	V VI VII	VIII IX X	XI XII I	Year.	
0—1	3.2	2.8	6.6	3.9	4.1	2.0	3.0	3.9	2.3	2.7	
1—2	5.7	5.2	8.7	6.4	6.4	3.3	3.0	7.8	2.3	3.7	
2—3	4.5	6.7	7.8	7.1	6.4	5.3	6.0	3.9	2.8	4.4	
3—4	7.5	8.3	8.4	10.1	8.9	8.2	10.1	7.8	2.0	6.7	
4—5	12.2	9.7	10.3	12.5	11.3	10.3	10.2	11.2	3.6	8.5	
5—6	18.0	14.7	14.1	17.1	16.2	11.7	13.4	6.6	4.4	8.9	
6—7	18.4	14.9	16.0	19.7	17.5	15.4	13.4	16.8	10.9	13.9	
7—8	2.0	13.7	21.4	27.3	29.1	19.8	15.6	25.5	24.2	21.2	
8—9	18.7	14.7	15.4	31.5	29.8	17.8	14.9	16.7	23.5	18.6	
9—10	18.6	15.1	14.9	25.9	19.1	15.0	14.5	12.9	19.1	15.8	
10—11	13.8	19.6	19.2	21.1	18.4	12.2	13.3	14.5	16.2	14.1	
11—12	15.8	20.8	29.3	22.3	19.9	12.5	16.4	7.8	16.9	14.0	
12—13	20.7	19.1	20.4	19.5	19.9	12.2	7.2	16.4	16.9	13.5	
13—14	19.2	21.8	29.8	16.1	19.3	13.3	6.7	15.9	16.5	13.5	
14—15	14.4	21.1	22.2	12.7	17.2	11.7	6.2	14.3	12.6	11.4	
15—16	11.6	15.5	10.8	9.9	11.8	4.4	4.7	7.8	8.1	6.3	
16—17	10.8	14.2	9.0	7.1	10.1	4.3	2.6	2.8	7.1	4.7	
17—18	6.8	10.4	9.2	10.3	9.2	2.9	0.6	4.1	7.0	4.0	
18—19	4.2	13.6	6.9	10.8	8.9	3.9	5.1	8.4	5.4	5.4	
19—20	5.3	12.8	6.8	6.6	7.8	4.2	6.1	7.0	2.9	4.8	
20—21	4.2	6.5	3.4	5.5	5.0	2.7	6.0	1.3	2.2	3.1	
21—22	5.5	5.3	3.4	5.6	5.0	2.3	3.7	1.9	3.0	2.7	
22—23	1.6	3.1	6.3	3.0	3.4	1.5	2.3	3.8	1.9	2.2	
23—24	3.2	4.0	6.3	3.8	4.3	1.6	3.3	5.1	0.7	2.4	

X.		50 <sup>s</sup> —70 <sup>s</sup>				Y.		50 <sup>s</sup> —70 <sup>s</sup>			
Month.	II III IV	V VI VII	VIII IX X	XI XII I	Year.	II III IV	V VI VII	VIII IX X	XI XII I	Year.	
0—1	8.6	7.9	12.2	7.4	8.9	3.6	3.5	10.2	3.8	4.8	
1—2	11.1	5.6	5.6	9.4	8.2	7.8	5.0	4.5	4.2	5.5	
2—3	7.5	8.6	10.4	15.2	10.6	9.3	5.5	6.5	5.5	6.4	
3—4	12.8	9.7	9.0	17.6	12.7	6.5	10.6	6.6	9.5	8.4	
4—5	11.4	12.6	7.6	15.2	12.0	11.2	11.7	7.4	8.3	9.8	
5—6	14.6	15.7	13.6	19.9	16.2	9.6	10.7	13.0	10.6	10.7	
6—7	19.2	20.3	16.6	14.7	17.6	11.2	17.2	18.2	6.7	12.5	
7—8	17.5	21.7	22.0	21.6	29.7	18.2	17.1	25.8	16.9	18.9	
8—9	19.6	16.6	16.1	25.5	19.8	16.9	11.8	19.9	23.5	18.3	
9—10	18.6	17.4	14.8	18.2	17.3	14.2	7.5	14.0	19.3	14.2	
10—11	16.2	18.2	16.1	17.1	17.0	9.4	13.3	11.6	17.6	13.2	
11—12	16.0	15.0	16.7	19.8	17.0	6.9	8.5	11.0	24.2	12.4	
12—13	15.8	16.4	14.4	19.8	16.4	10.3	5.2	13.2	17.8	12.4	
13—14	17.1	12.3	18.3	16.1	16.0	9.5	5.3	11.1	17.1	11.5	
14—15	13.5	12.6	15.6	13.9	14.3	9.3	3.4	6.8	14.4	9.4	
15—16	10.7	14.1	12.4	11.6	12.1	6.1	2.0	2.7	6.9	4.9	
16—17	7.8	9.5	8.0	8.9	8.5	1.7	2.6	3.3	7.0	4.0	
17—18	7.2	7.0	11.8	7.5	8.2	1.6	0.6	6.6	6.2	3.8	
18—19	6.6	11.4	10.8	9.0	9.3	3.9	6.6	7.0	4.6	5.3	
19—20	6.8	8.9	13.6	6.2	8.6	5.0	13.2	10.4	5.1	7.9	
20—21	5.0	7.0	12.6	5.9	7.3	2.7	10.6	11.0	5.1	6.8	
21—22	4.7	8.9	10.1	7.1	7.7	4.8	6.4	8.5	2.2	4.8	
22—23	4.3	6.7	7.8	7.2	6.4	3.1	5.1	6.8	5.9	5.1	
23—24	7.2	8.5	9.3	12.0	8.8	2.3	4.2	9.9	2.2	4.1	

TABLE II. (*continued*).

X.		70 <sup>s</sup> —90 <sup>s</sup>				Y.		70 <sup>s</sup> —90 <sup>s</sup>			
Month.	II III IV	V VI VII	VIII IX X	XI XII I	Year.	II III IV	V VI VII	VIII IX X	XI XII I	Year.	
0—1	10.2	9.3	11.1	12.0	10.7	7.2	3.0	6.4	5.0	5.4	
1—2	11.5	6.4	10.8	13.5	10.8	7.3	3.0	7.1	4.3	5.4	
2—3	11.2	9.9	9.4	18.8	12.7	8.9	4.5	7.1	6.7	6.9	
3—4	9.5	8.5	7.9	13.0	9.9	5.7	6.5	3.8	5.6	5.5	
4—5	12.7	11.5	8.7	12.9	11.6	5.0	6.1	5.3	6.4	5.7	
5—6	13.4	12.8	8.1	14.0	12.3	6.2	7.5	4.0	5.2	5.8	
6—7	12.2	9.2	8.3	10.8	10.3	6.2	4.8	6.0	3.6	5.1	
7—8	14.2	12.1	7.9	13.0	12.0	7.4	7.3	7.3	7.4	7.4	
8—9	10.6	8.8	9.6	13.3	10.8	10.1	6.7	6.7	12.1	9.3	
9—10	10.5	8.1	5.4	11.1	9.1	6.5	4.5	2.0	8.2	5.8	
10—11	8.1	9.6	6.8	9.5	8.6	4.5	5.5	2.2	8.3	5.5	
11—12	9.4	10.1	6.4	7.7	8.4	4.7	1.2	1.6	7.7	4.5	
12—13	12.0	10.4	10.4	7.6	10.0	5.1	2.6	0.8	10.2	5.6	
13—14	8.8	4.7	7.6	9.6	7.8	5.2	2.7	4.8	8.2	5.7	
14—15	9.3	9.7	10.9	8.9	9.6	5.6	2.0	3.0	7.5	5.1	
15—16	9.0	8.2	8.8	3.8	7.3	3.5	3.3	3.6	4.6	3.9	
16—17	3.5	4.9	4.0	2.6	3.7	0.9	1.3	1.4	3.7	2.0	
17—18	4.0	4.9	7.7	7.4	6.0	2.4	0.0	4.1	4.0	2.8	
18—19	4.6	8.0	9.4	5.4	6.6	5.1	4.1	7.1	4.3	5.0	
19—20	7.6	8.9	10.2	10.0	9.1	9.5	8.5	7.0	5.1	7.4	
20—21	5.0	6.4	9.3	7.0	6.8	3.8	7.4	11.3	4.8	6.3	
21—22	7.1	9.3	9.1	10.4	9.0	4.2	5.5	5.6	5.5	5.2	
22—23	7.9	9.8	9.7	9.8	9.3	5.4	4.2	4.5	4.1	4.6	
23—24	10.8	6.1	8.8	11.5	9.5	5.9	2.8	3.8	4.1	4.3	

X.						Y.					
90°—130°						90°—130°					
Month.	II III IV	V VI VII	VIII IX X	XI XII I	Year.	II III IV	V VI VII	VIII IX X	XI XII I	Year.	
Hours.											
0—1	19.6	9.6	10.6	24.8	16.8	8.8	7.0	8.3	11.5	9.1	
1—2	20.1	9.6	9.2	27.7	17.5	10.6	3.0	7.7	8.2	7.6	
2—3	18.2	9.3	8.8	21.8	15.2	8.9	2.5	7.1	11.1	7.7	
3—4	15.4	9.5	13.2	19.6	14.8	8.6	7.5	8.3	7.2	7.9	
4—5	13.9	10.6	8.0	16.4	12.6	7.4	6.6	8.6	6.8	7.3	
5—6	17.6	9.2	7.1	14.8	12.6	6.0	5.9	3.9	4.8	5.2	
6—7	10.4	7.0	5.0	12.8	9.1	3.8	4.3	4.7	5.3	4.5	
7—8	5.4	7.7	4.2	8.4	6.6	6.2	3.1	3.3	5.8	4.9	
8—9	9.0	6.8	7.6	10.0	8.5	8.1	3.1	6.7	12.5	8.0	
9—10	9.7	6.1	5.9	8.5	7.7	6.1	1.5	2.7	8.2	5.1	
10—11	5.7	8.1	7.8	12.0	8.5	4.5	0.6	1.5	3.9	2.9	
11—12	8.2	6.7	6.4	8.8	7.6	2.6	1.2	2.3	4.2	2.8	
12—13	9.1	6.8	6.5	6.4	7.2	1.9	1.3	0.0	5.1	2.5	
13—14	7.5	10.2	6.1	10.0	8.5	4.3	2.7	1.6	4.7	3.6	
14—15	11.4	7.5	9.4	6.3	8.5	2.8	1.4	0.8	4.8	2.8	
15—16	7.7	5.0	8.8	5.0	6.5	2.6	2.0	3.6	3.7	3.1	
16—17	5.2	8.5	4.0	5.6	5.8	0.9	2.0	0.7	4.1	2.1	
17—18	4.0	3.5	4.6	7.1	5.0	2.8	0.6	1.4	3.3	2.3	
18—19	5.4	7.0	11.4	8.9	8.1	7.0	6.6	4.5	5.4	6.0	
19—20	7.6	5.0	14.5	14.4	10.4	9.1	6.1	8.3	6.6	7.5	
20—21	8.1	8.1	12.2	12.1	10.1	8.0	10.1	10.7	7.8	8.9	
21—22	11.0	10.0	11.6	11.1	10.9	9.5	10.1	13.0	7.4	9.7	
22—23	12.3	6.4	10.2	19.6	12.5	11.2	8.8	7.7	9.3	9.5	
23—24	16.4	6.0	13.1	22.6	15.0	11.8	5.1	5.1	10.1	8.5	

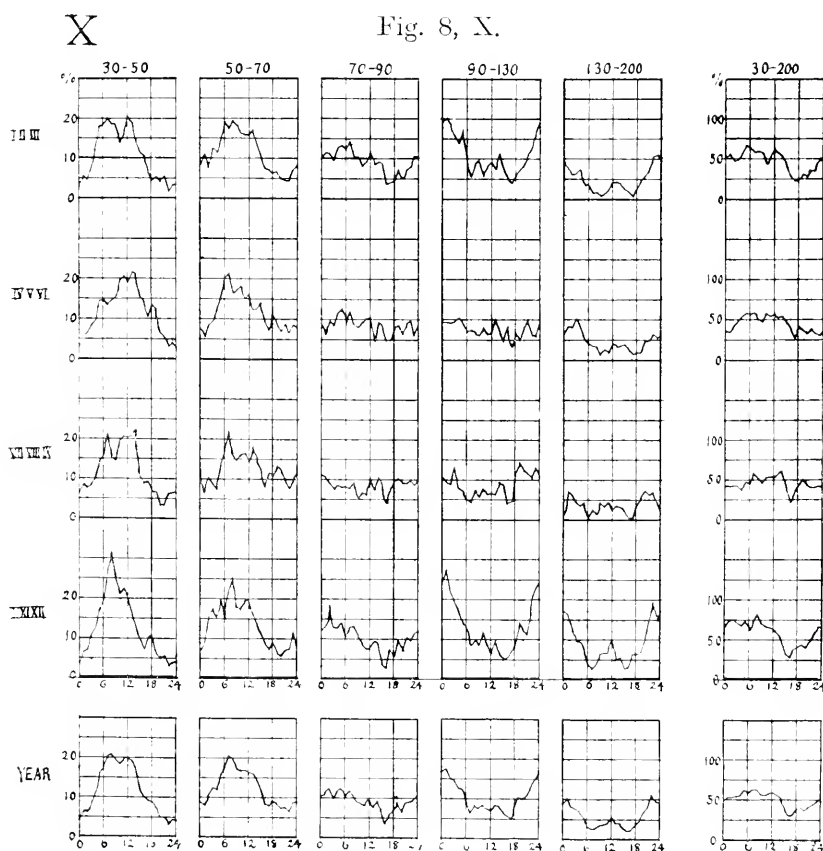
TABLE II. (*continued*).

X.		130 <sup>s</sup> —200 <sup>s</sup>				Y.		130 <sup>s</sup> —200 <sup>s</sup>			
Month.	II III IV	V VI VII	VIII IX X	XI XII I	Year.	II III IV	V VI VII	VIII IX X	XI XII I	Year.	
0—1	9.6	6.5	1.5	17.1	9.2	6.8	5.0	1.3	7.3	5.5	
1—2	7.6	8.5	7.2	16.7	10.3	4.9	5.0	3.2	5.8	4.9	
2—3	6.1	8.1	6.2	12.1	8.3	4.0	2.5	1.9	5.0	3.6	
3—4	6.5	10.2	4.7	9.8	7.9	1.2	3.5	3.2	3.6	2.8	
4—5	7.4	8.3	3.2	9.8	7.4	3.7	2.0	3.3	3.6	3.2	
5—6	3.3	5.4	4.4	8.2	5.4	4.6	4.3	3.9	4.8	4.5	
6—7	3.7	4.0	0.6	3.9	3.2	1.7	1.6	1.3	1.6	1.6	
7—8	1.2	3.3	2.6	2.7	2.4	0.8	0.5	0.7	2.3	1.2	
8—9	1.6	3.3	1.5	3.7	2.6	2.8	3.1	0.7	3.8	2.8	
9—10	0.8	1.4	4.4	6.3	3.3	2.0	0.5	2.0	4.1	2.3	
10—11	1.2	2.7	3.4	6.6	3.6	1.6	0.6	0.7	4.2	2.0	
11—12	2.4	1.8	4.4	6.6	3.9	0.4	0.6	0.0	1.9	0.9	
12—13	4.1	4.1	2.5	10.2	5.5	0.5	0.0	0.0	2.0	0.8	
13—14	4.1	3.2	3.6	5.0	4.0	1.9	2.0	0.8	1.6	1.6	
14—15	3.7	3.7	3.1	5.4	4.1	0.5	0.0	0.8	0.4	0.4	
15—16	2.5	3.8	2.1	2.7	2.8	0.0	0.7	0.7	1.5	0.8	
16—17	1.7	2.8	0.5	3.0	2.1	0.9	0.0	0.7	2.6	1.3	
17—18	0.4	1.4	0.5	6.4	2.4	0.8	0.0	0.0	3.7	1.4	
18—19	2.7	1.8	3.5	6.5	3.7	4.3	1.5	1.3	7.2	4.1	
19—20	4.1	1.8	5.3	6.9	4.6	4.2	4.2	6.4	8.0	5.7	
20—21	5.7	4.8	7.3	9.6	6.9	5.3	5.5	7.6	8.5	6.7	
21—22	6.9	4.9	6.2	14.6	8.4	7.6	10.6	3.7	5.9	7.1	
22—23	10.5	6.7	6.8	19.6	11.3	5.4	8.4	2.6	9.3	6.8	
23—24	11.0	5.8	4.4	15.3	9.5	6.6	2.8	5.1	10.1	6.5	

X.						Y.					
30 <sup>s</sup> —200 <sup>s</sup>						30 <sup>s</sup> —200 <sup>s</sup>					
Month.	II	V	VIII	XI	Year.	II	V	VIII	XI	Year.	
Hours.	III	VI	IX	XII		III	VI	IX	XII		
	IV	VII	X	I		IV	VII	X	I		
0—1	51.2	36.1	42.0	65.2	49.7	28.4	21.5	30.1	29.9	27.5	
1—2	56.0	35.3	41.5	73.8	53.2	33.9	19.0	30.3	24.8	27.1	
2—3	47.5	42.6	42.6	75.0	53.2	36.4	21.0	26.5	31.1	29.0	
3—4	51.7	46.2	43.2	70.1	54.2	30.2	38.2	29.7	27.9	31.3	
4—5	57.6	52.7	37.8	66.8	54.9	37.6	36.6	35.8	28.7	34.5	
5—6	66.9	57.8	47.3	74.0	62.7	38.1	41.8	31.4	29.8	35.1	
6—7	63.9	55.4	46.5	61.9	57.7	38.3	41.3	17.0	28.1	37.6	
7—8	58.3	58.5	58.1	73.0	61.8	52.4	43.6	62.6	56.6	53.6	
8—9	59.5	50.2	50.2	84.0	62.5	55.7	39.6	50.7	75.4	57.0	
9—10	58.2	48.1	45.4	70.0	56.5	43.8	28.5	33.6	58.9	43.2	
10—11	45.0	58.2	53.3	66.3	56.1	32.2	33.3	30.5	50.2	37.7	
11—12	51.8	54.4	54.5	65.2	56.8	27.1	27.9	22.7	50.9	34.6	
12—13	61.7	55.8	54.2	63.5	59.0	30.0	16.3	30.4	52.0	34.8	
13—14	56.7	52.2	56.4	56.8	55.6	34.2	19.4	34.2	48.1	35.9	
14—15	52.3	54.6	61.2	47.2	53.7	29.9	13.0	25.7	39.7	29.1	
15—16	41.5	46.6	42.9	33.0	40.5	16.6	12.7	18.4	24.8	19.0	
16—17	29.0	39.9	21.5	27.2	30.2	8.7	8.5	8.9	24.5	14.1	
17—18	22.4	37.2	33.8	38.7	30.8	10.5	1.8	16.2	24.2	14.3	
18—19	23.5	41.8	42.0	40.6	36.6	24.2	23.9	35.4	26.9	25.8	
19—20	31.4	37.4	50.1	44.1	40.5	32.0	38.1	39.1	27.7	33.3	
20—21	28.0	32.8	44.8	40.1	36.1	22.5	39.6	41.9	23.4	31.8	
21—22	35.2	38.4	40.4	48.8	41.0	28.4	36.3	32.7	24.0	29.5	
22—23	36.6	32.7	40.8	59.2	42.9	26.6	28.8	25.4	30.5	28.2	
23—24	48.6	30.4	41.9	65.2	47.1	28.2	18.2	29.0	27.2	25.8	

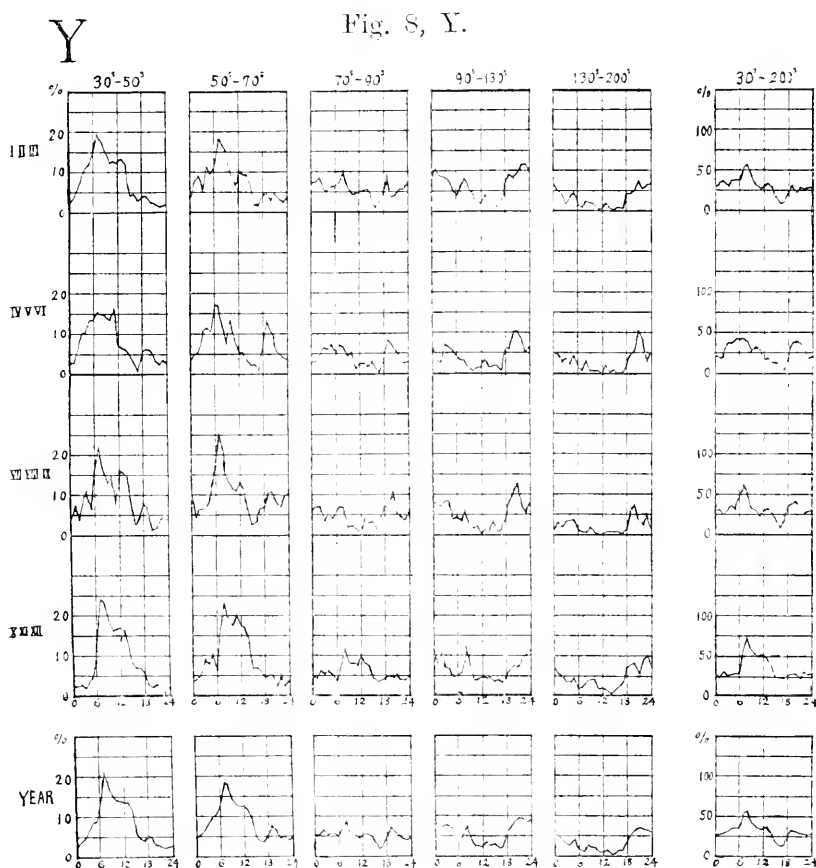


The results are also plotted in Fig. 8. As will be clearly seen, the waves with periods less than  $70^s$  show decided maximum frequency in the day time, more or less near noon, while those



longer than  $90^s$  are more frequent during the night. For  $30^s$ – $50^s$  waves, a tendency is suggested in the X-component that the hour of the maximum frequency is earlier in winter than in summer. Besides, for X- as well as for Y-components a secondary minimum near noon is suspected in spring and autumn. For  $50^s$ – $70^s$  waves, the hours of the day time maxima seem to fall somewhat earlier in the morning than for the shorter waves, and a secondary maximum in the early evening is suggested in some of the Y-diagrams.  $70^s$ – $90^s$  waves form apparently a transition stage to the still longer waves. For  $90^s$ – $130^s$  and  $130^s$ – $200^s$  waves, the

maximum frequencies fall decidedly in the night hours, mostly a little before midnight, while at the same time, a secondary maximum in the day time is suspected in some of the graphs.



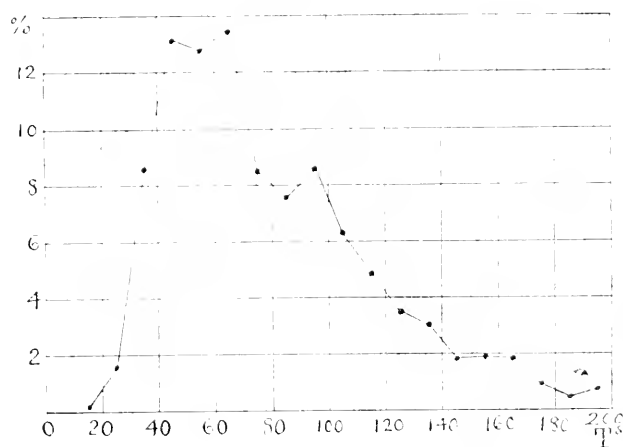
The frequency of all waves,  $30^{\circ}$ - $200^{\circ}$ , shows a maximum in the morning and a minimum in the evening.

It is to be remarked that the diurnal variation of the number of "spasms" as well as "pulsations" studied by W. van Bemmeln, and also that of the frequency of the disturbed hours, as could be deduced from the diagrams in Bidlingmeier's paper above cited, show a character quite similar to the variation of the frequency of the "longer waves" here studied, up to the appearance of the secondary daytime maxima.

On closer examination of the diagrams mentioned in p. 25 above, it is frequently found that wave trains with a certain period appear in almost the same isolated hours of two or three successive days, as if to repeat the particular program of the preceding days. This is interesting as one of the facts strongly suggesting that the agent producing these waves is intimately connected with the position of the earth relative to the sun. In some cases, it also happened that the hours of the successive days in which a particular train appears seemed to shift gradually in either direction.

9. *The "spectra" of the magnetic waves.* To find the most frequent period, the observed periods were at first classified second by second and the total number of *trains* (not that of days or hours in which they occurred) belonging to these groups were plotted in a diagram with the periods as abscissa. The diagram obtained showed a great number of maxima and minima with

Fig. 9.



intervals of several seconds. Most of these maxima and minima were, however, found to have no real physical meaning, being either due to chance,<sup>1)</sup> or due to some involuntary tendency of particular persons to prefer some par-

ticular fractions of the scale division when measuring the wave trains on the records with a millimeter scale.<sup>2)</sup> Hence, finally the following groups were taken: 20<sup>s</sup>-30<sup>s</sup>, 30<sup>s</sup>-40<sup>s</sup> *etc.* up to 190<sup>s</sup>-200<sup>s</sup>. The results are given in Table III. and also plotted in Fig. 9. As will be seen, the maximum frequency is generally

1) T. Terada, Proc. Tokyo Math.-Phys. Soc., 8, 1916, p. 492.

2) Note that a tenth of a millimeter corresponds to about 1.8 sec.

at the interval of periods 50<sup>s</sup>–60<sup>s</sup>. The curve reminds us rather of the energy distribution of the luminous spectra than the usual probability curves. A secondary maximum is seen near the period 90<sup>s</sup>. The results for other years are of quite similar character.

TABLE III.

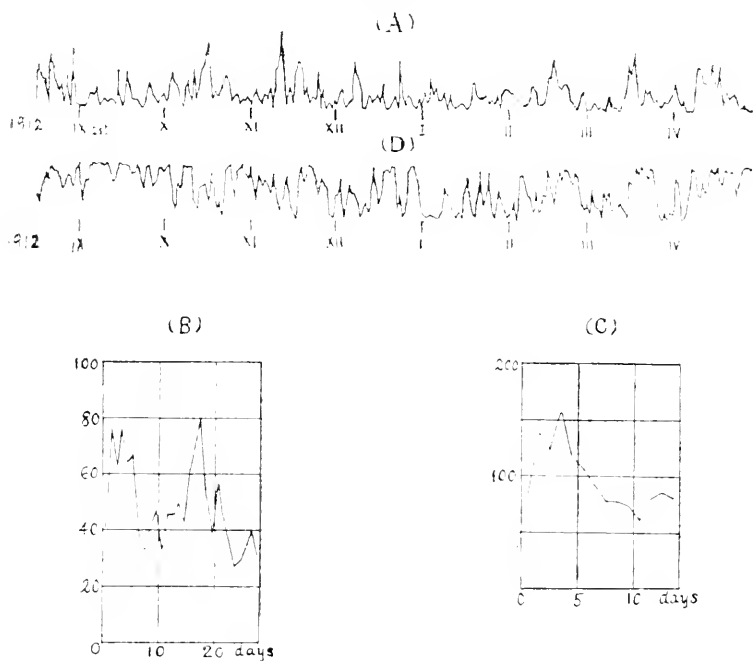
For each season, the first column gives the number of trains and the second the percentage of the total number.

1912. X.													
Season.		I II III		IV V VI		VII VIII IX		X XI XII		Year.			
Period.													
10s—	20s	3	0.3	2	0.2	0	0.0	2	0.1	7	0.1		
20 —	30	20	1.8	20	2.3	10	0.6	36	2.0	86	1.6		
30 —	40	120	10.9	75	8.8	126	7.8	143	7.8	464	8.6		
40 —	50	145	13.2	114	13.3	207	12.8	250	13.6	716	13.2		
50 —	60	134	12.2	106	12.4	231	14.3	224	12.1	695	12.8		
60 —	70	116	10.5	100	11.7	289	17.9	227	12.3	732	13.5		
70 —	80	85	7.7	63	7.4	168	10.4	145	7.9	461	8.5		
80 —	90	77	7.0	56	6.5	136	8.4	141	7.6	410	7.6		
90 —	100	107	9.7	66	7.7	139	8.6	154	8.4	466	8.6		
100 —	110	70	6.4	51	6.0	92	5.7	127	6.9	340	6.3		
110 —	120	59	5.4	36	4.2	56	3.5	114	6.2	265	4.9		
120 —	130	45	4.1	35	4.1	38	2.4	74	4.0	192	3.5		
130 —	140	33	3.0	36	4.2	34	2.0	62	3.4	165	3.0		
140 —	150	24	2.2	23	2.7	16	1.0	37	2.0	100	1.9		
150 —	160	21	1.9	20	2.3	29	1.8	35	1.9	105	1.9		
160 —	170	24	2.2	21	2.5	19	1.2	37	2.0	101	1.9		
170 —	180	8	0.7	9	1.1	17	1.1	17	0.9	51	0.9		
180 —	190	5	0.5	5	0.6	4	0.3	10	0.5	24	0.4		
190 —	200	5	0.5	18	2.1	7	0.4	10	0.5	40	0.7		
		1101		856		1618		1845		5420			

The result must not be hastily interpreted as showing that the *absolute* maximum of frequency is at the above mentioned interval. If we could multiply the sensibility of the instruments and turn at the same time the recording drum correspondingly faster, the waves most conspicuous in our case might possibly be replaced by others with a decidedly shorter periods. Besides,

it must be taken into account that the shorter the period, the greater will be the chance of revealing isolated trains in a given interval of time, even if the mean intensity and number of maxima of the trains be independent of the periods. This partially explains the falling off of the frequency curve toward the longer period in a form of hyperbola. Hence the real meaning of the above result can be simply interpreted as follows: As far as the sensibilities of the present instruments reveal, every period is rather evenly represented as in a continuous spectrum, showing no very sharply defined maximum, except two rather

Fig. 10.



flat relative maxima near  $60^\circ$  and  $90^\circ$ . The above holds good when we take the different hours of day and night altogether into account. When the different hours are taken separately, the results are somewhat different as already remarked in §8. This latter point will be referred to again later on, with respect to differently chosen materials. Here it may be remarked only

that the secondary maximum of frequency at about  $90^{\circ}$  corresponds to the most frequent waves observed during night hours.

No conspicuous group of waves with about  $10^{\circ}$  period, observed by Birkeland, could be confirmed in our records, though such waves might have been detected if the amplitudes were somewhat larger than  $0.2 \gamma$ .

10. *Fluctuation of frequency of regular waves in successive days.* The number of *hours* (not that of *trains*) disturbed by regular waves was counted for each of the successive days and plotted in a diagram with the days as abscissa. The results showed apparently very irregular fluctuations, either if we take all waves with the periods  $30^{\circ}$ – $200^{\circ}$ , or only  $30^{\circ}$ – $70^{\circ}$  waves. Though we must be very cautious in deducing any periodicity from such material, the results show nevertheless a remarkable tendency to suggest the existence of a period, or rather of an "interval" of about 25–30 days. The most conspicuous examples are illustrated by the interval from October, 1912, to April, 1913, especially when the waves with the periods  $30^{\circ}$ – $70^{\circ}$  alone are taken into account (Fig. 10, A). Fig. 10, B and C were obtained by superposing the successive series of 14 or 28 days<sup>1)</sup> respectively. These graphs seem to suggest the existence more of a 14 days period than a 28 days one, the amplitude amounting to the same order of magnitude as the mean value. The last procedure will however, have a definite meaning only when the phenomena are simply and purely periodic, but not when the frequency maxima are repeated with conspicuous amplitudes only a small number of times in a definite period, and then replaced by another of a similar kind, but setting in more or less abruptly with quite accidental time relation to the former. The general aspect of the frequency diagram here in question strongly suggests that the nature of the phenomena concerned is of the type above mentioned. In the above example, we may probably assume the accidental superposition of two independent series with the longer period, say 28 days. The lunar period is to be excluded, since the above fluctuation

---

1) 28 days instead of 27 days was taken simply because it is an even number, no weight being laid here on the exactitude of the period.

does not keep pace with moon's phases. It will be more plausible to suppose that the period in question is related to the sun's rotation.<sup>1)</sup>

It is to be regretted that our observations were not very adequate for investigations of the kind mentioned above, since in the warmer half of the year the records were occasionally defective. For the same reason, we must unfortunately refrain from carrying out the statistical investigations with respect to the *annual* or *seasonal* variation of the daily frequency.

11. *Probable relation of the frequency of waves with meteorological elements.* Since the phenomena of the magnetic pulsations were suspected of being closely related to some atmospheric phenomena as will be seen later on, it seemed possible that they might have a sensible correlation with some of the meteorological elements. Among the latter elements, cloudiness was considered as a most promising one for investigation, since its correlation with the solar activity is already acknowledged by some authorities,<sup>2)</sup> and moreover, considering the layer of cloud as a conducting sheet covering a considerable part of the earth's surface it may in some way or other play a sensible rôle where electromagnetic waves of not indefinitely long periods are in question. To carry out the comparison effectively, it will however, be necessary to take the cloudiness over a sufficiently wide area of the earth's surface in order to eliminate local irregularities of secondary nature which are very conspicuous in the case of this element. As the only available data in hand, the Monthly Reports of the Central Meteorological Observatory were used. Different groups of the local stations were taken and the average amounts of cloudiness were calculated. The results of comparison were not conclusive, though some correlation was suspected between the frequency of the magnetic pulsations and the average cloudiness for Tōkyō, Tyōsi, Mito and Maebasi.

---

1) Maunder and Marchand, *loc. cit.* Curiously enough, Schuster, on examining Maunder's data, also noticed a pronounced 14 days period. If the 14 days period was to be invariably found in allied phenomena, then the seat of the direct or indirect cause of magnetic disturbances may be sought in two antipodal portions of the sun's surface.

2) Hann, *Lehrbuch der Meteorologie*, 2nd. Ed., p. 476.

which is shown in Fig. 10.D. This point decidedly deserves further investigation.

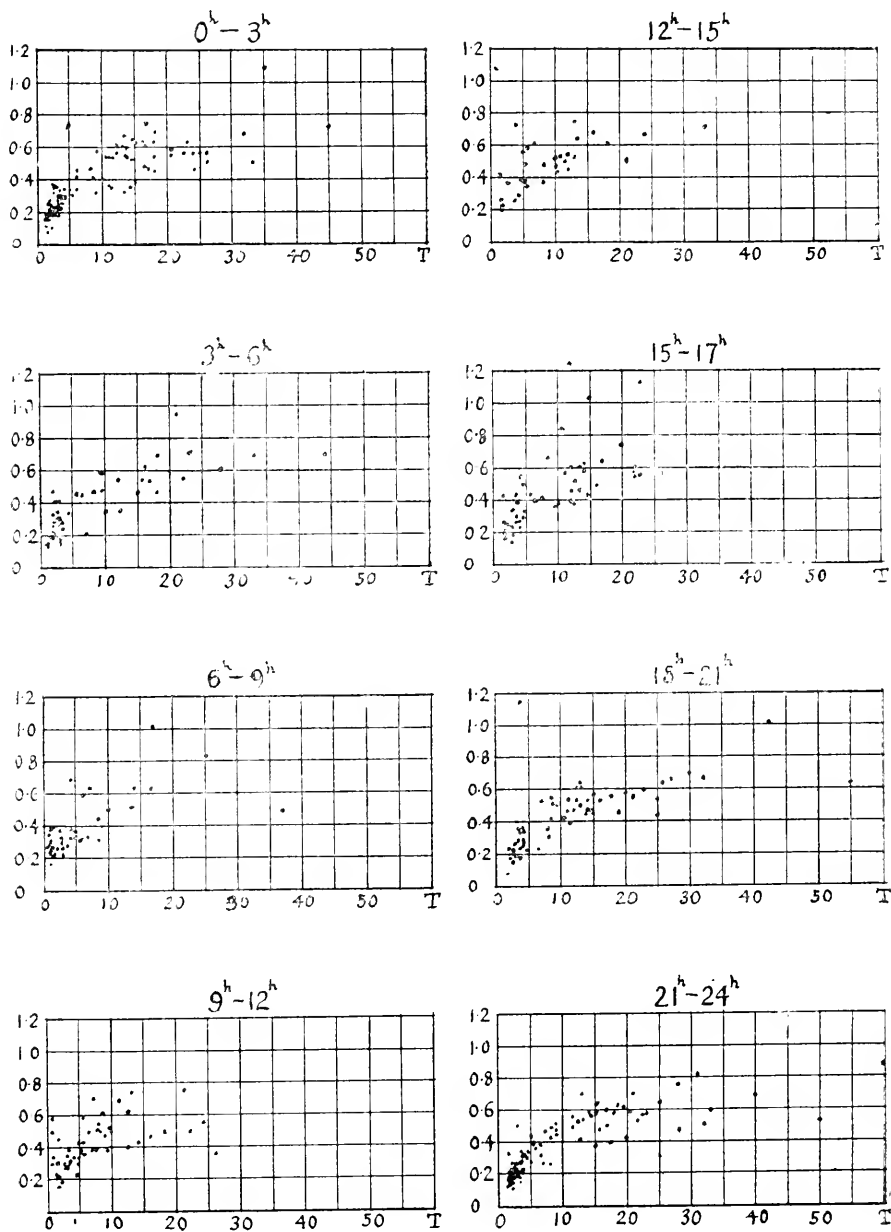
12. To carry out a more detailed quantitative investigation regarding the nature of the magnetic pulsations under consideration, the records of 1913 were specially chosen, since in this year the determination of the sensibilities of the instruments was most regularly made and hence most adequate for the quantitative comparison of the different components. It is, however, to be regretted that during the summer months the records were too frequently defective, chiefly due to damage to the photographic paper on account of the extreme dampness notwithstanding the use of the desiccator, and also due to the condensation of the atmospheric humidity in minute drops or mist which was especially dense in the daytime and caused a remarkable absorption of light. It must therefore be remarked that in some statistical studies to be described later, the winter season has a rather overweighing influence on the general results though the statistics extend over a full year. As far as the present investigations are concerned, no serious modification of the general results will, however, be required on that account.

13. *Ratio of amplitudes of X- and Z-components.* As already mentioned, the waves appearing in the Z-component are generally the reduced facsimiles of those in the X-component, except that the former always lags behind the latter in definite amounts depending on the periods, but usually less than a quarter of a period. In other words, the end of the magnetic vector representing the periodic disturbing field revolves on more or less elliptic orbits, with their major axes mostly dipping towards N. To find first a quantitative relation between the amplitudes of the two components, the following reductions were made. Specially regular portions of wave trains were carefully chosen out from among all the records of the year, and for each train the ratio of the mean amplitude of corresponding waves for the two components was calculated, the daily value of the sensibilities being duly taken into account. The results were tabulated together with the corresponding periods and the hours of



occurrence. Plotting the ratios as ordinates with the periods as abscissa in a diagram, the points representing different trains are

Fig. 11.



dispersed rather irregularly as shown in Fig. 11 in which the results are grouped with respect to the hours of occurrence. Next, the results were grouped according to the periods and the mean ratios were calculated for each group of the periods. The results are shown in the following Table and also plotted in Fig. 12 where the mean periods<sup>1)</sup> are taken as abscissa.

Fig. 12.

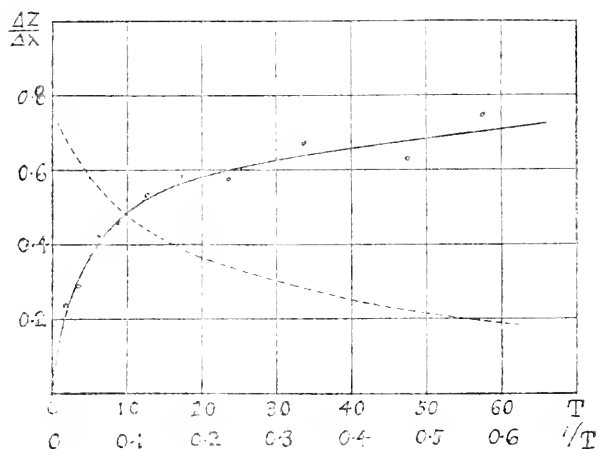


TABLE IV.

Range of $T$ .	$\frac{m}{0-2.5}$	$\frac{m}{2.6-5.0}$	$\frac{m}{5.1-7.5}$	$\frac{m}{7.6-10.0}$	$\frac{m}{10.1-15.0}$	$\frac{m}{15.1-20.0}$	$\frac{m}{20.1-30.0}$	$\frac{m}{30.1-40.0}$	$\frac{m}{40.1-50.0}$	$\frac{m}{51.0-60.0}$
Mean $T$ .	1.72	3.49	6.23	8.90	12.86	17.41	23.76	33.90	47.50	57.50
$\frac{\Delta Z}{\Delta X}$ .	0.235	0.291	0.421	0.459	0.536	0.580	0.574	0.672	0.621	0.745
$\text{tg}^{-1} \frac{\Delta Z}{\Delta X}$ .	13.°1	16.°1	22.°6	24.°5	28.°0	29.°9	30.°4	33.°4	31.°7	36.°5

As will be seen, the ratio increases at first rapidly with the periods, then gradually tends to an asymptotic value probably nearly equal to unity. The fact is rather remarkable and must serve as an important basis for explaining the phenomena in

1) The mean of the actual periods corresponding to the trains taken was calculated, not the simple mean of the interval of the period concerned.

question. For the purpose of a subsequent reference, the value of the ratios are also plotted with  $1/T$ , *i.e.* the reciprocal of the periods as abscissa (the dotted line in Fig. 12).

The irregular dispersion of the points in Fig. 11 is too remarkable to be considered as due to the inaccuracy of the measurements of the record or to the inconstancy of the instruments, but must be regarded as actually inherent to the nature of the phenomena. Neither is the irregularity at all eliminated, even if we take the ratio of the amplitude of  $Z$  to that of the *resultant* horizontal component,  $\sqrt{\Delta X^2 + \Delta Y^2}$  instead, which was actually calculated for the earlier period of the year.

Though we have not calculated the ratio  $\Delta Z / \sqrt{\Delta X^2 + \Delta Y^2}$  throughout the year, it will surely be an overestimation of the  $Y$ -component if we take  $\Delta Z / \sqrt{2} \Delta X$  for it, since, as will be seen later in §15, the azimuth of the horizontal component of the disturbing periodic field is generally less than  $45^\circ$  and about  $23.7^\circ$  on an average (see Fig. 16).

14. *Phase retardation of Z-component with respect to X-component.* Next, the phase relation of  $X$ - and  $Z$ -components were to be investigated. Since the corresponding waves in the two components appear as a rule widely apart on the photographic records where no special zero-line was recorded, a device was necessary to accurately mark off the corresponding time in each of the components at any part of the record. For this purpose, a kind of sliding T-square, originally constructed by Dr. Kadooka, was found very convenient. For the waves of shorter periods, utmost caution was still needed to avoid serious mistakes, very liable to be committed by the slight inclination of the sliding lineal which was to be kept parallel to the time-mark lines.

The mean retardation of the maxima and minima of  $\Delta Z$  relative to those of  $\Delta X$  were calculated in fractions of the periods. The corresponding values for maxima and minima respectively were often sensibly different, especially when the waves are not of simple form, in which case the mean of the two values was simply taken. Plotting the values for different trains with the periods as abscissa, the annexed figure was obtained (Fig. 13, A).

Classifying the period in the same groups as in the case of Fig. 12, we obtain the following Table and also Fig. 13, B.

Fig. 13, A.

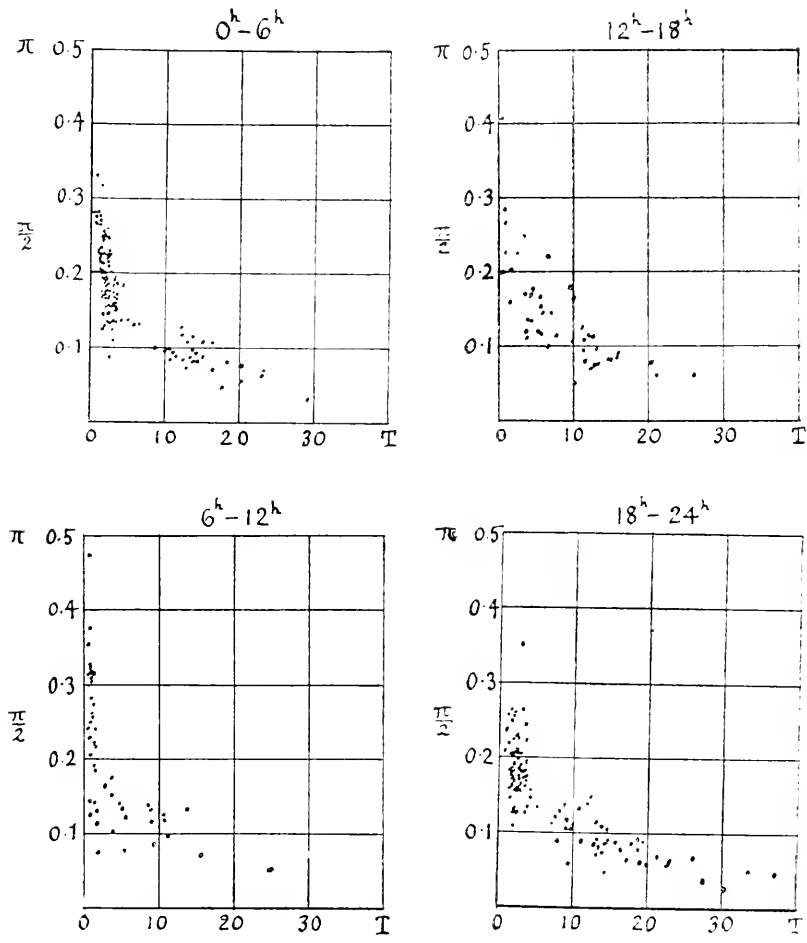
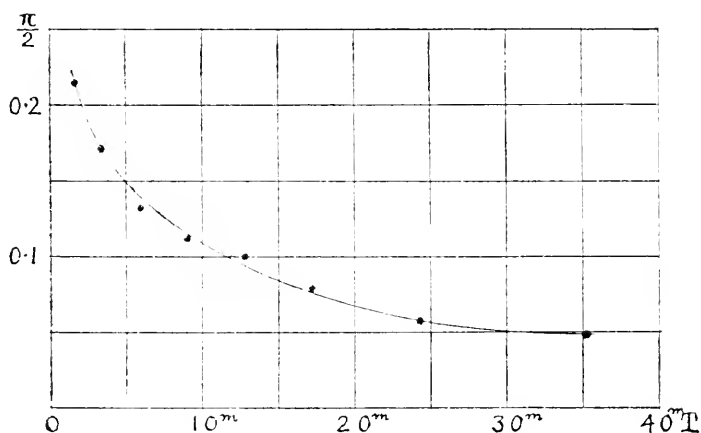


TABLE V.

Range of $T$ .	$\overset{m}{0}-\overset{m}{2.5}$	$\overset{m}{2.6}-\overset{m}{5.0}$	$\overset{m}{5.1}-\overset{m}{7.5}$	$\overset{m}{7.6}-\overset{m}{10.0}$	$\overset{m}{10.1}-\overset{m}{15.0}$	$\overset{m}{15.1}-\overset{m}{20.0}$	$\overset{m}{20.1}-\overset{m}{30.0}$	$\overset{m}{30.1}-\overset{m}{40.0}$
Mean $T$ .	$\overset{m}{1.59}$	$\overset{m}{3.34}$	$\overset{m}{5.35}$	$\overset{m}{9.11}$	$\overset{m}{12.80}$	$\overset{m}{17.22}$	$\overset{m}{24.45}$	$\overset{m}{35.15}$
Phase.	0.215	0.172	0.134	0.112	0.100	0.079	0.057	0.049

As will be seen from Fig. 13, the retardation is remarkable for shorter waves, sometimes amounting to decidedly more than

Fig. 13, B.



a quarter period in the case of 30<sup>s</sup> waves and gradually decreasing in a hyperbolic curve apparently tending to zero for longer waves over one hour. Combining the result with that obtained in the preceding article, we may trace the meridional projection of the elliptic orbit described by the end of the periodic disturbing vector of different periods.

15. *Azimuth of periodic disturbing fields, or the relation of amplitudes of X- and Y-components.* While the amplitude ratio between  $\Delta X$  and  $\Delta Z$  depends very much on the periods, but not sensibly on the hours of day, the ratio between the amplitudes of X- and Y-waves varies remarkably with the hours of occurrence, but not sensibly with the periods. To investigate the case more closely, the following procedures were adopted.

At first, all available records were examined and the number of regular trains were counted in which the two horizontal components are nearly parallel to each other, *i.e.* of phase difference zero, and also those in which the two are nearly inverted, *i.e.* of phase difference  $\pi$ . The results are given in the Table VI. and also in Fig. 14, regardless of the periods of the waves.

TABLE VI.

The numbers are given in % of all cases for each season.  
 + denotes the cases where  $\angle X$  and  $\angle Y$  are nearly parallel to each other,  
 - denotes the cases where  $\angle X$  and  $\angle Y$  are nearly inverted to each other.

Hours.	III IV V		VI VII VIII		IX X XI		XII I II		Year.	
	+	-	+	-	+	-	+	-	+	-
0-1	2.5	1.1	3.5	0.4	1.8	1.0	1.7	1.6	2.2	1.2
1-2	2.2	1.1	0.7	0.0	2.4	0.0	1.0	1.0	1.6	0.7
2-3	2.5	1.4	2.1	0.4	2.5	0.4	1.6	1.2	2.1	1.0
3-4	1.9	1.4	4.6	1.8	1.2	0.0	1.2	0.9	1.8	0.9
4-5	2.2	1.9	5.6	0.0	2.9	0.2	1.6	0.5	2.5	0.7
5-6	2.5	1.4	6.7	0.0	1.2	0.4	0.8	0.5	2.1	0.6
6-7	8.6	0.3	11.6	0.4	4.1	0.2	2.0	0.0	5.5	0.2
7-8	7.2	1.4	13.4	0.0	14.7	0.0	6.9	0.7	9.5	0.6
8-9	8.9	1.4	5.6	0.0	15.7	0.6	13.0	1.1	11.5	0.9
9-10	4.7	0.9	5.6	0.4	11.5	1.0	8.5	1.1	7.7	0.9
10-11	2.3	0.3	1.8	0.0	5.7	0.2	6.1	0.6	4.4	0.3
11-12	2.3	0.0	1.8	0.7	6.1	0.0	6.4	0.5	4.7	0.3
12-13	1.4	0.0	1.4	0.4	3.5	0.0	5.4	0.7	3.4	0.3
13-14	1.9	0.2	0.7	0.4	3.1	0.8	4.6	0.6	3.1	0.5
14-15	1.1	0.2	0.7	0.0	1.6	0.2	2.2	0.3	1.6	0.2
15-16	0.6	0.5	1.1	0.0	0.2	0.2	0.7	0.5	0.6	0.3
16-17	0.2	0.3	0.0	0.0	0.2	0.4	0.7	0.9	0.3	0.5
17-18	0.6	0.6	0.4	0.0	0.4	0.6	1.4	1.8	0.8	1.0
18-19	1.6	4.1	1.8	2.1	1.0	2.2	1.1	2.7	1.3	2.9
19-20	1.9	4.7	2.5	4.6	0.4	2.5	0.7	3.3	1.1	3.7
20-21	0.6	5.3	3.2	1.1	0.4	1.8	0.7	2.6	0.9	3.0
21-22	2.2	4.2	3.5	2.8	0.4	2.5	0.7	2.4	1.4	3.0
22-23	1.7	3.1	1.1	3.9	0.2	2.2	0.3	2.3	0.8	2.7
23-24	1.1	1.7	1.1	0.7	0.8	1.0	1.2	2.5	1.1	1.7

It will be seen that the number of cases with the phase difference zero attains a maximum in the early hours of morning, while that with the phase difference  $\pi$  shows a maximum in the evening (Fig. 14).

Secondly, those cases were chosen where either the one, X- or Y-component, is alone conspicuous, while the other is quite insignificant. The distribution of these special cases in different hours is given in Table VII. and plotted in Fig. 15.

As may be seen, the cases where X-waves are alone conspicuous, or in other words, the disturbing field is directed nearly in the meridian, are most frequent near midnight and noon, while the opposite cases, *i.e.* those in which the disturbance occurs nearly in the WE direction, are most frequent in the morning and evening.

Fig. 14.

— Parallel.  
 ---- Inverted.

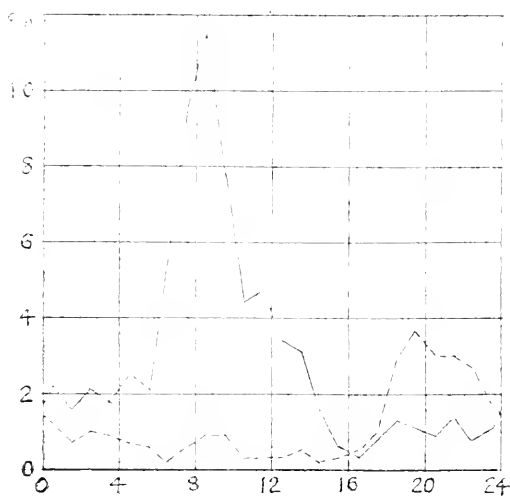


Fig. 15.

— X alone.      ---- Y alone.

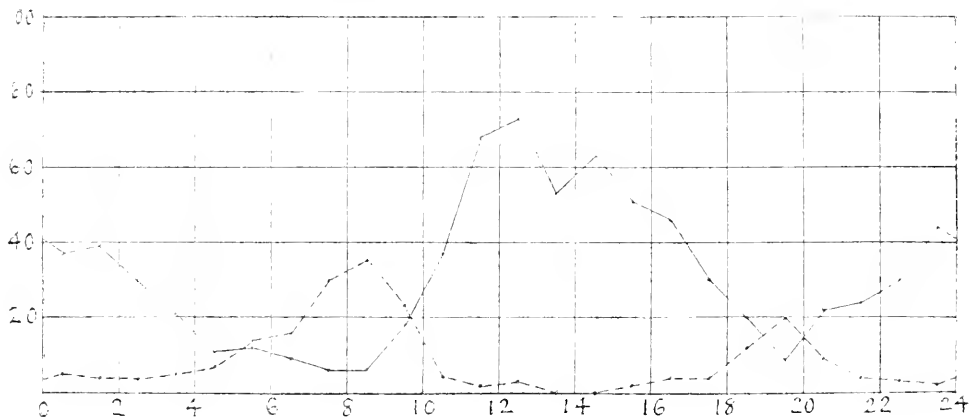
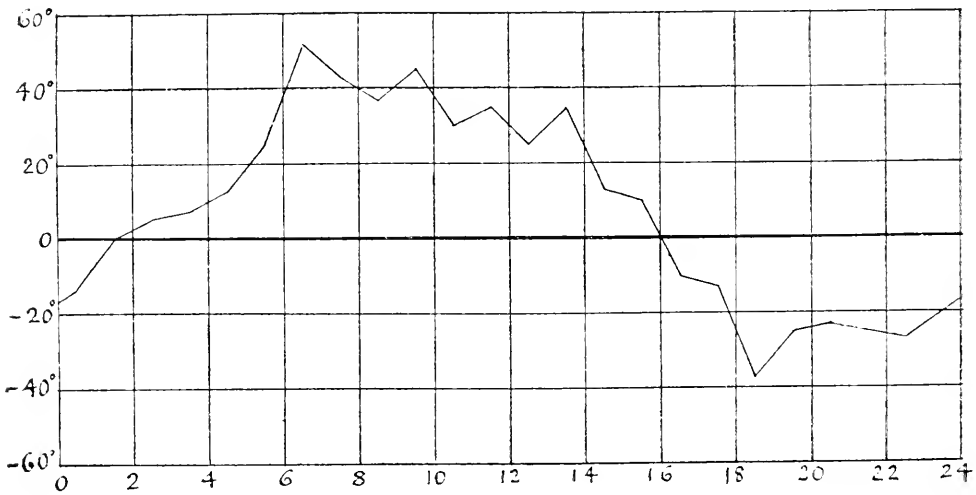


TABLE VII.

Hour.	X only.	Y only.	Hour.	X only.	Y only.	Hour.	X only.	Y only.	Hour.	X only.	Y only.
0-1	37	5	6-7	9	16	12-13	73	3	18-19	20	12
1-2	39	4	7-8	6	30	13-14	53	0	19-20	9	20
2-3	30	4	8-9	6	35	14-15	63	0	20-21	22	9
3-4	21	5	9-10	18	23	15-16	51	2	21-22	24	4
4-5	11	7	10-11	37	4	16-17	46	4	22-23	20	3
5-6	12	14	11-12	68	2	17-18	30	4	23-24	44	2

Thirdly, taking the records of 1913 only, those cases were chosen in which the phase difference of the two horizontal components was either 0 or nearly  $\pi$ , *i.e.* in which the periodic disturbance is “polarized” in a certain azimuth, and the ratio of the amplitudes was carefully determined which corresponds to the tangent of the azimuthal angle  $\alpha$ . The latter angle was counted from N. positive value taken toward W. The results, if plotted in a diagram, with the hours as abscissa, regardless of

Fig. 16.





the periods, show very irregular scattering of the points representing different trains. Nor is the irregularity lessened by choosing the waves of a definite period only.

The most frequent value of the azimuth for each hour was then determined, not by taking the simple mean value, but by plotting graphically the frequency of different azimuthal angles for each hour and taking the maximum point of the frequency curve thus obtained. The results are given in Table VIII. and plotted in Fig. 16, which generally confirms the result to be inferred from Fig. 15. Neither is the present result in contradiction with that shown in Fig. 19, since the maximum and minimum value of  $JY/JX$  must correspond to cases where the direction of the disturbing force makes the largest angle with the meridian, and the zero value of this ratio must correspond to the case where the field is nearly in the meridian. These results show that the azimuthal angle, on an average, undergoes a continuous and fairly regular diurnal variation. Though the present data are too defective for drawing conclusive inferences with respect to the seasonal difference of the above relation, they suggest that in summer, the azimuth has a secondary minimum near noon. Besides, it is suspected that the mean azimuthal angle in day time is somewhat less for longer periods than for shorter. These points must, however, be postponed for a future investigation.

TABLE VIII.

Hour.	$z^\circ$	Hour.	$z^\circ$	Hour.	$z^\circ$	Hour.	$z^\circ$
0-1	-13	6-7	52	12-13	25	18-19	-37
1-2	0	7-8	43	13-14	35	19-20	-25
2-3	5	8-9	37	14-15	13	20-21	-23
3-4	7	9-10	45	15-16	10	21-22	-25
4-5	13	10-11	30	16-17	-10	22-23	-27
5-6	25	11-12	35	17-18	-13	23-24	-20

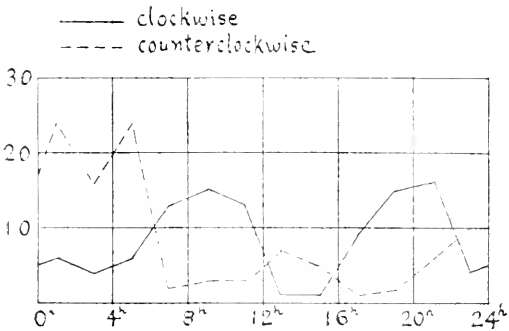
16. Since in the above investigations, the trains chosen from among the records of 1913 were those especially regular and moreover, the periods were determined with special care, the material seems appropriate for studying the frequencies of different periods in different hours of the day, in spite of the relatively small number of trains taken. The results of the examination are tabulated below, which show remarkable predominance of the *longer* waves in the night hours, as already remarked in §9.

TABLE IX. *Number of trains.*

Period in Hour.	0-0.5	0.5-1.0	1.0-1.5	1.5-2.0	2.0-2.5	2.5-3.0	3.0-3.5	3.5-4.0	4.0-4.5
0-4	0	19	26	29	29	7	20	6	0
4-8	4	66	39	21	22	10	7	3	1
8-12	4	93	49	20	15	7	5	5	3
12-16	1	45	40	10	8	7	2	1	1
16-20	0	14	12	19	16	6	3	5	6
20-24	0	6	25	41	31	24	13	6	8
Sum	9	243	191	140	121	61	50	26	19

17. *Rotatory character of the horizontal components.* As already mentioned, the horizontal components of the periodic disturbing field show as a rule more or less rotatory character.

Fig. 17.



the clockwise and in the counterclockwise sense respectively.

To investigate the relation in detail, regular waves with decidedly rotatory character were chosen from the records of 1913, at the same time with the investigation of the preceding article. The data obtained were classified into two groups, *i.e.* those which showed regular rotation in

The frequencies of the two groups in different hours were calculated, as shown in Table X, and also in Fig. 17.

TABLE X.

Hour.	Counter-clockwise.	Clockwise.	Hour.	Counter-clockwise.	Clockwise.
0-2	24	6	12-14	7	1
2-4	16	4	14-16	5	1
4-6	24	6	16-18	1	9
6-8	2	13	18-20	2	15
8-10	3	15	20-22	6	16
10-12	3	13	22-24	10	4

For each group, the frequency shows apparently a *semidiurnal* period. Comparing the result with Fig. 16, it may be noticed that the clockwise rotation predominates in those hours where the direction of the disturbing field is at the maximum deviation from the meridian, while the counterclockwise rotation falls most frequently in the intermediate hours. It must be also remarked that the sense of rotation during night hours is generally opposite to that determined by Sangster<sup>1)</sup> for disturbances of decidedly longer durations, and therefore also opposite to the sense in which the abrupt disturbing field described in §5 *e)* tends. In Sangster's case the sense of rotation showed a diurnal period, being of the same sense throughout twelve hours, while in the case of the short waves here in question, it shows a semidiurnal period as given above.

## PART IV.

### Discussion of the Results.

18. The results of the present investigations so far described seem to throw some light, however faint, on the actual origin

1) Sangster, *loc. cit.*

of the magnetic pulsations in question, though it is at the present stage rather difficult to draw anything like a conclusive inference, for even if the observations had been carried out for a much longer period with more reliable instruments, the data were in any case confined only to a single station. In the following, we will try, instead of hastening to any premature conclusion, to consider, merely by way of tentative suggestion, different possibilities regarding the probable cause of the phenomena in question. The considerations will inevitably be of a speculative character, but may serve at least as useful hints for projecting future investigations of allied phenomena, especially of the as yet very obscure nature of the electrical as well as mechanical behaviour of the upper atmosphere.

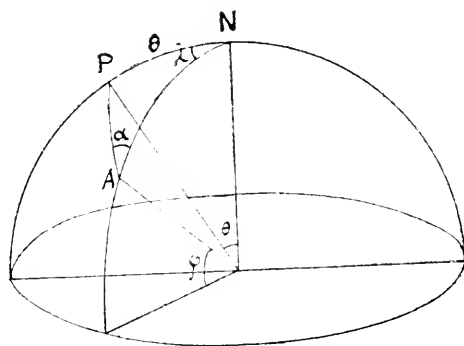
19. A fact strongly impressing us in the first place, is that the occurrence of the magnetic pulsations in question is subjected in more than one respect to a remarkable diurnal variation. This evidence alone is sufficient to infer the important rôle played by the sun, whether its influence be direct or indirect. The position of the sun, not only determines the length of the periods of the most frequent waves in different hours, but also affects the direction in which the periodic magnetic field fluctuates. It seems quite plausible to assume from the outset that the seat of the *primary* cause of the phenomena is chiefly to be sought in our atmosphere subjected to solar radiation of different kinds. The periodic heating of the superficial layer of the earth crust, though it may possibly cause a slow variation of the terrestrial magnetism, may scarcely account for the periodic nature of the disturbances in question. The direct magnetic influence of the sun itself<sup>1)</sup> seems also improbable, since if such be the primary cause, the more or less complete screening off of waves shorter than 50<sup>s</sup> during night hours must be explained, while 100<sup>s</sup> waves are so conspicuous in these hours. Moreover, the unsymmetrical distribution of the characteristic waves at noon is rather difficult to explain on this view. On the other hand, the existence of remarkable electric currents in the upper region

---

1) Bosler, Journal de Physique, [6] 2, 1912, p. 877.

of our atmosphere may be regarded as almost an established fact since the classical investigations of Schuster,<sup>1)</sup> Birkeland and Störmer.<sup>2)</sup> Now, according to Schuster and Bezold, there exists in the upper atmosphere a definite system of currents whose position is nearly fixed relative to the sun, which produces the remarkable diurnal variation of the terrestrial magnetic field. The first suggestion which naturally arises as to the cause of the magnetic pulsations, is the fluctuation of this permanent system of currents.<sup>3)</sup> This seems the more plausible, if we remember the very regular diurnal reiteration of the characteristic phenomena. The material nearest in hand for testing this conjecture is the daily variation of the azimuth of the horizontal components of the periodic disturbing field. Examination of Fig. 16 will show that a similar daily variation could be produced, if a nearly

Fig. 18.



circular zonal system<sup>4)</sup> of electric currents, fixed with respect to the sun and having its pole situated at a considerable distance from the earth's axis, undergoes some periodic fluctuations in its different parts. Referring to Fig. 18, let  $N$  be the earth's astronomical pole, while  $P$  is the pole of the zonal current. Denoting the latitude

of the point of observation  $A$  by  $\phi$ , and its longitude counted from the meridian containing  $P$ , by  $\lambda$ , the azimuthal angle  $\alpha$  of the

1) A. Schuster, *Philosophical Transactions*, **180 A**, 1889, p. 467; v. Bezold, *Gesammelte Abh.*, p. 404.

2) Birkeland, *loc. cit.*; *C. R.*, **147**, p. 539. C. Störmer, *Archiv for Math. og Naturvidenskab.*, **31**, 1911, Nr. 11; *Archiv des Sc. phys. et nat.*, **24**, 1907, pp. 5, 113, 221, 317; numerous papers in *C. R.*

3) The idea is not at all new, being expressed already by Eschenhagen, Birkeland, van Bemmeln *etc.*, though more or less vaguely.

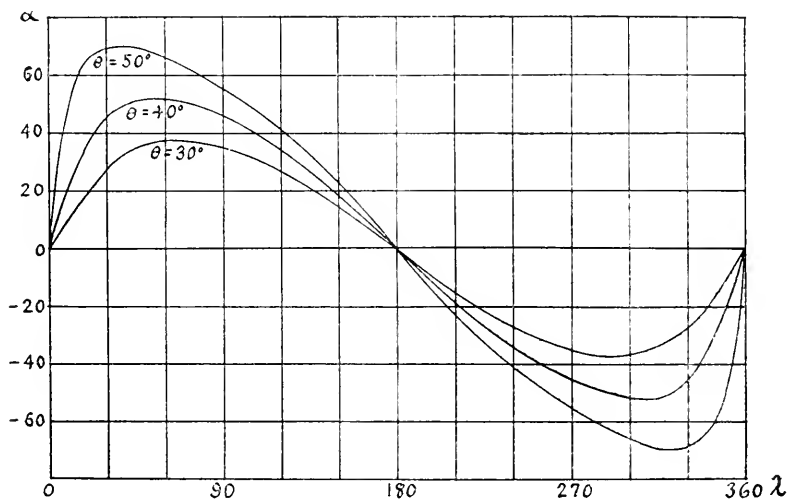
4) We do not necessarily mean a continuous system of current flowing in a given direction at the same time, but only that the directions of the different portions of the current causing pulsations, when put together, form the *portions* of a circular zone with a given pole.

magnetic field due to the current passing near the point  $A$ , counted positive toward W from N of  $A$ , is given by

$$\sin \alpha = \frac{\sin \theta \sin \lambda}{\sqrt{1 - (\cos \theta \sin \varphi + \sin \theta \cos \varphi \cos \lambda)^2}}$$

Putting for example,  $\varphi = 35^\circ$  and  $\theta = 30^\circ, 40^\circ$  or  $50^\circ$ , the variation of  $\alpha$  as the function of  $\lambda$  is shown in the annexed figure (Fig. 19).

Fig. 19.



To compare with Fig. 16, the present figure must be properly shifted along the axis of  $\lambda$ , which is equal to the hours, up to an additive constant. It seems that the meridian corresponding to the pole  $P$ , (*i.e.*  $\lambda=0$ ) of the assumed circular current may be placed somewhat in the early hours of the morning. The shapes of the curves, however, do not agree so well as to enable us to determine the most probable value of  $\theta$ . Indeed, it will be too much to infer at once the existence of such a simple circular current in view of the above consideration, based on the observation at a single station. Still the orientation of the different *portions* of the atmospheric current, of which the fluctuations may produce the magnetic pulsations, must resemble in some measure that of the corresponding portions of the ideal simple system above considered, and must in any case be directed

nearly SW-NE or reverse during the day time and NW-SE or reverse during night. The supposed system of currents can not be directly identified with that given by Schuster or Bezold, since in the latter case,  $\alpha$  passes the value  $\frac{\pi}{2}$  twice during 24 hours, and the corresponding curve of  $\alpha$  with the hour as abscissa shows no apparent resemblance either with Fig. 16 or with Fig. 19. Nor is the system of currents deduced by Birkeland<sup>1)</sup> from the disturbances of longer durations observed during his memorable auroral expedition similar to the supposed one. Remembering, however, that the daily variation of the terrestrial magnetic field can be represented in the first rough approximation by a system of currents having its axis considerably inclined to the earth's axis, we may regard provisionally the total current system given by Schuster and Bezold consisting of two parts, and that the one part which is the principal and represents a system of zonal currents, shows a more conspicuous regular fluctuation than the remaining secondary part more or less converging toward the pole (see § 28). As a matter of fact, Fig. 19 represents only the *average* distribution of the most frequent azimuth in different hours. In actual cases, the points corresponding to different trains of waves are so remarkably scattered that the adoption of the mean value evaluated in the usual manner seems scarcely justified for seeking the most frequent value. It is very probable that among these widely scattered points, there are many which actually correspond to the fluctuations of the part of the current belonging to the higher harmonics. At any rate, our conjecture seems to be justified in the first approximation, though the position of the pole of the circular current can not be determined with certitude.

20. As to the actual modes of fluctuation of the atmospheric current causing the magnetic waves concerned several possibilities are suggested at the same time. Firstly, we may consider the total intensity as well as the distribution of the current as constant, but oscillating as a whole about its mean position,

---

1) Birkeland, *loc. cit.*, Pl. X.

either vertically, horizontally or in a rotatory manner. Secondly, it is also possible that the current itself undergoes a periodic fluctuation, either in the total intensity or in the distribution in its different parts. More probable is the combination of the above two modes. Thirdly, we may suppose a system of parallel currents arranged at nearly equal intervals propagated perpendicular to itself, over the point of observation with a finite velocity, in which case the waves must show a time difference in difference stations. If the results of observations confirm the exact simultaneity of waves in widely distant stations beyond all doubt, the last hypothesis will naturally fall out. Birkeland, indeed, observed the approximate simultaneity of some waves with short periods in two stations so widely apart as Potsdam and Bossekop. The two examples reproduced in his report, however, refer only to nearly the same midnight hour, where the direction of the atmospheric current might well have been approximately parallel to the line joining the two stations. Again, according to the result of the simultaneous observations made at Kyôto, Misaki and Sendai, in April, 1909, by Dr. Kadooka and Prof. Tanakadate, a similar simultaneity is observed within the limit of experimental error; but in this case the distances were not very great. Though these two observations strongly speak against the progressive nature of the periodic disturbances, a further accumulation of evidence will not be considered superfluous for deciding the point beyond all doubt. On the other hand, some disturbances of a longer duration investigated by Ad. Schmidt<sup>1)</sup> were actually progressive. Birkeland also attributed a velocity of translation at the rate of 100 km. per minute to some class of perturbations. A possibility of occasional occurrence of progressive waves, if not of regular phenomena, seems to be not yet disproved. On this view, it will be of some theoretical interest to include the case of progressive waves among the possible cases and see how far the hypothesis is favourable or unfavourable for explaining the different peculiarities of the observed phenomena.

---

1. Ad. Schmidt, *Met. Zs.*, 16 1899, p. 385.



In the following, we will recapitulate some of the most remarkable results of the statistical investigations and try to review them in the light of the different hypothetical atmospheric currents.

21. First, take the relation between X- and Z-components which show such an intimate connection as regards their amplitudes and phases, as described fully in previous paragraphs. We will proceed to consider the influences of different possible ideal systems of atmospheric currents separately, and compare the results with the observed facts by way of seeking a most plausible explanation.

Since the disturbances with the short periods here in question most probably extend to a limited portion of the earth's surface, as may be judged from their remarkable dependency on the hours of the day, it will be allowed for a first approximation to consider both the surface of the earth and the atmospheric layer carrying the current as a plane.

22. *a)* Consider an infinite linear current  $i$  running perpendicular to the meridian at a height  $h$  from the earth's surface considered plane, and at a horizontal distance  $x$  from the point of observation A. Then the X- and Z-components will be given by

$$ZX = \frac{2ih}{x^2 + h^2}, \quad Z = \frac{2ix}{x^2 + h^2} \dots \dots \dots (1)$$

If the intensity of the current fluctuates in any manner, while its position remains unchanged with respect to the earth, the two components will follow the fluctuation simultaneously, provided that the variation is slow enough for neglecting the effect of the induced current. The ratio of the amplitudes being

$$\frac{Z}{X} = \frac{x}{h},$$

it may assume any value when  $x$  varies from  $-\infty$  to  $+\infty$ . Besides,  $Z$  will be of opposite phase on both sides of the current.

*b)* If the above current *moves* perpendicular to itself from  $x = -\infty$  to  $+\infty$ , X-component at A evidently attains a maximum at  $x=0$ , while  $Z$  is zero at  $x=0$  and has a maximum and

minimum at  $x=\pm h$  respectively. The end point of the vector describes a circle with the radius  $i/h$ .

c) Instead of a linear current, we consider next a current of uniform density  $i$ , with a rectangular section having a breadth of  $2l$  and a height of  $2b$ , the middle point lying at a height  $h$  and the horizontal distance  $x$  from A. The two components are respectively given by

$$\left. \begin{aligned} \frac{JX}{i} &= x \log \frac{(x+l)^2+(h+b)^2}{(x+l)^2+(h-b)^2} \cdot \frac{(x-l)^2+(h-b)^2}{(x-l)^2+(h+b)^2} \\ &+ l \log \frac{(x+l)^2+(h+b)^2}{(x+l)^2+(h-b)^2} \cdot \frac{(x-l)^2+(h+b)^2}{(x-l)^2+(h-b)^2} \\ &+ 2(h+b) \operatorname{tg}^{-1} \frac{2(h+b)l}{(h+b)^2+x^2-l^2} - 2(h-b) \operatorname{tg}^{-1} \frac{2(h-b)l}{(h-b)^2+x^2-l^2} \\ \frac{JZ}{i} &= 2(x+l) \operatorname{tg}^{-1} \frac{2(x+l)b}{(x+l)^2+h^2-b^2} - 2(x-l) \operatorname{tg}^{-1} \frac{2(x-l)b}{(x-l)^2+h^2-b^2} \\ &+ h \log \frac{(x+l)^2+(h+b)^2}{(x+l)^2+(h-b)^2} \cdot \frac{(x-l)^2+(h-b)^2}{(x-l)^2+(h+b)^2} \\ &+ b \log \frac{(x+l)^2+(h+b)^2}{(x-l)^2+(h-b)^2} \cdot \frac{(x+l)^2+(h+b)^2}{(x-l)^2+(h+b)^2} \end{aligned} \right\} \quad (2)$$

When the current degenerates into a current sheet of the horizontal breadth  $2l$  and the linear intensity  $i'$ ,

$$\left. \begin{aligned} JX &= 2i' \operatorname{tg}^{-1} \frac{2lh}{h^2+x^2-l^2} , \\ JZ &= i' \log \frac{(x+l)^2+h^2}{(x-l)^2+h^2} . \end{aligned} \right\} \dots\dots\dots (3)$$

Again, when the current sheet is vertical with a breadth  $2b$ ,

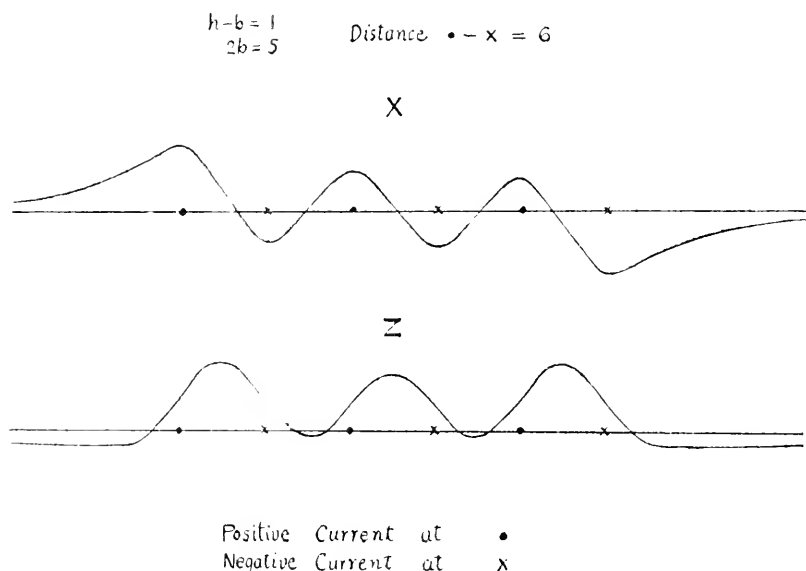
$$\left. \begin{aligned} JX &= i' \log \frac{x^2+(h+b)^2}{x^2+(h-b)^2} , \\ JZ &= 2i' \operatorname{tg}^{-1} \frac{2bx}{x^2+h^2-b^2} . \end{aligned} \right\} \dots\dots\dots (4)$$

In the former case (3), the maximum value of  $JZ$ ,  $JZ_m$  say, which is attained at  $x=\pm\sqrt{l^2+h^2}$ , will increase indefinitely, while the maximum value of  $JX$ , or  $JX_m$  tends to  $2\pi i'$ , when the ratio  $b/h$  increases indefinitely. For  $b=0$ , the ratio is  $1/2$ . In the latter case (4),  $JZ_m$  varies from 0 to  $\frac{\pi}{2}$  when  $2b$  increases from

0 to  $\infty$ ,  $h$  being kept constant, while  $\Delta X_m$  increases indefinitely with  $b$ . The ratio  $\Delta Z_m / \Delta X_m$  tends to  $1/2$  when  $b$  decreases indefinitely, as is already evident from the former results.

d) Let a number of such currents be arranged with the directions alternately positive and negative, and parallel to each other at definite intervals, each moving perpendicular to itself with a uniform velocity. Neglecting the effect of the induced current, the magnetic field at A will undergo a train of periodic variation as illustrated in the annexed figure (Fig. 20) for a special

Fig. 20.



case. As will be seen, the phase retardation of  $\Delta Z$  is somewhat similar to that in the actual case, though here at the same time with the short waves, a rather remarkable general swelling of the curves appears. The latter may probably be avoided by properly reducing the intensity of the currents toward both ends of the train. In this case, the pulsations must necessarily be *progressive*.

23. Next, we will consider the effect of the current induced

in the earth, especially for a simple case convenient for mathematical treatment, *i.e.* the case when the current is arranged in an *infinite train of waves*, either *stationary* or *progressive*.<sup>1)</sup>

Take the surface of the earth, considered plane as usual, as  $xy$ -plane and the positive direction of  $z$  downward. For the positive value of  $z$ , the space is considered to be filled with a conducting medium with the uniform specific conductivity  $k$  and the magnetic permeability  $\mu$ , while the negative side of  $z$  is regarded as a vacuum. Assuming the electric and magnetic force independent of  $y$  and denoting their components respectively by  $\mathfrak{E}_x$ ,  $\mathfrak{E}_z$ ,  $\mathfrak{H}_x$ ,  $\mathfrak{H}_z$ , the usual fundamental equations for the slow variations reduce to

$$\left. \begin{aligned} \mu \frac{\partial \mathfrak{H}_x}{\partial t} &= \frac{\partial \mathfrak{E}_y}{\partial z}, & 4\pi k \mathfrak{E}_y &= \frac{\partial \mathfrak{H}_x}{\partial z} - \frac{\partial \mathfrak{H}_z}{\partial x}, \\ -\mu \frac{\partial \mathfrak{H}_z}{\partial t} &= \frac{\partial \mathfrak{E}_y}{\partial x}, & \frac{\partial \mathfrak{H}_x}{\partial x} + \frac{\partial \mathfrak{H}_z}{\partial z} &= 0. \end{aligned} \right\} \dots\dots\dots (1)$$

since  $\mathfrak{E}_x = \mathfrak{E}_z = 0$ ,  $\mathfrak{H}_y = 0$ . Next, assume that the electromagnetic field varies periodically with the frequency  $n/2\pi$  and the distribution of the fields represents a two-dimensional wave with the wave length

$$\lambda = \frac{2\pi}{a}.$$

In the case of *stationary* waves, we may assume

$$\mathfrak{E}_y = e^{int - (\beta + i\gamma)z} \sin ax, \dots\dots\dots (2)$$

where  $\beta$  and  $\gamma$  are considered real. From

$$4\pi\mu k \frac{\partial \mathfrak{E}_y}{\partial t} = \frac{\partial^2 \mathfrak{E}_y}{\partial x^2} + \frac{\partial^2 \mathfrak{E}_y}{\partial z^2},$$

we obtain

$$4\pi\mu k in = -a^2 + (\beta + i\gamma)^2$$

or

$$\beta^2 - \gamma^2 = a^2, \quad 2\beta\gamma = 4\pi\mu kn, \dots\dots\dots (4)$$

---

1) The mathematical solution of the case was kindly carried out by Prof. S. Sano, to whom the best thanks of the author are due.

whence

$$\beta = \sqrt{\frac{1}{2}(\sqrt{a^4 + 16\pi^2 \mu^2 k^2 n^2} + a^2)}, \quad \gamma = \sqrt{\frac{1}{2}(\sqrt{a^4 + 16\pi^2 \mu^2 k^2 n^2} - a^2)}. \quad \dots (5)$$

From the first set of the fundamental equations results

$$\left. \begin{aligned} \mathfrak{G}_x &= \frac{(-\gamma + i\beta)}{\mu n} e^{int - (\beta + i\gamma)z} \sin ax, \\ \mathfrak{G}_z &= \frac{i\alpha}{\mu n} e^{int - (\beta + i\gamma)z} \cos ax. \end{aligned} \right\} \dots \dots \dots (6)$$

Taking the real parts and putting  $z=0$ , we obtain at last

$$\left. \begin{aligned} (\mathfrak{G}_y)_{z=0} &= \cos nt \sin ax, \\ (\mathfrak{G}_x)_{z=0} = \mathcal{A}X &= - \frac{(\gamma \cos nt + \beta \sin nt)}{\mu n} \sin ax, \\ (\mathfrak{G}_z)_{z=0} = \mathcal{A}Z &= - \frac{\alpha \sin nt}{\mu n} \cos ax. \end{aligned} \right\} \dots \dots \dots (7)$$

Similarly in the case of *progressive* waves, we may proceed by assuming

$$\mathfrak{G}_y = e^{(nt \pm \alpha x)i - (\beta \pm i\gamma)z} \dots \dots \dots (8)$$

and obtain

$$\left. \begin{aligned} \mathcal{A}X &= - \frac{1}{\mu n} \left\{ \gamma \cos(nt \pm \alpha x) + \beta \sin(nt \pm \alpha x) \right\}, \\ \mathcal{A}Z &= \mp \frac{\alpha}{\mu n} \cos(nt \pm \alpha x), \end{aligned} \right\} \dots \dots \dots (9)$$

where the values of  $\beta$  and  $\gamma$  are the same as above (5).

Putting

$$\beta = A \cos \varphi, \quad \gamma = A \sin \varphi,$$

or

$$A = \sqrt{\beta^2 + \gamma^2}, \quad \operatorname{tg} \varphi = \frac{\gamma}{\beta}, \quad \dots \dots \dots (10)$$

(7) becomes

$$\left. \begin{aligned} \mathcal{A}X &= - \frac{A}{\mu n} \sin(nt + \varphi) \sin ax, \\ \mathcal{A}Z &= - \frac{\alpha}{\mu n} \sin nt \cos ax. \end{aligned} \right\} \dots \dots \dots (7')$$

The same substitution makes (9), for progressive waves toward N.

$$\left. \begin{aligned} \mathcal{J}X &= \frac{A}{\mu n} \cos\left(nt - ax + \frac{\pi}{2} + \varphi\right), \\ \mathcal{J}Z &= \frac{a}{\mu n} \cos(nt - ax), \end{aligned} \right\} \dots\dots\dots (9')$$

and for retrograde waves toward S.

$$\left. \begin{aligned} \mathcal{J}X &= -\frac{A}{\mu n} \sin(nt + ax + \varphi), \\ \mathcal{J}Z &= -\frac{a}{\mu n} \sin\left(nt + ax + \frac{\pi}{2}\right). \end{aligned} \right\} \dots\dots\dots (9'')$$

Hence for the case of stationary waves (7'), the ratio of the amplitudes of Z and X is given by

$$\frac{\mathcal{J}Z_m}{\mathcal{J}X_m} = \frac{a}{A} \cotg ax \dots\dots\dots (11)$$

which can assume any value whatever between  $-\infty$  and  $+\infty$ , as we proceed normal to the wave ridges. Moreover,  $\mathcal{J}Z$  is retarded after  $\mathcal{J}X$  by  $\varphi$  given by (10).

Again, in the case of progressive and retrograde waves, the ratio of the amplitudes is

$$\frac{\mathcal{J}Z_m}{\mathcal{J}X_m} = \frac{a}{A} = \frac{a}{\sqrt{\beta^2 + \gamma^2}} \dots\dots\dots (12)$$

which is always less than, and tends to, unity as the frequency decreases, since

$$A^2 = \beta^2 + \gamma^2 = \sqrt{a^4 + 16\pi^2 \mu^2 k^2 n^2} \dots\dots\dots (13)$$

Besides,  $\mathcal{J}Z$  lags behind  $\mathcal{J}X$  by  $\varphi + \frac{\pi}{2}$  or  $\varphi - \frac{\pi}{2}$  according as the waves are progressive or retrograde.

Now, the angle determining the phase is given by

$$\tg \varphi = \frac{\gamma}{\beta} = \sqrt{\frac{\sqrt{a^4 + 16\pi^2 \mu^2 k^2 n^2} - a^2}{\sqrt{a^4 + 16\pi^2 \mu^2 k^2 n^2} + a^2}}$$

which becomes zero for small value of  $kn$  and tends to unity for large values. Hence, in the case of stationary waves, the retardation of the vertical component will increase from 0 to  $\frac{\pi}{4}$  when  $kn$  increases from 0 to  $\infty$ . In the case of progressive

waves, when  $kn$  increases from 0 to  $\infty$ , the retardation will vary from  $\frac{\pi}{2}$  to  $\frac{\pi}{2} + \frac{\pi}{4}$  or  $\pi - \frac{\pi}{4}$ , while in the case of retrograde waves, it may be considered as negative and varies from  $-\frac{\pi}{2}$  to  $-\frac{\pi}{4}$ .

Now, returning to the actual case, we will try to examine if either of these hypothetical waves could be reconciled with the observed facts regarding the relations between the horizontal and vertical components of magnetic pulsations.

If the stationary waves alone were concerned, we would have to assume that the distance of the observing station from the node of the electric current was in any case greater than  $\frac{\lambda}{8}$  but less than  $\frac{\lambda}{4}$ , in order to explain the fact that the ratio  $\Delta Z_m / \Delta X_m$  was always less than unity, at least in the case of the slow oscillations where  $a/\lambda$  in (11) is nearly equal to unity and  $\cotg ax$  may become less than unity only when  $ax$  or  $\frac{2\pi x}{\lambda}$  is greater than  $\frac{\pi}{4}$ . This will be a rather awkward, though not impossible assumption, if the wave length were small in comparison with the earth's quadrant, since we must then also assume that the location of the current is always limited to a rather narrow range favorable to the above relation. The only plausible hypothesis reconcilable with this assumption is that the wave length of the current producing the slow waves is of the order of magnitude of the earth's meridian, and also that the station lies always not far apart from the loop of the current. In such a case, however, either of our assumption as to the planeness of the earth's surface and the existence of the infinite train of waves, will fail to apply; but the case will rather approach that which was discussed in the preceding paragraph. The present result may be interpreted as merely indicating that the effect of the induced current has the tendency to retard the vertical component with respect to the horizontal one. For such a case, the mathematical calculation given by Lamb<sup>1)</sup> for spherical conductors will directly apply, which also shows the retardation tending to  $\frac{\pi}{4}$  for the large value of  $km$ . At any rate, the observed

---

(1) H. Lamb, Phil. Trans., 1883, p. 526; *ibid.*, 1889, p. 513.

waves with periods longer than  $10^m$  which show the retardation generally less than  $\frac{\pi}{4}$ , may easily be explained by a current of rather diffused character subject to fluctuations. Indeed, these longer waves are generally not very regular and rarely form a train with the number of successive maxima greater than three or four,—a decided contrast with the shorter waves of a few minutes periods which form as a rule remarkably regular trains and show occasionally phase retardation of  $\mathcal{JZ}$  greater than  $\frac{\pi}{4}$ . If the above conjecture be justified in some measure, the current, of which the local fluctuation produces these longer waves, may plausibly be identified with the circular current discussed in § 18 and compared with the principal part of the current causing the diurnal variation of the terrestrial field, since in this way, the variation of the azimuth of the disturbing field may also be explained satisfactorily, at least to the first approximation.

The maximum current intensity may be expected probably near the equator if the phase relation between  $\mathcal{JX}$  and  $\mathcal{JZ}$  is never inverted throughout the N-hemisphere. It will be interesting to see if the relation is actually opposite on the S-hemisphere. v. Bemmeln found  $\frac{\mathcal{JZ}}{\mathcal{JX}}$  in Batavia invariably insignificant.

On the other hand, the most regular waves with periods less than about  $4^m$  show as a rule remarkable phase retardation of the vertical component after the horizontal ones, generally greater than  $\frac{\pi}{4}$ . This seems apparently difficult to explain on the assumption of stationary waves, if we solely rely on the above calculation.

Next, turning for a while to the case of progressive waves, we remark that one fact seems at first sight to be in favour of this assumption. As described repeatedly above, the actual ratio of the amplitudes  $\mathcal{JZ}_m/\mathcal{JX}_m$  never exceeds unity and decreases gradually as the frequency of the wave increases. From (12) and (13), we have indeed



$$\frac{\Delta Z_m}{\Delta X_m} = \frac{a}{\sqrt[4]{a^4 + 16\pi^2 \mu^2 k^2 n^2}},$$

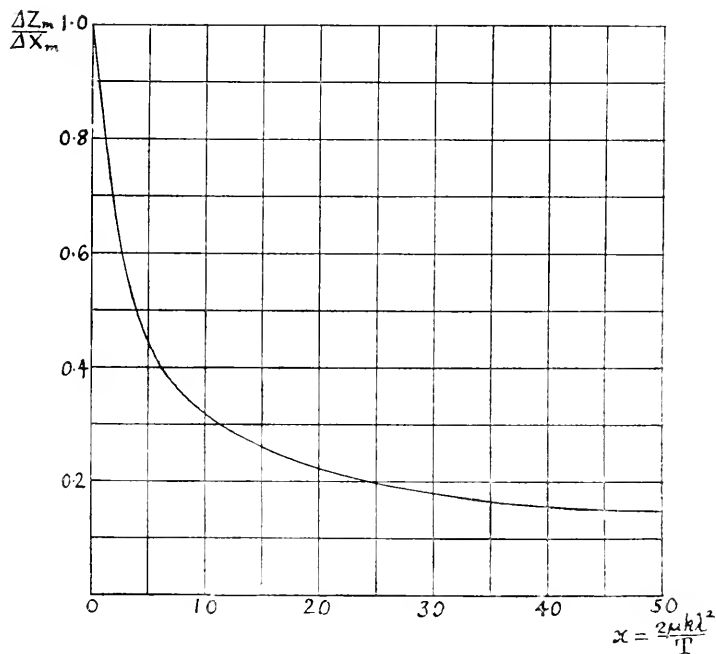
which may be written  $= \frac{1}{\sqrt[4]{1+x^2}},$

if we put  $x = \frac{4\pi\mu kn}{a^2} = \frac{2\mu k\lambda^2}{T},$

denoting the period by  $T$ , *i.e.* putting  $n = \frac{2\pi}{T}.$

The variation of the calculated ratio  $\Delta Z_m/\Delta X_m$  with  $x$  as abscissa, may be seen from the annexed figure (Fig. 21). Referring to

Fig. 21.



Figs. 11 and 12, and comparing the present theoretical curve with the curve of the observed ratio with  $1/T$  as abscissa, we may observe a striking resemblance, though the ratio of the scales for the two diagrams is not yet known. If we take, for example, the 3<sup>m</sup> wave for the purpose of comparison, the observed value of  $\Delta Z_m/\Delta X_m$  is nearly 0.28. Making a discount of 10 % on account of the reason discussed at the end of § 13,

we obtain 0.25. The corresponding value of  $x$  in Fig. 21 is found to be nearly 17. Hence, we must have, assuming for simplicity's sake  $\mu=1$ ,

$$2k\lambda^2 = 17 \times 180 = 3060 ;$$

hence  $\lambda^2 = \frac{1530}{k}$ , or  $\frac{2 \cdot 10^3}{k}$  in round number. Now assuming the conductivity of the earth to be  $10^{-13}$  as is suggested by the result of Schuster's investigation, we obtain

$$\lambda = 1.2 \times 10^8 \text{ cm. or } 1200 \text{ km., say.}$$

Nearly the same value may be obtained, if we take  $10^m$  waves instead. We have no theoretical ground at hand for assuming that the wave length varies with the periods; still, judging from the remarkable resemblance of the two diagrams above compared, it seems plausible to assume provisionally that the wave length is at least of the same order of magnitude, and the different periods are determined not so much by the difference of the wave length as of the velocity of propagation. In the above example, where  $\lambda = 1.2 \times 10^3$  km. for  $T = 180^s$ , the velocity of propagation  $v$  will be about  $7 \frac{\text{km.}}{\text{sec.}}$ <sup>1)</sup>. The above estimation was solely based on the assumption that the equations (11), (12) *etc.* hold rigorously. Judging from the analogy of the case investigated by Schuster, it is probable that the actual reduction of the vertical component will be decidedly more remarkable than the calculated value. If such be the case, the value of  $x$  and accordingly the values of  $\lambda$  and  $v$  will become less than those above estimated.

A closer examination of Fig. 12 shows that the asymptotic value of  $\Delta Z_m / \Delta X_m$  is not 1, but somewhat near 0.8. If we compare Fig. 12 with a diagram obtained by multiplying the ordinates of Fig. 21 by 0.8, the acceptable value of  $x$  become about 10 instead of 17. But this does not alter the order of magnitude of the results.

---

1) According to Birkeland, the lateral velocity of the current producing some disturbances was of the order of 100 km. per minute, while that of some auroral bands observed in the polar region was about 300 m. per sec., which is very small in comparison with the above calculated velocity of the hypothetical current.

As for the phase retardation of  $\mathcal{J}Z$  after  $\mathcal{J}X$ , the serious difficulty against the hypothesis of the progressive waves is that, in the theoretical result, the phase angle must be included within the range  $90^\circ$  to  $135^\circ$  or  $-45^\circ$  to  $-90^\circ$ , while in the observed results, it crowds most densely within the limit  $45^\circ$  to  $90^\circ$ . At present we are at a loss to judge whether the difficulty may be evaded by assuming the presence of more conducting layer below the earth's crust, as argued by Schuster to explain a similar discrepancy in the case of the diurnal wave.

On the other hand, if we once admit in the case of the *stationary* wave that  $\cotg \alpha x$  is somehow of the order of unity, the ratio of amplitude  $\mathcal{J}Z_m/\mathcal{J}X_m$  is just the same as in the case of the progressive waves, and the above calculations generally apply also to this case, except that part concerning the velocity of propagation which is zero in this case. The general mode of dependency of the ratio on the periods is equally favourable for the stationary waves, and we see no strong reason for preferring the theory of progressive waves, as far as the amplitude ratio is concerned. If we take  $\cotg \alpha x = 1$  or  $0.8$  and  $k = 10^{-13}$  the wave length estimated seems, however, too small.

At any rate too much weight must not be laid on the numerical results of the above calculations, since they have no claim to accuracy of the quantitative results, if we remember the utmost simplicity of the assumptions on which they are based, even if they may be legitimate in essential features.

24. Next, consider the ideal case where an atmospheric current is subject to a rotatory oscillation remaining parallel to itself. Taking the simplest case of a constant linear current running parallel to the  $y$ -axis and oscillating about the mean position, given by its elevation  $h_0$  above the surface of the earth and the horizontal distance  $x_0$  from the point of observation taken as the origin. Let the position of the current  $i$  be given by

$$\left. \begin{aligned} x &= x_0 + x_1 \cos nt, \\ h &= h_0 + h_1 \cos(nt - \varphi). \end{aligned} \right\} \dots\dots\dots (I)$$

We may obtain, neglecting the effect of induction

$$\left. \begin{aligned} \frac{X}{2i} &= \frac{h_0}{x_0^2 + h_0^2} + A_x \cos(nt - \phi_x), \\ \frac{Z}{2i} &= \frac{x_0}{x_0^2 + h_0^2} + A_z \cos(nt - \phi_z), \end{aligned} \right\} \dots\dots\dots (2)$$

where

$$\left. \begin{aligned} A_x \cos \phi_x &= \frac{h_0}{h_0^2 + x_0^2} \left\{ -\frac{2x_0x_1}{x_0^2 + h_0^2} + \left( \frac{h_1}{h_0} - \frac{2h_0h_1}{h_0^2 + x_0^2} \right) \cos \varphi \right\}, \\ A_x \sin \phi_x &= \frac{h_0}{h_0^2 + x_0^2} \left\{ \frac{h_1}{h_0} - \frac{2h_0h_1}{h_0^2 + x_0^2} \right\} \sin \varphi, \\ A_z \cos \phi_z &= \frac{x_0}{h_0^2 + x_0^2} \left\{ \frac{x_1}{x_0} - \frac{2x_0x_1}{h_0^2 + x_0^2} - \frac{2h_0h_1}{h_0^2 + x_0^2} \cos \varphi \right\}, \\ A_z \sin \phi_z &= -\frac{x_0}{h_0^2 + x_0^2} \cdot \frac{2h_0h_1}{h_0^2 + x_0^2} \sin \varphi. \end{aligned} \right\} \dots\dots\dots (3)$$

For the special case  $\varphi=0$ , *i.e.* when the oscillation is linear,

$$\left. \begin{aligned} A_x &= \frac{h_0}{h_0^2 + x_0^2} \left\{ \frac{h_1}{h_0} - \frac{2(x_0x_1 + h_0h_1)}{h_0^2 + x_0^2} \right\}, & \phi_x &= 0, \\ A_z &= \frac{h_0}{h_0^2 + x_0^2} \left\{ \frac{x_1}{x_0} - \frac{2(x_0x_1 + h_0h_1)}{h_0^2 + x_0^2} \right\}, & \phi_z &= 0, \end{aligned} \right\} \dots\dots\dots (4)$$

or

$$\left. \begin{aligned} \frac{A_x}{x_1} &= \frac{1}{1 + \xi^2} \left( a - \frac{2(\xi + a)}{1 + \xi^2} \right), & \phi_x &= 0, \\ \frac{A_z}{x^1} &= \frac{1}{1 + \xi^2} \left( 1 - \frac{2(\xi + a)}{1 + \xi^2} \right), & \phi_z &= 0, \end{aligned} \right\} \dots\dots\dots (5)$$

if we put  $h_0=1$ ,  $x_0=\xi$  and  $h_1/x_1=a$ .

$$\text{Hence,} \quad \frac{A_z}{A_x} = \frac{JZ_m}{JX_m} = \frac{(1 + \xi^2)a - 2(\xi + a)}{1 + \xi^2 - 2(\xi + a)} \dots\dots\dots (6)$$

This is greater or less than unity according as  $a >$  or  $< 1$ . Since  $\phi_x = \phi_z = 0$ , there is no difference of phase, neglecting the induction. If we take the induction into account,  $Z$ -component will probably lag behind  $X$ , though we are at present at a loss to carry out the calculation.

Again in the special case  $\varphi = \frac{\pi}{2}$ , *i.e.* when the current oscillates elliptically, with the axes of the ellipse horizontal and vertical respectively, we have

$$\left. \begin{aligned} \frac{A_x}{x} &= \frac{2\tilde{\xi}}{(1+\tilde{\xi}^2)^2} \sqrt{\left(\frac{\tilde{\xi}^2-1}{2\tilde{\xi}}\right)^2 a^2 + 1}, \\ \frac{A_z}{x} &= \frac{2\tilde{\xi}}{(1+\tilde{\xi}^2)^2} \sqrt{\left(\frac{\tilde{\xi}^2-1}{2\tilde{\xi}}\right)^2 + a^2}, \\ \tan \phi_x &= \frac{1-\tilde{\xi}^2}{2\tilde{\xi}} a, \\ \tan \phi_z &= \frac{2\tilde{\xi}}{\tilde{\xi}^2-1} a. \end{aligned} \right\} \dots\dots\dots (7)$$

It may be seen that

$$\frac{A_z}{A_x} = \frac{JZ_m}{JX_m} = \sqrt{\frac{(\tilde{\xi}^2-1)^2 + 4\tilde{\xi}^2 a}{(\tilde{\xi}^2-1)^2 a^2 + 4\tilde{\xi}^2}}, \dots\dots\dots (8)$$

which varies from  $1/a$  to  $a$ , and then from  $a$  to  $1/a$ , when  $\tilde{\xi}$  increases from 0 to 1 and 1 to  $\infty$ . The phase difference is given by

$$\tan(\phi_x - \phi_z) = \frac{a}{1-a^2} \cdot \frac{(1+\tilde{\xi}^2)^2}{2\tilde{\xi}(\tilde{\xi}^2-1)} \dots\dots\dots (9)$$

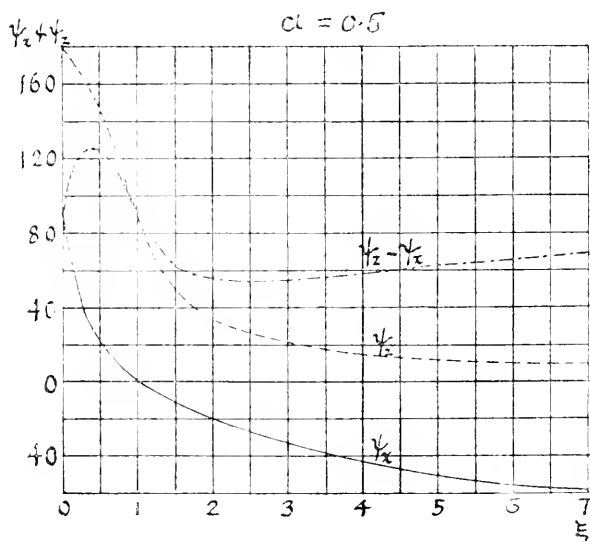
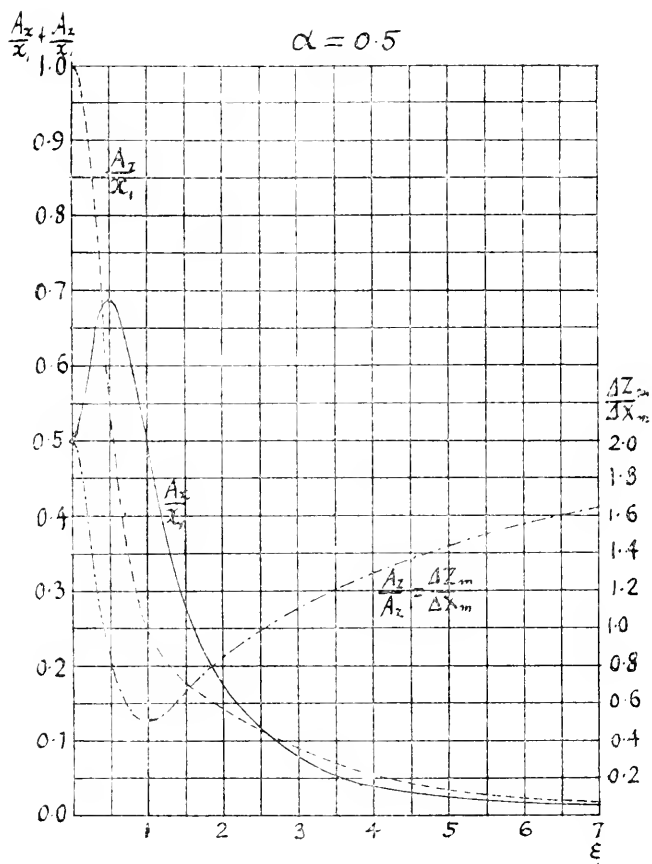
If  $\tilde{\xi} < 1$ , then  $\phi_x - \phi_z > \text{or} < 90^\circ$  according as  $a > \text{or} < 1$ .

If  $\tilde{\xi} > 1$ , then  $\phi_x - \phi_z < \text{or} > 90^\circ$  according as  $a > \text{or} < 1$ .

Thus we see in this case that the phase difference as well as the ratio of the amplitudes may assume different values according to the values of  $a$  and  $\tilde{\xi}$ . If the effect of the induced current be taken into account, these values will of course be altered considerably. Fig. 22 illustrates the variation of the amplitude ratio and phase difference as functions of  $\tilde{\xi}$  for a special case.

In the above discussion,  $i$  was considered constant. If it varies at the same time, the results will be more complicated, in some cases giving rise to a higher harmonic oscillation of the magnetic field. In the case treated in § 22, the external source of the disturbance was such as could be represented by the wave-like distribution of current in a *fixed* horizontal layer. If such current layer is disturbed into a wave motion simultaneous with the fluctuation of the intensity, each elementary current will be subjected to motion similar to that expressed by (1) of this paragraph. This motion will greatly modify the relations between the X- and Z-component waves discussed in the preceding paragraph as is suggested by the above simple example. It seems plausible

Fig. 22.



to consider that the difficulties met with in the preceding paragraph with regard to the phase relation may partly be accounted for by a similar *combination* of the motion and the variation in the intensity of the current. Such a combination is quite probable in view of the reciprocal action of the magnetic field on the conducting layer carrying the current. Though these points seem to suggest many interesting problems worth investigation, it will at present be rather too far fetched to introduce any further hypothesis.<sup>1)</sup>

25. The fact described in § 5, *g*) that two trains of waves with different periods sometimes appear simultaneously in the X- and Y-components respectively, may probably be explained by the combination of fluctuations in the direction as well as in the intensity of the current. Take the simplest case, when a linear current at a distance  $d$  from the point of observation A in its mean position, is fluctuating in its intensity as given by

$$i = i_0 \cos pt,$$

while it is oscillating stationarily about the position of equilibrium, in such a manner that it were always tangential to a string vibrating in a horizontal plane with its node at the foot of the perpendicular from A to its mean position. If the angle made by the current to its mean position at the time  $t$  be  $\alpha$ , then  $\tan \alpha$  will vary as  $C \cos(qt + \epsilon)$ , where  $C$  is the tangent of the maximum angle of inclination. If the mean position of the current be perpendicular to the meridian, the periodic variation of  $X$  and  $Y$  will be given by

$$dX = \frac{i_0}{d} \cos pt,$$

$$dY = \frac{i_0 C}{d} \cos pt \cos(qt + \epsilon).$$

Thus a "combination tone" will arise in the component parallel to the mean direction of the current. The effect of the induced current will probably enhance the "summation tone" in comparison with the "difference tone." If the oscillation is the

---

1) These points will be touched upon again later in § 28.

necessary result or cause of the fluctuation of the intensity,  $p$  must be equal to  $q$ , in which case the period of  $\Delta Y$  will be octave to that of  $\Delta X$ . This latter case was frequently observed, though not always.

The above consideration seems to explain the fact that the cases where the period of the X-waves is longer than that of Y are decidedly more frequent than the opposite cases, if we remember that the hypothetical current is generally inclined to the circle of latitude by an angle decidedly less than  $45^\circ$ . It is however strange to observe that the hourly distribution given in § 5 is rather conformable to the supposition of the "difference tone" being more conspicuous. This latter point requires further investigation.

Different facts remain still to be considered in the light of the above hypotheses, *i.e.* the dependency of the prevalent periods on the hours of occurrence, the rotatory character of the horizontal components, *etc.* We shall consider these points later, after having tried to ascertain the nature of the supposed atmospheric electric currents.

26. Thus far, we have tried to find some plausible explanations of the observed phenomena on the assumption of a system of fluctuating currents existing in the upper atmosphere, neither alluding to the possibility of such, nor giving hint as to the cause of the supposed fluctuations. It will be by far the more interesting physical problem to inquire into the origin of these remarkable periodic variations. Though we are not yet in a position to answer the question in any definite sense, it will not be quite out of place to say a few words on the subject, merely by way of suggesting many interesting problems regarding the electrical behaviour of the upper atmosphere.

The existence of a permanent system of atmospheric currents producing the remarkable diurnal variation of the terrestrial magnetism, first effectively elucidated by Schuster, may in these days be regarded as a universally accepted hypothesis and requires scarcely any further comment. It is the fluctuation of this current that we are here chiefly concerned with, and the



question is, why and in what manner these variations are produced. Schuster attributed the origin of the current to the induction caused by the daily oscillation of the upper atmosphere, which may be regarded as a conducting layer enveloping the entire earth. The first suggestion strongly appealing to us is that this diurnal wave may occasionally be accompanied by numerous trains of secondary waves with decidedly shorter periods compared with the daily or semidiurnal periods. An analogy is afforded in the case of the secondary undulations of oceanic tides.<sup>1)</sup> Whatever may be the cause, any mechanical wave motion produced in the upper atmosphere will produce corresponding waves of the induced current which will very much resemble the case discussed in § 23. Supposing such to be actually the case, let us see how far the assumption may be justified.

Taking first the case of the progressive waves, a serious difficulty confronting the assumption is to explain the enormous velocity of propagation as obtained in the preceding calculation which is far greater than the sound velocity, even if the upper atmosphere be entirely of hydrogen at the temperature of the stratosphere. The case would become more favorable only, if by any modification in the method of estimation, we could bring down the calculated velocity to a plausible range.

Another alternative hypothesis of the stationary wave, where the wave length is of the order of magnitude of the earth's meridian, must then be considered. If the atmospheric oscillation be purely mechanical and be one of the modes of the natural *tangential* vibration of the *whole* atmosphere, the period corresponding to such harmonics of low order can scarcely be of the order of a few minutes, as is most frequently observed, in so far as we can judge from the results of investigation<sup>2)</sup> on the phenomena of the daily variation of atmospheric pressure.

These considerations alone seem to lead us rather to

1) K. Honda, T. Teraoka, Y. Yoshida and D. Isitani, Secondary Undulations of Oceanic Tides, Journal of the Coll. of Sc., Imp. Univ., Tôkyô, **24**, 1908.

2) Rayleigh, Phil. Mag., 5<sup>th</sup> **29**, 1890, p. 173; M. Margules, Sitz. ber. d. kön. Akad. d. Wiss. z. Wien, **99**, 1890, p. 204, etc.; H. Lamb, Proc. Roy. Soc., A **84**, 1911, p. 551.

conviction, that if the fluctuations of the current be either of the kinds here considered, it is not merely due to the mechanical wave motion of the upper atmosphere. This leads the question towards the weakest side of our knowledge.

The natural period of the usual electrical oscillations cannot in any case be as long as several minutes, even if we take into account the effect of the upper atmospheric shell; nor can it be of such indefinite periods as actually observed.

Though it seems *so far* difficult to say anything definite about the physical cause which may produce the fluctuations in question, the existence of the fluctuations above considered seems to be suggested, on the other hand, by the phenomena of the aurora polaris. Firstly, the frequently observed auroral are vividly reminds us of our hypothesis of the diffused zonal current considered in § 23. According to the numerous descriptions of the phenomena, the luminosity seems to undergo different modes of variation, though we could find no record definitely stating a periodicity of a few minutes. Such a slow variation, even if present, would probably have eluded discovery by ordinary simple eye-observations, not equipped with special means for that purpose. A special investigation in this direction seems in any case desirable; for example a minute photometrical study of cinematographical records as obtained by Störmer.<sup>1)</sup> Again, among the numerous records of the auroral displays,<sup>2)</sup> we frequently meet with descriptions of peculiar bands of luminosity, running nearly perpendicular to the meridian and showing wave-like propagation mostly toward S. It is very probable that similar phenomena are of quite frequent, or rather of almost daily occurrence, although usually the intensity may be so weak that it rarely shows a luminosity strong enough to attract the attention of the naked eye. Indeed, it is well known that the characteristic "auroral lines" of spectra are almost invariably visible in different latitudes. If such bands of

1) C. Störmer, Videnskapsselskabets Skrifter, Math.-Naturv. Klasse, 1911, No. 17; Astrophys. Jour., **38**, 1913, p. 311; Bull. Soc. Astr. France, 1913, Nov.

2) E. E. Barnard, Observations of Aurora made at the Yerkes Obs., 1897-1902, Astrophys. Jour., **14**, 1902, p. 135. M. Brendel, Ueber das Nordlicht von 30. Juni, Met. Zs., 1908, p. 552.

luminosity correspond to the traces of the *horizontal* electric current, as Birkeland supposed,<sup>1)</sup> they remind us strongly of the hypothetical parallel currents considered above. It must be noticed that according to the calculation cited, the progressive motion must be S to N instead of N to S, in order to explain the observed phase relation of X- and Z-components. It might, however, be surmised that the motion of the current in the upper atmosphere is in many respects of opposite directions in the lower and higher latitudes, as is suggested by Schuster-Bezold's system of currents. A similar observation in a considerably high latitude will be in any case very desirable, especially with a reliable instrument for the vertical component.

27. As to the remarkable dependency of the periods of the most frequent waves on the hours of day, we may suggest first of all that it probably has some relation with the difference in the temperature as well as in the state of ionization of the upper atmosphere. According to Prof. Nagaoka,<sup>2)</sup> the thickness of the conducting layer in the atmosphere must also be decidedly greater during the day than in the night.

If the cause of the periodic fluctuation of the atmospheric current is to be sought in the purely *horizontal* oscillation of the atmosphere, the dependency of its periods on the hours of day is rather difficult to explain, even if we suppose the atmosphere consisting of different layers with remarkably different composition and temperatures.

Another, and probably the last possibility is that in the upper atmosphere there may occur a *vertical longitudinal* wave of limited extent, the period of which may sensibly depend on the effects of the solar radiations. That the vertical vibration of the atmosphere is possible, and may have a definite *natural period* depending on the sound velocity, has been fully

1) According to the recent investigations of Störmer, the auroral band is produced by the *vertical* inflow of *positive* corpuscles. If this be actually the case, the idea must be abandoned.

2) H. Nagaoka, Proc. Tōkyō Math.-Phys. Soc., 7, 1911, p. 103; Revue générale des Sciences pures et appliquées, 26, p. 570.

investigated by H. Lamb and also by Prof. S. Sano.<sup>1)</sup> Both authorities agree in the result that the period must be roughly of the order of *5 minutes*, if we assume a plane earth and take the ordinary value of the velocity of sound, which is assumed to be uniform throughout the atmosphere. According to S. Sano, the period is given by

$$T = \frac{4\pi c}{\gamma g}$$

where  $c$  is the velocity of sound and  $\gamma = 1.41$ . Since  $c = \sqrt{\gamma R\theta}$ , *i.e.* the period increases with the temperature, we must assume a lower temperature on the side of the upper atmosphere facing the sun than on the opposite side. This seems at first sight strange, but is in accordance with the fact that the diurnal variation of temperature in the upper layer shows a tendency to become opposite in phase compared with the lower layer<sup>2)</sup>; though the amplitude is of course small, a tendency is suspected, that it increases with height. The difficulty is to explain the actual *amount* of the difference of the characteristic periods, the night-wave being nearly twice as long as the day-waves. The absolute temperature must then be assumed nearly 4 times higher on the night side, if the difference of the periods is to be exclusively attributed to the difference of  $\theta$ . If the corpuscular radiation from the sun chiefly frequents the night side of our atmosphere, as is supported by different phenomena pertaining to aurora and magnetic storms, the effective temperature of that side of the atmosphere may be raised considerably by the presence of the additional kinetic energy of the free electrons. As to the increase of  $c$  due to the ionizations, no conclusive experimental evidence is yet afforded,<sup>3)</sup> especially for the highly rarefied state

1) H. Lamb, Proc. London Math. Soc., **2**] **7**, 1907, p. 122. S. Sano, Bull. of the Central Meteor. Obs., Japan, **2**, No. 2, 1913.

2) T. Reger, Arbeiten d. kön. preuss. aeronautischen Observatoriums bei Lindenberg, **8**, p. 229.

3) W. Küpper found a sensible increase of  $c$  for gases ionized by radiations of different kinds, Dissertation, Marburg, 1912; Ann. d. Phys. **[4]** **43**, 1914, p. 905. W. H. Westphal obtained, however, a negative result, Verh. d. deutsch. phys. Ges., 1914, p. 613. These results refer to gases at ordinary pressure.

of gases. In this respect, many interesting physical problems may be suggested which seem worth special consideration.

On the other hand, if a more or less limited portion of the atmosphere be subjected to the oscillation of vertical type, the period will surely depend on the extent of the area disturbed. According to a personal communication by Prof. Sano, such a mode is actually possible and the period will decrease with the area disturbed. At least, the periods shorter than five minutes may partly be explained in this way. The period of vertical vibration may, however, also depend on the modes of laminar structure of the atmosphere in the distribution of the temperatures and the wind velocities of the different layers. The inquiry in these directions involves many intricate problems for mathematical physicists, and may better be left for the specialists in these lines.

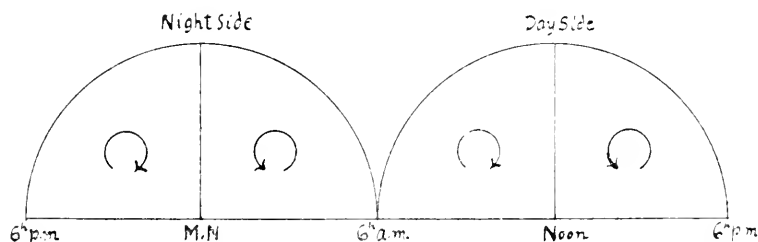
If the vertical vibration of the atmosphere be the actual cause of the magnetic pulsation as appears most probable, the investigations of the latter phenomena will in any case afford very valuable material for studying the actual physical conditions of the upper atmosphere, and may offer probably an unexpectedly wide field for new researches in different directions.

According to Prof. Sano, mechanical disturbances of any kind must gradually subside into a regular vertical natural vibration, which is comparatively slowly dissipated. This theoretical result is in harmony with the observed phenomena, *viz.*, the subsidence of an abrupt change of the terrestrial field into a train of regular damped waves, and also the peculiar persistent character of some trains. These points will be touched on once more in § 28.

28. Finally, let us consider the last crucial test of the different hypotheses, the peculiar behaviour of the *rotational* oscillation of the horizontal components. If we assume the observed sense of rotation for different hours, as generally applicable for the entire northern hemisphere, the distribution of the different senses of rotation in different hours will be roughly represented by the annexed figure (Fig. 23), where the semicircles

represent the hemispheres for day and night respectively. The distribution, expressed in other words, is such that when the periodic magnetic field is directed toward due south, the WE-component, just passing zero, is increasing toward the direction

Fig. 23.



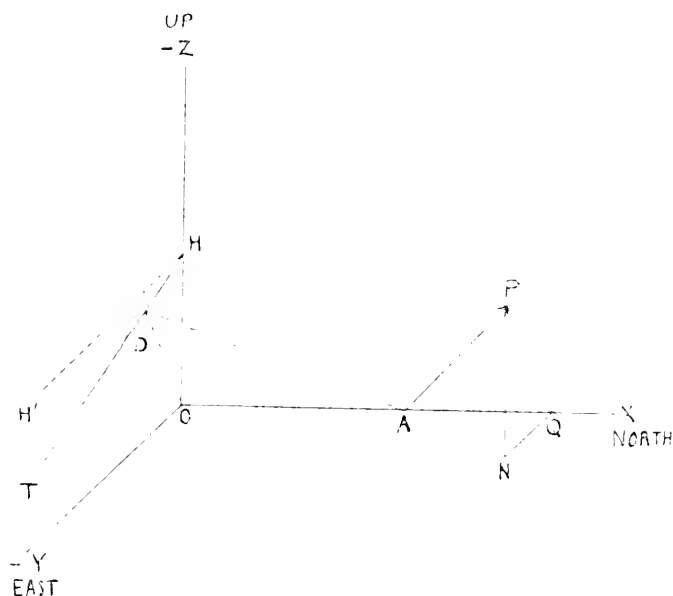
of the meridian at 6<sup>h</sup> a.m., or 6<sup>h</sup> p.m., for all points of a.m., or p.m. region respectively. A similar variation might have been produced, if there existed two sets of *horizontal* atmospheric oscillations corresponding to the zonal harmonics of the second order, the one having its axis at the earth's axis and the other in a direction passing through the equator at the meridians corresponding to 6<sup>h</sup> p.m. and 6<sup>h</sup> p.m.; the two component vibrations having a proper phase difference. Purely mechanical vibration of such a type must, however, have a more or less definite, and certainly much longer period, and is scarcely apt to explain the observed phenomena in the case of the most frequent short waves.

Another suggestion is that along the atmospheric current of more or less linear character, running near the place of observation, a sinuous motion is propagated, in which case the periodic disturbance may become rotatory and the sense of rotation will be opposite on both sides of the current. It seems to suffice, therefore, to assume a belt of current making no considerable angle with the meridian at 0<sup>h</sup> or 12<sup>h</sup> on which a sinuous motion is propagating with a proper velocity. The assumption is so far not utterly contradictory to the assumption of the circular current mentioned earlier, since the latter has

the pole in the morning hour, decidedly deviating from the earth's pole. But in this case the phase relation of  $JZ$  and  $JN$  must be opposite on both sides of the current which is never actually the case. If the above be the case, the magnetic waves will naturally be of progressive character.

Again, to explain the phenomena in question on the assumption of a progressive wave of the sort considered in § 23, it may probably suffice theoretically to consider two intersecting systems of waves propagated with proper velocities, though as a matter of fact, we have neither an evidence nor a physical ground for assuming the existence of such a complicated system of currents. The wave length of such waves must, however, be of the order of the earth circumference, in order to explain Fig. 23; hence the case is essentially similar to that considered at the outset of this paragraph.

Fig. 24.



Finally, we may suppose that the atmospheric electric current is *not purely horizontal* as was generally assumed in the above discussions, and also that the vertical component current is subjected to a periodic fluctuation with a proper phase relation

to that of the horizontal one; or less probably, to a rotatory oscillation of the kind considered in § 24, but in a horizontal elliptical orbit instead of the vertical one. These will probably remain the only admissible hypotheses, if the progressive nature of the magnetic waves be ultimately denied by the observations.

The simplest ideal case conceivable of this kind is that in which a linear current is subjected to a *see-saw motion in the vertical plane*, about its horizontal mean position. Referring to the annexed figure,<sup>1)</sup> where  $xy$ -plane corresponds to the earth's surface, let  $HH'$  be the mean position of the current  $i$ , at the height  $h$ , and let it be vibrating about its mean position in the vertical  $yz$ -plane, as if it were a tangent to a string subjected to a stationary vibration, at its node at  $H$ . Denote the frequency of vibration by  $\frac{p}{2\pi}$ .  $A$  is the point of observation at a distance  $x$  from the origin, and  $AD$  the perpendicular from it to the current  $HT$  at time  $t$ . If  $AP$  represents the magnetic field at  $A$  due to the current at  $t$ , it is perpendicular to  $AD$  in the plane perpendicular to  $HT$  and of the magnitude

$$\frac{2i}{AD} = \frac{2i}{\sqrt{x^2 + h^2 \cos^2 \theta}} ,$$

if we denote by  $\theta$  the inclination of  $HT$  to  $HH'$ . Let  $Q$  and  $N$  be the feet of the perpendiculars from  $P$  to  $Ox$  and  $xy$ -plane respectively. Then, denoting the angle  $\angle OAD$  by  $\phi$ ,

$$AQ = X = AP \sin \phi,$$

$$QN = -Y = PN \sin \theta,$$

$$PQ = -Z = PN \cos \theta,$$

since the angle  $\angle NPQ = \theta$ . But  $PN = AP \cos \phi$  and  $\operatorname{tg} \phi = \frac{h \cos \theta}{x}$ .

Hence, we have for the fields of the three components:

$$X = \frac{2ih \cos \theta}{x^2 + h^2 \cos^2 \theta} \quad \text{for N-component,}$$

$$-Y = \frac{2ix \sin \theta}{x^2 + h^2 \cos^2 \theta} \quad \text{for E-component,}$$

$$-Z = \frac{2ix \cos \theta}{x^2 + h^2 \cos^2 \theta} \quad \text{for Upward-component.}$$

1) The coordinates axes are chosen lefthanded to correspond to our initial convention.



According to our assumption,  $\theta$  is given by

$$\operatorname{tg} \theta = C \cos(pt + \varphi).$$

If  $C$  is small and we neglect the small quantities of the second order against unity, we may put  $\cos \theta \approx 1$  and  $\sin \theta \approx C \cos(pt + \varphi)$ .

Hence

$$X = \frac{2ih}{x^2 + h^2}; \quad Y = -\frac{2ix}{x^2 + h^2} C \cos(pt + \varphi); \quad Z = -\frac{2ix}{x^2 + h^2}.$$

Thus, the  $Y$ -component only will be sensibly affected while the others remain constant, if  $i$  be considered constant. If  $i$  be variable and given by

$$i = i_0 + i_1 \cos qt,$$

where  $i_0$  and  $i_1$  are constants and  $i_1$  is small compared with  $i_0$ , the periodic parts of the three components will be given by

$$\begin{aligned} \Delta X &= \frac{2i_1 h}{x^2 + h^2} \cos qt, \\ \Delta Y &= -\frac{2i_1 x C}{x^2 + h^2} \cos(pt + \varphi), \\ \Delta Z &= -\frac{2i_1 x}{x^2 + h^2} \cos qt, \end{aligned}$$

neglecting the small quantities of the second order in  $\Delta Y$ . If  $p=q$ , as may be the case when the see-saw motion is the direct cause or result of the fluctuation of the current and moreover if  $\varphi \neq 0$ , we will have a rotatory motion of the kind desired. Besides, we notice that the sense of rotation is opposite on both sides of the  $yz$ -plane. The relation of  $\Delta X$  and  $\Delta Y$  is just the same as in § 22 a), as is evident.  $\Delta Z$  must be of the opposite sign on both sides of the current. The results of observations show, however, that the phase relation between  $\Delta X$  and  $\Delta Z$  is generally the same all through,  $\Delta Z$  never being ahead of  $\Delta X$ . Hence the maximum intensity of the current in question can not be running largely in the meridional direction, but probably more or less near the equatorial zone, since otherwise we should expect that in some hours  $\Delta Z$  may run in advance of  $\Delta X$ . To reconcile the present case with the result shown in Fig. 23, it will be plausible to assume that in passing along the four

quadrants  $0^h-6^h$   $6^h-12^h$   $12^h-18^h$   $18^h-24^h$  the phase angle differs successively by  $\pi$ , if  $i_0$  be of the same sign throughout: or  $i_0$  changes the sign alternatively, if  $\varphi$  remains constant. It we are to identify  $i_0$  with the equatorial portion of the circular current assumed in § 19, then it will suffice to suppose that a *portion* of the circular belt or ring carrying the current is subjected to a *radial* vibration, as if it were a portion of the ring carrying out a *dilatatory* vibration in such a way that the amplitude is given by  $\cos^2\lambda$  say, where  $\lambda$  is the longitude counted from noon. The fluctuation of the intensity must be considered as keeping pace with the vibration and the period must be different for day and night.

Though the above solution is by no means unique, yet it may at least serve as a provisional explanation as far as the phenomena of rotatory pulsation are concerned. It is, moreover, not contradictory to the principal facts of observation already enumerated: *viz.*, not irreconcilable with the mode of the daily variation of the azimuth of the horizontal components, since the circular current assumed may be considered to have its maximum intensity always near the equator; and again not inconsistent with the observed amplitude ratio and phase relation of  $\mathcal{JZ}$  and  $\mathcal{JX}$ , since the see-saw motion chiefly affects  $\mathcal{JY}$ , and the discussions on these relations given earlier hold good here also without any essential modification.

According to van Bemmeln, the ratio  $\mathcal{JZ}/\mathcal{JX}$  at Batavia seems to be invariably of insensible magnitudes. This fact is in harmony with the above assumption that the maximum current is near the equator. On a theoretical ground, this seems also admissible if we may attribute the origin of the disturbing current to the vertical motion of the atmosphere, since general planetary circulation of the whole atmosphere must be in any case vertical in these regions, where the horizontal intensity of the magnetic field is also greatest.

29. The above taken as granted, it seems plausible to assume next that the *impulse* causing the vertical vibration, if not solely mechanical, is to be attributed to the reciprocal action

of the magnetic field on the change of the current,<sup>1)</sup> assuming the current already caused by other agents. In § 19 we have suggested that the zonal part of the atmospheric current seems to be more liable to the fluctuations than the part running in the meridional direction. This is in some measure favourable to the hypothesis.

If the mechanical vibration of the atmosphere be once started, the periodic fluctuation of current naturally results on account of the induction due to the general terrestrial field. The intensity of the induced current will be greatest at the equator for a given amplitude of the oscillation.

The cause of the initial impulsive increase of the current may on one hand be considered as the result of the motion of the atmosphere brought about in a purely mechanical way, for example, an abrupt advent of the vertical flow of the upper atmosphere caused by the release of some instability of equilibrium; or we may conceive a limited portion of the atmosphere excited to a vigorous vertical current, as in the centre of a cyclone, caused as a secondary disturbance accompanying the daily exchange of air between the day and night hemispheres.

On the other hand, the abrupt increase of current may also be attributed to an external agent, for example, a sudden increase of the conductivity of air caused by the inflow of the corpuscular radiation from the sun.<sup>2)</sup>

Among the above two possibilities, the latter is more plausible, being in accordance with the commonly accepted view as regards the origin of magnetic disturbances, which is strongly supported by the intimate relation existing between the solar activity and the disturbances in general. Fig. 10 is also favourable to this hypothesis. The former is rather doubtful.

1) In view of this consideration, an interesting physical problem presents itself: Consider a current passing through highly rarefied gases, acted upon by an external magnetic field; will the gases really flow *as a whole* as Fleming's rule specifies for a solid conductor? As far as we are aware, the answer is not yet given either experimentally or theoretically, especially for such a case as is analogous to the atmospheric currents.

2) A. Schuster concluded on the basis of energy consideration that the E.M.F. of the current causing magnetic disturbances is to be attributed to the motion of the atmosphere, the sun's radiation serving only as an agent increasing the conductivity.

since it is an open question whether in the higher part of our atmosphere there may occur any remarkable vertical *convection*, as is the case in the troposphere. At any rate, the fact that an abrupt increase of the general field is most frequently accompanied by a train of remarkable pulsations, is in harmony with the above idea that the increase of the current is associated with the increase of the vertical impulsive motion of the atmosphere which subsides into a vertical natural vibration. The characteristic disturbance of this type occurs as a rule near midnight. On the other hand, examples are by no means rare, especially in the evening, where an abrupt increase of the horizontal component occurs, but not at all accompanied by a train of waves. How is the fact to be explained? It may at first be suggested that in this case the abrupt increase of the current takes place in the direction of the general terrestrial field; but as a matter of fact, the increment of the Y-component in such a case is not generally of a different order of magnitude compared with that of the X- component. Another possible alternative is that in the hours which are near the boundary between the day and night hemispheres, the regular vertical vibration of the atmosphere is not so easy as at midnight. The latter assumption seems in some measure plausible, if we consider very probable heterogeneity of the atmosphere in that region forming the transition stage of the illuminated and non-illuminated halves. The minimum of the frequency of pulsations of all periods falls actually in the evening hours (Fig. 8). The morning hours are not necessarily in the same condition as the evening hours. In the former, the atmosphere is being rapidly heated up and ionized, but on the night side of the boundary a dormant homogeneity of the night-atmosphere may probably prevail; whereas in the latter, the gases are cooling down and the ions recombining, and gradually passing into the nightly condition. In the morning, the transition may therefore be abrupt and the area of the heterogeneous atmosphere comparatively small, while in the evening the heterogeneity may extend to a considerable area of the earth's surface.

Again, cases are quite common where remarkable trains of waves occur without any general swelling of the horizontal component. Among such trains, we may distinguish two types, *viz.*, those with the abrupt beginning and those gradually increasing in amplitudes. The former, which is most frequent during night, may probably be explained by a transient increase of the atmospheric current with a duration comparable with, or shorter than the natural period of the atmospheric oscillation. Indeed, the first wave of the train of this type is often sensibly shorter than the following regular waves. The latter class, which is generally the case with the shorter day-waves and also sometime with the longer night-waves, may be caused either by the mechanical disturbance of the atmosphere propagated from a remote region, or by some different agents. Among other conceivable causes of the vertical vibration of the upper atmosphere, we may cite the instability of the discontinuous horizontal motion of the higher layers. That the upper layer has a considerable angular velocity with respect to the earth's surface is well known from the observation of the "illuminated night cloud." It is then probable that a favorable vertical distribution of density may cause a remarkable wave motion of different types. The gravitational wave, as occurs in the case of an incompressible fluid, will not answer our purpose. But it is more than probable that a radial or vertical expansional wave which is the most persistent type, is excited in this way—a case somewhat analogous to the excitation of the organ pipe by the stream of air running along the loop of the vibrating air column. If the upper atmosphere be arranged in different layers with different temperatures and different general wind velocities, as is the case in the troposphere, different periods may occur at the same time. The irregularities of the pulsations during day time might well have been produced in this way, if we consider that the laminar structure may be enhanced in some way or other, by the influence of solar radiation. Beside the thermal effect, light pressure may also play some sensible

rôle in this respect, since it acts in differentiating the gases with different absorbing powers and molecular sizes.<sup>1)</sup>

Again, if there be present any sensible fluctuation of the solar radiation<sup>2)</sup> with a short duration, the thermal effect, and also the radiation pressure in some measure, may contribute to the initiation, if not the direct excitation of the vertical motion of the upper atmosphere. The remarkable irregularities of the day-waves may partly be accounted for in this way.<sup>3)</sup>

As to the origin of the magnetic waves with the periods longer than  $10^m$ , we may probably suggest the slow atmospheric waves possible in the case when two layers with different temperatures are superposed.<sup>4)</sup>

The fact described in § 17, that the hourly distribution of the senses of rotation of the disturbing magnetic vectors are quite different for the short waves and the long undulations, requires an explanation. It may only be suggested for the present that the difference is in any case due to the difference in the modes of atmospheric free vibration. Any further discussion must be postponed till the nature of the vibrations of the atmosphere has been more fully investigated from the theoretical side, especially for a *spherical* atmosphere.

---

1) Adopting Delye's approximate formula for an *absorbing* sphere (Ann. d. Phys., [4] **30**, 1909, p. 117), the pressure of the light wave with the wave length  $\lambda$  on a sphere of radius  $a$  may be put

$$1.83 \cdot \frac{2\pi a}{\lambda} \cdot \pi a^2 \frac{S}{c},$$

where  $S$  is the energy of the radiation per sec. per  $\text{cm}^2$ . Assuming  $a=10^{-8}$ ,  $\lambda=5 \times 10^{-5}$  and  $S = \frac{3}{60} \times 4 \cdot 10^7$ , we obtain a pressure  $0.48 \times 10^{-22}$  dynes. Taking the mass of the sphere as  $1.6 \times 10^{-24}$  gr. for a hydrogen atom, we obtain an acceleration of 30 cm/sec. The mean free path at the pressure of 0.007 mm. being about 1.76 cm, the mean velocity may be estimated to be of the order of 5.1 cm/sec. The path traversed is therefore only 184 m. per hour. This is probably too small to answer our purpose. But if we take a "Dipole" instead of the absorbing sphere, the value of the pressure may in some cases be estimated to be decidedly greater. Near 200 km. from the earth's surface, the pressure will vary rapidly with the height; in the higher layer, the path traversed by molecules or atoms may be enormously greater than the above estimation.

2) Together with the back-radiation from the earth.

3) The *corpuscular* radiation being deviated by the terrestrial field, will not be confined to the day hemisphere, or rather prefers the night side. The fluctuation of this radiation may be considered to be of the type considered in p. 79.

4) H. Lamb, Proc. R.S., A **84** 1911, p. 551.

30. From all we have discussed at length in the preceding paragraphs, we can as yet draw no convincing conclusion regarding the actual mechanism producing the magnetic pulsations in question. Many things, indeed, turn on the crucial observation regarding the universal *simultaneity* of the periodic phenomena. If it be *proved* ultimately beyond doubt as seems probable, there remain only those hypotheses at disposal, which lead to the simultaneous occurrence of the phenomena for an area of considerable extent. In that case, the magnetic waves may probably be explained by the *combination of periodic fluctuations, in intensity as well as in position and inclination of the atmospheric current*, which is then to be considered of rather diffused, but not of linear character, having the maximum intensity near the equator. The origin of these fluctuations might then very probably be sought in the *vertical stationary oscillation* of limited portions of the upper atmosphere accompanying the diurnal oscillation of the entire atmosphere.<sup>1)</sup>

At any rate, it must be admitted that the present results of observation refer to a single station, and the observations are far from being complete. A further study of the allied phenomena, especially the simultaneous observations in at least *three* stations, sufficiently apart from each other, will be desirable. The results will not fail to advance our knowledge on the nature of the atmospheric current of which we have at present only a very vague idea. The interest attached to the problem at hand is by no means confined to the limited subject of terrestrial magnetism. The phenomena have a much wider bearing than at first sight appears, on various interesting problems in different branches of physics, for examples those regarding solar physics, meteorology and also especially those regarding the electrical and mechanical behaviours of highly rarefied gases under the action of different kinds of radiation.

In conclusion, the author wishes to express his sincerest

---

1) In this case, however, the phenomena of the propagating auroral bands accompanied with no corresponding magnetic waves, become rather incomprehensible and throw some doubt on Birkeland's original conception pertaining to the nature of the luminous band.

thanks to Prof. A. Tanakadate, under whose supervision the entire work was carried out, for his kind guidance throughout the course of the investigations. Most cordial thanks are also due to Prof. H. Nagaoka and to Prof. S. Sano, for the interest shown in the investigations and for many valuable suggestions and instructions given. Last, but not least, we feel very much indebted to Prof. I. Ijima, the Director of the Marine Biological Laboratory, for his kindness and generosity in affording lodging and many other conveniences to the observers resident in Misaki, for which the best thanks of all the participators in the present work are due.

### Summary of the Results of Investigations.

1. The period of the magnetic pulsations has no sharply defined value, varying from about 20 seconds to nearly 1 hour. Nor is it exactly constant even in a coherent train.

2. During the day time, waves of 0.5–1 minute periods predominate, whereas during the night hours longer periods 1.5–2.5 minutes are most frequent.

3. A periodicity of 25–30 days is suspected in the daily frequency of the pulsations.

4. The vertical component of the waves is a reduced reproduction of the NS-component except the phase retardation. The shorter the period, the more remarkable is the reduction of the amplitude as well as the phase retardation.

5. The azimuth of the linearly pulsating magnetic field undergoes a remarkable diurnal variation, showing maximum deviations from the meridian a few hours before noon and midnight.

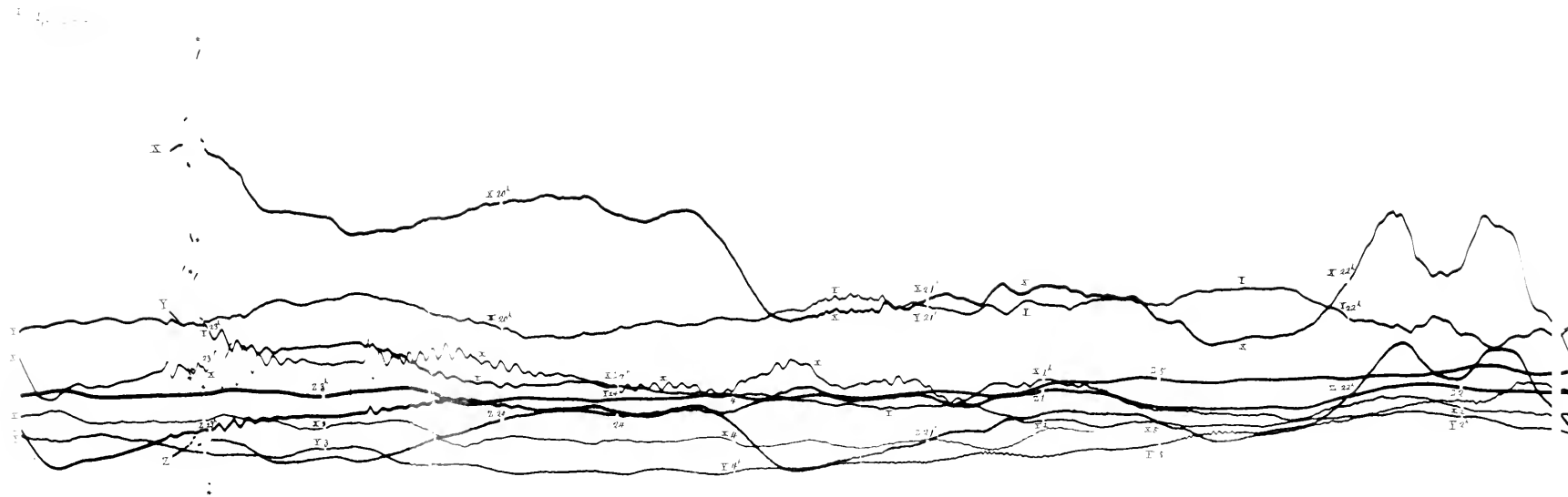
6. The disturbing field is generally more or less rotatory. The sense of rotation shows a semidiurnal variation. The clockwise rotation is most frequent during the hours between sunrise and noon, as well as between sunset and midnight, while the opposite rotation falls most frequently in the remaining hours.



7. The observed results may probably be explained by the fluctuations of the horizontal electric current existing in the upper atmosphere, and causing the diurnal variation of the terrestrial magnetism.

8. Two diverging lines of theoretical considerations intended for the explanation of the phenomena in question, are given: the one based on the assumption of the *simultaneity* of the phenomena in a wide area, and the other on the assumption of *a progressive nature* of the pulsations, though some evidences at hand seems to speak rather strongly against the latter assumption. The results of the discussions turn out rather favourable for the hypothesis of simultaneous disturbances than for that of progressive waves. If the simultaneity be universally established, the phenomena may probably be accounted for by the fluctuation of the atmospheric current, in its *intensity* as well as in its *location*. The fluctuation must then very probably be attributed to the more or less *vertical oscillation* of limited portions of the upper atmosphere. If such be actually the case, we have in the phenomena of the magnetic pulsations a very valuable clue for studying the physical conditions of the upper atmosphere unattainable by the usual means, and then, it may be hoped, for following the hourly or daily changes occurring in the remotest part of our atmosphere.





Light record on a comparatively calm day, with character of long waves in midnight and short waves in the morning. April 4, 1911. Reduced to  $\frac{1}{2}$  original size.



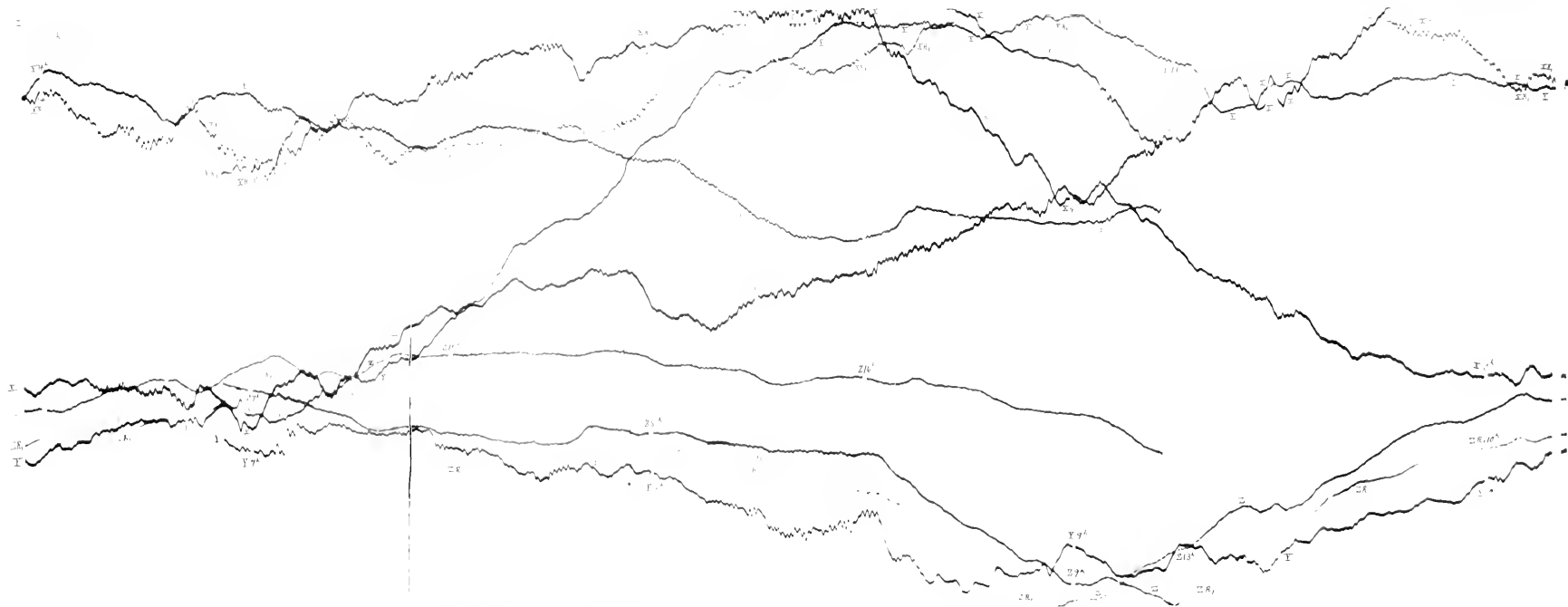
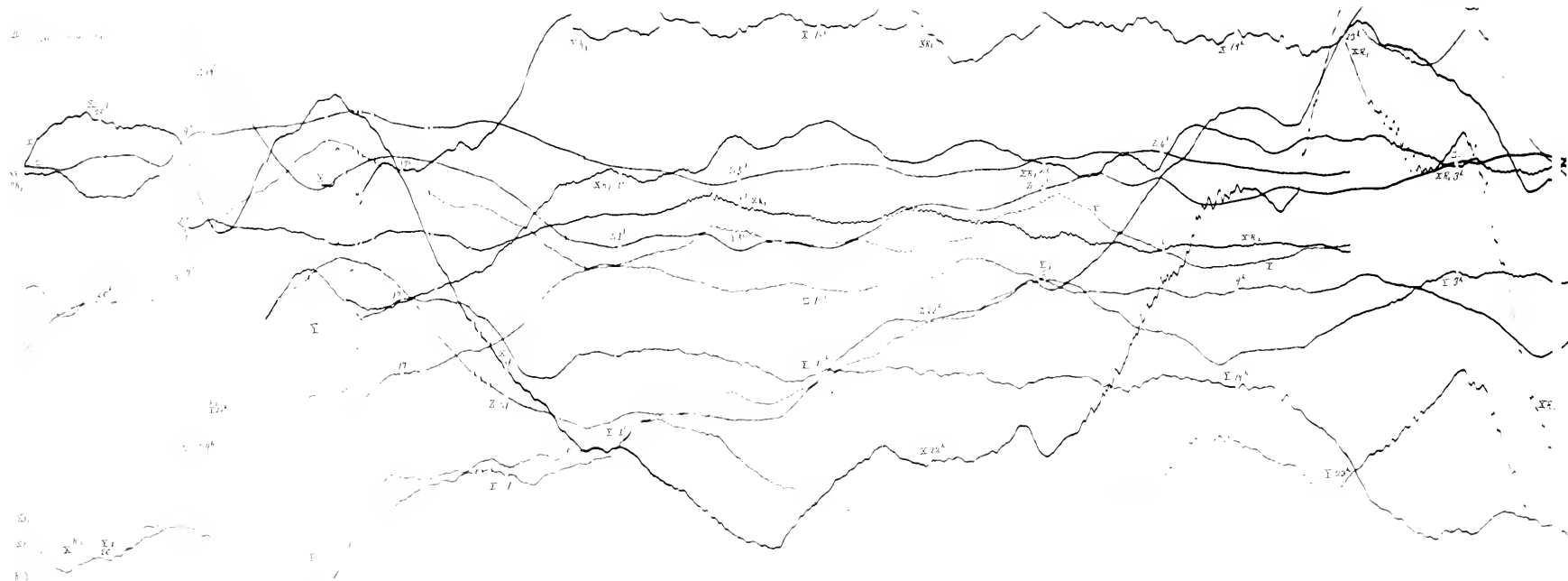


Fig. 1. Geologic cross-section of the T. T. Road, showing the relationship of the T. T. Road to the T. T. Road.





Detailed day. Regular long wave character but throughout not conspicuous, except of the remarkable disturbance of the general field. Note the morning trains of short waves, similar trains not occurring in the evening. (Jan. 24, 1912, 10.30 to 11.00 a.m.)



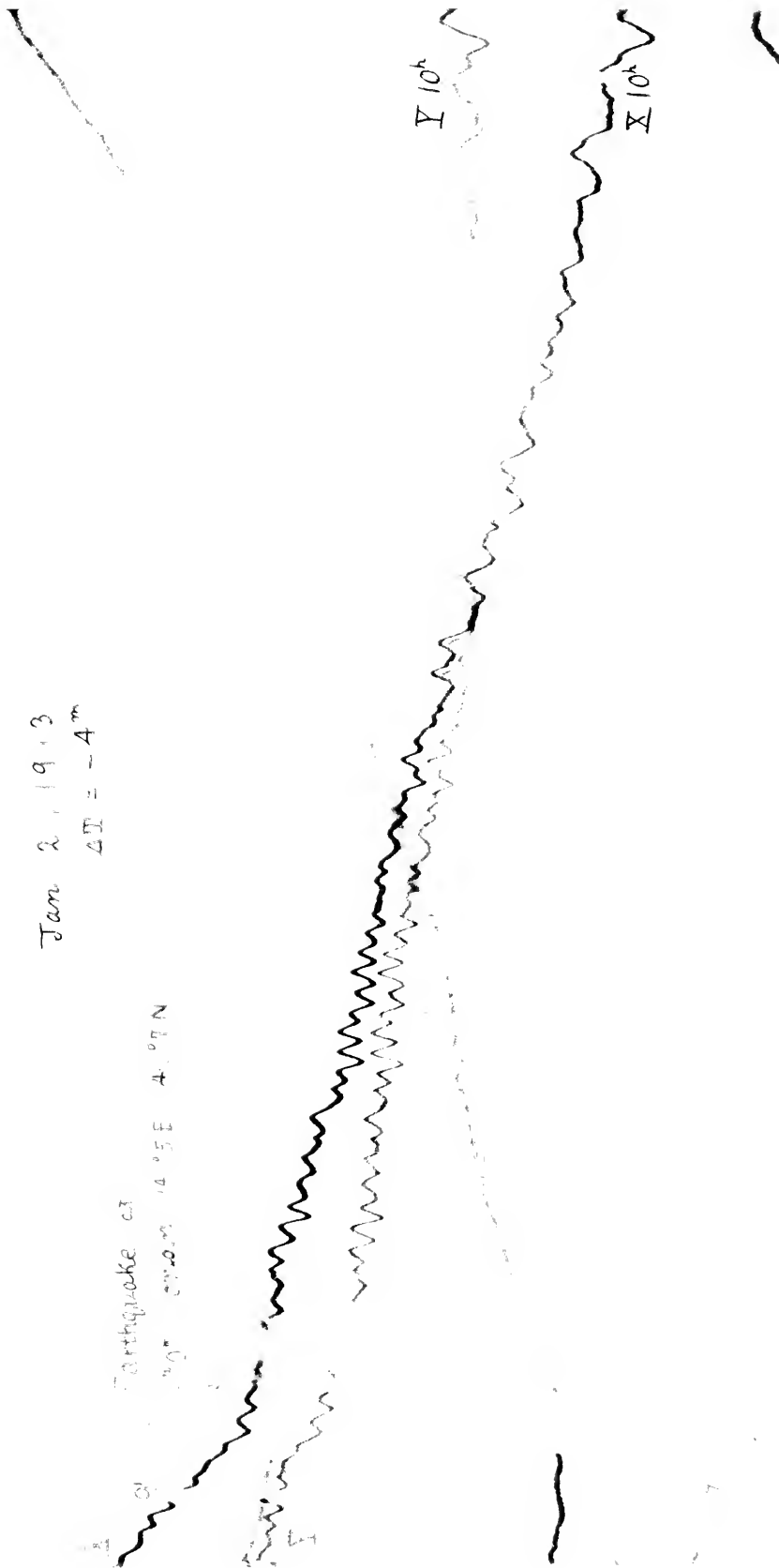






Jan 2, 1913  
 $\Delta T = -4^m$

Earthquake at  
 14.00 54.00 14.05 E 4.07 N



Note the approximate parallelism between X and Y. Record of a local earthquake indicated at 9 a.m. (Natural size).



## ERRATA.

p. 1, *For* **Hadime** **IKEUTI** *read* **Hazime** **IKEUT.**

p. 5, eighth line from bottom. *For* **outer** *read* **inner.**

„ seventh line from bottom. *For* **inner** *read* **outer.**

p. 10, fourteenth line from top, *For*  $c = \frac{\pi r_o}{1}$  *read*  $c = \frac{\pi r_o^2}{1}$

p. 12, eighth line from top, *For* **numbar** *read* **number.**



## On the Photographic Action of $\alpha$ , $\beta$ and $\gamma$ Rays emitted from Radioactive Substances.

By

**Suekichi KINOSHITA**, *Rigakuhakushi.*

and

**Hadime IKEUTI**, *Rigakushi.*

---

*With 5 Plates.*

---

1. *Introduction.* In 1909 one of the writers<sup>1)</sup> showed that whenever an  $\alpha$  particle strikes a grain of silver halide in the sensitive film of photographic plates, that grain becomes subsequently capable of development. It was also shown that this is the case throughout the whole range of  $\alpha$  rays, no matter what may be the quality of the plate. It is remarkable that the behaviour of the photographic plate regarding this phenomenon should obey such a simple law, when we take into consideration its complex behaviour with regard to light.

From the atomistic point of view, on the other hand, the above result is also highly interesting, as it affords a third independent method of recording the emission of a single  $\alpha$  particle, in addition to the electrical method devised by Rutherford and Geiger<sup>2)</sup>, and the scintillation method first systematically studied by Regener<sup>3)</sup>.

In the light of the above investigation, it was to be anticipated that if  $\alpha$  particles were projected tangentially on a photographic plate, the halide grains encountered by each  $\alpha$  particle would on development appear in a train. This effect

---

1) S. Kinoshita, Proc. Roy. Soc. A, **83** (1910), p. 432.

2) E. Rutherford and H. Geiger, Proc. Roy. Soc. A, **81** (1908), p. 141.

3) E. Regener, Verh. d. D. Phys. Ges. **10** (1908), pp. 78 and 351.

was examined first by Reinganum<sup>1)</sup>. On a photograph obtained in this way, silver grains were found arranged on distinct lines, showing themselves as the  $\alpha$  ray tracks. He also found that some of the tracks showed the effect of scattering. Experiments on this subject were later made in detail by Michl<sup>2)</sup> and by Mayer<sup>3)</sup>. Some microphotographs of the  $\alpha$  ray tracks showing deflexions were obtained by Walmsley and Makower<sup>4)</sup>.

For the last three years, we have been engaged in devising some simple methods of obtaining radial  $\alpha$  ray tracks and making some investigations upon them. The present paper contains the main results in this line of investigation, most of which appeared separately in other publications<sup>5)</sup>.

2. *Methods of obtaining radial  $\alpha$  ray tracks.* In investigating the photographic traces of  $\alpha$  rays it was thought most advantageous to work with the smallest possible source of the rays. For, if a point source be established and placed on a photographic plate, the expelled  $\alpha$  particles will leave on it a set of radial traces, which can be followed with greater ease and certainty<sup>6)</sup>.

The source which we first utilized was a fine needle point coated with a trace of active deposit of radium<sup>7)</sup>. This was prepared by lightly rubbing the point on a small ball of iron which had previously been exposed to a few millicuries of radium emanation. By bringing the needle in contact with a photographic plate, a part of the active deposit was detached from the needle and left on the plate at the point of contact. Leaving the plate for a certain time to allow a sufficient number of  $\alpha$  particles

1) M. Reinganum, Phys. Zeits. **12** (1911), p. 1076; Verh. d. D. Phys. Ges. **13** (1911), p. 848.

2) W. Michl, Akad. Wiss. Wien. Ber. **121**, 2a, (1912), p. 1431.

3) F. Mayer, Ann. d. Phys. **41** (1913), p. 931.

4) H. P. Walmsley and W. Makower, Proc. Phys. Soc. **26** (1914), p. 261.

5) S. Kinoshita and H. Ikeuti, Proc. Tokyo Math.-Phys. Soc. **7** (1914), p. 360; also Phil. Mag. **29** (1915), p. 420; H. Ikeuti, Phil. Mag. **32** (1916), p. 129; Proc. Tokyo Math.-Phys. Soc. **8** (1916), p. 465.

6) In the first publication, we have referred to the paper of Michl of which we learnt through the Beiblätter z. d. Ann. d. Phys. and the Science Abstracts, as the number of the Wien. Ber. containing the original paper could at that time not be found in our Library. In these reviews nothing was mentioned of the method by which  $\alpha$  ray tracks had been obtained. When we obtained the original paper afterwards, we found that the method employed by him had, in some ways, been similar to that of ours. However, his lines of investigation were different from ours.

7) For the case of polonium and of active deposits of thorium, R. R. Sahni's paper in Phil. Mag. **29** (1915), p. 831 may be referred to.



to emit, it was developed when a fine spot became visible to the naked eye. On examining the plate under a microscope, the said spot was found to consist of a multitude of separate trails of silver grains running radially from a common centre.

In the photographs taken in this way, however, there is around the centre a dark area, which is no doubt the portion where the active needle touched the plate during the above said process. In this case, the radial tracks do not emerge at the centre but at the rim of the dark area. Since the tip of the needle had the shape of a truncated cone terminating in a flat section of about  $10\mu$  in diameter, it was impossible to obtain by this method a photograph showing no central dark area. Still, this method was found useful when, as reference will be made later, deflexions of  $\alpha$  ray tracks had to be investigated.

Several trials were made to obtain photographs with nuclei as small as possible. When an iron ball coated with the active deposit was held above a photographic plate and knocked with a hammer or the like, some fine dust particles adhering to the iron ball seemed to be set free by the shock and to settle down on the plate, becoming thus the sources of the  $\alpha$  radiations. On developing the plate several spots appeared and some of them were found to possess nuclei whose linear dimensions are very small compared with the length of the  $\alpha$  ray track. The spots themselves were so small that they were hardly detected by the naked eye.

To obtain a large number of these spots, it was found effective to strike the photographic plate directly with the active iron ball on the film side. To illustrate the general feature of the photographs obtained in this way, one of the plates is reproduced in fig. 1, enlarged 120 diameters. The *irregular* dark areas seen in this figure are the spots where the plate was struck by the iron ball. Around these areas, there can be seen several circular spots, each of which consists of a set of  $\alpha$  ray tracks running radially from a common centre.

It may be remarked that, in a photograph in which a large number of  $\alpha$  ray tracks radiate from a common centre, each trail

does not appear distinct from the others along the whole length, but, in the vicinity of the centre, comes very close to or overlaps the neighbouring ones, even when the radiant nucleus is practically a point. This effect also gives rise to a dark area at the centre, which has no definite shape. The dimensions of the dark area vary of course with the number of the trails.

3. *Two different types of radial  $\alpha$  ray tracks.* As microscopic examinations at once show, the trails of grains may, in general, be divided into two different types.

In the first type, the trails emerge directly at the centre or, in case when the dark nucleus is present, at the rim of it. Consequently, when a set of homogeneous  $\alpha$  rays have been utilized, all the tracks terminate very nearly at the circumference of a circle drawn around the centre, and present themselves as a halo (figs. 2-8), resembling the pleochroic halo seen in minerals such as biotite, and investigated in detail by Joly<sup>1)</sup>.

Without question, the radial tracks do not all lie on planes parallel to the surface of the emulsion film, and as can be traced by focussing the microscope, some of them are running oblique to the surface. Since the film on ordinary photographic plates has a thickness equivalent to only about two centimetres of air in stopping  $\alpha$  rays, the photographic halo obtained on these plates can never be that of a complete sphere.

The trails belonging to the second type spread out around the centre over a wide region of no definite boundary, as can be seen in fig. 9, which is reproduced in the same magnification as the haloes in figs. 2-8. In this case, most trails are found to have their seat within the uppermost layer of the film, showing that they are the tracks of the  $\alpha$  particles projected tangentially to the surface of the film from the part of the source just above the surface. At first sight, some of the trails seem to be much longer than those constituting the haloes. Closer inspection, however, shows that this is only apparent and that each of them consists of two or more elementary trails following one another in succession.

---

1) J. Joly, Phil. Mag. **13** (1907), p. 381; **19** (1910), p. 327; J. Joly and A. L. Fletcher, Phil. Mag. **19** (1910), p. 630.

4. *Haloës due to radium C.* These can be obtained by utilizing as the source of  $\alpha$  rays the active deposit of radium, in which radium A has already disappeared. Figs. 2-4 are the microphotographs of these haloës, enlarged 500 diameters. It will be of interest to see the different stages of formation. In the halo in fig. 2 about 45 tracks are to be seen, this being of course the number of the tracks on a plane focussed in reproducing the microphotograph and forming therefore only a small fraction of the total. The haloës in figs. 3 and 4 are seen to contain about 70 and 120 tracks respectively.

The ends of the tracks constituting a halo do not lie strictly on a circle owing to the difference in the struggling of the rays through the medium. We have therefore taken as the radius of the halo the radius of the circle drawn so as to pass through the ends of most of the far reaching tracks. The radii of the haloës determined in this way vary slightly, but their smallest limit is found to be  $52\ \mu$ . Since, on the other hand, isolated tracks of this length are found in such photographs as fig. 9, this may be taken as the range of the  $\alpha$  rays from radium C in the substance, so that the radiant nuclei of these haloës must be very small.

5. *Haloës due to radium A and radium C.* To obtain haloës of this kind, we have exposed an iron ball to radium emanation for a few minutes and performed the above stated process as quickly as possible. These haloës are reproduced in figs. 5-8, in the same magnification as before. They indicate that the tracks of a set of homogeneous  $\alpha$  rays from radium A give rise to another concentric circle inside that due to radium C, as in the case of the pleochroic halo.

It will be seen that in fig. 5 the outer circle is more conspicuous than the inner one, while with fig. 6 the reverse is the case. Which of the circles comes out more conspicuously depends upon in what proportion radium A and radium C have been mixed in the source utilized.

The inner circle is in each case smaller than the outer by  $16\ \mu$  in radius. Thus the ratio of the ranges in the substance of the two  $\alpha$  rays becomes  $(52-16):52$  or  $.69$ , which is the same as its value

in air. According to Marsden and Richardson<sup>1</sup>, the above ratio for silver is much higher, amounting to .86. In the present case, the absorption of the  $\alpha$  rays is mainly due to gelatine, which is the main composition of the sensitive film, and this substance seems to be of a character similar to air concerning absorption.

6. *Number of silver grains along an  $\alpha$  ray track.* Silver grains along an  $\alpha$  ray track are naturally not equidistant. To find the distribution, Ikeuti has measured, by means of the ocular micrometer of a microscope, the distance  $d$  between successive grains on the track for a large number of pairs of the grains. When the number of pairs of grains was plotted against the corresponding values of  $d$ , and a mean curve was drawn, this showed a maximum at  $d=1.85 \mu$  in the case of Ilford Process Plates, falling quickly to zero on the side of the origin and somewhat slowly on the other side. From these measurements the mean value of  $d$  was calculated to be  $2.85 \mu$ . This corresponds to 350 grains per millimetre of the track. Since the longest tracks of the  $\alpha$  rays from radium A and radium C are 36 and  $52 \mu$  respectively, they will consist on the average of 12.6 and 18.2 grains respectively. It must, however, be remembered that the actual numbers are subjected to fairly large fluctuations.

7. *The nature of the photographic action of  $\alpha$  particles.* Alpha ray tracks obtained in a sensitive film do not exhibit even the slightest difference along their whole range; neither in the compactness of the grains nor in their size. This is a very important fact and confirms conclusively the previous experiment of Kinoshita<sup>2</sup>), in which the constancy of the photographic action of an  $\alpha$  particle along the whole range was photometrically established. Now, if it be considered that there are all possibilities of regarding ionisations in a solid and in a gas to be of a similar type, the question may arise, why the photographic action, which is nothing but the result of ionisation, should not be represented by the characteristic curve known as Bragg's ionisation curve. As a matter of fact, darkening in the pleochroic halo is particularly pronounced near the boundary, in spite of that the number of  $\alpha$

1) E. Marsden and H. Richardson, Phil. Mag. **25** (1918), p. 191.

2) *l. c.*

particles traversed, taken per unit volume, is least in that region, and this fact can be explained as the result of an intense ionisation near the extreme end of the range of the  $\alpha$  particles<sup>1)</sup>.

A theory put forward by Kinoshita to explain the singularity of the photographic action was that, if some of the halide molecules within a grain are initially ionised by one or more  $\alpha$  particles, the whole grain becomes subsequently capable of development, but the reduction cannot extend to other grains which have not been initially ionised. When the film is completely developed, all the grains struck by the  $\alpha$  particles are reduced to a constant limit, which depends on the size of halide grains in the emulsion film but not on the degree of the primary ionisation in them, and we thus obtain silver grains as a secondary consequence of the ionisation, so that the photographic action is constant throughout the whole range of the  $\alpha$  particles in the substance. A further consideration will be presented later<sup>2)</sup>.

In variance with the above theory, Michl<sup>3)</sup> states that only a part of the halide grains encountered by an  $\alpha$  particle become subsequently developable. This conclusion is based on a microscopic comparison between the compactness of silver grains on a photographic plate which was obtained by exposing it to light, and the diffuse arrangement of the grains on an  $\alpha$  ray track obtained on the same plate.

In order to show that the above reasoning is by no means adequate, the original paper of Kinoshita must be again referred to. It was shown that the photographic density  $D$  of a photographic plate produced by normally falling  $\alpha$  particles varies with their number  $n$  per unit area of the plate as

$$D=D_0(1-e^{-cn}), \quad (1)$$

where  $D_0$  is the maximum value of  $D$  attainable by an indefinitely large number of the  $\alpha$  particles, and  $c$  is a constant depending on the quality and the thickness of the emulsion film on the plate.

As is generally known, the photometric density of a plate is

1) J. Joly, *l. c.*; E. Rutherford, 'Radioactive Substances and their Radiations' (1913), p. 310.

2) *c. f.* p. 15.

3) *l. c.*

proportional to the mass of silver contained in a unit area of the plate. Therefore, if it be assumed, as a first approximation, that all the grains are of equal mass, the above equation may be written in terms of the number  $s$  of the grains per unit area in the plate.

$$s = s_0 (1 - e^{-cn}), \quad (2)$$

where  $s_0$  is the value of  $s$  for the plate for which  $D = D_0$  and would be the total number of the halide grains initially present in the emulsion film per unit area.

Consequently, the number of the falling  $\alpha$  particles required to increase one more developable grain will be

$$\frac{dn}{ds} = \frac{1}{c(s_0 - s)}. \quad (3)$$

If we take the corresponding values of  $s$  and  $n$  in a plate of very small density,  $s$  is negligibly small compared with  $s_0$ . In this case, the above equation reduces to

$$\frac{dn}{ds} = \frac{1}{cs_0}.$$

Giving values experimentally found:

$c = 1.18 \cdot 10^{-8}$  and  $s_0 = 1.16 \cdot 10^8$  for a Wratten Instantaneous Plate, and  $c = .93 \cdot 10^{-8}$  and  $s_0 = .97 \cdot 10^8$  for a Wratten Ordinary Plate,

$$\begin{aligned} \frac{dn}{ds} &= .73 \text{ for the Instantaneous Plate, and} \\ &= 1.1 \text{ for the Ordinary Plate.} \end{aligned}$$

On examining microscopically, it was found that the Instantaneous Plate of very high density was entirely covered with silver grains, while the Ordinary Plate of maximum density was almost covered with grains, but about one-tenth of the area was estimated as allowing  $\alpha$  particles to pass through without contact with the grains, and that in an Instantaneous Plate of small density about one-third of the grains were overlapping others, while in an Ordinary Plate the overlapping was practically negligible, so that one  $\alpha$  particle did not strike more than one halide grain.

Taking these facts into consideration, it can be concluded with certainty that the number of  $\alpha$  particles required to change one halide grain into the developable state is *one*, whenever it

strikes the grain. For, if, in the case of the Instantaneous Plate, the number of the overlapping be taken as 37 per cent. of the total, each  $\alpha$  particle would in the average change 1.37 grains on its passage through the film; in other words, the number of  $\alpha$  particles required to change one halide grain would be  $\frac{1}{1.37}$  or .73, which is the value of  $\frac{dn}{ds}$  calculated from the values of  $e$  and  $s_0$  for that plate. Similarly, in the case of the Ordinary Plate, if the area uncovered with the grains be taken as 10 per cent. of the totals, 1.1  $\alpha$  particles on average would be required to change one halide grain. We are thus lead to the conclusion that one  $\alpha$  particle is sufficient to change a halide grain into the developable state, whenever it encounters the grain and whatever may be the quality of the plate.

In dealing with an  $\alpha$  ray track, it must be remembered that we are observing those grains only, the centres of which lie, as will be directly shown, within a very narrow cylinder of a cross section equal to that of the halide grains, but not those having their centres outside the cylinder. Since grains at various depths, the difference of which is much greater than their linear dimensions, can be seen simultaneously in a microscopic vision even of fairly high magnification, mere comparison of the compactness of visible grains on the two different plates, one acted on by light and the other by individual  $\alpha$  particles, would never lead to the conclusion already stated.

8. *The size of grains.* The size of the silver grains has been determined, as far as we know, only by microscopic methods, visual, projecting or photographing. These methods, however, do not seem to give very reliable results, unless care is taken with regard to the diffraction phenomenon, because the grains to be measured are so small that their linear dimensions are of the same order of magnitude as the wave-lengths of the visible light. In the following, we shall describe two methods of deducing the size of halide grains from the data obtained in the investigation on the  $\alpha$  ray photographs. Although the methods are rather indirect, they may still be of use in practical application.

(a). Having proved that each halide grain is rendered capable of development whenever it is encountered by an  $\alpha$  particle, equation (3) which can be written in the form:

$$ds = c (s_0 - s) dn, \quad (3')$$

may be interpreted as: the rate at which the number of acted or developable halide grains increases with the falling  $\alpha$  particles is proportional to the number of halide grains not yet acted upon. And the proportional factor  $c$  will be the probability of one halide grain being struck by an  $\alpha$  particle, and consequently, the ratio of the area of the projection of each grain to a plane perpendicular to the direction of motion of the  $\alpha$  particles to a unit area.

Therefore, if  $r_0$  is the average radius of the halide grains, supposing these to be spherical,

$$c = \frac{\pi r_0^2}{1},$$

from which

$$r_0 = \left( \frac{c}{\pi} \right)^{\frac{1}{2}}. \quad (4)$$

Thus, from the values of  $c$  already given, we obtain:

$$\begin{aligned} r_0 &= 6.1 \mu \text{ for the Instantaneous Plate, and} \\ r_0 &= 5.4 \mu \text{ for the Ordinary Plate.} \end{aligned}$$

If each grain of silver bromide of radius  $r_0$  be completely reduced to metallic silver, its mass  $m$  and radius  $r$  would be

$$m = \frac{4}{3} \pi r_0^3 \rho_0 \times \frac{108}{188} = \frac{4}{3} \pi \left( \frac{c}{\pi} \right)^{\frac{3}{2}} \rho_0 \times \frac{108}{188}, \quad (5)$$

$$r = \left( \frac{108}{188} \frac{\rho_0}{\rho} \right)^{\frac{1}{3}} r_0 = \left( \frac{108}{188} \frac{\rho_0}{\rho} \right)^{\frac{1}{3}} \left( \frac{c}{\pi} \right)^{\frac{1}{2}}, \quad (6)$$

where  $\rho_0$  and  $\rho$  are the densities of silver bromide and metallic silver respectively.

As a verification of the result, the mass  $M$  of silver contained in a unit area of a plate deduced from the mass  $m$  calculated by equation (5) and the number  $s$  of the silver grains per unit area, viz.,

$$M = ms = \frac{4}{3} \pi \left( \frac{c}{\pi} \right)^{\frac{3}{2}} \rho_0 s \times \frac{108}{188} \quad (7)$$



may be compared with that deduced from its photometric density  $D$ , viz.

$$M=kD, \quad (8)$$

where  $k$  is the photometric constant, being for green light equal to  $1.03.10^{-1}$  gr. per sq. cm. of the plate.

Giving the following values experimentally found:

$s=1.29.10^7$  for an Instantaneous Plate, for which  $D=.412$ , and

$s=1.06.10^7$  for an Ordinary Plate, for which  $D=.210$ , we get

$M=4.52.10^{-5}$  gr. per sq. cm. by (7) and

$M=4.24.10^{-5}$  gr. per sq. cm. by (8) for the Instantaneous Plate, and

$M=2.55.10^{-5}$  gr. per sq. cm. by (7) and

$M=2.16.10^{-5}$  gr. per sq. cm. by (8) for the Ordinary Plate.

Bearing in mind the fact that the conversion of silver bromide to metallic silver is not carried out to completion, the agreement between the values obtained by the two methods is seen to be quite satisfactory.

The average radius of silver grains calculated by equation (6) corresponds, for the reason just stated, to the superior limit. It is

$r=.43 \mu$  for the Instantaneous Plate, and

$r=.38 \mu$  for the Ordinary Plate.

The size of the silver grains was actually measured under a microscope, by means of an ocular micrometer for a number of grains. It was found that the above calculated values of  $r$  are within the range over which the size of the observed grains varies.

(b). Ikenti showed that the average radius  $r_0$  of halide grains can also be deduced from the average number  $s_1$  of silver grains per unit length along an  $\alpha$  ray track, when the thickness of the emulsion film and the mass of silver halide contained per unit area of it are known from other determinations.

Remembering that every halide grain becomes subsequently developable whenever struck by an  $\alpha$  particle, it can easily be seen that silver grains presenting themselves as an  $\alpha$  ray track on a developed plate must have their centres within a circular

cylinder drawn round the path of the  $\alpha$  particle with radius equal to that of halide grains. Consequently,  $s_1$ , which is the reciprocal of the average distance  $d$  between successive grains along the track, will be the number of the halide grains having their centres within the cylinder of unit length; thus  $\frac{s_1}{\pi r_0^2}$  will be the total number of the halide grains initially present in the emulsion film per unit volume.

If  $t$  is the thickness of the film, the total number  $s_0$  of the halide grains in a unit area of the plate will be

$$s_0 = \frac{s_1 t}{\pi r_0^2}.$$

Another relation between  $s_0$  and  $r_0$  can be obtained from a consideration on the amount  $M_0$  of silver bromide contained in a unit area of the plate,

$$M_0 = \frac{4}{3} \pi r_0^3 \rho_0 s_0,$$

where  $\rho_0$  is, as before, the density of silver bromide.

From the above two equations, we obtain

$$r_0 = \frac{3}{4} \frac{M_0}{\rho_0 s_1 t}.$$

From a set of measurements made on an Ilford Process Plate, *e.g.*

$$s_1 = 3,500 \text{ per cm.},$$

$M_0 = 9.6 \cdot 10^{-4}$  gr. per sq. cm., which was determined by chemical analysis, and

$t = 15 \mu$ , which was measured by Zeiss's Dickenmesser, the average radius of the halide grain is found to be

$$r_0 = .22 \mu.$$

By using the relation in equation (6), the average radius of the silver grains becomes

$$r = \left( \frac{108}{188} \frac{\rho_0}{\rho} \right)^{\frac{1}{3}} r_0 = .15 \mu.$$

A suitable photometer being at present not at our disposal, we are unable to compare this result with that deduced from the photometric density. It may only be noted that the above

calculated value of  $r$  is also within the range over which the size of the grains actually measured by means of the microscope varies.

9. *Deflexions of  $\alpha$  particles on the passage through the emulsion film.* Evidences have already been given by the previously cited investigators that some of the  $\alpha$  particles suffer sudden deflexions on the passage through the emulsion film.

In dealing with the deflexions of  $\alpha$  rays, the importance of utilizing a single source may be emphasized. If a set of radial  $\alpha$  ray tracks are obtained with an active needle in the way already described, the possibility is excluded that two tracks, running in different directions, happen to fall at a common point and present themselves as if they were a single track suffering a sudden deflexion.

In the microphotograph in fig. 10, which is enlarged 1,500 diameters, the tracks of four  $\alpha$  particles, running from left to right, are visible. The source of the particles lies outside the figure to the left about 15 centimetres on this scale from the left end. We can see that while the second  $\alpha$  particle from the top passed straight on, the other three suffered sudden deflexions of  $10^\circ$  to  $15^\circ$  downwards after traversing some distances nearly parallel to one another.

We have examined hundreds of sets of the radial  $\alpha$  ray tracks, but so far we have not been able to find any which can be said with certainty to have suffered the deflexion of an angle so large as  $90^\circ$ . The smallness of the proportion of the largely deflected tracks to the total will not be inconsistent with the experimental results arrived at by Geiger<sup>1)</sup> and by Geiger and Marsden<sup>2)</sup>, and also with the theory worked out by Rutherford<sup>3)</sup>. It must be borne in mind that we are, in the present case, observing only such deflexions, which have taken place within a very thin layer bounded by planes parallel to the surface of the film, whereas the deflexions occur, in general, equally in all planes which contain the initial line of motion.

---

1) H. Geiger, Proc. Roy. Soc. A, **81** (1908), p. 174, and **83** (1910), p. 492.

2) H. Geiger and E. Marsden, Proc. Roy. Soc. A, **82** (1909), p. 495.

3) E. Rutherford, Phil. Mag. **21** (1911), p. 669.

When a photographic plate was placed in contact with a flat piece of glass coated with the active deposit of radium and thus exposed to the  $\alpha$  rays coming out of the source of large area, a considerable proportion of their tracks seemed to have suffered large deflexions. This is not in conformity with the result just stated. It appears likely that most, if not all, of the tracks which look as if they were deflected are only apparently so. This view is supported by the fact that there were as many tracks showing large deflexions as small ones.

Experiments made with the object of finding if the magnetic field has any influence upon the  $\alpha$  ray tracks gave negative results. In a field of ten thousand gauss, up to which the experiment was extended, an  $\alpha$  particle with a velocity of  $10^9$  cm. per sec. (one-half of the initial velocity of the  $\alpha$  particles from radium C) will describe a path for which the radius of curvature is as great as 20 centimetres. It would not be possible to recognize such a slight curvature, as the track under examination is only  $52 \mu$  at most in length.

10. *The photographic action of  $\beta$  particles.* It has long been known that  $\beta$  rays possess the property of acting on a photographic plate; but owing to difficulties involved in the experiments, very little is known about the effect of an individual  $\beta$  particle.

When the  $\alpha$  and  $\beta$  rays from the active deposit of radium were allowed to fall separately upon two areas on a thinly coated plate, the photometric density produced by the  $\beta$  rays was, for an equal number of the particles, found to be one-sixth to one-eighth of that produced by the  $\alpha$  rays. Therefore in going a unit distance through the emulsion film, a  $\beta$  particle brings out at most the above fraction only of the silver grains which an  $\alpha$  particle would, the actual path of the  $\beta$  particle being, on account of deflexions, greater than the thickness of the film. It is thus to be anticipated that the silver grains acted on by a  $\beta$  particle follow one another with too wide intervals to present themselves as the track of the particle, much more so when the liability of the particle in suffering deflexions through matter is considered. The difference shown by the tracks in air of  $\alpha$  and  $\beta$  particles in the photograph obtained by

C. T. R. Wilson in his well-known condensation experiment may, though not quite similar, serve as an analogy. While an  $\alpha$  ray track would still be detectable, if the number of water drops per unit length were reduced to one-thousandth, say, in a  $\beta$  ray track this would be far from being the case. It must be remembered that  $\beta$  particles will suffer greater deflexions in gelatine films than in air. A direct evidence for the above conclusion is found in the fact that it is possible to obtain a halo due to the  $\alpha$  particles from radium C, outside of which no perceptible track of any sort is present, although the source emits simultaneously  $\beta$  particles as well and the most of them travel far beyond the boundary of the halo.

The photographic action of  $\beta$  particles should be explained by an hypothesis of the kind we have made in the case of  $\alpha$  particles; for, in the latter the basis of the hypothesis is the ionisation of halide molecules, which is the effect also common to  $\beta$  particles. We shall consider that a halide grain becomes capable of development when it is encountered by a  $\beta$  particle, but only when the encounter takes place under certain favourable conditions. This seems plausible, because a  $\beta$  particle, while it would encounter on a path per unit length as many halide grains as an  $\alpha$  particle does, renders developable silver grains of only a small part compared with those similarly affected by an  $\alpha$  particle. Since it is very likely that, whenever a halide grain is encountered by a  $\beta$  particle, some halide molecules in it, however few in number, are ionised, we may assume that the process of development in the grain cannot start unless the number of initially ionised halide molecules exceeds a certain value. An analogous phenomenon is met with in the case of an electric discharge between two electrodes. The discharge is facilitated and starts at a lower but definite potential when the interposed gas is initially ionised beyond a certain degree. The above assumption apparently contradicts what has been said in the case of  $\alpha$  particles; but it seems quite possible to an  $\alpha$  particle, which in gases shows an ionising action several thousand times stronger than that of a  $\beta$  particle, to ionise a number of halide molecules over the threshold value, whenever it strikes a halide grain.

11. *Considerations on the photographic action of  $\gamma$  rays.* The general feature of the photographic action of  $\gamma$  rays may be inferred from the facts hitherto accumulated. As is well known, X rays do not directly ionise the molecules of a gas which the rays traverse, but liberate from them corpuscular radiation which is responsible for the ionisation<sup>1)</sup>. The velocity of the emitted corpuscles is independent of the nature of the emitter and depends only upon the wave-length of the exciting X rays, the smaller the wave-length the greater the velocity. The excitation of the corpuscular radiation by X rays is not limited to gases but is also true of solids and liquids.

There is every reason to believe that this is the case with  $\gamma$  rays, which, as we know, differ from X rays only in wave-length. It has already been shown that the corpuscular radiation set up by  $\gamma$  rays from a radium salt is nearly as swift as the primary  $\beta$  rays emitted by it<sup>2)</sup>. Thus, the effect of exposing a photographic plate to X or  $\gamma$  rays will be that corpuscular radiation is set up throughout the exposed portion of the plate. Since individual  $\beta$  particles leave no detectable tracks of silver grains on a photographic plate, it will be impossible to obtain a track of X or  $\gamma$  rays on a photographic plate similar to that of X rays illustrated by the photographs obtained by C. T. R. Wilson in the condensation method. It will be evident that the halide grains rendered capable of development by a flash of X or  $\gamma$  rays are scattered very diffusely throughout the volume of the emulsion film, but with no definite arrangement.

In an experiment we have exposed a plate to a flash of X rays through an extremely narrow slit between two thick brass plates, to see if any particular effects were produced in- and outside the region upon which the X rays fell. Microscopic examination of the plate gave negative results, as was naturally to be expected.

---

1) C. G. Barkla and L. Simons, *Phil. Mag.* **23** (1912), p. 317; C. T. R. Wilson, *Proc. Roy. Soc. A*, **87** (1912), p. 277; C. G. Barkla and A. J. Philpot, *Phil. Mag.* **25** (1913), p. 832.

2) A. S. Eve, *Phil. Mag.* **8** (1904), p. 669; S. J. Allen, *Phys. Rev.* **23** (1906), p. 65.

In conclusion, we wish to thank Professor Nagaoka for placing the resources of the Laboratory at our disposal and for his continual interest during the progress of this investigation.

Physical Laboratory, University of Tokyo.

### Explanation of the Plates.

- Fig. 1.** The general feature of a plate containing several spots, each of which consists of a number of radial  $\alpha$  ray tracks. The isolated spot at the top and the large one at the bottom of the figure are reproduced in figs 5 and 6 respectively in a higher magnification.
- Figs. 2-4.** Haloes due to radium C, at different stages of formation.
- Figs. 5-8.** Haloes due to radium A and C. In each halo two concentric circles are to be seen. The inner circle is due to radium A and the outer to radium C. In fig. 5 the inner circle is more conspicuous than the outer one, while in fig. 6 the reverse is the case.
- Fig. 9.** The tracks of  $\alpha$  particles emitted from a nucleus of radium C, reaching to various distances.
- Fig. 10.**  $\alpha$  ray tracks showing sudden bents. On this figure are visible the tracks of four  $\alpha$  particles which passed from left to right. Three of them suffered sudden deflexions.







Fig. 1.  $\times 120$ .

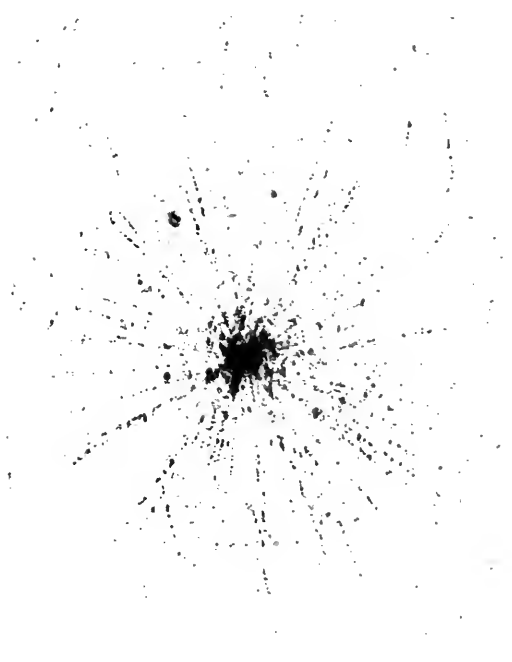


Fig. 2.  $\times 500$ .

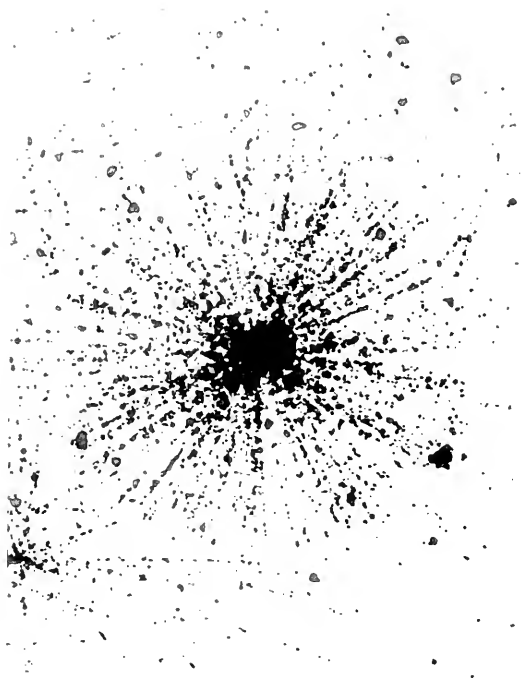


Fig. 3.  $\times 500$ .

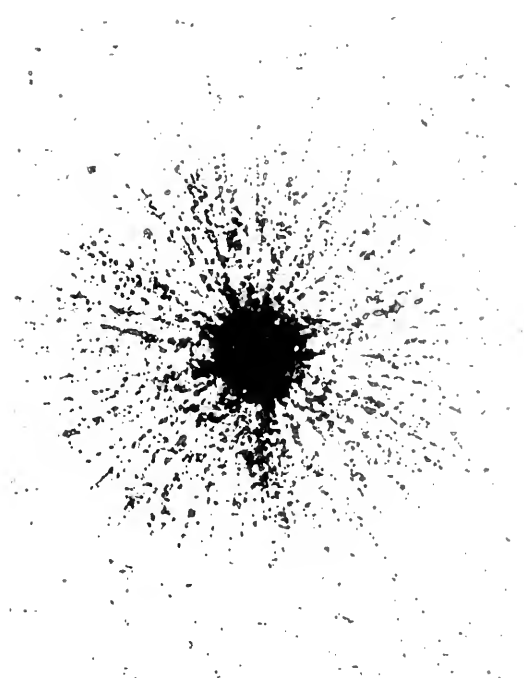


Fig. 4.  $\times 500$ .



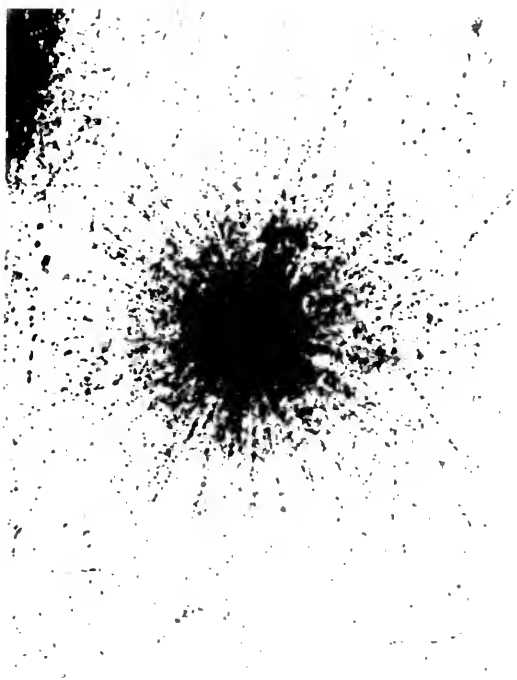


Fig. 5.  $\times 500$ .

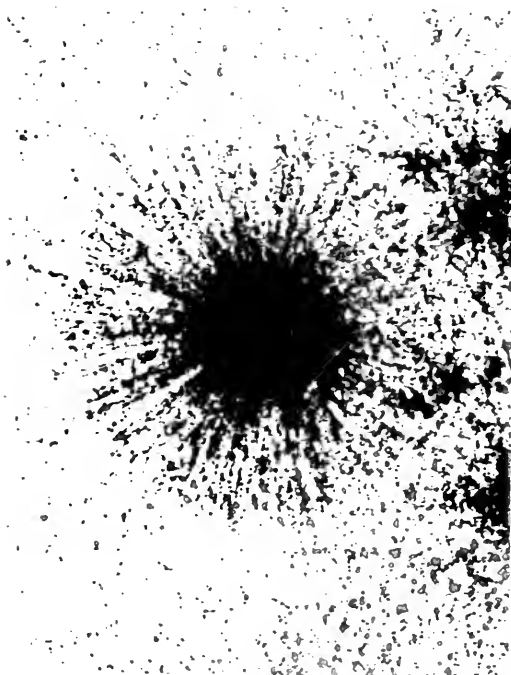


Fig. 6.  $\times 500$ .

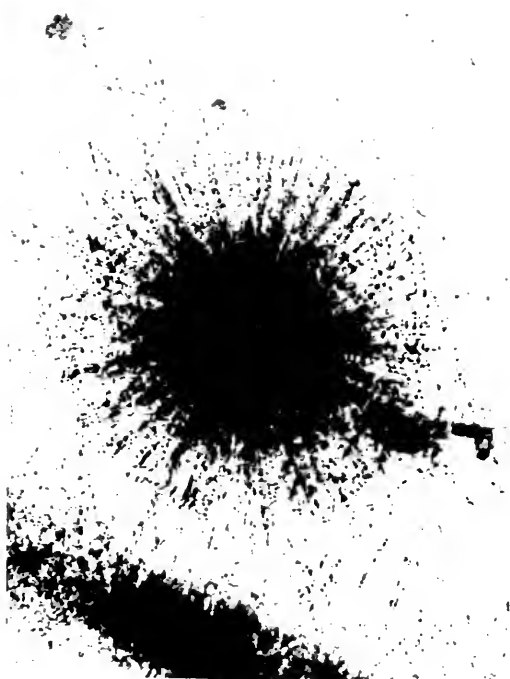


Fig. 7.  $\times 500$ .

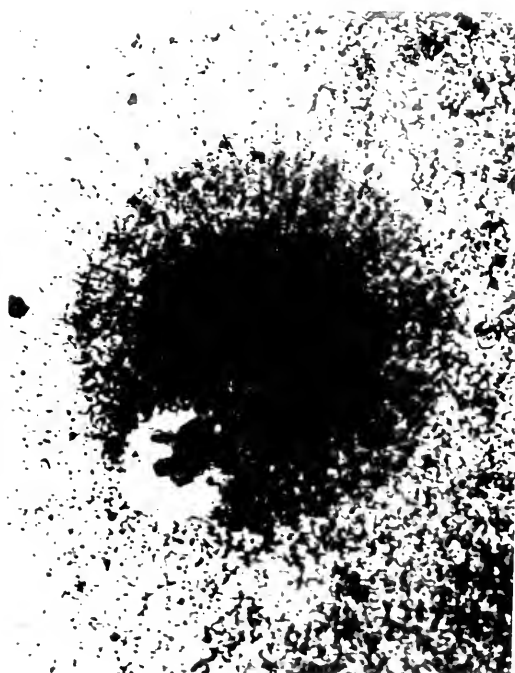


Fig. 8.  $\times 500$ .



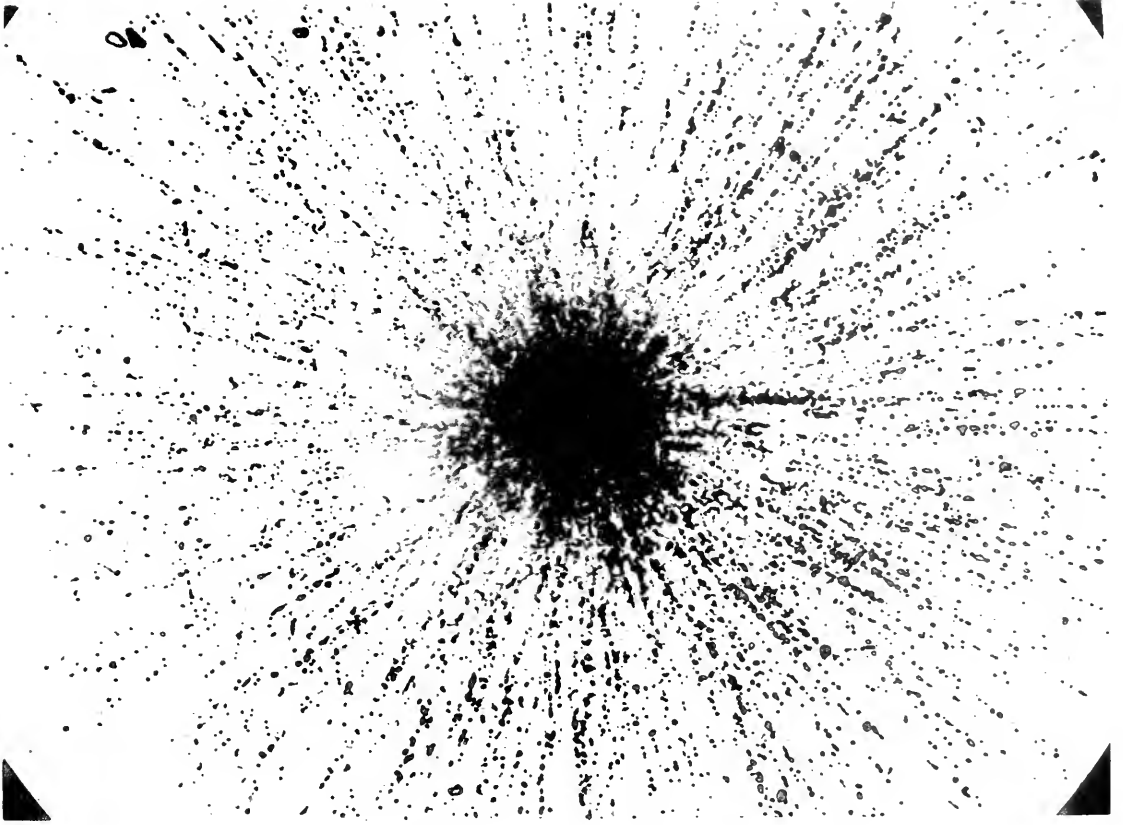


Fig. 9.  $\times 500$ .

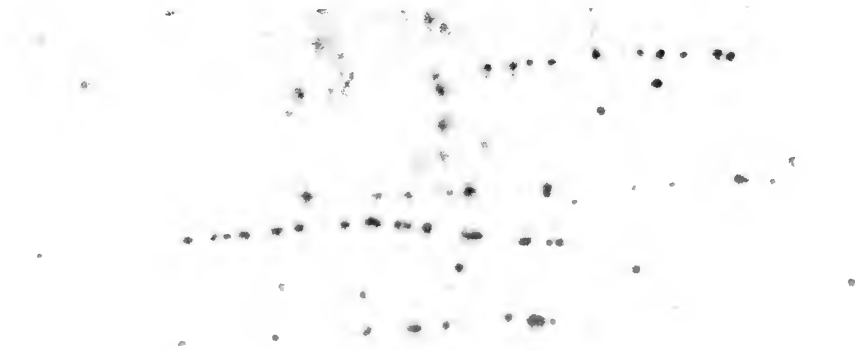


Fig. 10.  $\times 1,500$ .









MBL WHOI LIBRARY



WH 19KX Q

